

Simulation and systems management in crop protection

R. Rabbinge, S.A. Ward and
H.H. van Laar (Editors)



Simulation Monographs 32

**Simulation Monographs is a series on
computer simulation in agriculture and
its supporting sciences**

Simulation and systems management in crop protection

R. Rabbinge, S.A. Ward and
H.H. van Laar (Editors)



Pudoc Wageningen 1989

CIP-data Koninklijke Bibliotheek, Den Haag

Simulation

Simulation and systems management in crop protection /
R. Rabbinge, S.A. Ward and H.H. van Laar (eds.). –
Wageningen : Pudoc. – Ill. – (Simulation monographs ; 32)
With index, ref.

ISBN 90-220-0899-1 bound

SISO 632.6 UDC 632.9:681.3 NUGI 835

Subject headings: crop protection ; simulation models /
crop protection ; systems management.

ISBN 90 220 0899 1

NUGI 835

© Centre for Agricultural Publishing and Documentation (Pudoc), Wageningen,
the Netherlands, 1989.

No part of this publication, apart from bibliographic data and brief quotations embodied
in critical reviews, may be reported, re-recorded or published in any form including print,
photocopy, microfilm, electronic or electromagnetic record without written permission
from the publisher: Pudoc, P.O. Box 4, 6700 AA Wageningen, the Netherlands.

Printed in the Netherlands

CONTENTS

PREFACE

CONTRIBUTORS

1	THEORY OF MODELLING AND SYSTEMS MANAGEMENT	1
1.1	Systems, models and simulation - R. Rabbinge and C.T. de Wit	3
1.1.1	Introduction	3
1.1.2	Systems	3
1.1.3	Models	4
1.1.4	Explanatory models	5
1.1.5	The state-variable approach	6
1.1.6	Defining the boundaries	7
1.1.7	Steps in model building	8
1.2	Crop growth under optimal and suboptimal conditions	9
1.2.1	Production situations	10
1.2.2	Yield-reducing factors	11
1.3	Systems management	12
2	BASIC TECHNIQUES OF DYNAMIC SIMULATION	17
2.1	Some elements of dynamic simulation - P.A. Leffelaar and Th.J. Ferrari	19
2.1.1	Introduction	19
2.1.2	State variables, rate variables and driving variables	19
2.1.3	Analytical integration and system behaviour in time	21
2.1.4	Feedback and relational diagrams	23
2.1.5	Numerical integration and the time coefficient	24
2.1.6	Some numerical integration methods	30
2.1.7	Error analysis; a case study of integration with and without feedback	35
2.1.8	An example	39
2.2	Modelling of ageing, development, delays and dispersion - J. Goudriaan and H.J.W. van Roermund	47
2.2.1	Introduction	47

2.2.2	Development and delay	47
2.2.3	Simulation of development of a single generation	48
2.2.4	The boxcar train	49
2.2.5	The escalator boxcar train	51
2.2.6	The fixed boxcar train	53
2.2.7	The fractional boxcar train	56
2.2.8	Implementation of the boxcar train in CSMP	59
2.2.9	A practical application using the fractional boxcar train	71
2.2.10	Effect of the type of boxcar train on population growth	78
2.2.11	Discussion	79
3	POPULATION DEVELOPMENT IN TIME AND SPACE	81
3.1	Population models - R. Rabbinge, J.C. Zadoks and L. Bastiaans	83
3.1.1	Introduction	83
3.1.2	Exponential, logistic and paralogistic growth	83
3.1.3	Computation of the latency period (LP) and the infectious period (IP)	88
3.1.4	Computation of the maximum number of infectious sites (NMAX)	90
3.1.5	Computation of the relative growth rate	91
3.1.6	Another approach, leaf area instead of sites	95
3.1.7	Insects and mites	95
3.2	Dispersal and dispersion in space - S.A. Ward, P.S. Wagenmakers and R. Rabbinge	99
3.2.1	Introduction	99
3.2.2	Passive dispersal: fungal spores	99
3.2.3	Active dispersal in two dimensions	106
3.2.4	Descriptive models and the consequences of dispersion	109
3.2.5	Effect of dispersion on the dynamics of an aphid-parasite system, an example	114
3.2.6	Discussion and conclusions	116
3.3	Predator-prey models, stochasticity - R. Rabbinge and S.A. Ward	119
3.3.1	Introduction	119
3.3.2	Lotka-Volterra equations for predator-prey interactions	119
3.3.3	Prey preference and predator satiation	123
3.3.4	Stochastic and deterministic models	124
3.3.5	Modelling at the population level	128
3.3.6	Other methods	129
3.3.7	Equilibria	130

3.4	Population models for fruit-tree red spider mite and predatory mites - R. Rabbinge	131
3.4.1	Introduction	131
3.4.2	Fruit-tree red spider mite	131
3.4.3	Predatory mite, <i>Amblyseius potentillae</i>	136
3.4.4	Relations between predator and prey	137
3.4.5	Preference as a competitive process	138
3.4.6	Model testing	140
3.4.7	Stiff equations	143
4	COUPLING OF CROP GROWTH AND PESTS, DISEASES AND WEEDS	145
4.1	A simple and universal crop growth simulator: SUCROS87 - C.J.T. Spitters, H. van Keulen and D.W.G. van Kraalingen	147
4.1.1	Introduction	147
4.1.2	General structure of the model	147
4.1.3	Description of the model	158
4.1.4	Crop species and site characteristics	171
4.1.5	Applying the model	177
4.2	Weeds: population dynamics, germination and competition - C.J.T. Spitters	182
4.2.1	Introduction	182
4.2.2	Dynamics of soil seed population	182
4.2.3	Germination	190
4.2.4	Competition: distributing total growth rate among the competing species	199
4.2.5	Calculating growth rates from absorbed light	203
4.2.6	Competition for soil moisture	208
4.2.7	Competition for nutrients (N, P, K)	211
4.3	Combination models, crop growth and pests and diseases - R. Rabbinge and L. Bastiaans	217
4.3.1	Introduction	217
4.3.2	Statistical analysis and descriptive models	217
4.3.3	Dynamic explanatory models as a vehicle for development of EILs	220
4.3.4	SUCROS87 coupled with growth-reducing factors	224
4.3.5	A detailed study of an assimilation rate reducer, mildew in winter wheat	232
4.3.6	Discussion	238

4.4	Simulation of aphid damage in winter wheat; a case study - W.A.H. Rossing, J.J.R. Groot and H.J.W. van Roermund	240
4.4.1	Introduction	240
4.4.2	The life cycle of <i>Sitobion avenae</i>	241
4.4.3	Simulation of crop growth	242
4.4.4	Simulation of aphid damage	246
4.4.5	Simulation results	250
4.4.6	Application to management	260
5	DECISION MAKING AND MANAGEMENT	263
5.1	Decision making and data management - F.H. Rijdsijk, J.C. Zadoks and R. Rabbinge	265
5.1.1	Introduction	265
5.1.2	Tactical decision making in disease control	265
5.1.3	EPIPPE, a supervised control system of pests and diseases in wheat	266
5.1.4	Pathosystem management as part of crop management	276
5.2	Application of operations research techniques in crop protection - W.A.H. Rossing	278
5.2.1	Introduction	278
5.2.2	General structure of a decision problem	279
5.2.3	Linear programming	280
5.2.4	Dynamic programming	290
5.2.5	Simulation analysis of complex decisions	296
5.2.6	Final remarks	298
6	EPILOGUE	299
6.1	Prospects for simulation and computerized decision making - J.C. Zadoks and R. Rabbinge	301
6.1.1	Introduction	301
6.1.2	Agricultural knowledge and decision making	301
6.1.3	Levels of decision making	301
6.1.4	Knowledge in agriculture	302
6.1.5	Decisions in agriculture	302
6.1.6	Agro-computerization in the Netherlands - facts	303
6.1.7	Agro-computerization in the Netherlands - opinions	305
6.1.8	Simulation applied	307
6.1.9	Comprehensiveness	307
6.1.10	Conclusions	308

ANSWERS TO THE EXERCISES	309
APPENDIX 1	361
APPENDIX 2	362
APPENDIX 3	363
APPENDIX 4	364
APPENDIX 5	365
A.5 CSMP, Continuous System Modeling Program	365
A.5.1 Introduction	365
A.5.2 The structure of the model	365
A.5.3 Some elements of CSMP	370
A.5.4 Labels	375
A.5.5 Syntax	378
APPENDIX 6	379
APPENDIX 7	387
APPENDIX 8	393
REFERENCES	398
INDEX	416

PREFACE

Crop protection: technology or science?

Pests, disease and weeds have threatened crop production since man began agricultural activity. They are a nuisance to the farmer in every agricultural system, be it subsistence farming or the high input farming now practised in many parts of the Western world.

In the last decade, pest and disease management have become accepted terms in crop protection. This is due both to a revolution in thinking and to a considerable increase in knowledge. The rather simplistic concept of destruction or total exclusion of a plant pest or disease has changed, and made way for the concepts of supervised control and pest and disease management. In agricultural systems, disease or pest outbreaks are no longer disasters which must be accepted, but are now manageable and manipulable phenomena. Intensive agriculture is developing into a technological rather than a biological activity.

More and more techniques with well-understood effects have been developed and are beginning to dominate the less well-understood methods of biological control. This enables the farmer and his advisers to manage the agricultural system to meet a well-defined target, that of maximum economic return in the short term and sound agricultural practice in the long term.

Crop protection is incorporated into a cropping system to manipulate the pathosystem of a crop in a way that prevents economic loss. Crop protection research is following a similar trend: the accent is changing from the 'scientific', to the 'technological'. Both types of research focus on crop protection. Scientific and technological activities are not considered to be qualitatively different, nor can an appeal be made to concepts of 'pure' as opposed to 'applied' science. They are considered as points on a convenient spectrum that is defined in terms of the objectives and expectations of the practitioners.

This development in crop protection research – from studying and describing effects to understanding, governing and manipulating cropping systems – has been made possible by an enormous increase in our knowledge of the processes of crop growth and crop production, and by an improved understanding of how crops behave and can be affected.

Systems analysis and simulation have contributed considerably to this development by providing the insight which has led to crop management policies and techniques. Modern crop protection is a complicated affair in which risk, cost-effectiveness and environment must be considered. Genetic resistance, crop husbandry methods and weather determine the course of insect-pest outbreaks and disease epidemics. Pesticides are often effective against more than one harmful agent, but they may also induce pest and disease shifts or resistance.

Systems analysis is an intellectual tool that can be used to bring order to this bewildering complexity.

This book is intended for agriculturalists, biologists and crop-protection researchers wishing to use this tool in their work, and is organized such that the reader is introduced step by step to the modern techniques and how they can best be used in crop protection and management.

In Chapter 1, systems analyses, simulation and systems management are introduced as instruments for crop-protection management. The character and importance of crop protection at various production stages is described.

Chapter 2 gives an explanation of systems dynamics. The state-variable approach is introduced and the elementary concepts of systems dynamics are explained. Time coefficients, numerical integration methods and relative and absolute errors are discussed and the concept of delay in simulation models is explained. Dispersion in relation to time and space is also discussed and the methods used to mimic this dispersion are introduced.

Simulation models of epidemics are introduced in Chapter 3. Models of insect populations and fungal epidemics in relation to time and space are discussed. Stochastic elements in simulation models are considered, and the need, in some cases, to introduce stochasticity into simulation models is illustrated. Predator-prey relations or host-parasite relations, crucial in biological control, are also discussed in this chapter.

Chapter 4 concerns models combining crop growth with the reducing factors pests, disease and weeds. Summary models of crop growth are sufficient to be able to evaluate the effects of pests and disease on crop growth, but comprehensive combination models may be needed to give some insight into the reasons for the damage and to use this insight to formulate damage relations. Various examples of pests, disease and weeds are given to illustrate this.

In Chapter 5, techniques and methods are discussed which may be used to manipulate cropping systems and pathosystems to minimize yield loss and maximize economic return. As agriculture is an integration of knowledge from several areas and comprises a considerable amount of data, decision-making methods are introduced. Dynamic optimization techniques are illustrated by their use in decision-making in pest management and the provision of recommendations tailored to the specific needs of a farmer and his individual field.

Chapter 6 describes the development of agriculture from management to manipulation, and the use of the described techniques for defining crop-management options. Simulation is not a panacea. In some cases, systems analysis may deliver simulation models that are scientifically sound and useful; in other cases, the approach may be too costly, the detour too long or the result too inaccurate to be useful in solving practical problems. A summary of how the techniques can be used is given, present trends are indicated and possible future developments discussed.

The publication of this Simulation Monograph was motivated by the advanced international course 'Simulation and Systems Management in Crop

Production'. This course, held in Wageningen in 1983 and 1986, was organized by the Foundation of Post-Graduate Courses of the Agricultural University of Wageningen.

In the text, and in several exercises, dynamic simulation models are described. These models are also available on floppy disk. They can be used on mainframe VAX computers and IBM PC-AT's, or compatibles, with 512 KB working memory (RAM), 10 MB hard disk external memory, 1 floppy disk drive for 360 KB or 1.2 MB disks and using the DOS 2.11 operating system or later versions. On Personal Computers, the computer simulation language PCSMP (Jansen et al., 1988) should be used.

We wish to thank Lien Uithol-van Gulijk, who typed the manuscript many times, Herman van Roermund and Lammert Bastiaans for writing the exercises, and Co Engelsman for drawing the graphs. Professor C. T. de Wit critically read the manuscript and his advice is gratefully acknowledged.

R. Rabbinge
S.A. Ward
H.H. van Laar

CONTRIBUTORS

- Bastiaans, L., Department of Theoretical Production Ecology, Agricultural University, P.O. Box 430, 6700 AK Wageningen, the Netherlands.
- Ferrari, Th.J., Esserlaan 5, 9722 SK Groningen, the Netherlands.
- Goudriaan, J., Department of Theoretical Production Ecology, Agricultural University, P.O. Box 430, 6700 AK Wageningen, the Netherlands.
- Groot, J.J.R., Institute for Soil Fertility, P.O. Box 30003, 9750 RA Haren, the Netherlands.
- Keulen, H. van, Centre for Agrobiological Research, P.O. Box 14, 6700 AA Wageningen, the Netherlands.
- Kraalingen, D.W.G. van, Department of Theoretical Production Ecology, Agricultural University, P.O. Box 430, 6700 AK Wageningen, the Netherlands.
- Laar, H.H. van, Department of Theoretical Production Ecology, Agricultural University, P.O. Box 430, 6700 AK Wageningen, the Netherlands.
- Leffelaar, P.A., Department of Theoretical Production Ecology, Agricultural University, P.O. Box 430, 6700 AK Wageningen, the Netherlands.
- Rabbinge, R., Department of Theoretical Production Ecology, Agricultural University, P.O. Box 430, 6700 AK Wageningen, the Netherlands.
- Roermund, H.W.J. van, Department of Theoretical Production Ecology, Agricultural University, P.O. Box 430, 6700 AK Wageningen, the Netherlands.
- Rossing, W.A.H., Department of Theoretical Production Ecology, Agricultural University, P.O. Box 430, 6700 AK Wageningen, the Netherlands.
- Rijsdijk, F.H., Gen. Foulkesweg 18, 6703 BR Wageningen, the Netherlands.
- Spitters, C.J.T., Centre for Agrobiological Research, P.O. Box 14, 6700 AA Wageningen, the Netherlands.
- Wagenmakers, P.S., Research Station for Fruit Growing, Brugstraat 51, 4475 AN Wilhelminadorp, the Netherlands.
- Ward, S.A., Zoology Department, La Trobe University, Bundoora, Victoria 3883, Australia.
- Wit, C.T. de, Department of Theoretical Production Ecology, Agricultural University, P.O. Box 430, 6700 AK Wageningen, the Netherlands.
- Zadoks, J.C., Department of Phytopathology, Agricultural University, P.O. Box 8025, 6700 EE Wageningen, the Netherlands.

1 THEORY OF MODELLING AND SYSTEMS MANAGEMENT

1.1 Systems, models and simulation

R. Rabbinge and C.T. de Wit

1.1.1 Introduction

Systems analysis and simulation have been used by engineers for many years and their success with this approach has inspired biologists and agronomists to apply similar techniques in their disciplines. The approach can be characterized by the terms: systems, models and simulation. A system is a limited part of reality that contains interrelated elements. A model is a simplified representation of a system. Simulation can be defined as the art of building mathematical models and the study of their properties with reference to those of the systems they represent.

1.1.2 Systems

As described elsewhere (de Wit, 1970; 1982), a system is a limited part of reality, so a boundary must be selected. Ideally, this choice should be made so that the system is isolated from its environment, but in most situations this is impossible. In this case, one should select a boundary whereby the environment may influence the system, but where the system affects the environment as little as possible. To achieve this, it may be necessary to choose a system larger than is strictly necessary.

In agricultural systems, for instance, the microclimate is often part of the system, but the influence of the agricultural system on the macroclimate is neglected. However, the assumption that everything is related to everything else would paralyse research. In crop protection agricultural systems are well defined. Thus, four main system types are distinguished here: pathosystems, cropping systems, farming systems and agroecosystems. A pathosystem may include host and parasite populations, and vectors and their mutual interactions. The pathosystem is subject to the effects of climate and man. Pathosystems are parts of cropping systems, which include not only crop protection aspects but also crop agronomic activities. Cropping systems are restricted to one crop and, in principle, deal mainly with crop husbandry and its economics. Farming systems comprise the husbandry and economics of a variety of crops, and the interactions between them. Here, managerial aspects may dominate over the crop agronomic aspects. Farming systems are subsystems of agroecosystems. Agroecosystems are those ecosystems which have been affected or manipulated by man to serve his own needs. Ecosystems have organisms and non-biotic factors as their components, each with its own pattern or distribution in relation to space and

time, and with a recognizable structure consisting of functional relations among these components.

Systems management takes place at all four levels, i.e. pathosystems, cropping systems, farming systems and agroecosystems. The importance of good management of agroecosystems and farming systems is clear, but good management requires considerable ecological and economic information. This book deals with management at both pathosystem and cropping system levels.

Systems may be repeatable, recurring or unique. Examples of repeatable systems are found in microbiology (manufacture of vinegar), agriculture (growth of maize) or industry (manufacture of cars). Examples of recurring systems are stars, individuals of a species, and ecological systems with so much resilience that after disturbance the original course of development is restored (peat bogs). However there are also unique ecological systems, or ecological systems with unique aspects. These are systems whose development is not governed by negative feedback (Section 2.1), so their development is unpredictable, even though their initial conditions may be similar. Examples are evolutionary systems and weather systems. Other systems are unique because of their geographical situation, e.g. some estuaries, lakes or islands or, of course, the world as a whole. Models of unique systems cannot be validated experimentally. They can only be verified – more or less – by observing the behaviour of the real system over a period of time. They remain, therefore, speculative models.

It is characteristic of all systems discussed in this book that major elements (e.g. plant biomass) change only gradually with time or location (space), in response to changing external factors, for example weather or fertilization. Such systems are called ‘continuous’, in contrast to ‘discrete’ systems (cf. Brockington, 1979), which deal with whole numbers or discontinuities in time. This book introduces systems analysis and simulation of repeatable living systems. The elements of this approach will be introduced in Chapter 2, on systems dynamics.

Throughout the book, CSMP (Continuous System Modeling Program III, IBM, 1975) and FORTRAN are used as computer languages. A brief description of CSMP is given in Appendix 5.

1.1.3 Models

Models may be either static or dynamic. Dynamic models consider changes with time but static models represent relations between variables which do not involve time. An example of a static model is one containing all the calculations necessary to represent the relation between respiration and growth, derived from knowledge of the underlying biochemical processes. Another example is a model used to calculate the light distribution over leaves, based on knowledge of canopy architecture, leaf properties, solar position and so on. Such static models are often components of dynamic models. Dynamic models describe the way in which a system changes over time. An important distinction to be made is that between ‘descriptive’ and ‘explanatory’ models.

A file of data on an ecosystem may be called a descriptive model, but it lacks purpose and lucidity. Potential uses of the data may be formulated, and perhaps lucidity can be introduced by mathematical or statistical treatment of the data. This may result in maps that depict characteristics of the ecosystem, or in a summary of the statistical analysis. Such models are called descriptive, because they show only the existence of relations between elements, but do not explain the relations.

However in biology, it is possible to construct models to explain systems, since, as in many other natural sciences, various levels of organization can be distinguished. These different levels of organization may be classified, according to the size of the system, for example, molecules, cell structures, cells, tissues, organs, individuals, populations and ecosystems. Models developed for the purpose of explanation are bridges between levels of organization; they allow the understanding of systems on a higher level of organization through knowledge gained by experiments on a lower level. In this way, for example, the properties of membranes may be understood better by studying molecules, and the properties of ecosystems by studying species. In this book, such explanatory simulation models of pathosystems and cropping systems are introduced. The construction of these models and the study of their behaviour in comparison with the performance of the real systems is termed simulation. Simulation may aid the understanding of important aspects of complex systems in such a way that their behaviour is understood and a guide to their management obtained. But solutions are acceptable only if they can be verified or their usefulness proved. There are models that can be validated in this way, but only models of repeatable or recurring systems. Many agricultural systems are represented by repeatable systems. A growing crop or a population of a pest or a disease organism that develops, can be repeated under various conditions and at different times.

Recurring ecological systems appear to the observer in different places at the same time in different stages. A good field ecologist is able to interpret as a time series what is observed in different places at the same time. Repeatable systems can always be analysed by experiment, but recurring systems, only sometimes, by observation. Today, there is a strong emphasis on the experimental analysis of recurring ecological systems. This experimentation does not cause irreversible effects if the disturbances to the system are damped. Also, if there are many of these systems even destruction of the system during experimentation may be acceptable.

1.1.4 Explanatory models

If the knowledge on the level which is used to explain the system is sufficiently detailed and complete, a model of the system whose behaviour has to be explained can be designed. If all of the elements composing the model are well understood it may not be necessary to evaluate the model by comparing its results with those of the real system. For example, models for space travel are so

good that the 'proof of the pudding' – the journey itself – is unnecessary as a test of the model. Explanatory models in biology are so rudimentary, however, that proof of their usefulness is necessary. Good agreement between predictions and observations is still more the exception than the rule, and even when there is good agreement, there is room for doubt.

If there are discrepancies between the model and the real system, the model may be adjusted by tuning variables to obtain better agreement. Then, something that started as an explanatory model degenerates progressively into a cumbersome descriptive model. By which time it may be much more satisfying to use statistically efficient models designed for this purpose, such as the multivariate regression models used by Thompson (1969), Pitter (1977) and Bridge (1976) to describe cropping systems.

The appropriate approach in explanatory modelling is heuristic, by way of gradual improvement. If unacceptable discrepancies between model and system are observed, it may be possible to judge which aspects are then to be studied experimentally on the level used for explanation. On the basis of this renewed study, elements of the model may be replaced and a renewed confrontation between the results of the model and the real system may again be useful. This way of working is widely used to gain insight into the functioning of repeatable and recurring systems and has proved to be very productive.

1.1.5 The state-variable approach

For dynamic models that claim to be of the explanatory type, the state-variable approach is gaining wide acceptance. These models are based on the assumption that the state of each system can be quantified at any moment, and that changes in the state can be described by mathematical equations. This leads to models in which state, rate and driving variables are distinguished.

State variables are quantities such as biomass, number of individuals of a species, the amount of nitrogen in the soil, plant or animal and the water content of the soil.

Driving variables, or forcing functions, characterize the effect of the environment on the system at its boundaries, and their value must be monitored continuously. Examples are macrometeorological variables like rain, wind, temperature and irradiation, but also the food supply or migration of animals over the boundaries of the system.

Each state variable is associated with rate variables that characterize its rate of change at a certain instant, as a result of specific processes. These variables represent flows of material between state variables; for example, between vegetative biomass and grazing animals. Their values are calculated from the state and driving variables according to rules based on knowledge of the physical, chemical and biological processes involved.

After calculating the values of all rate variables, they are then used to calculate the state variables according to the scheme: state variable at time

$t + \Delta t$ equals state variable at time t plus the rate at time t multiplied by Δt . This procedure, called numerical integration, gives the new values of the state variables, from which the calculation of rate variables is repeated. The time interval Δt must be small enough, so that the rates do not change materially within this period to avoid instabilities. This is generally the case when the time interval of integration is smaller than one-tenth of the 'time coefficient' or 'response time'. This characteristic time of a system is equal to the inverse of the fastest relative rate of change of one of its state variables. The smaller the time coefficient, the smaller the time interval of integration.

Rates are not dependent on each other in these state determined systems. Each rate depends at each moment on the state and forcing variables only and is therefore computed independently of any other rate. Hence, it is never necessary to solve n equations with n unknowns. The concept is illustrated in the following example. It is clear that the growth rate of a plant, as measured by the increase in weight of its structural tissues, is closely related to the rate of photosynthesis of the leaves. In a state variable model, this dependency is a result of the simultaneous operation of two independent processes. Photosynthesis contributes to the amount of non-structural reserves, and this amount is one of the states that determine the rate of growth. At the onset of darkness photosynthesis stops, but growth proceeds until the non-structural reserves are depleted.

Simulation models are often depicted by relational diagrams, according to the method developed by Forrester (1961) to represent models of industrial systems. Examples of such relational diagrams may be found throughout this book. The state variables are represented by rectangles and the flow of material (water, carbon, nutrients) by solid arrows. The rate of these flows is represented by the valve symbol. Constants, driving variables or forcing functions are placed in parenthesis. The dotted arrows indicate the flows of information that are considered. Relational diagrams contain no quantitative information. Such a diagram of the simplest dynamic system is given in Figure 1. If the rate is mathematically described as $\text{RATE} = \text{CONSTANT} \cdot \text{STATE}$, it depicts exponential growth. It is the most simple information feedback loop, containing one state variable whose change is given by a rate variable which depends on information flowing from the state variable to the rate variable. In many cases more complicated relational diagrams are needed to represent living systems, and another type of variable, e.g. an auxiliary variable, is needed (Section 2.1).

1.1.6 *Defining the boundaries*

The number of state variables that may be distinguished in an ecosystem is depressingly large. They concern not only primary producers, consumers and decomposers, but also the various species, their number, size, age, sex, stage of development, etc. For plants, not only are the weight and surface area of the leaves of importance but also their nitrogen and mineral contents, their enzymes and other biochemical characteristics. One could continue in this way *ad in-*

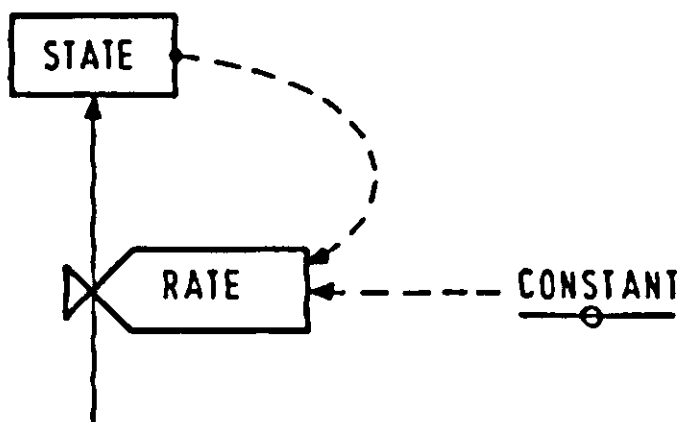


Figure 1. A relational diagram of exponential growth, drawn to the conventions of Forrester (1961).

finitum, so it is obviously not feasible to construct a model based on full knowledge of all biological, physical and chemical phenomena. Models are simplified representations of systems, and this simplification manifests itself in the limited number of state variables that are considered.

The number of state variables can be reduced considerably by limiting the boundaries of the model and by focussing only on important aspects. The number of state variables that can be considered in any model is limited, not so much by the size of the computer, or the cost of computer time, as by the research effort that can be invested in any one problem.

For each purpose there is an optimal number of state variables that should be considered. At first the applicability of the model to the real world increases with the number of state variables, but eventually the addition of new state variables diverts attention from more important state variables already present in the model. The heuristic process of obtaining a set of state variables in order of importance takes time, and many modelling efforts in ecology are explicitly, or more often implicitly, directed towards this goal.

1.1.7 Steps in model building

We may distinguish three types of models, expressing different levels, or phases of development, knowledge and insight. At the frontiers of knowledge, preliminary or conceptual models are very common. These are useful in the quantification and evaluation of hypotheses but are seldom of lasting value. Many different hypotheses may be expressed quantitatively in these models, and their consequences may be calculated and used for an evaluation. These models may help as guidelines in experimental research. Comprehensive models may be developed from these preliminary models as a result of scientific progress: more knowledge and insight become available and may clarify the processes in the system studied.

To evaluate the relative importance of the various parameters and relations and the structure, these models are subjected to a numerical sensitivity test, by changing parameter and input values, and to a structural sensitivity test, by altering the structure of the model. After these sensitivity tests, summary models

may be developed by simplifying the structure of the model. These summary models serve as vehicles for communication, instruction and may sometimes be used for management purposes. Since summary models are derived from comprehensive models, different forms may be constructed depending on the objective and interest of the user.

Various steps in model building may thus be distinguished: (a) the conceptual phase or model, (b) the comprehensive model and (c) the summary model.

Within the conceptual phase, the following steps may be distinguished:

1. Formulation of objectives;
2. Definition of the limits of the system;
3. Conceptualization of the system (states, rates, auxiliary variables, forcing variables, etc.).

In the comprehensive modelling phase, steps 4 to 6 may be distinguished:

4. Quantification through literature, process experiment or estimation of the relations between rate and forcing variables, state or auxiliary variables;
5. Model construction (definition of the computer algorithm);
6. Verification of the model, i.e. testing the intended behaviour of the model.

Finally, the model is used to set research priorities and to develop management tools:

7. Validation, i.e. testing the model in parts or as a whole, using independent experiments on system level;
8. Sensitivity analysis, numerical or structural;
9. Simplification, development of a summary model;
10. Formulation of decision rules or forecasting models to be used in management.

These ten steps may be seen in any modelling effort, although very often incomplete or not exactly in this order. In steps 1 to 3 there is a clear emphasis on conceptualization, steps 4 to 6 stress explanation and should therefore be considered as scientific effort, whereas the management or instructive aspects are merely seen in steps 7 to 10.

In many cases it is possible to work at the same time with comprehensive explanatory models and simple universal summary models which are used to derive management methods. Mutual interaction may improve the quality of both. This iterative improvement of both types of models may improve insight and stimulate better management schedules.

1.2 Crop growth under optimal and suboptimal conditions

The factors that influence crop production may be divided into three broad categories: (1) factors that determine potential yields, such as light, temperature and the main crop physiological properties, (2) factors that limit yields such as the availability of water and nutrients and (3) factors that reduce yields such as weeds, pests and diseases, hail and other disasters. To study the effects of yield-determining and yield-limiting factors, and their interactions, different

production situations are distinguished, whereas the effect of the yield-reducing factors are superimposed on these factors (de Wit & Penning de Vries, 1982).

1.2.1 Production situations

In many studies it suffices to distinguish the following four production situations:

– **Production Situation 1**

This is the potential production situation reached in conditions with ample plant nutrients and soil water throughout growth. The growth rate of the crop in these conditions is determined by weather conditions, and in terms of dry matter amounts to $150\text{-}350\text{ kg ha}^{-1}\text{ d}^{-1}$ when the canopy fully covers the soil. In these conditions the absorbed radiation is often the factor limiting growth rate during the growing season. Major state variables are the dry weight of leaves, stems, reproductive or storage organs and roots, and the surfaces of photosynthesizing tissues; major processes are CO_2 assimilation, maintenance and growth, assimilate distribution and leaf area development. This production situation can be created in field and laboratory experiments, and is approached in practice in glasshouses and in the intensive production of sugar beet, potato and wheat on some Western European farms and on some sugar cane plantations in South America.

– **Production Situation 2**

Growth is limited by water shortage for at least part of the time, but when sufficient water is available the growth rate increases up to the maximum rate set by the weather. Such situations can be created experimentally by fertilization in temperate climates and in semi-arid zones. They are approached in practice in non-irrigated but intensively fertilized fields, such as many Dutch pastures. Additional state variables are the water balances of the plant and soil; crucial processes are transpiration and its coupling to CO_2 assimilation, and the loss or gain of water by the soil through evaporation, drainage and run-off. The heat balance of the canopy needs detailed consideration in this production situation because of its relation to the water balance.

– **Production Situation 3**

Growth is limited by shortage of nitrogen (N) for at least part of the time, and by water or weather conditions for the remainder of the growth period. Minerals are well supplied. This is quite a common situation in agricultural systems even with ample fertilization, N shortage commonly develops in crops at the end of the growing season. Important elements in these systems are the various forms of N in both soil and plant; important processes are the transformations of nitrogenous compounds in the soil to forms which are available to plants, leaching, denitrification, N absorption by roots, uptake

and redistribution of N within the plant from old organs to growing ones and its growth response.

– **Production Situation 4**

Growth is also limited by the low availability of phosphorus (P) or by other minerals such as potassium (K) for at least part of the time. Growth rates are typically only 10-15 kg ha⁻¹ d⁻¹ of dry matter. This situation often occurs in heavily exploited areas where no fertilizer is used, such as in the poorest parts of the world. Important elements of this class of system are mineral contents of the soils and plants; important processes are their transformation into organic and inorganic forms of differing availabilities, absorption of minerals by roots, and the response of plant growth to their supply. The availability of P relative to that of N is of special interest.

It is rare to find cases that fit exactly into one of these four production situations, but it is a useful simplification to reduce specific cases to one of them. It focusses attention on the dynamics of the principal environmental factor and on the plant's response. Other factors can be neglected, because they do not determine the growth rate; or rather, it is the growth rate that sets the rate of absorption or efficiency of utilization of the non-limiting factor.

If, for example, plant growth is limited by the availability of N, there is little use in studying CO₂ assimilation or transpiration to understand the current growth rate. All emphasis should then be on N availability, the N balance and the response of the plants to N.

1.2.2 Yield-reducing factors

Pests and diseases are the main yield-reducing factors considered in this book. They may affect the growth of a crop in all production situations. However, the nature of the relation between crop and pest or disease organism may be considerably different and crop losses, both qualitative and quantitative, depend on the way crop growth is affected.

Many diseases and pests work in a complicated way through shifts in carboxylation resistances, e.g. mildew (Rabbinge et al., 1985), phloem blockage (e.g. mites), shifts in N balances (e.g. aphids), or injection of hormones or viruses (e.g. aphids and white flies). The simulation of these processes may help to formulate specific damage relations for the various yield situations that are distinguished.

In a detailed study on crop losses due to cereal aphids, Rabbinge et al. (1983) demonstrated that the effect of a constant aphid load on the wheat plant differs considerably among the different production situations. Yield loss (kernels in kg ha⁻¹) is correlated with the maximum aphid density per kernel, typically reached when crops have milk-ripe seeds. At a wheat production level of about 5000 kg ha⁻¹, a maximum aphid density of 15 tiller⁻¹ caused yield depression of about 250 kg ha⁻¹; whereas the same population density at a yield level of 7500 kg ha⁻¹

caused a yield loss of 700 kg ha^{-1} . In the analysis of this damage relation, it was demonstrated that the major reason for the progressive damage relation was the importance of indirect effects on yield loss, such as honeydew on the leaves.

Comparison of leaf damage by mutilation and by the formation of necrotic tissue provides another example. In the case of mutilation, the light that passes through is not lost but intercepted by lower leaves, provided that the canopy is well developed and closed. Only in situations where production is already low, is the light likely to be lost. However, light that falls on a necrotic area is always lost, irrespective of whether the canopy is closed or not.

These examples demonstrate the importance of defining the yield or production situation at which the crop-pathogen relation is studied.

1.3 Systems management

The main processes and phenomena involved in crop growth and pest and disease development are schematically presented in Figure 2. They all centre around the plant-pathogen interaction but are, nevertheless, related to various fields of knowledge that have developed rather independently of each other: plant physiology, biochemistry, meteorology, plant pathology, entomology, plant ecology and weed science. The integration of knowledge from these different fields is done by the comprehensive models which may, depending on the focus of interest, be worked out in more detail in various parts. Submodels have been developed for various processes, and can be combined to study the interaction of various aspects. This hierarchical modelling (de Wit, 1982) permits linkage of

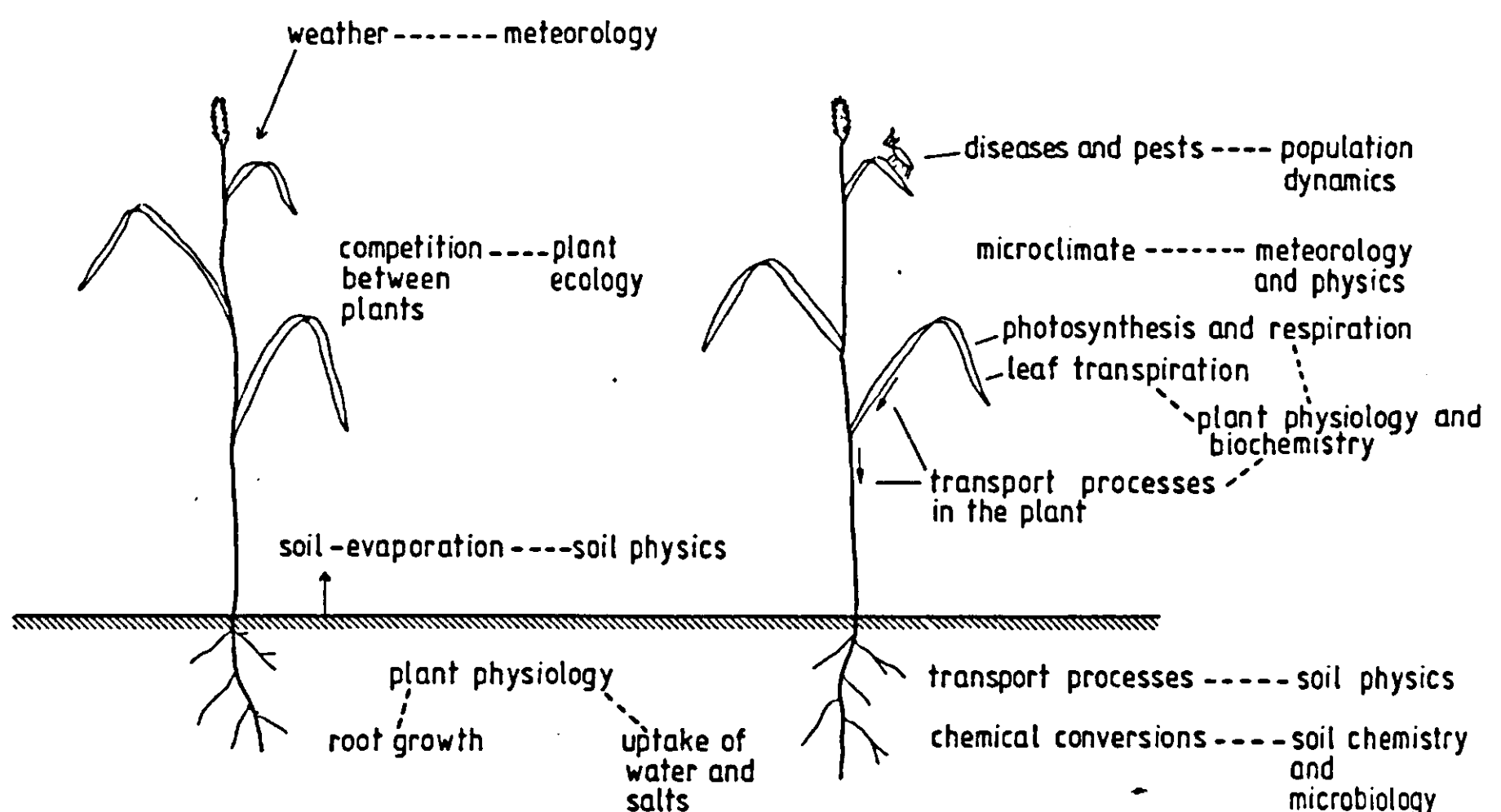


Figure 2. Fields of knowledge that need consideration in a study of plant growth. (Source: de Wit, 1982).

models at different organizational levels. Linkage of models at a similar level of organization but with different points of focus is also possible. This linkage between organization levels and between fields of interest is the task of combination models of pests and diseases and crop growth.

For example, submodels can be produced for the uptake, distribution and redistribution of nitrogen in a wheat plant after flowering. The consequences of an extra N drain, for example, due to aphids can be evaluated by these submodels in terms of assimilation rate reduction or shortening of leaf area duration. This information is then used in crop growth models as an input relation.

Pest, disease and weed management (pathosystem management) form part of all systems. It incorporates knowledge of crop growth, pathogen dynamics and economy of the production process in programs that help to maintain pest populations below economic damage thresholds.

Options for production may be designed and offered to the farmer through various combinations of yield-limiting and yield-reducing factors. Depending on the farmers objectives different combinations are optimal. Some farmers like to gamble and do not care much about a high chance of loss, provided it is compensated by high returns in case the gamble pays off. Others are extremely averse to taking risks, and are willing to pay a high premium to reduce the chances of substantial loss.

Pathosystem management may be applied for one single pest or disease, but is of little use, since the farmer is concerned about all pests, diseases and weeds in a specific crop, and about their interaction. Control of various combinations of diseases and pests requires different control strategies to minimize damage. Zadoks & Schein (1979) expressed the possible control strategies for plant diseases in a simple diagram (Figure 3). It shows how a disease may be delayed or set back by (a) sanitation, (b) change in planting time, (c) partial resistance, (d) treatment with eradicant fungicide, (e) treatment with protective fungicide, or (f) residual adult plant resistance or repeated fungicide treatment. The same diagram holds for insect pests if biological control measures with natural enemies like bacteria or fungi is applied. In cases of biological control with parasites or predators the aim is not completely to eradicate the disease organism or the prey, but to maintain it at a low level that is acceptable to both farmer and natural enemy.

In the summarizing diagram of Zadoks & Schein (1979) the concept of damage threshold or economic injury level is incorporated. This is the lowest population density that causes economic damage and justifies the cost of control measures. When the damage threshold is known and the disease or pest is present the farmer must know how and when to act. For this purpose it is necessary to define an action threshold, which is reached earlier than the damage threshold. Both damage threshold and action threshold depend on the pathosystem's reaction to environmental conditions such as temperature, humidity and irradiation and the crop production situation. In most cases, the damage threshold is not constant but depends very much on time, growing conditions and expected yield. It is often

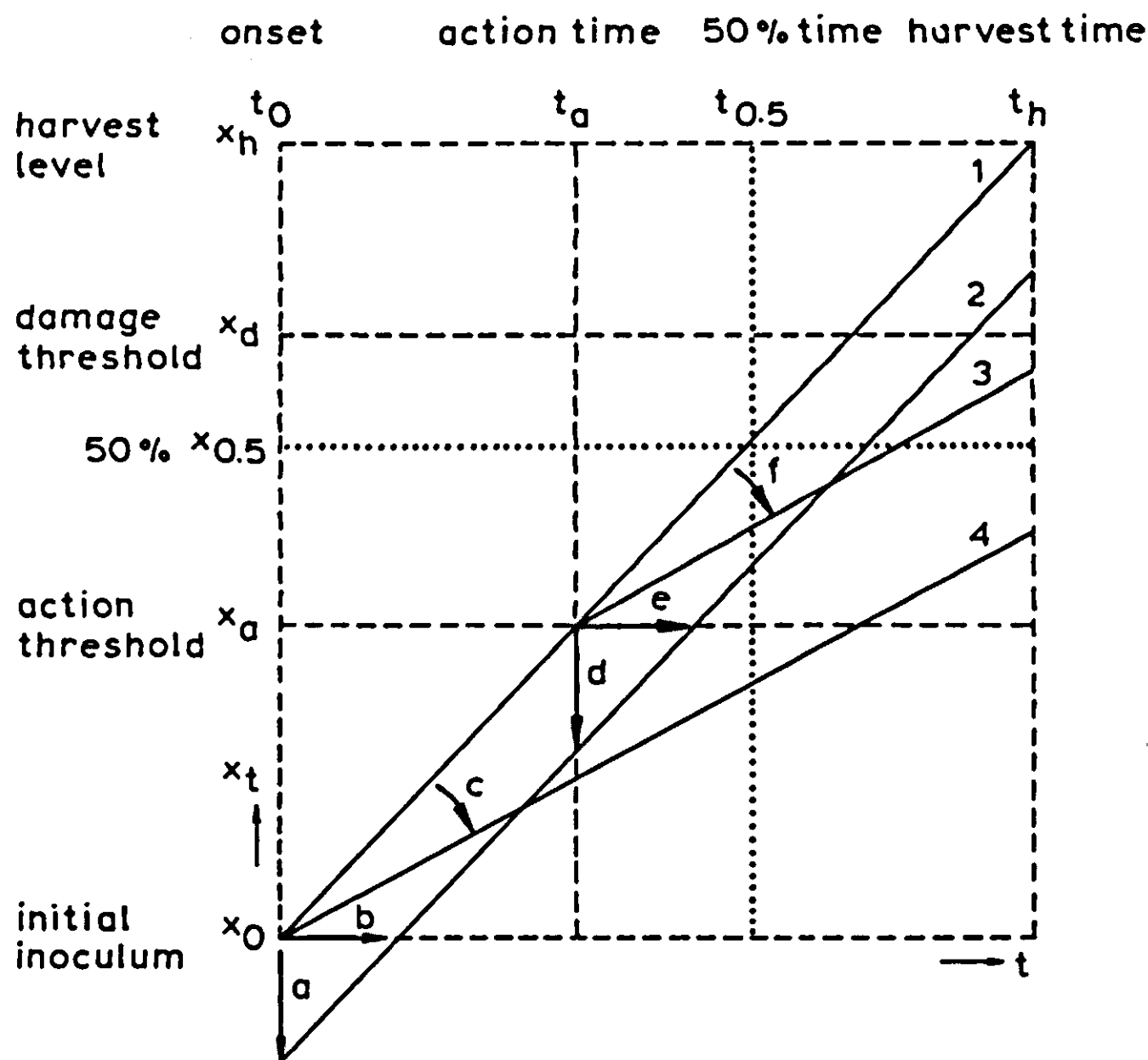


Figure 3. A model demonstrating the effects of various control actions in terms of the equivalence theorem, reduction of r , the slope, and x_0 or x_t . Relation between time (t) and disease severity (x_t). Entries: (1) original disease progress curve, (2) same after reduction of x_0 or x_t (actions a and d) or delay of the epidemic (actions b and c), curves 1 and 2 have the same r value, (3) r changed after action f taken at action time, (4) r changed from the beginning of the season by action c . Actions (examples only); a : sanitation, b : change of planting time, c : partial resistance, d : treatment with eradicant fungicide, e : treatment with protective fungicide, f : residual resistance in the adult stage, or regular treatments with fungicides. (Source: Zadoks & Schein, 1979).

very loosely quantified and therefore difficult to incorporate in crop management. Decision making thus becomes a complicated affair in which intuition generally plays an important role. The value of good intuition and experience in farm management is considerable and determines in many cases whether a farmer has 'green fingers' or not. However, such characteristics are non-transferable, and can be explained only with hindsight.

As decision making is such a complicated affair, information processing equipment may help in handling the relevant data, simulating and/or predicting population dynamics and estimating damage or yield loss (Section 5.1). To optimize decisions and to determine appropriate damage thresholds for various objectives, e.g. profit maximization, pesticide minimization or yield maximization, dynamic optimization techniques are also developed (Section 5.1).

These techniques should enable the farmer or his adviser to improve decision making. However, it should be kept in mind that the quality of the decision is in general not limited by such technical constraints but by the availability of basic biological knowledge. In crop protection, this concerns information on the population dynamics of the pests and diseases and their interactions with the host crop, and with each other.

Population models used for these purposes are discussed in Chapter 3. These models have proved to be reliable predictors of pest or disease development but their value as quantitative predictors of injury to the crop is limited. For that purpose, combination models of the population dynamics of the pest or disease organism and of the growing crop are needed. Such combined models have been developed for situations in specific crops, such as cotton, alfalfa, apple and wheat (Gutierrez et al., 1975; Gutierrez et al., 1976; Rabbinge, 1976; Rabbinge et al., 1981; Section 4.3). In some cases, these comprehensive simulation models have led to simplified models that contain sufficient economic elements to form a management instrument for decision making about sprayings. However, they require considerable input information on various processes and a great deal of parameterization to be more reliable than the simpler approaches.

2 BASIC TECHNIQUES OF DYNAMIC SIMULATION

2.1 Some elements of dynamic simulation

P.A. Leffelaar and Th.J. Ferrari

2.1.1 Introduction

When analysing systems, one is usually interested in the status of the system at a given moment and in its behaviour as a function of time. A system, which can be defined as a limited part of reality that contains interrelated elements, may be too complex to study directly. However, a model, which can be defined as a simplified representation of a system that contains the elements and their relations that are considered to be of major importance for the system's behaviour, may be easier to study. The design of such models and the study of the model properties in relation to those of the system is called simulation; if these models change with time they are called dynamic simulation models.

Dynamic simulation models are based on the assumption that the state of each system – at any given moment – can be quantified, and that changes in the state can be described by mathematical equations: rate or differential equations. This leads to models in which state, rate, and driving variables can be distinguished.

The purpose of this Section is to introduce the method of constructing models according to the state variable approach by using the very elementary system units described in Subsection 2.1.2. Subsection 2.1.3 shows how the appropriate differential equations may be integrated analytically to obtain the state variables as a function of time in these simple system units. The concept of feedback, and the possibility of visualizing the available knowledge of a system by means of relational diagrams, will be discussed in Subsection 2.1.4. Slight changes in differential equations make analytical solutions impossible, so solutions must be obtained by numerical integration methods. These solutions are based on the assumption that the rate of change is constant over a short period of time, Δt . The principle of numerical integration, the relation between the time interval of integration, Δt , and the time coefficient of an equation, are discussed in Subsection 2.1.5. Some numerical integration methods are presented in Subsection 2.1.6. During a time interval of integration, rates will usually change, so numerical integration methods introduce errors in the solution of differential equations. This will be demonstrated in Subsection 2.1.7, and relations between these errors and the time coefficient of the system will also be discussed. Finally, in Subsection 2.1.8 a more complex system is analysed using the methods presented.

2.1.2 State variables, rate variables and driving variables

To introduce the method of constructing models according to the state-variable approach, the following elementary system units are used (Figure 4):

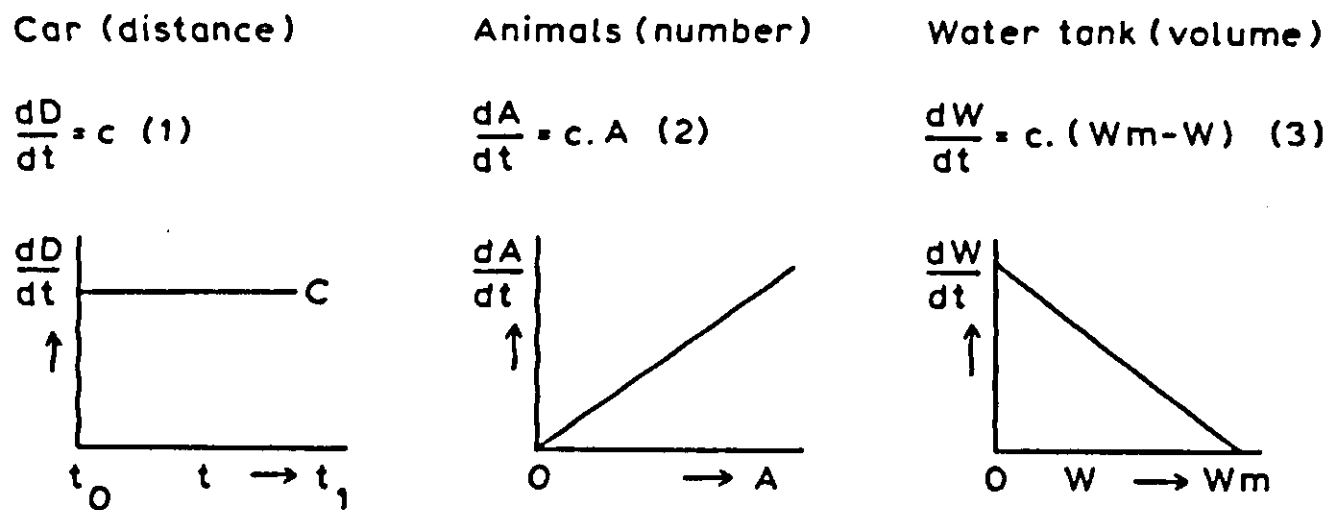


Figure 4. Rate or differential equations (Equations 1, 2 and 3), and their graphs, for three elementary system units. D , A and W stand for the state variables, t for time and c is a constant that may be different in each equation. W_m is the maximum water level that can be reached.

1. A car driving at a constant speed;
2. A number of animals that increases every year by a certain fraction;
3. A tank which is filled by a flow of water through an adjustable valve until a certain water level is reached.

The state variables in these examples are the distance covered by the car, the number of animals, and the amount of water in the tank, respectively. Generally, state variables have dimensions of length, number, volume, weight, energy or temperature. Such quantities can be measured directly.

The ultimate status of a system is not the only feature of interest; we are also concerned with its behaviour in time. Thus, the rate of change of the state variables in time, as well as the direction of change must be known. If these rates have a clear pattern, they may be formalized by means of rate equations or differential equations. The rate equations and their graphical representation for the three elementary system units are given in Figure 4. Rate variables, on the left hand sides of Equations 1, 2 and 3, have the dimension of a state variable per time, i.e. length time^{-1} , number time^{-1} and volume time^{-1} , respectively. These variables cannot be measured directly and are usually calculated from state variables. For instance, when both the distance covered by the car and the time are measured, the (average) speed is given by their ratio. In Equations 2 and 3 the rate variables are functions of the state variables, A and W , respectively, whereas in Equation 1 the state has no effect on the rate. The influence of a state on its rate of change is called feedback and will be discussed in Subsection 2.1.4. The proportionality coefficients, c , in Equations 2 and 3 are important with regard to the behaviour of the state variables and are often given special names. In biological systems c is called the relative growth rate; in technical systems the inverse of c is used, and is called the time coefficient. Time coefficients and their effect on numerical integration are crucial in dynamic simulation, which is discussed in Subsection 2.1.5. The constant c in Equation 1 is a driving variable

with the dimension for speed. Driving variables, or forcing functions, characterize the effect of outside conditions on a system at its limits or boundaries, and their value must be monitored continuously. Driving variables may have the dimension of rate variables, as in Equation 1, or of state variables, depending on their nature. When the driving variable is temperature, e.g. when the fraction by which the number of animals increases each year depends on temperature, it has the dimension of a state variable. It is good practice to check the dimensions of all variables in a particular model.

Exercise 1

- a. What are the dimensions of c in Equations 1, 2 and 3 in Figure 4?
 - b. Which general rules form the basis of dimensional analysis?
-

2.1.3 Analytical integration and system behaviour in time

Differential equations summarize the existing knowledge of a system, i.e. they relate rate variables to state variables, driving variables and parameters. Hence, they form a model for that system. When the differential equations are formulated, and when the state of the model at a certain moment is known, then its future state can be calculated. For this purpose, the differential equation must be solved with respect to its state variable. This process of integration can be visualized for the simplest case of Equation 1 by determining the distance covered by the car after a certain period of time when its speed is constant and known. Here, the speed is multiplied by the time. Thus, the value of the state variable equals the area (Figure 4) delimited by the time axis, the line parallel to this time axis at the value c on the rate axis, and the two lines, parallel to the rate axis, at two points of time, t_0 and t_1 , indicating the period. This does not apply to Equations 2 and 3 as the rate variables depend on the state; they are not expressed as functions of time. The formal process to obtain the state variable as a function of time must be applied. This is shown in Figure 5 for all three models. Integration of Equation 2 produces the familiar exponential growth curve (Equation 5). The relationship between the rate variable, dA/dt , and time is obtained by differentiating Equation 5 with respect to time. This yields Equation 2a, which has the same form as Equation 5. The graph depicting Equation 2a may be used to obtain the state variable. It may seem trivial to state this, since the analytical solution is already available in the form of Equation 5. The graph may, however, be used to illustrate the errors introduced by numerical integration methods when these are used to solve differential equations (Subsection 2.1.7).

In the case of the water tank, it is assumed that the rate of water inflow decreases linearly with the difference between a known maximum water level, W_m , and the actual water level, W (Equation 3). Integration yields Equation 6, which shows that the amount of water in the tank approaches W_m exponentially.

Car

Animals

Water tank

$$\frac{dW}{dt} = -c \cdot (W - W_m)$$

$$\frac{d(W - W_m)}{dt} = -c \cdot (W - W_m)$$

$$\int dD = c \cdot \int dt$$

$$\int \frac{dA}{A} = c \int dt$$

$$\int \frac{d(W - W_m)}{W - W_m} = -c \int dt$$

$$D = c \cdot t + Q$$

$$\ln A = c \cdot t + Q$$

$$\ln(W - W_m) = -c \cdot t + Q$$

initial value of the state variable at $t = 0$:

$$D = D_0 \text{ so } Q = D_0$$

$$A = A_0 \text{ so } Q = \ln A_0$$

$$W = W_0 \text{ so } Q = \ln(W_0 - W_m)$$

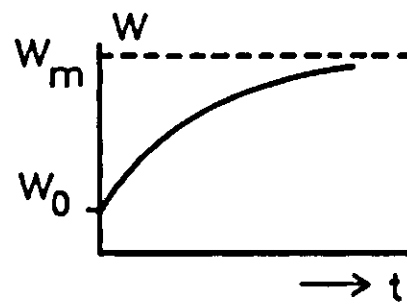
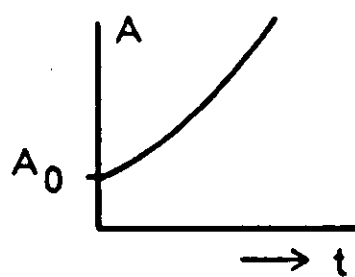
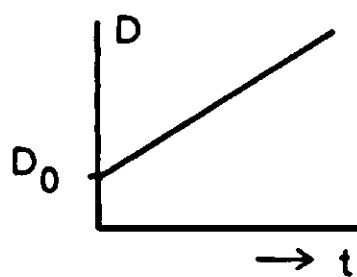
$$\ln \frac{A}{A_0} = c \cdot t$$

$$\ln \left(\frac{W - W_m}{W_0 - W_m} \right) = -c \cdot t$$

$$D = c \cdot t + D_0 \quad (4)$$

$$A = A_0 e^{c \cdot t} \quad (5)$$

$$W = W_m - (W_m - W_0) \cdot e^{-c \cdot t} \quad (6)$$



$$\frac{dD}{dt} = c \quad (1)$$

$$\frac{dA}{dt} = A_0 c \cdot e^{c \cdot t} \quad (2a)$$

$$\frac{dW}{dt} = (W_m - W_0) c \cdot e^{-c \cdot t} \quad (3a)$$

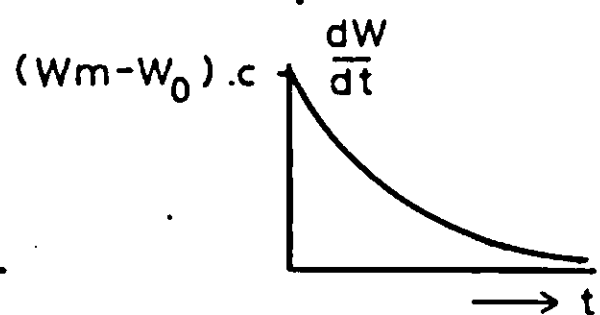
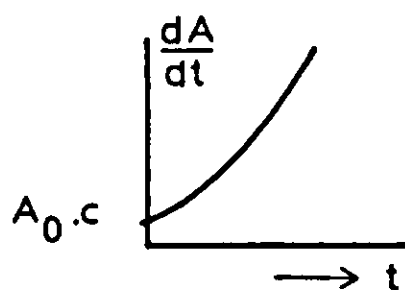
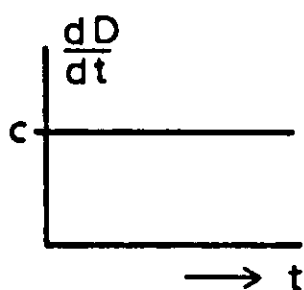


Figure 5. Upper half: analytical solutions (Equations 4, 5 and 6) to differential Equations 1, 2 and 3, respectively, and their graphs.

Lower half: rate variables (Equations 1, 2a and 3a) as a function of time, derived from Equations 4, 5 and 6, respectively, and their graphs. For an explanation of variables see Figure 4. Q stands for a general integration constant, and D_0 , A_0 and W_0 are the initial values of the state variables in the particular models.

Equation 3a, obtained by differentiating Equation 6, shows that the rate of inflow decreases exponentially.

Exercise 2

Consider the graphs depicting Equations 4, 5 and 6 in Figure 5.

- What do the slopes of the different lines represent?
 - What is the dimension of the slope in each case?
 - How do the numerical values of the slopes change as a function of time?
 - Are your findings in accordance with the graphs depicting Equations 1, 2a and 3a?
-

As long as differential equations are simple, they may be solved analytically to study the behaviour of the models. Slight changes in these equations, e.g. if c in Equation 2 is a function of temperature, make analytical solutions impossible. The equations should then be solved numerically. Before the principle of numerical integration is discussed (Subsection 2.1.5), and some integration methods presented (Subsection 2.1.6), the concept of feedback and the possibility of representing state, rate and driving variables in the form of relational diagrams is considered.

2.1.4 Feedback and relational diagrams

The rate variables in Equations 2 and 3 (Figure 4) are, respectively, a function of the state variables A and W , whereas the rate in Equation 1 is independent of the distance covered. When a rate variable, dX/dt , of a differential equation depends on the state variable X , there is a feedback loop, i.e. the state of the variable determines the degree of action or rate of change of this state. This process takes place in a continuously circulating loop. There are two types of feedback loops.

In a negative feedback loop, the rate may be either positive or negative, but will decrease as a function of the state variable. For instance, in the case of the water tank, Equation 3, the rate is positive, but decreases linearly with the increasing volume of water in the tank. An example of a negative rate which decreases the state variable, and vice versa, is obtained when the sign of the coefficient c in Equation 2 is made negative. Then, the number of animals decreases each year by a certain fraction. This denotes exponential mortality. A negative feedback loop can be recognized in a differential equation when the rate of change of the state variable is negatively related to that state variable (Equation 3). Negative feedback causes the system to approach equilibrium. Such an equilibrium state is stable: if the system is perturbed it returns to its equilibrium state. In the case of the water tank, the equilibrium state is the maximum level of water, W_m , whereas in the case of exponential mortality the state variable approaches zero.

In a positive feedback loop, the rate enhances the state, and vice versa, so that both become greater and greater. The exponential growth of the animals that is described by Equations 2 and 5 is an example of positive feedback. In nature, however, there are limits to growth. For instance, there may be a shortage of food. Then, the simple Equations 2 and 5 no longer describe the system and the model needs revision. A positive feedback loop can be recognized in a differential equation when the rate of change of the state variable is positively related to that state variable (Equation 2).

Relational diagrams are used to visualize feedback loops, rate and state variables and, more generally, the available knowledge about a system. They depict the most important elements and relationships of a system and form qualitative models of systems. Relational diagrams may be especially helpful at the start of the research in order to simplify the formulation of rate and state variables. They also make the content and characteristics of a model easily accessible. Relational diagrams for the three systems are given in Figure 6. They are drawn according to Forrester (1961), as shown in Figure 7. Figure 6 shows that feedback is absent in the case of the car, and that there is positive and negative feedback in the case of the animals and the water tank, respectively. When a parameter turns out to be variable, it must be replaced by a table or by an auxiliary equation. For instance, if the coefficient c , in the relational diagram for the animals, is temperature dependent, it can be replaced by a so-called auxiliary variable which contains information concerning this temperature dependence, and from which information flows to the rate variable.

Relational diagrams of more complex models may often be analysed in terms of the elementary units of Figure 6.

2.1.5 Numerical integration and the time coefficient

The differential equations considered so far can be solved analytically in order to study the state variable as a function of time. When model computations do not agree with the behaviour of the system, more complex (sub-)models are needed, based on new knowledge of the system. The resulting set of differential equations cannot be integrated analytically; instead, numerical integration methods must be used.

In numerical integration the assumption is made that the rate of change of a state variable is constant over a short period of time, Δt . To calculate the state of a model after that short period, one must know the state of the system at time t , $state_t$, and the value of the rate variable, $rate_t$, calculated from the differential equation. By multiplying the $rate_t$ by Δt , and adding this product to the value of the state variable according to

$$state_{t+\Delta t} = state_t + \Delta t \cdot rate_t \quad \text{Equation 7}$$

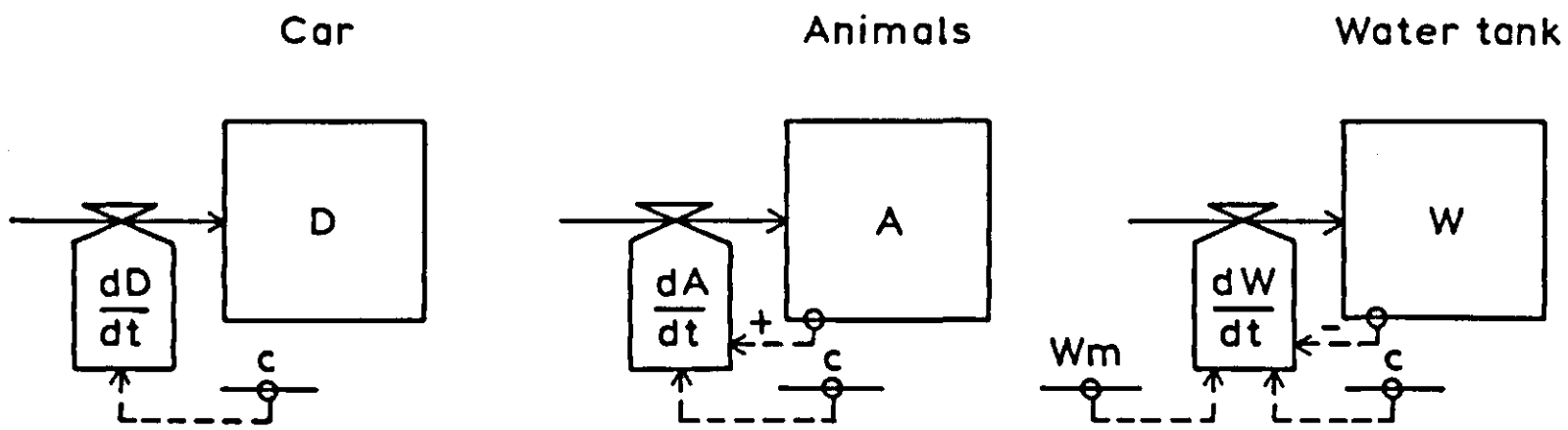


Figure 6. Relational diagrams for three elementary systems. Variables and symbols are explained in Figures 4 and 7, respectively.

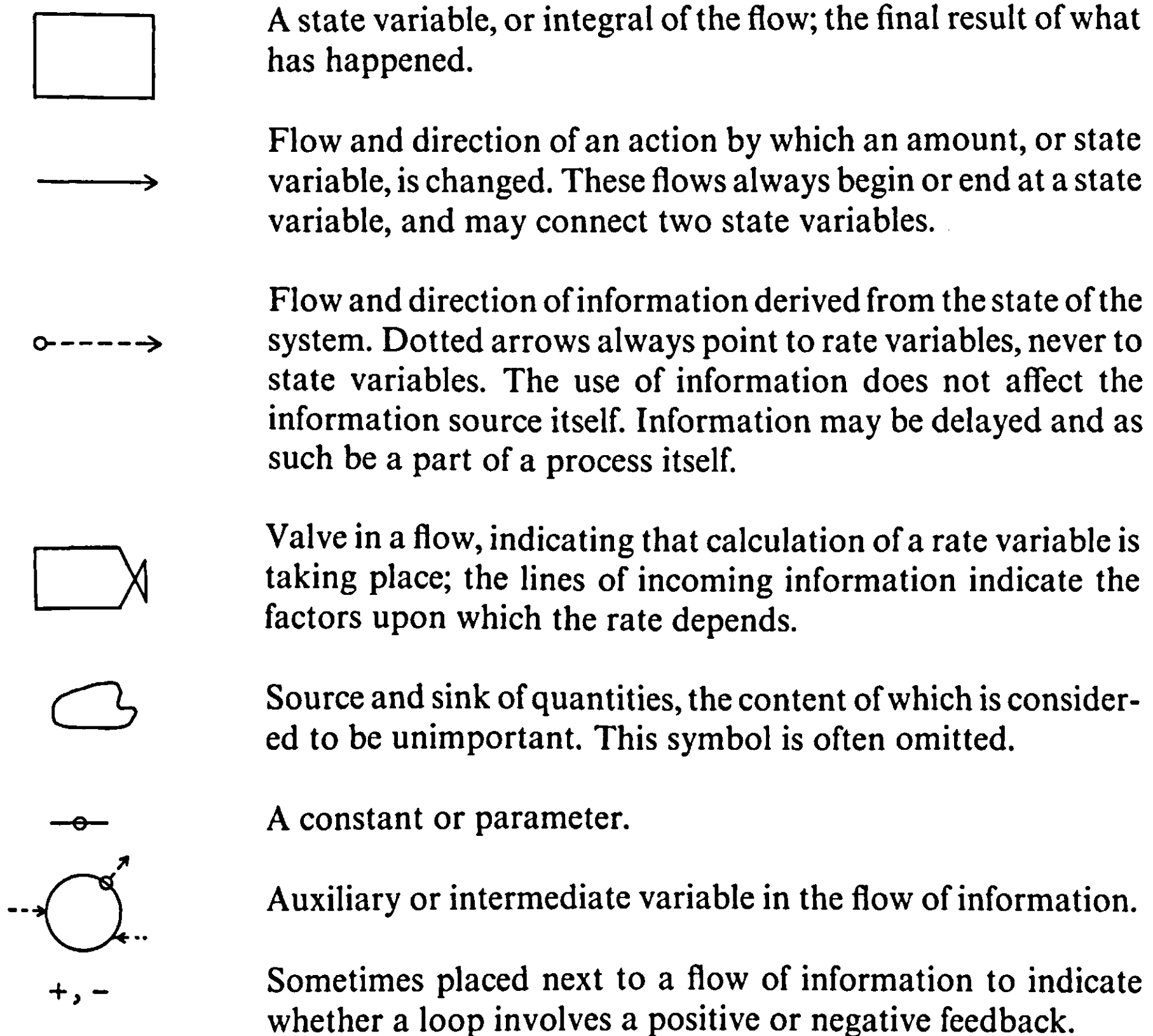


Figure 7. Basic elements of relational diagrams. Abbreviated names of variables represented by these elements are usually written inside the symbols. Note that driving variables are often underlined or placed in parenthesis. Intermediate variables are often characterized by circles.

the new state, state_{t+Δt}, of the system is determined. From this new state, a new rate is calculated which holds for the next interval Δt, and so on. Much can be said about the 'short period', Δt, especially in the context of its relation to the time coefficient of a particular model (see below), and with respect to errors introduced by numerical integration methods (see Subsection 2.1.7). The calculation of rate, will be discussed further in Subsection 2.1.6.

Numerical integration is first applied to the example of the water tank, Equation 3. Assume that there is no water in the tank at t = 0 s, so W₀ = 0 l; coefficient c equals ¼ s⁻¹, and the maximum water level W_m = 16 l. The rate at which water flows into the tank at t = 0 is calculated from the rate equation

$$(dW/dt)_t = c \cdot (W_m - W_t) \quad \text{Equation 8}$$

as 4 l s⁻¹. If the time interval Δt, or the 'short period' equals 2 s, the volume of water at time t + Δt is obtained from the state equation

$$W_{t+\Delta t} = W_t + \Delta t \cdot (dW/dt)_t \quad \text{Equation 9}$$

as 8 l. During the following time interval of 2 s, the rate is: ¼ · (16 - 8) = 2 l s⁻¹. Thus, during this time interval, 4 l of water will flow into the tank and the total quantity of water after 4 s equals 8 + 4 = 12 l. The calculations thus proceed according to Equations 8 and 9, and can be facilitated by the following diagram:

times	s	0	← Δt →	2	4	6	8	10
W	l	0		8				
dW/dt	l s ⁻¹	4		2				

Exercise 3

Complete the calculation and plot the amount of water in the tank against time. Calculate the amount of water in the tank using Equation 6 and the same parameters, and plot the results in the same graph.

- What do you notice about the difference between the numerical and analytical solution?
- When is the rate of inflow zero?
- What happens if coefficient c is 1/8 instead of 1/4?

In the case of the water tank the rate of filling decreases (see Figure 5 depicting Equation 3a), so that the numerical integration, where the rate variable is kept constant during the time interval Δt, overestimates the amount of water in the tank compared to the analytical solution (see also Exercise 3). The difference between the value of the state variable obtained by the numerical method, and the analytical value, will be smaller when Δt is smaller. The lower limit of Δt is set

by the technical (rounding errors) possibilities of performing the calculations over large time spans.

Exercise 4

The parameters in Equations 8 and 9 are:

$$W_0 = 0 \text{ l}; W_m = 16 \text{ l}; c = \frac{1}{4} \text{ s}^{-1}.$$

- Perform numerical integration up to about 30 s for the filling of the water tank using the following time intervals:
 $\Delta t = 1 \cdot c^{-1}$; $\Delta t = 1\frac{1}{2} \cdot c^{-1}$; $\Delta t = 2 \cdot c^{-1}$; $\Delta t = 2\frac{1}{2} \cdot c^{-1}$.
- Plot your results in the graph of Exercise 3.
- What can you say about the ratio of the time interval and the value of c^{-1} ?
- What upper limit would you set to this ratio? (Also consider your calculations for Exercise 3.)

The upper limit to Δt is determined by the inverse of coefficient c in the differential equation. The inverse of c is called the time coefficient, τ , which has the dimension of time. It is a measure of the reaction rate of a model. In models containing more than one time coefficient, a first approximation to the time interval is obtained by taking Δt smaller than one-tenth of the smallest τ in that model. The time coefficient appears equal to the time that would be needed by the model to reach the equilibrium state, if the rate of change were fixed. This applies to any point on the integrated function, as shown in Figure 8.

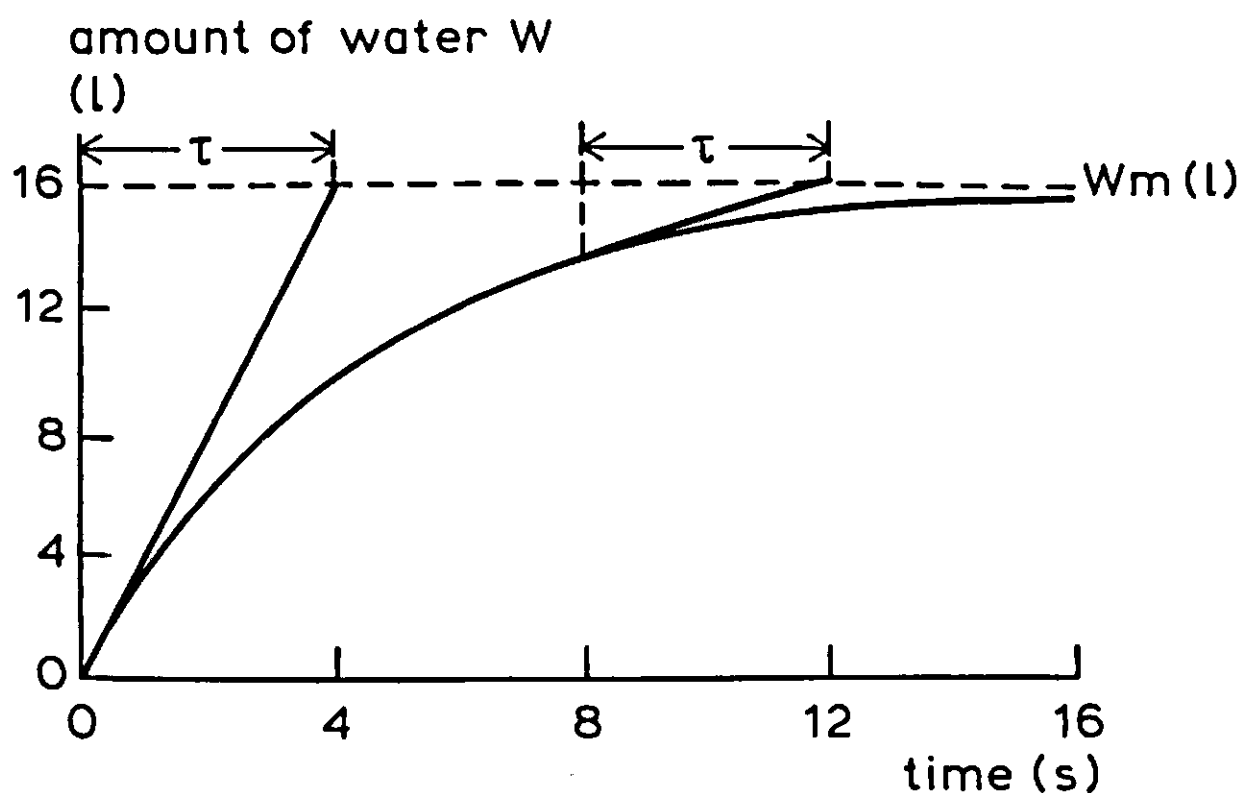


Figure 8. The amount of water as a function of time, according to Equation 6, with $W_0 = 0 \text{ l}$, $W_m = 16 \text{ l}$ and $c^{-1} = \tau = 4 \text{ s}$, yields $W = W_m \cdot (1 - e^{-t/\tau})$. The time interval over which the tangent must be extended to intercept the line of equilibrium is the time coefficient, τ .

Exercise 5

- a. Prove this last statement by using Equation 8 for the water tank case.
 - b. This is also correct for a positive feedback loop, but the formulation is different. Explain this for the case of exponential growth.
-

Biological models are often characterized by a relative growth rate (rgr), i.e. coefficient c in Equation 2, with dimension t^{-1} . This name is clarified by writing c explicitly: $c = (dA/dt)/A$.

Exercise 6

- a. Calculate the time coefficients when the relative growth rates are 1.5, 0.2, and 0.05 per year.
 - b. What time intervals would you use for numerical integration in these cases? Also take into account the practical aspect of numerical calculations.
 - c. Compute the number of animals after 5 years, when $c = 0.2$, $A_0 = 100$, by using
 1. The analytical solution to the problem, Equation 5;
 2. The numerical solution to the problem, using Equation 2 and $\Delta t = c^{-1}/10$.
 - d. Plot your results on graph paper.
 - e. Explain the underestimate of the numerical solution compared with the analytical one.
-

A note of caution may be appropriate here. The time coefficient is defined as the inverse of the relative growth rate (see also Exercise 6). The growth percentage (i.e. the relative increase in the number of animals after one year, or annual relative increase) is often used to calculate τ , but this gives incorrect results. A growth rate of, for example, 20% per year is not equivalent to an rgr of 0.2 per year. The relative growth rate is less: when $A_0 = 100$, A equals 120 after one year and Equation 5 can be used to calculate the relative growth rate as follows: $A = 120 = 100 \cdot e^{rgr \cdot 1}$, so $rgr = \ln 1.2 = 0.182 \text{ yr}^{-1}$ and $\tau = 5.48 \text{ yr}$ instead of $1/0.2 = 5 \text{ yr}$. The relative growth rate (rgr) may be expressed in the annual relative increase (ari) as: $A_0 + A_0 \cdot ari = A_0 \cdot e^{rgr \cdot 1}$ or $rgr = \ln(1 + ari)$. For an exponential decline, one can derive $rdr = -\ln(1 - ard)$, rdr and ard being the relative death rate and the annual relative decrease, respectively. The differences between ari and rgr, or that between ard and rdr, will be substantial when the annual relative increase or decrease is large.

Other names for the time coefficient and related concepts are time constant, transmission time (in control-system theory), average residence time, delay time,

extinction time and relaxation time; this indicates the significance of the time coefficient in various sciences. Doubling time, the time needed to double an amount, is sometimes used to characterize a system but it is not synonymous with the time coefficient.

Exercise 7

The relationship between doubling time, $t(2)$, and the time coefficient in exponential growth is $t(2) \cong 0.7 \cdot \tau$. Why?

Relaxation time, a term often used in physics, is the time needed in exponential increase to change the state by a factor e , or in exponential decrease, to change the state by a factor $1/e$: it is equivalent to the time coefficient. For an example of average residence time, consider an exponentially decreasing population of animals without the effects of birth or migration. Then, the average residence time equals the time coefficient.

Exercise 8

Prove this last statement mathematically by using the definition of the average residence time:

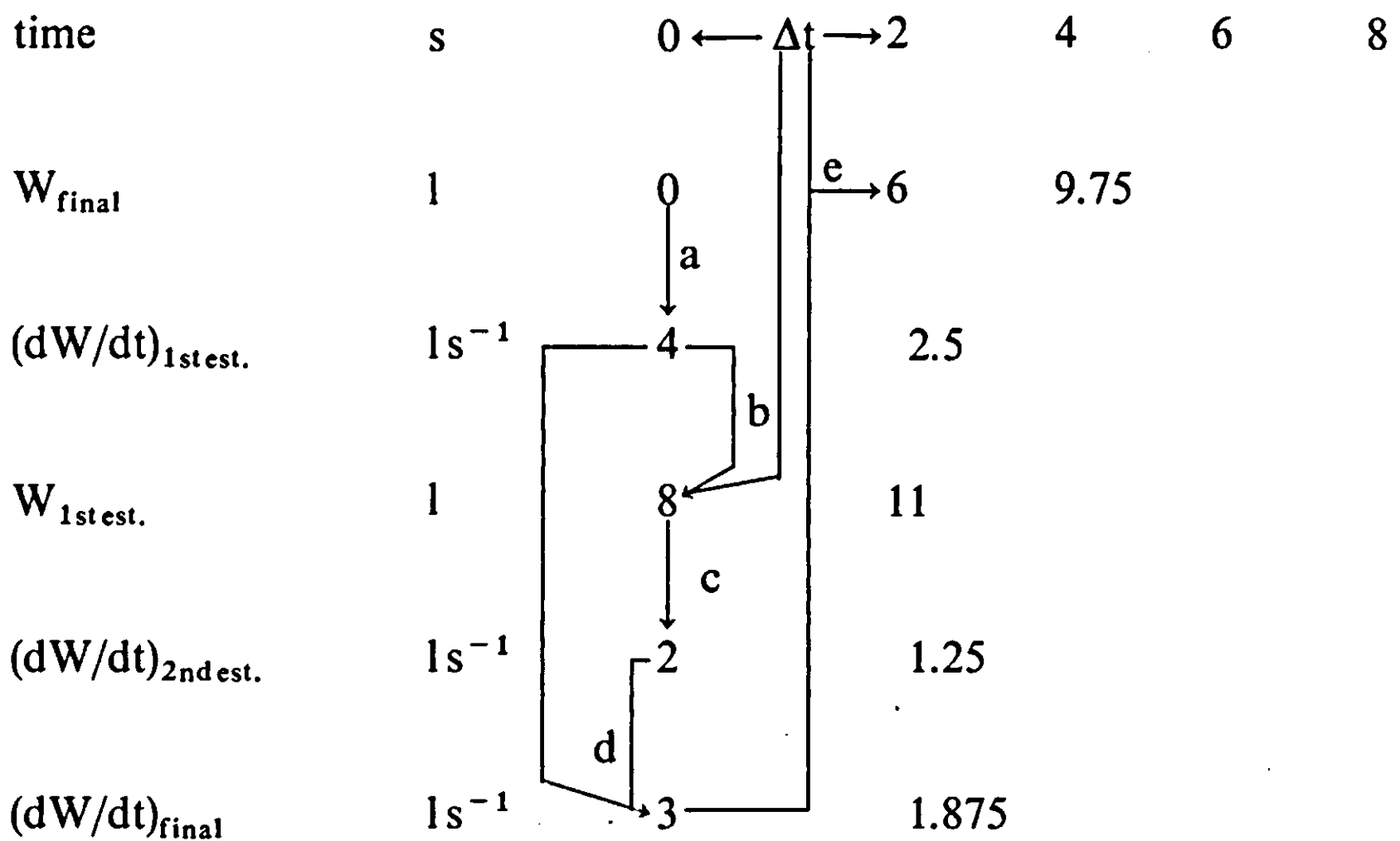
$$-\frac{1}{A_0} \int_0^{\infty} t \cdot \frac{dA}{dt} \cdot dt = \frac{1}{A_0} \int_0^{A_0} t \cdot dA = \frac{1}{A_0} \int_0^{\infty} A \cdot dt,$$

and the analytical equation describing exponential decrease: $A = A_0 \cdot e^{-t/\tau}$.

In nature many processes occur simultaneously. Calculations in simulation models of such processes, however, take place one after another. But since dynamic simulation is based on the principle that rates of change are mutually independent (i.e. they depend individually on state variables and driving variables), all rates applicable to any one moment can be calculated in series; they can then be integrated (in series) to obtain the values of the state variables a moment (Δt) later. In this way the model operates in a semi-parallel fashion, and simulates simultaneously occurring processes. It is convenient to use special simulation languages to describe parallel processes in a semi-parallel fashion. If other computer languages are used, this requirement should still be met.

2.1.6 Some numerical integration methods

The principle of numerical integration was illustrated using the simplest and most straightforward, rectangular integration method of Euler. Rectangular integration gives the poorest agreement with an analytical solution (if available). Other, more sophisticated methods, e.g. the trapezoidal method and the Runge-Kutta method, are more accurate, but cannot always be used. These two sophisticated methods will now be considered in more detail. Their computation schemes are given in Table 1. The example of the water tank will be used to illustrate the trapezoidal integration method. A first estimate of the rate variable, R1, and the state variable, A1, is calculated using the rectangular integration method, yielding (for a 2 s time step): $R1 = (dW/dt)_{t=0} = 4 \text{ l s}^{-1}$ and $A1 = W_{t=2} = 8 \text{ l}$. The estimated final state, A1, is used to calculate a second rate, R2, pertaining to $t = 2 \text{ s}$: $R2 = (dW/dt)_{t=2} = \frac{1}{4} \cdot (16 - 8) = 2 \text{ l s}^{-1}$. The rate which is integrated is the arithmetic average of R1 and R2; thus, the final amount of water, after 2 seconds, is: $0 + 2 \cdot ((4 + 2)/2) = 6 \text{ l}$. The following diagram clarifies the calculations:



where the sequence, a to e, indicates the computational sequence. At a and c, the rate equation is used (Equation 3 from Figure 4); at b and e, integration takes place and, at d, the arithmetic average is calculated; est. stands for estimate.

Exercise 9

Complete the calculation above and plot the amount of water in the tank against time on the graph from Exercise 3.

- What do you notice about the difference between the numerical and analytical solutions?
 - Show graphically that the trapezoidal integration method underestimates the analytical solution, and explain why; make use of the graph depicting Equation 3a, and the appropriate numerical values.
-

In this method, the differential equation had to be evaluated twice to obtain the state of the model after one time interval. The larger computation effort is more than compensated for by the larger ratio of $\Delta t/\tau$ that can be taken to reach the same accuracy as in the rectangular method (see Subsection 2.1.7). This is even more so for the Runge-Kutta integration method. This method will not be

Table 1. Summary of the rectangular, trapezoidal and Runge-Kutta integration methods; t stands for time, R for rate and A for state. The equals sign is not used here algebraically but as an assignment.

Euler's rectangular method

$$\begin{aligned}R &= f(A_t, t) \\A_{t+\Delta t} &= A_t + \Delta t \cdot R \\t &= t + \Delta t\end{aligned}$$

Trapezoidal method

$$\begin{aligned}R1 &= f(A_t, t) \\A1 &= A_t + \Delta t \cdot R1 \\R2 &= f(A1, t + \Delta t) \\A_{t+\Delta t} &= A_t + \Delta t \cdot (R1 + R2)/2 \\t &= t + \Delta t\end{aligned}$$

Runge-Kutta method

$$\begin{aligned}R1 &= f(A_t, t) \\A1 &= A_t + \Delta t \cdot R1 \cdot 0.5 \\R2 &= f(A1, t + 0.5 \cdot \Delta t) \\A2 &= A_t + \Delta t \cdot R2 \cdot 0.5 \\R3 &= f(A2, t + 0.5 \cdot \Delta t) \\A3 &= A_t + \Delta t \cdot R3 \\R4 &= f(A3, t + \Delta t) \\A_{t+\Delta t} &= A_t + \Delta t \cdot (R1 + 2 \cdot R2 + 2 \cdot R3 + R4)/6 \\t &= t + \Delta t\end{aligned}$$

explained in detail, but its scheme, given in Table 1, shows that four estimates are necessary to calculate the final rate.

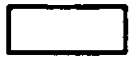
Exercise 10

Calculate the amount of water in the tank after a time interval of 2 s using the numerical integration scheme of Runge-Kutta. Use the numerical values from Exercises 3 and 9.

So far, the integration routines have had a fixed time interval, which was set arbitrarily to one-tenth of the time coefficient of the model. If the time coefficient changes during simulation, and its smallest value is known, one can fix the time interval to one-tenth of that value. This, however, implies that during periods with large τ values, the accuracy of integration would be greater than that during periods with small τ values. In models intended to quantify natural systems, it is preferable to preset the accuracy of integration and to vary the time interval to meet this accuracy. This is done by combining the integration methods of Runge-Kutta and Simpson. (The Simpson method, the accuracy of which lies somewhere between that of the trapezoidal and the Runge-Kutta methods, is discussed in detail in IBM, 1975.) Two integration routines, Runge-Kutta's and Simpson's are applied to integrate the differential equations. Their results are compared and, if they differ by more than a preset error, the time interval of integration, Δt , is halved. If the deviation is much smaller than required, Δt is doubled for the next time step. Because of the constancy of the integration error, this method is to be recommended as standard.

Exercise 11

The principle of the combined Runge-Kutta and Simpson methods is demonstrated in the program given in Figure 9, for the example of exponential population growth (for numerical constants see Exercise 6c). For simplicity, the Runge-Kutta and Simpson methods are replaced by the trapezoidal and rectangular methods, respectively. Also, Δt (DELTA) is doubled at the beginning of each new time interval. The program is written in FORTRAN and the results given in Table 2.

- a. Draw a flow diagram of the program listed in Figure 9, indicating decisions by  and calculations, etc., by 

Note that the purposes and symbols of a flow diagram are completely different from those of the relational diagram. The first is a technical scheme of how calculations are arranged, whereas the second expresses the conceptualization of the system.

Figure 9. Program demonstrating the principle of an integration method that adapts its time interval to meet a pre-set error criterion, using the rectangular and the trapezoidal integration methods.

```

C Demonstration program of a variable time-step integration method
C   using the rectangular- and trapezoidal methods.
C Timer variables 1) DELT should not become smaller than a certain small
C   value (DELMIN) or larger than the print interval (PRDEL)
C   2) timer variables have been set double precision to
C   avoid rounding errors on the PRDEL-timings.
C INITIAL PART.
  DOUBLE PRECISION TIME,PRDEL,FINTIM,DELT,DELMIN,DELTIM,COUNT3
  TIME =0.D00
  FINTIM=5.D00
  PRDEL =5.D00
  DELMIN=1.D-5
  DELT  =5.D00
  ERROR =1.E-5
C Relative growth rate and initial amount.
  A    =100.
  RGR  =0.2
C Counter one gives number of times that algorithm has been executed.
C Counter two gives number of times final integration has been performed.
C Counter three gives the number of times that output has been written.
  COUNT1=0.
  COUNT2=0.
  COUNT3=0.D00
C DYNAMIC PART.
5  IF(TIME.EQ.COUNT3*PRDEL) GOTO 10
   IF(TIME.GT.FINTIM) STOP 'FINTIM'
   DELT  =2.D00*DELT
   DELTIM=COUNT3*PRDEL-TIME
   IF(DELT.GT.DELTIM) DELT=DELTIM
C Remember current amount 'A' in memory 'B'.
15  B    =A
     GR1 =RGR*A
     A1  =A+DELT*GR1
     GR2 =RGR*A1
     A   =A+((GR1+GR2)/2.)*DELT
C RELERR=ABSolute value of (A(RECT)-A(TRAPZ))/A(TRAPZ)
     RELERR=ABS((A1-A)/A)
     COUNT1=COUNT1+1.
     IF(RELERR.GT.ERROR) GOTO 20
     TIME  =TIME+DELT
     COUNT2=COUNT2+1.
     GOTO 5
20  CONTINUE
C Restore current amount 'A' again in memory A, because
C calculation is not accurate enough and should be done again
C starting with the previous final amount and a halved DELT.
     A    =B
     DELT =DELT/2.
     IF(DELT.LT.DELMIN) STOP 'DELMIN'
     GOTO 15
C PRINT PART.
10  WRITE(21,25)TIME,A,A1,RELERR,DELT,COUNT3,COUNT1,COUNT2
25  FORMAT(/10H TIME  =D12.7,10H  A    =F12.5,10H  A1    =F12.5/
$10H RELERR =E12.7,10H  DELT  =D12.7,10H  COUNT3=F9.2/
$10H COUNT1 =F8.2,14H          COUNT2=F8.2)
     COUNT3=COUNT3+1.
     GOTO 5
END

```

Table 2. Results of the program shown in Figure 9.

Symbols mean:

A, A1 : Results of integration by the trapezoidal and the rectangular methods, respectively.

RELERR : Absolute value of the relative error between methods.

DELT : Δt .

COUNT1, 2 and 3: See Comments in Figure 9 (lines starting with C in first column).

TIME = .0000000D+00	A = 100.00000	A1 = 0.00000
RELERR = .0000000E+00	DELT = .5000000D+01	COUNT3 = 0.0
COUNT1 = 0.00	COUNT2 = 0.00	

TIME = .5000000D+01	A = 271.82767	A1 = 271.82559
RELERR = .7634231E-05	DELT = .1953125D-01	COUNT3 = 1.00
COUNT1 = 518.00	COUNT2 = 256.00	

The combined methods of Runge-Kutta and Simpson cannot be used at discontinuities of the state variable in time. For instance, when a crop is harvested, the contents of the state variable in the model must be removed instantaneously. In principle, states can only be changed by integration of rates over time. If a state variable's content, A_t , must be removed instantaneously, i.e. in one time interval Δt , the rate of change must be defined as $R_t = A_t/\Delta t$, and the rectangular integration method should be used. Rewriting Equation 7 for the moment of harvesting yields:

$$A_{t+\Delta t} = A_t - \Delta t \cdot (A_t/\Delta t)$$

Exercise 12

Let A_t be 100, Δt be 2, and define the rate of change R_t as $R_t = A_t/\Delta t$:

- Compute the amount $A_{t+\Delta t}$ according to the rectangular and trapezoidal integration routines.
- What do you conclude about the method of integration to be applied when division by Δt occurs in a rate variable?

There are many more numerical integration routines available, but the methods discussed here are usually sufficient to tackle the problems encountered in biological models.

Figure 10 summarizes the line of reasoning to be followed in order to select the appropriate integration method.

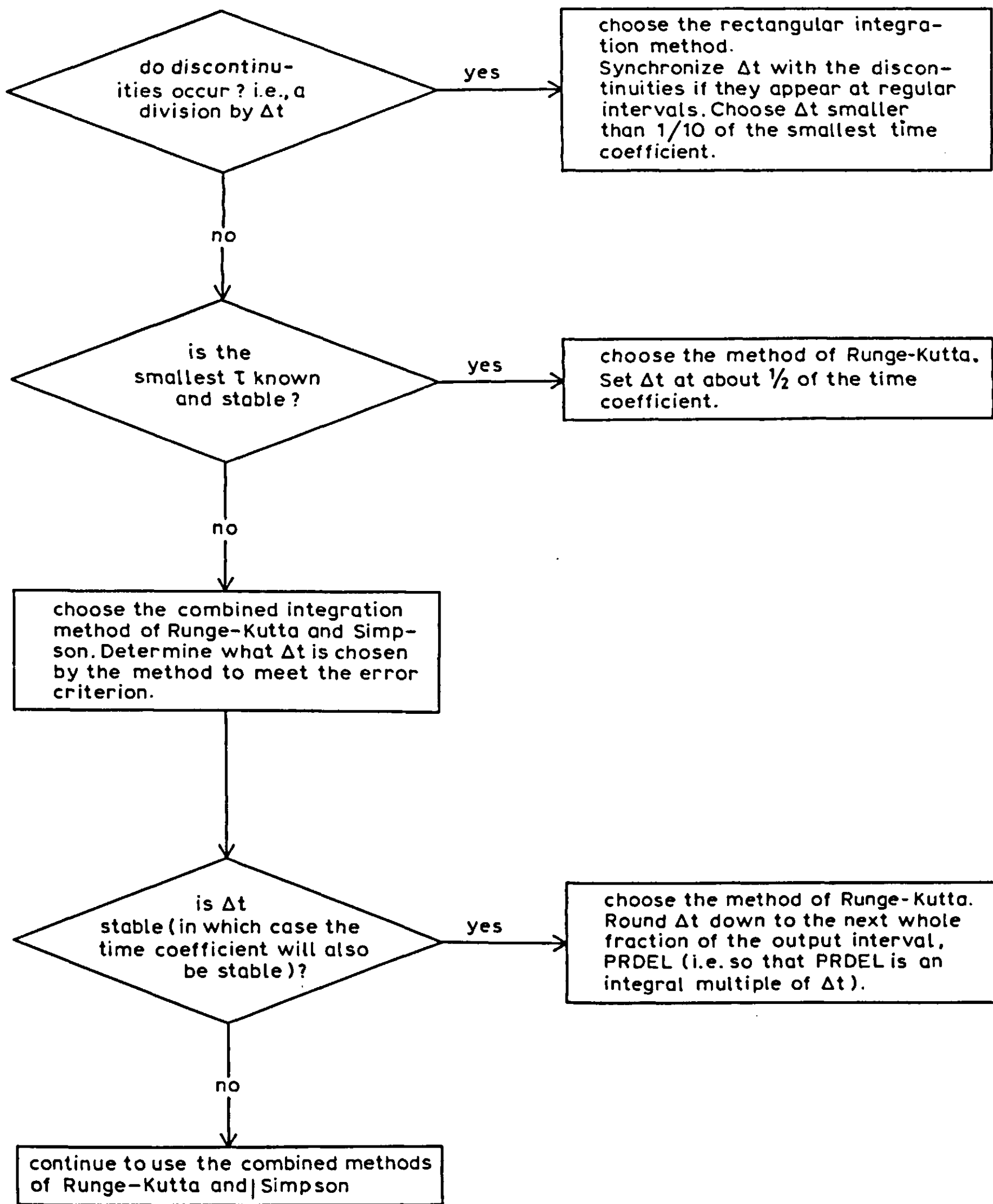


Figure 10. Flow diagram for choosing the appropriate integration method.

2.1.7 Error analysis; a case study of integration with and without feedback

The accuracy of numerical integration is influenced by the choice of Δt (Subsection 2.1.5). An error criterion was introduced in Subsection 2.1.6 (see Figure 9) to determine which Δt should be chosen to obtain integration results with errors smaller than, or equal to, this preset limit. Error analysis is used to

quantify these errors in terms of Δt and τ . As many rates in nature are proportional to the amounts present, the error analysis will be demonstrated for the model of exponential growth (Equations 2, 2a, 5 and Figure 6).

In the analysis of propagation of errors in integration, two situations should be distinguished. In the first situation, rate as a function of time is known in advance, e.g. a driving force. Then, results of integration are independent of the state variable that is changed by integrating the rate (situation without feedback), and the same relative error is made each time interval. In the second situation, the rate depends at each moment on the state of the system. This situation usually occurs in simulation, and the error in the calculations will accumulate: in exponential growth, an underestimation of the state will cause an underestimation of the rate, and hence state (situation with feedback).

Integration of a driving force (no feedback) When a driving force is integrated, its value is known in advance as a function of time; for instance, a series of data of rates of change which may be represented by an exponential curve. Figure 11 shows such a curve (solid line), drawn according to Equation 2a, with $A_0c = v_0$, the initial velocity. Integration by the rectangular and trapezoidal methods yields the hatched areas. In this case, the exact error in the result obtained by the rectangular integration method could be derived, but a good approximation is given by the area of the triangles that are included using the trapezoidal integration method.

The relative error in an integration method of order n is defined as

$$E_{rel,n} = \frac{A(n^{th} \text{ order method}) - A((n + 1)^{th} \text{ order method})}{A((n + 1)^{th} \text{ order method})} \quad \text{Equation 10}$$

where A stands for surface area. (This definition has already been used in the program in Figure 9.) Examples of first, second, third and fourth order integration methods are the rectangular, trapezoidal, Simpson and Runge-Kutta methods, respectively.

Applying Equation 10 to calculate the relative error in the first order rectangular integration method gives:

$$E_{rel,1} = \frac{v_0 \cdot \Delta t}{(v_0 + v_0 \cdot e^{c \cdot \Delta t}) \cdot \Delta t / 2} - 1$$

From the numerator and denominator, $v_0 \cdot \Delta t$ cancels, and $e^{c \cdot \Delta t}$ can be written according to a Taylor expansion: $1 + c \cdot \Delta t + \frac{1}{2}(c \cdot \Delta t)^2 + \dots$ (see Appendix 1 for details). Since $c \cdot \Delta t$ is much smaller than 1, higher order terms can be omitted, and, after some algebra, one obtains:

$$E_{rel,1} \cong -\frac{1}{2} \cdot c \cdot \Delta t = -\frac{1}{2} \cdot \frac{\Delta t}{\tau} \quad \text{Equation 11}$$

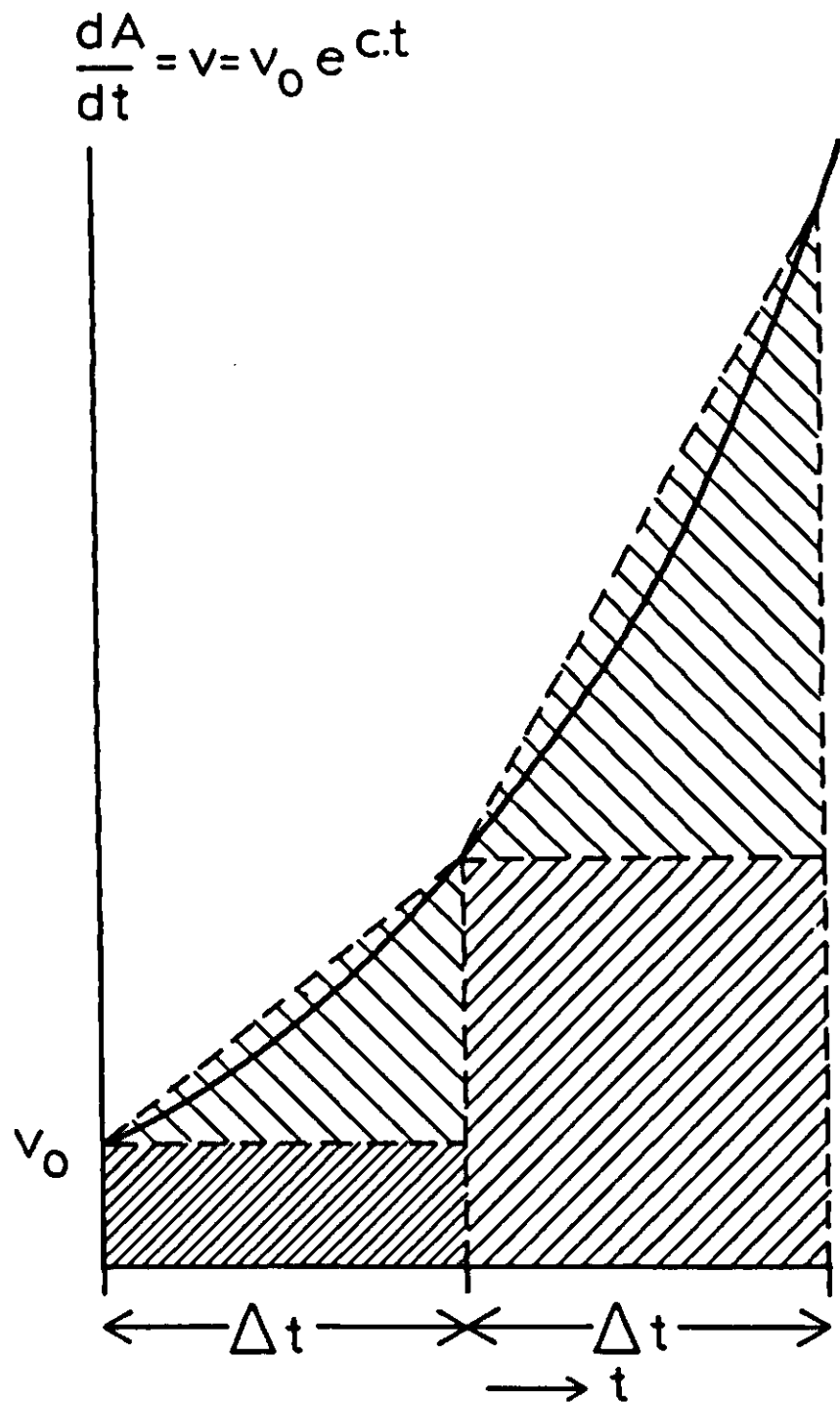


Figure 11. Graphical representation of the surface areas that are calculated by the rectangular integration method () and by the trapezoidal integration method ( + ), when the exponential rate curve is given as a function of time (solid curved line).

This derivation is given in detail in Appendix 1. Equation 11 shows that the relative error is proportional to the ratio of the time interval of integration and the time coefficient of the model. The minus sign reveals the underestimation of the surface area beneath the curved solid line in Figure 11. As the rate of change grows exponentially, the same relative error is added each time interval. Thus, the final absolute error is $E_{abs,1} = -\frac{1}{2} \cdot (\Delta t / \tau) \cdot A$. In the trapezoidal integration method, the triangles are taken into account, so the error is much smaller. The remaining error is estimated from the area between the straight line that is formed by connecting the corners of the vertical bars and the parabola constructed through the values of the exponential rate function at times t , $t + \frac{1}{2} \cdot \Delta t$ and $t + \Delta t$. The relative errors for the trapezoidal and Runge-Kutta integration methods have been calculated by Goudriaan (1982) and are given in Table 3. Note that for integration without feedback, the relative error is independent of the simulation time.

Exercise 13

- Use the estimates of the relative errors without feedback from Table 3 to calculate which Δt (expressed as a fraction of τ) must be chosen to yield a relative error of 1% in the integration of an exponential curve, for all three methods.
 - Calculate analytically the area beneath an exponential curve between $t = 0$ and $t = 1$, with $v_0 = 1$ and $c = 1$. Also, calculate this area using the three numerical methods with $\Delta t = 1$. Since in integration without feedback all rates are known in advance, it is neither necessary to know the initial condition nor to calculate the intermediate areas.
 - From the answer to b, calculate the exact absolute and relative errors in the integration results using the three numerical methods, with respect to the analytical solution. Compare these exact relative errors with the estimates from Table 3.
-

Table 3. Estimates of the relative errors of three integration methods.

Method	Without feedback	With feedback
rectangular	$-(\Delta t/\tau)/2$	$-(t \cdot \Delta t/\tau^2)/2$
trapezoidal	$(\Delta t/\tau)^2/12$	$-(t \cdot \Delta t^2/\tau^3)/6$
Runge-Kutta	$(\Delta t/\tau)^4/2880$	$-(t \cdot \Delta t^4/\tau^5)/120$

Integration of a differential equation with feedback In dynamic simulation, the rate variable is usually not known as a function of time; instead, new values are calculated from the current state, as for example in Equations 2 and 3. For instance, in the case of exponential growth of an animal population, an underestimate of the growth rate will result in an underestimate of the population at time $t + \Delta t$, and thus also of the growth rate at that moment. This occurs in numerical integration of differential equations with feedback, and a new error will be added each time interval. Thus, in contrast to the integration of a driving force, relative errors increase during the time of simulation. The error analysis is slightly different from that for a driving force, because the relative error will refer to the total integral value, which consists of the integrated amount together with the initial value.

For the rectangular method this implies the following. The rate at time t equals (Equation 2): $(dA/dt)_t = c \cdot A_t$. So the value of the integral after one time interval is $A_{t+\Delta t} = A_t + \Delta t \cdot c \cdot A_t$. To calculate the value of the integral according to the trapezoidal method, the rate at $t + \Delta t$ is calculated:

$$(dA/dt)_{t+\Delta t} = c \cdot A_t \cdot (1 + \Delta t \cdot c).$$

It then follows that

$$A_{t+\Delta t} = A_t + \Delta t \cdot (c \cdot A_t + c \cdot A_t \cdot (1 + \Delta t \cdot c))/2.$$

All the terms required to calculate $E_{rel,1}$ according to Equation 10 are now available. After some algebra, and neglecting higher order terms, the relative error in the rectangular integration method is determined as

$$E_{rel,1} \cong -\frac{1}{2} \cdot (\Delta t \cdot c)^2 = -\frac{1}{2} \left(\frac{\Delta t}{\tau} \right)^2 \quad \text{Equation 12}$$

This derivation is given in detail in Appendix 2. The relative error occurs in each integration step and, in contrast to the situation without feedback, these errors accumulate. At time t , when $t/\Delta t$ integration steps have been performed, the relative error is

$$E_{rel,1} \cong -(t \cdot \Delta t / \tau^2) / 2$$

Interestingly, the relative error is proportional to Δt , as for integration without feedback, but is now also linearly dependent on the simulation time. The relative errors for integration with feedback for the trapezoidal and Runge-Kutta integration methods, as derived by Goudriaan (1982), are also given in Table 3.

Exercise 14

- Perform the calculations in Exercise 13a for the situation with feedback and a simulation time equal to τ .
- For the situation with feedback, the differential equation is $dA/dt = v = c \cdot A$ (Equation 2). Calculate A at $t = 1$ when the initial condition, A_0 , equals 1, $c = 1$, and $\Delta t = 1$, using the three numerical methods. Also calculate A at $t = 1$ for this situation, analytically.
- Perform the calculations in Exercise 13c for the situation with feedback.

At a discontinuity, no derivative exists. When an integration interval overlaps a discontinuity, the error in any integration method will be large, as seen in Exercise 12 where an attempt was made to nullify a state variable in one time step, using the trapezoidal integration method. Error analysis as described above can, however, be applied before and after such discontinuities. The numerical error due to the discontinuity itself is avoided by using the rectangular integration method and synchronizing the time interval with the discontinuity.

2.1.8 An example

The different steps which are distinguished in systems analysis of living systems are demonstrated below.

Objectives and definition of the system A microbiologist plans to develop a technical system in which yeast can be grown continuously. To do this he wishes to use a vessel of constant volume, through which a sugar solution will flow. To gain insight into the proper technical system parameters, such as the volume of the vessel (v, m^3), the concentration of sugar in water ($c_s, kg\ kg^{-1}$) and the flow rate of water ($q, m^3\ d^{-1}$), he decides to design a model of the system.

The physiological parameters pertaining to the yeast cannot be adjusted like the technical parameters. Therefore, some experiments are performed which reveal that the absolute growth rate of the yeast ($dy/dt, kg\ d^{-1}$) is proportional to the amount of yeast (y, kg) present, and to the sugar concentration. At a sugar concentration of 10%, $c_{s,10}$, the relative growth rate and amount of sugar in the vessel are termed μ_{10} and s_{10} , respectively. The rate of sugar consumption per unit yeast ($s_y, kg\ kg^{-1}\ d^{-1}$) is known. The maximum possible quantity of sugar (s_m, kg) in the vessel is determined by the incoming sugar concentration and the volume of the vessel.

Exercise 15

The following table gives fictitious data on the changing amount of yeast at different constant sugar concentrations.

sugar concentration in water ($kg\ kg^{-1}$)	time (h)			
	0	2	4	10
0	2000	2000	2000	2000
0.02	1950	2119	2304	2958
0.05	1900	2340	2882	5384
0.10	2050	3110	4717	16464

- Derive the relative growth rate of yeast, μ , at these four different sugar concentrations.
- Plot the relative growth rate, in units of day^{-1} , against the sugar concentration, c_s . Express μ in terms of c_s , $c_{s,10}$ and μ_{10} .
- Rewrite the expression for μ in terms of the current amount of sugar, s , and s_{10} .

The relational diagram Figure 12 shows the relational diagram of the model. Note that this figure is constructed from the elementary system units used throughout this text. For instance, the lower left input rate together with the integral of the sugar (s, kg) is equivalent to the relational diagram of the car from Figure 6; and the upper integral of the yeast, together with the right output rate, forms an exponential decrease. The representation of the model by one integral

$$s_{10} = c_{s10} \cdot v \cdot 1000 \quad \text{Equation 15}$$

$$\tau = \frac{v}{q} \quad \text{Equation 16}$$

By analogy, the net flow rate for sugar is

$$\frac{ds}{dt} = c_s \cdot q \cdot 1000 - y \cdot s_y - \frac{s}{\tau} \quad \text{Equation 17}$$

Exercise 16

- Examine the dimensions of all variables and constants in Equations 13 to 17.
- What does the number 1000 denote in Equations 15 and 17?

Further analysis of Equations 13 to 17 To study the dynamic behaviour of the yeast-sugar model, Equations 13 and 17 should be solved by numerical integration. However, several model properties can be analysed without a computer; for example by studying simplified equations or equilibrium properties.

An example of needing to simplify equations, is the calculation of the time needed to equilibrate a water-filled vessel, which is initially free of sugar, with the sugar solution but in the absence of yeast. The relational diagram for this problem is represented by the lower half of Figure 12 when the outflow of sugar, due to consumption by the yeast, is omitted. The differential equation for the sugar, when $y = 0$, is $ds/dt = c_s \cdot q \cdot 1000 - s/\tau$, which can be solved analytically. For the condition that at $t = 0$, $s = 0$, this gives

$$s = s_m \cdot (1 - e^{-t/\tau}) \quad \text{Equation 18}$$

where $s_m = c_s \cdot v \cdot 1000$, which is the maximum amount of sugar that can be achieved with given c_s and v .

Equations 18 and 6, when $W_0 = 0$, are similar in form, although their differential equations describe quite different systems and express a dynamic and a static flow model, respectively.

Exercise 17

Derive from Equation 18, in general terms, the time needed to reach 95% of the final equilibrium level of sugar in the vessel.

Such equilibrating processes may take a long time when large time coefficients are involved. It is preferable, therefore, to start an experiment by filling an empty vessel with the desired sugar solution.

Exercise 18

How much time, expressed in terms of the time coefficient, is needed to reach 100 % of the equilibrium level of sugar when an empty vessel is filled at a constant rate with the sugar solution? There is no outflow until the vessel is full.

Equations 13 and 17 can be analysed to determine whether equilibrium levels of yeast and sugar can be reached, and if so, what levels. In a dynamic equilibrium the state variables are constant, and the sum of the inflow rates is equal to the sum of the outflow rates. Thus, the net rate of change of the state variable is zero. In the case of the continuous culture, this means that dy/dt and ds/dt in Equations 13 and 17, respectively, are zero. The equilibrium levels of sugar and yeast can be calculated from

$$s = \frac{s_{10}}{\mu_{10} \cdot \tau} \quad \text{Equation 19}$$

and

$$y = \frac{1}{\tau \cdot s_y} \cdot (s_m - s) \quad \text{Equation 20}$$

A special case of dynamic equilibrium is obtained when y is zero. Such a dynamic equilibrium is established when the yeast culture is washed out, because the time coefficient for the vessel is smaller than that for the yeast. This is the case when $q > c_s \cdot v \cdot \mu_{10}/c_{s10}$.

Exercise 19

Derive Equations 19 and 20 from Equations 13 to 17.

Equation 20 shows that the equilibrium level of yeast depends on the (manipulable) time coefficient for the vessel.

The microbiologist is interested in the combination of manipulable parameters yielding maximum yeast production with the minimum amount of sugar. The only manipulable variables in Equation 20 are s_m and τ . From Equation 19 it follows that s is a hyperbolic function of τ , indicating that at very low τ values s will be very large, and at high τ values s will be small; i.e. there is no practical minimum value of the amount of sugar. To investigate whether a maximum exists in the curve of yeast production against the time coefficient, Equation 19 is inserted into Equation 20, which is then differentiated with respect to τ , to obtain

$$\frac{dy}{d\tau} = \frac{1}{\tau^2 \cdot s_y} \cdot \left(\frac{2 \cdot s_{10}}{\tau \cdot \mu_{10}} - s_m \right) \quad \text{Equation 21}$$

Exercise 20

- Derive Equation 21.
- At what value of τ is there a maximum or minimum value of y ?

If the second derivative of y with respect to τ is negative at the τ value found in Exercise 20b, y is at a maximum. The second derivative is

$$\frac{d}{d\tau} \left(\frac{dy}{d\tau} \right) = \frac{d^2y}{d\tau^2} = \frac{2}{\tau^3 \cdot s_y} \cdot \left(s_m - \frac{3 \cdot s_{10}}{\tau \cdot \mu_{10}} \right) \quad \text{Equation 22}$$

Substituting the answer from Exercise 20b into Equation 22 yields a negative value for the second derivative. The maximum yeast level, at that value of τ , can be calculated from Equation 20 as

$$y = \frac{1}{4} \cdot \frac{\mu_{10}}{s_{10} \cdot s_y} \cdot s_m^2 \quad \text{Equation 23}$$

The quantity of sugar is then

$$s = \frac{1}{2} \cdot s_m. \quad \text{Equation 24}$$

Equations 23 and 24 show that at the optimum value of τ ($= v/q$), the amounts of yeast and sugar can still be changed by adjusting the inflow concentration of sugar which determines s_m .

Exercise 21

- Check the dimensions of Equations 19 to 24.
- Express the water flux q in terms of the other parameters to calculate the inflow rate resulting in the maximum amount of yeast at a given sugar concentration and vessel volume.

It has been shown which tools are needed to develop and solve simple models. Although the treatise is far from complete, it will be seen that most of the models described in the following chapters are composed of the elementary feedback loops discussed in this chapter, and that the above simple mathematical tech-

niques are adequate to solve them. Analysing and solving more complex problems, requires more knowledge, especially about the relationships that may characterize system structure, rather than sophisticated mathematics. Today, the lack of such knowledge is the major restriction, but is also the major challenge, of future research.

2.2 Modelling of ageing, development, delays and dispersion

J. Goudriaan and H.J.W. van Roermund

2.2.1 Introduction

In a model designed for a population with only one generation, the development stage can be treated as a single state variable (Subsection 2.2.3). However, when there is a distribution of ages, or stages of development, the boxcar train is a suitable method that can be used to simulate the development process of the entire population (Subsection 2.2.4). During the simulation process, some dispersion (variability) may occur within the development rates of different individuals. Three types of boxcar train are possible, differing mainly in this dispersion of development rate. In the escalator boxcar train, dispersion is virtually absent (Subsection 2.2.5). In the fixed boxcar train, dispersion is quite substantial and rigidly determined by the number of boxcars (Subsection 2.2.6). The fractional boxcar train includes a parameter which allows the dispersion to be varied between these two extremes, and to be altered during the simulation process itself (Subsection 2.2.7).

The CSMP statements (see Appendix 5), and FORTRAN subroutines used to implement these methods are given, and the approach is illustrated with a simple application.

2.2.2 Development and delay

A good example of a stable and well measurable rate of development can be found in a bird's egg; the time between laying and hatching is rather fixed. Both moments are two clearly marked milestones in the life of a bird. Because the duration of time between these moments is rather stable, the rate of hatching in a population of birds is the same as the rate of laying, delayed over the period of brooding. Such delays are quite common in the description of biological processes. For instance, the well-known equation for exponential growth:

$$\frac{dy}{dt} = r \cdot y \quad \text{Equation 25}$$

can be written more specifically to describe adult birds only as:

$$\frac{dy}{dt} = r \cdot y_{t-p} \quad \text{Equation 26}$$

where p stands for the duration of egg and juvenile stages combined. The value of the relative growth rate, r , is not the same in Equations 25 and 26. In the

development of disease for example, latency periods can often cause delays (see Chapter 3).

When the delay period is always the same, a simple CSMP function (see Appendix 5) can be used to implement the delay:

$$\text{OUTFL} = \text{DELAY}(\text{N}, \text{PERIOD}, \text{INFLOW})$$

where the rate *INFLOW* is delayed over a period *PERIOD* to produce the outflow rate *OUTFL*. *N* stands for the number of sampling points describing the shape of the inflow rate during the delay period, and should typically be of the order of *PERIOD/DELTA* (*DELTA* is the time step of integration, Δt).

Exercise 22

Use this *DELAY* function to simulate hatching 20 days after laying. During days 1 and 2, 100 eggs are laid, and no more afterwards.

A major limitation of the *DELAY* function is that it cannot be used with variable delay periods. Another limitation is that operations on the quantities delayed, such as mortality or emigration, are not possible.

2.2.3 *Simulation of development of a single generation*

In warm-blooded animals, development and ageing can hardly be distinguished, but in other organisms these rates can be completely different. For instance, plants of the same species may flower at moments that are more determined by temperature and day length than by time since emergence. Usually, at low temperatures the developmental processes run much slower than at high temperatures.

Discernible stages of development have been given names, for instance 'anthesis', 'dough-ripe' (in wheat), 'silking' (in maize), and are largely species specific. Numbers have also been given to these stages, so that they can be more easily quantified. For instance, in the general scale of development, as used in the crop growth model *SUCROS87* (Section 4.1), 'anthesis' was given the value 1, and 'maturation' the value 2. In the literature, more refined scales have been developed, e.g. for wheat (Zadoks et al., 1974; Reinink et al., 1986), maize (Groot et al., 1986) and rape seed (Remmelzwaal & Habekotté, 1986).

Rate of development can be defined as the numerical distance between two stages, divided by the time required to pass from one stage to the other. The problem with empirical scales is that the time intervals between subsequent stages are often not equal, even under constant conditions. Then, the empirical scale must be projected onto a fictive scale that meets this requirement of

a homogeneous rate. Alternatively, the rate of development varies with the stage of development.

In the following example (Remmelzwaal & Habekotté, 1986), a simulation approach will be shown for the development of rape seed from stage 9 (end of flowering) to stage 15 (maturation). Over this range, the development rate (DEVR) is proportional to temperature above 6°C, but it is assumed here that above 25°C no further acceleration occurs. This means that the response between 6°C and 25°C can be quantified in terms of degree-days with a base temperature of 6°C. 490 degree-days are needed to proceed from stage 9 to stage 15.

Exercise 23

How long would this period be at 10°C and how long at 20°C? What would be the rate of development at these temperatures?

The state variable 'stage of development' (STAGE) can now be simulated by the following CSMP statements:

```
STAGE = INTGRL(9., DEVR)
DEVR = AFGEN(DEVTB, TA)
FUNCTION DEVTB = (0., 0.), (6., 0.), (25., 0.233), (30., 0.233)
```

where TA stands for air temperature in °C, and DEVTB for DEVelopment TaBle with the development rate as a function of temperature.

Exercise 24

Check the consistency of this model and the manual calculation of Exercise 23 by running this simple model for 10°C and for 20°C.

2.2.4 *The boxcar train*

Using the above method, it is only possible to keep track of the stage of development of the entire population, because all individuals are synchronized. This situation is quite common in field crops. In insect populations, especially if they are polyvoltine, several stages of development occur simultaneously. Each stage would then require its own simulation. Also, new generations are continuously being born, which adds to the complexity.

The boxcar train technique provides for all possible development stages simultaneously. Before simulation starts, the developmental axis of one stage is broken up into a number of classes or boxcars, each with identical development

widths. If necessary, several separate boxcar trains may be chained; for instance, one to allow for all egg stages, one for all juvenile stages and one for all adult stages. This separation may be necessary to fulfil the requirement of homogeneity of development rate within a boxcar train. It is then much easier to acquire boxcars of identical development widths, at least within the boxcar train.

After this classification, each boxcar is initialized with the number of individuals contained in it. In principle, a histogram can now be drawn for the development distribution of the population in the stage considered (Figure 13a).

If a higher resolution of the development axis is required, the number of boxcars in the boxcar train should be increased (Figure 13b). In Figure 13b, the vertical axis is scaled so that the total area is still the same as in Figure 13a. This can be achieved by plotting vertically not just the number per boxcar, but this number divided by its development width γ . The number obtained in this way is a boxcar-averaged concentration c , as an approximation of the 'true' concentration which could vary with stage g , given by the broken line in Figure 13b.

If there is no mortality, this concentration-distribution function simply shifts to the right without any change in shape. Of course, new individuals may enter at $g = 0$, and at $g = g_f$ individuals are removed from the scene. Theoretically, it is possible to store the shape of the graph of $c(g)$ into a computer with a very high degree of resolution and, accordingly, to simulate the development process. However, computer limitations prevent this procedure, and we have to live with a representation as given by histograms in Figure 13a.

The question now is how to allow for the continuously occurring development drift, which shifts all individuals to a higher stage of development at the same rate. In principle, there are two options available to simulate this process:

1. Continuously shift the entire distribution, shown by the histogram in Figure 13, to higher values of development, including the boxcar boundaries. Only the beginning ($g = 0$) and the end ($g = g_f$) are fixed. This system is called the escalator boxcar train.

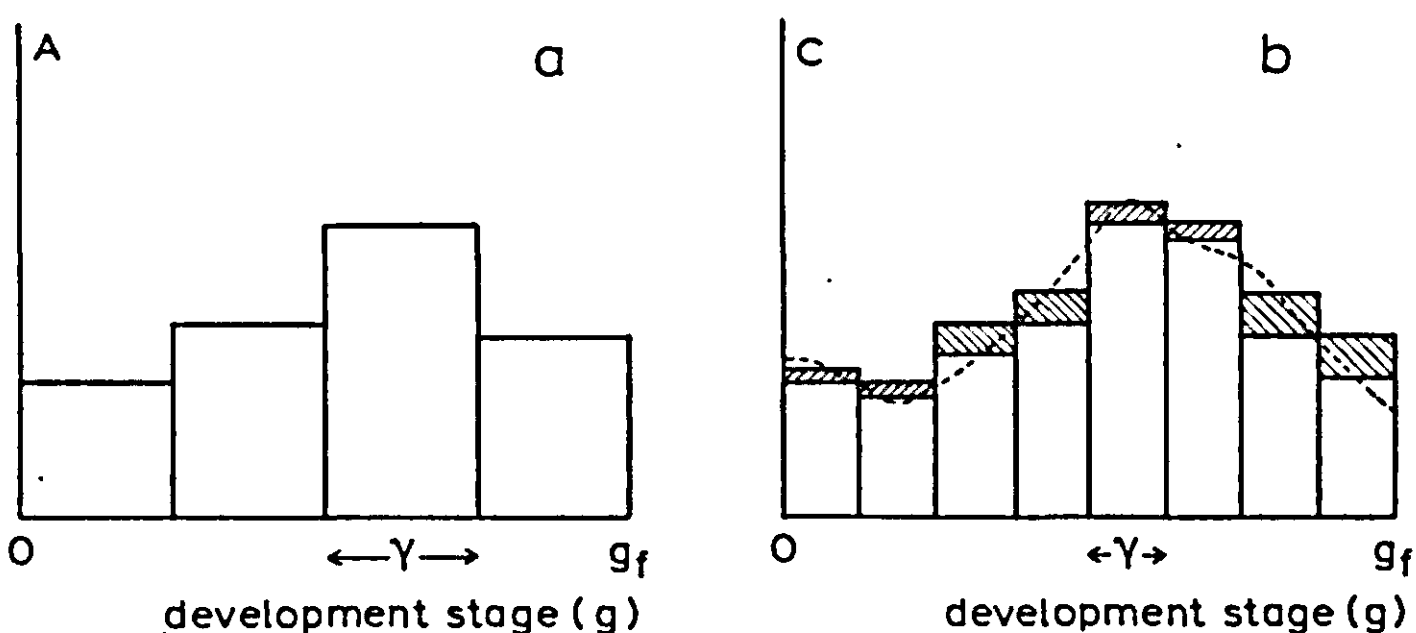


Figure 13. Distribution of numbers of individuals (A) or of concentrations (c) with stage of development (g). g_f stands for the final value of g, and γ for the width of a single boxcar. For explanation see text.

2. Keep the location of the boundaries of the boxcars (the bars in the histogram) fixed, but allow the individuals to flow from one boxcar to the next. The rate of movement is proportional to the rate of development, and also to the concentration (height of the bar). This system is called the fixed boxcar train.

These two types of boxcar train do not differ in mean delay time. However, in the escalator boxcar train all individuals are about equally delayed, whereas in the fixed boxcar train some are more and others less delayed. The reason for this variability is that for each individual the probability of flowing to the next boxcar is the same, whether that individual has just arrived or has been waiting quite a while. Due to this stochastic process, there is variance in the residence time in each boxcar. The variance of duration of through-flow through the fixed boxcar train, causes a levelling of peaks and dips originally present in the inflow curve (Berger & Jones, 1985). An intensive but brief pulse will be buffered in the relatively long residence time of the boxcars, and will result in dispersion during development. This so-called numerical 'dispersion' is an artefact of the system, but is a useful by-product of the boxcar train. Whenever such variance is observed in nature, the fixed boxcar train may help to simulate this phenomenon, although it does not add any explanatory value about its causes.

It will be explained later that it is possible to hybridize both systems into the fractional boxcar train. Using this hybrid method, the degree of variance of through-flow can be controlled to match the observed variance.

2.2.5 *The escalator boxcar train*

In the escalator boxcar train, the developmental process is simulated by a continuous developmental drift of the boxcar boundaries. It is essential that these boundaries are chosen so that each boxcar covers the same developmental width; this means that the duration between adjacent boundaries are made equal for all of them. After the developmental process has completed one such sub-unit of development, boxcar width γ (Figure 14), the entire population will have gradually shifted to the right by exactly one boxcar, and so all boxcar numbers can be reset.

This process is schematically given in Figure 14. An escalator boxcar train with 4 boxcars is presented here, so that the total development range covered (g_f) is equal to 4γ . Although the rate of development is not necessarily constant, it should change simultaneously for all boxcar boundaries.

Immediately following the start of simulation, a gap opens between $g = 0$ and the lower boundary of boxcar 1. This gap is filled by a new boxcar, with number 0, which will receive the newcomers into the boxcar train. As far as the functioning of the boxcar train is concerned, it does not matter where these newcomers have come from, whether they have been generated as an external driving force, been produced as offspring from the boxcar train itself, or have simply come from a preceding boxcar train.

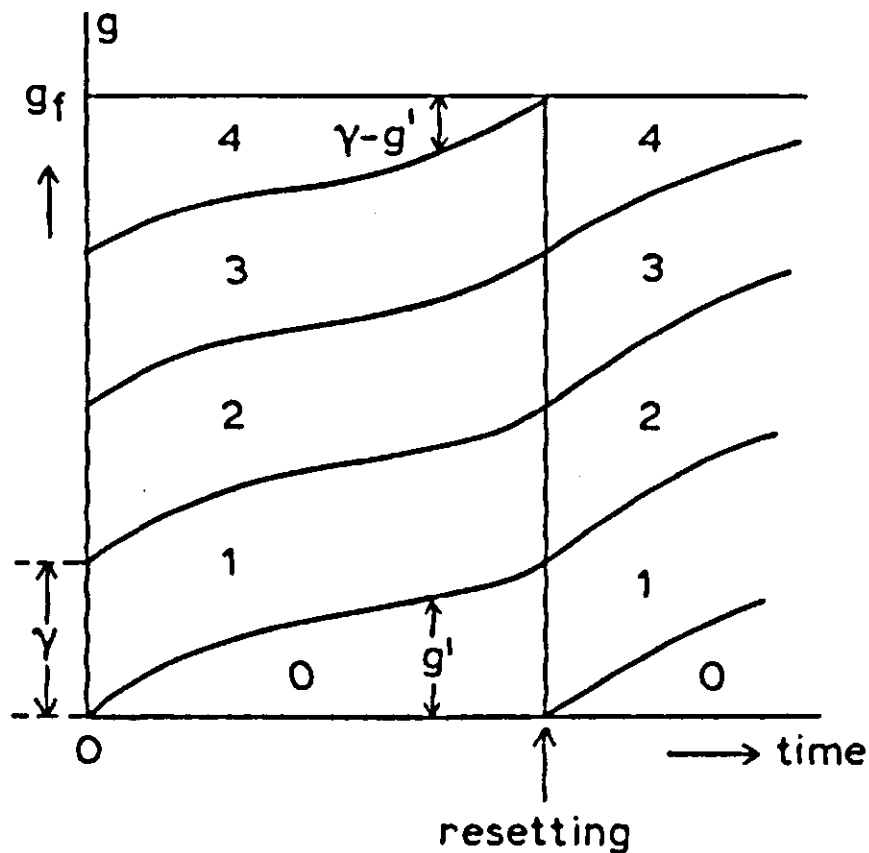


Figure 14. The escalator boxcar train. Time dependence of position of the boxcars and their numbering. For explanation see text.

At the other end of the boxcar train, the last boxcar is contained between a fixed end boundary and an upward-moving lower boundary. The distance between them ($\gamma - g'$) keeps shrinking, and so without outflow the concentration in the last boxcar, c_N , would grow beyond limit. Such unlimited compression is prevented because there is also a rate of outflow, Q_{out} , defined as:

$$Q_{out} = v \cdot c_N$$

with

$$c_N = A_N / (\gamma - g')$$

where v is the rate of development, A_N is the amount in the last boxcar and g' the cyclic development stage ($0 < g' < \gamma$, Figure 14).

When there is no mortality, the relative rate of decrease of amount A_N and of the remaining width $\gamma - g'$ are equal, and so the concentration c_N does not change. The rate of outflow Q_{out} is then proportional to the rate of development v , exactly as we want it to be.

When there is mortality, Q_{out} decreases within each development cycle. In fact all boxcars, including the zero boxcar and the last one, may or may not lose individuals due to mortality, but they do not exchange them. This lack of exchange preserves the shape of the development distribution curve.

The resetting event occurs when the development process has covered one sub-unit γ , the width of one boxcar. At that moment, each boxcar has reached the position occupied by its successor at the start of the simulation. The boxcar numbers are then reset, the last boxcar is removed entirely and a new zero boxcar is opened.

A calculation of the delay values and residual dispersion in the escalator boxcar train is given in Appendix 3.

Exercise 25

If the escalator boxcar train is used to describe the development of rape seed from stage 9 to stage 15, in 4 boxcars, what is then the value of γ ? How would you formulate the development rate DEVR? If the degree-day simplification is permitted ($6 < T_a < 25^\circ\text{C}$), on how many degree-days does the resetting (or 'shift') event occur?

2.2.6 The fixed boxcar train

With fixed boundaries between the boxcars, there is a continuous forward flow from each boxcar into the next to allow for the development drift. Water, cascading from tanks can be used as a physical model to visualize how the fixed boxcar train operates. The flow from a boxcar is proportional to the concentration c in it, and to the development rate, v :

$$Q_{i+1} = v \cdot c_i \quad \text{Equation 27}$$

where Q_{i+1} is the flow rate from boxcar i to boxcar $i + 1$. The concentration c_i is given by:

$$c_i = A_i/\gamma \quad \text{Equation 28}$$

To understand the behaviour of the population contents in the fixed boxcar train, it is best to consider first the simplified situation under a constant development rate v . Then, each boxcar will act as a first order exponential delay, which means that a single sharp input pulse will give rise to an exponentially declining output flow (Figure 15). Of course, the total area of both pulses must be the same.

The exponential shape of the decline can be derived as follows. Imagine that at time zero the boxcar considered is empty, and that consequently the output flow is also zero. Suddenly, a very brief, sharply peaked input flow fills the boxcar with an amount A_0 . According to Equations 27 and 28, the output flow Q_{out} is directly proportional to the contents A :

$$Q_{\text{out}} = A \cdot v/\gamma$$

In the situation described, the inflow will be zero immediately after the passage of the brief pulse, and so the differential equation for the contents A is:

$$\frac{dA}{dt} = -A \cdot v/\gamma \quad \text{Equation 29}$$

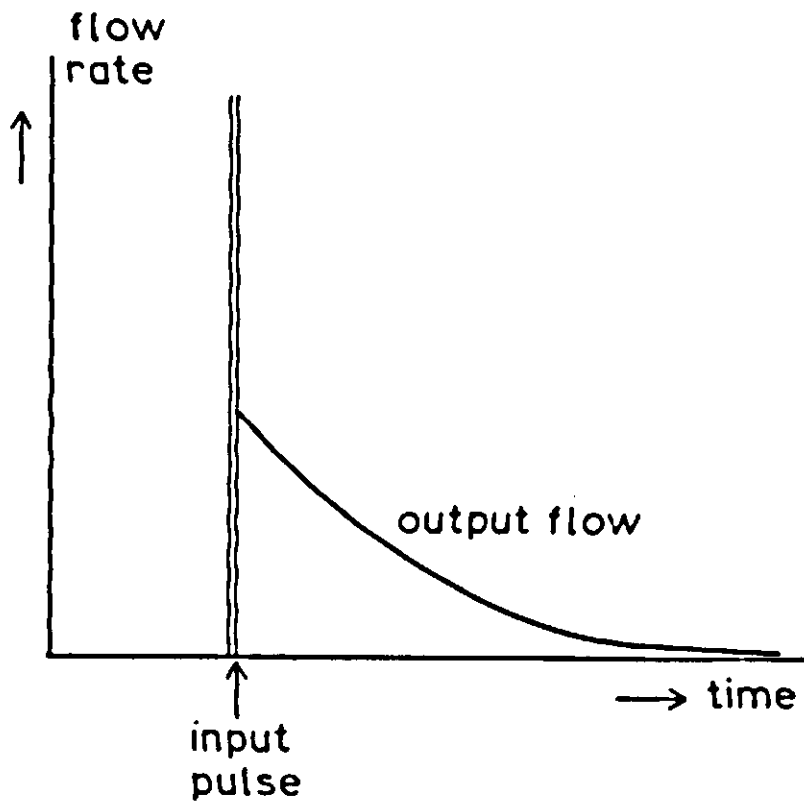


Figure 15. Output flow of a sub-unit in the fixed boxcar train in response to a sharply peaked input pulse.

Since v and γ are constant in this simplified situation, the solution of this differential equation for A is an exponentially declining function:

$$A = A_0 \exp(-v \cdot t/\gamma)$$

with A_0 as the initial value of A , and the outflow Q_{out} given by:

$$Q_{out} = (v/\gamma) A_0 \exp(-v \cdot t/\gamma) \quad \text{Equation 30}$$

With regard to the relationship between the inflow peak and the outflow function (Figure 15), two observations can be made: (1) on average, the outflow is delayed with respect to the inflow; (2) the shape of the outflow is more dispersed over time than the inflow.

To find the value of the average delay we should remember that the inflow pulse was localized at time zero, and so the average delay is equal to the mean of time t of outflow in Equation 30. To find this mean time τ , time t should be integrated between zero (start) and infinity, weighted with the value of Q_{out} :

$$\tau = \int_0^{\infty} t Q_{out} dt / A_0$$

Substitution of Q_{out} according to Equation 30 gives:

$$\tau = \int_0^{\infty} t \cdot (v/\gamma) \exp(-v \cdot t/\gamma) dt$$

which has the solution:

$$\tau = -\exp(-v \cdot t/\gamma)(t + \gamma/v)]_0^\infty$$

or $\tau = \gamma/v$. In fact, this answer is not surprising since γ/v is the time coefficient in the argument of the exponential function in Equation 30, and also in differential Equation 29. This is similar to the derivation in Subsection 2.1.5.

So far, the derivation has only concerned a single infinitely sharp inflow pulse, and one might wonder whether the value of the delay is independent of the shape of the inflow. This simple thought is correct, since any shape of the inflow can be broken up into a series of sharp pulses, each giving rise to its own exponentially delayed outflow. Since the whole system is linear (meaning that outflow is proportional to contents, Equation 29), the contents and outflows due to the subsequent pulses can simply be added together. Therefore, the average delay is also equal to γ/v (or τ), independent of the shape of the inflow. Each boxcar will add this delay to result in the total delay of the entire boxcar train:

$$T_{\text{total}} = N \cdot \tau \quad \text{Equation 31}$$

With regard to the average value of the total delay, the fixed boxcar train and the escalator boxcar train are similar. The difference between these methods appears in the effect on the shape of the outflow. Whereas the outflow is identical in shape to the inflow in the escalator boxcar train, it is much more dispersed in the fixed boxcar train. This means that a considerable amount of variance has been added to the time distribution of the inflow.

Statistically, the variance σ^2 is the second order moment of the time of outflow, which can be calculated as the mean value of $(t - \tau)^2$, weighted with Q_{out}/A_0 :

$$\sigma^2 = \int_0^\infty (t - \tau)^2 Q_{\text{out}} dt / A_0$$

With Q_{out} given by Equation 30, and using $\gamma/v = \tau$, σ^2 can be written as

$$\sigma^2 = \int_0^\infty (t - \tau)^2 (1/\tau) \exp(-t/\tau) dt$$

By using of a table of indefinite integrals, and some algebra, this expression can be shown to lead to (see Appendix 4):

$$\sigma^2 = \tau^2$$

Since each boxcar will add this amount of variance, irrespective of the other boxcars and of its own position in the cascade, the total amount of variance added by the entire boxcar train is given by:

$$\sigma_{\text{total}}^2 = N \cdot \tau^2$$

Combining this expression with the one for total delay (Equation 31) gives the interesting result for relative 'dispersion' RD:

$$\sigma_{\text{total}}/T_{\text{total}} = 1/\sqrt{N}$$

The relative 'dispersion' RD (or 'coefficient of variation CV') of the outflow time, in response to a peaked inflow decreases with the number of boxcars N. This result could be understood more easily if one were to imagine more (but narrower) boxcars in the boxcar train.

Exercise 26

How many boxcars are needed to simulate a delay of 20 days with a 'dispersion' of 2 days (RD = 0.1)?

A system of N fixed boxcars is often termed an Nth order delay. The dynamic response of the outflow after a stepwise change in inflow is given in Figure 16 for different values of N (Ferrari, 1978).

2.2.7 The fractional boxcar train

Compared with the DELAY function of CSMP, both the escalator and the fixed boxcar trains are much more flexible, in that they permit variable development rates. However, they still lack flexibility in the relative 'dispersion' (or RD) of outflow. The escalator boxcar train has almost no dispersion (except for the small amount due to the distribution over a single boxcar) and the fixed boxcar train has a fixed RD of $1/\sqrt{N}$ which, once chosen, cannot be changed during the simulation. But in several experimental data sets there is evidence that delay and dispersion are not equally influenced by e.g. temperature, and so the relative

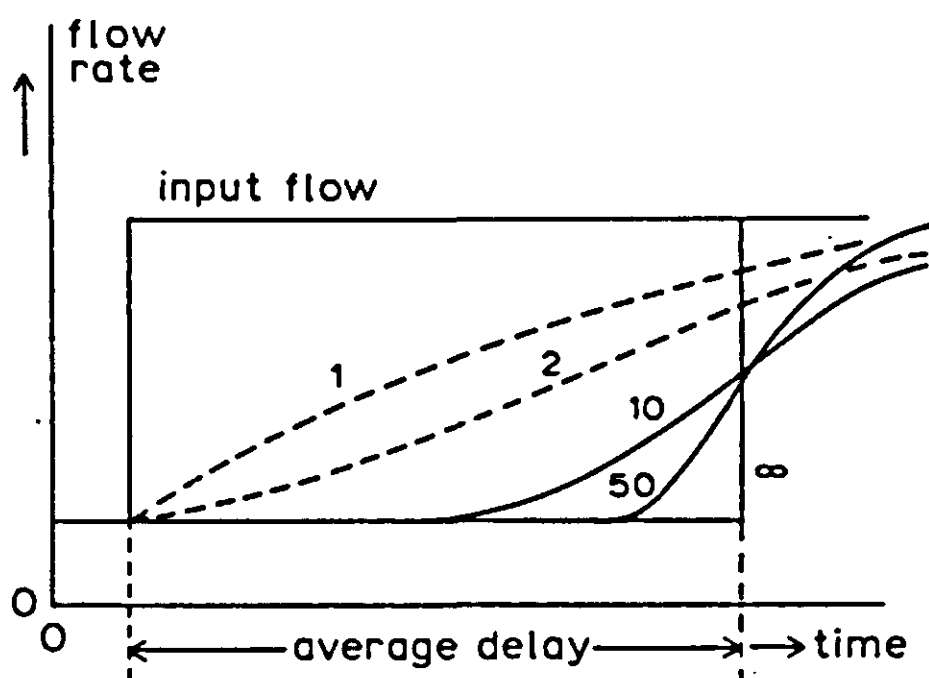


Figure 16. Response of outflow to a stepwise change in inflow for a fixed boxcar train with different numbers of boxcars.

dispersion also varies. To allow for this change during simulation, a more flexible method than that of the fixed boxcar train is needed. Such a flexible method can be obtained by hybridizing the methods of both the fixed and the escalator boxcar trains. This method will be termed the fractional boxcar train, because it is based on a fractional repeated shift.

In the escalator boxcar train, a complete shift to the next boxcar occurs at the moment of resetting. In the fractional boxcar train, it is not the complete contents that are shifted, but only a fraction F of each boxcar's contents. To compensate for the smaller amount, the shift must occur more frequently. In the escalator boxcar train the renumbering (or shift) occurs upon completion of a full development cycle, γ . In the fractional boxcar train method, the fractional shift occurs upon completion of a fraction F of the development cycle. This fraction ranges between 0 and 1 and can be changed during simulation. A possible time path of the boundaries between the boxcars is illustrated in Figure 17.

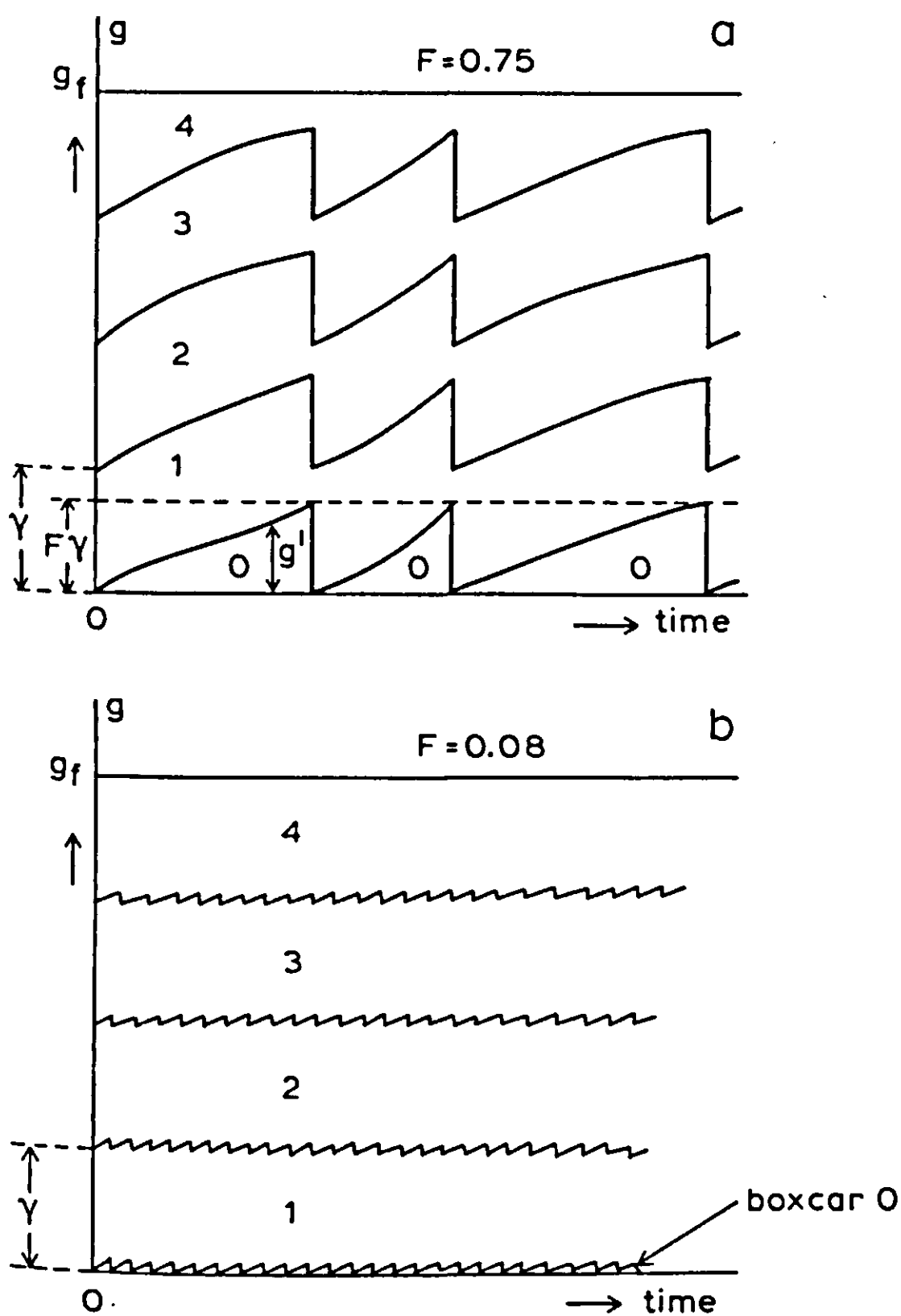


Figure 17. Sawtooth shape of time path of the boxcar boundaries in the fractional boxcar train. For explanation see text.

The value of the fraction F determines how often resetting and partial transfer of contents occurs. When F is equal to 1, the escalator boxcar train is effectively restored (Figure 14). On the other hand, when F approaches zero, the sawtooth shape of the boundaries between the boxcars is practically straight, so that the fixed boxcar train is approached. During simulation, the value of F can be varied anywhere between these two extremes, so that gradual adaptations can be made in the value of the desired dispersion.

Since movement through the boxcars is pulsewise, the differential equations must be replaced by difference equations. The cyclic development stage, g' , stands for the development elapsed since the last resetting occurred. In the escalator boxcar train, g' triggers the renumbering when it exceeds γ . Here, in the fractional boxcar train, the trigger level is set at $F\gamma$. When this level is exceeded, fractional shift occurs and g' is decreased by $F\gamma$. The contents of boxcar i are also reduced:

$$A_{i,j} = A_{i,j-1} - F \cdot A_{i,j-1}$$

where j counts the number of shifts since the start. Here, as for Equation 29, it is assumed that inflow into A_i is zero. $A_{i,j}$ is then given by

$$A_{i,j} = A_{i,0}(1 - F)^j$$

A special situation occurs in the zero boxcar. The contents of this boxcar are entirely transferred to the first one, so that after the shift,

$$A_{0,j} = 0.$$

The delay in the fractional boxcar train The first fractional shift does not occur at time zero, but only when g' equals $F\gamma$. When the development rate, v , is constant, this occurs at time $F\gamma/v$, or at time $F\tau$. The expression for the average residence time, $\bar{\tau}$, is:

$$\bar{\tau} = \frac{1}{A_0} \sum_{j=1}^{\infty} j F \tau A_0 (1 - F)^{j-1} F \quad \text{Equation 32}$$

time quantity transferred

This expression can be evaluated using the general expression for the sum of the series

$$\sum_{j=1}^{\infty} j r^{j-1} = \frac{1}{(1 - r)^2} \quad 0 < r < 1$$

In this equation, r can be replaced by $1 - F$, and Equation 32 then yields

$$\bar{\tau} = \tau$$

This result shows that the delay per boxcar is independent of the value of F . Also, the total delay T_{total} of the boxcar train is independent of F , and equal to $N\tau$.

The variance in the fractional boxcar train The variance can be evaluated from

$$\sigma^2 = \frac{1}{A_0} \sum_{j=1}^{\infty} (jF\tau - \tau)^2 A_0(1-F)^{j-1}F \quad \text{Equation 33}$$

deviation quantity transferred

By using the sum of the series given above, and also the following one:

$$\sum_{j=1}^{\infty} j^2 r^{j-1} = \frac{1+r}{(1-r)^3} \quad 0 < r < 1$$

we find that Equation 33 can be simplified to:

$$\sigma^2 = \tau^2(1-F)$$

This result shows that the variance is linearly related to the value of the fraction F. This variance occurs in each boxcar, so that the total variance of the whole boxcar train is

$$\sigma_{\text{total}}^2 = N\tau^2(1-F) \quad \text{Equation 34}$$

2.2.8 Implementation of the boxcar train in CSMP

The fixed boxcar train (see Figure 18) First, the three types of boxcar train will be applied in a simple example. There will be 5 boxcars with initial content zero:

A = INTGRL(AI, RA, 5)
state initial rate number of
state integrals

In the rest of the program, A and RA can be referred to as indexed variables, just as in FORTRAN: A(I) stands for element I of the array A. The array AI (initial values) is set at zero. It is convenient to use DO loops to calculate rates and concentrations:

```
DO I = 1,5
    C(I) = A(I)/GAMMA (see Equation 28)
ENDDO
```

Here, GAMMA is the name for the mathematical symbol γ , the width of a boxcar in development units, and is defined as $1/N$. This implies that the full range of development has the numerical value of unity. This is an arbitrary choice which could have been 100 or any other figure. In the case of another value for the full range of development, the width of the boxcars is adapted proportionally.

The rate of flow from boxcar I to boxcar I + 1 is given by the rate of development, v (DEV), multiplied by the concentration C(I):

$$\text{FLOW}(I + 1) = \text{DEV} * C(I) \quad \text{(see Equation 27)}$$

An inflow pulse of total size UNITY occurring at time PTIME can be obtained by:

$$\text{INFL} = \text{IMPULS}(\text{PTIME}, \text{FINTIM}) * \text{UNITY} / \text{DELT}$$
$$\text{PARAM PTIME} = 0., \text{UNITY} = 1.$$

The rate of development (DEV R), is also integrated to yield the physiological time, G, which can be considered to be the state of development of an immortal individual born at time zero:

$$G = \text{INTGRL}(0., \text{DEV R})$$

It should be noted that G always increases.

The inflow into the boxcar train, generated somewhere else, is used here.

$$\text{FLOW}(1) = \text{INFL}$$

and the outflow is made equal to FLOW(N + 1):

$$\text{OUTFL} = \text{FLOW}(N + 1)$$

The net flow of a boxcar is given by:

$$\text{NETFLO}(I) = \text{FLOW}(I) - \text{FLOW}(I + 1)$$

and, since there is no mortality so far,

$$\text{RA}(I) = \text{NETFLO}(I)$$

The outflow can be collected in a separate integral

$$\text{AOUT} = \text{INTGRL}(0., \text{OUTFL})$$

In this example the inflow was kept at zero, except for a single pulse at time zero with height UNITY/DELT. This discontinuous behaviour of the inflow requires the use of the rectangular integration method:

METHOD RECT

The following optional statements for monitoring purposes would normally not be included in a model, but study of their formulation and behaviour improves the understanding.

For this simple situation, the average delay period (ADP) can also be calculated numerically:

$$\text{ADP} = \text{INTGRL}(0., (\text{TIME} - \text{PTIME}) * \text{OUTFL}) / \text{UNITY}$$

The expression for the variance (VAR) is given by:

$$\text{VAR} = \text{INTGRL}(0., (\text{TIME} - \text{PTIME} - \text{ADPG}) ** 2 * \text{OUTFL}) / \text{UNITY}$$

ADPG must be a constant and, in fact, be equal to the final value of ADP at time FINTIM. Therefore, two runs are required, the first one to find ADP and the second one to find VAR. Fortunately, in normal simulations, there is no necessity

to calculate both ADP and VAR. Here, it is done simply to check our model and to compare it with the theoretical results. The timing is defined in a TIMER statement:

```
TIMER FINTIM = 1000., PRDEL = 100., DELT = 1.
```

Here, we require the variables AOUT, ATOT, A(1 – 5), ADP and VAR as printed output on intervals PRDEL. The variables ATOT and BALANC are used only to check the balances. Although they may seem unnecessary, in more complicated models these balance variables are extremely useful to detect omitted or twice-defined flows.

The development rate (DEVR) is given in a PARAMeter statement as 0.005, and N as 5. The variables N and I are declared fixed, and for the arrays NETFLO, FLOW and C, ample space is reserved by a STORAGE statement. For variables in the array integral this reservation is done by default.

Exercise 27

Use this program to generate the curves of Figure 16 for $N = 1, 2, 5$ and 10.

Exercise 28.

Run the simulation model of Figure 18. Compare the simulated (mimicked) delay period (ADP) and its variance (VAR) with the values calculated arithmetically (T_{total} respectively σ_{total}^2). When are the simulated values significant?

The escalator boxcar train (Figure 19) Most statements are the same as for the fixed boxcar train, so here only the differences will be mentioned. The criterion for renumbering (shifting) is when the cyclic development stage, g' , (GCYCL) has reached the value GAMMA (the width of a boxcar):

```
IF (GCYCL.GE.GAMMA) CALL SHIFT(N, GAMMA, GCYCL, A, A0)
```

The subroutine 'SHIFT' is explained at the end of this Subsection. The use of the IF statement requires a preceding NOSORT label. The shift is formulated in a FORTRAN subroutine with the necessary arguments N (number of boxcars), and the names of the treated integrals. Here, the zero boxcar (A0) appears separately because, unfortunately, the indexing of array integrals begins with one and not with zero. In the main program, A0 must also be formulated separately:

```
A0 = INTGRL(0., RA0)
```

and

```
RA0 = INFL
```

Figure 18. Listing of a program, including the fixed boxcar train.

```
TITLE FIXED BOXCARTRAIN
STORAGE FLOW(6), NETFLO(5), C(5)
FIXED N,I

INITIAL

TABLE AI(1-5)=5*0.
PARAM DEVR=0.005, N=5
GAMMA = 1./N
PARAM PTIME=0.,UNITY=1.

DYNAMIC
NOSORT

*Calculation of the states
G =INTGRL(0.,DEVR)
A =INTGRL(AI,RA,5)
AOUT=INTGRL(0.,OUTFL)

*Calculation of the rates
INFLF =IMPULS(PTIME,FINTIM)
INFL =UNITY*INFLF/DELT
FLOW(1)=INFL
DO I=1,N
    C(I)=A(I)/GAMMA
    FLOW(I+1)=DEVR * C(I)
    NETFLO(I)=FLOW(I) - FLOW(I+1)
*   no mortality
    RA(I) =NETFLO(I)
ENDDO
OUTFL =FLOW(N+1)

* Balance should be zero
ATOT=0.
DO I=1,N
    ATOT=ATOT + A(I)
ENDDO
BALANC=ATOT + AOUT -INTGRL(0.,INFL)

*Optional statements for study and checking purposes:
ADPG=1./DEVR
ADP =INTGRL(0.,(TIME-PTIME)*OUTFL)/ UNITY
VAR =INTGRL(0.,(TIME-PTIME-ADPG)**2 * OUTFL)/ UNITY
S =SQRT(VAR)

TIMER FINTIM=1000.,PRDEL=100.,DELT=1.
METHOD RECT
PRINT AOUT,ATOT,A(1-5),ADP,VAR,S,BALANC

END
STOP
ENDJOB
```

Figure 19. Listing of a program, including the escalator boxcar train.

```
TITLE ESCALATOR BOXCARTRAIN
STORAGE C(5)
FIXED N,I
```

```
INITIAL
```

```
TABLE AI(1-5)=5*0.
PARAM DEVR=0.005, N=5
GAMMA =1./N
*The cyclic development starts halfway
GCYCLI=0.5*GAMMA
PARAM PTIME=0.,UNITY=1.
```

```
DYNAMIC
NOSORT
```

```
*Calculation of the states
GCYCL =INTGRL(GCYCLI,DEVR)
G      =INTGRL(0.,DEVR)
AO     =INTGRL(0.,RA0)
A      =INTGRL(AI,RA,5)
AOUT   =INTGRL(0.,OUTFL)
```

```
IF(GCYCL.GE.GAMMA) CALL SHIFT(N,GAMMA,GCYCL,A,A0)
```

```
*Calculations of the rates
INFLF  =IMPULS(PTIME,FINTIM)
INFL   =INFLF*UNITY/DELT
RA0    =INFL
```

```
DO I=1,N-1
*   no mortality
   RA(I)=0.
```

```
ENDDO
C(N)   =A(N)/(GAMMA-GCYCL)
```

```
*To prevent a negative value of A(N), the AMIN1-function is used
OUTFL  =AMIN1(DEVR * C(N),A(N)/DELT)
RA(N)  =-OUTFL
```

```
* Balance should be zero
```

```
ATOT   =A0
```

```
DO I=1,N
   ATOT=ATOT + A(I).
```

```
ENDDO
```

```
BALANC=ATOT + AOUT - INTGRL(0.,INFL)
```

*Optional statements for study and checking purposes:

ADPG=1./DEV

ADP =INTGRL(0.,(TIME-PTIME)*OUTFL) / UNITY

VAR =INTGRL(0.,(TIME-PTIME-ADPG)**2 *OUTFL) / UNITY

S =SQRT(VAR)

TIMER FINTIM=200.,PRDEL=20.,DELT=1.

METHOD RECT

PRINT A0,A(1-5),AOUT,ATOT,BALANC,G,GCYCL,ADP,VAR,S

END

STOP

SUBROUTINE SHIFT(N,GAMMA,GCYCL,A,A0)

DIMENSION A(N)

DO I =N,2,-1

A(I)=A(I-1)

ENDDO

A(1) =A0

A0 =0.

GCYCL=GCYCL-GAMMA

RETURN

END

ENDJOB

Since the flows between boxcars are zero (by definition in the escalator boxcar train), the names FLOW and NETFLO are not required. Only the outflow from the last boxcar must be defined (see Subsection 2.2.5):

$OUTFL = AMIN1(DEV * C(N), A(N)/DELT)$

and

$RA(N) = -OUTFL$

The other rates of change in the boxcars are zero (no mortality yet):

DO I = 1,N - 1

RA(I) = 0

ENDDO

which can be stated in the INITIAL segment. The concentration C(N) of the last boxcar must be calculated in a different way than in the fixed boxcar train:

$C(N) = A(N)/(GAMMA - GCYCL)$

The cyclic development stage, GCYCL, is formulated in exactly the same way as G:

$GCYCL = INTGRL(GCYCLI, DEV)$

It is not equal to G, however, because GCYCL is modified in the subroutine SHIFT.

The subroutine 'SHIFT' This subroutine definition is placed between the CSMP labels STOP and ENDJOB.

The list of arguments transfers the values from the main program to the subroutine and vice versa. A separate DIMENSION declaration of A is necessary in the subroutine. With ample memory space available, over-dimensioning is convenient. The DO loop must be a backward one, because a forward loop would fill all array elements with the first one.

```
DO I = N, 2, -1
  A(I) = A(I - 1)
ENDDO
A(1) = A0
A0 = 0.
GCYCL = GCYCL - GAMMA
```

It is important that GCYCL is decreased by GAMMA, and not reset to zero. The shift is triggered when g' reaches γ , but this does not necessarily occur at an exact multiple of DELT. The excess value of g' above γ before the shift must be retained.

The escalator boxcar train, applied to a demographic problem The best method for solving demographic problems is the escalator boxcar train, because age, which is used as a characteristic, does not disperse. To illustrate its use, the same example will be given for the growth of the Dutch population, described by de Wit & Goudriaan (1978). For reasons of clarity, only the female proportion of the population is simulated, the male proportion being taken for granted. The ratio of boys to girls at birth (FRBOY), is used to calculate the fraction of girls (FRGIRL). The age dependence relating to relative death rate and relative birth rate is given in Figure 20. The corresponding fraction of survival (FS) is found by simulating a single cohort from birth onwards. Mathematically, the relative death rate (RDR) and the fraction survival (FS) are related by:

$$\text{RDR} = -(\text{d}(\text{FS})/\text{d}A)/\text{FS}$$

where A stands for age.

The listing of the CSMP program used is given in Figure 21. Data concerning the initial age distribution of the population are supplied. This is done by a TABLE specifying the contents of the twenty 5-year classes of the population array AI. Then, two FUNCTIONS with a list of coordinate points of the relationship between relative death and birth rates and age are supplied. In the INITIAL segment some computations are done for the discretization of age and development scale. This is necessary before the actual simulation in the DYNAMIC segment occurs. The simulation itself requires computation of the rates

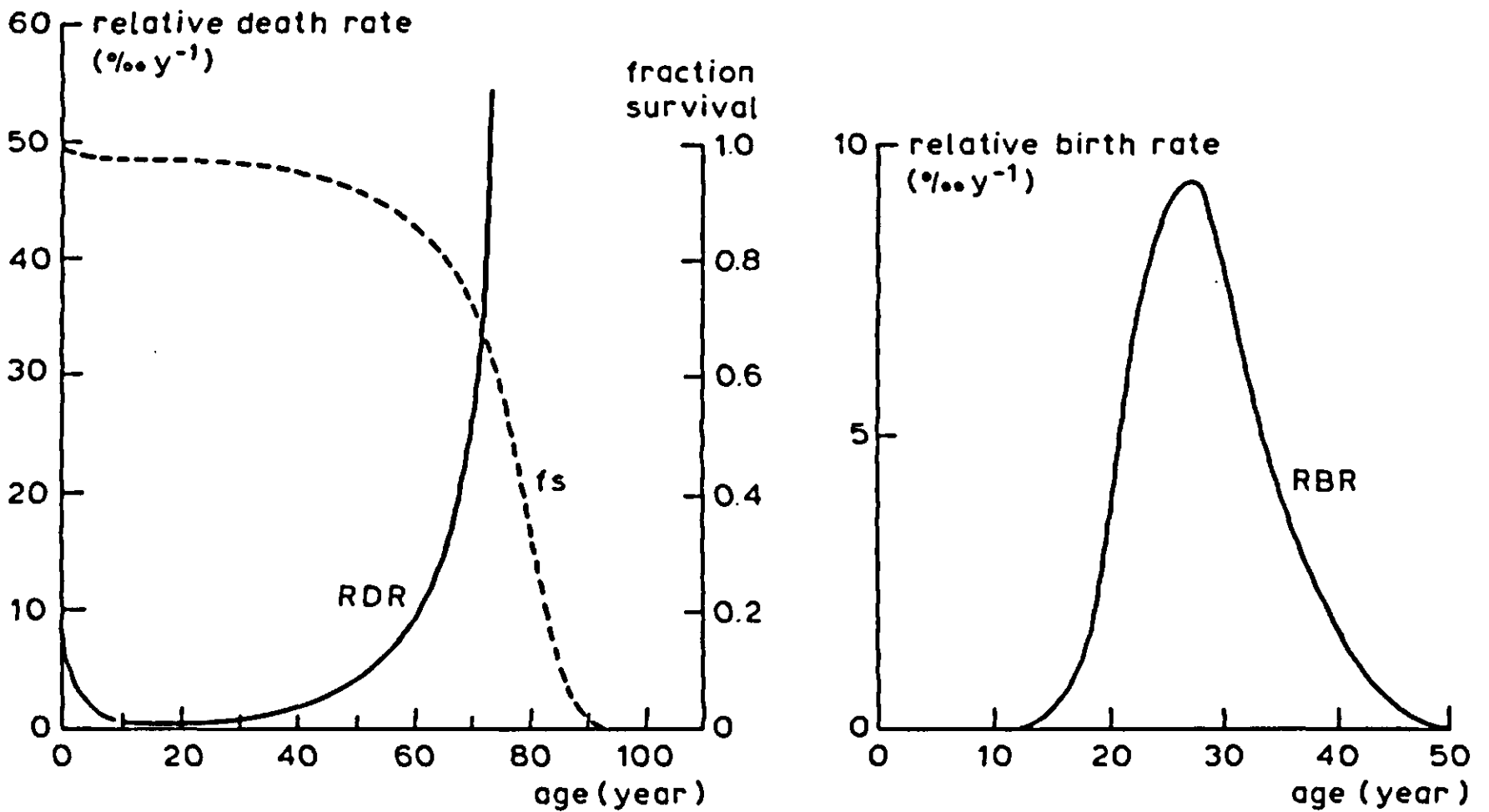


Figure 20. The age dependence of relative death rate (RDR) and of relative birth rate (RBR). The fraction survival (fs, dashed line) is a function of RDR.

Figure 21. Listing of the program of the model simulating the growth of the Netherlands population.

```

TITLE GROWTH OF THE NETHERLANDS POPULATION
STORAGE AGE(20),MORR(20),FRACA(20)
FIXED I,N

INITIAL
NOSORT
*   Relative death rate, in promille per year, as a function of age
    FUNCTION RMRTB= 0.,10., 2.5,4., 5.,1.8, 7.5,0.8, 10.,0.5, ...
                  15.,0.3, 20.,0.3, 30.,0.6, 40.,1.6, 50.,4.9, ...
                  60.,8.5, 65.,14., 70.,25., 75.,55., 82.5,180., ...
                  87.5,380., 92.5,760., 97.5,900., 105.,900.
*   Relative birth rate per year, as a function of age
    FUNCTION RBRTB= 0.,0., 12.5,0., 17.5,.02, 22.5,.137, 25.,.166,...
                  27.5,.188, 30.,.166, 32.5,.113, 37.5,.055, ...
                  42.5,.016, 47.5,.002, 50.,0., 105.,0.
*   Fraction young born boys
    PARAM FRBOY=0.512
*   100 years of age (AGETOT=ADP) is covered in 20 classes (N)
    PARAM AGETOT=100.,N=20
*   Residence time in one age class
    TC =AGETOT/N
*   Development rate is standardized and constant
    DEVR =1./AGETOT
*   Development width covered by one ageclass
    GAMMA =1./N
*   The fraction girl of the young borns
    FRGIRL=1.-FRBOY
* Calculation of the initial amounts

```

```

* Initial contents of ageclasses of 5 years wide, expressed in thousands
TABLE AI(1-20)=582.,587.,553.,543.,554.,420.,380.,381.,378., ...
                376.,330.,323.,298.,226.,226.,150.,70.,25.,13.,0.
* Initialization of integrals
ATOTI=0.
DO I=1,N
    AI(I)=AI(I)*1000.
    A(I) =AI(I)
    ATOTI=ATOTI + AI(I)
ENDDO
AO =0.
G =0.
GCYCL=0.

DYNAMIC
NOSORT
* Calculation of the states
* Development
G =INTGRL(0.,DEVR)
GCYCL =INTGRL(0.,DEVR)
* Calculation of the number of each boxcar
AO =INTGRL(0.,RA0)
A =INTGRL(AI,RA,20)
AOUT =INTGRL(0.,OUTFL)
* When GCYCL exceeds GAMMA, the shift is applied.
* In this situation, this is after every 5 years
PUSH =IMPULS(5.,5.)
IF(PUSH.EQ.1.) CALL SHIFT(N,GAMMA,GCYCL,A,AO)
* Calculation of the rates
* The total birth rate of girls is first set to zero
TBR =0.
**The zero's boxcar
* The age of the centre
AGE0 = 0.5 * GCYCL*AGETOT
* The mortality rate
MORRO =AO * 0.001*AFGEN(RMRTB,AGE0)
TMORT =MORRO
**The 1 - (N-1)'s boxcar
DO I=1,N-1
* The age of the centre of each boxcar
AGE(I) =TC*(I-0.5)+GCYCL*AGETOT
* Mortality rate of each class
MORR(I)=A(I)*0.001*AFGEN(RMRTB,AGE(I))
* Total mortality
TMORT =TMORT + MORR(I)
* The 1 - (N-1)'s class only change by death
RA(I) =-MORR(I)
* Total birth rate of girls
TBR =TBR + A(I) * AFGEN(RBRTB,AGE(I))*FRGIRL
ENDDO
**The N's boxcar
AGE(N) =TC*(N-0.5)+0.5*GCYCL*AGETOT
RMRN =0.001*AFGEN(RMRTB,AGE(N))
MORR(N)=A(N)*RMRN
TMORT =TMORT + MORR(N)
* The zero's class increases by birth, and decreases by death
RA0 =TBR - MORRO
* The N's boxcar decreases by death and by an outflow of people

```

```

* older than 100 years old.
  CN    =A(N)/(GAMMA-GCYCL)
  OUTFL =AMIN1(DEVR*CN*(1.-RMRN),A(N)/DELT)
  RA(N) =-OUTFL - MORR(N)
* The balance should be zero:
  ATOT  =A0
  DO I=1,N
    ATOT  =ATOT+A(I)
  ENDDO
  TOTMOR=INTGRL(0.,TMORT)
  TOTBIR=INTGRL(0.,TBR)
  BALANC=ATOT +TOTMOR + AOUT - ATOTI - TOTBIR
* Calculation of the age-distribution
  FRACAO=A0/ATOT
  DO I=1,N
    FRACA(I)=A(I)/ATOT
  ENDDO
* Time is expressed in years
  TIMER FINTIM=1000.,DELT=1.,PRDEL=100.
  PRINT A0,A(1-20),AOUT,ATOT,FRACAO,FRACA(1-20),TBR, TMORT, BALANC
  METHOD RECT
END
STOP
SUBROUTINE SHIFT(N,GAMMA,GCYCL,A,A0)
DIMENSION A(N)
DO I=N,2,-1
  A(I)=A(I-1)
ENDDO
A(1) =A0
A0   =0.
GCYCL=GCYCL-GAMMA
RETURN
END
ENDJOB

```

of change and, of course, the integration of these rates, which is done by the INTGRL statement. Also, whole population totals are computed by summation over all age classes in a regular FORTRAN DO loop. The data supplied for the FUNCTIONS are read by an AFGEN statement.

Exercise 29

Find FS (Figure 20) by simulation. Make the birth rate constant, for instance 1000 per year, and after 100 years the age distribution will have the same shape as the fraction FS.

Exercise 30

In the normal simulation, with the birth rate coupled to the number of fertile women, the population size will not be constant. After a long enough period of

simulation, exponential growth will result, with a corresponding age distribution and relative growth rate. To find these, run the model, as given here, for 1000 years. Compare the age distribution with FS found in Exercise 29.

The fractional boxcar train (see Figure 22) This boxcar train can be used when the relative dispersion of through-flow is known to vary during simulation, so both the desired delay and dispersion must be computed in the DYNAMIC segment of the main program. The rate of development, v or DEVR, often has a simpler relation with environmental conditions than the delay (germination period, longevity, etc.) itself:

$$\text{DEVR} = \text{AFGEN}(\text{DEVT}, \text{TEMP})$$

In this example, the rate of development is a function of temperature. The shape of the function must be specified in a separate list of paired numbers with the name DEVT. In a similar way, the relative dispersion RD ($\sigma_{\text{total}}/T_{\text{total}}$) is a function of temperature:

$$\text{RD} = \text{AFGEN}(\text{RDT}, \text{TEMP})$$

The procedure of the fractional boxcar train is described in a subroutine called 'BOXCAR' which can be used as a separate module. In the main program, this subroutine is called:

```
A0,A,ATOT,MORFL,OUTFL,GAMMA,GCYCL = ...  
BOXCAR(1,AI,DEVR,RD,RMR,INFL,N,DELT,TIME)
```

Inputs for this subroutine are: a number which serves to identify the boxcar train in the event of a computing error, the initial amount in the boxcars of the train ($\text{AI}(1 - \text{N})$), the development rate (DEVR), the relative dispersion (RD), the relative mortality rate (RMR), the inflow into the zero boxcar (INFL), the number of boxcars in the train (N), DELT and TIME, respectively. These inputs must be given or calculated in the main program. Time is available by default. Outputs of this subroutine are the amount in the zero boxcar (A0), the amount in the other boxcars ($\text{A}(1 - \text{N})$), the total amount in the boxcar train (ATOT), the total mortality rate in the boxcar train (MORFL), the outflow of the last (N^{th}) boxcar (OUTFL), the development width (GAMMA) and the cyclic development stage (GCYCL). In the main program, memory storage should be reserved for two array variables AI and A, e.g. when N equals 10:

```
STORAGE AI(10), A(10)
```

N, the number of boxcars, should be declared integer

```
FIXED N
```

In the initial segment of the main program, the initial amount in the boxcar train and the number of boxcars should be given:

TABLE AI(1 - 10) =
PARAM N = 10

In the subroutine 'BOXCAR', the boxcar train is initialized by calling subroutine 'BOXINI'. In this subroutine, A0 and GCYCL are set to zero, GAMMA is computed as $1/N$ and $A(1 - N)$ is initialized.

The fraction F for the fractional boxcar train is calculated by Equation 34, written with F on the left:

$$F = 1 - N * RD * RD$$

When this computed value of F is used, the fractional boxcar train will produce the desired dispersion.

Although this method is flexible, it cannot be stretched beyond its limits. An undue imbalance between the number of boxcars N and the desired RD will be revealed in nonsense values of F. Theoretically, it is immediately clear that F must lie between zero and unity. The upper end of this range is exceeded if the number of boxcars N is too small for the low RD that we wish to simulate. To select an appropriate value for N, it should be kept in mind that a minimum amount of dispersion cannot be avoided. Even when F is set at unity, some dispersion remains within the boxcar width. Usually this amount can be neglected.

The lower end of the range of F is zero, but a closer inspection indicates that F must also be larger than the fraction that would normally be transferred in each integration interval in the fixed boxcar train: $DEL T * DEVR / GAMMA$. If F is smaller than this value, the chosen number of boxcars N was too high. N must be smaller than 1 divided by the maximally occurring value of RD squared. About three-quarters of this maximum number is usually sufficient. If this does not solve the problems, it could mean that DELT is too large. It is good practice to include finish conditions for these sorts of criteria:

```
IF (DEL T.GT.(F * GAMMA/DEVR)) THEN  
  CALL EXIT  
ENDIF
```

Both time-interval of integration and residence-time in the boxcars of a boxcar train characterize the degree of temporal resolution required in the model. Therefore, there is little point in choosing Δt much smaller than the residence time γ/v . In this case, the general rule that Δt must not exceed one-tenth of the time coefficient of the fastest model component can be relaxed a little. The requirement here is less stringent, thanks to the negative feedback within the boxcar train: a numerical error in the rate of transition only affects the distribution among adjacent boxcars and has hardly any effect on removal from the boxcar train as a whole. The conclusion is that Δt should not exceed $F\gamma/v$, but may well be greater than $1/10$ of γ/v .

If the program is aborted on account of one of these finish conditions, the programmer should first search for bugs in the data set such as AFGEN functions, or in other parts of the program before trying to repair the failure by adapting of N or DELT. Now that F has been adequately defined, it is used in the trigger for the shift:

```
IF (GCYCL.GE.F*GAMMA) CALL SHIFT...  
  (N, F, A0, A, GAMMA, GCYCL)
```

In the subroutine SHIFT, the list of arguments is repeated, and the array declaration follows:

```
DIMENSION A(N)  
A(N) = A(N) + A(N-1) * F  
DO I = N - 1, 2, -1  
  A(I) = A(I) * (1 - F) + A(I-1) * F  
ENDDO  
A(1) = A(1) * (1 - F) + A0  
A0 = 0.  
GCYCL = GCYCL - F * GAMMA
```

These lines suffice to implement the theory of Subsection 2.2.6. There are no further changes in comparison to the escalator boxcar train.

2.2.9 *A practical application using the fractional boxcar train*

The fractional boxcar train can be used to simulate the population development of insects. This will be illustrated with an example of an orchard tortricid moth *Pandemis heparana* (DENN. et SCHIFF.), which is an important pest in European apple orchards. Control of these insects mainly relies on the use of broad-spectrum insecticides, but since these also kill beneficial insects, research has been directed towards more specific insect growth-regulators. These prevent metamorphosis but are only effective if applied at the right time: at emergence of the last-instar larvae. The best application time can be well predicted using a simulation model of population development.

P. heparana usually has one generation per year. Adult female moths deposit their eggs in August. Second or third larval instars hibernate until the end of March when they become active; the sixth larval instar pupates in June. Adult moths are, therefore, found from June to August.

The model presented in Figure 22 is a simplified version of that described by de Reede & de Wilde (1986), which simulates the post-hibernation phenology of *P. heparana* (in 1982 in Wageningen, the Netherlands). Each development stage (diapause-stage, 3-5th stage larvae, 6th stage male and female larvae, and male and female pupae) is described by a fractional boxcar train, which mimics the mean delay and temporal dispersion. Experiments showed temperature to be the only important determinant of the development rate. Temperature is computed as

Figure 22. Listing of a program, including the fractional boxcar train.

TITLE DEVELOPMENT PANDEMIS HEPARANA 1982

STORAGE DIAINI(4) , DIA(4) , ...
L3INI(10) , L3(10) , ...
L4INI(8) , L4(8) , ...
L5INI(3) , L5(3) , ...
ML6INI(10) , ML6(10) , ...
FL6INI(4) , FL6(4) , ...
MPINI(10) , MP(10) , ...
FPINI(10) , FP(10)

INITIAL

*Initial numbers in boxcartrains

TABLE DIAINI(1-4) = 4*25.
TABLE L3INI(1-10)=10* 0.
TABLE L4INI(1-8) = 8* 0.
TABLE L5INI(1-3) = 3* 0.
TABLE ML6INI(1-10)=10* 0.
TABLE FL6INI(1-4) = 4* 0.
TABLE MPINI(1-10)=10* 0.
TABLE FPINI(1-10)=10* 0.

*Total initial amount of diapause larvae
TINDIA=100.

*Fraction male
PARAM SEXR=0.5

*Fraction DIA3/DIA2
PARAM G=0.7

PI=ATAN(1.)*4.

DYNAMIC

*Temperature

TEMP =AVTEMP + AMPTMP*(-COS(2.*PI*TIME))
AVTEMP=0.5 * (MAXT+MINT)
AMPTMP=0.5 * (MAXT-MINT)
MAXT =AFGEN(MXTT,DAY)
MINT =AFGEN(MNTT,DAY)

DAY =STDAY + TIME
PARAM STDAY= 32.

*Relative Mortality Rate

PARAMETER RMRL3 =0., RMRL4=0., RMRL5=0., RMRML6=0., ...
RMRFL6=0., RMRDIA=0., RMRMP=0., RMRFP =0.

*Development Rate

DRDIA =AFGEN(DRDIAT,TEMP)
DRL3 =AFGEN(DRL3T ,TEMP)
DRL4 =AFGEN(DRL4T ,TEMP)
DRL5 =AFGEN(DRL5T ,TEMP)
DRML6 =AFGEN(DRML6T,TEMP)
DRFL6 =AFGEN(DRFL6T,TEMP)
DRMP =AFGEN(DRMPT ,TEMP)
DRFP =AFGEN(DRFPT ,TEMP)

*Relative Dispersion

RDDIA =AFGEN(RDDIAT,TEMP)
RDL3 =AFGEN(RDL3T ,TEMP)
RDL4 =AFGEN(RDL4T ,TEMP)
RDL5 =AFGEN(RDL5T ,TEMP)
RDML6 =AFGEN(RDML6T,TEMP)

RDFL6 =AFGEN(RDFL6T,TEMP)
RDMP =AFGEN(RDMPT ,TEMP)
RDFP =AFGEN(RDFPT ,TEMP)

*Subsequent boxcar calls must be done in a nosort section

NOSORT

PIDIA=0.

DIA0,DIA,DIATOT,MRDIA,PDDIA,GAMMA1,GCYCL1=...
BOXCAR(1,DIAINI,DRDIA,RDDIA,RMRDIA,PIDIA , 4,DELT,TIME)

PIL3=(1.-G)*PDDIA
L30, L3, L3TOT, MRL3, PDL3, GAMMA2,GCYCL2=...
BOXCAR(2, L3INI, DRL3, RDL3, RMRL3, PIL3 ,10,DELT,TIME)

PIL4=G *PDDIA + PDL3
L40, L4, L4TOT, MRL4, PDL4, GAMMA3,GCYCL3=...
BOXCAR(3, L4INI, DRL4, RDL4, RMRL4, PIL4 , 8,DELT,TIME)

PIL5=PDL4
L50, L5, L5TOT, MRL5, PDL5, GAMMA4,GCYCL4=...
BOXCAR(4, L5INI, DRL5, RDL5, RMRL5, PIL5 , 3,DELT,TIME)

PIML6=SEXR * PDL5
ML60,ML6,ML6TOT,MRML6,PDML6,GAMMA5,GCYCL5=...
BOXCAR(5,ML6INI,DRML6,RDML6,RMRML6,PIML6,10,DELT,TIME)

PIFL6=(1.-SEXR) * PDL5
FL60,FL6,FL6TOT,MRFL6,PDFL6,GAMMA6,GCYCL6=...
BOXCAR(6,FL6INI,DRFL6,RDFL6,RMRFL6,PIFL6 ,4,DELT,TIME)

PIMP=PDML6
MPO, MP, MPTOT, MRMP, PDMP, GAMMA7,GCYCL7=...
BOXCAR(7, MPINI, DRMP, RDMP, RMRMP, PIMP ,10,DELT,TIME)

PIFP=PDFL6
FPO, FP, FPTOT, MRFP, PDFP, GAMMA8,GCYCL8=...
BOXCAR(8, FPINI, DRFP, RDFP, RMRFP, PIFP ,10,DELT,TIME)

SORT

CUML3 =INTGRL(0.,PIL3)
CUML4 =INTGRL(0.,PIL4)
CUML5 =INTGRL(0.,PIL5)
CUMML6=INTGRL(0.,PIML6)
CUMFL6=INTGRL(0.,PIFL6)
CUMMP =INTGRL(0.,PIMP)
CUMFP =INTGRL(0.,PIFP)
CUMMM =INTGRL(0.,PDMP)
CUMFM =INTGRL(0.,PDFP)

CUPL3 =100.*CUML3/(TINDIA*(1.-G))
CUPL4 =100.*CUML4/TINDIA
CUPL5 =100.*CUML5/TINDIA
CUPML6=100.*CUMML6/(TINDIA*SEXR)
CUPFL6=100.*CUMFL6/(TINDIA*(1.-SEXR))
CUPMP =100.*CUMMP/(TINDIA*SEXR)
CUPFP =100.*CUMFP/(TINDIA*(1.-SEXR))
CUPMM =100.*CUMMM/(TINDIA*SEXR)
CUPFM =100.*CUMFM/(TINDIA*(1.-SEXR))

* Balance should be zero:
 TMORR=MRDIA + MRL3 + MRL4 + MRL5 + MRML6 + MRFL6 + MRMP + MRFP
 ATOT =DIATOT+ L3TOT+L4TOT +L5TOT + ML6TOT+ FL6TOT+ MPTOT+FPTOT ...
 + CUMMM + CUMFM
 BALANC=ATOT-TINDIA+INTGRL(0.,TMORR-PIDIA)

PRINT DAY,DIATOT,CUPL3,CUPL4,CUPL5,CUPML6,CUPFL6,...
 CUPMP,CUPFP,CUPMM,CUPFM,BALANC
 TIMER FINTIM=220.,DELT=0.0417,PRDEL=2.
 METHOD RECT

*Development Rate

FUNCTION DRDIAT = -10.,0.0000, 6.0,0.0000, 11.,0.0181, 13.,0.0251,...
 16.,0.0412, 19.,0.0621, 22.,0.0831, 25.,0.1015,...
 35.,0.1015
 FUNCTION DRL3T = -10.,0.0000, 9.4,0.0000, 16.,0.1093, 25.,0.2585,...
 35.,0.2585
 FUNCTION DRL4T = -10.,0.0000, 8.0,0.0000, 16.,0.1155, 25.,0.2460,...
 35.,0.2460
 FUNCTION DRL5T = -10.,0.0000, 7.2,0.0000, 16.,0.1088, 25.,0.2204,...
 35.,0.2204
 FUNCTION DRML6T = -10.,0.0000, 6.3,0.0000, 16.,0.0704, 25.,0.1355,...
 35.,0.1355
 FUNCTION DRFL6T = -10.,0.0000, 7.8,0.0000, 16.,0.0594, 25.,0.1246,...
 35.,0.1246
 FUNCTION DRMPT = -10.,0.0000, 8.2,0.0000, 16.,0.0551, 25.,0.1190,...
 35.,0.1190
 FUNCTION DRFPT = -10.,0.0000, 8.2,0.0000, 16.,0.0551, 25.,0.1190,...
 35.,0.1190

*Relative Dispersion

FUNCTION RDDIAT = -10.,0.00, 6.0,0.00, 11.,0.23, 13.,0.32, 16.,0.18,...
 19.,0.45, 22.,0.20, 25.,0.24, 35.,0.24
 FUNCTION RDL3T = -10.,0.00, 9.4,0.00, 13.,0.04, 16.,0.11, 19.,0.11,...
 22.,0.10, 25.,0.13, 35.,0.13
 FUNCTION RDL4T = -10.,0.00, 8.0,0.00, 13.,0.30, 16.,0.19, 19.,0.18,...
 22.,0.24, 25.,0.30, 35.,0.30
 FUNCTION RDL5T = -10.,0.00, 7.2,0.00, 11.,0.23, 13.,0.57, 16.,0.15,...
 19.,0.23, 22.,0.11, 25.,0.13, 35.,0.13
 FUNCTION RDML6T = -10.,0.00, 6.3,0.00, 11.,0.25, 13.,0.16, 16.,0.14,...
 19.,0.14, 22.,0.07, 25.,0.08, 35.,0.08
 FUNCTION RDFL6T = -10.,0.00, 7.8,0.00, 11.,0.25, 13.,0.06, 16.,0.49,...
 19.,0.10, 22.,0.13, 25.,0.16, 35.,0.16
 FUNCTION RDMPT = -10.,0.00, 8.2,0.00, 11.,0.03, 13.,0.06, 16.,0.08,...
 19.,0.06, 22.,0.22, 25.,0.26, 35.,0.26
 FUNCTION RDFPT = -10.,0.00, 8.2,0.00, 11.,0.03, 13.,0.06, 16.,0.08,...
 19.,0.06, 22.,0.22, 25.,0.26, 35.,0.26

*Maximum daily temperature

FUNCTION MXTT= 1., 7., 2., 11., 3., 11.6, 4., 11.4, 5., 9.8 , ...WAG1982
 etc. weatherdata Wageningen, 1982

*Minimum daily temperature

FUNCTION MNTT= 1., 2.1, 2., 4.5, 3., 6.4, 4., 7.4, 5., 0.2, ...WAG1982
 etc. weatherdata Wageningen, 1982

END
 STOP

```

C*****C
  SUBROUTINE BOXCAR(COUNT, AI, DEVR, RD, RMR, INFL, N, DELT, TIME,
    $              AO, A, ATOT, MORFL, OUTFL, GAMMA, GCYCL)
C*****C
C   To use this subroutine, memory storage has to be reserved for
C   the initial- and actual values of each boxcar of a particular boxcar
C   train by typing in the INITIAL-part: STORAGE AI(N), A(N)
C   in which AI and A are the names of the arrays of that boxcar train.
C   For N, the total number of boxcars in that boxcar train has to be
C   substituted. N is an integer, which has to be declared by: FIXED N
C   The initial conditions of AI can be given by means of a
C   TABLE statement: TABLE AI(1-N)=..., ..., or can be calculated in
C   a DO loop.
C   N has to be calculated as a function of the residence time and
C   its standard deviation and has to be given as a parameter in the
C   main program. For a fractional boxcar train:
C       N < minimum of 1/RD**2
C   Usually 3/4 * minimum of 1/RD**2 is taken. (In practice a value of
C   N=4 usually seems to mimick delay and dispersion very well).

  IMPLICIT REAL(A-Z)
  INTEGER      I, N, COUNT
  DIMENSION    AI(N), A(N), MORR(50)

C-----C
C   Initiation of the boxcar train                               C
C-----C
  IF (TIME.EQ.0.) CALL BOXINI(AI, N, AO, A, GAMMA, GCYCL)

C-----C
C   Calculation of fraction F                                     C
C-----C
  CALL FRACT(COUNT, DEVR, RD, N, DELT, GAMMA, F)

C-----C
C   Calculation of the rates                                     C
C-----C
  IF (TIME.EQ.0.) GO TO 10
C-----the rate of inflow (INFL) is given or calculated in the main program
C-----mortality rate (MORR) and total mortality flow (MORFL)
  MORRO = RMR * AO
  MORFL = MORRO
  DO I=1, N
    MORR(I) = RMR * A(I)
    MORFL = MORFL + MORR(I)
  ENDDO

C-----the rate of outflow (OUTFL) is calculated
C-----note the outflow is also subject to mortality
  CN = A(N) / (GAMMA - GCYCL)
  OUTFL = DEVR * CN * (1. - RMR * DELT)

C-----C
C   Calculation of the states (integrals)                       C
C-----C
C-----development
  GCYCL = GCYCL + DEVR * DELT

```

```

C-----amount in each boxcar (A), after mortality flow and
C-----inflow and outflow in respectively AO and A(N)
      AO =AO - MORRO*DELT + INFL*DELT
      DO I=1,N-1
          A(I) =A(I) - MORR(I)*DELT
      ENDDO
      A(N) =A(N) -MORR(N)*DELT - OUTFL*DELT

C-----amount in each boxcar (A), after shift (discontinuous process)
      IF(GCYCL.GE.F*GAMMA) CALL SHIFT(N,F,AO,A,GAMMA,GCYCL)

10  CONTINUE

C-----total amount in boxcar train (ATOT)
      ATOT= AO
      DO I=1,N
          ATOT =ATOT + A(I)
      ENDDO

      RETURN
      END

C*****C
      SUBROUTINE BOXINI(AI,N,AO,A,GAMMA,GCYCL)
C*****C
      IMPLICIT REAL(A-Z)
      INTEGER      I,N
      DIMENSION    AI(N),A(N)

      GCYCL =0.
      GAMMA =1./FLOAT(N)

      AO =0.
      DO I=1,N
          A(I) = AI(I)
      ENDDO

      RETURN
      END

C*****C
      SUBROUTINE FRACT(COUNT,DEVR,RD,N,DELT,GAMMA,F)
C*****C
      IMPLICIT REAL(A-Z)
      INTEGER      N,COUNT

      F = 1. - N * RD * RD

C-----DELT has to be smaller than a fraction F of the smallest time coefficient
C of one boxcar
      IF (DELT.GT.(F*GAMMA/(DEVR+1.E-10))) THEN
          WRITE (6,'(A,I2,A)') ' Delt too large for boxcar no: ',COUNT
          $           ', ' or too many boxes N: F too small '
          CALL EXIT
      ENDIF

      RETURN
      END

```

```

C*****C
  SUBROUTINE SHIFT(N,F,AO,A,GAMMA,GCYCL)
C*****C
  IMPLICIT REAL(A-Z)
  INTEGER      I,N
  DIMENSION   A(N)

  A(N) = A(N) + A(N-1)*F
  DO I=N-1,2,-1
    A(I)=A(I)*(1.-F) + A(I-1)*F
  ENDDO
  A(1)=A(1)*(1.-F) + AO
  AO = 0.

  GCYCL =GCYCL - F*GAMMA

  RETURN
  END
C-----C
ENDJOB

```

a simple sinusoidal curve through the daily maximum and minimum temperatures, which were measured in a Stevenson screen, 1.5 m high. The time step for numerical integration is one hour ($1/24 = 0.0417$ day), to allow for diurnal fluctuations in temperature. The model is started by initializing the total number of diapause larvae entering the first boxcar trains; the numbers of all other stages are set to zero. Input data are the development rates and relative dispersions of the various stages at different temperatures, the relative mortality rate, the sex ratio, the initial ratio of the numbers of L_3 and L_2 larvae in diapause, the startday and the minimum and maximum daily temperatures. For each development stage (except the adult stage), the subroutine BOXCAR is called at each time step. The inputs for this subroutine are: the initial content of each boxcar, which is an array variable (...INI); the development rate (DR...); the relative dispersion (RD...); the relative mortality rate (RMR...); the inflow into the boxcar train (PI...); the number of boxcars (N); DELT and TIME.

The outputs of the BOXCAR subroutine are: the content of the zero boxcar (...0); the content of the other boxcars, which is an array variable (e.g. L3(I) in which I is the number of the boxcar from 1 – N); the total content of the boxcar train (...TOT), which equals the sum of the contents of each boxcar (from 0 – N); the total mortality rate (MR...); the outflow of the boxcar train (PD...); the cyclic development stage (GCYCL.) and the width of the boxcar in development units (GAMMA.).

Figure 23 compares the simulation results with field sample data on L_5 , L_6 , pupae and adult moths (in which the sexes are combined). From this figure, it is clear that phenology can be simulated well, using the fractional boxcar train when the temperature fluctuates.

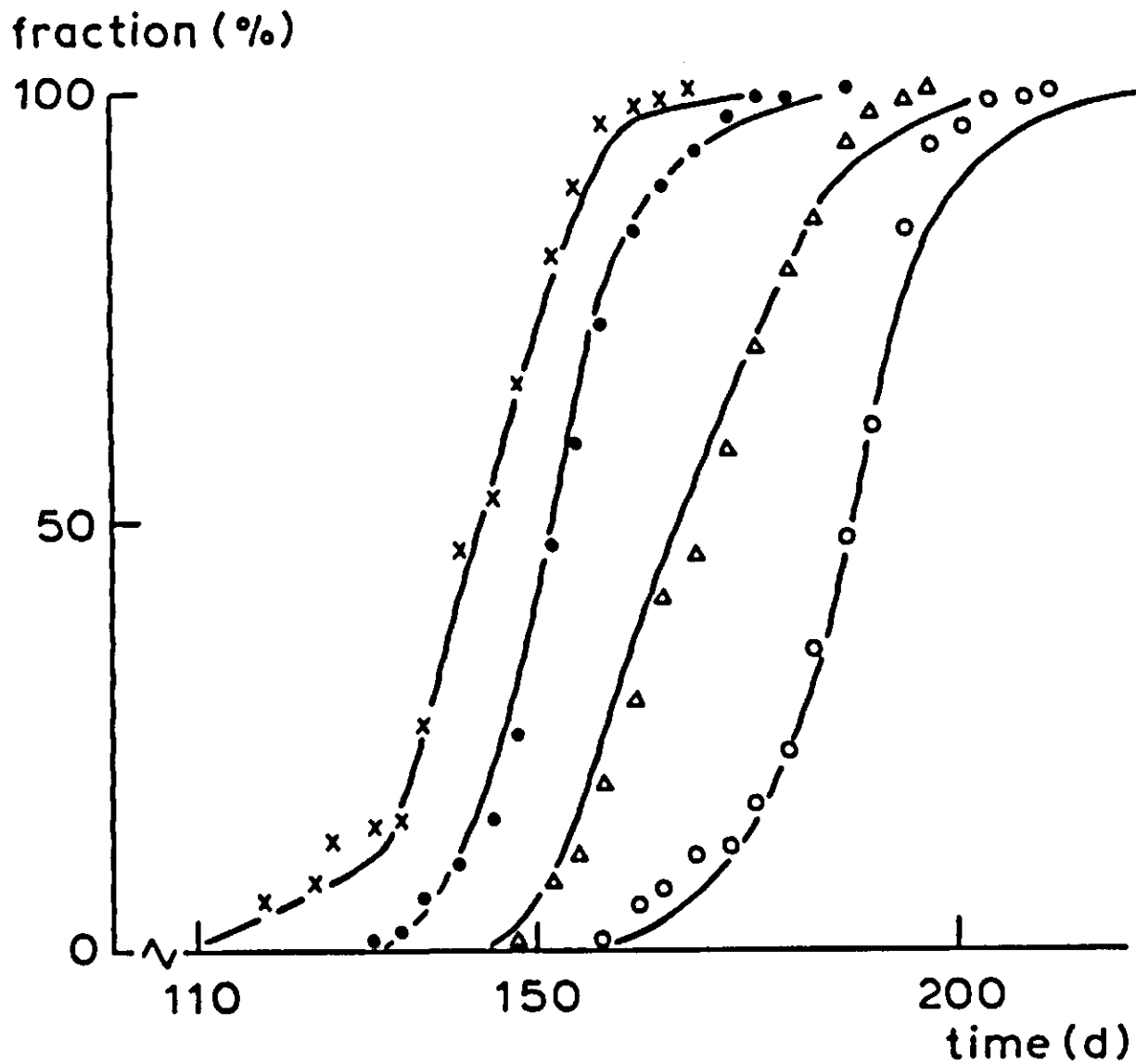


Figure 23. Simulation (—) and measured phenology of L_5 (x), L_6 (●), pupae (Δ) and adult moths (\circ) of *Pandemis heparana*.

2.2.10 Effect of the type of boxcar train on population growth

With the fractional boxcar train being intermediate, the greatest difference can be expected between the escalator boxcar train and the fixed boxcar train types. To evaluate the effect of the chosen method, the demographic example (Figures 20 and 21) was used. To establish a control, the fixed boxcar train was also run with 1-year classes, to find an accurate estimate of the equilibrium age distribution and of the relative growth rate corresponding to the used mortality and fertility distributions. This equilibrium age distribution was then used as input for both the fixed and the escalator boxcar trains with 5-year classes. The 1-year control yielded an equilibrium relative growth rate of $8.29 \cdot 10^{-3} \text{ yr}^{-1}$, which was closely approximated by the 5-year escalator boxcar train ($8.27 \cdot 10^{-3} \text{ yr}^{-1}$). The 5-year fixed boxcar train resulted in a lower simulated relative growth rate: $7.24 \cdot 10^{-3} \text{ yr}^{-1}$. The explanation for this underestimation is the numerical dispersion in the fixed boxcar train method. In a growing population, as simulated here, the younger age groups will contain many more individuals, so that the numerical dispersion will cause an apparent artificial 'ageing', slowing down the simulated population growth.

The price for the high accuracy of the escalator boxcar train is a slight irregularity in the simulated relative growth rate (RGR) following a 5-year cycle around the mean value of $8.27 \cdot 10^{-3} \text{ yr}^{-1}$, and ranging between 7.97 and 8.59

10^{-3} yr^{-1} . This irregularity is caused by the sawtooth ageing tendency of the 5-year classes.

2.2.11 Discussion

Clearly, the fixed boxcar train method is the simplest and, if possible, should be preferred for that very reason. As shown in the demographic example, it is much easier to use 1-year classes in combination with a time interval of integration of one year than to use the escalator boxcar train with 5-year classes. Simplicity of program formulation is then bought for computer time, which is often a profitable deal. In both methods, numerical dispersion is avoided.

Compelling reasons for using the more complicated boxcar train versions may be found in the desire to simulate fluctuating rates of development and dispersion. However, one must still remain aware of the unpleasant fact that dispersion is simply mimicked by a numerical tool, and that it is not really simulated from the underlying processes. This should stimulate further research so that the true reasons for the dispersion can be explained.

The merit of the methods presented here is that they enable effects of the observed characteristics of population dynamics in other situations to be evaluated, and can also serve as a tool for prognostic and management purposes.

3 POPULATION DEVELOPMENT IN TIME AND SPACE

3.1 Population models

R. Rabbinge, J.C. Zadoks and L. Bastiaans

3.1.1 Introduction

This Section presents some widely-used population models and elaborates on a numerical model that can be used to simulate epidemics in relation to time. First, a summary of models is presented, describing plant disease epidemics (van der Plank, 1963). After demonstrating the limitations of these simple models the pathosystem, powdery mildew-wheat is used to illustrate the development of a simulation model. Various important features will be added to improve the accuracy.

3.1.2 Exponential, logistic and paralogistic growth

Consider a population of size Y , in which each individual has a constant rate of reproduction, λ (in units of t^{-1}) and a constant rate (probability) of dying, μ . The rate of change in the population is then

$$\frac{dY}{dt} = (\lambda - \mu) \cdot Y \quad \text{Equation 35}$$

The size of the population at time t is thus

$$Y_t = Y_0 e^{rt} \quad \text{Equation 36}$$

where $r = \lambda - \mu$, the intrinsic per capita rate of increase, or the population's relative growth rate (RGR).

This exponential growth model assumes that the relative reproduction rate and relative mortality rate of the population are independent of the number of individuals. In many species, however, this is simply not true. For example, as the number of fungal lesions increases, the number of sites available for new lesions declines; and pest insects often compete for food. In these cases, reproduction will decline or mortality will increase with density. This is introduced into the rate equation by using a density-dependent reduction factor. The simplest assumption is that the relative growth rate declines linearly with the population size:

$$\frac{dY}{dt} = r \cdot Y \cdot (1 - Y/Y_m) \quad \text{Equation 37}$$

where the actual growth rate (dY/dt) equals the growth rate under non-limiting conditions ($r \cdot Y$) times reduction factor ($1 - Y/Y_m$).

Y_m is the maximum possible population size, r is the relative growth rate of the population under non-limiting conditions; the net result of birth and mortality. The growth of a population in time can now be described by a logistic growth equation:

$$Y_t = \frac{Y_m}{1 + K \cdot e^{-rt}} \quad \text{Equation 38}$$

Exercise 31

K (Equation 38) is a scaling factor. Express this factor in Y_m and Y_0 , the initial value of Y at time $t = 0$.

When Y_t is plotted against time, a typical S-shaped curve appears. In phytopathology, such S-shaped curves are found in epidemic diseases; logit transformation yields straight lines, representing the relation between the logit value

$$\text{logit } Y_t = \ln(Y_t / (Y_m - Y_t)) \quad \text{Equation 39}$$

and time. This logit value is a way of representing disease intensities that takes into account an upper limit for the amount of disease.

However, it is a serious mistake to think that all S-shaped curves found in phytopathology are produced by logistic growth. The logistic growth process assumes that the effect of population density on population growth is instantaneous, i.e. newly-born individuals reproduce immediately. This is true only for processes like the growth of yeast, where, when cell division is completed, the two newly formed cells can begin to divide again immediately, without a substantial lag time. For populations of plant pests and diseases, however, considerable waiting times exist: e.g. latency periods, p , in fungi, and non-reproductive periods in insects – such as the egg, larval and pupal stages in holometabola. Furthermore, the length of the reproductive period is finite: e.g. infectious periods, i , in fungi and reproductive periods in insects. Therefore, a more accurate description of the growth of a population may be expected when the relative growth rate is related to the reproductive part of the population only.

For a fungal disease – where an individual can be defined as a site with the area of a lesion – this means that the total number of infected sites (Y in Equation 37) should be replaced by the number of infectious sites:

$$\frac{dY_t}{dt} = R_c \cdot (Y_{t-p} - Y_{t-p-i}) \cdot \left(1 - \frac{Y_t}{Y_m}\right) \quad \text{Equation 40}$$

The three components of the right hand side of the equation represent:

R_c , the multiplication factor or relative growth rate;
 $Y_{t-p} - Y_{t-p-i}$, an activator representing the number of sporulating lesions;

$1 - \frac{Y_t}{Y_m}$, a correction factor to prevent double infections and to introduce an upper limit for the lesion density.

The growth model represented here is called paralogistic (Zadoks & Kampmeyer, 1977). In Table 4, the various descriptive formulae for population development in relation to time, from the exponential growth model to the paralogistic growth model, are summarized.

In several fungal diseases, the definition of an individual is rather arbitrary and, therefore, it is more convenient to work with the fraction diseased-leaf tissue. After replacing the number of infected sites by the fraction diseased-leaf tissue, we obtain the equation produced by van der Plank (1963):

$$\frac{dy_t}{dt} = R_c \cdot (y_{t-p} - y_{t-p-i}) \cdot (1 - y_t) \quad \text{Equation 41}$$

where y is the fraction diseased-plant tissue.

The differential equation for paralogistic growth (Equation 40) cannot be solved analytically, as i and p are not constant and depend on various environmental factors. Therefore, numerical integration techniques must be used. As a first step, the principle of paralogistic growth is translated into a simple relational diagram (Figure 24). The host is represented by a number of sites, vacant (NI) or infected. Infected sites are divided into three classes, latent (LAT), infectious (INF) and no longer infectious sites or removed sites (NLINF). The total number of sites is computed from the leaf area and the space needed for one lesion. For powdery mildew on wheat, with a site size of 3.5 mm^2 , each hectare of leaf area contains $10^{10}/3.5 = 2.9 \cdot 10^9$ sites (NMAXHA). Thus, a field of wheat with a leaf area index of 3 (LAI, ha ha^{-1}) contains $8.6 \cdot 10^9$ sites (NMAX). This maximum number, of course, is never reached as this would mean that all leaf area is completely covered by lesions. R is the relative growth rate of the population, and LP and IP the latency and infectious periods, respectively.

Exercise 32

Write a CSMP model for paralogistic growth, without using the subroutine BOXCAR, Section 2.2. Use one state variable per class and test the model for sensitivity to R , LP and IP .

Table 4. A family of logistic equations; differential form, integral form (when available) and rate equations.

No	Differential equations (T^{-1})	Integral equations (I)	Rate equations (T^{-1})
1	exponential growth $\frac{dx_t}{dt} = r \cdot x_t$	$x_t = x_0 \cdot e^{r \cdot t}$ $f(x_t) = \ln x_t = \ln x_0 + r \cdot t$	$r = \frac{\ln(x_2) - \ln(x_1)}{t_2 - t_1}$
2	logistic growth $\frac{dx_t}{dt} = r \cdot x_t \cdot (1 - x_t)$	$x_t = \frac{x_0 \cdot e^{r \cdot t}}{1 - x_0(1 - e^{r \cdot t})}$ $f(x_t) = \ln \frac{x_t}{1 - x_t} = r \cdot t + c = \text{logit}(x_t)$	$r = \frac{\text{logit}(x_2) - \text{logit}(x_1)}{t_2 - t_1}$
3	introduction of latency period p ($i = \infty$) $\frac{dx_t}{dt} = R \cdot x_{t-p} \cdot (1 - x_t)$		
4	paralogistic growth: introduction of p and a limited infectious period i $\frac{dx_t}{dt} = R_c \cdot (x_{t-p} - x_{t-i-p}) \cdot (1 - x_t)$		

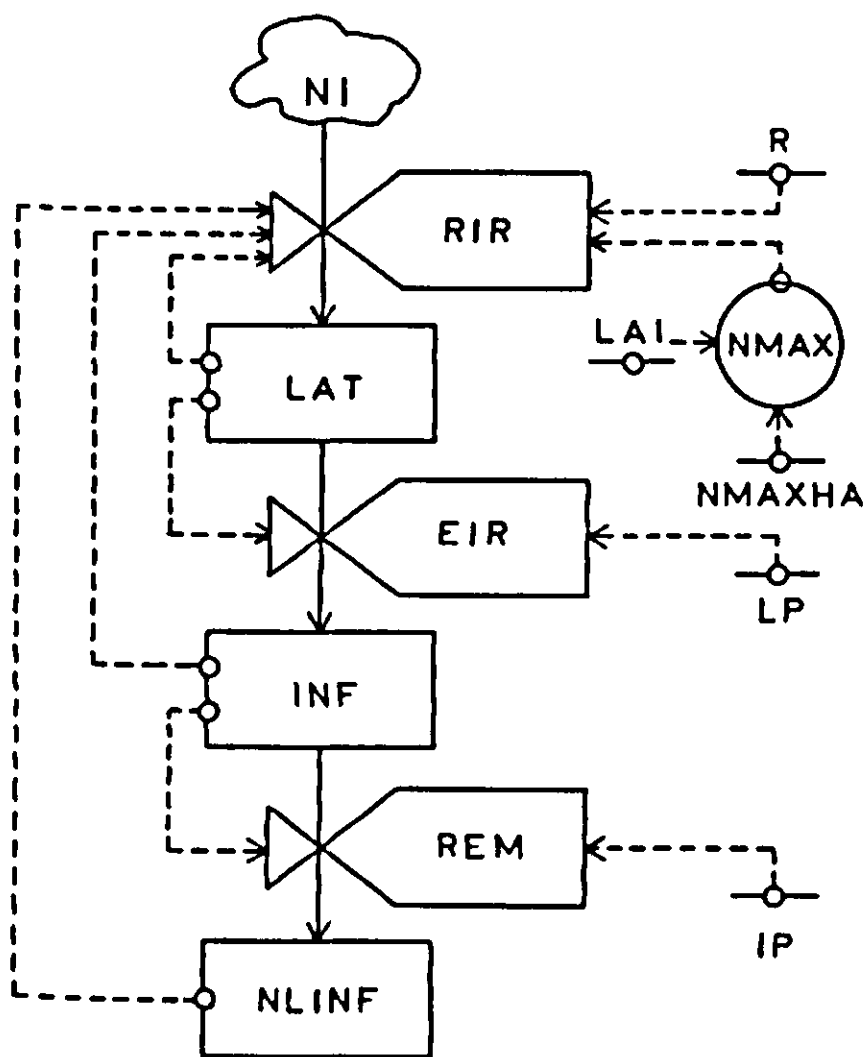


Figure 24. Relational diagram for the life cycle of a fungal disease such as *Erysiphe graminis*. NI = vacant sites, LAT = latent lesions, INF = infectious lesions, NLINF = no longer infectious lesions, RIR = real infection rate, EIR = effective infection rate, REM = rate of removal of infectious lesions, R = relative growth rate, NMAX = maximum number of infections, LP = latency period, IP = infectious period, LAI = leaf area index, NMAXHA = maximum number of lesions per ha of leaf area.

The results of Exercise 32 are given in Figure 25 as log number of infections versus time. The increase on a logarithmic scale is linear, and flattening occurs only when NMAX is limited (Figure 25b).

The model in its present form is useful for demonstration purposes only. It shows that the latency period is of major importance for the growth rate of an epidemic.

Exercise 33

Express LAT, INF, and NLINF in terms of the elements of Equation 40.

The paralogistic growth of an epidemic (Equation 40) is governed by four parameters: the latency period p (days), the infectious period i (days), the maximum number of sites Y_m (number) and the relative growth rate of the epidemic R (day^{-1}). In real epidemics, these four parameters are not constant. They depend on environmental conditions such as temperature and leaf wetness, on

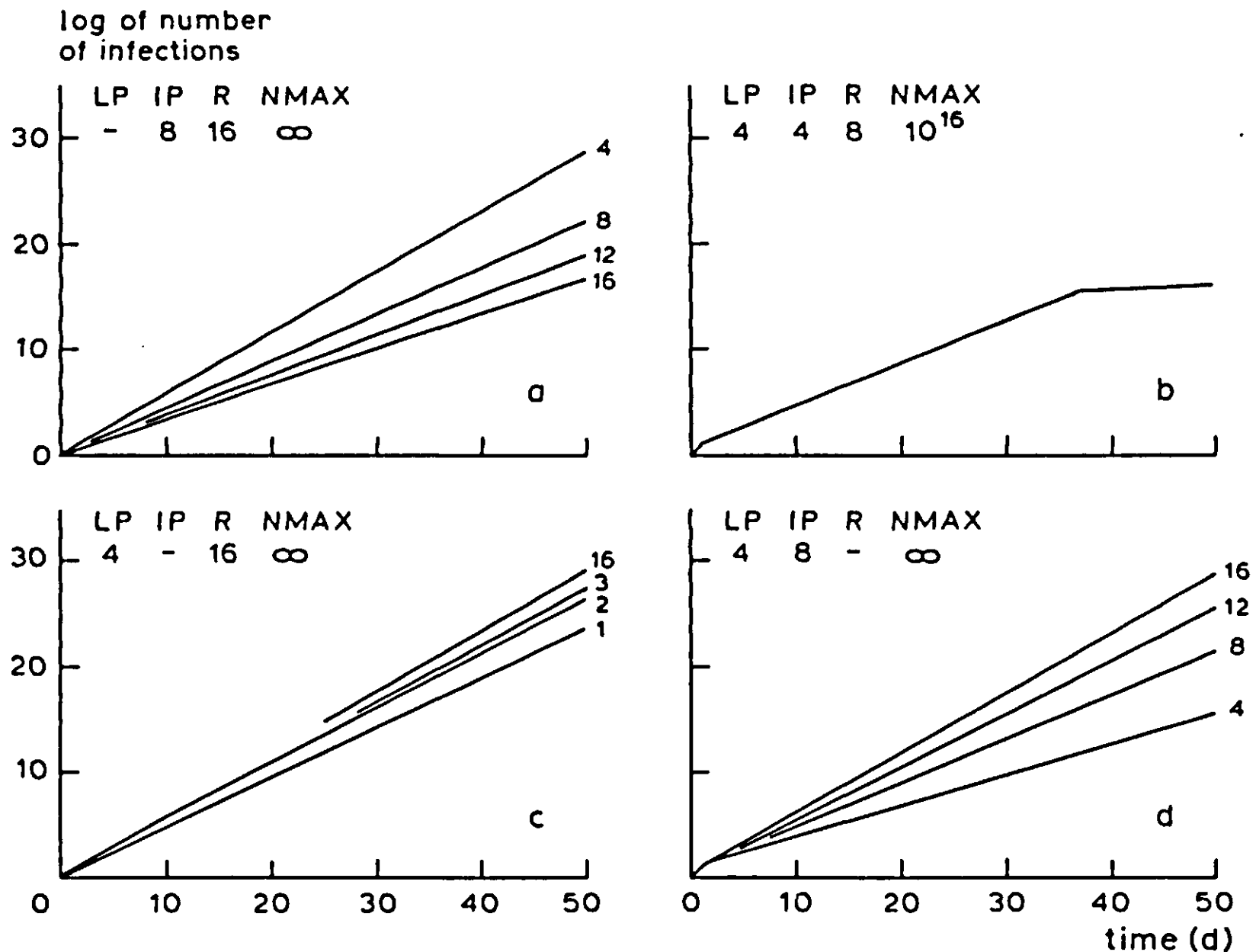


Figure 25. The increase of an epidemic over time, vertical axis: log (number of infections); horizontal axis: time. a) Effect of length of latency period (LP), in days, on upsurge of the epidemic. b) Effect of a finite number of possible infections (NMAX). c) Effect of length of infectious period (IP). d) Effect of daily reproduction rate or relative growth rate (R).

crop growth and on the condition of the various parts of the crop. In the next Subsections, these factors will be considered and incorporated step by step in the model of Exercise 32, finally resulting in a more accurate simulation model of a powdery mildew epidemic.

3.1.3 Computation of the latency period (LP) and the infectious period (IP)

In many fungal pathogens, the latency period and the infectious period depend on temperature, humidity and crop condition. If humidity does not limit development and the crop condition is optimal, both periods are computed from functions which describe their relations with temperature (TEMP):

$$LP = f(TEMP)$$

$$IP = f(TEMP)$$

These relations may be used, but they are often replaced by their inverses, since, at suboptimal temperatures, there is often an approximate linear relation between the rate of development and temperature. The model implicitly assumes that

development reacts instantaneously to changes in temperature. If this assumption is not true, considerable errors may result.

Exercise 34

Table 5 shows the duration of the latency period of powdery mildew, *Erysiphe graminis*, on winter wheat at different temperatures. At 5 °C the development rate equals zero, the temperature threshold is 7 °C. Express the development during latency in units from 0 to 1.

- Compute the development stage of the fungus after 3 days at a constant temperature of 15 °C.
- Compute the development stage after the same period when 12 h at 12 °C is alternated with 12 h at 18 °C.
- Perform the same calculation when the temperature varies between 2 °C and 18 °C and compare this with the results for a constant temperature of 10 °C. Explain the results of these comparisons of development at constant and fluctuating temperatures.

The nitrogen status of the crop (or nitrogen content of the leaves) may affect development considerably (Aust, 1981). To incorporate this plant effect, another state variable should be introduced by coupling a crop growth simulator to the epidemiological model. For the sake of simplicity, this nitrogen effect is neglected here. This simplification seems reasonable when crop husbandry practices are such that potential yield levels are reached. In this case, nitrogen is always abundantly available and nitrogen levels in the leaves are quite high. In Section 4.4 of this textbook, an approach will be described in which the nitrogen status of the crop is considered.

Table 5. Duration of the latency period (LP), infectious period (IP) and their standard deviations (SD) for powdery mildew, *Erysiphe graminis*, on winter wheat grown with abundant nitrogen at various temperatures.

Temperature (°C)	Length latency period (days)		Length infectious period (days)	
	X	SD	X	SD
10	16	3	10	3
15	8	2	4	2
20	4	1.5	3	1
25	2.5	1.	2	0.5
30	2.2	1.	1	0.25

The latency period and the infectious period were both simulated with one boxcar, thus assuming that in both stages relative dispersion equals unity. This is not realistic, as dispersion in time is not constant. Controlled dispersion is now introduced into the program by means of a BOXCAR subroutine (see Section 2.2). The inverse of the average latency and infectious periods and their relative dispersions should now be introduced explicitly into the model and used in these BOXCAR subroutines, which mimic dispersion in time. Using an AFGEN function, the inverse of the latency and infectious periods and their relative dispersions are read from tables DRLATT, DRINFT, RDLATT and RDINFT, respectively.

3.1.4 Computation of the maximum number of infectious sites (*NMAX*)

In the model of the paralogistic growth, the maximum number of sites was introduced as a parameter and held constant throughout the growing season. This is an unrealistic simplification, since the leaf area increases and decreases with time. To take this into account, leaf area can be introduced in a table that gives the actual leaf area values at different times. Another method would be the coupling of the epidemic simulator to a crop growth model (see Section 4.3).

In the present model, total leaf biomass (TLBM, kg ha^{-1}) is introduced by way of a forcing function (Table 6). This total leaf mass is converted to leaf area by multiplying the mass by a constant specific leaf area (SLA, ha kg^{-1}). The number of sites is found directly from the leaf area (LAI, ha ha^{-1}) and is used in the model of paralogistic growth:

$$NMAX = LAI/SI.ES$$

Table 6. Leaf mass (TLBM) of a wheat crop in relation to the start of the epidemic.

TIME (Julian days)	TLBM (kg ha^{-1})
70	75
90	100
115	200
130	1250
150	2200
180	2250
200	2000
220	1300
240	0

in which SLES expresses the Surface occupied by one LESion, for mildew 3.5 mm^2 .

Since leaf area is no longer a constant, the rate of dying leaf area is required to compute the rate of dying lesions. For simplicity, it is assumed that the probability of death due to leaf senescence is equal for all four categories of sites, i.e. NI, LAT, INF and NLINF. The death rate of the canopy can be computed from the forcing function by calculating the derivative of biomass with respect to time: $\text{RDYING} = -\text{DERIV}(0., \text{TLBM})$. To prevent an increase in the number of lesions due to the growth of leaf mass, a provision is needed that sets a lower limit of zero, so:

$$\text{RDYING} = -\text{AMIN1}(0., \text{DERIV}(0., \text{TLBM}))$$

The relative mortality rate of both leaf area and number of different categories of sites is now $\text{RMRLA} = \text{RDYING}/\text{TLBM}$. The area of dead leaves is accumulated using the CSMP integral function:

$$\text{DEADLA} = \text{INTGRL}(0., \text{RDYING} * \text{SLA}).$$

Further, RMRLA is introduced into the boxcar trains for latent and infectious sites. The number of sites that are no longer infectious is now calculated as:

$$\text{NLINF} = \text{INTGRL}(0., \text{REM} - \text{RMRLA} * \text{NLINF})$$

3.1.5 *Computation of the relative growth rate*

Each infectious site produces spores, but these must disperse, land, germinate and infect before new lesions can be produced. Although some models of dispersion and germination have been developed (Chamberlain, 1972; Legg & Powell, 1979; Waggoner in de Wit & Goudriaan, 1978; see Section 3.2), the data available on most fungal epidemics are insufficient for such a detailed, realistic approach. Unfortunately, therefore, it is often necessary to compact all these processes into a single variable: the 'effective spore' – the number of daughter lesions per mother lesion. In the previous model of Subsection 3.1.2, this single variable is expressed as the relative growth rate of the epidemic (R, number of daughter infections per mother lesion per day). In this way, a substantial amount of biological information is lumped together, which may decrease the value of the model as an explanatory tool. Some attempts have, however, been made to model the process of spore formation, spore emergence, spore dispersal, spore landing and spore germination. Attempts in cereal rusts have resulted in a submodel on spores. In these cereal rusts, the majority of spores die during dispersal or fail to germinate, and no more than 0.1 % of the spores produce lesions. The proportion of 'effective spores' depends on environmental conditions and on the condition and characteristics of the crop. For example, leaf wetness has a considerable effect on spore germination in wheat rusts, and therefore greatly influences the number of daughter lesions per mother lesion per day. This effect of leaf wetness may be a 'yes/no' reaction; for example, in potato

late blight, *Phytophthora infestans*, germination occurs only if there is free water on the leaves. In many cases, the reaction of the fungus is less abrupt, and the number of effective spores gradually declines as leaf wetness decreases.

Another important factor is temperature. Temperature affects the germination period, spore mortality and rate of infection. These processes are incorporated into the one variable that comprises all the sporal processes: the relative growth rate. In our simple simulator of a mildew epidemic, a preliminary model of spore production, spore death and spore germination is incorporated (Figure 26). Spores are produced at a particular rate. After dispersal, a fraction of these spores is caught. The number caught depends on the leaf area index, LAI and the fraction of intercepted spores per leaf layer FINTLL. Only the spores landing on a site that has not yet, been infected have a chance to establish an infection. The number of caught spores on a vacant site (INTSPO) increases with:

$$\text{IRPSP} = R * \text{INFTOT} * \text{FINTLL} * \text{LAI} * (1 - \text{OCC}/\text{NMAX})$$

in which IRPSP is the interception rate of produced spores, R the spore production rate per infectious lesion, INFTOT the number of infectious lesions and OCC the number of occupied sites. The spores that have been caught begin to germinate, at a rate that is dependent on the average germination period and the number of spores available:

$$\text{GRISP} = \text{RGRISP} * \text{INTSPO}$$

in which GRISP is the germination rate of intercepted spores, RGRISP the inverse of the germination period (Table 7) and INTSPO the number of intercepted spores. Not all spores germinate, some die during development. The relative spore mortality rate per day is often calculated from the experimentally determined fraction of germinated spores as:

$$\text{RMRISP} = (1 - \text{GF})/\text{GP}$$

in which GF is the germinated fraction and GP the germination period.

Figure 26. Relational diagram of a model of a fungal epidemic.

State variables: LATTOT = latent lesions, INFTOT = infectious lesions, NLINF = no longer infectious lesions, INTSPO = intercepted spores, GERSPO = germinated spores.

Rate variables: RIR = real infection rate, EIR = effective infection rate, REM = rate of no longer infectious lesions, MR... = mortality rates, IRPSP = interception rate of produced spores, GRISP = germination rate of intercepted spores.

Auxiliary variables: CP = colonization period, LP = latency period, IP = infectious period, GP = germination period, RMR... = relative mortality rates, R = spore production rate per lesion, FINTLL = fraction intercepted spores per leaf layer, TLBM = total leaf biomass, LAI = leaf area index, SLES = surface of a single lesion, NMAX = maximum number of sites, OCC = occupied sites, SLA = specific leaf area, TEMP = temperature.

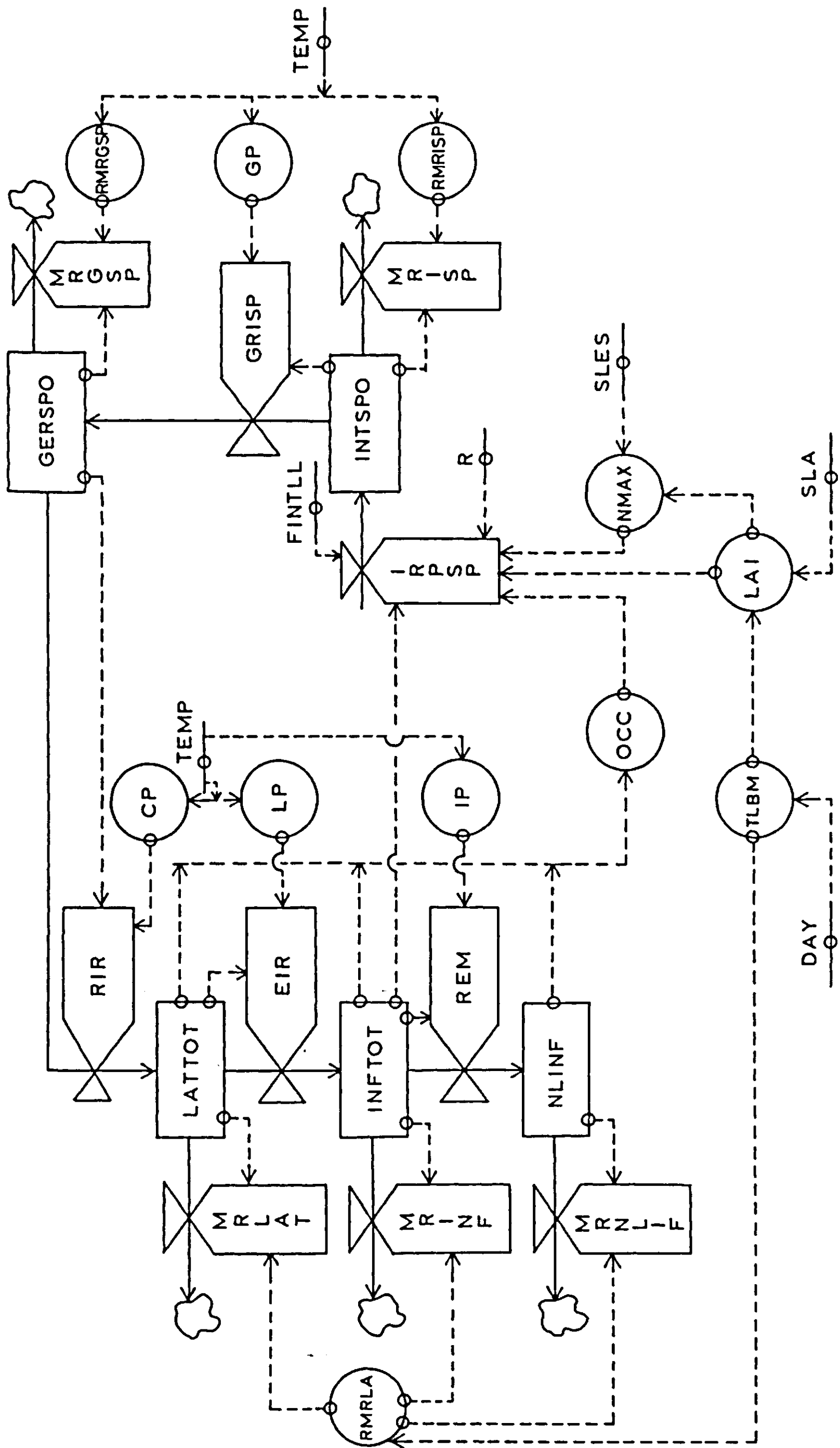


Table 7. Relation between temperature and germination period (days) for mildew spores.

Temperature (°C)	Germination period (days)
10	30
15	10
20	8
25	4
30	3

Exercise 35

What is wrong with this method of computing relative mortality? Illustrate the consequences of this incorrect computation method and give the correct method.

The real infection rate (RIR, number $\text{ha}^{-1} \text{day}^{-1}$) is now calculated from the number of germinated spores (GERSPO):

$$\text{RIR} = \text{RIRGSP} * \text{GERSPO}$$

in which RIRGSP is the inverse of the time it takes a germinated spore to colonize the host tissue.

Not all germinated spores are successful, some die. Like germinating spores, the relative mortality rate per day of germinated spores can be calculated from the fraction of successful spores and the time it takes a germinated spore to colonize the host tissue. The number of infected sites per germinated spore is called the colonization ratio.

A first concept for modelling spore germination has now been presented, although germination is not considered in detail in the model presented here. For instance, the germinating spores are lumped in one development class; but not all spores, produced at one moment, germinate at the same time: there are delays and dispersion in time. Again, the subroutine BOXCAR may be used to mimic this dispersion (see Section 2.2).

The model can now be used to simulate a polycyclic fungal epidemic. One important, implicit assumption may yet be incorrect: the leaves are all assumed to be equally sensitive to the fungus, but in many cases ageing leaves are less

sensitive than those that have just appeared. To include this effect, the epidemiological model should be coupled to an appropriate crop model. Various examples of coupling are presented in Section 4.3.

3.1.6 *Another approach, leaf area instead of sites*

The arbitrary unit of fungal density, number of lesions and the relation with the host plant is a considerable simplification. However, observations are seldom made in terms of the number of pustules or sites, but rather in the fraction-infected leaf area. To bring the model more in line with these observations, it is probably better to express disease intensity in leaf area infected instead of number of lesions.

The leaf area may contain four characteristics: sound leaf area, leaf area with latent lesions (TLATLA), leaf area with sporulating lesions (TINFLA) and leaf area with old, no longer sporulating lesions (NLIFLA). Spore production is still computed in a way similar to that in the 'site' model:

$$\text{IRPSP} = R * \text{INFTOT} * \text{FINTLL} * \text{LAI} * (1 - \text{DISLA}/\text{LAI})$$

INFTOT has now to be computed from the leaf area with sporulating lesions:

$$\text{INFTOT} = \text{TINFLA}/\text{SLES}$$

The diseased leaf area (DISLA) is calculated as:

$$\text{DISLA} = \text{TLATLA} + \text{TINFLA} + \text{NLIFLA}$$

The real infection rate is multiplied by the leaf area of a single lesion (SLES) to change the growth of the number of infected sites into growth of infected leaf area:

$$\text{RIRLA} = \text{RIR} * \text{SLES}$$

A complete listing of the simulation program of this epidemic simulator is given in Figure 27.

Exercise 36

Study the listing of the epidemic simulator. If possible, run the program with the given values of the parameters, and with other selected values.

3.1.7 *Insects and mites*

The example given above was based on a fungal epidemic. A more detailed example of the simulation of a fungal epidemic, *Helminthosporium maydis*, is described by Waggoner, in de Wit & Goudriaan (1978). Simulation of the

Figure 27. Listing of a program to simulate a powdery mildew epidemic. The same BOXCAR subroutine has to be used as in Figure 22, Section 2.2.

TITLE EPIDEMIC POWDERY MILDEW

STORAGE ILATLA(4),LATLA(4),IINFLA(3),INFLA(3)
FIXED N1,N2

INITIAL

*crop-parameters

PARAM SLA=20.E-4

*parameters connected with the fungus

PARAM STDAY=100.,N1=4,N2=3

TABLE ILATLA(1-4)=5.E-4,3*0., IINFLA(1-3)=3*0.

PARAM SLES=3.5E-10,R=1.E3,FINTLL=0.01

DYNAMIC

DAY =STDAY + TIME

TEMP =AFGEN(TEMPT,DAY)

*the crop

TLBM =AFGEN(TLBMT,DAY)

LAI =TLBM * SLA

* TLBM:Total Leaf BioMass in kg(leaf)/ha(soil)

RDYING=-AMIN1(0.,DERIV(0.,TLBM))

RMRLA =RDYING/TLBM

* RMRLA:Relative Mortality Rate Leaf Area in 1/day

DEADLA=INTGRL(0.,RDYING*SLA)

* DEADLA:DEAD Leaf Area in ha(leaf)/ha(soil)

*the fungus

**spores

INTSPO=INTGRL(0.,IRPSP-MRISP-GRISP)

GERSP0=INTGRL(0.,GRISP-MRGSP-RIR)

* INTSPO:INTERcepted SPOres in number/ha

* GERSP0:GERminated SPOres in number/ha

* IRPSP:Interception Rate of Produced SPOres in number/ha/day

* MR-,GRISP:Mortality and Germination Rate of Intercepted

* SPOres in number/ha/day

* MRGSP:Mortality Rate of Germinated SPOres in number/ha/day

* RIR:Real Infection Rate in number/ha/day

IRPSP =R * INFTOT * FINTLL*LAI * (1.-DISLA/LAI)

INFTOT=TINFLA/SLES

* R:spore production rate in number/infectious lesion/day

* TINFLA:Total INFectious Leaf Area in ha/ha

* SLES:Surface of a single LESion in ha

* INFTOT:TOTAL number of INFectious lesions in number/ha(soil)

* FINTLL:Fraction INTERcepted spores per Leaf Layer

* DISLA:DISEased Leaf Area in ha/ha

MRISP =RMRISP*INTSPO

RMRISP=AFGEN(RMRIST,TEMP)

* RMRISP:Relative Mortality Rate Intercepted SPOres in 1/day

GRISP =RGRISP*INTSPO

RGRISP=AFGEN(RGRIST,TEMP)

* RGRISP:Relative Germination Rate Intercepted SPOres in 1/day

MRGSP =RMRGSP*GERSP0

RMRGSP=AFGEN(RMRGST,TEMP)

* RMRGSP:Relative Mortality Rate Germinated SPOres in 1/day

RIR =RIRGSP*GERSP0

RIRGSP=AFGEN(RIRGST,TEMP)

* RIRGSP:Relative Infection Rate Germinated SPOres in 1/day

**infected leaf area
 RIRLA =RIR*SLES
 * RIRLA:Real Infection Rate expressed in Leaf Area in ha/ha(soil)/day

*Development Rate

DRLAT =AFGEN(DRLATT,TEMP)
 DRINF =AFGEN(DRINFT,TEMP)
 *Relative Dispersion
 RDLAT =AFGEN(RDLATT,TEMP)
 RDINF =AFGEN(RDINFT,TEMP)

NOSORT
 LATO,LATLA,TLATLA,MRLAT,EIRLA,GAMMA1,GCYCL1=...
 BOXCAR(1,ILATLA,DRLAT,RDLAT,RMRLA,RIRLA,N1,DELT,TIME)

INFO,INFLA,TINFLA,MRINF,REMLA,GAMMA2,GCYCL2=...
 BOXCAR(2,IINFLA,DRINF,RDINF,RMRLA,EIRLA,N2,DELT,TIME)

SORT

NLIFLA=INTGRL(0.,REMLA - RMRLA*NLIFLA)
 DISLA =TLATLA+TINFLA+NLIFLA

FUNCTION TLBMT = 0.,75., 70., 75., 90., 100., 115., 200.,...
 130.,1250., 150.,2200., 180.,2250., 200.,2000.,...
 220.,1300., 240.,1., 300.,1.
 FUNCTION RMRIST= 0.,0.12, 10.,0.12, 15.,0.36, 20.,0.46, 25.,0.92,...
 30.,1., 35.,1.
 FUNCTION RGRIST= 0.,0., 7.,0., 10.,0.0333, 15.,0.1000, 20.,0.1250,...
 25.,0.2500, 30.,0.3333
 FUNCTION RMRGST= 0.,20., 10.,16., 15.,18., 20.,20., 30.,24.
 FUNCTION RIRGST= 0.,1., 10.,1.8, 15.,2., 20.,2.2, 30.,2.4
 FUNCTION DRLATT= 0.,0., 7.,0., 10.,0.0625, 15.,0.1250, 20.,0.2500,...
 25.,0.4000, 30.,0.4540
 FUNCTION DRINFT= 0.,0., 7.,0., 10.,0.1000, 15.,0.2500, 20.,0.3333,...
 25.,0.5000, 30.,1.0000
 FUNCTION RDLATT= 0.,0., 7.,0., 10.,0.1875, 15.,0.2500, 20.,0.3750,...
 25.,0.4000, 30.,0.4545
 FUNCTION RDINFT= 0.,0., 7.,0., 10.,0.3000, 15.,0.5000, 20.,0.3333,...
 25.,0.2500, 30.,0.2500
 FUNCTION TEMPT = 0.,2., 60.,8., 120.,15., 180.,28., 240.,15., 300.,2.

METHOD RECT
 TIMER FINTIM=120., DELT=0.05, PRDEL=5.
 PRINT DAY,TLBM,LAI,DISLA,TLATLA,TINFLA,NLIFLA,DEADLA,RMRLA,...
 INTSPO,GERSP0,RIR,RIRLA

END
 STOP

```
C*****C
  SUBROUTINE BOXCAR(COUNT,AI,DEVR,RD,RMR,INFL,N,DELT,TIME,
    S          AO,A,ATOT,MORFL,OUTFL,GAMMA,GCYCL)
C*****C
```

population dynamics of a pest is roughly similar to that of a fungal epidemic, so this model can also be used to simulate the population growth of insects or mites. This will be illustrated in Section 3.4 where a detailed predator-prey model for an acarine system is discussed, and in Section 4.4 which considers a model for a pest epidemic (cereal aphids) combined with a crop growth model for wheat.

3.2 Dispersal and dispersion in space

S.A. Ward, P.S. Wagenmakers and R. Rabbinge

3.2.1 Introduction

The models and techniques presented in Section 3.1 can be used to simulate the development of pest populations or disease epidemics during the course of a year, but they include no spatial component. It was assumed implicitly that the pests or diseases are distributed evenly among the sampling units (e.g., wheat tillers, potato leaves, etc.). This assumption, however, is rarely or never true: most pests or diseases are found in clusters or patches.

The effects of such aggregation can be extremely important, especially when the population's growth rate is influenced by local density-dependent factors such as predation or intra-specific competition for food or sites (Section 3.3).

This Section begins by considering two recent models simulating the dispersal processes which result in observed distributions of fungal spores and actively moving insects. It then discusses a number of commonly used simple descriptive models of dispersion, one of which is then used to examine the consequences of spatial distributions on the dynamics of an aphid-parasitoid system.

3.2.2 Passive dispersal: fungal spores

As in Section 3.1, most models of fungal epidemics simulate the process of spore production and dispersal by means of a single rate variable: the effective number of spores per mother lesion per day. Clearly, this involves considerable simplification (in any case, often unavoidable, owing to the lack of quantitative data on the biological and physical backgrounds). However, the dispersal process itself depends on a wide range of physical factors, and is sufficiently complex to justify the use of numerical simulation methods.

This section considers such a more detailed model of the dispersal process alone. It simulates the dispersal of airborne spores of the basidiomycete, *Chondrostereum purpureum* in woodland (Wagenmakers, 1984). The basidiomycete *Chondrostereum purpureum* is a common fungus in temperate regions. It occurs as a saprophyte on many deciduous trees, and as a parasite of fruit trees and various ornamentals, where it causes silver leaf disease. Spores landing on fresh wounds develop into mycelia, which obstruct the sieve tubes and, as a result, the plant produces gum in the sapwood. The fungal toxins cause senescence and release of the leaf epidermis, resulting in the characteristic silver leaf disease symptoms.

In the autumn, basidiocarps are produced (these are visible as a purple crust on the wood). These basidiocarps produce spores, which are ejected and subsequently dispersed by air currents.

Prunus serotina Erhr (American black cherry) is a tree species, introduced into Europe in the first part of this century from the United States, to improve the understory of woodlands on poor sand soils. This species, however, has become a serious pest, as it prevents native species from germinating and developing.

P. serotina is sensitive to *C. purpureum* and can be controlled by cutting the trees and treating the wounds with a suspension of mycelium or spores (de Jong & Scheepens, 1985; de Jong, 1988). Newly-formed shoots show the characteristic silver leaf disease symptoms, and die off in a few months; 60 to 70% of the uninfected branches on treated trees also die.

Before introducing *C. purpureum* as a biological control agent, however, plant protection authorities considered it necessary to estimate the increased chance of adjacent plots becoming infected. The 'normal' dispersal of *C. purpureum* should, therefore, be compared with the dispersal in areas infested as a result of control of *P. serotina*. Large-scale field trials are laborious and risky, so instead, small-scale trials were combined with theoretical calculations to evaluate the consequences of this way of control. Computer models were used to simulate spore dispersal. In the small-scale trials, results of the computer model are tested against experimental results. The validated computer model can be used to calculate infection risks at various times and under various conditions.

The model presented here is based on the micrometeorological studies of Goudriaan (1977), which simulates the dispersal of *C. purpureum* spores in a coniferous forest, but can be easily adapted to simulate other conditions.

Structure of the model To simulate the dispersal of *C. purpureum* correctly, the forest must be divided into at least four spatial sections; a spore production layer, a stem layer, a crown layer and the air above the canopy. The layers are schematically represented in Figure 28. Each layer is characterized by its own specific biological and aerodynamic properties.

Spore production takes place on the stumps that have been infected with a sporal substrate. An epidemiological model of the fungus (Section 3.1) could be used to study the epidemic on the stumps within this spore production layer.

Spore production and dispersal processes are schematically represented in Figures 28 and 29. Spore production is held proportional to the amount of sporulating area on the cut stumps: the basidiocarp area. The relation between temperature and spore production rate per unit of basidiocarp area is derived from the data of Grosclaude (1969).

Wind is responsible for the dispersal of spores to other air layers outside the forest. Spores are exchanged vertically between the layers of air by turbulent air movements.

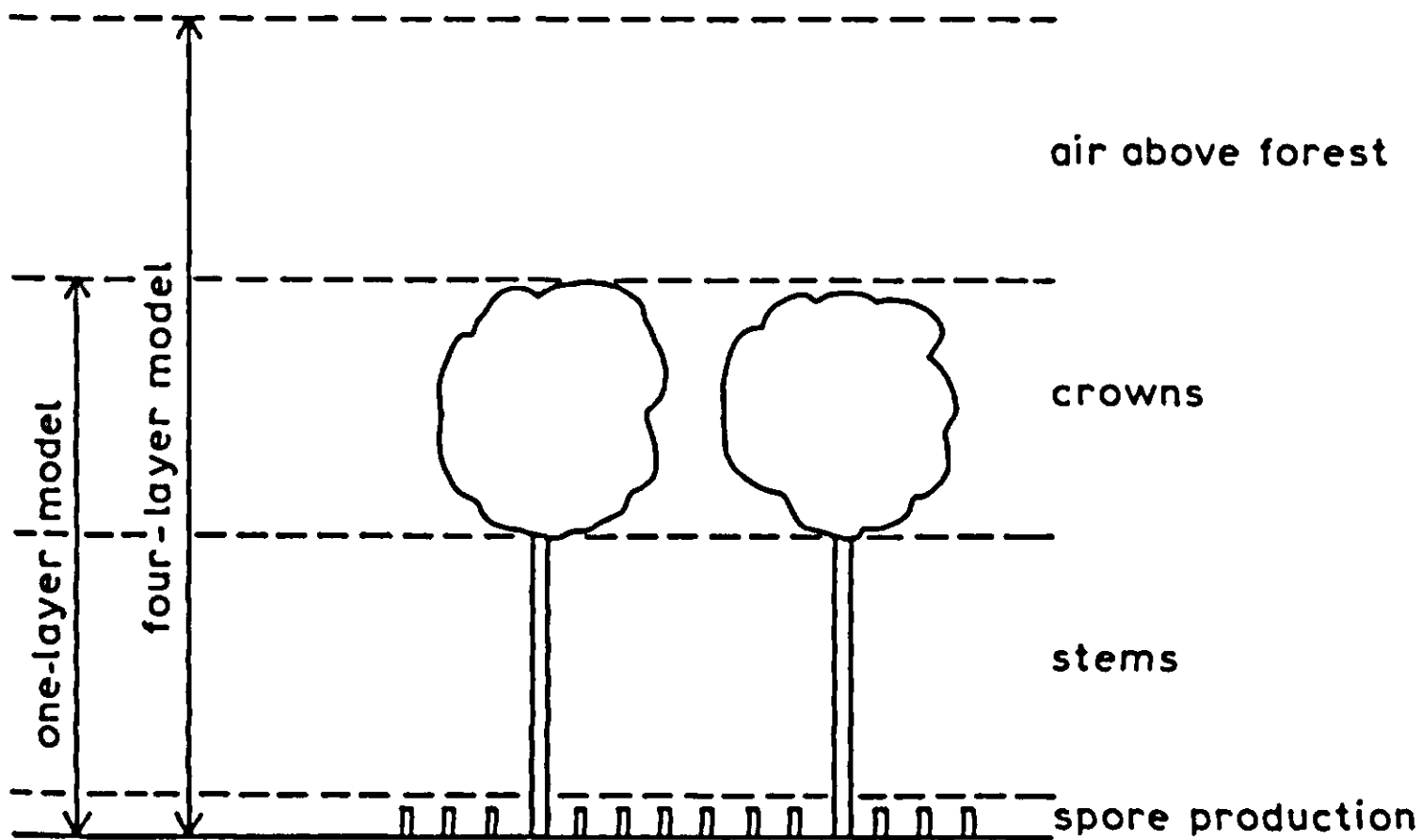


Figure 28. Layer structure of the forest.

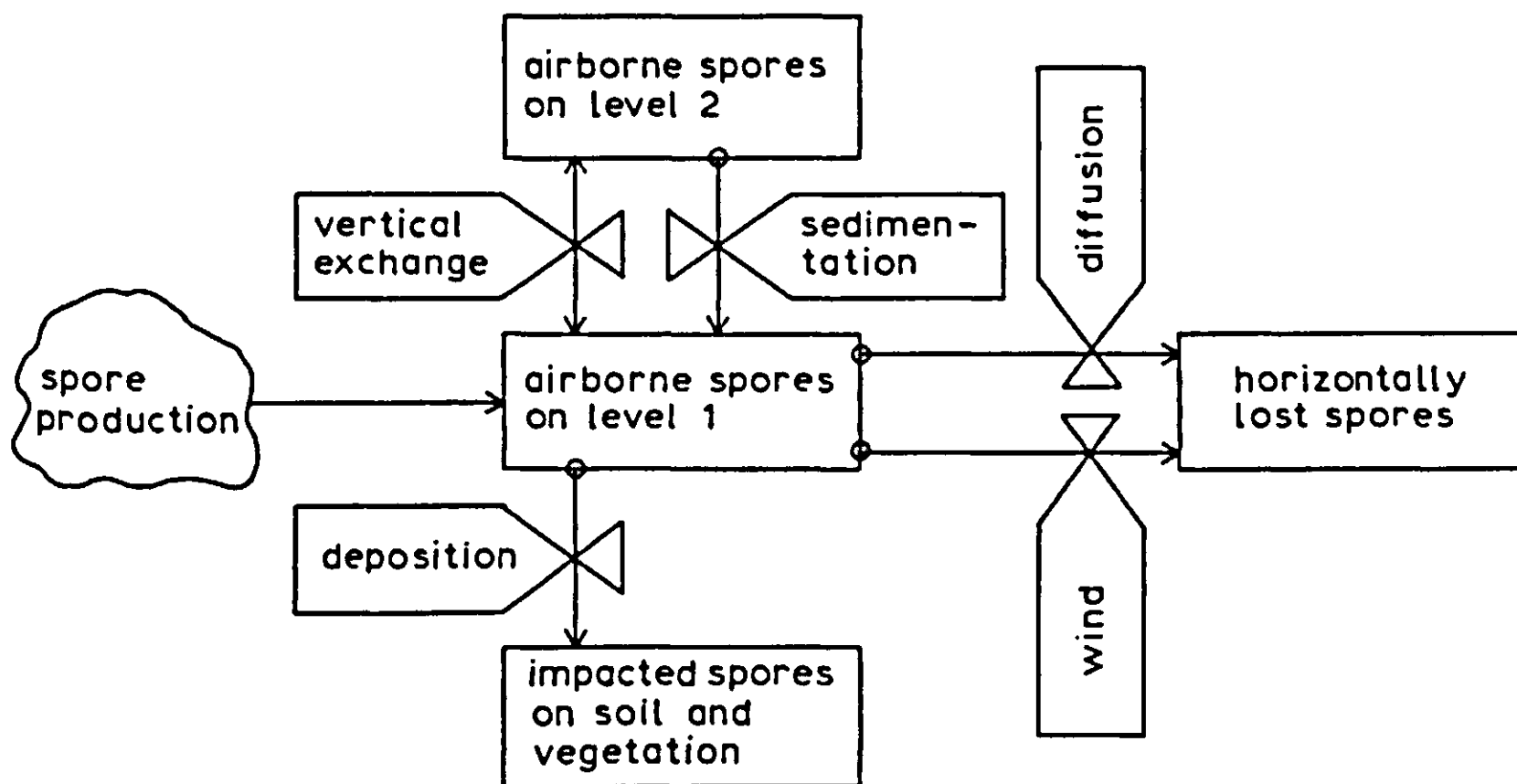


Figure 29. Relational diagram of the transport processes.

The rate of exchange is determined by exchange resistances, which have the units m^{-1} . The spore flux between two adjacent layers ($\text{spores m}^{-2} \text{s}^{-1}$) is found by dividing the difference between the spore densities by the exchange resistance.

A multi-layer model requires a lot of information on the various exchange rates, together with a detailed description of the aerodynamics of a canopy. Therefore, a simplified approach, using a one-layer model, is used in this book.

One-layer model The multi-layer model can be developed later from a simplified one-layer model in which the crown, stem and stump layers are grouped together

into one mixed layer, exchanging spores with the open air above (Figure 28). In this simplified model, the net rate of change in the number of spores inside the forest is summarized as

$$\frac{dS}{dt} = R_{\text{prod}} + R_{\text{ex}} + R_{\text{sed}} + R_{\text{dep}} \quad \text{Equation 42}$$

where S is the number of spores per m^2 of ground area, R_{prod} the rate of spore production on the stumps in numbers $\text{m}^{-2} \text{s}^{-1}$, R_{ex} the net rate of exchange by turbulent air movements in numbers $\text{m}^{-2} \text{s}^{-1}$, R_{sed} the rate of sedimentation due to settling of spores in numbers $\text{m}^{-2} \text{s}^{-1}$, and R_{dep} the rate of deposition of spores on leaves, branches etc. in numbers $\text{m}^{-2} \text{s}^{-1}$.

The concentration of spores inside the forest c_i (m^{-3}) is the number of spores per m^2 ground area divided by the thickness L of the layer (the height of the forest):

$$c_i = S/L$$

The rates R can be formulated as:

$$R_{\text{ex}} = (c_a - c_i)/r_{\text{ex}}$$

$$R_{\text{sed}} = -v_{\text{sed}} c_i$$

$$R_{\text{dep}} = -u \varepsilon_{\text{dep}} \text{LAI} c_i$$

where c_i is the spore concentration in the layer (m^{-3}), c_a the background concentration of spores in the air above the forest (m^{-3}), r_{ex} the exchange resistance between the open air and the forest (s m^{-1}), v_{sed} the sedimentation velocity (m s^{-1}), u the wind speed inside the forest (m s^{-1}), ε_{dep} the deposition efficiency of leaves (-), and LAI the leaf area index ($\text{m}^2 \text{m}^{-2}$).

Typical values for the parameters in these equations are: $R_{\text{prod}} = 20 \text{ m}^{-2} \text{ s}^{-1}$; $L = 17 \text{ m}$; $c_a = 100 \text{ m}^{-3}$; $r_{\text{ex}} = 20 \text{ s m}^{-1}$; $v_{\text{sed}} = 0.001 \text{ m s}^{-1}$; $u = 2 \text{ m s}^{-1}$; $\varepsilon_{\text{dep}} = 0.01$; and $\text{LAI} = 2$.

Equation 42 can now be rewritten in a form that groups the influx and efflux:

$$L \frac{dc_i}{dt} = \left(R_{\text{prod}} + \frac{c_a}{r_{\text{ex}}} \right) - \left(\frac{1}{r_{\text{ex}}} + v_{\text{sed}} + u \varepsilon_{\text{dep}} \text{LAI} \right) c_i \quad \text{Equation 43}$$

or, more briefly:

$$L \frac{dc_i}{dt} = b - ac_i \quad \text{Equation 44}$$

Exercise 37

Find the values of b and a by substituting the given parameters. What are their units? What is the value of the time coefficient of this equation?

At equilibrium the rate of change is zero, so spore concentration in the layer is given by:

$$c_{eq} = b/a \qquad \text{Equation 45}$$

Exercise 38

Calculate the value of c_{eq} using Equations 43, 44 and 45 with the given typical parameter values. How long does it take before c_i lies within 5% of c_{eq} , when it starts at the value c_a .

This model, despite its simplicity, gives a good impression of the relative importance of the different processes of spore dispersal. The coefficient, a , is the result of exchange, sedimentation and deposition. The sedimentation rate appears to be dwarfed by turbulent exchange and deposition. These latter two processes are of roughly equal importance, so about half the spores produced are deposited.

Above the forest, the spore concentration is set arbitrarily at $100 \text{ spores m}^{-3}$. The concentration inside the forest depends on both the concentration above the forest and on the spore production rate.

For a forest with no sporulating surface, the removal processes will reduce c_{eq} below c_a . Here, when R_{prod} is zero, so that $(R_{prod} + c_a/r_{ex})$ equals $0 + 100/20 = 5$, c_{eq} will reach a value of $5/0.091$, or only 55 spores m^{-3} . Thus, the concentration inside the forest, will be about half that in the air above.

Losses of spores downwind The model developed so far has considered an infinitely extended forest, for which c_{eq} is not a function of horizontal distance. However, at the upwind side of the forest, air blows into the forest carrying spores at the background concentration c_a (Figure 30). On a transect through the forest, in the downwind direction, spore concentration will gradually rise, until it finally reaches the equilibrium concentration c_{eq} , calculated above. The time coefficient of this process depends on the variables L and a (see Exercise 37). After about three of these time coefficients have elapsed, equilibrium will be practically established. In the meantime, the wind will have traversed a distance to be

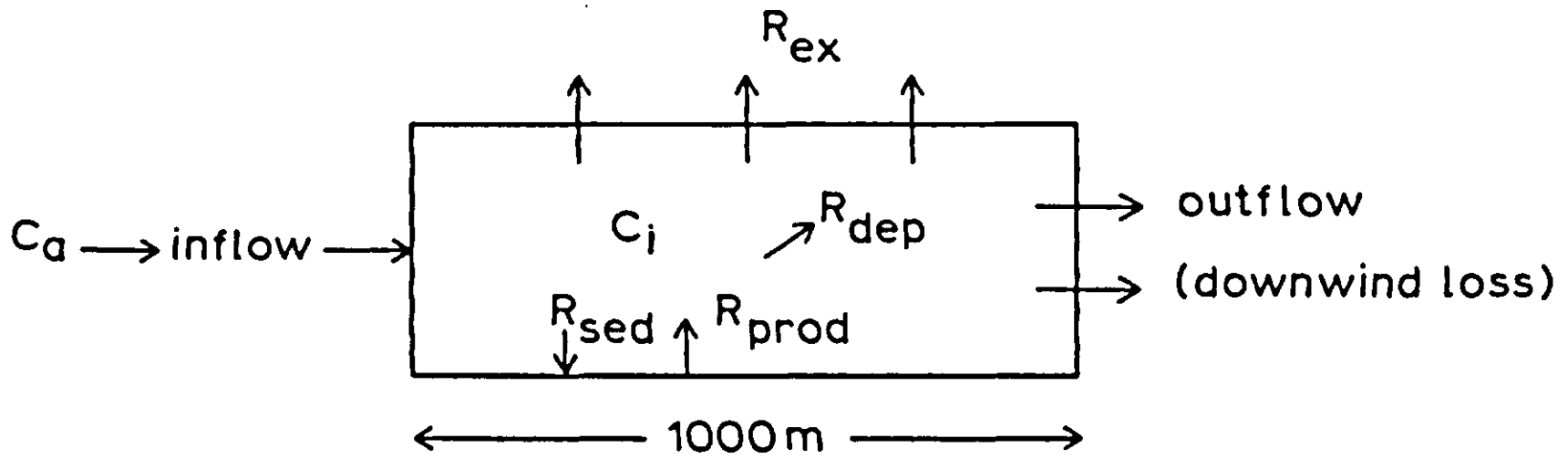


Figure 30. Rates of inflow, outflow, upward exchange (R_{ex}), sedimentation (R_{sed}), deposition (R_{dep}), and production (R_{prod}) of spores in a forest with a one-layer model.

calculated as $3 \cdot u \cdot L/a$, or about 1000 m. This means that for a forest of less than about 1000 m wide, c_{eq} is not reached.

The inflow of spores at the upwind side is about $L \cdot u \cdot c_a$, and the outflow at the leeward side about $L \cdot u \cdot c_{eq}$, so that the net downwind loss is about $L \cdot u \cdot (c_{eq} - c_a)$. This quantity can be calculated to be $5950 \text{ m}^{-1} \text{ s}^{-1}$, for the parameters chosen above. The unit m^{-1} in this expression means that the rate is expressed per m of forest width, perpendicular to the wind direction. Total spore production over a forest that is 1000 m wide is in the same units $R_{prod} \cdot 1000$ or $20000 \text{ m}^{-1} \text{ s}^{-1}$. The lateral loss thus amounts to more than a quarter of the total production. The upward loss is more difficult to calculate, since c_i actually varies over the forest width from c_a to c_{eq} . Horizontal compartmentalization would be required to find the horizontal gradients, and the total loss in a vertical direction.

This model accounts for the finite limits of a forest and is thus more appropriate for application in actual situations. Another extreme is a very small forest, i.e. a point source of spore production. This situation is not considered, as the widely used Gaussian plume model can then be applied. The one-layer model is used as a first approximation and is adequate if only temperature and humidity are to be considered, but is inadequate for spores that are produced in the spore production layer. Therefore, a four-layer model, or other more complicated model, has to be used.

Four-layer model Although the processes are essentially the same, a four-layer model (Figure 28) is complicated by spore exchange between the layers. This means that in a rate equation like Equation 43, spore concentrations must appear in adjacent layers. The system must now be represented as a set of four equations, which can be written in matrix form as:

$$\vec{L} \cdot \frac{d\vec{c}}{dt} = \vec{B} - |A| \vec{c} \quad \text{Equation 46}$$

The various elements of the matrix are derived from the geometric and agronomic characteristics of the canopy. At equilibrium, the rate of change is zero, so

$$|A| \vec{c} = \vec{B} \text{ or} \quad \text{Equation 47}$$

$$\vec{c} = |A^{-1}| \vec{B} \quad \text{Equation 48}$$

The matrix $|A|$ contains the removal processes, and the exchange resistances between the layers. The vector \vec{B} contains the source terms which are independent of the spore concentrations inside the forest. These source terms represent the rate of spore production in the bottom layer and the gross influx of spores from the air above. When the terms of A and B are substituted, Equation 47 becomes

$\frac{1}{r_1} + v_{sed}$	$-\frac{1}{r_1} - v_{sed}$	0	0	×	=	c_1	R_{prod}
$-\frac{1}{r_1}$	$\frac{1}{r_1} + \frac{1}{r_2} + v_{sed}$	$-\frac{1}{r_2} - v_{sed}$	0			c_2	0
0	$-\frac{1}{r_2}$	$\frac{1}{r_2} + \frac{1}{r_3} + v_{sed} + u_3 \epsilon_{dep} LAI$	$-\frac{1}{r_3} - v_{sed}$			c_3	0
0	0	$-\frac{1}{r_3}$	$\frac{1}{r_3} + \frac{1}{r_4} + v_{sed}$			c_4	$\left(v_{sed} + \frac{1}{r_4}\right) c_a$

The subscripts, 1 to 4, refer to the stump, stem and crown layers and an open air layer above. Typical values for the resistances r_{1-4} are $r_1 = 200$, $r_2 = 50$, $r_3 = 10$, $r_4 = 4 \text{ s m}^{-1}$, respectively; u_3 will be about 2 m s^{-1} . The other parameters are the same as before.

Exercise 39

Substitute these parameters (r_{1-4} , u_3) into Equation 47 and set up the numerical form of the equation. Determine the vector c , preferably using an existing software package.

The resulting vector c , which can be calculated by matrix inversion from Equation 48, gives the spore concentrations in the four layers. As shown by Wagenmakers (1984), these concentrations differ by factors of 10. The one-layer model is, therefore, a gross oversimplification.

Influence of weather and forest structure The exchange resistances are approximately inversely proportional to windspeed. Since v_{sed} is small, the entire matrix A is almost proportional to windspeed, so c_{eq} will be roughly inversely proportional to windspeed. Temperature and humidity affect the system, mainly as a result of their influence on the rate of spore production. Other parameters being constant, $(c_{eq} - c_a)$ will be proportional to R_{prod} .

In a denser forest, the intercepting area (LAI) will be larger, but windspeed in the crown layer will fall. The product $u_3 \cdot LAI$ may change either way. The exchange resistances will be larger, so a steeper spore gradient will develop. An extensive sensitivity analysis is given by Wagenmakers (1984).

3.2.3 Active dispersal in two dimensions

Unlike fungal spores, animals move actively. Therefore, spatial dispersal of these organisms should be considered in a different way. In predator-prey systems, the movement of prey and predator is decisive for the number of encounters between them, and this determines the predation rate of individual predators. Acarine systems are well-studied predator-prey systems. They are found in various crops and, in many cases, enable feasible biological control. To understand such systems, the individual predator's dispersal is studied. It appears that the movement of an individual predatory mite is determined by its condition, often expressed in gut content. The more a predatory mite has eaten, the less its linear displacement. This is explained in a simulation study of predatory mite movement by Sabelis (1981), based on a detailed analysis of walking patterns in relation to gut content.

The model presented in this Subsection simulates the walking patterns of predatory mites searching for spider mites, *Tetranychus urticae*, on rose leaves. The formulation, however, can be used for a wide range of organisms. The resulting simulation models can be used as a basis for determining predation rates of individual predators, when predation rate is mainly determined by encountering rate and success ratio. These individual predation rates may be used in models of pest population dynamics. The mite's continuous movement is modelled as a series of linear steps of constant length. This allows separation of the two determinants of the walking pattern: speed and direction. Here, we will consider only the directional component.

Figure 31 illustrates the division of the mite's curved path into linear steps of fixed length. The angular deviation between the directions of steps $s-1$ and s is denoted by A_s (in radians). It is important to note that A_s expresses the change in direction, rather than the direction itself.

The angular deviation per step can be used as follows, to generate a two-dimensional walking pattern. The direction (a state variable) is calculated in a CSMP program as (see Appendix 5):

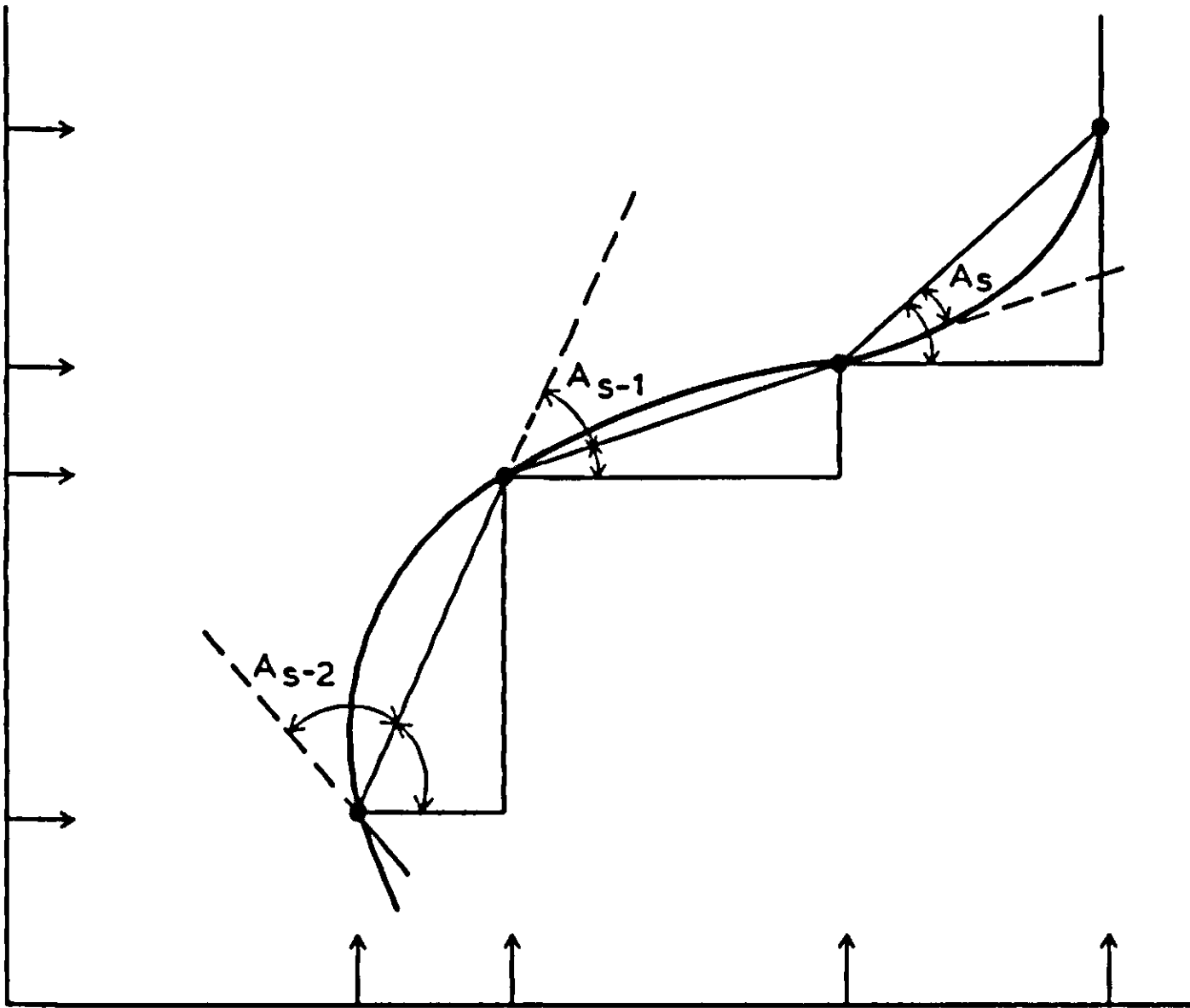


Figure 31. Determination of three consecutive angular deviations (A_{s-2} , A_{s-1} , A_s) after pacing linear distances of fixed length. (Source: Sabelis, 1981).

$$\text{DIR} = \text{INTGRL}(\text{DIRI}, A/\text{DEL T}) \text{ or mathematically } \text{DIR} = \int (A/\Delta t) dt$$

where DIRI is the initial direction in radians, relative to a reference direction, A is the angular deviation (A_s) and DELT is the time step of integration (DEL T).

To calculate movement in two dimensions, we write in CSMP:

$$\text{CSDR} = \text{COS}(\text{DIR})$$

$$\text{SNDR} = \text{SIN}(\text{DIR})$$

$$X = \text{INTGRL}(X_0, \text{CSDR}/\text{UNIT}) \text{ or mathematically } X_t = \int_0^t (\text{CSDR}/\text{UNIT}) dt$$

$$Y = \text{INTGRL}(Y_0, \text{SNDR}/\text{UNIT}) \text{ or mathematically } Y_t = \int_0^t (\text{SNDR}/\text{UNIT}) dt$$

The term UNIT is required because the magnitudes of CSDR and SNDR cannot exceed unity, whereas X and Y are the distances from the start of the step. The time step DELT dictates the physical time step taken by a predator, so that this

time step of integration should be based on the step size of the predator. UNIT thus determines the organism's speed of movement.

We can now consider the simulation of the successive values of A_s , the angular deviation. First, it should be noted that A_s is the angular deviation per step. This means that the measurements used in constructing the model cannot be analysed until the step length has been decided. The modelling approach is thus required early on in the study; it is not sufficient to collect data first and make the model later.

The rate of turning is described in terms of two components, one of which depends on previous movements, the other being considered as a random 'error term'. A_s can be expressed as the dependent variable of a multiple auto-regression:

$$A_s = a_1 \cdot A_{s-1} + a_2 \cdot A_{s-2} + \dots + a_m \cdot A_{s-m} + E_s$$

where a_1, a_2, \dots, a_m are the regression coefficients, and E_s is the random 'error term'; m is called the order of the process, and is a measure of the length of the animal's 'memory'. These higher order terms account for the memory of the animal that affects its present step direction.

Exercise 40

Give the equation for a first-order walking process. What is the effect of changing the sign of the coefficient from negative to positive?

In the simulation, E_s may be drawn at random from a specified distribution. The Tukey distribution is most appropriate since, by changing its three parameters, it can be made to approximate several other well-known distributions (Sabelis, 1981). This distribution can be generated as follows:

$$E_s = \mu + \sigma \cdot Y_p$$

$$Y_p = \begin{cases} (p^\lambda - (1-p)^\lambda)/\lambda & \lambda \neq 0 \\ \ln(p/(1-p)) & \lambda = 0 \end{cases}$$

where μ is a parameter determining the mean change in direction (independent of previous turns), σ determines the variance in the angular deviations, and λ is a parameter related to the distribution's kurtosis. (A distribution with high kurtosis has a relatively sharp peak and long flat tails.) The variable p is the cumulative frequency, and is drawn at random from a uniform distribution ($0 \leq p \leq 1$). The approximated distribution depends on the value of λ (Snedecor & Cochran, 1980), as follows:

$\lambda = 1$	uniform
$\lambda = 0.14$	normal
$\lambda = 0$	logistic
$\lambda = -0.85$	Cauchy

Exercise 41

How well does the Tukey approximation compare with a uniform distribution? What are the maximum and minimum values of E_s ? What behaviour is expressed by μ ?

The angular deviation in a first-order walking process is now given by

$$A_s = a \cdot A_{s-1} + \mu + \sigma \cdot (p^\lambda - (1-p)^\lambda) / \lambda$$

In fact, many observed walking patterns are 'zero order' (i.e. the change in direction during step s is independent of previous turns) so the coefficient a equals 0. A_s can thus be calculated as follows in CSMP:

$$P = \text{RNDGEN}(U)$$

$$A = \text{MU} + \text{SIGMA} * (P ** \text{LAMBDA} - (1. - P) ** \text{LAMBDA}) / \text{LAMBDA}$$

where $\text{MU} = \mu$, $\text{SIGMA} = \sigma$, $\text{LAMBDA} = \lambda$; $U =$ an odd integer, so that $0 \leq P \leq 1$.

Figure 32 presents some examples of the walking patterns generated by this model, with different values of σ and λ . These figures represent the patterns of single individuals, although they were generated using parameters which describe the range of behaviours measured in a population (e.g. μ , σ , the regression coefficients a_i).

The use of such a model to determine the effects of an individual's behaviour on changes at the population level (e.g., dispersion, effects on prey density etc.), involves two main steps. First, the consequences of an individual's action must be calculated; then these effects must be summed or averaged over the whole population.

Clearly, an individual's behaviour has a wide range of consequences: dispersal, rate of encounter with prey individuals (which also depends on the distribution of the prey population) or mates, etc. The consequences to be modelled thus depend on the purpose of the model.

3.2.4 Descriptive models and the consequences of dispersion

The previous two Subsections have considered techniques for modelling dispersal – the process by which a population's dispersion pattern develops. In many cases, however, quantitative data at the process level are insufficient to

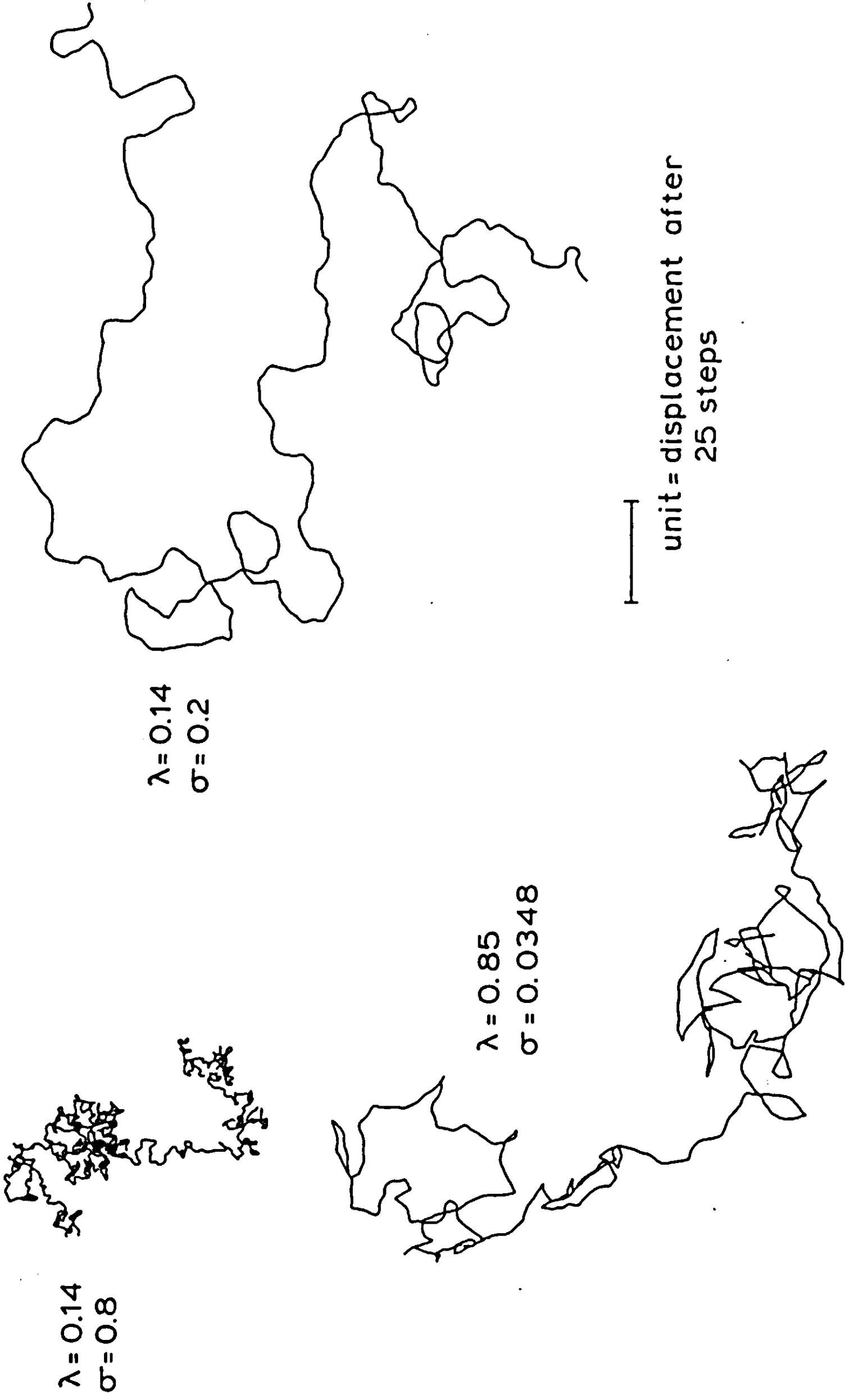


Figure 32. Some walking pattern matched by simulation. (Source: Sabelis, 1981).

construct an explanatory model of the resulting behaviour and dispersion. It is also usually unnecessary to use detailed explanatory models of individuals behaviour to predict effects at the population level: simpler descriptive models of the distribution of individuals in space are often sufficient as a basis for models of population dynamics (see Section 3.3). Although these descriptive functions may be summaries of the results of more detailed explanatory simulation models, the lack of appropriate behavioural measurements often means that simple statistical distributions must be used as a basis for studying the consequences of dispersion. Such consequences may concern the possibilities of biological control in various distributed prey populations. This is illustrated in Subsection 3.2.5.

Before presenting some of the more commonly used models, three cases should be distinguished:

1. A population of distinct individuals, distributed among discrete sample units (e.g. aphids distributed among wheat tillers);
2. Distinct individuals distributed over a continuous area or volume (e.g. mites on a leaf, nematodes in soil, or weed seeds in a field);
3. Indistinct 'individuals' distributed over a continuous area (e.g. fungal lesions on leaves).

In models simulating the consequences of dispersion, cases (2) and (3) are often considered as if they were populations of type (1); continuous areas are divided into 'discrete' squares. The reason for this is that most distribution models can be applied only to case (1).

We can now consider some of the statistical distributions commonly used to describe the spatial distributions of pest and disease populations.

Spatial distributions Considerable information on spatial distribution of individuals is given in most ecological textbooks; e.g. Southwood (1978). Here, only the most common distributions will be discussed.

The Poisson distribution This arises if organisms are distributed at random i.e., the probability of an individual being 'placed' in a particular sample unit is independent of the number of individuals already there, and does not vary among sample units. The probability that a sample unit contains x individuals is given by:

$$P_x = \mu^x \cdot e^{-\mu} / x!$$

where μ is the mean density per unit. An important feature of this distribution is that the between-unit variance in density is equal to the mean.

Generalized distributions These can arise if individuals are clustered. The most commonly used such distribution is the Negative Binomial Distribution (NBD), in which cluster size follows a logarithmic distribution, and clusters are distrib-

uted at random (Poisson). Here, the probability that a cluster contains i individuals is

$$P_i = -a^i / (i \cdot \ln(1 - a)) \quad \text{Equation 49}$$

where a is a constant ($0 < a < 1$). The number of clusters per sample unit is a Poisson variable.

The main features of the NBD are, in terms of its two parameters μ (mean density) and k (which describes the degree of clustering),

$$V = \mu \cdot (1 + \mu/k) \quad \text{Equation 50}$$

$$P_x = \frac{(k + x - 1)! \cdot \mu^x}{k^x \cdot (k - 1)! \cdot x!} \cdot (1 + \mu/k)^{-(k+x)}$$

where V is the between-sample unit variance in the number of individuals, and P_x the probability that a sample unit contains x individuals.

The full NBD can be generated from:

$$P_0 = (1 + \mu/k)^{-k} \quad \text{Equation 51}$$

$$P_{x+1} = \frac{P_x \cdot \mu \cdot (k + x)}{k \cdot (x + 1) \cdot (1 + \mu/k)} \quad \text{Equation 52}$$

For the derivation of Equations 51 and 52 the reader should refer to the ecology textbooks already mentioned.

Fitting a distribution to observed data Clearly, before testing whether field data can be described by one of these distributions, it is necessary to estimate the parameters. Estimation of the mean, μ , from the sample mean (m), e.g. the number of individuals per tiller, per leaf, m^{-2} , or per plant, is sufficient to generate a Poisson distribution; but the NBD requires additional parameters. Besides estimating the mean, the k -value characterizing the level of clustering should also be estimated.

Three methods are commonly used to estimate k for an observed distribution (Southwood, 1978). The first uses iteration to solve the equation (see Equation 51):

$$\log P_0 = -k \cdot \log(1 + m/k) \quad \text{Equation 53}$$

where m is the sample mean (an estimate of μ) and P_0 is the proportion of unoccupied sampling units (e.g. wheat tillers carrying no aphids). The second method uses the relation (see Equation 50):

$$k = m^2 / (V - m), \quad \text{Equation 54}$$

where V is the between-tiller variance in aphid density. Finally, a maximum likelihood estimate of k can be found by iterative solution of the equation

$$N \cdot \ln(1 + m/k) = \sum_x \left(\frac{A_x}{k + x} \right) \quad \text{Equation 55}$$

where N is the number of sample units, and A_x the number of sample units carrying more than x individuals (e.g. $A_6 = f_7 + f_8 + f_9 + \dots$). Equations 53–55 are derived from the ecological textbooks.

Having estimated the appropriate parameter values, the measured data can be compared with the predicted distribution. The simplest way of showing to what extent the data fit the predictions, involves comparing the moments (variance, skewness and kurtosis) of the observed distribution with those of the predicted form.

If the data conform to a Poisson distribution, the sample variance will be equal to the sample mean, i.e. $V/m = 1$. This is easily tested, since $N \cdot V/m$ is distributed approximately as a χ^2 variate with $N - 1$ degrees of freedom (N is the number of sample units).

To test whether observed data conform to an NBD with known k , either the sample variance or the skewness can be used, depending on the values of m and k . Details of these methods are again given in Southwood (1978).

Exercise 42

Table 8 gives data on the frequency of *Drosophila melanogaster* (Meigen) containing various numbers of eggs of the parasitoid *Pseudeucoila bochei* (Weld) from an experiment described by van Lenteren et al., 1978. Do these data support the hypothesis that all hosts, whether previously infested with parasites or not, are equally attractive to the parasitoids?

Table 8. Distribution of eggs of the parasite *P. bochei* among larvae of *D. melanogaster*. (Source: van Lenteren et al., 1978).

Number of egg per host larvae	Frequency
0	0
1	8
2	19
3	19
4	4
5+	0

The comparison of observed and predicted distributions can only be used to test the descriptive accuracy of a particular model. If the data differ significantly from the predictions, then at least one of the model's assumptions must be untrue. A close correspondence between observations and predictions, however, does not confirm the assumptions underlying the theoretical distribution, and cannot be used as a basis for inferring that the mechanisms result in an observed distribution. For example, a Negative Binomial Distribution may result from the random distribution of clusters (whose size is distributed according to Equation 49) among identical sample units, or from the random distribution of individuals among sample units of varying suitability (see Pielou, 1977).

3.2.5 *Effect of dispersion on the dynamics of an aphid-parasite system, an example*

The system to be considered here involves the cereal aphid, *Sitobion avenae* on winter wheat, and its hymenopterous parasitoid *Aphidius rhopalosiphi*. The original model of population dynamics assumed implicitly that the aphids and parasites were distributed uniformly among wheat tillers. To test the effects of introducing more realistic assumptions about the spatial distributions of the two species, a simulation model that takes the measured distributions into account was developed (Rabbinge et al., 1984a).

A series of steps is involved:

1. Selecting the appropriate statistical distribution, for describing the populations' dispersion;
2. Calculating the distribution parameters;
3. Determining a method for predicting these parameters;
4. Generating the populations' distribution; and
5. Calculating the resulting parasitism rate.

Choice of a distribution (1) Field data on *S. avenae*, when compared with the results predicted by the Poisson, Negative Binomial, and Neyman A distributions, have been shown in most cases to be best described by the Negative Binomial Distribution (Rabbinge & Mantel, 1981). The model, therefore, assumes that this is the appropriate form.

The parasites are assumed to be dispersed according to one of two extreme distributions: either uniformly (i.e., the likelihood that a parasite is present on a tiller is independent of the number of aphids present) or in proportion to the number of aphids on each tiller.

Estimation of the parameters (2) As stated above (Subsection 3.2.4), the Negative Binomial Distribution is characterized by two parameters: the mean, μ , and k , which determines the degree of aggregation of the population. The mean density will be generated by the population model, so need not be estimated here. The parameter, k , however, must be determined on the basis of field observations.

Modelling the changes in k (3) Three methods have been used in various studies. The first relies on a descriptive relation between m and V , of the form:

$$V = a \cdot m^b \quad \text{Equation 56}$$

where a and b are constants to be estimated by regression from a series of observations on cereal aphid distribution (Taylor, 1961). This has been shown to describe the mean-variance relation for a wide range of species (Taylor et al., 1978). One parameter k can then be calculated from m (by substituting Equation 56 into 54)

$$k = m^2 / (am^2 - m) = m / (am^{b-1} - 1)$$

Alternatively, k can be estimated using Equation 53, by substituting a descriptive relation between m and P_0 (e.g. those found by Rabbinge & Mantel, 1981; Nachman, 1981).

The simplest method, which will be used here, relies on a regression of the maximum likelihood estimates of k on the mean density. Using sample data on cereal aphids, Rabbinge et al. (1984a) calculated the regression:

$$k = 0.3128 + 0.0724 \cdot m \quad \text{Equation 57}$$

Generation of the dispersion of the aphid population (4) The dispersion of the aphid population is generated in this example from the theoretically formulated curve for a Negative Binomial Distribution, which is characterized by the mean and the clustering parameter k . Within the theoretically defined distribution of individuals, various density classes are distinguished, within which the assumption of linearity for parasite-infestation rate is valid.

In this example, five density classes are considered: 0, 1–5, 6–25, 26–125, and > 126 aphids tiller⁻¹, respectively. The proportion of tillers in each class is calculated with Equations 51 and 57, using FORTRAN DO loops in a NOSORT section of the program. The mean aphid density is used first, to calculate the dispersion parameter, k . The frequencies in the various density classes are then generated.

```

K = 0.313 + 0.072* MEAN
P0 = (1. + MEAN/K)** (-K)
SUM1 = 0
P = P0
DO 1 I = 1,5
  Q = P* MEAN*(K + I - 1.)/(I*(K + MEAN))
  SUM1 = SUM1 + Q
  P = Q
1 CONTINUE

```

Here, P_0 is the frequency of tillers bearing no aphids; the final value of SUM1 is the sum of the frequencies in classes 1 to 5. Similar methods are used to calculate the frequencies of tillers in the other three groups of density classes.

The parasites can then be allotted to the various groups of tillers, either uniformly or in proportion to aphid density. Generation of the spatial distributions requires considerable computation time. Fortunately, the form of the distribution changes only gradually (Kroon & Driessen, 1982); this means that the aphids and parasites need not be redistributed each DELT (in this case, $\text{DEL T} = 0.01$ day). Instead, the dispersion section of the program is used only twice per simulated day. (This approach to the problem of 'Stiff equations' will be considered in Subsection 3.4.6).

Calculating the resulting rate of parasitism (5) Having modelled the distribution of aphids and parasites at the start of a time step, the total rate of parasitism can be calculated for the whole population. The parasitism rate (per parasitoid per day) increases with the number of aphids present on a tiller. This is modelled here using an AFGEN statement to describe the experimental results of Shirota et al. (1983) (Figure 33). The processes which determine this 'functional response' will be considered in Section 3.3. Its main features are that at low prey densities, parasitism is limited by the number of hosts available, while at higher densities it depends on the maximum rate at which a parasitoid can oviposit. The mean rate of oviposition is calculated for each density class, and averaged over all tillers (the weighting of individual rates depends on the proportion of tillers in the various density classes). The resulting mean rate of parasitism is then used to calculate the rate of transition from 'living' aphids to 'parasitized' aphids, which then forms a component of the mortality rate.

Figure 34 shows the results of three models: (1) aphids and parasites both uniformly distributed, (2) aphids distributed according to a Negative Binomial – parasites distributed uniformly, and (3) aphids distributed according to a Negative Binomial – parasites distributed in proportion to local aphid densities; i.e. most parasitoids are on the tillers with highest aphid densities.

Clearly, aggregation of parasitoids in areas of high aphid density increases the rate of parasitism, and thus reduces the peak aphid population. The magnitude of the effect, however, is small. In the conditions simulated here, therefore, increasing the parasitoids' searching efficiency does not have a significant influence on the growth of the aphid population; parasitism is thus unlikely to be a useful natural control method unless the density of parasites can be increased considerably.

3.2.6 *Discussion and conclusions*

The models introduced in this Section were chosen to illustrate approaches to modelling some of the aspects of dispersal and dispersion. Clearly, the range of phenomena covered by the term 'spatial heterogeneity' is far too great to review

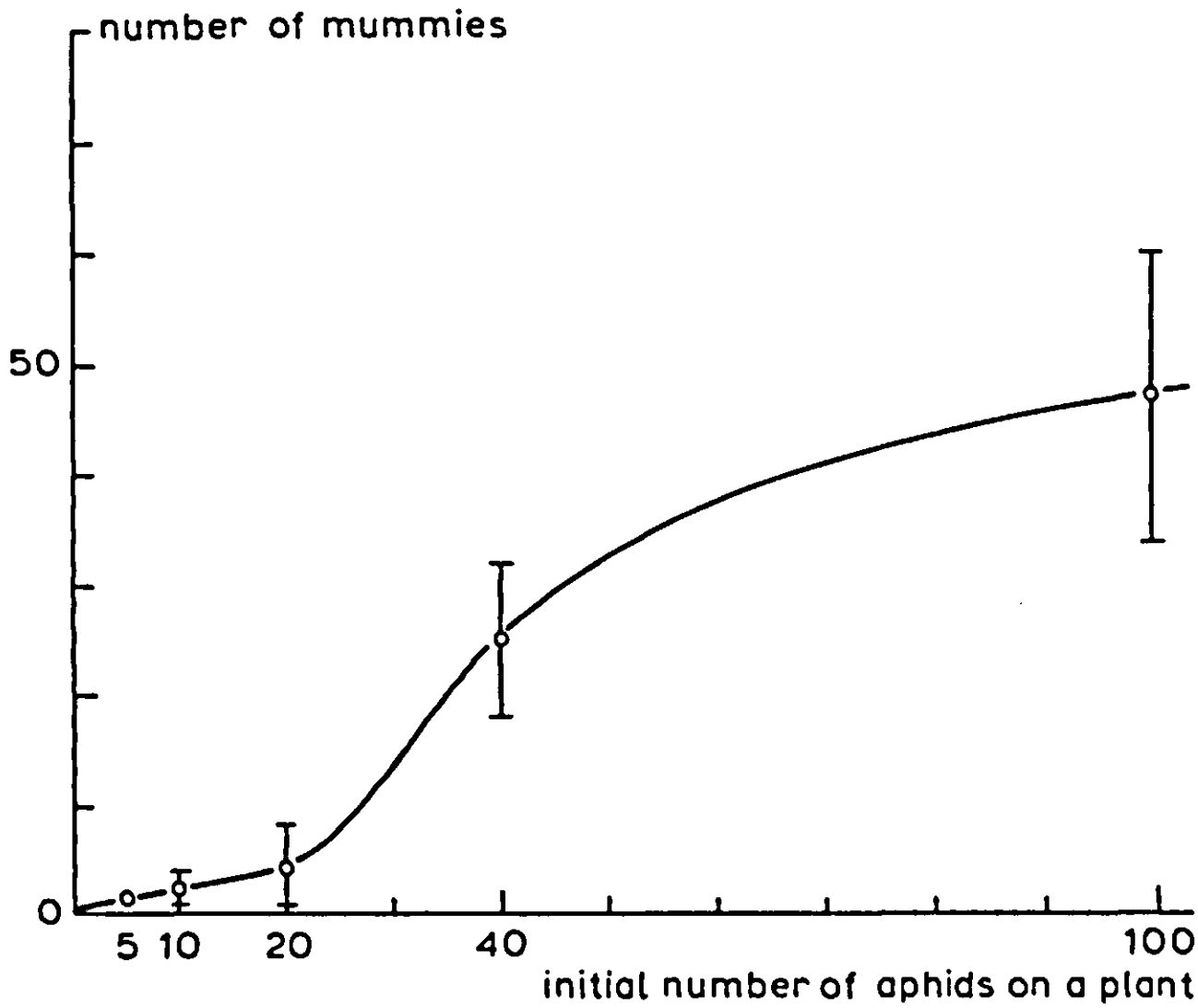


Figure 33. The functional response of *Aphidius rhopalosiphi* to changes in host density. (Source: Shirota et al., 1983).

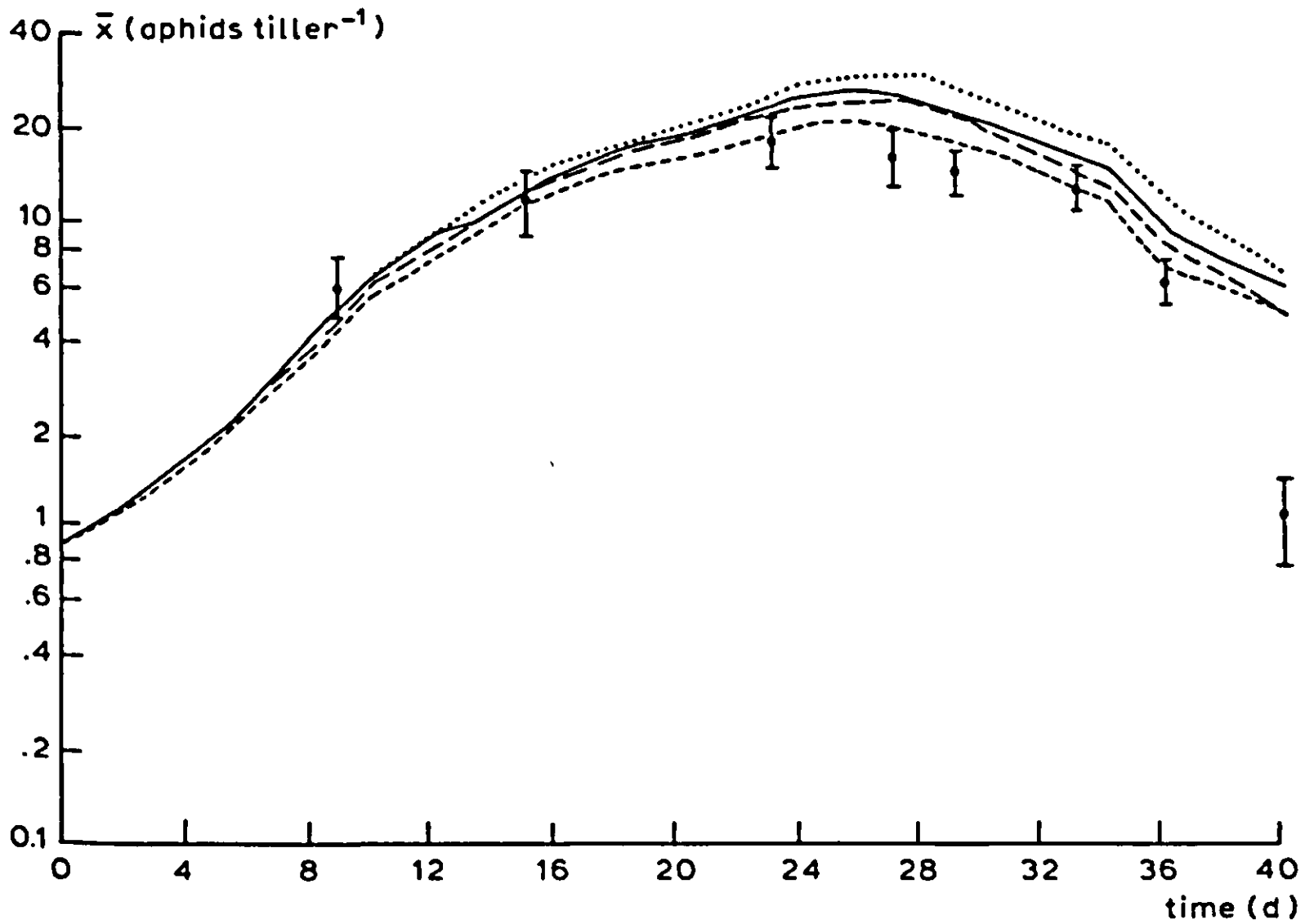


Figure 34. Mean aphid density (\bar{x}) in the field (I bar with 95% confidence intervals), and the results of simulations 1 (—), 2 (---) and 3 (-.-) (see text) and without parasitoids (....). (Source: Rabbinge et al., 1984a).

thoroughly in a single Section, but the models chosen certainly illustrate a number of important groups of features.

First, it is important to decide (in advance) whether the model is to be used to simulate dispersal (the process by which spatial distribution is produced) or the consequences of dispersion (the pattern resulting from dispersal).

Secondly, dispersal can be simulated at the level of either the individual or the population. Thus, Wagenmakers' model (1984) for passive dispersal of fungal spores simulates the process of dispersal in a system described in terms of features of the spore population; while the model for active dispersal simulates the behaviour of individual mites (Sabelis, 1981).

The other main aspect of modelling introduced in this Section, was that of evaluation of the consequences of a particular spatial distribution on the population dynamics of an organism. This was done using the model described in Subsection 3.2.5. Here, compound simulation (see also Section 3.3) was used to overcome problems of Monte Carlo analysis. The latter is needed in case stochastic processes are introduced in the models. This was not done in this Section but will be discussed in the next Section 3.3.

The very different levels and approaches of the examples considered in this Section, show that there is no standard 'right way' of simulating dispersal and dispersion. As in most of the other areas treated in this book, the choice of methods must depend on the aims of the study, the biological or physical processes concerned, and the information available.

3.3 Predator-prey models, stochasticity

R. Rabbinge and S.A. Ward

3.3.1 Introduction

Population growth in time and space can be simulated using the techniques presented in Chapter 2, and is illustrated for polycyclic epidemics in Section 3.1. Applying these methods to predator-prey or host-parasite systems would result in population models for either predator and prey, or host and parasite. In such models, the interaction between predator and prey, or host and parasite, determines the decrease in prey numbers due to predation, and the growth in the number of predators as a result of feeding.

Predator-prey or host-parasite relations are probably the most frequently modelled phenomena in population biology. Predator-prey models, at all levels of detail and complexity, can be found in the literature. These models vary from differential equations expressing predator-prey relations in terms of a single variable, to very detailed predator-prey models at individual and population levels; incorporating much ethological and physiological information. Stochastic elements are often included. In this Section, a simple model of the population dynamics of prey and predators is presented. The behavioural and physiological factors influencing predation rate are then considered at the level of the individual. Finally, methods are introduced which can be used to calculate population changes using models of predation rates for individuals.

3.3.2 Lotka-Volterra equations for predator-prey interactions

The logistic growth equation (Section 3.1, Equation 37) can be applied in predator-prey systems to both prey and predator. The predation process is then introduced as a reduction in the growth rate of the prey population, and the increase in predator numbers is made dependent on the availability of prey. Lotka (1925) and Volterra (1931) proposed the following equations for changes in prey and predator numbers:

$$\text{for the prey, } \frac{dx}{dt} = (a - b \cdot x) \cdot x - c \cdot x \cdot y; \quad \text{Equation 58}$$

$$\text{for the predator, } \frac{dy}{dt} = -e \cdot y + d \cdot x \cdot y. \quad \text{Equation 59}$$

In these equations, the following implicit assumptions are made:

1. Densities of prey and predators can be expressed as single variables;

2. Interaction between prey and predator responds instantaneously to changes in density;
3. In the absence of predation (i.e. with $c \cdot x \cdot y = 0$), the prey population grows according to a logistic growth equation;
4. In the absence of prey, the predator population declines exponentially;
5. The rate of consumption of prey is proportional to the product of prey and predator densities;
6. The effects of predator satiation are negligible.

None of these assumptions is valid in real predator-prey systems. Nevertheless, these equations may help to provide some insight into the operation of predator-prey systems. It is possible, for example, to use them to study the behaviour of such systems at equilibrium. Here, the rates of change are zero, so conditions at equilibrium can be defined as:

for the prey: $\frac{dx}{dt} = 0$, so $a - b \cdot x - c \cdot y = 0$;

for the predator: $\frac{dy}{dt} = 0$, so $-e + d \cdot x = 0$.

Figure 35 shows the trajectory of the system when $b/c > 0$. When the densities of prey or predator, x and y respectively, are below their equilibrium, the rates of change are positive and their numbers increase (Equations 58 and 59). When prey or predator densities are above their equilibrium, the rates are negative and the numbers of x and y decrease. As a result, the numbers of x and y approach an equilibrium value at the junction of both equilibrium lines. The system moves in an anti-clockwise spiral towards stable equilibrium. If $b/c < 0$, however, the system spirals away from equilibrium, until either the predator population or both prey and predators become extinct. Apparently, the ratio between the parameter which expresses intraspecific effects of the prey population (b) and the parameter which expresses predation activity (c), determines whether stable equilibrium, or extinction of prey or predator populations, will be reached. This ratio determines the position of both equilibrium lines; the graphical representation helps to explain the consequences of the change in b/c .

Exercise 43

Plot the changes in the populations of prey, x , and predators, y , as functions of time, for $b/c < 0$, $b/c = 0$ and $b/c > 0$. Try to explain these phenomena.

To evaluate the consequences of changing various parameter values for population fluctuations of prey and predator, a simple simulation model may help.

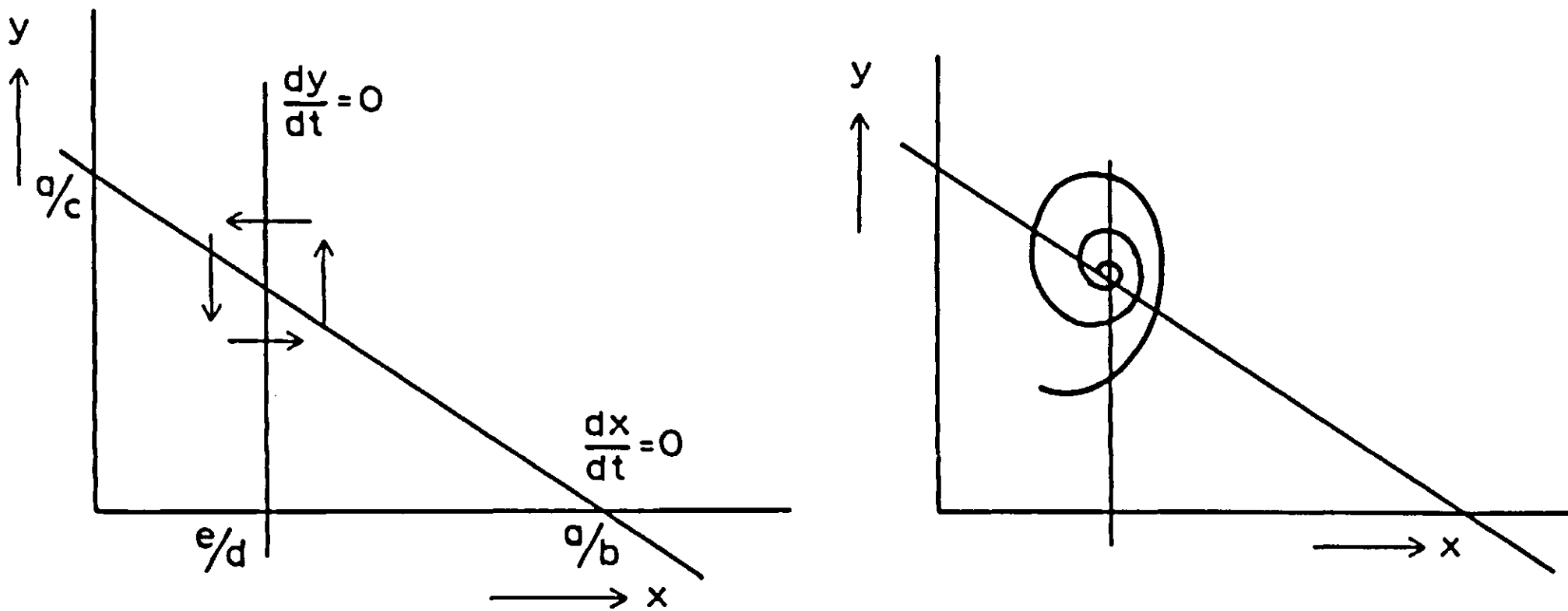


Figure 35. Equilibrium conditions for prey and predator populations; when $b/c > 0$ there will be a stable equilibrium.

This is formulated in the simulation language CSMP (see Appendix 5). Such a program reads as follows:

TITLE PREDATOR-PREY

INITIAL

INCON PREYI = 10., PREDI = 2.

PARAM A = 0.1732, B = 0.0577, C = 0.0867, D = 0.1540, E = 0.2310

DYNAMIC

PREY = INTGRL(PREYI, RPREY)

PRED = INTGRL(PREDI, RPRED)

RPREY = (A - B * PREY) * PREY - C * PREY * PRED

RPRED = -E * PRED + D * PREY * PRED

TIMER FINTIM = 50., DELT = 0.4, OUTDEL = 5.

OUTPUT PREY,PRED

METHOD RECT

END

STOP

ENDJOB

Exercise 44

Give the time coefficients of this simple system. What are the dimensions of A, B, C, D and E? Test the sensitivity of the output to changes in the values of these parameters. Explain the outcomes of the model. Run the model with various combinations of parameter values.

This simple predator-prey model may offer some insight into the functioning of predator-prey systems. It is a conceptual model, which can be used at the very beginning of the scientific approach to the problem. The addition of further detail may improve the model's realism and, ultimately, yield a comprehensive simulation model. This 'top-down' approach is different from the 'bottom-up' approach used in Section 3.1 for the epidemiological models. Here, we can proceed by modifying the model's assumptions. This increases its realism but does not imply that it is now a comprehensive explanatory model. It is still conceptual and various other ways of improvement, discussed below, are possible. For example, assumption 2, that both prey and predator react instantaneously to changes in density, is unrealistic as there is generally a considerable time delay in the numerical response of predator density to changing prey density. To take this delay into account, a separate state variable is introduced which accumulates the numbers of recently consumed prey. The state variable PREYP is emptied, and its content multiplied by the inverse of a time coefficient of, for example, 3 days, so that an exponentially weighted average of prey consumption rate is found:

$$\text{PREYP} = \text{INTGRL}(0., C * \text{PREY} * \text{PRED} - \text{PREYP}/3.)$$

This state variable, expressing predation activity, is used as the independent variable of the table from which D is read:

$$D = \text{AFGEN}(\text{DT}, \text{PREYP})$$

Thus, as far as numerical response is concerned, the model has become more realistic. Even so, the changes are arbitrary and lack experimental quantitative support.

Assumptions 5 and 6 are equally unrealistic, since a predator cannot continue to eat indefinitely. Long before its appetite is satisfied, the predator becomes more selective and tends to accept only the most attractive prey, which may then be only partially consumed. This selective behaviour, which depends on satiation, can be introduced into the Lotka-Volterra equations by inserting a state variable representing, for example, the gut content. The predation rate is then dependent on this gut content.

3.3.3 Prey preference and predator satiation

Several animal ecologists have tried to quantify the physiological conditions determining predator behaviour. Holling (1966), Fransz (1974) and many other workers quantified the influence of physiological conditions on predation activity. They determined the effect of this state variable on predator behaviour, and its consequences for the interactions between prey and predator populations.

Detailed observations have shown the presence of a functional response; as the number of prey per unit area increases, predation activity also increases until a certain plateau is reached. Holling (1966) distinguishes three basic functional responses (Figure 36). Type 1 includes a linear increase in predation rate per predator, as prey density increases, until a maximum predation rate is reached. This type of response is found only in a few filter-feeding crustaceae. As prey density increases, predation rate also increases until the filters are completely full; at that level, increases in prey density do not result in a further increase in predation rate.

Type 2 is often found in arthropod predators. Predation increases at a decreasing rate with increasing prey density, until a plateau is reached. The flattening is due either to satiation, which decreases predation activity, or to the time needed for the various components of the predation process to accumulate. Prey handling, prey consumption, and prey searching; all require time, which becomes a limiting factor at higher prey densities. Thus, time limitation and satiation together limit the predation rate. The predator gradually reaches satiation and, as a result, the predation rate steadily approaches its maximum value. The type 2 functional response can be described with a hyperbolic function, or may be tabulated with an Arbitrary Function GENERator (in CSMP: AFGEN).

Exercise 45

Introduce the type 2 functional response into the Lotka-Volterra equations. Adapt the simulation program and run it with various self-chosen values for the parameters.

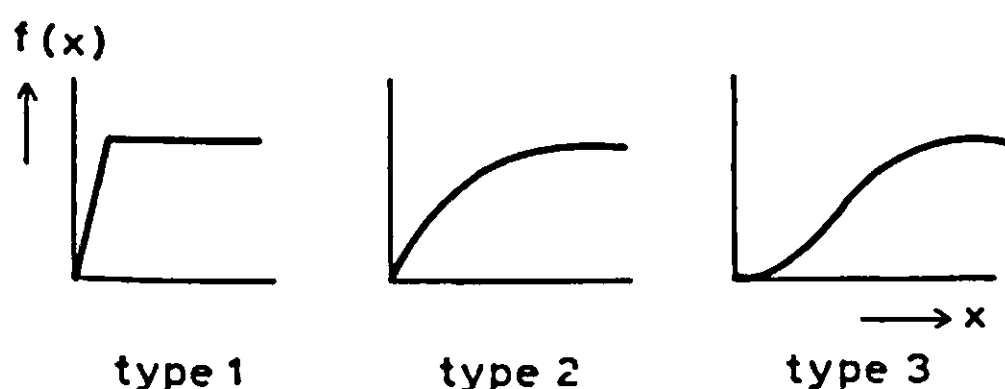


Figure 36. Three functional responses of predation rate with regard to prey density. (Source: Holling, 1966).

The type 3 functional response is often found in vertebrate predators. It differs from the type 2 response in that the predation rate at low prey densities, shows a more than proportional increase with prey density. This could be due to several reasons. First, if the prey occurs in clusters or patches, the predator may leave low-density patches, but remain for a longer time in dense prey clusters (e.g. the parasitoid, *Aphelinus thomsoni* (Collins et al., 1981)). Second, predators may 'switch' from one habitat type to another, depending on the densities of prey available (e.g., the predatory groundbeetle, *Pterostychus coerulescens* (Mols, 1989)). Finally, some predators may develop a 'search image' for a particular prey species if this species is abundant (e.g. the great tit, *Parus major* searching for caterpillars or aphids (van Balen, 1973)).

At high prey densities, satiation or handling time again limit the predation rate. Type 3 is thus sigmoid (Figure 36). Other factors, which can be important in determining the predation rate, include mutual interference between searching predators (Hassell & May, 1973) and the spatial distribution of prey and predators (see Subsection 3.2.4).

In addition to the effects of predation on prey mortality rate, the second main component of the predator-prey interaction (at the population level) is the effect of predation on the predators' rate of increase. In many insect parasitoids, each act of 'predation' (i.e. oviposition in a host) results in the production of a new 'predator' (parasitoid). In true predators, however, this relation is less direct; for example, a predator's feeding rate may determine either its rate of reproduction or its probability of surviving to maturity (Dixon, 1959).

Although the likely effects of these relations have been widely studied using general analytical models (Hassell, 1978), the complexity of real systems often means that numerical models must be used to study particular examples.

There is another reason for developing simulation models. During the predation process, some stochastic phenomena play a role; e.g. a certain probability for predator-prey encounters (which are discrete events) occurring within a limited time period. The effects of these stochastic elements on the predation process, and their consequences for the predation rate, can be evaluated using a numerical simulation model.

3.3.4 Stochastic and deterministic models

Many phenomena in ecology are stochastic: the appearance of a spore from a pustule, its arrival at a particular place at a particular time, the sampling of a population, or the killing of a prey by a predator. All these events occur with a certain probability. However, it is not the event as such that is important (except for the individual concerned), but its consequences for the overall rates. Thus sporulation rate, landing rate, predation rate etc., must be examined. Simulation models of the predation process are used to compute the expected number of prey killed, over time. The expected values are the means of many simulation experiments with individual predators. As the interval between the

captures is a state variable with a certain probability distribution, each experiment is a stochastic process with a variable number of captures in a well-defined time interval. The expected number of captures is estimated by dividing the total number of catches in a collection of experiments by the number of experiments. There may be important differences between the results of deterministic and stochastic models. In deterministic models, computations are based on the expected values of the parameters. However, this may introduce errors, since the mean of the values computed, using unprocessed values of the components, does not necessarily equal the value calculated using the expected values of the components: $\varepsilon(f(x)) \neq f(\varepsilon(x))$. In addition, stochastic models compute both the mean and the variance. Thus, generally, there are two reasons for using stochastic models:

1. Curvilinear relations between stochastic characteristics and rate variables mean that the use of mean values introduces a significant bias into the results;
2. Stochastic models can provide estimates of the variation in the system's behaviour. Sampling errors, for example, may have important consequences in interpreting the results.

To illustrate the consequences of deterministic and stochastic simulation of the predation process, simple deterministic and stochastic models of the predation process will be described and their results compared.

A computer model Assume that P is the number of prey killed by a predator in a certain time. The predation rate, dP/dt , depends on the predator's velocity, V , which has a uniform probability distribution between 0 and 1, so $0 \leq V \leq 1$.

If the rate of predation, dP/dt , is proportional to V , then $dP/dt = cV$, where c is a parameter whose value expresses predation efficiency; here $c = 10$.

A deterministic simulation of predation during the course of a day can be written in CSMP as:

TITLE DETERMINISTIC PREDATION

INITIAL

INCON PI = 0.0

PARAM V = 0.5, C = 10.0

DYNAMIC

P = INTGRL(PI, C * V)

TIMER FINTIM = 24., DELT = 1., OUTDEL = 1.

METHOD RECT

OUTPUT P

END

STOP

ENDJOB

Alternatively, this process can be modelled stochastically (with the velocity changing at random every hour) using the following program:

```
TITLE STOCHASTIC PREDATION
```

```
INITIAL
```

```
FIXED M
```

```
M = 315
```

```
INCON PI = 0.
```

```
PARAM C = 10.0
```

```
DYNAMIC
```

```
P = INTGRL(PI, C * V)
```

```
V = RNDGEN(M)
```

```
NOSORT
```

```
M = M + 2
```

```
TIMER FINTIM = 24.0, DELT = 1.0, OUTDEL = 1.
```

```
METHOD RECT
```

```
OUTPUT P
```

The statement $V = \text{RNDGEN}(M)$ is a CSMP function, which draws (each time interval of integration, DELT) a number at random from a standard uniform probability distribution between 0 and 1. M is an arbitrary odd integer chosen to initialize the random number generator. PI is the initial value of P, and C is a constant. The program uses time steps of 1 hour and continues the calculations for one day (24 hours). The expected value of P (ϵP) is the mean result of many replicates of the experiment (in this case 1000). The commands to repeat the performance 1000 times and to calculate the expectation value are given below in FORTRAN.

```
TERMINAL
```

```
PARAM NREP = 1000.
```

```
INCON SUMP = 0., COUNT = 0.
```

```
    SUMP = SUMP + P
```

```
    COUNT = COUNT + 1.
```

```
    IF (COUNT.GE.NREP) GOTO 1
```

```
    CALL RERUN
```

```
    GO TO 2
```

```
1 EP = SUMP/COUNT
```

```
    WRITE (6,100) EP
```

```
100 FORMAT (H1, F10.4)
```

```
    2 CONTINUE
```

```
END
```

```
STOP
```

```
ENDJOB
```

This TERMINAL section is performed once per run, when TIME reaches the value FINTIM.

With a uniform probability distribution, an analytical solution of $\varepsilon(P)$ is possible because P is the sum of a number of stochastic variables:

$$\varepsilon(P) = PI + 24 \cdot \varepsilon(cV)$$

$$\varepsilon(cV) = \int_0^1 cV dV = \frac{1}{2} \cdot cV^2 \Big|_0^1 = 5$$

$$\varepsilon(P) = 0 + 24 \cdot 5 = 120$$

The deterministic computation of this model is found by accumulating the expected values during the observation period.

$$P = PI + 24 \cdot c \cdot \varepsilon(V)$$

$$\varepsilon(V) = 0.5$$

$$P = 0 + 24 \cdot 10 \cdot 0.5 = 120$$

Thus, with dP/dt proportional to V , the deterministic model (using \bar{V}) yields the same result as the stochastic version, since $\varepsilon(f(x)) = f(\varepsilon(x))$. If the relation between dP/dt and V is non-linear, however, the deterministic model introduces important errors.

Consider the following simple example. We wish to determine the mean rate of predation by a predator whose velocity varies at random as assumed above. The individual predation rate is

$$dP/dt = c \cdot V^{\frac{1}{2}}$$

and V has a uniform distribution between 0 and 1. A deterministic model, using the population's mean V gives

$$P = PI + 24 \cdot c \cdot (\varepsilon(V))^{\frac{1}{2}}$$

where $\varepsilon(V) = 0.5$, so

$$P = 0 + 240 \cdot (0.5)^{\frac{1}{2}} = 169.7$$

A stochastic model, however, which allows for variation in V , yields:

$$P = PI + 24 \cdot c \cdot \varepsilon(V^{\frac{1}{2}})$$

$$\varepsilon(V^{\frac{1}{2}}) = \int_0^1 V^{\frac{1}{2}} dV = \frac{2}{3} V^{3/2} \Big|_0^1 = 0.67,$$

so $P = 0 + 240 \cdot 0.67 = 160.8$

The use of $\varepsilon(V)$ in the deterministic model, thus results in an overestimation of the total predation. This is because the curvilinear relation, between the predation rate and the velocity of the individual predators, means that

$$d(\varepsilon(P))/dt \neq c \cdot (\varepsilon(V))^{\frac{1}{2}}$$

Exercise 46

Use a deterministic model and a stochastic model to calculate the number of prey killed per day when the relationship between the number of prey killed per hour and the predator's velocity is described by $dP/dt = cV^{3/2}$; c equals 8 and V has a standard uniform probability distribution. Make these calculations both numerically and analytically.

The case of the stochastic simulation is described above. When the parameters are dependent upon environmental factors or a relation, such as the dependency of predation rate on velocity, more complicated simulation models are needed. However, the basic structure remains the same.

Basically, the process of sampling from a population, needed in many population studies, is the same. This is explained by de Wit & Goudriaan (1978) for a population model of protozoa growing on a bacterial culture.

3.3.5 Modelling at the population level

The model STOCHASTIC PREDATION simulates prey mortality caused by a predator moving with a velocity that changes unpredictably during the 24 hour foraging period. When the relation between V and dP/dt is non-linear, models that fail to account for the variation in V yield erroneous results.

Similar problems are encountered in modelling changes at the population level. For example, the effects of a population of predators cannot be accurately modelled by using the population mean of the search parameters (velocity, handling time, etc.), unless these parameters are the same for all individual predators; in which case, stochastic models can be used to simulate the consequences of individual variation.

Areas where true stochasticity is important at the population level include, for example, mortality in small populations and the effects of sampling. For examples and discussion of these areas see Pielou (1974) and de Wit & Goudriaan (1978). An example based on the predation process above: in the stochastic model for a population of individuals the assumption is made that velocity has a well-defined probability distribution. The average velocity is:

$$V = \sum_{i=1}^n V_i/n_i$$

where V_i is the velocity of individuals in one predation experiment. When V_i is constant, then a deterministic model could be used. However, this is virtually never true; therefore, calculations using various individual velocities should be done. The mean and variance may be computed because the rates in a single predation experiment have a uniform probability distribution. Therefore, the mean velocity is computed as: $\varepsilon(V_i) = 0.5$, and its variance computed as:

$$\text{var}(V_i) = \int_0^1 V_i^2 dV_i - \left(\int_0^1 V_i dV_i \right)^2 = 1/3 V_i^3 \Big|_0^1 - (1/2 \cdot V_i^2 \Big|_0^1)^2 = 1/3 - 1/4 = 1/12$$

In a population of n individuals the mean velocity is thus:

$$\varepsilon(V) = n/n \cdot 0.5 = 0.5$$

and its variance is computed as

$$\text{var}(V) = n/n^2 \cdot 1/12 = 1/(12n)$$

As with the 'individual' model, the results of this 'population' model differ from the deterministic model of an individual predation process because of the curvilinear relationship between stochastic variables and the state or rate variables. Also, the variance of the model is different.

The results in this section serve to emphasize an important problem in the use of experimental data on individuals to construct models to simulate the dynamics of populations. Unless features of population dynamics depend linearly on components of individuals' behaviour (e.g. velocity), the use of the mean behaviour may introduce significant errors into simulations at the population level. Therefore, where rate variables depend non-linearly on variable or stochastic state (or rate) variables, deterministic models are often inadequate.

3.3.6 *Other methods*

The model STOCHASTIC PREDATION illustrates the use of Monte Carlo analysis to obtain results at the population level using information about individual predators. Effectively, it 'samples' 1000 predators at random, and uses each predator in a simulated experiment. In principle, therefore, it solves the problem of stochasticity in the same way as the model of dispersal, described in Subsection 3.2.3 (Sabelis, 1981).

Repeated use of stochastic models, however, is time-consuming and expensive, so other methods, such as the queuing approach of Curry & De Michele (1977) and the compound simulation of Fransz (1974), have been developed to mimic stochasticity. The queuing technique requires only a limited amount of computer time. Basically, this method may be compared with calculating the waiting time of a patient in the dentist's waiting room. The patient may enter the waiting room (be encountered by a predator) with a certain expectance of service (being eaten).

Compound simulation is an intermediate approach between the stochastic model, which gives correct results but requires a lot of computing time, and the deterministic model, which requires less computer time but gives erroneous results. In this intermediate approach, deterministic simulation is applied to classes of the stochastic variables. The classes in this method of compound simulation, are chosen in such a way that within the classes the relation between velocity and predation rate is approximately linear. The number of classes depends on the balance required between accuracy and computer time. The calculation, for each class of individuals, is made at each time step of integration, after which the contents of the classes are updated and another computation starts with the redistributed classes of individuals. In this way, only one simulation needs to be carried out for each set of conditions, instead of 1000 runs, as required for the Monte Carlo method. Replication of all computations is omitted, and replaced by a complicated, but not time-consuming, system of book-keeping of predators, distributed each time interval among classes of individuals.

Sabelis (1981) described the application of Fransz's compound simulation, Monte Carlo techniques and queuing techniques to the predation process of mites. He showed that all three methods produced results that were within the confidence intervals of the measurements. The queuing techniques required the least computing time, whereas the deterministic model gave erroneous results. Although these mimicking procedures have contributed a great deal to the accurate simulation of predation rates, they are still too complicated to be applied to population models of prey and predators.

3.3.7 *Equilibria*

Simulation of individual predators shows that if prey density is kept roughly constant, the predator population reaches equilibrium. In that situation, the physiological condition of the predator oscillates, with low amplitudes, around a constant level. Changes in this equilibrium level are slow in comparison with changes in population composition. The time coefficient of this change is thus large in comparison with those for other changes in the system, such as development and growth. This equilibrium level is determined by prey and predator densities, and by temperature. At equilibrium, velocity and other variables determining predation rate also vary slightly, relative to the system as a whole. This characteristic of many predator-prey systems permits the computation of the predation rate at each level of the motivation state or physiological condition of the predator, using the expected values of the component variables. Use of this approach in population models for predator-prey systems will be illustrated for an acarine system in Section 3.4.

3.4 Population models for fruit-tree red spider mite and predatory mites

R. Rabbinge

3.4.1 Introduction

This Section describes a basic model for simulating the population dynamics of the harmful fruit-tree red spider mite, *Panonychus ulmi* (Koch), and one of its natural enemies, the predatory mite *Amblyseius potentillae*. The model, its results and evaluation are briefly presented; a more detailed description of the model, its construction and parameter values, verification and evaluation are given in another monograph in this series (Rabbinge, 1976).

The fruit-tree red spider mite belongs to the family Tetranychidae, a subgroup of the class of Acarina. The members of this vast family are found almost all over the world and cause damage in several types of plants. The fruit-tree red spider mite is one of the most harmful organisms in deciduous orchards, and its control is the major task of the fruit grower. In the last twenty years or so, the mites have become increasingly resistant to the various biocides, so the development of other control techniques has been stimulated. Biological control is an attractive alternative. It is already being practised in several places, and field experiments on the release of predatory mites have proved to be successful.

3.4.2 Fruit-tree red spider mite

Figure 37 shows the life cycle of the fruit-tree red spider mite. The mites develop from eggs through several juvenile stages into adults. The female adults deposit their eggs on leaves and a new generation starts; there may be up to six generations a year. Due to a combination of daylength, average daily temperature and food quality, some juveniles may develop into the 'winter form' which oviposit in sheltered places on branches and twigs, but are otherwise indistinguishable from the 'summer form'. (The transition to the winter form, which is partly reversible, is a complicated process and is not discussed here.) Their eggs, winter eggs, have a thicker scale and are redder than the summer eggs. The winter eggs do not hatch until after the winter.

To mimic dispersion in hatching, development classes of the eggs are distinguished. The number of classes and the method of simulation depend on the relative dispersion at different temperatures (see Section 2.2). The start of the hatching process is induced by a combination of external variables: length of cold period, daylength and temperature. Some mites die during the hatching process; their relative mortality rate depends on temperature.

The eggs hatch into juveniles which moult several times during their development into adults. During each juvenile stage, different development classes can

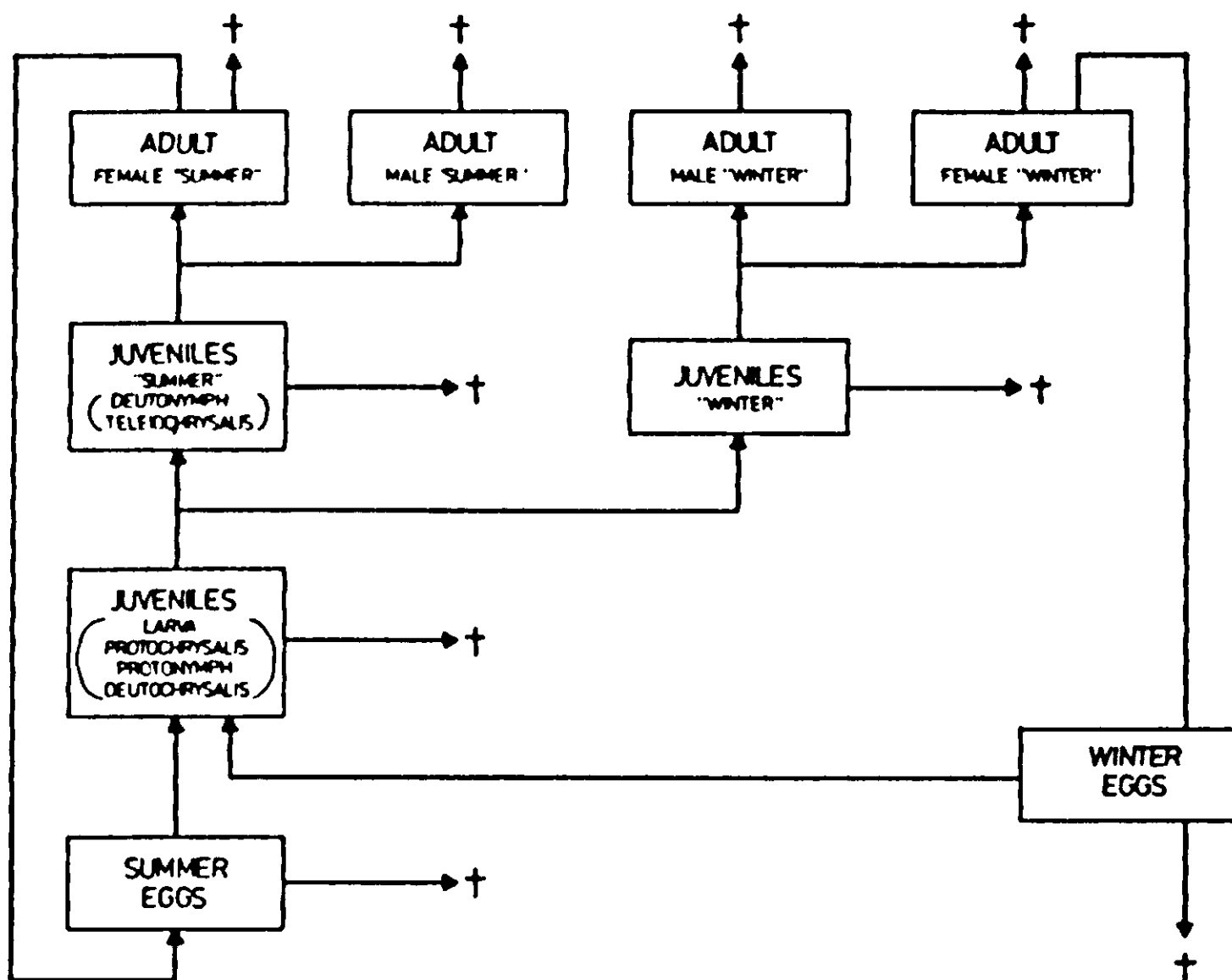


Figure 37. Life cycle of fruit-tree red spider mite (*Panonychus ulmi* Koch), symbols are not in Forrester notation. (Source: Rabbinge, 1976).

be distinguished. A relational diagram for the development of *P. ulmi* during the juvenile phase from larva to deutonymph is given in Figure 38. This part of the juvenile phase is distinguished, and treated separately because the winter form is induced only in the later juvenile stages. Table 9 gives the length of the development period and its dispersion for the juvenile stages (J and JS) and for winter eggs (EGG), in relation to temperature.

Exercise 47

Calculate the number of classes required to mimic the dispersion of stages EGG, J and JS using a boxcar train with constant relative dispersion (see Section 2.2). Why can this method be used only when the temperature is constant? Which method must be used when the temperature varies? Write a simulation program for the hatching process of winter eggs, assuming an initial quantity of 1000 and a daily sinusoidal temperature fluctuation between 15°C and 30°C. Mortality during this development process may be neglected. Calculate the relative rate of mortality in the juvenile stage for a constant temperature of 30°C, if the experimental results on mortality show that at this temperature, 50% of the juveniles die during their development from egg to deutonymph.

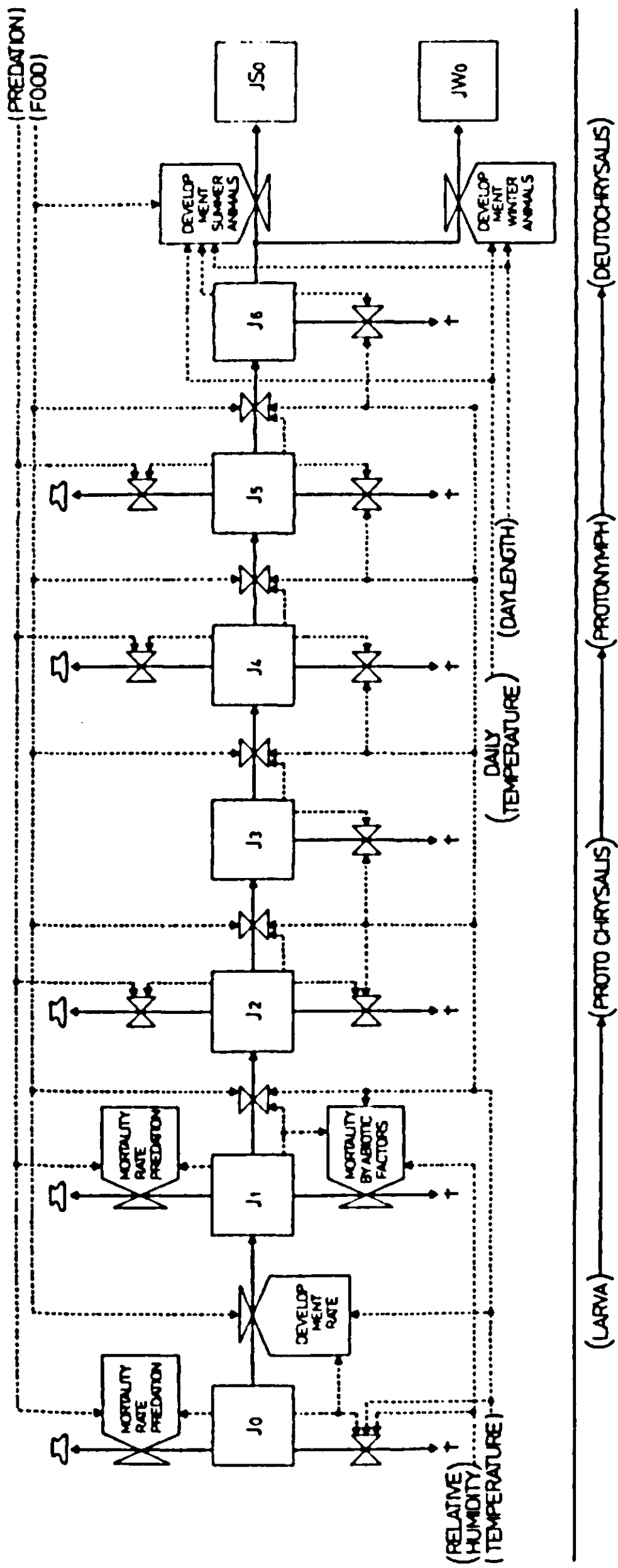


Figure 38. Growth and development of the juvenile stages of the fruit-tree red spider mite *P. ulmi* (larva, protochrysalis, protonymph, deutochrysalis). (Source: Rabbinge, 1976).

Table 9. Duration (x) of different development stages of fruit-tree red spider mite in days at various temperatures with standard deviation (s(x)).

	Temperature							
	15°C		18°C		25°C		30°C	
	x	s(x)	x	s(x)	x	s(x)	x	s(x)
Egg	18.0	3.0	10.0	1.6	6.3	1.06	5.0	1.25
J	10.1	2.0	6.5	1.3	4.0	0.8	2.5	0.62 ³
JS	5.5	1.1	4.3	0.85	2.4	0.6	2.0	0.5

J = Juveniles insensitive to diapause-inducing conditions (larva, protochrysales, protonymph, deutochrysales).

JS = Juveniles Sensitive to diapause-inducing conditions (deutonymph, teleiochrysales).

Development of both eggs and juveniles is simulated by the BOXCAR subroutine developed by Goudriaan & van Roermund (Section 2.2). This subroutine is added at the end of a program and then called upon in the program by inserting the statement:

```
A0,A,ATOT,MORFL,OUTFL,GAMMA,GCYCL = ...
  BOXCAR(1,AI,DEV,RD,RMR,INFL,N,DELT,TIME)
```

In this statement the variables A0 to GCYCL express the output of the subroutine, OUTFL is the rate of outflow of the last integral of the train and ATOT the sum of the contents of the integrals in the train with initial value AI. The variable RD (relative dispersion) is the standard deviation divided by the total residence time (development period) and RMR is the relative rate of mortality during this development period. INFL is the rate of flow into the first boxcar and N the number of boxcars in the train.

Exercise 48

Write a simulation program for the development of fruit-tree red spider mite into adults using the data of Table 9. Use the subroutine BOXCAR. Temperature is the only changing external variable.

Females and males emerge from the last juvenile stage in equal proportions. After copulation, the fertile females mature during a temperature-dependent pre-oviposition period and then start laying eggs. The oviposition rate and

ageing rate of the females depend directly on temperature (Table 10). The oviposition rate also depends on temperature, indirectly through the physiological age of the females.

This age-dependence normally means that the oviposition rate of young females is above average, while that of old females is much less than the mean. When calculations are performed using the average oviposition rate during the whole life span of a female, the simulated total number of produced eggs may be correct, but the course of the cumulative egg production curve is wrong. At the beginning, egg production per day is underestimated, and at the end it is overestimated.

Exercise 49

Explain why the subroutine BOXCAR cannot be used to mimic the ageing process when oviposition rate is dependent on physiological age.

Ageing of the reproducing female is simulated using the basic method described in Section 2.2, taking into account temperature-dependent and age-dependent relative mortality rates. These relative mortality rates are calculated as follows.

The maximum life span is arbitrarily defined as the mean life span plus three standard deviations. The residence time in a single class is the maximum period, just defined, divided by the number of classes N . The percentages of animals alive at the end of each age class are now read from the cumulative frequency distribution drawn on probability paper. This is done by dividing the total

Table 10. The oviposition rate ($\overset{\text{mean}}{x}$) and its standard deviation ($\overset{\text{std. dev.}}{s(x)}$) in eggs per day for each age class, and the total oviposition period in days of *P. ulmi*, as a function of temperature.

Age class	Temperature									
	10°C		15°C		20°C		25°C		30°C	
	x	$s(x)$	x	$s(x)$	x	$s(x)$	x	$s(x)$	x	$s(x)$
1	0.6	0.15	1.2	0.2	1.9	0.7	3.1	0.8	4.2	1.1
2	0.5	0.1	1.2	0.2	2.2	0.7	3.7	0.8	5.5	1.2
3	0.5	0.1	1.1	0.2	1.8	0.6	3.1	0.6	3.8	1.1
4	0.4	0.08	1.0	0.2	1.4	0.4	2.0	0.4	1.4	0.4
5	0.2	0.05	0.8	0.15	0.8	0.2	1.0	0.2	0.8	0.1
Oviposition period	24	14.5	25	12	13	5.0	9.0	3.7	7.5	2.4

residence time in, for example, five equal classes and interpolating the line that describes the relation between residence time and frequency. At the ordinate, the percentage that survives in each class can now be derived. The relative mortality rate per age class is calculated with the formula used in Exercise 47. This yields the results given in Table 11.

The only function of the males is to copulate, for which task their number is not limiting; more than one copulation being possible. For this aspect, they can be disregarded. However, they act as a source of food for predators, so they cannot be omitted from the simulation. The ageing process of the males is described by inserting the statement:

```
M0,M,MTOT,MORFLM,OUTFLM,GAMMAM,GCYCLM =...
  BOXCAR(5, MI, DEVRM, RDM, RMRM, INFLM, NM, ...
    DELT, TIME)
```

The females lay either winter eggs, that overwinter on twigs or branches, or summer eggs that give rise to a new generation of mites during that summer. The hatching process of summer eggs is again mimicked by a boxcar train.

Exercise 50

Extend the simulation program of Exercise 48 to include oviposition and ageing of females, using the data of Tables 10 and 11.

3.4.3 Predatory mite, *Amblyseius potentillae*

The life cycle of the predatory mite is very similar to that of the fruit-tree red spider mite (Figure 37). The only difference is that it overwinters as a mated adult female and not as an egg. The sensitive period for induction of either summer or

Table 11. Relative mortality rate (day^{-1}) of female *P. ulmi* per age class in dependence of temperature.

Age class	Temperature				
	10°C	15°C	20°C	25°C	30°C
1	0.011	0.011	0.005	0.005	0.003
2	0.033	0.031	0.049	0.050	0.027
3	0.088	0.089	0.061	0.245	0.273
4	0.15	0.138	0.360	0.504	0.709
5	0.2	0.15	0.4	0.6	0.8

winter adults is the same: the older juvenile stage. Therefore, the structure of the program is also almost the same, and need not be given here.

3.4.4 Relations between predator and prey

The food source does not affect reproduction and development of the fruit-tree red spider mite, as long as crop functions are optimal and densities so low that interference between individuals is absent. For the predatory mite, however, food supply is restricted. The availability of prey affects development rate, reproduction rate and fecundity (total number of eggs produced during the life of a female) of the predator. When prey is scarce, the relative mortality rates of the predators in the different stages may increase.

The motivation state of the predatory mite is characterized by its gut content (Figure 39) which determines the relative predation rate and prey utilization by the predator. The relative predation rate is the absolute predation rate per unit area divided by prey density; this variable has the dimension time^{-1} . Hungry predators have a high relative predation rate, activity increases with decreasing gut content, their encounters with prey are nearly always successful (fatal for the prey), and the dead prey is completely consumed. Well-fed predators, on the other hand, are less active, have a low success ratio (successful encounters divided by total number of encounters) and only partly consume the prey that are killed. A predator kept at a constant prey density, rapidly reaches a steady state (Fransz, 1974; Section 3.3) in which a unique relation exists between gut content and temperature on the one hand, and the relative predation rate and prey utilization on the other, provided that prey stage and prey composition are fixed. The stochastic models of Section 3.3 can, therefore, be omitted in this situation.

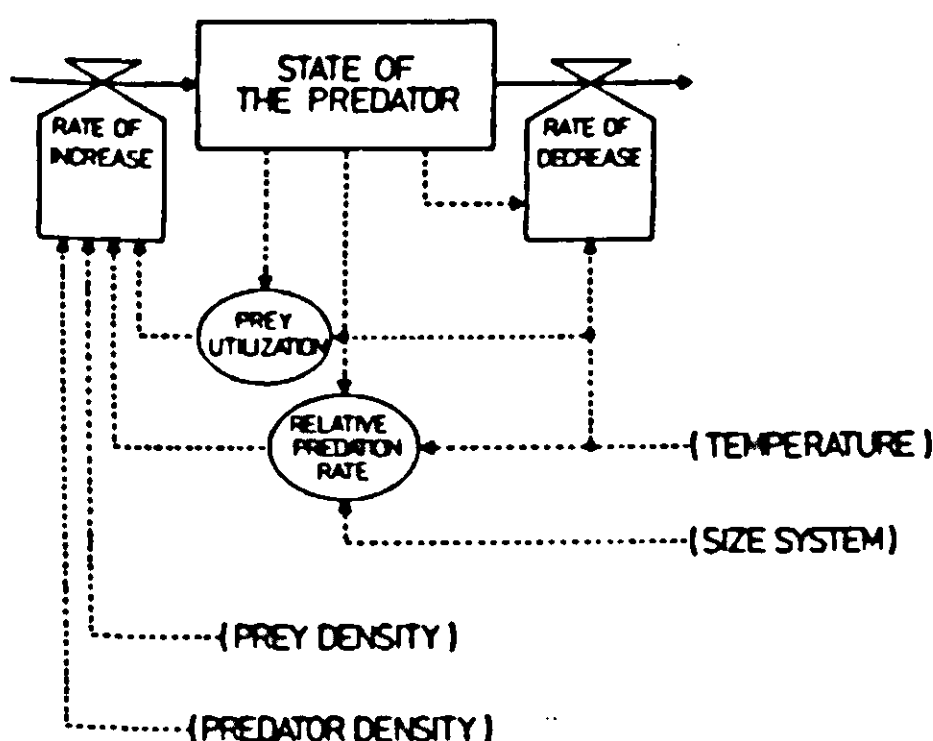


Figure 39. A predator-prey system, one predator versus a fixed number of prey of one stage. (Source: Rabbinge, 1976).

Old adult female predators eat all stages of prey except eggs, and show a clear preference for the younger stages, especially at higher gut contents. Young predator juveniles can kill only larvae and young prey juveniles, because the older prey stages are too vigorous. The gut contents are digested at a rate proportional to the content; there is thus a relative rate of digestion which depends only on temperature.

Exercise 51

Write a simulation model for the state (gut content) of a predator based on the relations presented above. Assume that temperature and densities of prey and predators are constant. You can fill in the required data yourself. Give the dimensions of all parameters and variables.

3.4.5 Preference as a competitive process

So far, preference of the predator for some types of prey has been treated as a difference in relative predation rate. At higher gut contents, relative predation rate of an unattractive prey type drops to zero. This relative predation rate is introduced into the simulation model as a variable, dependent on temperature and gut content. The relative predation rate is easily determined from the functional response curve (predation rate as a function of prey density (Figure 40)). Each prey density corresponds to a well-determined level of gut content of the predator, so the relative rates of predation on different prey types can be related through this gut content. Thus, the response to various prey species may be different but they are all related to the same state variable 'gut content'. This approach is straightforward and its validity can be tested in experiments using replacement series of two prey types (Rabbinge, 1976). The results support the assumption that the density of one prey type can affect the predation rate on another, only through the gut content of the predator.

Another approach, in which simulation is not needed and which allows us to bypass the gut content of the predator, is to consider predation and preference as competitive processes. Prey 'compete' for space in the gut of the predator, so it should be possible to derive the predation rates in mixed prey populations from the predation rates in pure populations (monocultures, see also Section 4.2). The predation rate (PR) as a function of prey density (Figure 40) is described by

$$PR = \frac{B \cdot D}{B \cdot D + 1} \cdot PRM \quad \text{Equation 60}$$

where D is prey density, PRM the maximum predation rate and B an apparent area per prey. PRM and B are determined for each combination of prey type and predator type from the functional response curve. Inversion of Equation 60 gives:

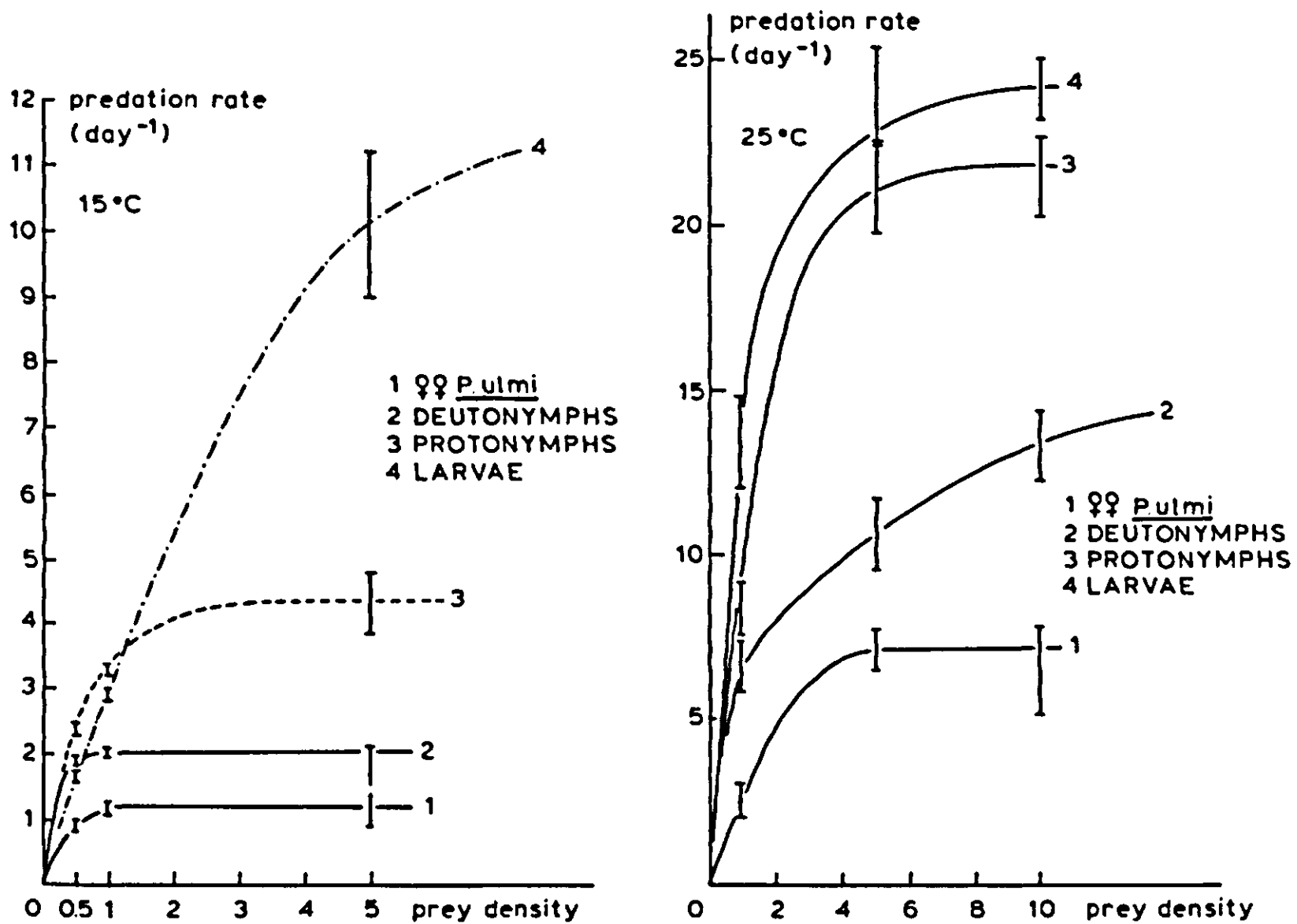


Figure 40. Functional response curves of the adult female stage of the predatory mite *Amblyseius potentillae* feeding on the fruit-tree red spider mite *P. ulmi* at 15°C and 25°C. (Source: Rabbinge, 1976).

$$\frac{1}{PR} = \frac{B \cdot D + 1}{B \cdot D} \cdot \frac{1}{PRM} = \frac{1}{PRM} + \frac{1}{B \cdot D} \cdot \frac{1}{PRM}$$

The corresponding graphical representation of $1/PR$ versus $1/D$ is a straight line that crosses the ordinate at $1/PRM$ and has a slope of $1/(B \cdot PRM)$. Maximum predation rate and apparent area per prey can be derived directly from the lines produced. An analogy to the competition of cereal-weed mixtures can be shown (Section 4.2). It is tempting, therefore, to describe predation on a mixture of prey with the same equations used to compute yield of one of the species in a cereal-weed mixture

$$PR_1 = \frac{B_1 \cdot D_1}{B_1 \cdot D_1 + B_2 \cdot D_2 + 1} \cdot PRM_1$$

and, similarly, for the rate of predation on prey type 2. Comparison of experimental and simulation results with the computations for mixtures, show that the various approaches give satisfactory results (Figure 41). Of course, the validity of the computation can be confirmed only with the restriction that the gut content of the predator must be in equilibrium with the available density and composition of prey.

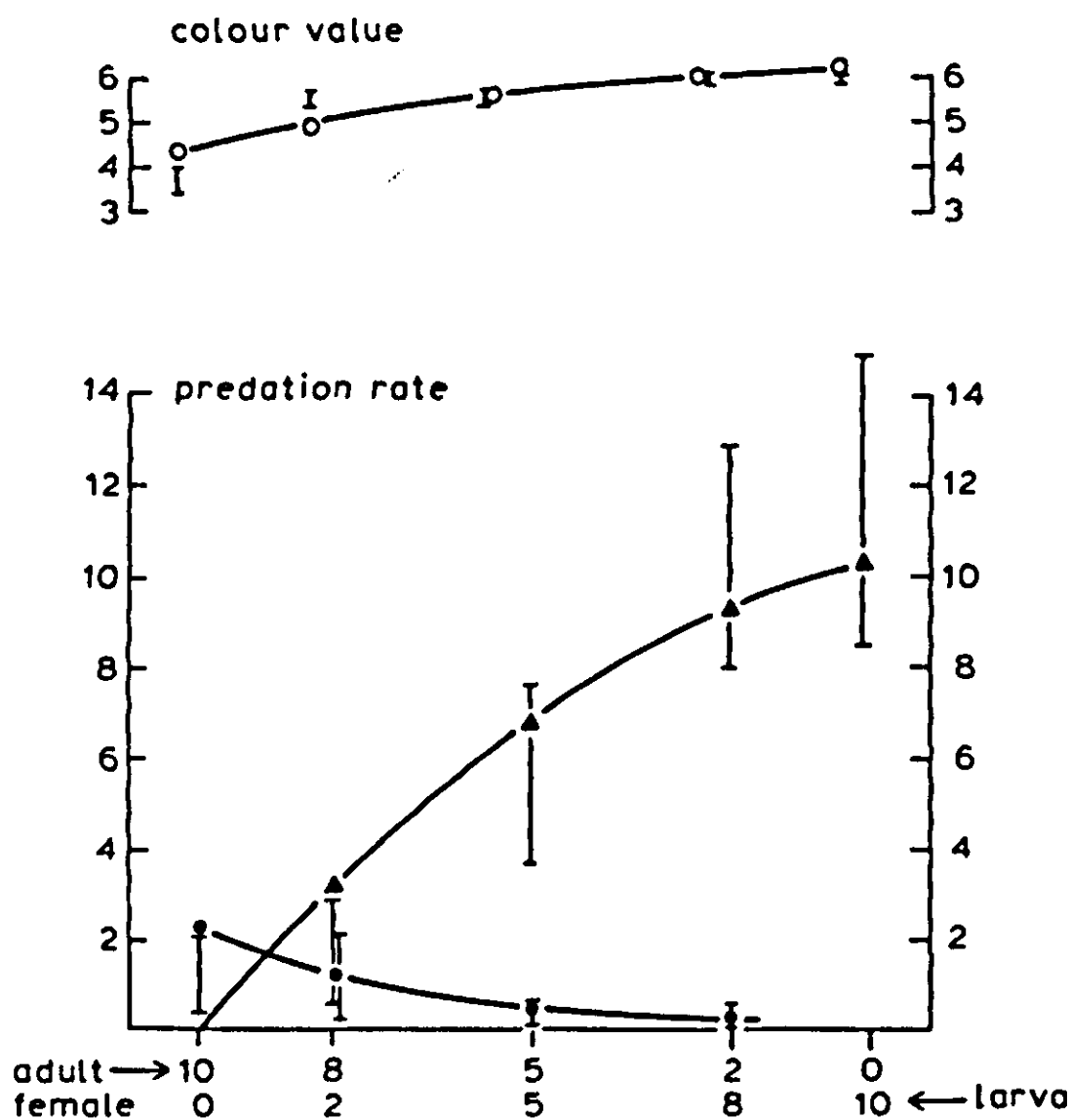


Figure 41. Simulated and experimental results of a replacement series of larvae and adult females of *Panonychus ulmi*, with one adult female of *Amblyseius potentillae* at 15°C. Simulated results (—), and experimental results (I bar with 95% confidence intervals). (Source: Rabbinge, 1976).

3.4.6 Model testing

Model building is a futile exercise unless the model output is compared with the results of independent experiments. Such tests are preferably done at different levels. One such level is mixed prey predation, as derived from predation on single prey types. This can be used to test the assumption about the interaction between different prey types as discussed in Subsection 3.4.4.

A second level of testing involves population experiments with prey and predator in a larger system with well-defined boundaries, under controlled conditions; e.g. a small apple tree in a greenhouse. The comparison of such measurements with simulated results indicates a reasonable correspondence (Figure 42), so a third phase of validation is justified: the apple orchard. Some results of simulations for orchards, together with experimental results, are given in Figure 43. The reasonable agreement increases confidence in the model. Validation at different levels can pinpoint errors in model structure or parameter values. Another important tool in error-spotting is sensitivity analysis, which shows which parameters have the greatest influence and might thus be responsible for deviations between measurements and results. The results of a sensitivity analysis can also help in deciding research priorities. For instance, sensitivity

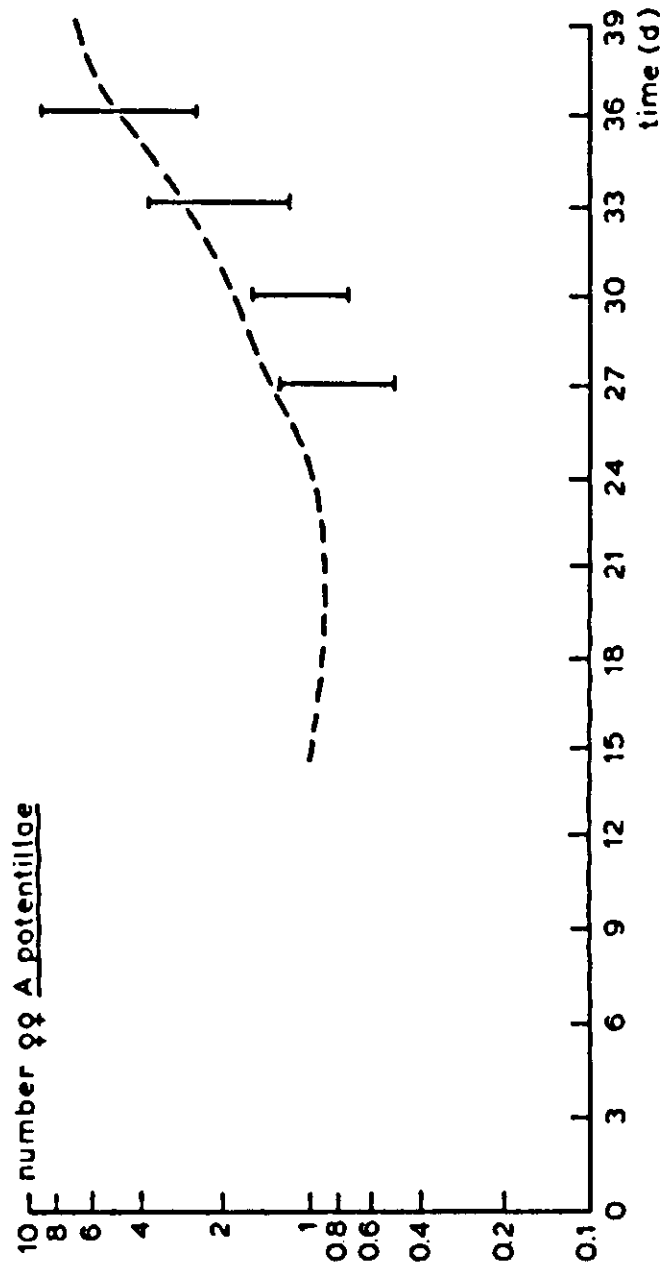
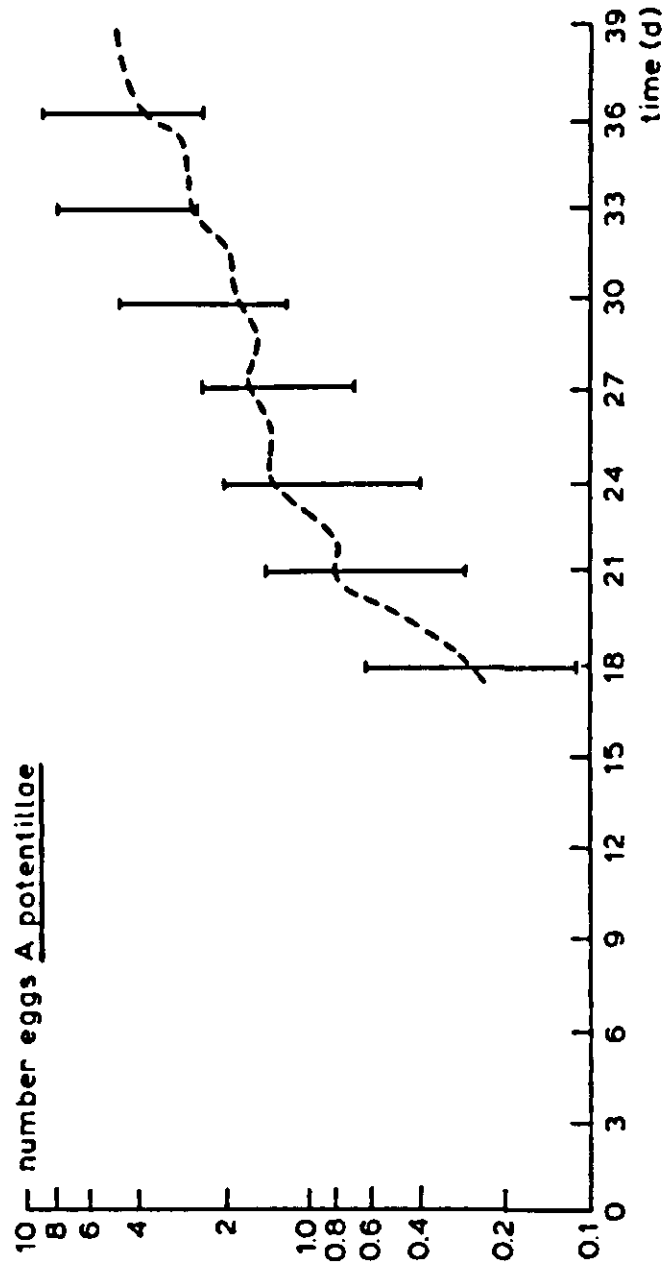
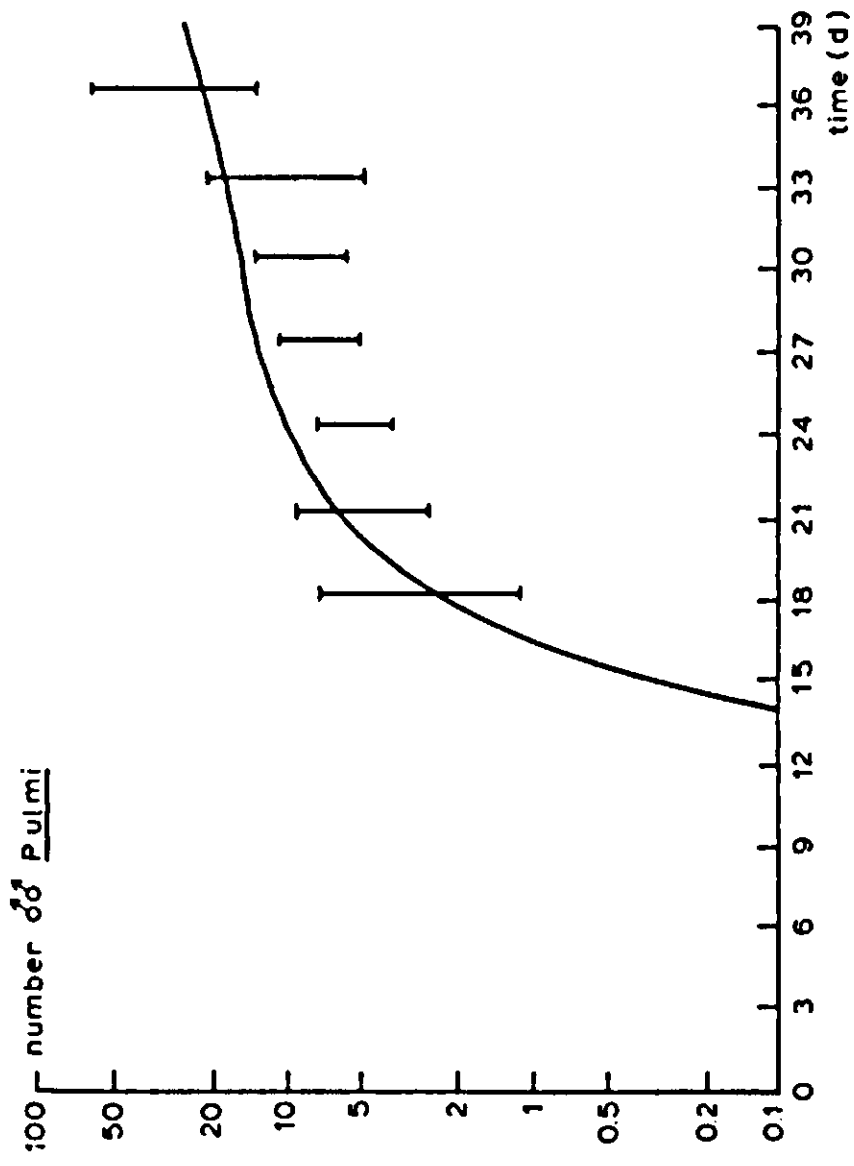
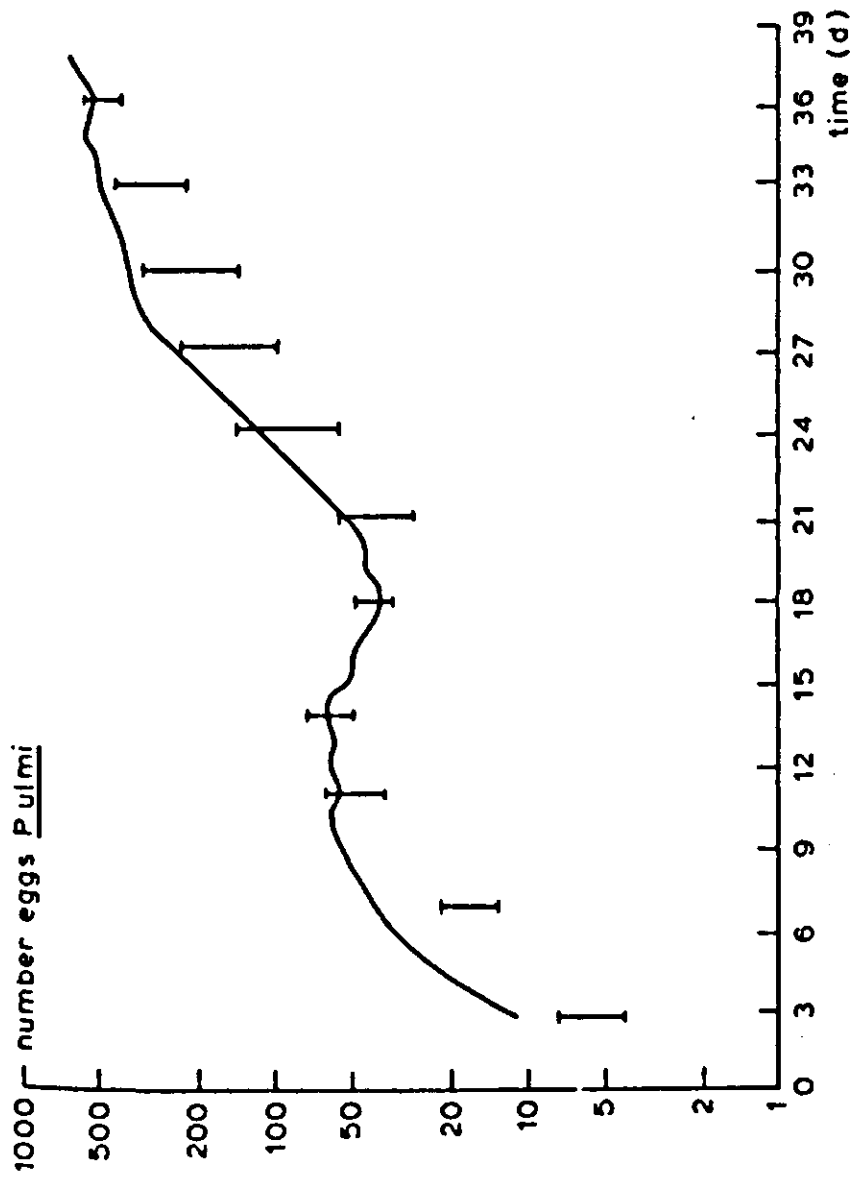


Figure. 42. Simulated and experimental results of a population experiment of *P. ulmi* and *A. potentillae* in a greenhouse; simulated number of *P. ulmi* (—), simulated number of *A. potentillae* (----), and experimental results (I bar with 95% confidence intervals). (Source: Rabbinge, 1976).

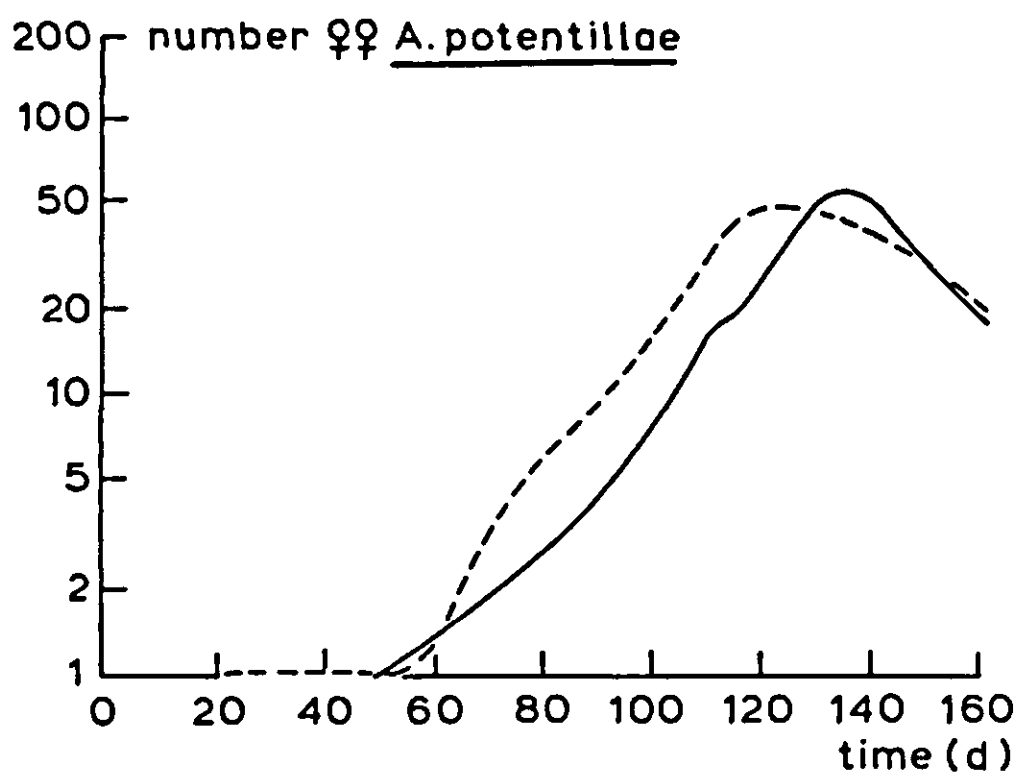
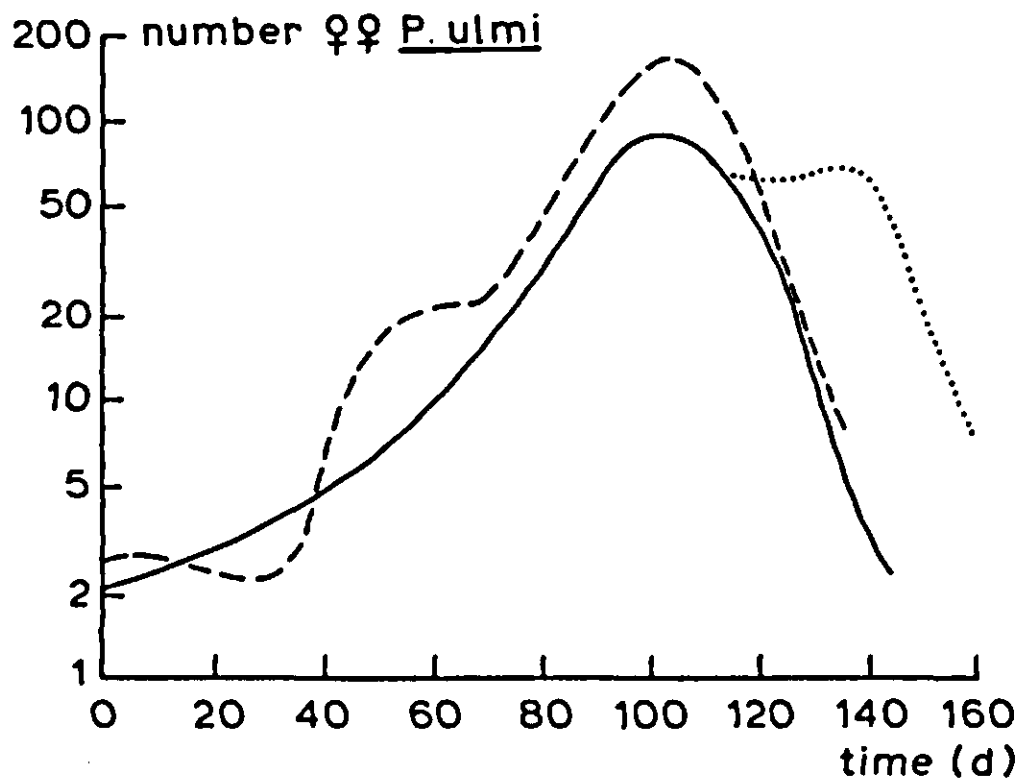


Figure 43. Simulated (----) and experimental (—) results of *P. ulmi* and *A. potentillae* in an orchard. The experimental results are the means for several orchards. (Source: Rabbinge, 1976).

analysis shows that in this model the abiotic mortality of prey and predator are of minor importance. The most important factors are the oviposition rate, the predation rate of the adult female predator and the length of the juvenile period of the prey. The gut content, especially when it is low, also has quite an important effect on the predator's rates of development and reproduction. Experimental data on these relations are scarce and inaccurate, so more research in this direction is required.

The model described here has also been used for the development of a practical pest management method. When, rather arbitrarily, an economic injury level of 3 mites per leaf is assumed (Rabbinge, 1985), model computations demonstrate that predator-prey ratios may vary from 3 to 0.3 without leading to a risk of local extinction of the predator or of very high prey densities (Rabbinge, 1976). The

preset damage threshold can be tested by the use of combination models (as described in Section 4.3) in which crop growth models are combined with population models of phytophagous and predatory arthropods. After quantification of the relation between the host plant and the phytophagous pest, these combined models may be used to calculate reduction in yield. With a preset limit for acceptable yield reduction, threshold levels for the density of the pest can then be determined, and can replace the arbitrary threshold values currently used to decide whether the introduction of control of predatory mites should be recommended.

3.4.7 *Stiff equations*

In the case of the predatory mites, the physiological state of an individual predatory mite approaches equilibrium with a very small time coefficient in minutes, while the time coefficient for the changes in the prey population is many orders of magnitude greater, in days. This is called a model with 'stiff equations'. Such a population model, which includes a dynamic model of the individual predator's gut contents would, therefore, require a very short time step of integration, and a large amount of computing time. The assumption of physiological equilibrium thus reduces the cost of a simulation run by an order of magnitude of 100, but need not involve any important loss of accuracy.

Two other approaches can be used to deal with models with stiff equations. First, if the period over which the system is to be simulated is short, relative to the time coefficient of the slow process, then this process can be omitted or simplified (i.e. input as parameters or calculated only once). This method, however, can be used only if the simulation's timescale was initially overestimated (Goudriaan, 1977).

A more generally method is to calculate the effects of the slow process less frequently than those of the rapid process. Thus, for example, the spatial distribution of the cereal aphids and parasitoids modelled in Subsection 3.2.4 is calculated once every 50 time steps (Rabbinge et al., 1984a).

Figure 44 shows a scheme for combining the two main methods of reducing the computation time needed to simulate systems involving processes with very different time coefficients.

Clearly, the use of short cuts of this type introduces some inaccuracy into the model. As pointed out by Goudriaan (1977), however, errors in the data used in agricultural models mean that extremely precise integration methods may be an expensive luxury. Short cuts, therefore, can yield dramatic reductions in computation time without resulting in significant errors in the model's results.

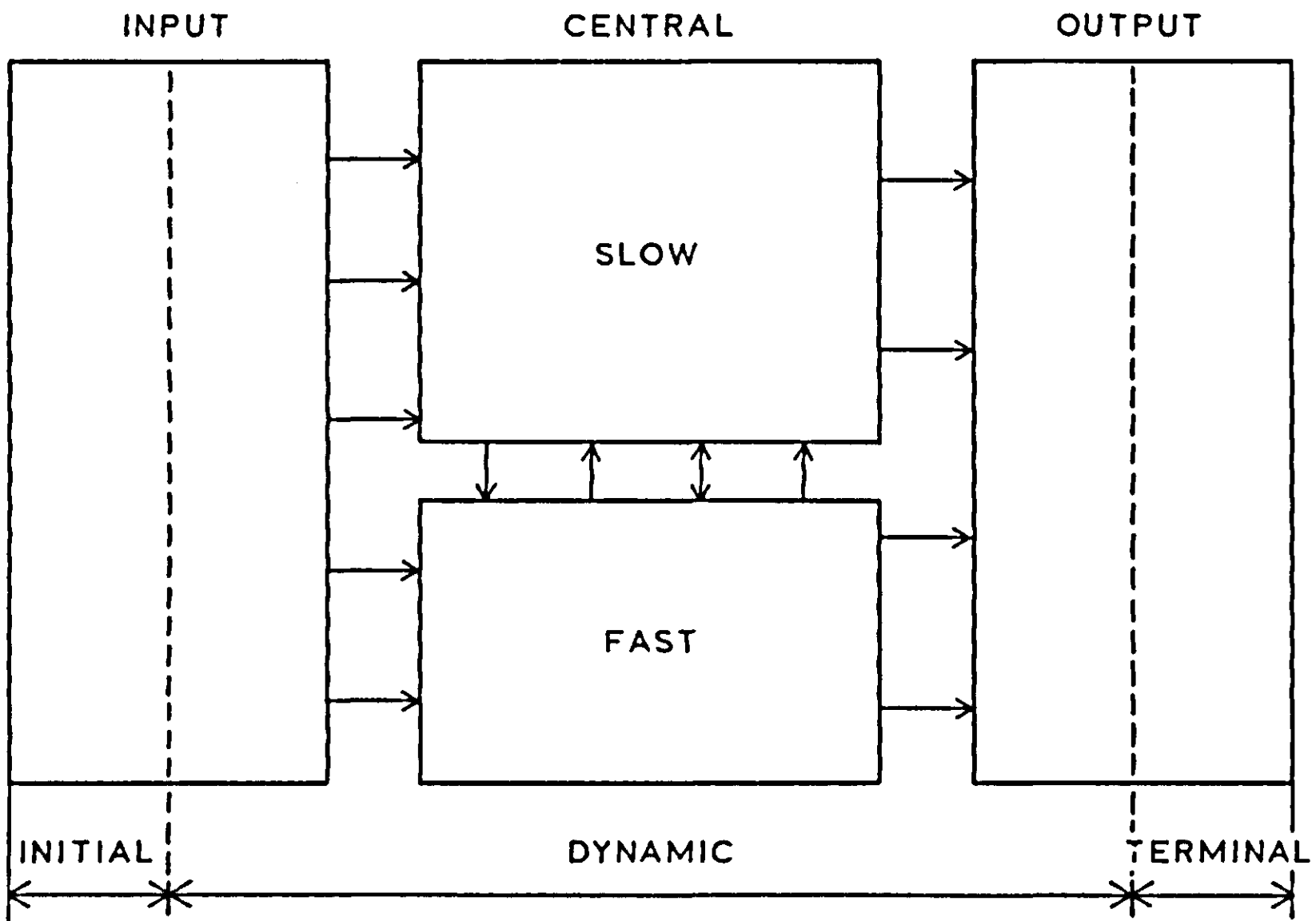


Figure 44. The main parts of a dynamic simulation model. The words 'INITIAL', 'DYNAMIC' and 'TERMINAL' refer to the CSMP terms that are used to indicate the segments of a simulation model. The input part contains those calculations connected with initial values and forcing functions, in as far as they are not subject to a feedback from state variables of the model. The output part contains those calculations connected with output variables, from the point where they no longer influence state variables. (Source: Goudriaan, 1973).

4 COUPLING OF CROP GROWTH AND PESTS, DISEASES AND WEEDS

4.1 A simple and universal crop growth simulator: SUCROS87

C.J.T. Spitters, H. van Keulen and D.W.G. van Kraalingen

4.1.1 Introduction

Pathogen and host mutually affect each other's growth. However, in most phytopathological and entomological studies, fungal and insect epidemics are not considered in relation to their close interaction with the growth of the host plant. To study the complex interference between a crop and its diseases and pests, models that simulate the growth of the crop, the population dynamics of the pathogen, and the interaction between both, are useful.

In this Section, a crop growth model is described, designated SUCROS87 (Simple and Universal CROp growth Simulator, version 1987). SUCROS87 simulates the potential growth of a crop; i.e. its dry matter accumulation under ample supply of water and nutrients in a pest, disease and weed-free environment under the prevailing weather conditions.

The version of SUCROS87 presented here, differs substantially from that published by van Keulen et al. (1982). Canopy photosynthesis is calculated using a different method, which is more mechanistic and more accurate and flexible (Spitters, 1986; Goudriaan, 1986; Spitters et al., 1986). An improved method to simulate leaf area growth of the crop is introduced.

4.1.2 General structure of the model

The model simulates dry matter accumulation of a crop as a function of irradiation, temperature and crop characteristics. The calculation procedure is presented schematically in Figure 45.

The basis for calculating dry matter production, is the rate of gross CO₂ assimilation of the canopy. This rate is dependent on the radiation energy absorbed by the canopy, which is a function of incoming radiation and crop leaf area. From the absorbed radiation and the photosynthetic characteristics of single leaves, the daily rate of CO₂ assimilation of the crop is calculated. Part of the carbohydrates produced (CH₂O) are used to maintain the present biomass. The remaining carbohydrates are converted into structural dry matter. In this conversion, some of the weight is lost as growth respiration. The growth rate (ΔW in kg DM ha⁻¹ d⁻¹) is thus obtained as

$$\Delta W = C_f(A - R_m) \quad \text{Equation 61}$$

in which A is the gross assimilation (kg CH₂O ha⁻¹ d⁻¹), R_m the maintenance respiration (kg CH₂O ha⁻¹ d⁻¹), and C_f the conversion efficiency (kg DM kg⁻¹ CH₂O).

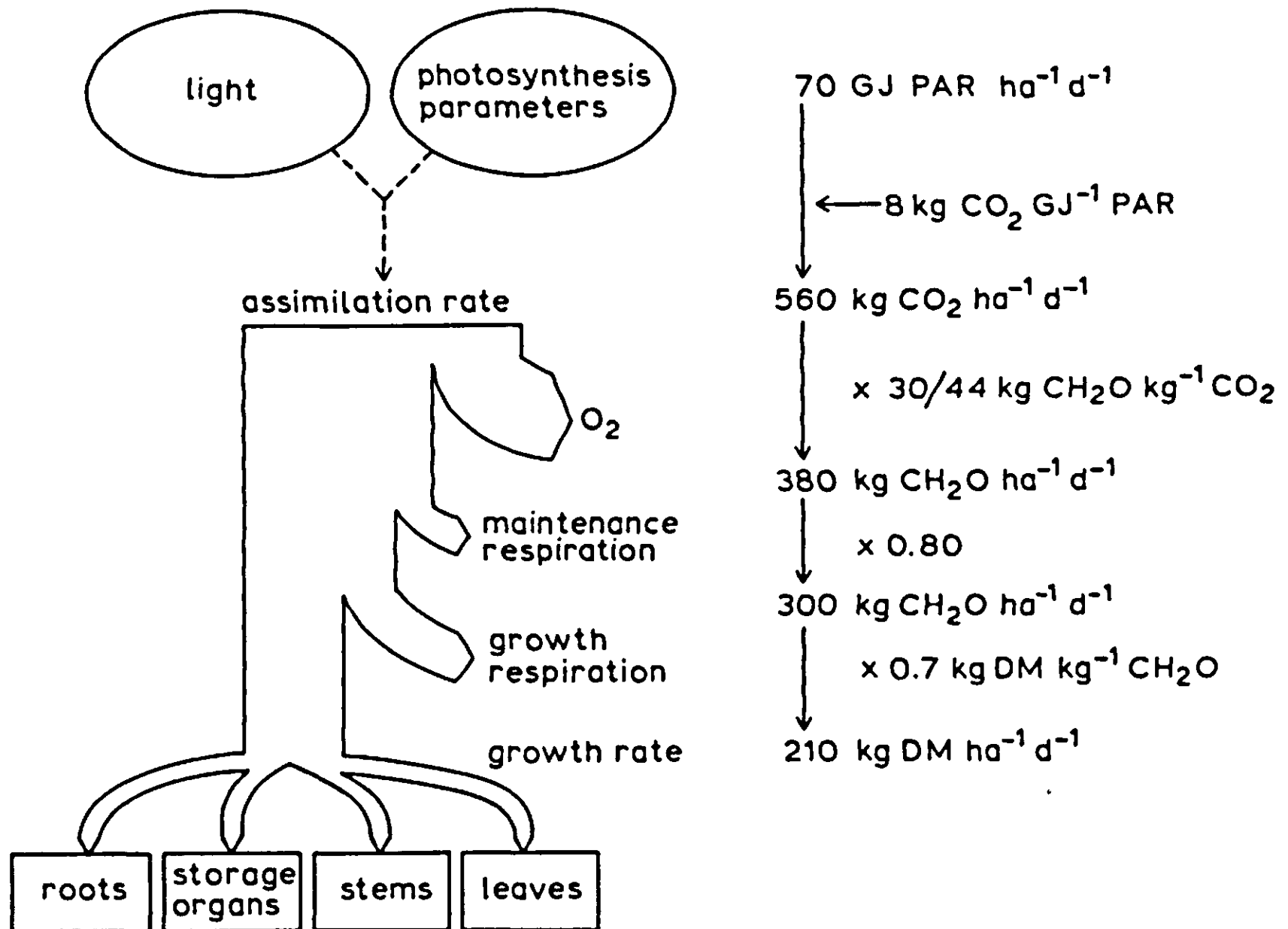


Figure 45. Diagram illustrating schematically the calculation procedure for daily crop growth rate. The numerical values given are typical for a crop that fully covers the ground, growing under average potential conditions in a temperate climate.

The dry matter produced is partitioned amongst the various plant organs, using partitioning factors introduced as a function of the phenological development stage of the crop. The dry weights of the plant organs are obtained by integrating their growth rates over time. The phenological development stage is calculated as a function of ambient temperature.

The model requires as input, data to describe the crop species or cultivar and the site. The site is characterized by its geographical latitude and by daily values of irradiation and temperature.

The computer program (Figure 46; Table 12) is structured in a small main program, followed by a block of parameters and functions to characterize the crop, and another block to characterize the site. Daily CO₂ assimilation and leaf area growth are calculated in separate modules.

Figure 46. Listing of the program of the model SUCROS87.

TITLE SUCROS87 SPRING WHEAT

- * Dry weights of leaves(green,dead,total), stems, storage organs, roots
- * and total above-ground biomass (kgDM/ha) as integrals of growth rates

```

WLVG = INTGRL(0.,GLV-DLV)
WLVD = INTGRL(0.,DLV)
WLV  = WLVG + WLVD
WST  = INTGRL(0.,GST)
WSO  = INTGRL(0.,GSO)
WRT  = INTGRL(0.,GRT)
TADRW = WLV + WST + WSO
    
```

- * Leaf area index (ha leaf / ha soil) as integral of leaf area growth rate

```

GLAI = GLA(DAY,DAYEM,DTEFF,DVS,NPL,LAO,RGRL,DELTA,SLA,LAI,GLV)
LAI  = INTGRL(0.,GLAI - DLAI)
    
```

- * but in wheat + 0.5 * ear area index:

```

LAI = 0.5 * EAI + INTGRL(0.,GLAI - DLAI)
    
```

- * Development stage: 0 = emergence, 1 = anthesis, 2 = dead ripeness

```

DVS = INTGRL(0.,DVR)
DVR = INSW(DVS-1.,AFGEN (DVRVT,DAVTMP),AFGEN (DVRRT,DAVTMP)) ...
      * INSW(DAY-DAYEM,0.,1.)
    
```

- * Daily total gross assimilation (DTGA, kg CO2/ha/d)

```

DTGA,DSO = DASS(DAY,LAT,DTR,KDF,SCP,LAI,AMAX,EFF)
    
```

- * Leaf photosynthesis rate at light saturation (kg CO2/ha leaf/h)

```

AMAX = AMX * AMDVS * AMTMP
AMDVS = AFGEN(AMDVST,DVS)
AMTMP = AFGEN(AMTMPT,DDTMP)
    
```

- * Conversion from assimilated CO2 to CH2O

```

GPHOT = DTGA * 30./44.
    
```

- * Maintenance respiration (kg CH2O/ha/d)

```

MAINT = AMIN1(GPHOT, MAINTS * TEFF * MNDVS)
MAINTS = 0.03*WLV + 0.015*WST + 0.015*WRT + MAINSO*WSO
MNDVS  = WLVG / (WLV+NOT(WLV))
TEFF   = Q10**((DAVTMP-25.)/10.)
    
```

PARAM Q10 = 2.

- * Fraction of dry matter growth occurring in shoots, leaves, stems,

- * storage organs and roots

```

FSH = AFGEN(FSHTB,DVS)
FLV = AFGEN(FLVTB,DVS)
FST = AFGEN(FSTTB,DVS)
FSO = 1. - FLV - FST
FRT = 1. - FSH
    
```

- * Assimilate requirements for dry matter conversion (kgCH2O/kgDM)

```

ASRQ = FSH *(1.46*FLV + 1.51*FST + ASRQSO*FSO) + 1.44*FRT
    
```

- * Total growth rate (kg DM/ha/d) and

- * growth rates of shoots (leaves, stems, storage organs) and roots

```

GTW = (GPHOT - MAINT) / ASRQ
GSH = FSH * GTW
GLV = FLV * GSH
GST = FST * GSH
GSO = FSO * GSH
GRT = FRT * GTW
    
```

* Death rate of leaves (DLAI in ha/ha/d, DLV in kg DM/ha/d)
 $DLAI = LAI * (1. - EXP(-RDR * DELT))$
 $DLV = WLVG * DLAI / (LAI + NOT(LAI))$

* Daily global radiation (J/m2/d)
 $DTR = AFGEN(DTRT, DAY) * 1.E6$

* Daily temperature (°C): maximum, minimum, average, daytime, effective

$DTMAX = AFGEN(TMAXT, DAY)$
 $DTMIN = AFGEN(TMINT, DAY)$
 $DAVTMP = 0.5 * (DTMAX + DTMIN)$
 $DDTMP = DTMAX - 0.25 * (DTMAX - DTMIN)$
 $DTEFF = AMAX1(0., DAVTMP - TBASE)$

* Temperature sum after emergence
 $TSUMEM = INTGRL(0., DTEFF * INSW(DAY - DAYEM, 0., 1.))$

* Simulation run specifications
 $DAY = AMOD(TIME, 365.)$
FINISH DVS = 2.
TIMER TIME = 90., FINTIM=271., DELT=1., PRDEL=5.
METHOD RECT
PRINT DVS, TADRW, WLV, WST, WSO, LAI, DTR, DTGA, GPHOT, GTW, MAINT, AMAX

*** WEATHER DATA ***

* Wageningen 1951 - 1980
* Daily global radiation (MJ/m2/d)
FUNCTION DTRT = 15,2.1, 46,4.4, 74,7.8, 105,13.0, 135,16.3, ...
166,17.5, 196,15.6, 227,13.8, 258,10.0, 288,5.8, 319,2.7, 349,1.7
* Daily maximum and minimum temperature (°C)
FUNCTION TMAXT = 15,4.3, 46,5.4, 74,8.9, 105,12.4, 135,17.3, ...
166,20.5, 196,21.4, 227,21.5, 258,18.9, 288,14.3, 319,8.6, 349,5.5
FUNCTION TMINT = 15,-0.7, 46,-0.6, 74,1.2, 105,3.3, 135,7.3, ...
166,10.3, 196,12.2, 227,12.0, 258,9.7, 288,6.5, 319,2.9, 349,0.6

*** FIELD PARAMETERS ***

* Latitude of the site
PARAM LAT = 52.
* Plant density (plants/m2) and day of emergence
PARAM NPL = 210., DAYEM = 100.

*** SPECIES PARAMETERS SPRING WHEAT ***

* Initial leaf area (cm2/plant) and relative leaf growth rate (cm2/cm2/°C d)
PARAM LAO = 0.57, RGRL = 0.0140, TBASE = 0.
* Specific leaf area of new leaves (ha leaf / kg leaf)
PARAM SLA = 0.0022

* Potential photosynthesis rate at light saturation (kg CO2/ha leaf/h)
PARAM AMX = 40.
* Effect of DVS on AMX
FUNCTION AMDVST = 0.,1., 1.,1., 2.,0.5, 2.5,0.
* Effect of daytime temperature on AMX
FUNCTION AMTMPT = 0.,0., 10.,1., 25.,1., 35.,0.01, 50.,0.01
* Initial light use efficiency ((kg CO2/ha leaf/h)/(J/m2/s))
PARAM EFF = 0.45

```

* Pre-anthesis and post-anthesis development rate(1/d) as a function of temp.
FUNCTION DVRVT = -10.,0., 0.,0., 30.,0.0377
FUNCTION DVRRT = -10.,0., 0.,0., 30.,0.0330

* Extinction coefient for diffuse PAR
PARAM KDF = 0.6
* Scattering coefficient for PAR
PARAM SCP = 0.20

* Maintenance coeficient for storage organs (kg CH2O/kg DM/d)
PARAM MAINSO = 0.01
* Assimilate requirement for d.m. conversion in storage organs (kgCH2O/kgDM)
PARAM ASRQSO = 1.41

* Fraction of total dry matter growth allocated to shoots (FSH)
* fraction of shoot d.m. growth allocated to leaves (FLV) and stems (FST)
* as a function of DVS
FUNCTION FSHTB = 0.,.50, .10,.50, .20,.60, .35,.78, .40,.83, ...
.50,.87, .60,.90, .70,.93, .80,.95, .90,.97, 1.,.98, 1.1,.99, ...
1.20,1.0, 2.5,1.0
* Leaf blades:
FUNCTION FLVTB = 0.,.65, .10,.65, .25,.70, .50,.50, .70,.15, .95,0.,...
2.5,0.
* Stems + leaf sheaths + chaff:
FUNCTION FSTTB = 0.,.35, .10,.35, .25,.30, .50,.50, .70,.85, ...
.95,1.0, 1.05,0., 2.5,0.

* Relative death rate of green leaf area (1/d)
* due to developmental ageing (RDRDV) and self-shading (RDRSH)
RDR = AMAX1(RDRDV, RDRSH)
RDRDV = INSW(DVS-1.0, 0., AFGEN(RDRT,DAVTMP))
RDRSH = LIMIT(0., 0.03, 0.03 * (LAI-LAICR) / LAICR)
FUNCTION RDRT = 0.,.03, 10.,.03, 15.,.04, 30.,.09
PARAM LAICR = 4.

* Ear area index (ha ears/ha ground)
EAI = INTGRL(0., EAR * TADRW * ...
INSW(DVS-0.8,0.,1.) * INSW(-EAI,0.,1.) - INSW(DVS-1.3,0.,RDR*EAI))
* Ear area ratio (ha ears (2* one-sided projection) /kg shoot)
PARAM EAR = 6.3E-5
* EAR: awnless 6.3 and awned cultivars 11.0 cm2/g shoot at anthesis

* Main references to the crop characteristics of wheat:
* van Keulen & Seligman (1987): AMTMPT,FSHTB,FLVTB,FSTTB,DVRVT,DVRRT
* Spitters & Kramer (1986): LAO, RGRL,SLA,FLVTB,FSTTB,EAR,DVRVT
* Groot (1987): FLVTB,FSTTB; van Keulen & de Milliano (1984): RDRT
END
STOP

```

```

* -----
* Subroutine GLA:
* computes daily increase of leaf area index (ha leaf/ ha ground/ d)
* -----
FUNCTION GLA (DAY, DAYEM, DTEFF, DVS, NPL, LAO, RGRL, DELT, SLA,
$ LAI, GLV)
IMPLICIT REAL (A-Z)
* during mature plant growth:
GLA = SLA * GLV
* during juvenile growth:
IF ((DVS.LT.0.3).AND.(LAI.LT.0.75)) THEN
GLA = LAI * (EXP(RGRL * DTEFF * DELT) - 1.)

```

```

ENDIF
* at day of seedling emergence:
IF ((DAY.GE.DAYEM).AND.(LAI.EQ.0.)) GLA = NPL * LAO * 1.E-4
* before seedling emergence:
IF (DAY.LT.DAYEM) GLA = 0.
RETURN
END

```

```

* -----
* Subroutine DASS
* computes potential daily assimilation (DTGA, kg CO2/ha/d)
* -----
SUBROUTINE DASS (DAY,LAT,DTR,KDF,SCP,LAI,AMAX,EFF,
$ DTGA,DSO)
IMPLICIT REAL (A-Z)
INTEGER T
* distances and weights in Gaussian integration
DIMENSION GSDST(3), GSWT(3)
DATA GSDST /0.112702, 0.5, 0.887298/
DATA GSWT /0.277778,0.444444,0.277778/
* daylength (h) and daily extra-terrestrial radiation (J/m2/d)
CALL ASTRO (DAY,LAT,
$ DAYL,SINLD,COSLD,DSINB,DSINBE,DSO)
* daily radiation above the canopy (J/m2/d)
CALL DRADIA (DSO,DTR,
$ FRDF,DPAR)

DTGA = 0.
DO T = 1,3
HOUR = 12. + DAYL*0.5*GSDST(T)
CALL ASS (HOUR,DAYL,SINLD,COSLD,DSINB,DSINBE,DTR,
$ FRDF,DPAR,KDF,SCP,LAI,AMAX,EFF,
$ FGROS)
* integration of instantaneous assimilation to a daily total (DTGA)
DTGA = DTGA + FGROS * DAYL * GSWT(T)
ENDDO
RETURN
END

```

```

* -----
* Subroutine ASTRO
* computes daylength and daily extra-terrestrial radiation
* from daynumber and latitude
* -----
SUBROUTINE ASTRO (DAY,LAT,
$ DAYL,SINLD,COSLD,DSINB,DSINBE,DSO)
IMPLICIT REAL (A-Z)
* conversion factor from degrees to radians
PI = 3.1416
RD = PI / 180.
* declination (DEC, degrees) of the sun as a function of daynumber(DAY)
DEC = -ASIN(SIN(23.45*RD) * COS(2.*PI*(DAY+10.)/365.))/RD
SINLD = SIN(LAT*RD) * SIN(DEC*RD)
COSLD = COS(LAT*RD) * COS(DEC*RD)
* daylength (DAYL, h)
DAYL = 12. * (1.+2. * ASIN(SINLD/COSLD)/PI)
* daily integral of sine of solar inclination (DSINB)
DSINB=3600.*(DAYL*SINLD+24.*COSLD*SQRT(1.-(SINLD/COSLD)**2)/PI)
* daily integral of SINB with a correction for lower
* atmospheric transmission at lower solar elevations (DSINBE)
DSINBE=3600.*(DAYL*(SINLD+0.4*(SINLD*SINLD+0.5*COSLD*COSLD)) +

```

```

$ 12.*COSLD*(2.+3.*0.4*SINLD)*SQRT(1.-(SINLD/COSLD)**2)/PI)
* daily extra-terrestrial radiation (DSO, J/m2/d) from
* corrected solar constant (SC, J/m2/s)
SC = 1370. * (1.+0.033*COS(2.*PI*DAY/365.))
DSO = SC * DSINB
RETURN
END

* -----
* Subroutine DRADIA:
* computes daily photosynthetically active radiation (DPAR) and
* diffuse fraction of incoming radiation (FRDF)
* from atmospheric radiation transmission
* -----
SUBROUTINE DRADIA (DSO,DTR,
$ FRDF,DPAR)
IMPLICIT REAL (A-Z)
* daily photosynthetically active radiation (J/m2/d)
DPAR = 0.50 * DTR
* fraction diffuse radiation(FRDF) from atmospheric transmission(ATMTR)
ATMTR = DTR / DSO
FRDF = 0.23
IF(ATMTR.LE.0.75) FRDF=1.33-1.46*ATMTR
IF(ATMTR.LE.0.35) FRDF=1.-2.3*(ATMTR-0.07)**2
IF(ATMTR.LE.0.07) FRDF=1.
RETURN
END

* -----
* Subroutine ASS
* calculates instantaneous assimilation (FGROS, kg CO2/ha/h)
* -----
SUBROUTINE ASS (HOUR,DAYL,SINLD,COSLD,DSINB,DSINBE,DTR,
$ FRDF,DPAR,KDF,SCP,LAI,AMAX,EFF,
$ FGROS)
IMPLICIT REAL (A-Z)
INTEGER I,L
DIMENSION GSDST(3), GSWT(3)
DATA GSDST /0.112702, 0.5, 0.887298/
DATA GSWT /0.277778,0.444444,0.277778/
* radiation above the canopy: PAR (J/m2/s)
CALL RADIAT (HOUR,SINLD,COSLD,DSINB,DSINBE,FRDF,DPAR,
$ PARDF,PARDR,SINB)

* selection of canopy depths (LAIC from top)
FGROS = 0.
DO L = 1,3
LAIC = LAI * GSDST(L)
* absorbed radiation fluxes (J/m2/s)
CALL RADPRF (PARDF,PARDR,SINB,KDF,SCP,LAIC,
$ PARLSH,PARLSL,PARLPP,FSLLA)
* assimilation of shaded leaf area (kg CO2/ha leaf/hr)
ASSSH = AMAX * (1.-EXP(-EFF*PARLSH/AMAX))
* assimilation of sunlit leaf area (kg CO2/ha leaf/hr)
ASSSL = 0.
DO I = 1,3
PARLSL = PARLSH + PARLPP * GSDST(I)
ASSSL = ASSSL + AMAX*(1.- EXP(-PARLSL*EFF/AMAX)) * GSWT(I)
ENDDO
* hourly total gross assimilation (kg CO2/ha soil/hr)
FGROS = FGROS + ((1.-FSLLA)*ASSSH + FSLLA*ASSSL)*LAI*GSWT(L)

```

```
ENDDO
RETURN
END
```

```
* -----
* Subroutine RADIAT
* computes instantaneous radiation above the canopy (J/m2/s)
* -----
```

```
  SUBROUTINE RADIAT (HOUR,SINLD,COSLD,DSINB,DSINBE,FRDF,DPAR,
$                   PARDF,PARDR,SINB)
  IMPLICIT REAL (A-Z)
  PI    = 3.1416
  * sine of solar inclination (SINB)
  SINB  = AMAX1(0.,SINLD+COSLD*COS(2.*PI*(HOUR+12.)/24.))
  * diffuse PAR (PARDF) and direct PAR (PARDR) in J/m2/s
  PAR   = DPAR * SINB * (1.+0.4*SINB) / DSINBE
  PARDF = AMIN1(PAR, FRDF * DPAR * SINB/OSINB)
  PARDR = PAR - PARDF
  RETURN
  END
```

```
* -----
* Subroutine RADPRF
* computes the radiation profile within the canopy and gives
* instantaneous values of absorbed radiation for successive leaf layers
* -----
```

```
  SUBROUTINE RADPRF (PARDF,PARDR,SINB,KDF,SCP,LAIC,
$                   PARLSH,PARLSL,PARLPP,FSLLA)
  IMPLICIT REAL (A-Z)
  * canopy reflection coefficient (REFL)
  REFL  = (1. - SQRT(1.-SCP)) / (1. + SQRT(1.-SCP))
  * extinct.coeff. for direct component(KBL) and total direct flux(KDRT)
  * cluster factor as ratio between empirical and theoretical value of KDF
  CLUSTF = KDF / (0.8*SQRT(1.-SCP))
  KBL    = (0.5/SINB) * CLUSTF
  KDRT   = KBL * SQRT(1.-SCP)
  * absorbed radiation fluxes per unit leaf area (J/m2/s):
  * diffuse flux, total direct flux, direct component of direct flux
  PARLDF = (1.-REFL) * PARDF * KDF * EXP(-KDF * LAIC)
  PARLT  = (1.-REFL) * PARDR * KDRT * EXP(-KDRT * LAIC)
  PARLDR = (1.-SCP) * PARDR * KBL * EXP(-KBL * LAIC)
  * absorbed fluxes (J/m2 leaf/s) for shaded and sunlit leaves
  PARLSH = PARLDF + (PARLT - PARLDR)
  PARLSL = PARLSH + (1.-SCP) * KBL * PARDR
  * direct par absorbed by leaves perpendicular on direct beam
  PARLPP = PARDR * (1.-SCP)/SINB
  * fraction sunlit leaf area
  FSLLA = EXP(-KBL*LAIC) * CLUSTF
  RETURN
  END
```

```
ENDJOB
```

Table 12. Definition of the abbreviations used in the model SUCROS87, as listed in Figure 46.

Name	Description	Unit
AMAX	actual CO ₂ assimilation rate at light saturation for individual leaves	kg ha ⁻¹ h ⁻¹
AMDVS	factor accounting for effect of development stage on AMX	–
AMTMP	factor accounting for effect of daytime temperature on AMX	–
AMX	potential CO ₂ assimilation rate at light saturation for individual leaves	kg ha ⁻¹ h ⁻¹
ASRQ	assimilate (CH ₂ O) requirement for dry matter production	kg kg ⁻¹
ASRQSO	assimilate requirement for dry matter production of storage organs	kg kg ⁻¹
ASSSH	CO ₂ assimilation rate of shaded leaf area	kg ha ⁻¹ h ⁻¹
ASSSL	CO ₂ assimilation rate of sunlit leaf area	kg ha ⁻¹ h ⁻¹
ATMTR	atmospheric transmission coefficient	–
CLUSTF	cluster factor	–
COSLD	intermediate variable in calculating solar declination	–
DAVTMP	daily average temperature	°C
DAY	day number since 1 January	d
DAYEM	day of crop emergence	d
DAYL	daylength	h d ⁻¹
DDTMP	daily average daytime temperature	°C
DEC	solar declination	degrees
DLV	death rate of leaves	kg ha ⁻¹ d ⁻¹
DPAR	daily photosynthetically active radiation	J m ⁻² d ⁻¹
DS0	daily extra-terrestrial radiation	J m ⁻² d ⁻¹
DSINB	integral of SINB over the day	s d ⁻¹
DSINBE	as DSINB, but with a correction for lower atmospheric transmission at lower solar elevations	s d ⁻¹
DTEFF	daily effective temperature	°C
DTGA	daily total gross CO ₂ assimilation of the crop	kg ha ⁻¹ d ⁻¹
DTMAX	daily maximum temperature	°C
DTMIN	daily minimum temperature	°C
DTR	daily total solar radiation	J m ⁻² d ⁻¹
DVR	development rate	d ⁻¹
DVRRT	development rate in pre-anthesis phase as a function of temperature	d ⁻¹
DVRVT	development rate in post-anthesis phase as a function of temperature	d ⁻¹

DVS	development stage of the crop	–
EFF	initial light use efficiency for individual leaves	(kg ha ⁻¹ h ⁻¹) (J m ⁻² s ⁻¹) ⁻¹
FGROS	instantaneous CO ₂ assimilation rate of the crop	kg ha ⁻¹ h ⁻¹
FLV	fraction of shoot d.m. increase allocated to leaves	–
FRDF	diffuse radiation as a fraction of total solar radiation	–
FRT	fraction of total d.m. increase allocated to roots	–
FSH	fraction of total d.m. increase allocated to shoots	–
FSLLA	fraction of sunlit leaf area	–
FSO	fraction of shoot d.m. increase allocated to storage organs	–
FST	fraction of shoot d.m. increase allocated to stems	–
GLA	dummy for GLAI	ha ha ⁻¹ d ⁻¹
GLAI	growth rate of leaf area index of the crop	ha ha ⁻¹ d ⁻¹
GLV	d.m. growth rate of leaves	kg ha ⁻¹ d ⁻¹
GPHOT	daily total gross assimilation (CH ₂ O)	kg ha ⁻¹ d ⁻¹
GRT	d.m. growth rate of roots	kg ha ⁻¹ d ⁻¹
GSDST	distance in Gaussian integration	–
GSH	d.m. growth rate of shoots	kg ha ⁻¹ d ⁻¹
GSO	d.m. growth rate of storage organs	kg ha ⁻¹ d ⁻¹
GST	d.m. growth rate of stems	kg ha ⁻¹ d ⁻¹
GSWT	weighting factor in Gaussian integration	–
GTW	total d.m. growth rate of the crop	kg ha ⁻¹ d ⁻¹
HOUR	hour during the day	h
KBL	extinction coefficient for direct component of direct PAR flux	ha ha ⁻¹
KDF	extinction coefficient for diffuse PAR flux	ha ha ⁻¹
KDRT	extinction coefficient for total direct PAR flux	ha ha ⁻¹
L	counter in DO loop	–
LA0	extrapolated leaf area at field emergence	cm ² plant ⁻¹
LAI	leaf area index	ha ha ⁻¹
LAIC	partial cumulated leaf area index at various canopy depths	ha ha ⁻¹
LAICR	critical LAI beyond which death due to self-shading occurs	ha ha ⁻¹
LAT	latitude of the site	degrees
MAINSO	maintenance respiration coefficient of storage organs (CH ₂ O per unit d.m.)	kg kg ⁻¹
MAINT	maintenance respiration (CH ₂ O) of the crop	kg ha ⁻¹ d ⁻¹
MAINTS	maintenance respiration (CH ₂ O) of the crop at reference temperature	kg ha ⁻¹ d ⁻¹
MNDVS	factor accounting for effect of development stage on maintenance respiration	–
NPL	plant density	plants m ⁻²

PAR	instantaneous flux of incoming photosynthetically active radiation	$\text{J m}^{-2} \text{s}^{-1}$
PARDF	instantaneous diffuse flux of incoming PAR	$\text{J m}^{-2} \text{s}^{-1}$
PARDR	instantaneous direct flux of incoming PAR	$\text{J m}^{-2} \text{s}^{-1}$
PARLDF	absorbed diffuse PAR per unit leaf area	$\text{J m}^{-2} \text{s}^{-1}$
PARLDR	absorbed direct component of direct PAR per unit leaf area	$\text{J m}^{-2} \text{s}^{-1}$
PARLPP	direct PAR absorbed by leaves perpendicular to direct beam	$\text{J m}^{-2} \text{s}^{-1}$
PARLSH	absorbed PAR for shaded leaves (per unit leaf area)	$\text{J m}^{-2} \text{s}^{-1}$
PARLSL	absorbed PAR for sunlit leaves (per unit leaf area)	$\text{J m}^{-2} \text{s}^{-1}$
PARLT	absorbed total direct PAR per unit leaf area	$\text{J m}^{-2} \text{s}^{-1}$
PI	ratio of circumference to diameter of circle	–
Q10	factor accounting for increase in maintenance respiration with a 10°C rise in temperature	–
RD	factor to convert degrees to radians	radians degree ⁻¹
RDR	relative death rate of leaves	d ⁻¹
RDRDV	relative death rate due to developmental ageing	d ⁻¹
RDRSH	relative death rate due to self-shading at high LAI	d ⁻¹
REFL	crop reflection coefficient for PAR	–
RGRL	relative growth rate during exponential leaf area growth	$\text{cm}^2 \text{cm}^{-2}$ $^\circ\text{C}^{-1} \text{d}^{-1}$
SC	solar constant, corrected for varying distance sun-earth	$\text{J m}^{-2} \text{s}^{-1}$
SCP	scattering coefficient of leaves for PAR	–
SINB	sine of solar inclination above the horizon	–
SINLD	intermediate variable in calculating solar declination	–
SLA	specific area of new leaves	ha(leaf) kg^{-1}
T	counter in DO loop	–
TADRW	total above-ground dry weight	kg ha^{-1}
TBASE	base temperature for juvenile leaf area growth	$^\circ\text{C}$
TEFF	factor accounting for effect of temperature on maintenance respiration	–
TSUMEM	temperature sum after emergence	$^\circ\text{C d}$
WLV	dry weight of leaves (green + dead)	kg ha^{-1}
WLVD	dry weight of dead leaves	kg ha^{-1}
WLVG	dry weight of green leaves	kg ha^{-1}
WRT	dry weight of roots	kg ha^{-1}
WSO	dry weight of storage organs	kg ha^{-1}
WST	dry weight of stems	kg ha^{-1}

4.1.3 Description of the model

Daily gross assimilation: an outline of the approach Rates of gross CO₂ assimilation are calculated from the absorbed light energy and the photosynthesis-light response of individual leaves. If illumination intensities, averaged over the day and over the canopy, were applied, daily canopy assimilation would be seriously overestimated, because photosynthesis responds to light intensity in a non-linear, convex way. In the model, the temporal and spatial variation in illumination intensity over the leaves is, therefore, taken into account.

First, the instantaneous radiation flux at the top of the canopy is derived from measured daily irradiance. A distinction is made between diffuse skylight and direct sunlight because of the large difference in illumination intensity between shaded leaves, receiving only diffuse radiation, and sunlit leaves, receiving both direct and diffuse radiation. Subsequently, the vertical profiles of the radiation fluxes within the canopy are characterized. From these profiles, the absorbed radiation for each horizontal leaf layer is derived. On the basis of the photosynthesis-light response of individual leaves, the assimilation rate in a leaf layer is calculated for sunlit and shaded leaves separately. Daily crop assimilation is obtained by integrating these assimilation rates over the leaf layers and over the day.

This comprehensive approach for calculating crop assimilation rate is discussed here only in general terms. Detailed discussions are given by Spitters et al. (1986) for calculating the diffuse and direct radiation fluxes above the canopy, by Spitters (1986) for calculating assimilation rates from these fluxes, and by Goudriaan (1986) for the Gaussian integration method used to integrate assimilation rates over the canopy and over the day. Simplified approaches for calculating crop assimilation rates are discussed in Subsections 4.2.4 and 4.2.5.

The model SUCROS87 can be applied, without a thorough understanding of the subroutines used, to calculate the daily crop assimilation rate. Readers not interested in the details can, therefore, proceed directly to the section on carbohydrate production.

Radiation fluxes above the canopy Measured daily total irradiance (wavelength 300-3000 nm) is used as input for the model. Incoming radiation is partly direct, with the angle of incidence equal to the angle of the sun, and partly diffuse, with incidence under various angles. The diffuse flux is the result of the scattering of sun rays by clouds, gases and dust in the atmosphere. The proportion of diffuse radiation in the total radiation is, thus, dependent on the degree of scattering. To characterize this, the measured daily total radiation is compared with the quantity that would have reached the earth's surface in the absence of an atmosphere; a value that can be calculated from theoretical considerations. The ratio of both values is called the atmospheric transmission. The proportion of diffuse radiation is derived from the atmospheric transmission on the basis of an empirical relationship.

Irradiance intensity changes during the day according to the sine of the elevation of the sun above the horizon ($\sin \beta$). On the basis of this relation, the instantaneous flux densities of diffuse and direct radiation are calculated from their daily totals.

Only half the incoming radiation is photosynthetically active (PAR, wavelength 400-700 nm). This visible fraction, usually called 'light', is used to calculate CO_2 assimilation.

Radiation profiles within the canopy Incoming radiation is partly reflected by the canopy. The reflection coefficient (ρ) of the canopy is a function of solar elevation, leaf angle distribution, and reflection and transmission properties of the leaves. The complementary fraction ($1 - \rho$) is potentially available for absorption by the canopy.

Radiation fluxes decrease more or less exponentially with increasing leaf area within the canopy:

$$I_L = (1 - \rho) I_0 e^{-kL} \quad \text{Equation 62}$$

in which I_0 is the flux at the top of the canopy ($\text{J m}^{-2} \text{ ground s}^{-1}$), L the cumulative leaf area index (counted from the top of the canopy downwards) ($\text{m}^2 \text{ leaf m}^{-2} \text{ ground}$), I_L the net flux at depth L , and k the extinction coefficient. The diffuse and direct fluxes each attenuate at a different rate, i.e. they are characterized by radiation-specific extinction coefficients. The extinction coefficients are calculated as a function of solar elevation, leaf angle distribution, and the scattering coefficient of individual leaves.

Part of the direct flux intercepted by the leaves is scattered (i.e. reflected or transmitted). Hence, the direct flux segregates inside the canopy into a scattered, diffused component and a direct component. Both are treated separately in the model.

The decline of the radiation flux is a measure for its absorption. The rate of absorption at a depth L in the canopy is obtained by taking the derivative of Equation 62 with respect to cumulative leaf area index in the canopy:

$$I_{aL} = -dI_L/dL = k(1 - \rho) I_0 e^{-kL} \quad \text{Equation 63}$$

in which the subscript a refers to absorbed radiation ($\text{J m}^{-2} \text{ leaf s}^{-1}$).

Instantaneous assimilation rate per leaf layer The photosynthesis-light response of individual leaves can be described by the exponential function:

$$A_L = A_m (1 - e^{-\epsilon I_{aL}/A_m}) \quad \text{Equation 64}$$

in which A_L is the gross assimilation rate ($\text{kg CO}_2 \text{ m}^{-2} \text{ leaf s}^{-1}$), A_m the gross assimilation rate at light saturation ($\text{kg CO}_2 \text{ m}^{-2} \text{ leaf s}^{-1}$), and ϵ the initial slope or light use efficiency ($\text{kg CO}_2 \text{ J}^{-1} \text{ absorbed}$). Substituting the appropriate value for the absorbed photosynthetically active radiation (I_{aL} in Equation 63) yields the assimilation rate for each specific leaf layer.

Instantaneous assimilation rates for each leaf layer are calculated for shaded leaf area and sunlit leaf area separately. The shaded leaf area receives the diffuse flux and the scattered component of the direct flux. The sunlit leaf area receives both diffuse and direct flux. Illumination intensity of sunlit leaves varies strongly with leaf angle. In the model, the assimilation rate of the sunlit leaf area is, therefore, integrated over the leaf angle distribution.

The assimilation rate per unit leaf area in a canopy layer, is the sum of the assimilation rates of sunlit and shaded leaves, taking into account their proportion in each layer. The proportion of sunlit leaf area at depth L in the canopy equals the proportion of the direct component of the direct flux reaching that depth. This proportion is calculated in analogy to Equation 62, introducing the extinction coefficient of the direct radiation component.

Daily gross assimilation of the canopy The daily rate of CO_2 assimilation of the crop is obtained by integrating the instantaneous rates per leaf layer over the canopy leaf area index and over the day. This is achieved by using the Gaussian integration method, a simple and fast method of numerical integration (Scheid, 1968). The Gaussian integration method specifies the discrete points at which the value of the function to be integrated has to be calculated, and the weighting factors that must be applied to these values to attain minimum deviation from the analytical solution. To integrate numerically a continuous function over the standardized interval (0,1) of the independent variable, using the 3-point algorithm, the function value is calculated at the discrete points $0.5 - \sqrt{0.15}$, 0.5 and $0.5 + \sqrt{0.15}$. The integrated value is obtained by applying a weighting factor of 1.6 to the value at 0.5 and 1.0 to both other values. (In Figure 46, the Gaussian distances and weighting factors are implemented as DATA statements). For calculating daily total assimilation, the 3-point method performs very well (Goudriaan, 1986; Spitters, 1986). The assimilation rates at three depths in the canopy are calculated three times daily (Figure 47).

The three canopy depths selected according to the Gaussian criteria are:

$$L = (0.5 + p\sqrt{0.15}) \text{LAI} \quad p = -1, 0, 1 \quad \text{Equation 65}$$

where LAI is the total leaf area index of the crop. The assimilation rates (A') at these depths are calculated according to Equation 64. The weighted average of these assimilation rates is:

$$A_h = \text{LAI}(A'_{-1} + 1.6 A'_0 + A'_1)/3.6 \quad \text{Equation 66}$$

where A_h is the hourly canopy assimilation rate ($\text{kg CO}_2 \text{ ha}^{-1} \text{ h}^{-1}$).

To integrate over the day, three points in time are selected in the period from noon to sunset:

$$t_h = 12 + 0.5D(0.5 + p\sqrt{0.15}) \quad p = -1, 0, 1 \quad \text{Equation 67}$$

where D is the daylength (h). Daily total canopy assimilation is obtained as the

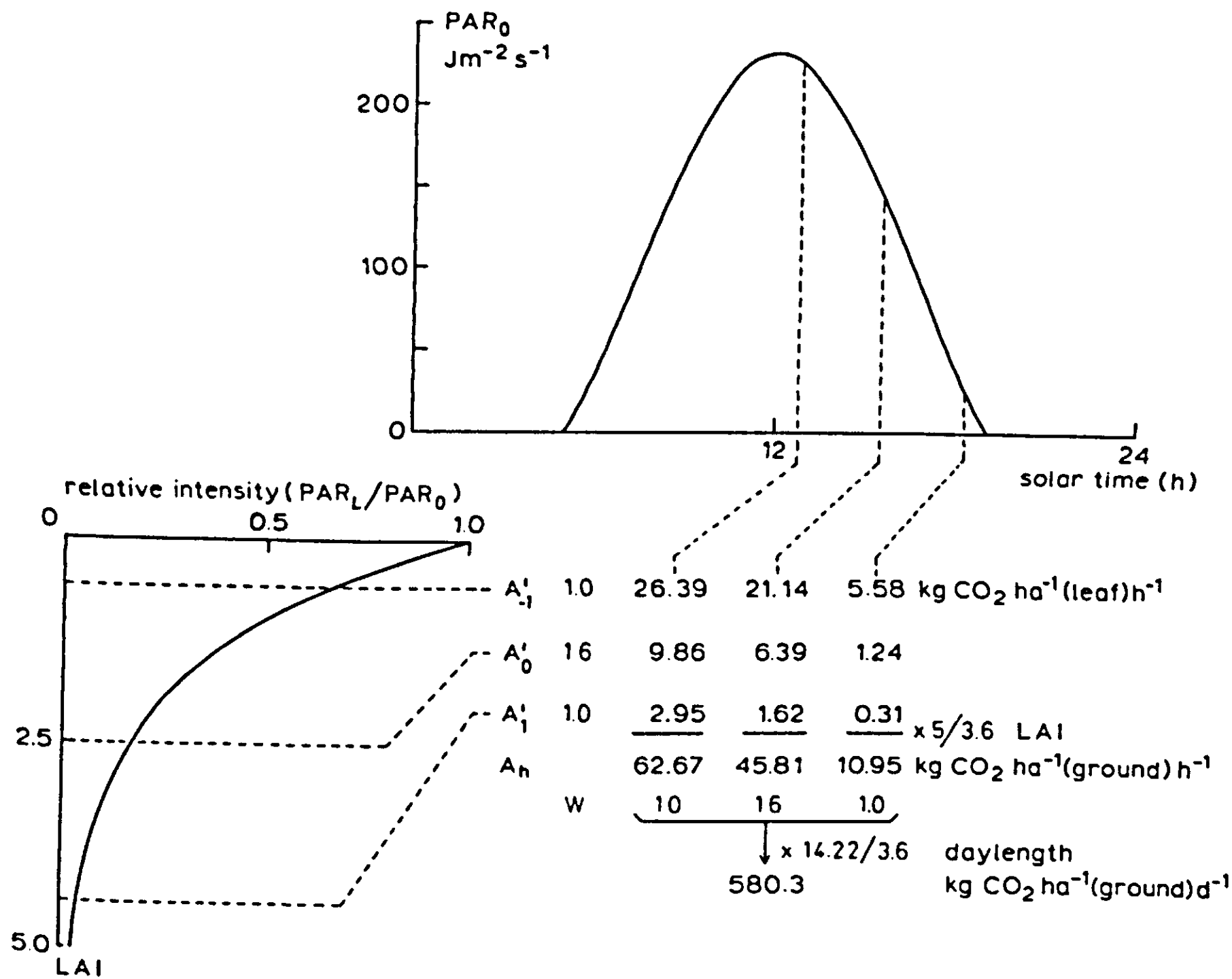


Figure 47. Summary of the Gaussian integration procedure. At three selected moments of the day, incident photosynthetically active radiation (PAR_0) is computed. Using this radiation, assimilation is computed at three selected depths in the canopy. Integration is performed following the Gaussian algorithm, i.e. a summation using certain weighting factors (w) (Equations 65-68). The daily assimilation rate of a standard crop ($LAI = 5$, $k = 0.72$, $A_m = 40 \text{ kg ha}^{-1} \text{ h}^{-1}$, $\epsilon = 0.45 \text{ kg ha}^{-1} \text{ h}^{-1} (\text{J m}^{-2} \text{ s}^{-1})^{-1}$) is presented for an average day in the Dutch growing season (18 August, 52° NL, $PAR = 7.07 \text{ MJ m}^{-2} \text{ d}^{-1}$).

weighted average of the instantaneous assimilation rates (Equation 66) at the three points in time:

$$A_d = D(A_{h,-1} + 1.6A_{h,0} + A_{h,1})/3.6 \quad \text{Equation 68}$$

where A_d is the total daily gross assimilation ($\text{kg CO}_2 \text{ ha}^{-1} \text{ d}^{-1}$).

Carbohydrate production In the photosynthesis process, CO_2 is reduced to carbohydrates (CH_2O) using the energy supplied by the absorbed light. This reaction can be written as:



For each kg of CO_2 absorbed, 30/44 kg of CH_2O is formed, the numerical values representing the molecular weights of CH_2O and CO_2 , respectively.

Maintenance respiration Some of the carbohydrates formed are respired to provide energy for maintaining the existing biostructures. The maintenance processes include resynthesis of degraded proteins (especially enzyme turnover) and maintenance of ionic gradients across cell membranes. The higher the metabolic activity of the plant, the higher the maintenance costs (Penning de Vries, 1975); probably due to a higher enzyme turnover and higher transport costs.

The maintenance costs may be estimated on the basis of the quantities of proteins and minerals present in the biomass, and crop metabolic activity, as presented by de Wit et al. (1978). This method, however, requires information on the nitrogen and mineral contents of the vegetation.

Based on the results of this analysis, typical values for the maintenance coefficients of various plant organs have been derived by Penning de Vries & van Laar (1982). In the model SUCROS87, these coefficients are used to calculate the maintenance requirements of the crop according to:

$$R_{m,r} = 0.03 W_{lv} + 0.015 W_{st} + 0.015 W_{rt} + 0.01 W_{so} \quad \text{Equation 69}$$

in which $R_{m,r}$ is the maintenance respiration rate ($\text{kg CH}_2\text{O ha}^{-1} \text{ d}^{-1}$) at a reference temperature of 25°C , and W is the organ dry weight (kg ha^{-1}) with the subscripts referring to leaves, stems, roots and storage organs, respectively. The numerical values in Equation 69, representing the maintenance coefficients, have the dimension $\text{kg CH}_2\text{O kg}^{-1} \text{ DM d}^{-1}$.

Higher temperatures accelerate the turnover rates in plant tissue and hence the costs of maintenance. An increase in temperature of 10°C increases maintenance respiration by a factor of about 2 ($Q_{10} = 2$) (Penning de Vries & van Laar, 1982; Kase & Catský, 1984). The rate of maintenance respiration at temperature, T , is thus:

$$R_m(T) = R_{m,r} \cdot 2^{(T-T_r)/10} \quad \text{Equation 70}$$

The reference (T_r) is assumed to be 10°C higher for tropical species than for

species from temperate climates, because the maintenance requirements of a crop are likely to be adapted to the growth temperatures.

When the crop ages, its metabolic activity and, therefore, its maintenance requirements decrease. This effect could be accounted for by relating the maintenance coefficients to the N content of the tissues (van Keulen & Seligman, 1987). However, N contents are not simulated in the model. Therefore, maintenance respiration is assumed to be proportional to the fraction of the accumulated leaf weight that is still green. This reduction factor is also applied to the maintenance respiration of the other plant organs, as it is assumed that dying of stem tissue and roots proceeds simultaneously to dying of leaves.

For the storage organs, a storage component and a non-storage component are distinguished. The storage component (mainly carbohydrates) is metabolically inactive and does not require maintenance. For the non-storage component, the maintenance coefficient is assumed to be identical to that of the stem. For instance, in sugar beet, the sugar content is about 80% on a dry weight basis, so the maintenance coefficient of the beet is $(1 - 0.80) \cdot 0.015 + 0.80 \cdot 0 = 0.003 \text{ kg-CH}_2\text{O kg}^{-1} \text{ DM d}^{-1}$.

It should be emphasized that modelling of maintenance respiration is still in a preliminary phase. The physiological basis is rather weak and measurements of maintenance costs are scarce and inaccurate.

Growth respiration The primary assimilates in excess of the maintenance costs, are available for conversion into structural plant material (Equation 61). In this conversion process of the glucose molecules, CO_2 and H_2O are released. This is a partial combustion of glucose to provide energy required in the various biochemical pathways. Hence, biosynthesis of the various structural compounds can be considered as a process of cut and paste, the scraps representing the weight lost in growth respiration.

Each structural compound is formed along a distinct, non crop-specific pathway. Following these reactions, the weight of glucose required to produce a unit weight of the compound can be calculated (Penning de Vries et al., 1974). The transport costs of the molecules are included. Two active passages of membranes are assumed. Each active passage requires 1 ATP, which is provided by respiring 1/38 molecule of glucose. The assimilate requirements are presented in Table 13 for the following groups: structural carbohydrates, proteins, lipids (including fats and oils), lignin and organic acids. Minerals require assimilates only for uptake and transport. The data in Table 13 show, for example, that lipids are more expensive to produce than proteins.

Table 13. Average chemical composition of leaves, stems, roots and wheat grains, and the assimilates required to form the distinguished groups of compounds (top line) and to form a unit weight of the various plant organs (right column). The assimilate requirement of leaves, for example, is calculated as:

$0.52 \cdot 1.275 + 0.25 \cdot 1.887 + 0.05 \cdot 3.189 + 0.05 \cdot 2.231 + 0.05 \cdot 0.954 + 0.08 \cdot 0.120 = 1.46 \text{ kg CH}_2\text{O kg}^{-1} \text{ DM}$. (Modified after Penning de Vries & van Laar, 1982, according to Penning de Vries, pers. commun.).

	Carbo- hydrates	Proteins	Lipids	Lignin	Organic acids	Minerals	Assim. req.
Assim. req.	1.275	1.887*	3.189	2.231	0.954	0.120	kg CH ₂ O kg ⁻¹ DM
% Composition							
Leaves	52	25	5	5	5	8	1.46
Stems	62	10	2	20	2	4	1.51
Roots	56	10	2	20	2	10	1.44
Wheat grain	76	12	2	6	2	2	1.41

* 2.784 for leguminous crops with N₂ fixation by Rhizobium.

The assimilates required to produce a unit weight of a certain plant organ can now be calculated from its chemical composition and the assimilate requirements of the various chemical compounds. Typical values for leaves, stems and roots are given in Table 13. Storage organs (grains, tubers, etc.) vary too much in composition among species for one general value of their assimilate requirements to be given. The conversion efficiency (Equation 61, kg DM kg⁻¹ CH₂O) represents the inverse of the assimilate requirement (kg CH₂O kg⁻¹ DM).

At higher temperatures, the conversion processes are accelerated, but the pathways are identical. Hence, the assimilate requirements do not vary with temperature.

Phenological development The pattern of dry matter distribution over the various plant organs is closely related to the development stage of the crop. Development is defined as progression in the successive phenological stages. It is characterized by the formation rate of the various vegetative and reproductive organs and their order of appearance.

For many annual crops, the development stage can conveniently be expressed in a dimensionless variable, having the value 0 at seedling emergence, 1 at flowering and 2 at maturity. The development stage (D) is calculated as the integral of the development rate (D_r). The development rate has the unit d⁻¹, and is equal to the inverse of the time, in days, required to complete one unit

development. If it takes 100 days from emergence ($D = 0$) to flowering ($D = 1$), the average development rate over that period equals $1/100$ or 0.01 d^{-1} .

Temperature is the main environmental factor affecting the rate of development. This rate responds to temperature according to a curvilinear relationship. It has, however, often been demonstrated, that over a wide range of temperatures, the development rate increases more or less linearly with temperature (van Dobben, 1962; van Keulen & Seligman, 1987). Within this linear region, the rate of development can be defined as a function of average daily temperature:

$$D_r = (\bar{T} - T_b) / \Sigma(\bar{T} - T_b) \quad \text{Equation 71}$$

in which \bar{T} is the average temperature, T_b the base temperature below which the development rate equals zero, and $\Sigma(\bar{T} - T_b)$ the temperature sum or 'heat sum' ($^{\circ}\text{C d}$) required to complete a unit development. The periods from emergence to flowering and from flowering to maturity are each characterized by their own temperature sum.

When temperatures fall partly outside the linear region, the rate of development is introduced in the model as a non-linear function of temperature (Figure 46: wheat, Figure 51: maize), or accumulated effective temperatures are used (Figure 51: potato, sugar beet).

For certain species or cultivars, effects of photoperiod and vernalization must also be taken into account. Approaches that describe such effects quantitatively are given by, among others, Weir et al. (1984), Hadley et al. (1984) and Reinink et al. (1986).

Pattern of dry matter distribution In the model, total dry matter growth is partitioned over the various plant organs according to fixed distribution factors, defined as a function of the development stage. Dry matter is first partitioned between shoots and roots, and then the shoot fraction is further subdivided between leaves, stems and storage organs.

The growth rate of a certain plant organ is thus obtained by multiplying the overall growth rate of the crop (Equation 61) by the fraction allocated to that organ. Its dry weight is obtained by integrating this growth rate over time.

This approach to the partitioning of dry matter is descriptive, as the distribution keys are defined as a function of the development stage of the crop only. The influence of environmental factors could be included by applying modification factors to these keys, depending on temperature, water and nutrient status of the crop, and its reserve level (Loomis et al., 1979; van Keulen & Seligman, 1987). In more mechanistic models, one or more reserve pools of free sugars are defined. Primary photosynthates enter these reserve pools, which are depleted by respiration and structural growth of the various organs, differing in sink strength (Thornley, 1972; Fick et al., 1973; Cooper & Thornley, 1976; Ng & Loomis, 1984). It is emphasized, however, that modelling of assimilate partitioning is still in a preliminary phase.

Redistribution of dry matter within the plant (sink-source relationships) Storage organs may not only be filled from current assimilates but also from carbohydrates and proteins that have been stored temporarily in other organs. Neglecting this relocation may lead to a substantial underestimate of the yield of storage organs. A simple procedure is discussed to elaborate the basic model to take into account the influence of carbohydrate reserves on the rate of kernel growth in cereals.

During the pre-anthesis phase, and in the early phase of kernel growth, not all primary assimilates are converted into structural plant material. Reserves in the form of non-structural carbohydrates (starch, fructans, di- and monosaccharides) are accumulated, especially in the stems. Together with the current assimilates, these temporary reserves form the carbohydrate 'source' available for kernel growth.

Dry matter accumulation in the grains proceeds according to an S-shaped curve, in which three phases can be distinguished: (1) the lag phase, in which cell division takes place and growth is about exponential, (2) the linear phase with an approximately constant growth rate and (3) the maturation phase with a gradual decline in the growth rate (Figure 48). Growth rate of the grains is relatively independent of the current rate of assimilation, as long as sufficient reserves are available. The growth rate of the grains is then determined by their demand for carbohydrates; i.e. by their 'sink' size. When the reserves are exhausted, the size of the 'source' limits growth rate. For further discussions on the sink-source relations in grain yield formation in cereals, see Tollenaar (1977) and Spiertz & van Keulen (1980).

A simple calculation procedure for grain yield formation is presented in Figure 49. The demand of the grains for carbohydrates (the size of the sink) and the availability of carbohydrates as the sum of current assimilates and reserves (the size of the source) are defined. The actual growth rate of the kernels is then calculated as the minimum of the potential growth rate (G_p) and the rate that can be realized by the available carbohydrates (G_a): $\text{Min}(G_p, G_a)$.

The potential rate of grain growth (G_p) is the product of the number of grains (N_g) and the potential growth rate of the individual grains (P). In maize, the number of kernels is mainly related to the current flux of assimilates around silking (Edmeades & Daynard, 1979), and in wheat to the net photosynthesis per unit degree-day in the period from ear initiation to anthesis (Rawson & Bagga, 1979). However, in both crops, kernel number can often be estimated satisfactorily on the basis of the amount of biomass at anthesis (Stapper & Arkin, 1980; Spiertz & van Keulen, 1980).

The potential rate of dry matter accumulation of individual kernels is a function of their development stage (Figure 48) and usually increases with temperature. The exponential increase in the growth rate during the lag phase is approximated here by a linear increase from zero when 1/3 of the lag phase has elapsed, to the maximum value at the end of this phase (Figure 48). An estimate of the

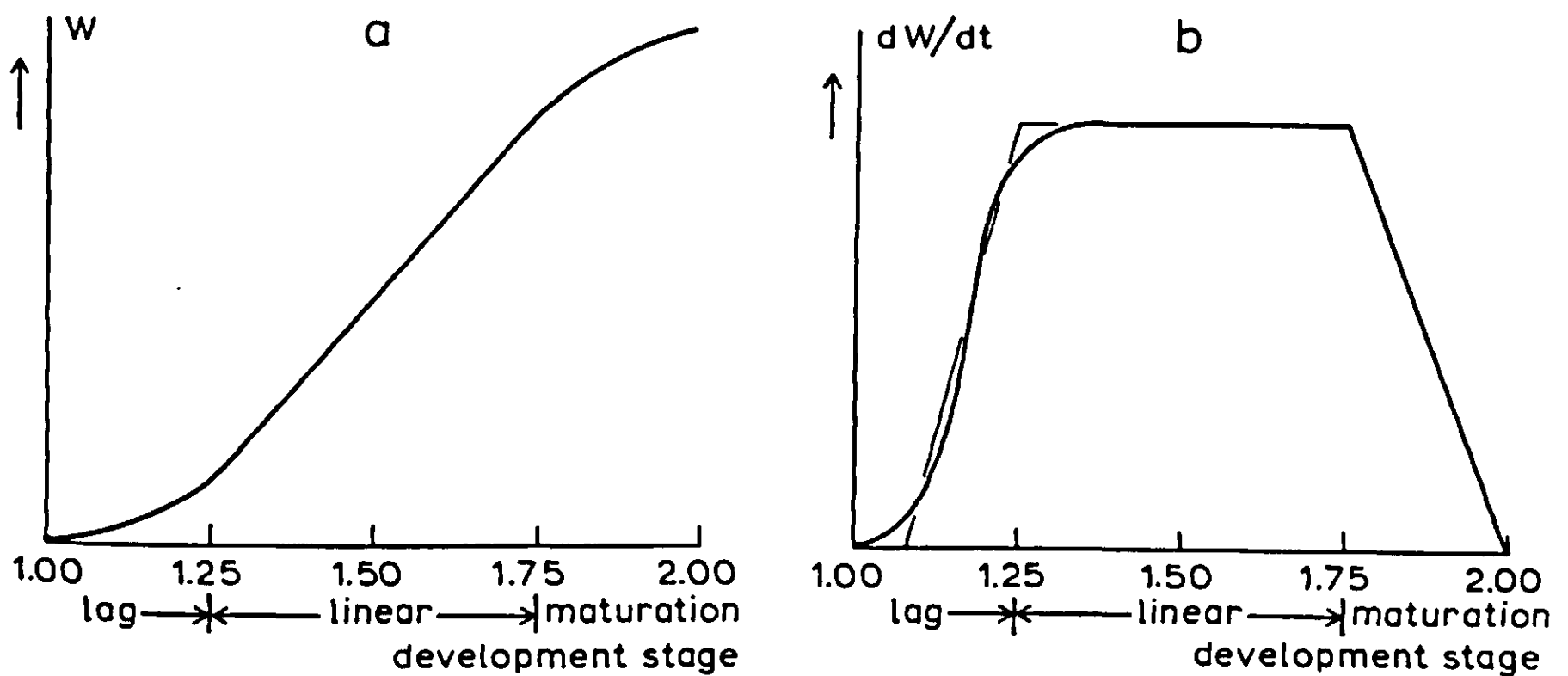


Figure 48. Schematic representation of cumulative weight (W) and growth rate (dW/dt) of individual grains as a function of development stage (1 = flowering, 2 = ripeness). The broken line represents the simplification used in the model.

Figure 49. Procedure to be included in the model SUCROS87 to account for sink-source relationships in grain growth. In the source-limited version of the model SUCROS87 (Figure 46), the statements used to calculate GPHOT, ASRQ, FST, GST, GSO, and WSO and FSTTB must be omitted. Parameters given are for spring wheat and maize.

- * Weight of grains (kg/ha)
 $WSO = \text{INTGRL}(0., GGR)$
- * Actual growth rate of the grains (kgDM/ha/d)
 $GGR = \text{AMIN1}(GGRP, GGRA)$
- * Potential growth rate of the grains (kgDM/ha/d)
 $GGRP = \text{NGRAIN} * 0.01 * \text{PGRI} * \text{GRTMP} * \text{GRDVS}$
- * No. of grains / m² as a function of above-ground biomass at anthesis
 $\text{NGRAIN} = \text{INTGRL}(0., (\text{NGA} + \text{NGB} * \text{TADRW}) * \dots$
 $\text{INSW}(\text{DVS}-1., 0., 1.) * \text{INSW}(-\text{NGRAIN}, 0., 1.))$
 $\text{PARAM NGA} = 0., \text{NGB} = 2.0$
- * Potential growth rate of individual grains (mg/kernel/d) at 16 °C
 $\text{PGRI} = \text{PKRWT} / ((\text{F2} + 0.5 * (0.67 * \text{F1} + \text{F3})) * \text{GFD16})$
- * Potential kernel weight (mgDM/kernel)
 $\text{PARAM PKRWT} = 45.$
- * Relative duration of lag, linear and maturation phase, resp.
 $\text{PARAM F1} = 0.11, \text{F2} = 0.61, \text{F3} = 0.28$
- * Grain fill duration (days at 16 °C), derived from DVRR
 $\text{PARAM GFD16} = 56.8$
- * Influence of temperature and development stage on PGRI
 $\text{GRTMP} = \text{AFGEN}(\text{GRTMPT}, \text{DAVTMP})$
 $\text{GRDVS} = \text{AFGEN}(\text{GRDVST}, \text{DVS})$
- FUNCTION GRTMPT = 0,0., 8,0., 10,0.37, 16,1.00, 20,1.22, 25,1.37, ...
 30,1.48, 35,1.48
- FUNCTION GRDVST = 0.,0., 1.07,0., 1.11,1., 1.72,1., 2.0,0., 2.5,0.
- * Growth rate of the grains that can be sustained by available assimilates
 $\text{GGRA} = \text{WRES} / \text{ASRQSO} / \text{TC}$
- * Time constant (d) for translocation of carbohydrate reserves
 $\text{PARAM TC} = 2.$

and maturation phase, respectively. Typical values for f_1 , f_2 and f_3 are 0.25, 0.50 and 0.25, respectively. \bar{P} refers to the storage capacity of the grains and is dependent on the environmental conditions during the period of cell division (Reddy & Daynard, 1983). When the duration of grain fill (D_g) is expressed in $^{\circ}\text{C d}$, a linear relationship between rate of grain fill and temperature is assumed, which is applicable for maize (Figure 49; Stapper & Arkin, 1980). For wheat, a non-linear relationship is used (Figure 49; van Keulen & Seligman, 1987).

The foregoing defines the capacity of the sink. The size of the carbohydrate source is calculated from the current CO_2 assimilation (Figure 46) complemented by the pool of reserve carbohydrates, which is obtained as the integral of the rates of replenishment and depletion of the reserves. During the pre-anthesis period, some of the primary assimilates are allocated to this reserve pool according to fixed keys (van Keulen & Seligman, 1987). After grain set, the changes in the reserve pool are treated more mechanistically. All current assimilates, not used for structural growth of leaves, stems or inflorescence frame, contribute to the reserves. Dividing the amount of reserves that can be mobilized each day by the carbohydrate requirement per unit grain weight, gives the rate of grain growth that could be sustained by the available carbohydrates (G_a). The storage capacity of the plant for carbohydrate reserves is limited, and leaf photosynthesis is reduced as the maximum capacity is approached (Barnett & Pearce, 1983). In the model, therefore, a maximum content of reserves in the stem is defined and the rate of canopy photosynthesis is reduced when this content is approached (Figure 49).

The actual growth rate of the grains takes either the value of the source-determined growth rate (G_a) or that of the sink-determined growth rate (G_p), whichever is the lowest. This actual growth rate also determines the rate of depletion of the reserves.

Leaf area The area of green leaves is the major determinant for light absorption and photosynthesis of the crop. Under optimum conditions, light intensity and temperature are the environmental factors influencing the rate of leaf area expansion. Light intensity determines the rate of photosynthesis and hence the supply of assimilates to the leaves. Temperature affects the rates of cell division and extension.

During the early stages of crop growth, temperature is the overriding factor. The rate of leaf appearance and final leaf size are constrained by temperature through its effect on cell division and extension, rather than by the supply of assimilates.

In these early stages, leaf area increases more or less exponentially over time. In the model, the leaf area index (ha leaf ha^{-1} ground) of the crop is calculated by multiplying the leaf area per plant by the planting density. The leaf area per plant (L , $\text{m}^2 \text{ plant}^{-1}$) is described by the exponential function:

$$L_t = L_0 \cdot e^{R_L \cdot t} \quad \text{Equation 73a}$$

so that the daily increase in leaf area is:

$$L_{t+\Delta t} - L_t = L_0 \cdot e^{R_L \cdot (t+\Delta t)} - L_0 \cdot e^{R_L \cdot t} = L_t(e^{R_L \cdot \Delta t} - 1) \quad \text{Equation 73b}$$

in which L_0 is the leaf area at emergence, R_L the relative growth rate of leaf area (d^{-1}), t the time after emergence (d), and Δt the integration interval (d). Note that in calculating the increase in leaf area over the discrete time interval Δt , a difference equation is used rather than a differential equation (see Answer to Exercise 52 in Section 4.2).

The relative growth rate is defined as a function of temperature. For the relatively wide range of temperatures where R_L responds more or less linearly to temperature (van Dobben, 1962; Causton & Venus, 1981; Hunt, 1982), R_L can be defined per degree-day rather than per day (Figure 46). Some unpublished field data have shown that the exponential model should be restricted to the situation where the development stage $D < 0.3$ and LAI < 0.75 .

In the later development stages, leaf area expansion is increasingly restricted by assimilate supply. Branching and tillering generate an increasing number of sites per plant, where leaf initiation can take place and mutual shading of plants further reduces the assimilate supply per growing point. For these later stages, the model calculates the growth of leaf area by multiplying the simulated increase in leaf weight by the specific leaf area ($m^2 g^{-1}$) of new leaves.

Various ways of expanding this simple approach can be envisaged. Relative growth rate can be defined as a function of temperature, irradiance and development stage. The specific area of new leaves can be defined in relation to temperature and irradiance (Acock et al., 1978; Sheehy et al., 1980; Ng & Loomis, 1984). In a more mechanistic approach, leaf area growth can be simulated from leaf appearance rate and rate and duration of expansion of individual leaves; all in relation to environmental factors (Stapper & Arkin, 1980; Jones & Hesketh, 1980).

To account for leaf senescence, a constant relative death rate of leaves is defined, starting from a certain point in the crop's development and affected by temperature. Leaf death rate ($ha ha^{-1} d^{-1}$) is calculated from the area of green leaves ($ha ha^{-1}$) and this relative death rate (d^{-1}) by a difference equation similar to Equation 73b used for the daily increase in leaf area. The net growth rate of green leaves is obtained by subtracting the death rate from the leaf area growth rate. In a more comprehensive approach, various leaf classes can be defined according to their time of appearance. For each class, leaf age is followed in time and when a certain age is reached, the class is aborted (Section 2.2; Johnson & Thornley, 1983).

In addition to this developmental ageing, leaf senescence also occurs due to shading at high LAI. A relative death rate due to self-shading is therefore defined that increases linearly from zero at a certain, critical LAI, to its maximum value at twice this LAI. Typical values for the maximum relative death rate and the critical LAI are $0.03 d^{-1}$ and $4 ha ha^{-1}$, respectively.

In some crops, organs other than leaves contribute significantly to crop assimilation (e.g. the ears in wheat). In such situations, the CO₂ assimilation of these organs must be taken into account in the model.

4.1.4 *Crop species and site characteristics*

The crop species, or cultivar, is characterized by a set of parameters and functions. Estimation of their numerical values from experimental data is discussed in this Subsection in some detail.

Distribution and absorption of light in the canopy The radiation flux incident on a leaf is partly absorbed and partly scattered. Scattering consists of reflection and transmission. Species differ in the optical properties of their leaves (Gausman & Allen, 1973). In the model, a value of 0.20 is used for the scattering coefficient of individual leaves for PAR ('light').

The light distribution within the canopy is characterized by the extinction coefficient (k in Equation 62). As a reference, we consider the situation where the leaves show a spherical angle distribution (i.e. as if they were placed on the surface area of a sphere), and are distributed randomly within the canopy volume. Assuming the above scattering coefficient of 0.20, the theoretical value of the extinction coefficient for the diffuse radiation flux is 0.72 (Goudriaan, 1977).

Actual values, however, can deviate substantially from this theoretical value. Crops with more erect leaves have lower k values, whereas crops with more prostrate leaves show higher values of k . In the model, a spherical leaf angle distribution is assumed. Alternative distributions can easily be implemented using the procedure described by Goudriaan (1988). A clustered distribution of leaves increases mutual shading, resulting in reduced light absorption and hence a lower value for k . However, especially in dicotyledons, new leaves are formed, preferably in gaps within the canopy, thus increasing the value of k . In the model, an actual value for the extinction coefficient for diffuse radiation is used. The ratio between this actual value and the above theoretical value is used as a cluster factor. The various extinction coefficients and the fraction sunlit leaf area are multiplied by this factor.

Light absorption by organs other than leaves results in a calculated extinction coefficient that is too high, if the measured extinction is related to leaf area only. If light absorption and assimilation by these organs are important, as for ears and panicles in cereals, these processes should be accounted for explicitly in the model; e.g. by treating them as competing assimilators (Appendix 7). This is also necessary for other factors, such as foliar diseases, that affect the photosynthetic capacity of the leaves and are distributed non-uniformly over canopy depth.

Typical values of k are 0.4 to 0.7 for monocotyledons and 0.65 to 1.1 for broadleaved dicotyledons (Monteith, 1969). The extinction coefficient can be estimated from measurements of PAR above and below a canopy with a known LAI (Equation 62), making sure that PAR is measured rather than total global

radiation. The extinction coefficient for total radiation is about 2/3 that of PAR. The extinction coefficient is best measured under a uniform overcast sky; then all radiation is diffuse so that the extinction coefficient is not affected by solar elevation.

Photosynthesis-light response of individual leaves The response of leaf photosynthesis to light intensity is characterized by its slope at low light intensity (ϵ) and its maximum rate at light saturation (A_m) (Equation 64). With respect to the photosynthetic pathway, three groups of species can be identified: C_3 and C_4 species and CAM plants. Lists of C_4 species have been published by Downton (1975) and Raghavendra & Das (1978).

At a leaf temperature of 20°C, both C_3 and C_4 species have an *initial light use efficiency* (ϵ) of approximately 12.5 $\mu\text{g CO}_2 \text{ J}^{-1}$ absorbed PAR or 0.45 $\text{kg CO}_2 \text{ ha}^{-1} \text{ leaf h}^{-1} (\text{J m}^{-2} \text{ s}^{-1})^{-1}$ (Ehleringer & Pearcy, 1983). In C_3 species, ϵ decreases with increasing temperature due to accelerated photorespiration. This temperature effect is relatively small: ϵ changes by about 1% with each change of 1°C in temperature (Farquhar et al., 1980; Ehleringer, 1978; Leverenz & Oquist, 1987). In C_4 species, ϵ is not affected by temperature because photorespiration is suppressed in the C_4 pathway.

Among both C_3 and C_4 species, there is hardly any variation in ϵ (Ehleringer & Pearcy, 1983). However, when ϵ is expressed per unit of incident PAR, instead of per unit of absorbed PAR, apparent differences may be due to differences in the absorption coefficient of the leaves (Hunt et al., 1985). Yellowing of leaves results in increased reflection and transmission and, therefore, in an apparent decrease of ϵ .

A large variation shows up in measured values of the *gross assimilation rate of leaves at light saturation* (A_m). The main sources of variation are differences in measurement conditions of temperature and ambient CO_2 concentration, differences in physiological and anatomical properties of the leaves as a result of differences in leaf age and pre-treatment, and variation among species and cultivars.

The influence of temperature on the rate of leaf photosynthesis is described in the model by multiplying the value of A_m by a temperature-dependent factor. The relationship between temperature and A_m is based on Versteeg & van Keulen (1986), where various reaction types are distinguished according to crop species and habitat (Figure 50).

The photosynthetic capacity of the leaves is affected by the preceding conditions of radiation and temperature to which they were exposed: leaves adapt their photosynthetic capacity to the environment. Therefore, A_m shows a seasonal course, which correlates with the time course of radiation and temperature (Parsons & Robson, 1981; Hodanova, 1981). This adaptation may be mimicked by using a seven-day running average of the value of A_m which has been adjusted for the environmental conditions (Schapendonk & Gaastra, 1984; Acock et al., 1978). A consequence of this adaptation is that the photosynthetic characteristics

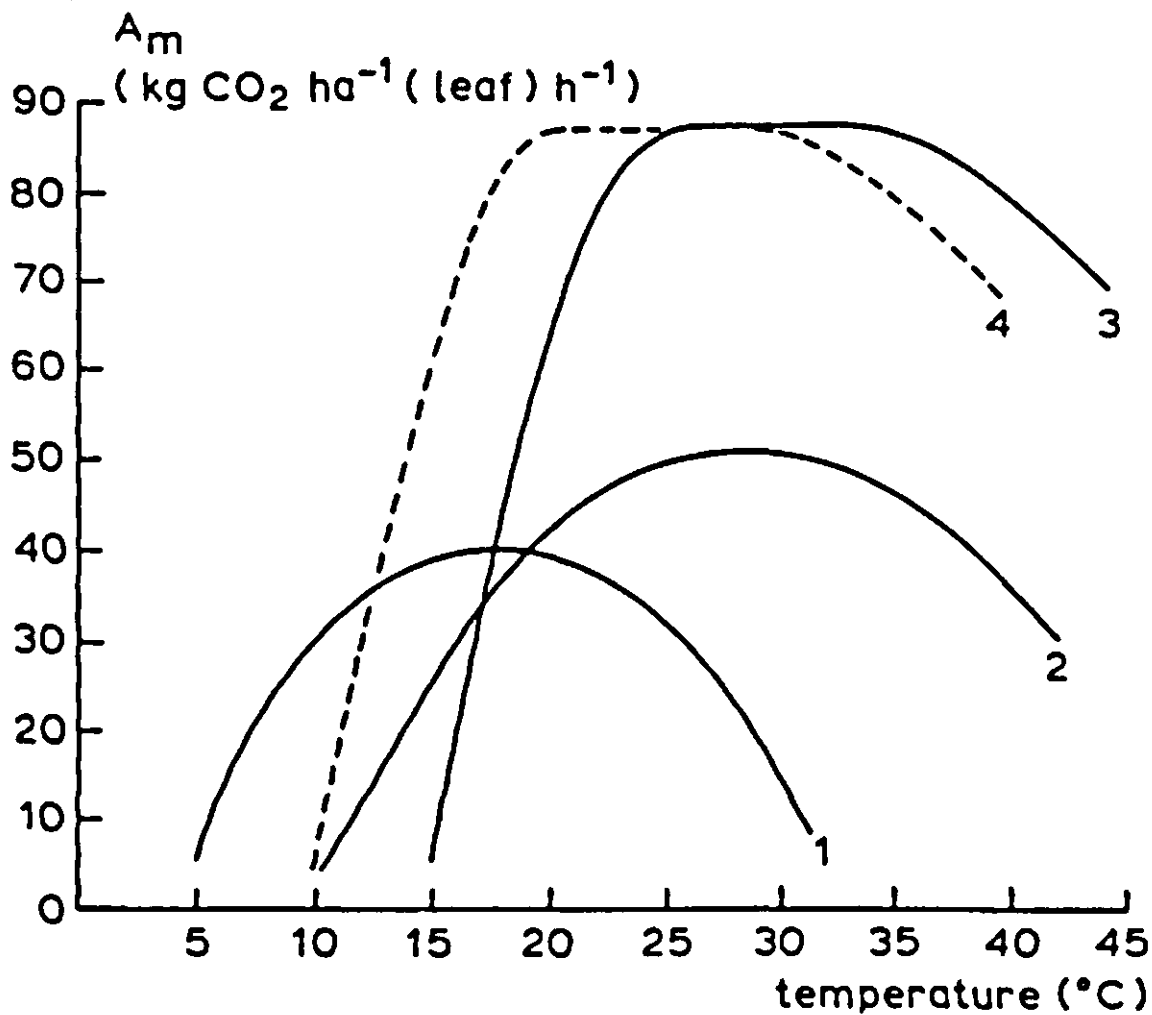


Figure 50. Average relationship between maximum assimilation rate of single leaves at light saturation (A_m) and temperature for (1) C_3 crops from temperate climates, (2) C_3 crops from warm climates, (3) thermophile C_4 crops, and (4) cultivars of C_4 crops adapted to temperate climates. (Source: Versteeg & van Keulen, 1986).

of leaves of plants grown in climate rooms, are not representative of those for plants grown in the field.

The photosynthetic capacity of a leaf is also affected by its age: A_m reaches a maximum shortly after full expansion of the leaf, followed by a gradual decline with ageing (Rawson et al., 1983; Dwyer & Stewart, 1986). Differences in photosynthetic capacity of the leaves are closely related to their nitrogen content, whether these variations are due to age, growing conditions or fertilizer application (van Keulen & Seligman, 1987). Leaves lower in the canopy have a lower photosynthetic capacity because they are older, have adapted to lower radiation levels (Acock et al., 1978; Williams, 1985) and also have lower nitrogen concentrations. The value of A_m used in the model, refers to the photosynthetic capacity of full-grown leaves at the top of the canopy, as these leaves absorb most of the radiation. Effects of canopy senescence are introduced by a multiplication factor which is a function of development stage.

Non-structural carbohydrate contents in leaves increase when the rate of conversion of assimilates into structural biomass is lower than the rate of assimilation. Such an increase in reserve content reduces the rate of photosynthesis. This feedback mechanism occurs at low night temperatures, under nutrient or water stress, and when sink size is small. The latter occurs in development phases where growth of stems and leaves is limited and the storage organs have not attained their potential growth capacity.

The photosynthetic capacity of leaves varies with crop species and cultivar. The coefficient of variation in A_m among genotypes within a species is of the order of 5–10% (Spitters & Kramer, 1986). Species can be grouped according to C_3 and C_4 types. Characteristic values range from 15–50 kg CO₂ ha⁻¹ leaf h⁻¹ for C_3 species and from 40–90 kg CO₂ ha⁻¹ h⁻¹ for C_4 species. Species from ruderal habitats show higher values than species from shaded habitats. In the model, estimates of ϵ and A_m must be used, which are found by fitting the exponential function (Equation 64) to data of gross photosynthesis of individual leaves. Such estimates may deviate from the measured values of photosynthetic efficiency at low light and photosynthesis at light saturation. If no firmly based value of A_m is available, a value of 40 kg CO₂ ha⁻¹ h⁻¹ for C_3 species and 70 kg CO₂ ha⁻¹ h⁻¹ for C_4 species is, in general, a reasonable estimate.

Maintenance respiration Respiration is usually measured as CO₂ evolution in the absence of light energy. This dark respiration can be partitioned into growth and maintenance respiration; estimation procedures being reviewed by Amthor (1984). Typical values for the maintenance coefficients of leaves, stems, roots and storage organs were given in Equation 69. As mentioned previously, these coefficients are affected by temperature, nitrogen content and mineral content of the plant tissue, and by the metabolic activity of the crop.

Measured rates of dark respiration of full-grown leaves, showed a large variation among species and among cultivars (M.J. de Kock, CABO, Wageningen, unpubl.).

The maintenance coefficients applied in the model are not based on conclusive evidence. This introduces a significant uncertainty in simulating the rate of crop growth, especially when the standing biomass is large compared to the current rate of photosynthesis, as at the end of the growth period.

Growth respiration The assimilate requirements to produce structural biomass are a function of the chemical composition of the biomass only. Assimilate requirements for the various groups of constituents are given in Table 13. Typical values for leaves, stems and roots are derived from their chemical composition, which is relatively constant. Storage organs of different species vary considerably in composition as indicated by Sinclair & de Wit (1975) and Penning de Vries et al. (1983).

Chemical analysis of plant material according to the specified groups of constituents is cumbersome. Elaborating on the approach of McDermitt & Loomis (1981), Vertregt & Penning de Vries (1987) developed a simpler, but still accurate method to determine the efficiency of the conversion processes. The assimilate requirement for the synthesis of plant biomass is calculated from its carbon and ash content by the empirical equation:

$$Q = (5.39 C + 0.80 \text{ ash} - 1.191) \cdot 1.0526 \quad \text{Equation 74}$$

in which Q is the carbohydrate requirement (kg CH₂O kg⁻¹ DM), C the carbon

content ($\text{kg C kg}^{-1} \text{ DM}$), and ash the ash content after ashing at 550°C ($\text{kg ash kg}^{-1} \text{ DM}$). The factor 1.0526 represents the transport costs which are assumed to be 2/38 molecules of glucose for each molecule transported.

Phenological development The rate of phenological development is mainly determined by temperature. The temperature response can be evaluated in field experiments planted at intervals, or in climate rooms where the plants are grown at various temperatures. Dates of the major phenological events (e.g. emergence and anthesis) are observed. The development rate, being the inverse of the time between two phenological events, is plotted against average temperature. The resulting relationship is, in general, linear over a wide range of temperatures. For this range, the temperature response can be characterized by slope and intercept of the linear regression (Equation 71). The intercept with the temperature axis is the base temperature (T_b), below which the development rate is zero. The inverse of the slope represents the temperature sum (ΣT in $^\circ\text{C d}$) required to complete the development phase.

Species originating from temperate regions show a base temperature of 0°C – 3°C , while species of sub-tropical and tropical origins have a base temperature of 9°C – 14°C (Angus et al., 1981). Within a species, cultivars may vary substantially in their temperature requirements. The temperature sum, therefore, must be characterized for each cultivar or group of cultivars (maturity classes).

Pattern of dry matter distribution In the model, the total daily dry matter increment is distributed over the various plant organs, according to key values dependent on the phenological development stage only. These key values can be estimated from experiments in which the crop is harvested at regular intervals during its growing period. At each harvest, the total dry weight is separated into the various plant organs. For each harvest interval, the growth in dry weight of a certain organ is expressed as a fraction of the total dry weight increment over that interval. These fractions are plotted against the average development stage or temperature sum for each harvest interval, and the dry matter distribution pattern is inferred. The fractions obtained show a substantial error variation, because each value is calculated on the basis of four dry weights, each having its own error.

As the distribution functions refer to total growth, the data must be adjusted to allow for weight loss due to fallen leaves. Redistribution of dry matter later in the growth period must also be taken into account. Growth of storage organs occurs partly from the translocation of carbohydrate reserves mainly from stems, and nitrogenous compounds mainly from leaves.

Leaf area. For the early growth stages, leaf area expansion is described by an exponential function, whereas for the later stages it is calculated by multiplying the simulated leaf weight increment by the specific leaf area of the new leaves.

Specific leaf area can be obtained from the same experiments used to derive the

pattern of dry matter distribution. Specific leaf area (SLA, ha leaves kg^{-1} leaves) of new leaves is estimated for each harvest interval by dividing the increase in LAI over the harvest interval by the increase in dry weight of green leaves. SLA is expressed as a function of development stage.

For the early, exponential stage (Equation 73), the relative growth rate of leaf area is defined as a function of temperature. The temperature response can be derived from field experiments planted at intervals. Over the range of temperatures where the relative growth rate increases more or less linearly with temperature, the logarithm of leaf area per plant is a linear function of the accumulated temperature after emergence:

$$\ln L_t = \ln L_0 + R'_L \Sigma T_t \quad \text{Equation 75}$$

in which L_0 is the extrapolated leaf area at emergence ($\text{m}^2 \text{ plant}^{-1}$), R'_L the relative growth rate of leaf area ($^{\circ}\text{C}^{-1} \text{ d}^{-1}$), and ΣT the temperature accumulated above the base temperature ($^{\circ}\text{C d}$). L_0 and R'_L are estimated from intercept and slope of the linear regression of $\ln L$ on accumulated temperature. In the case of non-linear temperature relationships, the relative growth rate (d^{-1}) can be defined as an empirical function of temperature.

The relative death rate of leaves can be estimated from the slope of the linear regression of the logarithm of the green leaf area index on time in days or degree-days. This is true for crops where leaf expansion and leaf senescence are separated in time, such as those with a determinate growth habit like cereals. When new leaf formation and senescence proceed concurrently, as in indeterminate species, calculating the relative death rate must take account of leaf growth. Apart from the development-related senescence, leaf senescence is accelerated by most stress conditions, and functioning of the foliage may be terminated by killing frosts.

Initialization The model is initialized with the LAI at crop emergence. This initial value is obtained by multiplying the extrapolated leaf area per plant at emergence (L_0 in Equation 75) by the plant density. Date of emergence, if not given, can often be well predicted from the date of planting and from a fixed temperature sum required for emergence (Subsection 4.2.3; Tamm, 1933; Bierhuizen & Wagenvoort, 1974; Angus et al., 1981).

Site characteristics The site is defined by its latitude (negative values for the Southern hemisphere) and by daily values of global radiation and average temperature. Weather data measured at a nearby meteorological station are generally sufficient. If no records of global radiation are available, daily global radiation can be estimated from relative sunshine duration (Frère & Popov, 1979). If no daily values of the weather characteristics are available, but only weekly or monthly averages, these averages can be used. However, due to the non-linear relations in the model, such as the response of assimilation to absorbed radiation, use of average values may lead to biased results. If this is the case, it

may be advisable to allow for the variation between days by generating daily values from the average data (Geng et al., 1985a, b).

4.1.5 Applying the model

SUCROS87 simulates the daily potential rate of crop growth, i.e. the growth rate under ample supply of water and nutrients in a pest, disease and weed free environment under the prevailing weather conditions. Extensions can be made to account for the effects of water and nutrient deficiencies (Section 4.2; van Keulen, 1982b; Stroosnijder, 1982; van Keulen & Wolf, 1986) and for the presence of weeds, diseases and pests (Sections 4.2.6, 4.2.7, 4.3 and 4.4).

To run the model, crop species and site must be characterized. The site is defined by its latitude and by data from standard meteorological stations for daily weather. Crop species and cultivar are characterized by a set of tables and parameters. In Figure 51, typical values are given for various crop species. The model is formulated in terms of the basic growth processes and is, therefore, widely applicable. Nevertheless, the species characteristics are to some extent dependent on environment and cultivar. To improve the accuracy of the model predictions, it may therefore be necessary to adjust the parameters on the basis of field experiments carried out in the target environment. An example of the performance of the model illustrated for potatoes is given in Figure 52.

Crop growth is often described by an empirical model, consisting of a regression equation (e.g. a logistic function). Sometimes, environmental variables, such as radiation and rainfall, are incorporated in the regression. These models can generate accurate yield predictions, especially when the regression parameters are estimated on the basis of extensive sets of experimental data. The predictions are restricted to the same environment on which the regression is based. These empirical, descriptive models, however, give little insight into the causes of the observed variation in yields.

SUCROS87 is a mechanistic model that explains crop growth on the basis of the underlying processes, such as photosynthesis and respiration, and how these processes are influenced by environmental conditions. The predictive ability of mechanistic models does not always live up to expectation. It should be realized, however, that each parameter estimate and process formulation has its own inaccuracy, and that these errors accumulate in the prediction of final yield. However, yield prediction is a secondary aim of these models. Their primary aim is to improve insight into the studied system by integrating the present knowledge quantitatively in terms of a simulation model. By studying the behaviour of the model, better insight into the real system is gained.

Figure 51. Parameters and functions to characterize winter wheat, maize, potato and sugar beet, respectively. These sets were implemented in the SUCROS87 model (Figure 46) and validated against the results of experiments conducted in the Netherlands under favourable growing conditions. Estimates of parameters and functions are, if not recorded elsewhere, mainly based on Dutch field experiments (Spitters et al., unpubl. data).

```

***                WINTER WHEAT                ***
* Initial leaf area (cm2/plant) and relative leaf growth rate (cm2/(cm2 °C d))
PARAM LAO = 6.5, RGRL = 0.0070, TBASE = 0.
* spring growth starts at 200 °C d after 1 Jan. (TIMER TIME=1.)
* in subroutine GLA:
  IF (TSUM.LT.200.) GLA = 0.
  IF ((TSUM.GE.200.).AND.(LAI.LE.0.)) GLA = NPL * LAO * 1.E-4
TSUM = INTGRL(0., AMAX1(0., DAVTMP-0.))
PARAM SLA = 0.0020
FUNCTION AMTMPT = 0.,0.01, 8.,0.01, 10.,0.4, 15.,0.9, 25.,1.0, 35.,0.

* Pre-anthesis and post-anthesis development rate as a function of temp.(1/d)
FUNCTION DVRVT = -10.,0., 0.,0., 30.,0.0239
FUNCTION DVRRT = -10.,0., 0.,0., 30.,0.0330
* simplified relationship DVRV based on 1254 °C d from 1 Jan. to anthesis
* For a subroutine to calculate DVR of winter wheat in relation to
* vernalization, photoperiodicity and temperature see Weir et al.(1984)
* and Reinink et al.(1986)

* Relative death rate of leaves (1/d) as a function of temperature and DVS
RDRDV = AFGEN(RDRT,DAVTMP) * AFGEN(RDRDST,DVS)
* Relative death rate of leaves (1/d) as a function of temperature
FUNCTION RDRT = 0.,.03, 10.,.03, 15.,.04, 30.,.09
* Multiplication factor for RDRDV as a function of DVS
FUNCTION RDRDST = 0.,0., 0.59,0., 0.60,0.085, 0.89,0.085, ...
                0.90,0.5, 1.09,0.5, 1.10,1.0, 2.5,1.0
* Other parameters and functions are identical to those given for spring wheat

* Main references:
* LAO, RGRL, SLA, DVRV, RDRDST: estimated from a collection of
* winter wheat data given by Groot (1987)
* AMTMPT: function accounts for reduction in leaf photosynthesis due to
* increased contents of non-structural carbohydrates at low spring
* temperatures (Groot, 1987)
* RDRT: van Keulen & de Milliano (1984)

```

```

***                MAIZE                ***
PARAM NPL = 11.11, DAYEM = 135.
PARAM LAO = 6.69, RGRL = 0.0294, TBASE = 10.
* Exponential growth ends at DVS=0.3 or when LAI>0.75
PARAM AMX = 70., EFF = 0.45
FUNCTION AMDVST = 0.,1.0, 1.3,1.0, 1.6,0.5, 2.0,0.25, 2.5,0.25
FUNCTION AMTMPT = -10.,.01, 9.,.05, 16.,.80, 18.,.94, 20,1., 30,1., 40,.75
PARAM KDF = 0.65, SCP = 0.20
PARAM MAINSO = 0.01, ASRQSO = 1.49
FUNCTION DVRVT = 0.,0., 10.,0., 30.,0.0471
FUNCTION DVRRT = 0.,0., 10.,0., 30.,0.0471
* emergence to silking 425 °C d (Tbase=10 °C) or 730 °C d (Tbase=6 °C)
* silking to maturity 425 °C d (Tbase=10 °C) or 730 °C d (Tbase=6 °C)
* fractional allocation to shoots (FSH), leaf blades (FLV),

```

* stems + leaf sheaths (FST), cobs (excl.grains) (FCOB)
 FUNCTION FSHTB = 0.0,0.60, 0.1,0.63, 0.2,0.66, 0.3,0.69, 0.4,0.73, ...
 0.5,0.77, 0.6,0.81, 0.7,0.85, 0.8,0.90, 0.9,0.94, 1.0,1.0, 2.5,1.0
 FUNCTION FLVTB = 0.,.70, .25,.70, .80,.15, .95,0., 2.5,0.
 FUNCTION FSTTB = 0.,.30, .25,.30, .80,.85, .95,.45, 1.1,0., 2.5,0.
 FUNCTION FCOBTB = 0.,0., .80,0., .95,.55, 1.1,1.0, 1.2,0., 2.5,0.
 FUNCTION SLAT = 0.,0.0040, 0.7,0.0010, 2.5,0.0010
 * SLA as a function of DVS
 RDR = INSW(DVS-1.0,0.,AMAX1(RDRDV,RDRSH,RDRLT,0.001))
 RDRDV = RDRSL * (DAVTMP - 8.)
 RDRSL = INSW (DVS-1.35, 0.0005, 0.0030)
 RDRLT = INSW (DVS-1.25, 0., LIMIT(0.,1.,(6.-DAVTMP)/6.))
 * RDR according to concept of Jones & Kiniry (1986): death due to
 * ontogenetic development (RDRDV), self-shading (RDRSH) and low, chilling
 * temperatures (RDRLT). RDRSL calibrated on Dutch field data.
 * Main references:
 * AMDVST: inferred from measurements of crop photosynthesis by
 * W.Louwerse (unpubl.)
 * AMTMPT: Versteeg & van Keulen (1986)
 * FSHTB: Foth (1962)
 * FLVTB,FSTTB: Dutch field data with cv. LG11; Hanway (1962,1963)
 * DVRV: Dutch field data with the early cv. LG11

*** POTATO ***
 PARAM NPL = 3.8, DAYEM = 137.
 PARAM LAO = 155., RGRL = 0.012, TBASE = 2.
 * Exponential growth ends at 450 °C d after emergence or when LAI>0.75
 PARAM SLA = 0.0030
 PARAM AMX = 30., EFF = 0.45
 FUNCTION AMTMPT = -10.,0.01, 3.,0.01, 10.,0.75, 15.,1.0, 20.,1.0, ...
 26.,0.75, 33.,0.01, 45.,0.01
 PARAM KDF = 1.00, SCP = 0.20
 PARAM MAINSO = 0.0045, ASRQSO = 1.28

* Fractions of dry matter growth allocated to:
 * 'shoots'(FSH) = leaves(FLV) + stems (incl. stolons)(FST) + tubers(FSO)
 FSH = LIMIT(0.80,1.00, 0.80 + 0.20 * (TSUME-IND)/430.)
 FLV = LIMIT(0.,0.75, 0.75 - (TSUME-IND)/430.)
 FSO = LIMIT(0.,1., (TSUME-IND)/430.)
 IND = 1. / (0.0015 + 0.00079 * MATR)
 PARAM MATR = 7.
 * Maturity class (MATR) 2.5 for very late cv's to 9.5 for very early cv's
 * (cv. Bintje: MATR = 7.)
 TSUME = INTGRL(0.,DTEFFT * INSW(DAY-DAYEM,0.,1.))
 DTEFFT = LIMIT (0.,11.,INSW(DAVTMP-13.,DAVTMP-2.,29.-DAVTMP))
 * Temperature sum (°C d) after emergence for tuber initiation and growth
 * Relative death rate due to developmental ageing (1/d)
 RDRDV = INSW(TSSNC, 0., AMAX1(8., DAVTMP - 2.) ...
 * EXP(-11.7+0.68*MATR) * EXP(TSSNC * (0.0068 - 0.00060*MATR)))
 TSUMEM = INTGRL(0.,DTEFFL * INSW(DAY-DAYEM,0.,1.))
 DTEFFL = AMAX1 (0.,DAVTMP-2.)
 TSSNC = TSUMEM - 725.
 * Leaf senescence starts after 725 °C d (Tbase=2 °C) after plant emergence
 * and is affected by temperature and maturity class of the cultivar

* Main references:
 * FSH,FLV,FSO: Spitters & Neele (1986,unpubl.), van Heemst (1986)
 * RDRDV: Spitters & Neele (1986,unpubl.)

- * MAINSO:
- * 0.70 (starch content) * 0. + 0.30 * 0.015 (non-sugar='stem'maintenance)
- * in line with measurements of Burton (1963,1964,1974) 48 h after harvest
- * AMTMPT: Versteeg & van Keulen (1986)
- * DTEFFT: inferred from Ingram & McCloud (1984)

*** SUGAR BEET ***

PARAM NPL = 7.8, DAYEM = 121.
 PARAM LAO = 0.845, RGRL = 0.0156, TBASE = 3.
 * Exponential growth ends at 450 °C d after emergence or when LAI>0.75
 PARAM SLA = 0.0020
 PARAM AMX = 45., EFF = 0.45
 FUNCTION AMDVST = 0.,0.50, 500.,1.0, 700.,1.0, 1700.,0.80, 3000.,0.60
 * DVS in °C d (Tbase=2 °C)
 FUNCTION AMTMPT = -10.,0.01, 3.,0.01, 10.,0.75, 15.,1.0, 20.,1.0, ...
 26.,0.75, 33.,0.01, 45.,0.01
 PARAM KDF = 0.69, SCP = 0.20
 PARAM MAINSO = 0.003, ASRQSO = 1.29

- * Fractions of dry matter growth allocated to the various plant organs
- * as a function of temperature sum after emergence (Tbase=2 °C)
- TSUM2 = INTGRL(0., LIMIT(0.,19.,DAVTMP-2.) * INSW(DAY-DAYEM,0.,1.))
- * shoots (leaves + crown):
- FUNCTION FSHTB = 0.,0.8, 400.,0.7, 900.,0.52, 901.,0.22, 3000.,0.22
- * the data suggest for TSUM2 > 900 °C d FSH=0.20 to 0.25
- * (for N rates as standard in practice) to 0.35 (for a continuous N-supply)
- * leaf laminae:
- FUNCTION FLVTB = 0.,0.85, 370.,0.85, 665.,0.48, 820.,0.23, 3000.,0.23
- * petioles + midribs:
- FUNCTION FSTTB = 0.,0.10, 370.,0.10, 665.,0.43, 820.,0.67, 3000.,0.67
- * crown:
- FUNCTION FCRTB = 0.,0.05, 370.,0.05, 665.,0.09, 820.,0.10, 3000.,0.10
- * fibrous roots (as a fraction of below-ground growth):
- FUNCTION FRTTB = 0.,1.,400.,1.,500.,0.5,1000.,0.1,2000.,0.03,3000.,0.03
- * Relative death rate of leaves in relation to temperature sum (1/°C/d)
- RDRDV = AFGEN(RDRT,TSUM2) * LIMIT(0.,19.,DAVTMP-2.)
- FUNCTION RDRT = 0,0., 600,0., 1000,.00022, 1500,.00050, 2500,.00075

- * Main references:
- * KDF: Tanaka (1983)
- * AMTMPT: Versteeg & van Keulen (1986)
- * ASRQSO:
- * 0.80 (sugar content) * 0. + 0.20 * 0.015 (non-sugar='stem'maintenance)
- * The value of 0.003 corresponds with respiration measurements one or two
- * days after harvest by Koster et al., Vanstallen, Vanstallen & Vigoureux,
- * Devillers, Wyse (all: Inst. Int. Rech. Betteravieres, 1980)

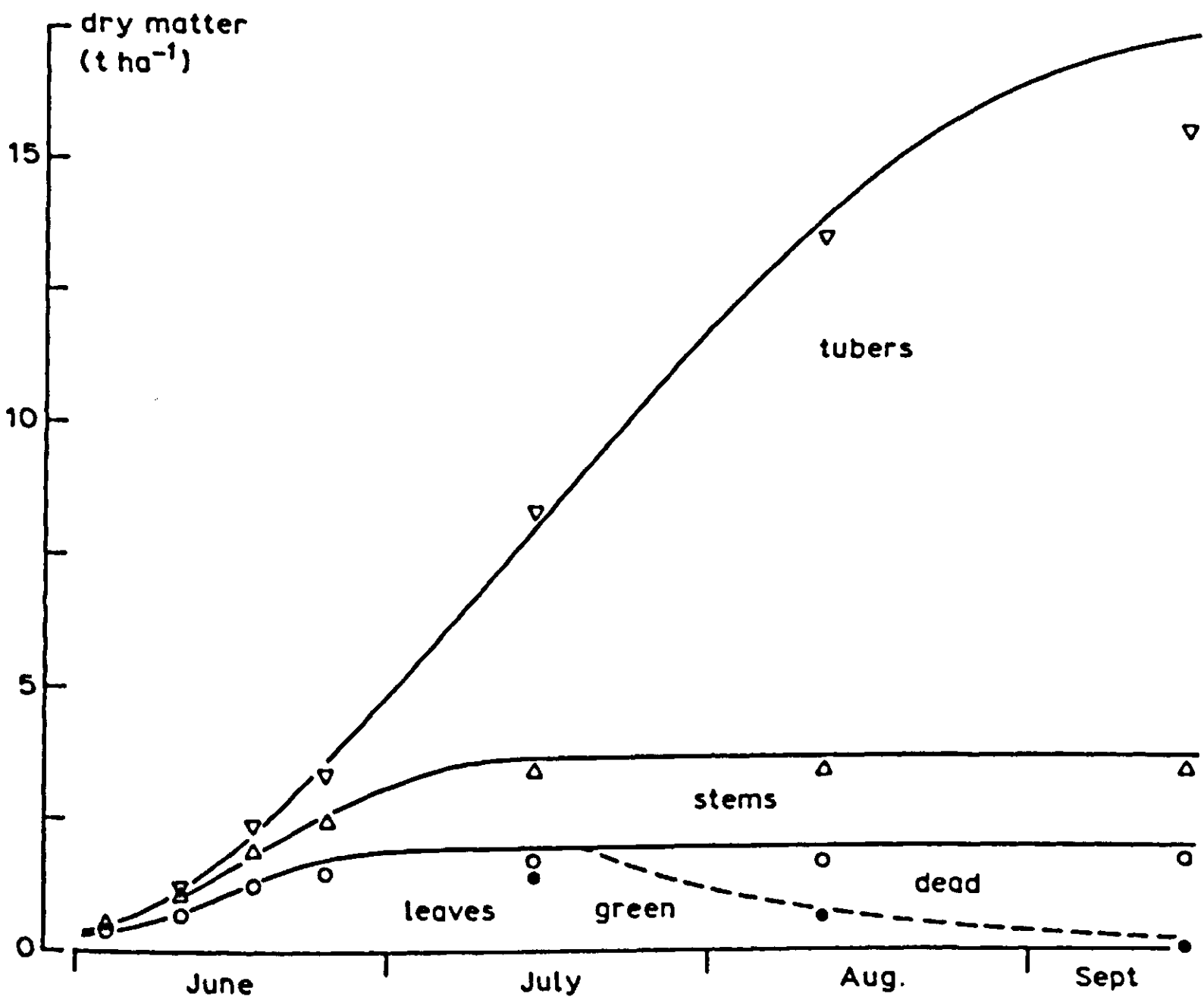


Figure 52. Cumulative organ dry weights as simulated with the SUCROS87 model version for potato. Data points refer to an experiment with cultivar Bintje in 1985 at Flevopolder, the Netherlands.

4.2 Weeds: population dynamics, germination and competition

C.J.T. Spitters

4.2.1 Introduction

Weeds are plants which interfere adversely with the production aims of the grower. These adverse influences: (1) reduce crop growth and yield, mainly due to competition for the growth-limiting resources light, water and nutrients; (2) reduce the financial value of the harvested product, mainly by contaminating the crop produce; and (3) hamper husbandry practices, especially harvesting operations, which increases the costs. Thus, weeds reduce the financial profits by lowering output (kg yield per hectare x price per kg) or increasing expenses. Weeds, therefore have to be controlled to minimize their adverse influence in the current crop ('tactics') and to anticipate these effects in future crops ('strategy').

The models presented in this Section are simple. Some summarize more comprehensive models, such as the competition models. Others, like the models of germination and seed bank dynamics are more preliminary. They are primarily instructive and directed towards providing insight into the underlying mechanisms of crop-weed interaction, and focus mainly on the biology of annual arable weeds. The models presented may also be useful for developing more effective advisory systems for practical weed management.

The long-term changes in weed seed reservoirs are discussed first. Weed infestation begins in this reservoir, from which the seeds germinate. The number of seeds and the time at which they emerge determine their starting position in competition with the crop. Germination is, therefore, the second topic to be discussed. The third section treats the modelling of crop and weed growth as determined by competition for the growth-limiting resources, providing more insight into how crop yield is reduced during the growing season and how it is affected by the various crop and weed characteristics. Attention is paid to how seed bank dynamics, germination and competition can be controlled by weeding and soil cultivation.

4.2.2 Dynamics of soil seed population

Changes in the soil seed population of annual, arable weeds are described using a dynamic population model, and the influence of control measures is discussed. The parameter values used here are typical for wild oats (*Avena fatua* L.) in barley, and are mainly derived from Wilson (1981) and Wilson et al. (1984). The global structure of this dynamic population model, where seed production per weed plant is treated as a constant, was also taken from these references. The model is a typical example of those applied when describing weed population

dynamics (Murdoch & Roberts, 1982; Mortimer, 1983). The model is eventually extended to include the effects of weed and crop density on weed seed production, and to estimate crop yield loss.

The sequential boxcar approach used in the preceding Sections to model the population dynamics of polycyclic diseases and pests is, in general, unnecessarily complex for weeds. Annual weeds usually accomplish only one, discrete generation a year, and plants of the same generation are quite synchronized in their development.

A simple flow diagram The population cycle of an annual weed is represented in Figure 53 in a simplified form. Each box denotes a state through which the seeds or plants pass during their life cycle. These state variables are expressed in numbers per unit ground area. Arrows represent transitions from one state to the other. The numbers change with the transitions and each transition is characterized by a discrete multiplication factor.

The soil seed population is exhausted by a fraction of P_g per year, so that a fraction $1 - P_g$ survives and contributes to the soil seed population of the following year. A fraction P_e of the removed seeds gives rise to established plants, which produce, on average, S_N seeds per year. A fraction P_b of these seeds is incorporated in the soil seed population. Hence, the net annual increment of the seed population is written as:

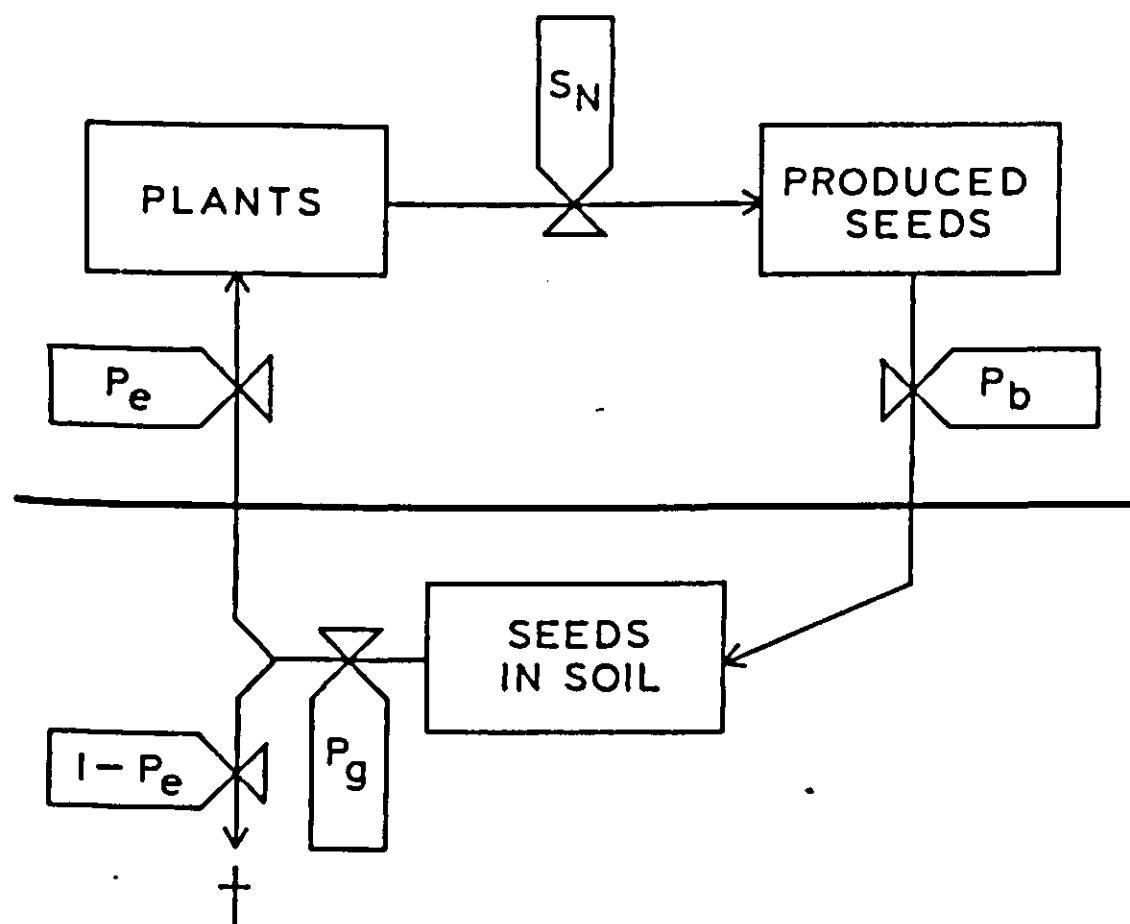


Figure 53. A simple flow diagram for the population cycle of an annual weed. The boxes represent state variables, expressed in numbers per unit area. P_g , P_e and P_b are fractions of exhaustion, seedling emergence and seed burial, respectively (yr^{-1}) and S_N represents the number of seeds produced per plant.

$$\Delta n_t / \Delta t = (-P_g + P_g P_e S_N P_b) n_t$$

Equation 76

where n_t is the number of seeds per unit area at time t , and Δt the time interval.

Exercise 52

Make a CSMP program for the population dynamics of wild oat according to Figure 53. Typical values for wild oat are $P_g = 0.68 \text{ yr}^{-1}$, $P_e = 0.15 \text{ yr}^{-1}$, $P_b = 0.60 \text{ yr}^{-1}$, and $S_N = 50 \text{ seeds plant}^{-1}$. Calculate the course of the soil seed population over a period of 15 years starting with an initial density of 1000 seeds m^{-2} .

In this simple model, each parameter is independent of population size. Soil seed population increases, therefore, by a constant percentage per year, resulting in an exponential growth of the population (straight line on the logarithmic scale in Figure 54). Many models on weed population dynamics are of this simple, exponential type.

Density dependence of seed production The greater the plant density, the smaller the plants and the lower the average number of seeds produced per plant. Hence, the seed population increases in time according to an S-shaped curve rather than exponentially. Effects of intra-specific and inter-specific competition are often accounted for in population dynamic models using a Lotka-Volterra approach

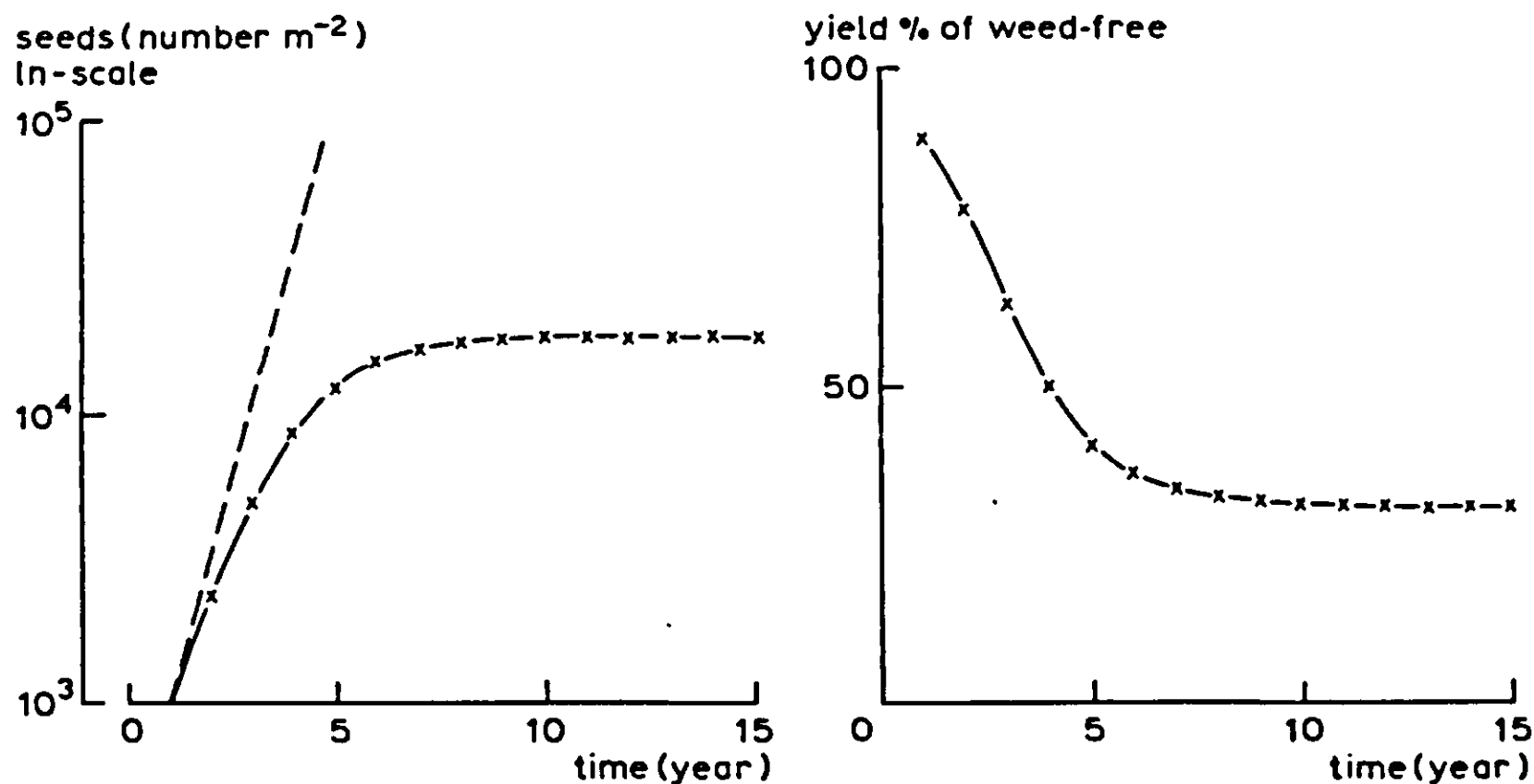


Figure 54. Simulated time course of soil seed population of wild oat, and the concomitant yield loss of spring barley. The broken line represents the exponential build-up of the seed population if density dependence of seed production is neglected. See also Exercises 52 and 53.

(e.g. Begon & Mortimer, 1981). Here, a more comprehensive model is presented where the influence of plant density is introduced by means of a descriptive competition model, based on a hyperbolic relation between biomass yield and plant density. For a review and further discussion of this type of competition model see Spitters (1983). Related descriptive equations for weed competition have been discussed by Cousens (1985). Spitters & Aerts (1983) and Firbank et al. (1984) proposed the use of this type of competition equation in models of weed population dynamics, to allow for the density dependence of weed seed production and to arrive at an estimate of concomitant crop yield loss.

The simplest form of interplant competition is that between plants of the same species. This intra-specific competition is generally characterized by a rectangular hyperbola:

$$Y = N/(b_0 + b_1N) \quad \text{or} \quad 1/W = N/Y = b_0 + b_1N \quad \text{Equation 77}$$

in which Y is the biomass yield (g m^{-2}), N the plant density (plants m^{-2}), W the average weight per plant (g plant^{-1}), and b_0 and b_1 are regression coefficients. When N approaches zero, $1/W$ approaches b_0 , so $1/b_0$ is the apparent weight of an isolated plant. When N approaches infinity, Y approaches $1/b_1$, so this quantity denotes the apparent maximum yield per unit area.

Equation 77 shows that $1/W$ is influenced additively by adding plants of the same species. This suggests that adding plants of another species also affects $1/W$ additively. Hence, for a crop in the presence of weeds:

$$1/W_{cw} = b_{c0} + b_{cc}N_c + b_{cw}N_w \quad \text{Equation 78a}$$

and for the associated weeds

$$1/W_{wc} = b_{w0} + b_{ww}N_w + b_{wc}N_c \quad \text{Equation 78b}$$

where the first subscript denotes the species whose yield is being considered, and the second subscript its associate. Subscript c refers to the crop and w to the weed. Adding one crop plant has the same effect on $1/W_{cw}$ as adding b_{cc}/b_{cw} weed plants. We could say that the crop is a b_{cc}/b_{cw} times stronger competitor against itself than the weed is against the crop. The ratio b_{cc}/b_{cw} measures the relative competitive ability of crop and weed, with respect to the effect on crop yield.

If more than one weed species is involved, the term $b_{cw}N_w$ is expanded linearly:

$$b_{cw}N_w = b_{c1}N_1 + \dots + b_{cn}N_n \quad \text{Equation 79}$$

and the term $b_{ww}N_w$ is similarly expanded. This also provides a method for calculating long-term changes in species composition within a multi-species weed vegetation.

The competition coefficients can be estimated from Equation 78 by multiple linear regression, but this results in biased estimates because the error variance of $1/W$ is much smaller at low values than at high values of $1/W$. When applying a linear regression, the data must therefore be weighted by their squared expectation value (Spitters, 1984). With the available statistical packages, however, it is

more convenient to estimate the coefficients by a least-squares procedure of non-linear regression of yield on the plant densities. To fulfil the assumption of homogeneity of variances, it is often necessary to apply a logarithmic or square root transformation of the yields when a wide yield range is covered; both sides of the equation being transformed before regression.

Usually, the crop is grown at constant plant density, so that Equation 78a simplifies to

$$1/W_{cw} = a_0 + b_{cw}N_w \quad \text{and} \quad 1/W_{cc} = b_{c0} + b_{cc}N_c = a_0 \quad \text{Equation 80}$$

where $1/a_0$ is the average weight per plant in the weed free crop. The yield of the weedy crop (Y_{cw}) relative to the weed free yield (Y_{cc}) is then

$$Y_{cw}/Y_{cc} = a_0/(a_0 + b_{cw}N_w) = 1/(1 + N_w b_{cw}/a_0) \quad \text{Equation 81}$$

Thus, the percentage reduction of crop yield in relation to weed density is characterized by the single parameter b_{cw}/a_0 . This parameter, being the initial slope of Equation 81, represents the apparent percentage yield loss caused by the first weed plant added to the crop stand. The aggregate yield reduction due to a multi-species weed infestation can be calculated, using Equation 81, from the 'damage coefficients' b_{cw}/a_0 of the individual weed species $w = 1, \dots, n$ because the effects of the different weed species accumulate additively (Equation 79). Due to the concave shape of the crop yield-weed density function (Equation 81), a non-uniform, clustered spatial distribution of the weed plants over the field gives a smaller yield reduction than a uniform distribution of the same average density.

Part of the total dry matter is invested in seeds. This ratio of seed weight to total biomass is called 'seed ratio' or 'net reproductive effort' (R_E). Although for many species, R_E remains fairly constant over a wide range of conditions, it may be influenced by genotype, environment (e.g. de Ridder et al., 1981) and plant density. A decrease in R_E with increasing density may be accounted for by extending the equation relating weed seed yield to density, to a power function (e.g. Firbank & Watkinson, 1985). These authors also propose a descriptive equation allowing for density-dependent self-thinning of seedlings, i.e. they distinguish initial and surviving plant densities.

Seed production of the weed is obtained from its biomass production as

$$n = Y_w R_E/S_w = N_w W_w R_E/S_w \quad \text{Equation 82}$$

in which n is the number of seeds produced (m^{-2}), and S_w the average weight per seed (g). Seed production is estimated much better in this way than by using a fixed value for the number of seeds produced per plant (S_N in Exercise 52).

It is emphasized that this simple population dynamic model uses average values for the parameters, and that these values can vary considerably from field to field and from year to year. Part of the variation is explained in relation to environmental variability by the germination model and the dynamic competition model still to be discussed.

Exercise 53

- a. Estimate the competition coefficients of spring barley and wild oat for the following situation. The competitive ability of plants of similar growth habits and similar times of seedling emergence, is closely related to their seed weights. Assume, therefore, that the degrees of intra-specific competition (b_{cc}/b_{c0} and b_{ww}/b_{w0}) and inter-specific competition (b_{cc}/b_{cw} and b_{ww}/b_{wc}) of barley and wild oat are proportional to their seed weights of 45 mg and 14 mg, respectively. Assume also that both use the available resources with an equal efficiency ($1/b_{cc} = 1/b_{ww}$). The density response of barley is characterized by a curvature b_{cc}/b_{c0} of $0.057 \text{ m}^2 \text{ plant}^{-1}$ and with the yield at a commercial density of $250 \text{ plants m}^{-2}$ amounting to 94% of the asymptote. Assume that at this density, the weed free grain yield amounts up to 5 t ha^{-1} (85% DM) with a grain yield/biomass ratio of 0.45.
 - b. Extend the model of Exercise 52 to allow for competition effects. Use the estimated competition coefficients to calculate soil seed population and crop yields for a period of 15 years when the field is sown each year with spring barley. Reproductive effort of wild oat is 0.42.
-

Weeding (herbicides) In the absence of control measures, the weed population builds up rapidly. Population increase is, however, strongly retarded by weeding.

In modern agriculture, weed control measures are, in general, applied early in the growing season, before the time when the weeds would significantly reduce crop growth. The efficiency of weeding can be characterized by the percentage reduction in soil cover or total leaf area of the weeds. The complementary percentage measures the degree of weed survival. Weeding operations are allowed for in the model by dividing the state variable 'plants' (Figure 53) into two state variables: 'plants before weeding' and 'plants after weeding', and by using the fraction of surviving weed plants as a multiplication factor for the transition.

Exercise 54

Calculate the influence of a post-emergence herbicide application – having an efficiency of 95%, and applied annually – on the system in Exercise 53. Evaluate also the effects of herbicide application once every 2, 3 and 4 years.

In the typical situation described in Exercise 54, weeding wild oat once every second year restricted yield losses to about 5% or less (Figure 55). Thus, annual weeding resulted in yield benefits of less than 5%. In general, with yield benefits of less than 5%, the profits of herbicide application do not outweigh the costs. The present example supports the opinion that in cereals, wild oat is controlled not so

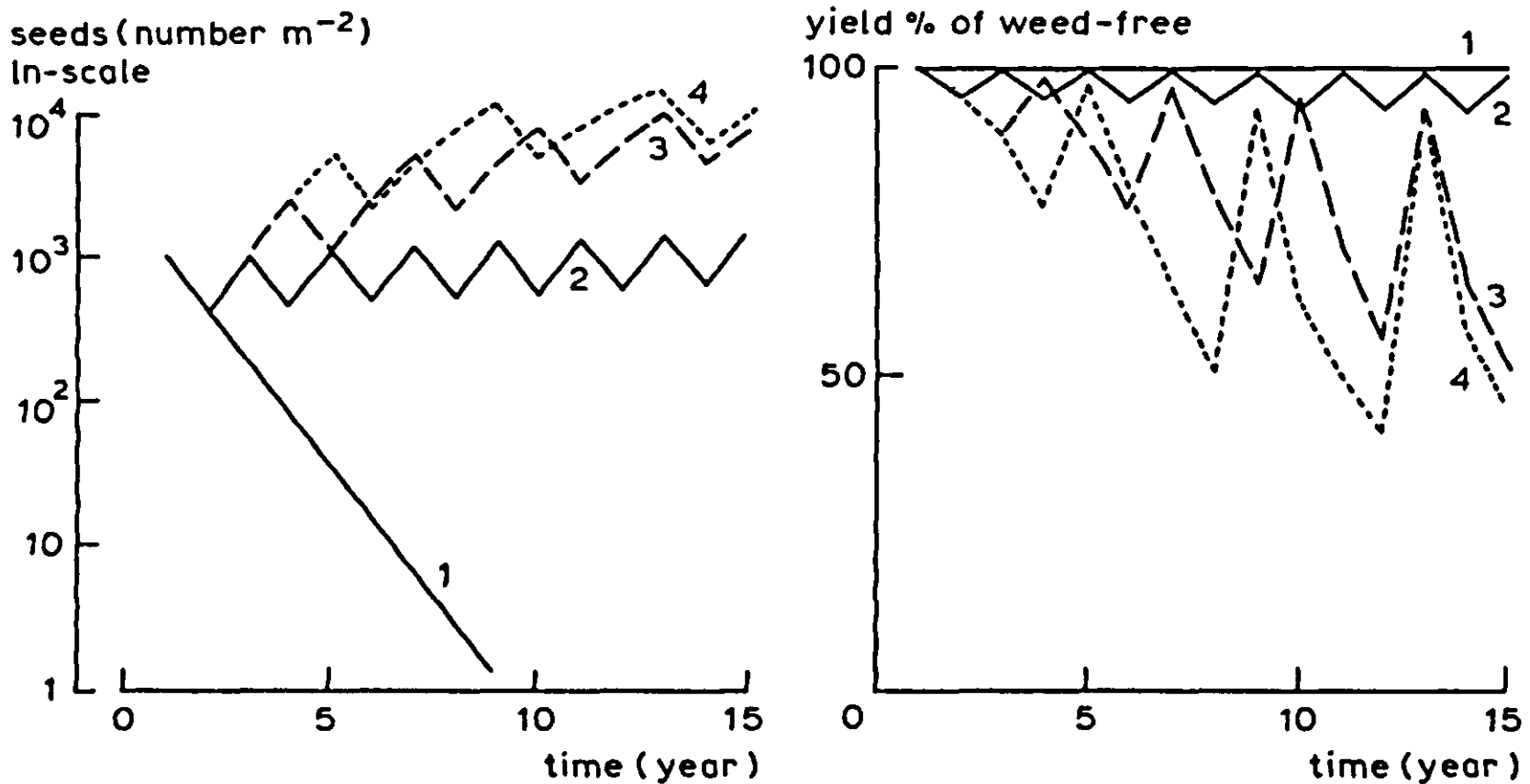


Figure 55. Simulated time course of soil seed population of wild oat, and the concomitant yield loss of spring barley. Herbicides are sprayed either annually or once every 2, 3 or 4 years.

much to prevent a yield reduction of the current crop (short-term tactics), but primarily to restrict increases in the weed seed population and thus to minimize the risks of having to take cumbersome and more expensive measures against large infestations in future crops (long-term strategy).

Sources of seed losses In the diagram of Figure 53, the seed population is depleted by recruitment of seedlings, losses of viability of seeds in the soil from one year to the next, and by losses prior to the incorporation of newly-produced seeds into the soil population.

Seed losses on the soil surface, the 'stubble losses', are mainly due to germination, removal by predators and attack by micro-organisms. Seeds become buried due to disturbance of the soil surface; soil cultivation being the main cause of soil disturbance in agricultural situations. After burial, seeds are lost much less rapidly: predation and parasitism are negligible; germination remains the principal factor, but is usually less than on the soil surface.

In Figure 56, a scheme is presented to introduce some more detail into calculating depletion of the soil seed population. Down to plough depth D_p , seeds are assumed to be distributed uniformly throughout the soil profile. The number of seeds below D_p is small and, therefore, ignored. Depletion of the soil seed population is primarily due to germination, either fatal or leading to successful emergence (Roberts, 1972; Murdoch & Roberts, 1982). Germination is, therefore, the only depletion process involved in the model. In Figure 56, a simple situation is represented where the probability of germination (P'_g) is

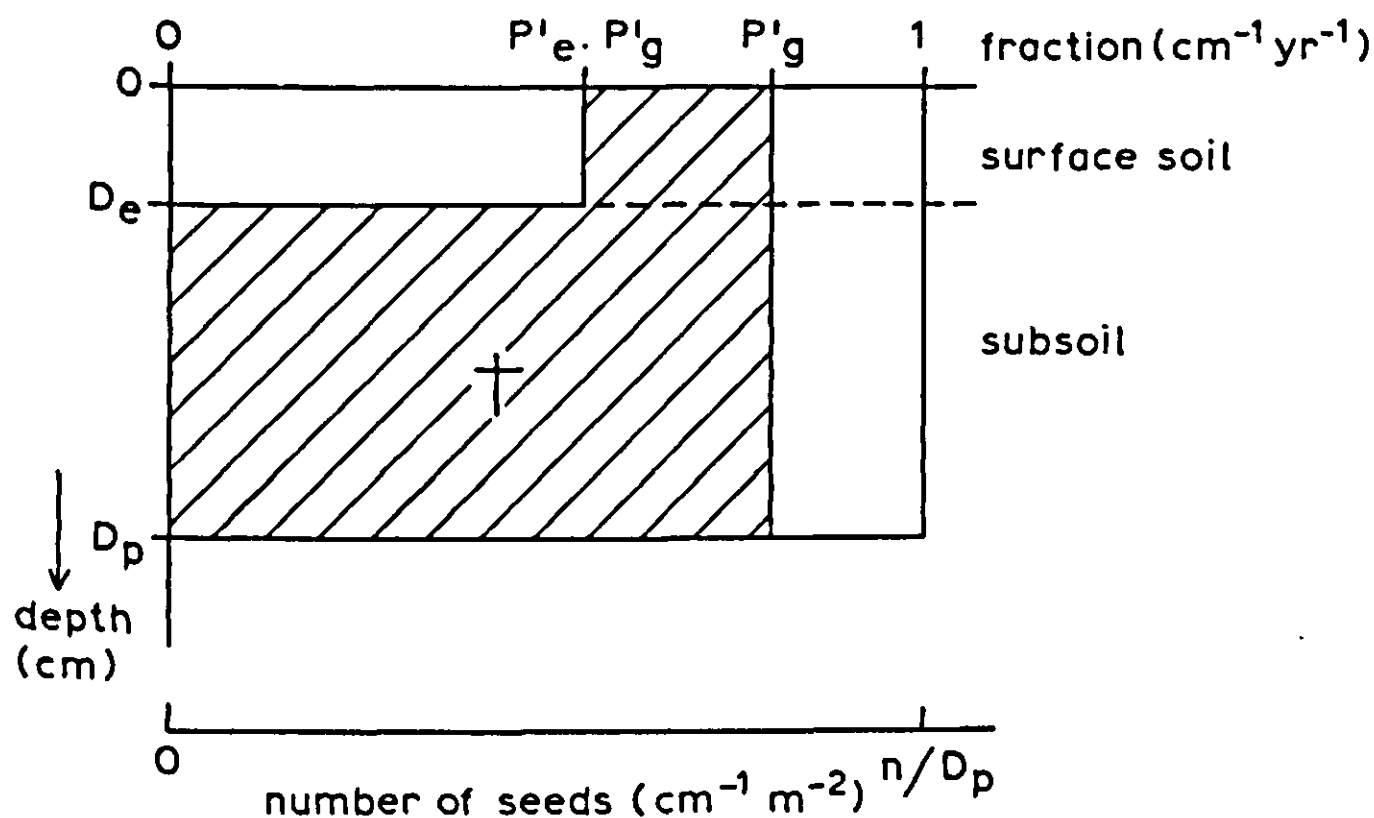


Figure 56. Fractions of germination (P'_g) and establishment (P'_e) in relation to soil depth. At a given depth, a fraction P'_g of the seeds germinates, of which a further fraction P'_e produces seedlings. All seeds are above plough depth D_p and successful emergence is only possible from depths less than D_e .

independent of soil depth. Successful emergence only takes place from depths less than D_e , with a uniform probability of $P'_e P'_g$.

The probability of seed survival from one year to the next equals $1 - P'_g$. The probability of emergence of germinated seeds (P_e in yr^{-1} , Figure 53) equals $P'_e D_e / D_p$. Alternative relations between P'_g , P'_e and soil depth can easily be accounted for in the model. (The primed probabilities have the dimension $\text{cm}^{-1} \text{yr}^{-1}$, while the unprimed probabilities are cumulated over the soil profile and have the dimension yr^{-1} .)

The depth D_e from which seedlings can emerge, strongly depends on the species and is especially related to seed size. Within a species, D_e is smaller in heavier soils. Few species emerge from depths in excess of 5 cm, but large-seeded species such as *Galium aparine* are able to emerge from up to 20 cm (Froud-Williams et al., 1984). With an emergence depth of, for instance, 2 cm and a plough depth of 20 cm, only 10% of the seeds are able to emerge successfully.

Species with a transient seed bank may be distinguished from those with a persistent seed bank (Thompson & Grime, 1979). In a transient seed bank, the major part of the soil seed population is depleted each year by germination, so the soil seed population in the following year mainly consists of newly produced seeds. Grasses in particular, such as wild oat, belong to this group. In a persistent seed bank, only a small part of the soil seed population is exhausted every year by germination. Many arable weeds are of the persistent type, especially species with hard seed coats, e.g. *Chenopodium album*. Not only do persistent species show a smaller P'_g , but the P'_g of their subsoil seed bank is also usually much smaller than that of their surface soil seed bank. This greater persistence of deeply buried

seeds is due to a higher degree of dormancy. Germination of these species is strongly stimulated by light, a large daily temperature amplitude and high nitrate concentration. The intensity of these dormancy-breaking factors decreases sharply with soil depth.

Exercise 55

Perform a separate calculation of the changes in the surface and subsoil seed bank of wild oat in the system described in Exercise 54 with annual herbicide application. Assume an emergence depth of 4 cm and a plough depth of 20 cm. Assume that after ploughing, the seeds are distributed at random throughout the soil profile down to plough depth. Germination and emergence probabilities are 0.68 and 0.75 $\text{cm}^{-1} \text{yr}^{-1}$, respectively. Calculate the changes also for an efficiency of herbicide application of 100%. What are the trends for a species with a persistent seed bank, characterized by a germination and emergence probability of 0.25 and 0.75 $\text{cm}^{-1} \text{yr}^{-1}$, respectively?

Exercise 55 demonstrates that eradication might be a possibility only for species with a transient seed bank, such as wild oat. Persistent seed banks are exhausted much more slowly, even with complete weed removal. In addition, since 100% efficiency of weed control is neither technically nor economically feasible, persistent species cannot be eradicated and containment of the species at low infestation levels is necessary (Murdoch & Roberts, 1982).

4.2.3 Germination

Weed infestation is recruited from the soil seed population by the processes of germination, emergence and establishment. Germination characteristics of the seeds in response to the environment, determine the initial extent of weed infestation and the timing of its occurrence. Both extent and timing are major determinants of the weeds' competitive ability, and thus of crop yield loss.

Germination accumulates over time; its rate is influenced mainly by temperature, availability of moisture, and seasonal periodicity. Periodicity of germination occurs in most weed species and is reflected in a well-defined, seasonal pattern of seedling emergence. Germination of weed seeds is often stimulated by light, daily fluctuations in temperature and high nitrate concentrations. These requirements are most intense close to the soil surface, so germination is greatest in the surface layer, and the seed bank is built up mainly in the subsoil. On the soil surface, germination may be inhibited by light (photo-inhibition) and by the low red/far-red ratio of radiation which has passed through a vegetation cover. When the seeds are buried, germination may be inhibited by a lack of stimulatory

factors (light, alternating temperature, nitrate), by a low oxygen tension or a high carbon dioxide tension, and by plant exudates.

The complex relations between seed germination and the environment have been reviewed by Heydecker (1973), Bewley & Black (1982) and Karssen (1982). In the present Subsection, the main processes of germination and seedling emergence are summarized in terms of a simulation model.

Three types of models can be distinguished for the simulation of seed germination and seedling emergence in the field. First, models in which germination is forecast on the basis of a certain average time required to germinate. Time is usually expressed as accumulated degree-days (e.g. Tamm, 1933; Bierhuizen & Wagenvoort, 1974). A second group includes models in which allowances are made for the time variation among seeds to germinate. This is done by using the cumulative frequency distribution of germination as a functional relationship in the model. Models of the third type, mimic dispersion by assuming that the germination process is composed of several arbitrary stages or boxcars. The different stages are successively passed through before reaching the final stage of visible germination (Janssen, 1974; Section 2.2). Although such a sequential boxcar approach provides a flexible model, it will often be unnecessarily complex for modelling the germination of weeds. Weed seed germination is triggered by certain, occasional events, mainly soil cultivation. In this Subsection, therefore, the second type of model is planned to simulate seed germination.

In the model, the time progression of germination and emergence is characterized by a cumulative frequency distribution function. This function is defined by three parameters. The influences of temperature, soil moisture and seed dormancy are quantified by multiplication factors for these germination parameters. The model is still in its preliminary phase, and the focus here is on its general structure. To arrive at a more accurate description of the multiplication factors, more research is needed on emergence under field conditions.

Time course The cumulative number of germinated seeds proceeds in time according to an S-shaped curve. Several equations have already been suggested to describe this distribution of time to germination. The model is described using a negative exponential function (Milthorpe & Moorby, 1974), being the simplest of the suggested functions. More sophisticated functions can, however, easily be substituted. In using a negative exponential, it is assumed that the seed population is depleted exponentially due to germination:

$$N_t = N_m(1 - \exp(-P(t - i))) \quad t \geq i \quad \text{Equation 83}$$

where N_t is the cumulative number of germinated seeds at time t , N_m the maximum number of germinable seeds, i the incubation time, being the time to first germination, and P the instantaneous germination probability. Equation 83 corresponds to a boxcar approach having only one boxcar.

Differentiating Equation 83,

$$dN_t/dt = P(N_m - N_t) \quad \text{or} \quad P = (dN_t/dt)/(N_m - N_t) \quad \text{Equation 84}$$

Thus, the germination rate, P , characterizes the fraction of the remaining, but germinable seed population that germinates within a short time interval dt . P determines the dispersion of the time to germination. Constancy of P with time is a feature of an exponential depletion function. Expressing the increment rate dN_t/dt independent of time, as in Equation 84, provides a flexible model where the influence of environment can easily be quantified by multiplication factors for the germination parameters.

The germination parameters can be estimated by fitting Equation 83 to the observations of N_t , using a least-squares procedure. It is easier, however, to estimate N_m from the maximum level of the cumulative germination curve and, subsequently, to estimate P and i from the linear regression of $\ln(1 - N_t/N_m)$ on t . The regression line has slope $-P$ and intersects the time axis at i . The linear regression approach is, however, less accurate, because the variation around the regression strongly increases as N_t approaches N_m .

Initialization of time For a crop, the germination process is started at the time of sowing. For weeds, initialization is more complex. In field populations of weeds, seedling flushes appear mainly after soil disturbance (Roberts, 1984). The main reason probably being that the seeds are exposed to conditions near the soil surface which overcome dormancy and promote germination. Under arable conditions, soil cultivation is the major source of soil disturbance so, for weeds, the time is started at the time of the last cultivation.

Temperature The maximum germination percentage (N_m) remains fairly constant over a wide range of temperatures (Figure 57a). The inclining sections of the temperature relation reflect the variation within the seed population in the limit temperatures for germination of the different seeds; they can be described using a cumulative normal frequency distribution (Washitani & Takenaka, 1984). For simplicity, they are approximated here by straight lines (Figure 57a). It can be derived that each inclining section embraces a temperature range of about three times the standard deviation of the population for the limit temperature.

The established temperature relation is used as a multiplication factor (f_T) for the final germination percentage at optimum temperatures ($N_{m,o}$):

$$N_m(T) = f_T N_{m,o} \quad \text{Equation 85}$$

(The stable and reproducible relationships which are usually obtained when cumulative seedling emergence in the field is plotted against accumulated degree-days, suggest that a long-term average of f_T should be used – e.g. a running average of f_T over the preceding 5 days – rather than an instantaneous effect of temperature on N_m .)

Like any metabolic process, germination is accelerated at higher temperatures. The time required to reach a certain percentage of germination, say 50%,

decreases, therefore, with an increase in temperature. Usually, the inverse of this time increases more or less linearly with temperature (e.g. Bierhuizen, 1973). Thus, the incubation rate – being the reciprocal of time to first germination – is given by:

$$1/i(T) = (T - T_b)/S = T/S - T_b/S \quad \text{for } T \geq T_b \quad \text{Equation 86}$$

where T_b is the base temperature (i.e. apparent temperature below which the germination process stops), and S the temperature sum to reach first germination ($^{\circ}\text{C d}$) (Figure 57b). The linearity of the relation implies that, independent of temperature, the first seeds germinate after a fixed temperature sum, S , has accumulated. If supra-optimum temperatures are involved, effective degree-days can be defined (Subsection 4.1.3: phenological development).

Acceleration of the germination process at higher temperatures, reduces variation among the seeds in germination time, so the germination probability (P) increases. The linear relation between the inverse of time to germination and temperature, indicates a linear increase in P with temperature (Figure 57c). The germination probability (P in d^{-1}) on any given day is thus defined as the product of slope (dP_0 in $^{\circ}\text{C}^{-1} \text{d}^{-1}$) and the increase in the temperature sum over that day:

$$P(T) = dP_0 \cdot (T - T_b) \quad \text{for } T \geq T_b \quad \text{and} \quad \Sigma(T - T_b) \geq S \quad \text{Equation 87a}$$

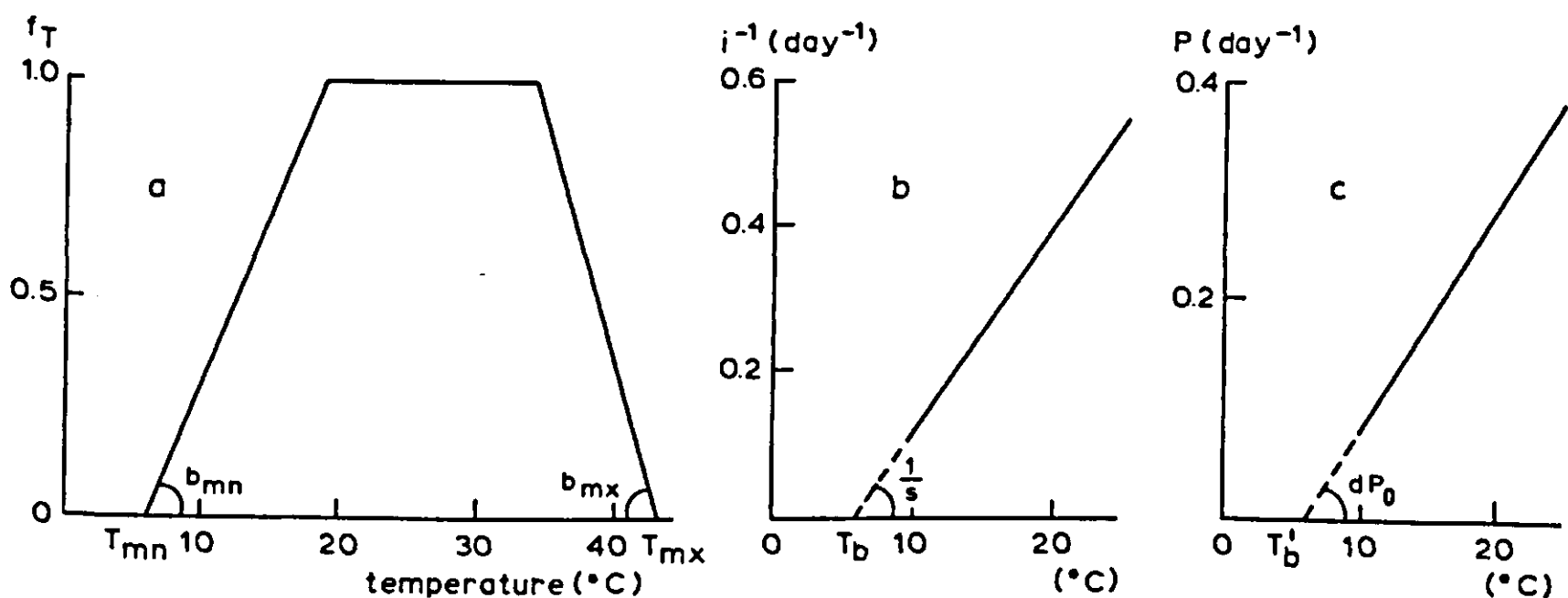


Figure 57. Influence of temperature on (a) maximum germination, represented by the multiplication factor f_T for maximum germination under optimum temperatures ($N_{m,o}$), (b) incubation rate (i.e. the inverse of time to first germination) and (c) germination probability. Intercepts with the temperature axis are $T_{mn} = 6^{\circ}\text{C}$, $T_{mx} = 43^{\circ}\text{C}$, $T_b = T'_b = 6^{\circ}\text{C}$ and slopes are $b_{mn} = 0.077^{\circ}\text{C}^{-1}$, $b_{mx} = -0.111^{\circ}\text{C}^{-1}$, $S = 35^{\circ}\text{C d}$, $dP_0 = 0.02^{\circ}\text{C}^{-1} \text{d}^{-1}$. Relationships are based on data for field emergence in natural seed populations of *Echinochloa crus-galli* (Spitters & Graveland, in prep.).

As long as the incubation time has not yet been passed, P equals zero:

$$P(T) = 0 \quad \text{for } \Sigma(T - T_b) < S \quad \text{Equation 87b}$$

The linear regression of P on temperature is characterized by a base temperature (T'_b in Figure 57c) which may differ from that of the incubation rate.

Exercise 56

Write a CSMP program to simulate field emergence in relation to temperature, according to the relations depicted in Figure 57. Assume an incubation time of 35°C d after last soil cultivation, a probability of emergence of $0.020^\circ\text{C}^{-1}\text{d}^{-1}$ ($T_b = 6^\circ\text{C}$), and 100 germinable seeds per m^2 . These values are typical for *Echinochloa crus-galli*, a C_4 type grass and one of world's major weeds. Assume that soil temperature increases linearly from 10°C at seedbed preparation to 20°C 30 days later.

Soil moisture Germination requires water. Weed seedlings usually emerge from the surface soil layers only, with a maximum depth of 2 cm being typical for many weed species. The surface layers dry out rapidly, so field emergence of weeds is strongly affected by the rainfall pattern.

The average moisture content in the soil compartment from which seedling emergence takes place is tracked by a very simple model of the water balance (Figure 58). The rate of change of soil moisture (dSM) over time interval, dt, equals the infiltrated rain minus the water that percolates to deeper soil layers and the water evaporated from the soil surface:

$$dSM/dt = \text{RAIN} - \text{PERC}_d - \text{EVAP}_d \quad \text{Equation 88}$$

The soil compartment is replenished by rainfall up to, at the most, field capacity. The excess of infiltrated rain above field capacity percolates to deeper soil layers:

$$\text{PERC}_d = \text{SM}_{\text{act}} + \text{RAIN} - \text{EVAP}_d - \text{SM}_{\text{fc}} \quad \text{PERC}_d \geq 0 \quad \text{Equation 89}$$

where SM_{fc} is the amount of soil moisture at field capacity, and SM_{act} the actual amount ($\text{kg H}_2\text{O m}^{-2}$ or mm). Field capacity (SM_{fc}) is the amount of moisture contained by the soil after initial drainage; i.e. about 2 to 3 days after heavy rain. From standard weather data, evaporation from an open water surface is usually calculated using the Penman (1948) equation. This evaporation rate is either calculated in the model itself or obtained from a nearby weather station. (If reference-crop evapotranspiration of short grass is given, this value must be multiplied by 1.25 to obtain the value for open water.) Evaporation from moist soil is, on average, 0.75 times the Penman evaporation for open water (H. van Keulen, pers. commun.). In the model, soil evaporation is reduced by a factor (f_2) depending on the relative moisture content of the top 2 cm of the soil. The

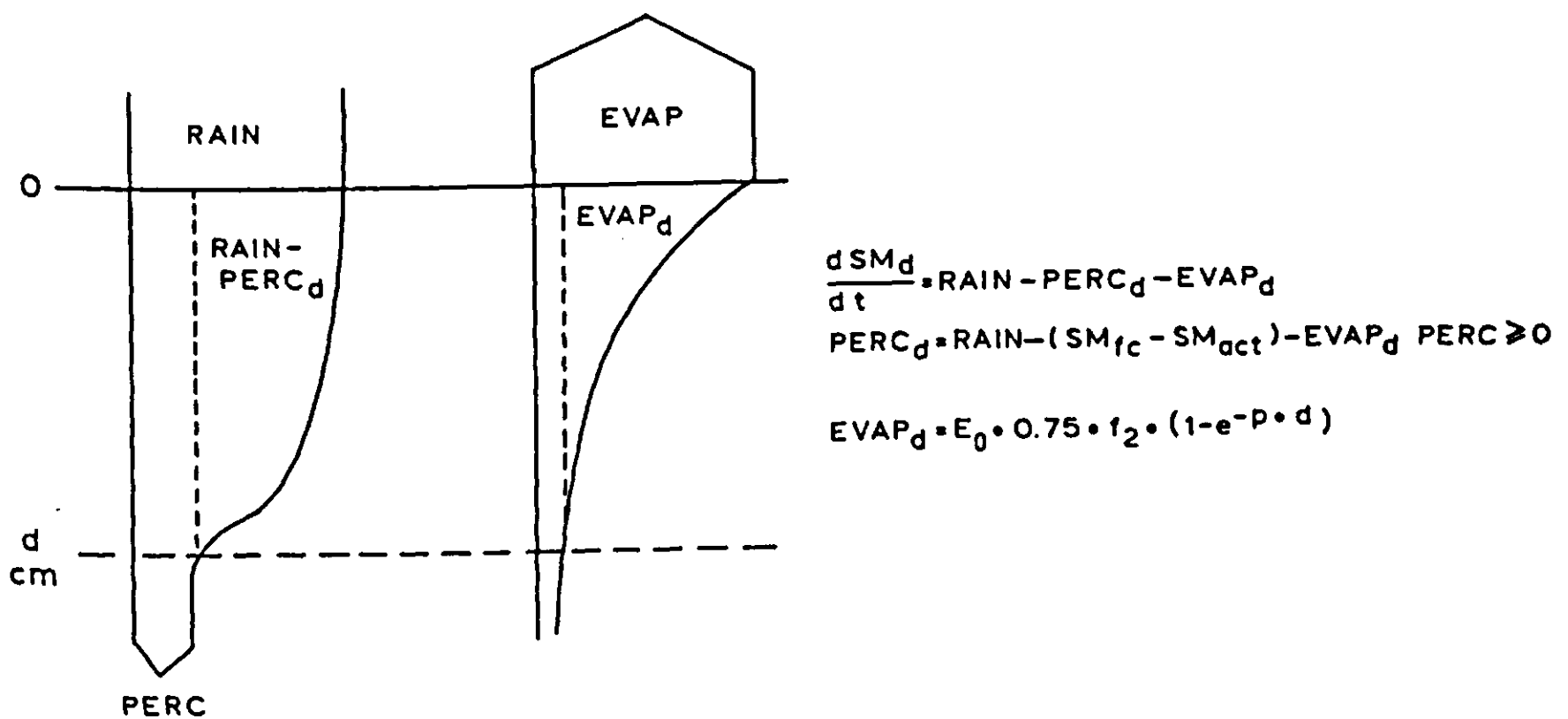


Figure 58. A simple water balance for the soil compartment of depth d from which seedling emergence takes place. The rate of change in the amount of soil moisture (dSM/dt) equals the infiltrated rain minus the water that percolates to deeper soil layers and the water evaporated from the soil surface. Equations are explained in the text.

function used to formulate the reduction is borrowed from van Keulen & Seligman (1987) and defined in the program listing given in the answer to Exercise 57. The relative moisture content is the ratio between the amount which can actually be withdrawn by evaporation ($SM_{act} - SM_{dry}$) and that which could potentially be withdrawn ($SM_{fc} - SM_{dry}$). The moisture content of air-dry soil (SM_{dry}) equals about 1/3 of that at wilting point (SM_{wp}), the point below which plants are no longer able to withdraw moisture from the soil. The moisture content of the top 2 cm is calculated separately, but by the same procedure as that used for the compartment from which seedling emergence takes place. The procedure requires daily data of rainfall as input.

As a result of capillary rise, the evaporated water is extracted over a certain soil depth. The contribution of a soil layer is assumed to decrease exponentially with its depth (van Keulen, 1975). Thus, the amount of moisture withdrawn from a compartment by evaporation ($EVAP_d$) is obtained by multiplying potential soil evaporation ($0.75 E_0$) by the factor (f_2) accounting for the drying out of the top 2 cm, and by the fraction withdrawn from the compartment:

$$EVAP_d = 0.75 E_0 f_2 (1 - \exp(-p \cdot d)) \quad \text{Equation 90}$$

where p is the extinction factor and for a sandy soil about of 10 m^{-1} , and d the thickness of the top compartment (m).

Soil moisture tension, the pF-value, is expressed logarithmically in mbars (at 100 mbar, $pF = \log 100 = 2.0$). There are very few studies relating seedling emergence to soil moisture tension in the field, so the soil moisture function (f_{SM} in Figure 59) applied to the three germination parameters (N_m , $1/i$ and P) is still

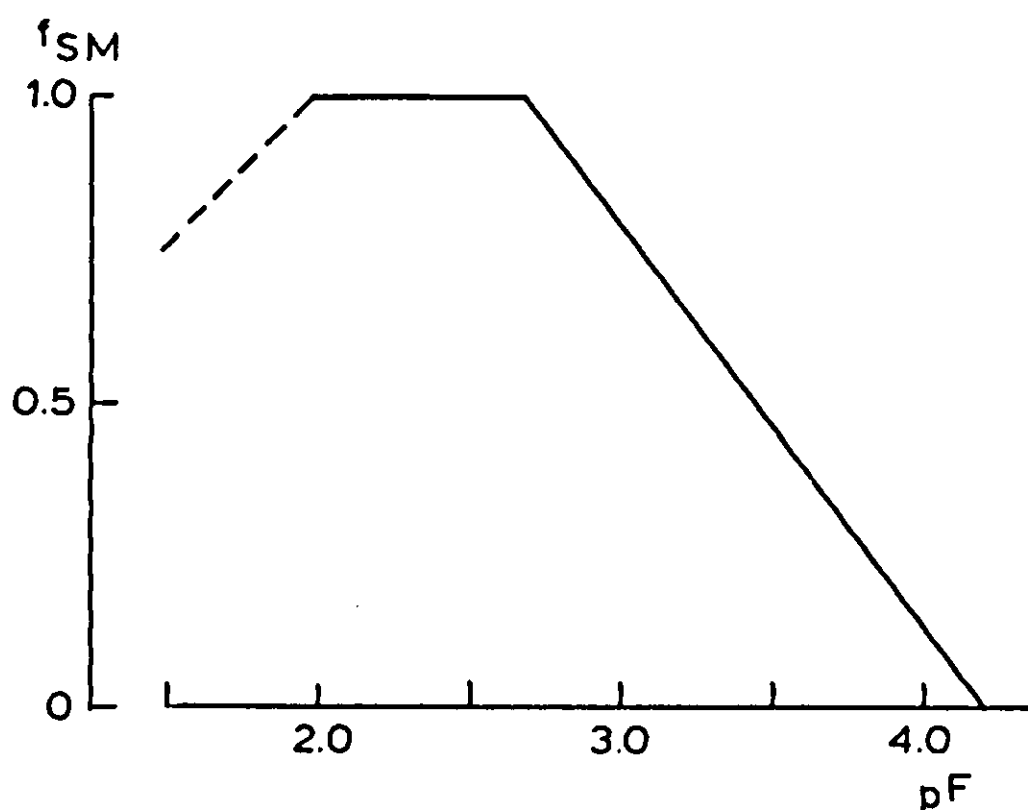


Figure 59. Influence of soil moisture tension ($pF = \log \text{mbar}$) on the three germination parameters (N_m , $1/i$, P) is characterized by the factor f_{SM} by which their values at optimum moisture supply must be multiplied. The relation presented is typical for seedling emergence in the field.

somewhat speculative. Field emergence is unrestricted at soil moisture tensions between roughly pF 2.0 and 2.7 (Bierhuizen, 1973; Bierhuizen & Feddes, 1973). At lower pF -values, emergence is inhibited by anaerobiosis, whereas at higher values drought reduces emergence to zero at wilting point (pF 4.2). The cardinal points depend on species and soil type.

Often, the relationship between soil moisture tension and moisture content of the soil is unknown. Then, as an approximation, the effect of drought on germination and plant growth has usually been related to the relative moisture content ($RMC = (SM_{act} - SM_{wp}) / (SM_{fc} - SM_{wp})$). The linear relationship between f_{SM} and pF (Figure 59) results in an approximately linear relation between f_{SM} and RMC . This relation is remarkably consistent over different soil types, although the function relating soil moisture tension to soil moisture content varies greatly with soil type. In calculating RMC , field capacity (SM_{fc}) is set at typical values of 1.7, 2.0 and 2.3 for clay, loam and sand, respectively. The breaking value of pF 2.7 is then replaced by an RMC of 0.50.

After a rain shower following a dry spell, new seedlings do not emerge immediately. Some of the processes will have been reversed during the preceding dry period (Hegarty, 1978). Therefore, some of the germination processes in the seed, and the phase of pre-emergence seedling growth must be repeated, and a new incubation time is required. In order to allow for partial moisture stress as well, a maximum is set to the rate of recovery of N_m , which is related to the incubation rate: $df_{SM}/dt \leq (1 - f_{SM})/i$.

Exercise 57

Extend the model of Exercise 56 to include the influence of soil moisture. *Echinochloa*, with its relatively large seeds, is capable of emerging from depths down to 12 cm. Assume that the soil has a volumetric moisture content of 0.20 at field capacity and 0.05 at wilting point. On Day 0, the soil is at field capacity. Potential evaporation amounts to 3 mm d^{-1} and rain showers of 10 mm occur on Days 3, 6 and 9, and of 15 mm at Days 22 and 25.

Cycles of drying and wetting reduce the number of seedlings that finally emerge. First, they promote the induction of secondary dormancy. Second, drought causes mortality among those seeds whose germination and emergence processes are too far advanced. Extent of pre-emergence mortality depends on the length of the susceptible phase and on the number of seeds in that phase. A susceptible period can be defined in terms of degree-days. Seeds at this stage, just prior to emergence, are subject to a probability of mortality (P_d) which is presumably proportional to $1 - f_{SM}$. Dead seeds are then subtracted from the population of germinable seeds (N_m).

Dormancy The specific, seasonal periodicity in the emergence pattern of a species is invoked by dormancy phenomena. For detailed reviews of this topic see Vegis (1964), Roberts & Totterdell (1981), Karssen (1982) and Bewley & Black (1982).

With relief of dormancy, the range of environmental conditions over which seeds are capable of germinating becomes progressively wider; while as seeds become more dormant, the range narrows again. Dormancy is a mechanism that prevents germination when environmental conditions do not provide a reasonable chance for the germinated seed to survive to reproductive maturity; e.g. in an unfavourable season or under a dense vegetation cover. By responding to environmental signals, germination can be triggered to occur in the right place at the right time.

Seeds of many species are dormant at the time they are shed from the mother plant. This primary dormancy is then released in the course of time. Such an 'after-ripening' occurs in winter annuals and postpones their germination until autumn. In summer annuals, winter cold (moist chilling or stratification) is the main dormancy-breaking factor, so that germination is in spring.

If, for some reason, hydrated seeds are prevented from germinating, secondary dormancy may be induced. In summer annuals, secondary dormancy is induced by high summer temperatures and released by winter cold, so that germination occurs in spring or early summer. The reverse holds for the autumn-germinating winter annuals. Light, alternating temperatures, and high nitrate concentrations are the other main factors leading to a release from the dormant state.

The most typical feature of dormancy is a narrowing of the temperature range over which seeds are able to germinate. The average temperature amplitude of

the population for germination can be characterized by the minimum and maximum temperatures at which N_m is reduced to half its potential value. The slopes of the temperature relationship of N_m (Figure 57a) reflect the variation among seeds in temperature amplitude. In the model, both cumulative frequency distribution functions are approximated by straight lines, so the temperature effect on N_m is characterized by:

$$N_m(T) = f_T N_{m,o} = N_{m,o} \min(b_{mn}(T - T_{mn}), b_{mx}(T_{mx} - T))$$

with $0 \leq f_T \leq 1$

Equation 91

where T_{mn} and T_{mx} are the apparent minimum and maximum temperatures for germination, and b_{mn} and b_{mx} the slopes of the temperature relationship (Figure 57a). The minimum value of the two regression equations is used. Again, f_T is best referred to a running average of several days.

The regression coefficients change during the season with the degree of dormancy, and this periodicity can be determined empirically. To do this, seeds are buried in the field at a time coinciding with normal dispersal from the mother plant. At regular time intervals, samples are dug up and germination is tested under controlled conditions over a range of temperatures. Plotting the observed temperature amplitude against the time of sampling yields the germination window of the species (Figure 85; Karssen, 1982). Superpositioning the variation within the population on that window (Equation 91), quantifies the influence of the seasonal dormancy pattern on N_m .

Exercise 58

Make a CSMP program for the annual course of germination of the summer annual *Ambrosia artemisiifolia* and the 'winter' annual *Lamium amplexicaule* in both dark and light. The coefficients characterizing their temperature relations were derived from data of Baskin & Baskin (1980, 1981) and are tabulated in the program listing (see answer). The annual temperature wave is depicted in Figure 85. Assume an incubation time of 80°C d and a germination probability of $0.003^\circ\text{C}^{-1}\text{d}^{-1}$ at a base temperature of 0°C . Assume an initial population of 100 viable seeds, shed in mid-July.

The simulation results (Figure 60) clearly illustrate the effect of soil cultivation. Soil cultivation exposes a fraction of the seed population to light, and in some species an exposure of one minute or less is enough to satisfy the light requirement of the seed (Baskin & Baskin, 1980). Since the temperature window of seeds exposed to light is, in general, much wider than that of those which remain in the dark, a flush of seedlings is generated after soil cultivation. Soil cultivation can easily be introduced in the model, by shifting a fraction of the seed population to

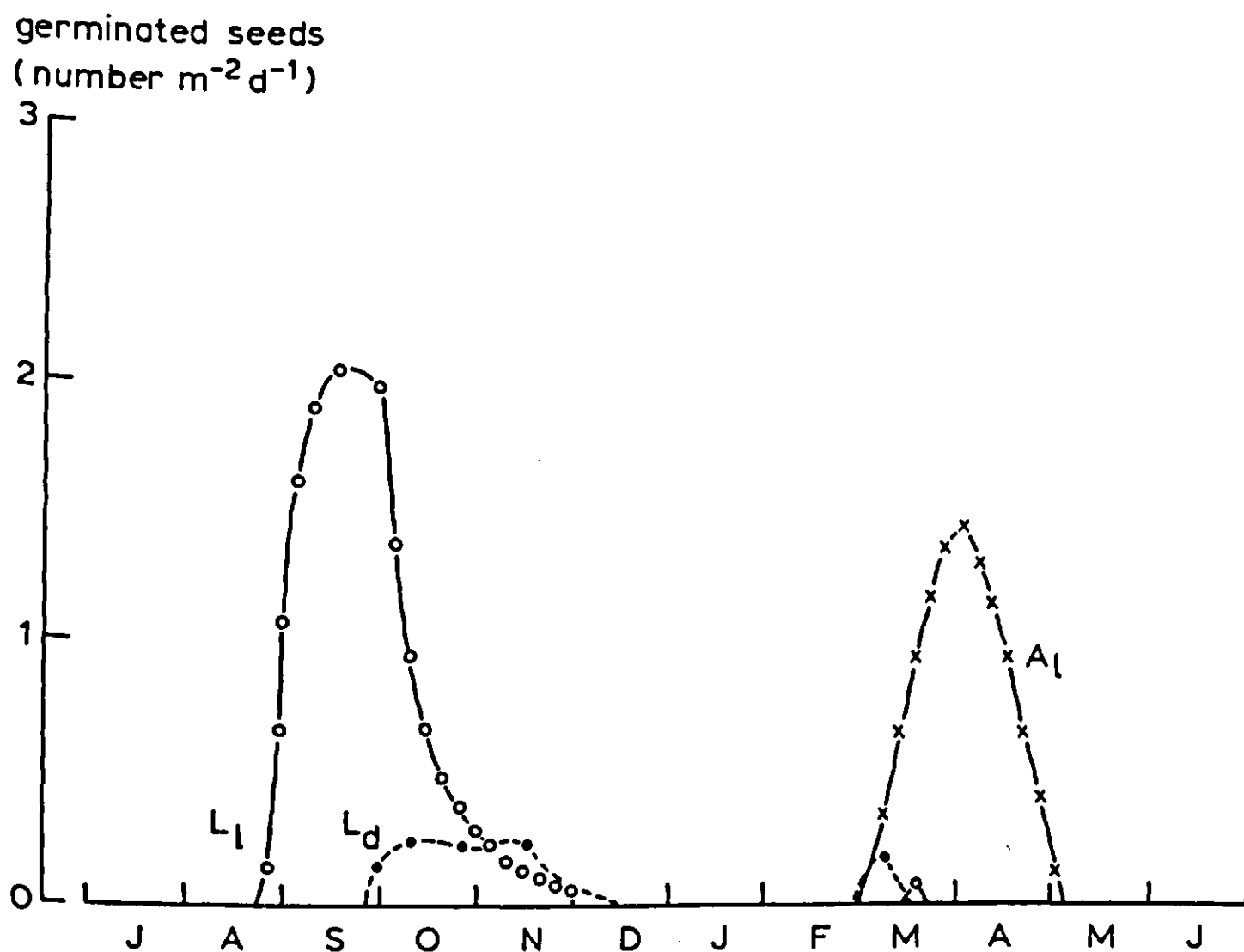


Figure 60. Simulated seasonal pattern of germination of *Ambrosia artemisiifolia* in light (x, A_l) and *Lamium amplexicaule* in light (o, L_l) and dark (●, L_d). The model predicted that *A. artemisiifolia* was unable to germinate in the dark because the seasonal temperature wave did not overlap the temperature window of this species in the dark. *L. amplexicaule* showed little germination in spring because its seed population had already been considerably depleted in the autumn. See also Exercise 58.

a new class of 'seeds exposed to light'. These start with a new incubation time.

The above model is based on an average, observed trend over the year. Forecasting seedling flushes would be improved if more causality were introduced in the model, by storing the degree of dormancy as an integral; having the value 0 for non-dormant seeds and 1 for fully dormant seeds. This state variable changes in time according to rates of induction and relief of dormancy. These rate variables depend on the factors controlling dormancy. In addition, induction and relief of secondary dormancy are influenced by temperature, similar to other metabolic processes, for which the relation of Figure 57b may be representative.

4.2.4 Competition: distributing total growth rate among the competing species

Weeds reduce yield by competing with the crop for environmental resources that are in short supply. Instead of describing these competition effects by an empirical, static regression model, as done in Equation 78, a dynamic, mechanistic model is now presented, in which distribution of the growth-limiting resources

among crop and weed, and the way each species uses the acquired resources, are simulated over time.

As an introduction, a very simple model is discussed, in which the total growth rate of the vegetation is calculated and distributed among the species composing the vegetation, according to their weighted share in total leaf area. The general crop growth model of Section 4.1 is then modified and extended to simulate competition for light, soil moisture and nitrogen.

The growth rate of a crop well supplied with water and nutrients is roughly proportional to its light interception (review by Gosse et al., 1986). The rate of crop growth can thus be estimated from intercepted light and the average efficiency (E) with which the crop uses the intercepted light in dry matter production. Light interception is calculated from incoming solar radiation (R) and the leaf area index (L) of the crop. Since the light flux penetrating a canopy decreases exponentially with the leaf area, the growth rate at time t is given by:

$$\Delta Y_t = \{1 - \exp(-0.7 L_t)\} \cdot 0.5 R \cdot E \quad \text{Equation 92}$$

where 0.7 is the light extinction coefficient. The factor 0.5 indicates that only 50% of the incoming solar radiation (R) is photosynthetically active. The light utilization efficiency (E) is of the order of 2.5 to 3 g DM MJ⁻¹ intercepted light for ruderal C₃ species. For C₄ species, E is about 4.5 g DM MJ⁻¹ at optimum temperature.

The leaf area index (L , ha leaf ha⁻¹ ground) is obtained by multiplying the biomass (Y , kg ha⁻¹) by the leaf area ratio (LAR, ha leaf kg⁻¹ biomass):

$$L_t = \text{LAR}_t \cdot Y_t \quad \text{Equation 93}$$

In a mixture of several species, all having an equal plant height, light interception and growth rate of each species are proportional to its share in the total leaf area. Hence, the growth rate of species 1 in a mixture becomes:

$$\Delta Y_{1,t} = \frac{L_{1,t}}{\Sigma L_t} \{1 - \exp(-0.7 \Sigma L_t)\} \cdot 0.5 R \cdot E \quad \text{Equation 94}$$

where ΣL is the total leaf area index of the mixed vegetation.

Crop yield is calculated by multiplying simulated final crop biomass by a fixed 'harvest index', which is the ratio between the yield of the desired parts (e.g. grains) and the total biomass of the crop.

Exercise 59

Write a CSMP program to simulate the growth of two species growing together in a mixture. Use for incoming solar radiation a value of 14 MJ m⁻² d⁻¹ and for the light utilization efficiency a value of 3 g DM MJ⁻¹. Species 1 starts with an initial biomass of 30 kg ha⁻¹ and species 2 begins with 20 kg ha⁻¹. Assume that LAR decreases linearly from a value of 0.0015 ha kg⁻¹ at emergence (Day 0), to

zero at full ripeness (Day 101). Compute the biomass production of both species over a period of 100 days. How does the biomass ratio (Y_1/Y_2) of the species change in time?

Species with a higher light extinction coefficient absorb more light per unit leaf area. It can be shown that these differences are allowed for by weighting the leaf areas by their extinction coefficients (k):

$$\Delta Y_{1,t} = \frac{k_1 L_{1,t}}{\Sigma(k L_i)} \{1 - \exp(-\Sigma(k L_i))\} \cdot 0.5 R \cdot E \quad \text{Equation 95}$$

In a mixture, a tall plant absorbs more light per unit leaf area than its shorter neighbour. In comparison to a detailed model of light competition (Appendix 7), a good approximation is obtained by setting the growth rates of the species proportional to the light intensities at half their plant heights. Extending Equation 95 gives for the growth rate of species 1 in a mixture:

$$\Delta Y_{1,t} = \frac{k_1 L_{1,t} l_{1,t}}{\Sigma(k L_i l_i)} \{1 - \exp(-\Sigma(k L_i))\} \cdot 0.5 R \cdot E \quad \text{Equation 96}$$

Assuming the leaf area of each species is evenly distributed over its plant height (Figure 61), the relative light intensity of species 1 at half its height (H) gives:

$$l_{1,t} = \exp \left\{ - \sum_{j=1}^n \left(k_j \frac{H_{j,t} - \frac{1}{2} H_{1,t}}{H_{j,t}} L_{j,t} \right) \right\} \quad \text{where } H_j \geq \frac{1}{2} H_1 \quad \text{Equation 97}$$

Exercise 60

Extend the simulation model by including the above equations to account for differences in extinction coefficient and plant height. Assume that plant height increases linearly in time from 1 cm at emergence up to 100 cm at an age of 80 days, after which time the height remains constant. Simulate first a situation where the two species are identical, and use reruns to model both monocultures. Set the total initial biomass for all vegetations to 50 kg ha^{-1} . In each subsequent simulation run, reduce one attribute value for the second species by 20% so that in any run the species differ in only a single trait. Consider the following attributes: initial biomass, plant height, leaf area ratio, light extinction coefficient, and light use efficiency. For solar radiation, use the average values from the meteorological station De Bilt, the Netherlands:

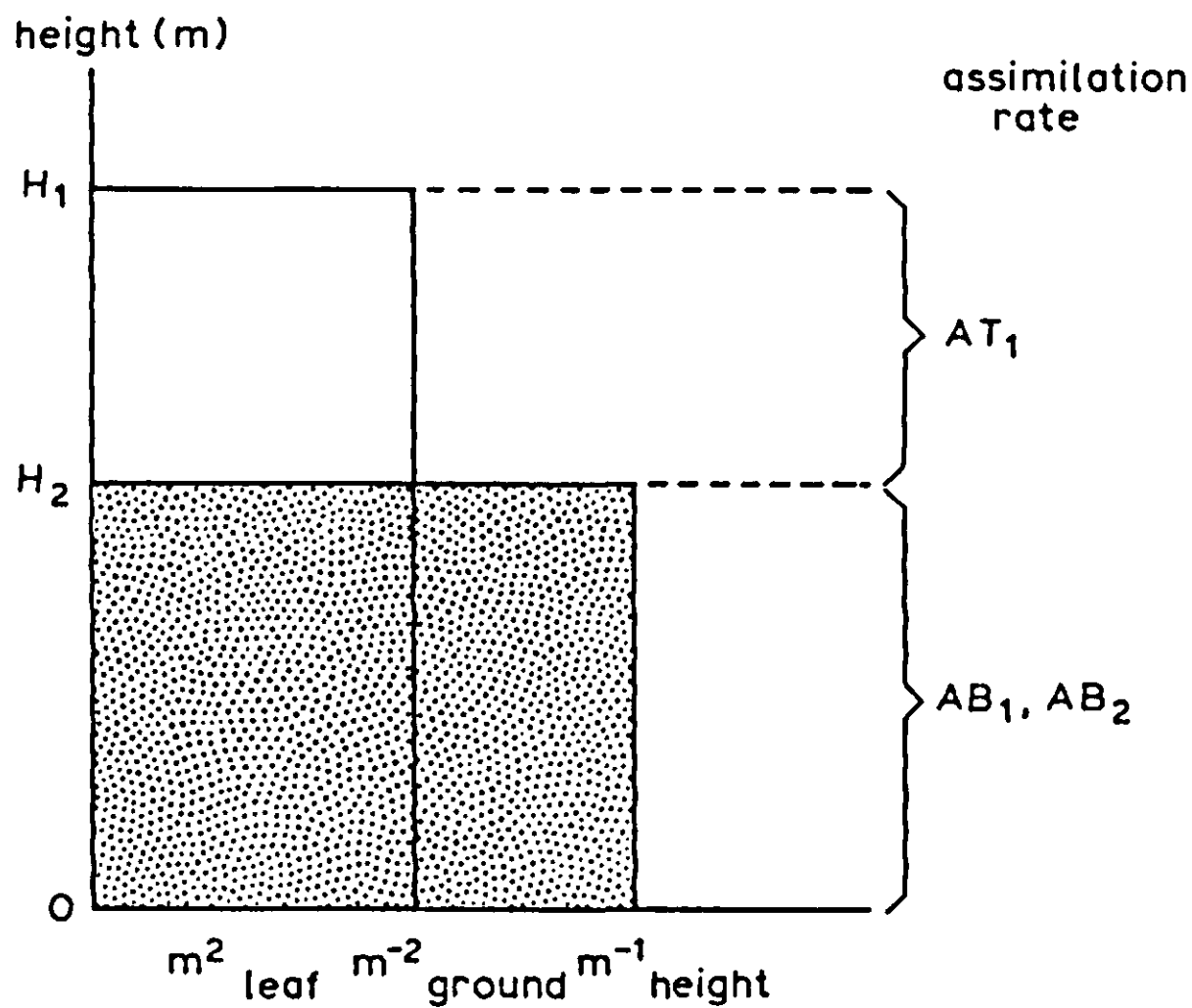


Figure 61. Schematic representation of a mixture of species 1 and 2. The canopy is divided into a top layer monopolized by the tall species 1 and a bottom layer shared by both species. Assimilation rates in the top layer (AT) and those in the bottom layer (AB) are calculated for each species separately.

Days since 1 January	105	135	166	196	227	258
Solar irradiance ($MJ m^{-2} d^{-1}$)	12.4	16.4	18.3	16.2	14.6	10.2
Assume seedling emergence to be at Day 120.						

The sensitivity analysis performed in Exercise 60 (Table 14) demonstrates the relative influence of the various parameters on the competitive ability of a species. The effect of differences in initial biomass shows the importance of the starting position and emphasizes the necessity for accurate initialization of the competition model (e.g. by the relative degrees of soil coverage of crop and weeds monitored in the field early in the season, when forecasting crop yield loss). The effect of plant morphology is reflected in plant height (priority for the growth-limiting factor light), leaf area ratio (pattern of dry matter allocation within the plant) and extinction coefficient (leaf angle distribution and clustering of the leaves). Physiology is reflected in the light use efficiency (photosynthesis and respiration). Stress conditions, such as shortage of water and nutrients, can be accounted for in a simplified way by multiplying the light utilization efficiency by a site index ($0 \leq SI \leq 1$). This index can be estimated by calibrating simulated crop yield against the observed or expected yield level.

Table 14. Simulated effect of single attributes on the ratio in biomass production Y of two isogenic species when grown alone in monoculture or together in a mixture. For species 2, only the attribute mentioned in each line was reduced to a value of 80% of that of species 1. Monoculture yield of species 1 is 20.2 t ha^{-1} .

	$Y_{2,\text{mono}}/Y_{1,\text{mono}}$	$Y_{2,\text{mix}}/Y_{1,\text{mix}}$
Initial biomass	0.98	0.80
Plant height	1.00	0.39
Leaf area ratio	0.90	0.30
Light extinction coefficient	0.90	0.30
Light use efficiency	0.73	0.30

Exercise 61

Evaluate the effect of the timing of herbicide application on yield, using the program of Exercise 60. Assume for both crop and weed an initial biomass of 50 kg ha^{-1} and a rate of plant height increment of 1 cm d^{-1} . Assume that the herbicide reduces biomass and plant height of the weed to 10% of their values before application.

Herbicides In practice, the effects of herbicide application are much more complex than is suggested by the preceding exercise. New seedling flushes of weeds may appear, especially at low leaf area index. After regrowth, the weeds may show a pattern of dry matter distribution that differs from that without spraying. The effectiveness of spraying strongly depends on the type of chemical, its dose, species composition of the weed infestation, development stage of the weeds, and weather and soil conditions. Frequently, some damage also occurs to the crop, depending on crop development stage.

Present decision making models for weed control are primarily concerned with herbicide retrieval systems, where the farmer is advised on the choice of chemical to be used. This advice is based mainly on the species composition of the weed infestation and the development stage of the crop (e.g. Aarts & de Visser, 1985).

4.2.5 Calculating growth rates from absorbed light

To gain more insight into the underlying mechanisms of competition, distribution of the major growth-limiting resources over the competing species and the way each uses the acquired resources are modelled. Competition for light is discussed first.

Growth of the crop alone Simulation of daily growth rate of the weed-free crop is based largely on the crop growth model described in Section 4.1. For purposes of simplicity, however, a simpler procedure is used here to calculate canopy photosynthesis.

Daily totals of incoming radiation are input for the model. Daily photosynthetically active radiation (usually called 'light', 400-700 nm) is obtained as 50% of total solar radiation. The light intensity at each canopy depth is obtained from the exponential light profile:

$$I_L = (1 - \rho)I_0 \exp(-k \cdot L) \quad \text{Equation 98}$$

in which I_L is the light intensity at height L , with L counted from the top of the canopy downwards ($\text{J m}^{-2} \text{h}^{-1}$), I_0 the light intensity at the top of the canopy, ρ the crop reflection coefficient, k the extinction coefficient and L the leaf area index ($\text{m}^2 \text{leaf m}^{-2} \text{ground}$).

Light absorption per unit leaf area at a depth L in the canopy is obtained by taking the derivative of the exponential light profile (Equation 98) with respect to L :

$$I_{aL} = -dI_L/dL = (1 - \rho)I_0 \cdot k \cdot \exp(-k \cdot L) \quad \text{Equation 99}$$

where I_{aL} in $\text{J m}^{-2} \text{leaf h}^{-1}$.

This concise model uses the daily average of light intensity at given canopy depth. Thus, spatial and diurnal variation in illumination among the leaves within a canopy layer are neglected. Use of averaged illumination intensities in an instantaneous assimilation-light response function of single leaves would, however, overestimate the actual assimilation rate, because of the convexity of the response function. As demonstrated by Spitters (1986), a reasonable approximation is arrived at by using the more gradual hyperbolic function for leaf photosynthesis instead of the asymptotic exponential which normally characterizes the instantaneous assimilation-light response of single leaves. Calculated crop assimilation rates deviate within -10% and $+5\%$ of those computed by the detailed model presented in Figure 46 ($\text{LAI} > 0.75$). The rectangular hyperbola is written as

$$A = \frac{\varepsilon I_{aL}}{\varepsilon I_{aL} + A_m} A_m \quad \text{Equation 100}$$

in which A is the assimilation rate ($\text{g CO}_2 \text{m}^{-2} \text{leaf h}^{-1}$). The hyperbola is used only to approximate an average assimilation rate over the day. Therefore, the values characterizing the instantaneous, negatively exponential, assimilation-light response of single leaves should be used for the initial slope ε and the saturation level A_m .

Substituting the absorbed light energy (Equation 99) into the assimilation-light response of single leaves (Equation 100) gives the assimilation rate at each depth of the canopy. Integration over canopy leaf area index L yields

$$A_d = D \frac{A_m}{k} \ln \left(\frac{A_m + \epsilon \bar{I} k}{A_m + \epsilon \bar{I} k \exp(-k \cdot L)} \right) \quad \text{Equation 101}$$

where A_d is the daily canopy assimilation ($\text{g CO}_2 \text{ m}^{-2} \text{ ground d}^{-1}$), $\bar{I} = (1 - \rho)I_d/D$ the incoming light flux averaged over the daylight period and corrected for crop reflection ($\text{J m}^{-2} \text{ h}^{-1}$), I_d the daily total of incident light, D the daylength, and \ln the natural logarithm.

Typical parameter values are: $\rho = 0.08$; $\epsilon = 12\frac{1}{2} \cdot 10^{-6} \text{ g CO}_2 \text{ J}^{-1}$ (at 20°C , Ehleringer & Pearcy, 1983); $A_m = 4 \text{ g CO}_2 \text{ m}^{-2} \text{ h}^{-1}$ for ruderal C_3 species and $7 \text{ g CO}_2 \text{ m}^{-2} \text{ h}^{-1}$ for C_4 species; $k = 0.72$ for a canopy with leaves randomly distributed within the canopy volume and having a spherical leaf angle distribution. Estimation of the parameter values is discussed in Subsection 4.1.4.

Assimilates are used for maintenance of standing biomass, and the remainder is converted into structural dry matter. Thus, daily crop growth rate is given by

$$\Delta Y_t = C_f(30/44 A_d - R_m) \quad \text{Equation 102}$$

where ΔY_t is the growth rate ($\text{g DM m}^{-2} \text{ d}^{-1}$), C_f the conversion efficiency ($\text{g DM g}^{-1} \text{ CH}_2\text{O}$), and R_m the maintenance requirements ($\text{g CH}_2\text{O m}^{-2} \text{ d}^{-1}$); $30/44$ represents the ratio of the molecular weights of CH_2O and CO_2 . The conversion efficiency of carbohydrates into dry matter is about 0.7. Maintenance requirements amount to roughly $0.015 \text{ g CH}_2\text{O g}^{-1} \text{ biomass d}^{-1}$ (at 25°C , $Q_{10} = 2$) (Section 4.1).

Total daily dry matter increment (ΔY_t) is allotted to the different plant organs: leaves, stems, roots and storage organs, according to empirical distribution factors which are a function of the development stage of the species. Time progression of the development stage is calculated in relation to temperature (Section 4.1).

Leaf area index is calculated as the integral of the rate of leaf area growth over time, obtained by multiplying the simulated increase of leaf dry weight with the specific leaf area ($\text{m}^2 \text{ g}^{-1}$) of new leaves, assuming that leaf area growth is limited by the supply of photosynthates and thus mainly affected by irradiation. However, during the early stage of crop growth, temperature is the overriding factor due to its effect on rates of cell division and expansion. For this early stage, leaf area growth is assumed to be exponential, with the relative growth rate being a function of temperature (Section 4.1).

Growth of crop and weed in competition Under potential growing conditions, light is the growth-limiting factor; weeds reduce crop growth because they capture part of the incoming light flux. The procedure used to calculate the assimilation rate of the weed-free crop (Equation 101) can now be extended to allow for crop and weed growing together in competition. A mixture of two species, differing in plant height, is considered (Figure 61). The canopy is divided into a top layer, monopolized by the tall species, and a bottom layer shared by both species. The

top layer is a monospecies canopy, so the assimilation rate of the tall species in that layer is given by Equation 101.

Assimilation rates of the species in the common bottom layer are slightly more difficult to derive. The light flux passing across an arbitrary horizon of the bottom layer is

$$I = IB_0 \exp(-k_1 L_1 - k_2 L_2) \quad \text{Equation 103}$$

where IB_0 is the light intensity incident at the top of the bottom layer ($J m^{-2} h^{-1}$). Subscripts refer to species 1 and 2. Differentiation with respect to L_1 gives the decrease in the downward light flux penetrating dL_1 deeper into the canopy. Of this total amount, species 1 absorbs a fraction proportional to its share in the canopy at that horizon. The leaf areas are weighted by their extinction coefficients in order to account for differences in light absorption per unit leaf area. Hence, the amount of light absorbed by species 1 in the horizon under consideration becomes

$$\begin{aligned} I_{aL,1} &= - \frac{dI_L}{dL_1} \frac{k_1 L_1}{k_1 L_1 + k_2 L_2} = \\ &= \frac{k_1 L_1}{k_1 L_1 + k_2 L_2} I_0 \left(k_1 + k_2 \frac{dL_2}{dL_1} \right) \exp(-k_1 L_1 - k_2 L_2) \quad \text{Equation 104} \end{aligned}$$

where I_{aL} in $J m^{-2} \text{ leaf } h^{-1}$.

Assuming that the leaf area of each species is evenly distributed over its plant height (Figure 61), dL_2/dL_1 equals L_2/L_1 for any horizon of the bottom layer. Applying this simplification to Equation 104 gives

$$I_{aL,1} = I_0 k_1 \exp(-k_1 L_1 - k_2 L_2) \quad \text{Equation 105}$$

Substituting the absorption intensity into the assimilation-light response function (Equation 100) and integrating over the leaf area index of the bottom layer (LB_1) yields the assimilation rate of species 1 in that layer:

$$\begin{aligned} AB_{d,1} &= \frac{k_1 LB_1}{k_1 LB_1 + k_2 LB_2} D \frac{A_{m,1}}{k_1} \cdot \\ &\cdot \ln \left(\frac{A_{m,1} + \varepsilon_1 IB_0 k_1}{A_{m,1} + \varepsilon_1 IB_0 k_1 \exp(-k_1 LB_1 - k_2 LB_2)} \right) \quad \text{Equation 106} \end{aligned}$$

where LB is the leaf area of the subscripted species in the bottom layer. This equation can be related directly to Equation 101 for a single-species stand, as the exponential describes the fraction of light transmitted through the bottom layer, while the first term gives the share of species 1 in the light absorption of the bottom layer.

The total daily assimilation rate of species 1 is obtained as the sum of its rates in the top and bottom strata (Figure 61):

$$A_{d,1} = AT_{d,1} + AB_{d,1} \quad \text{Equation 107}$$

in which $A_{d,1}$ is the daily assimilation rate of species 1 ($\text{g CO}_2 \text{ m}^{-2} \text{ d}^{-1}$).

Calculations for species 2 are similar. In the program listed in Appendix 6, a general formulation is used, referring to a mixture of n species with the canopy stratified into n layers bounded by the plant heights of the different species. Light absorption and photosynthesis by non-leaf organs, e.g. stems and panicles, may be treated as though these organs represented another species.

The above approach accounts, analytically, for the exponential light profile within the mixed canopy layers. A more detailed, numerical model of light competition is presented in Appendix 7. This model is an extension of the elementary crop photosynthesis model discussed in Section 4.1, and can easily be linked to the model given in Appendix 6.

Plant height Height increases in time according to an S-shaped curve. It is expressed as a function of development stage (or accumulated temperature) rather than chronological time. Richards (1959, 1969; Causton & Venus, 1981) defined a family of sigmoid curves. Applied to plant height:

$$H_D = H_m(1 \pm b \cdot \exp(-sD))^{-1/v} \quad \text{Equation 108}$$

where H_D is the plant height at development stage D , H_m the maximum plant height, and b , s and v are constants. The plus sign applies when $v > 0$, the minus sign when $-1 \leq v < 0$, while the function is not defined for $v < -1$ or for $v = 0$. The rate of height increment is given by the derivative of H_D :

$$\frac{dH_t}{dt} = \frac{dD}{dt} \frac{dH_D}{dD} = \pm \frac{dD}{dt} \frac{s}{v} H_m b \cdot \exp(-sD) (1 \pm b \exp(-sD))^{-(1+v)/v}$$

$$\text{Equation 109}$$

where dH_t/dt is the rate of height increment (m d^{-1}), and dD/dt the rate of development (stages d^{-1}). The coefficients are obtained by fitting Equation 108 to data on height and development stage, using a least squares procedure. The logistic function ($v = 1$) is often satisfactory. Sub-optimal conditions reduce plant height. As a simplifying approach, the height increment rate is then multiplied by a reduction factor which is the same as that calculated for the growth rate (Equations 113 and 117). Equation 109 assumes that a reduction of the height increment rate during a certain stage does not affect the increment rate at later stages.

In the model, height is obtained as the integral of the height increment rate.

Initialization In a mixture, the growth rate (dY_t/dt) of a species tends to be proportional to its leaf area and so to its present biomass (Y_t). This is especially true when the species differ only slightly in plant height and in the ratio of leaf area to plant weight. Thus, the relative growth rate ($R = (dY_t/dt)/Y_t$) tends to be

the same for all species when grown together in a mixture. The relative differences then remain constant in time so that the competitive status of a species is fully explained by its initial leaf area (Exercise 59). This emphasizes the prime importance of a correct initialization in competition models, especially when the species show a similar plant habit.

Leaf areas of the species, as measured at an early harvest, may be used to initialize the model. This is useful when simulation is applied to interpret experiments, but it has little predictive value. For a predictive model, the species are characterized by plant density and initial leaf area per plant; the latter being estimated by logarithmic extrapolation of leaf area per plant at seedling emergence (Section 4.1).

4.2.6 Competition for soil moisture

The above model is concerned with potential growing conditions, i.e. situations where light is the main growth-limiting factor. In the following sections, the model will be extended by simple procedures to account for growth reduction due to shortage of soil moisture and nutrients. The demand of the species is calculated by its rate of uptake with no shortage of moisture or nutrients. The degree to which the available soil stocks can cover the demand determines the actual uptake and the reduction in growth rate of the species.

Potential transpiration The demand for soil moisture by a species is characterized by its transpiration rate with ample moisture supply. The potential rate of transpiration of a foliage that fully covers the ground is proportional to the evaporation rate of an open water surface (E_0), which can be calculated from standard weather data using the Penman (1948) equation. E_0 is calculated in the model either by this equation or by using data of E_0 from a nearby weather station. The proportionality factor, called crop factor (F_c), is about 0.9 for C_3 species (Feddes, 1987). C_4 species transpire nearly half as much water per unit of produced dry matter as C_3 species. In temperate climates, their growth rate is only slightly higher than that of C_3 species, but in semi-arid climates their growth rate can be almost twice that of C_3 species (van Keulen, 1982a; Pearcy & Ehleringer, 1984). For C_4 species, therefore, F_c is set at 0.7 for temperate climates and 0.9 for warm climates.

Instead of taking the evaporation of a hypothetical water surface as a reference, one can also take the evapotranspiration rate of a reference crop, i.e. short grass, actively growing and well supplied with water (E_r). This rate can be calculated from a modified Penman-Monteith equation (Monteith, 1965; Doorenbos & Pruitt, 1977). In the model listed in Appendix 6, a simplified expression developed by Makkink (1957) is used, which gives an accurate description for Dutch conditions (de Bruin, 1987). It has the advantage of requiring only data of solar radiation and temperature. The reference evapotranspiration of a short grass cover (E_r) is, on average, 0.8 times the Penman evaporation of open water

(E_0). So the new crop factor (F'_c) referring to E_r is about 1.1 for C_3 species, depending somewhat on crop and climatic conditions (Doorenbos & Kassam, 1979; Feddes, 1987).

Transpiration of a crop is reduced by incomplete soil coverage. Transpiration requires energy from absorbed radiation. The rate of transpiration is, therefore, approximately proportional to the fraction of incoming solar radiation intercepted by the foliage. This fraction is calculated from the exponential radiation profile (Equation 98). All incoming solar radiation is potentially available for vapourization. Therefore, the extinction coefficient (k) for total solar radiation (300-3000 nm) is used, which has a value of about 0.7 of that for photosynthetically active radiation (400-700 nm). In a mixed vegetation, the potential transpiration rate of each species is proportional to the radiation it intercepts in the mixture, which is calculated in a similar way to its interception of PAR in a mixture.

Thus, the potential transpiration rate of the foliage is calculated as:

$$T_{\text{pot}} = E_0 F_c (1 - \exp(-0.7 kL)) / 0.85 \quad \text{Equation 110}$$

where T_{pot} is the potential transpiration rate (mm d^{-1}), E_0 the evaporation from an open water surface (mm d^{-1}) and F_c the crop factor (—). The third term is the fraction of incoming radiation actually intercepted by the foliage, relative to the fractional interception at full ground coverage. At full ground coverage, LAI is about 4 and the foliage intercepts about 85% of incoming radiation. The term $E_0 F_c$ can be replaced by $E_r F'_c$, where E_r is the evapotranspiration of a reference crop and F'_c the adjusted crop factor. (Note that the above references use the term 'crop coefficient' or 'crop factor' for the ratio T_{pot}/E_0 or T_{pot}/E_r as a whole rather than for F_c or F'_c alone.)

Available moisture The amount of soil moisture is tracked using a modified version of the simple water balance model discussed in the germination section (Equations 88-90). Equation 88, however, needs to be expanded to incorporate water uptake by the vegetation. The soil compartment considered, is the depth to which the roots finally penetrate. This maximum rooting depth is often dictated by soil attributes rather than being a species characteristic. The rooted profile is, in general, of such depth that the term $\exp(-p \cdot d)$ of Equation 90 can be neglected. Vertical root penetration proceeds rapidly: 2-4 cm d^{-1} , depending on soil temperature. If substantial water shortage is expected to occur early in the season, the extended procedure of van Keulen (1986a) can be included to allow for the feature that rooting has not yet reached its final depth. Field capacity and wilting point refer to their values averaged over the rooted compartment.

To account for reduction in soil evaporation caused by the canopy cover, the term EVAP in Equation 90 is multiplied by the radiation transmission of the canopy, being $\exp(-0.7 kL)$. Use of the drying factor (f_2) relies strictly upon daily data of rainfall. As a simple approximation, reduction in soil evaporation due to drying is, therefore, set linearly proportional to the relative moisture content of

the root zone rather than as a function of that of only the top 2 cm (van Keulen, 1986a).

In situations with a shallow water table and high soil conductivity, capillary rise from soil layers below the root zone substantially adds to soil moisture availability and must be taken into account; in which case, the procedure outlined by Driessen (1986a) can be used.

Actual transpiration When water is in short supply, plants reduce loss of water vapour from the leaves by closure of the stomata. Actual transpiration is then less than the potential value. The multiplication factor (f_{SM}) which must then be applied to the potential transpiration rate (Equation 110) is assumed to decrease linearly from a value of 1 at a critical soil moisture content to a value of 0 at wilting point:

$$f_{SM} = (SM_{act} - SM_{wp}) / (SM_{cr} - SM_{wp}) \quad 0 \leq f_{SM} \leq 1 \quad \text{Equation 111}$$

where the critical soil moisture content is defined as

$$SM_{cr} = SM_{wp} + (1 - P)(SM_{fc} - SM_{wp}) \quad \text{Equation 112}$$

By convention, soil moisture between field capacity (SM_{fc}) and permanent wilting point (SM_{wp}) is considered to be the maximum quantity available for uptake by the crop. The factor P measures to what extent this maximum available soil moisture can be depleted until transpiration is reduced. At a greater evaporative demand of the atmosphere, plants rapidly fail to cover the demand by uptake of soil moisture; species differ in their reaction (Hagan & Stewart, 1972). For temperate climates, the soil moisture depletion factor (P) varies between 0.6 and 0.4 (or pF 2.90 and 2.55) for an evaporative demand of 1 and 5 mm d⁻¹, respectively. For climates with a high evaporative demand, the approach of Doorenbos & Kassam (1979; Driessen 1986a) may be followed. The evaporative demand decreases about exponentially with depth in the canopy. Thus, the demand is lower for a short species than for a tall species in a mixture. Evaporative demand should, therefore, refer to the values at the respective plant heights of the species in the mixture. However, this is not applied in this summary model and partly compensates for the reduced root/shoot ratio of shaded species.

The role of rooting density is discussed in the section on competition for nutrients (model listing in Exercise 62). The errors introduced in the model by neglecting the roots will usually be small, because the share of a species in the total rooting system closely correlates with its share in total leaf area, and so with its share in canopy transpiration.

Actual growth rate Stomatal closure with water shortage restricts not only water loss of the plant but also CO₂ uptake. For a wide range of environmental conditions, reduction in CO₂ assimilation is approximately proportional to reduction in transpiration:

$$A_{act}/A_{pot} = T_{act}/T_{pot} \quad \text{or} \quad A_{act} = (T_{act}/T_{pot})A_{pot} \quad \text{Equation 113}$$

Reduction in total growth rate, therefore, is calculated by multiplying the potential rate of growth by the reduction factor T_{act}/T_{pot} .

Program listing of the competition model A complete listing of the competition model is presented in Appendix 6. Parameter values are for maize and barnyard grass (*Echinochloa crus-galli* (L.)P.B. var *crus-galli*). The presented method of calculating daily assimilation rates, per species in a mixture, and the soil moisture balance, are both relatively simple, and primarily aim to illustrate the principles of competition for light and water. The description of competition for light is improved by replacing subroutine XDASSH in Appendix 6 by subroutine XDASS (Appendix 7). The latter is an extension of the model SUCROS87 described in Section 4.1 for monocultures to a mixed vegetation. The resulting model for growth of different species in a mixture is designated COMPETITOR.

4.2.7 Competition for nutrients (N, P, K)

Shortage of soil nutrients reduces the rate of crop growth. The presence of weeds reinforces this reduction because they capture nutrients which would otherwise be used for crop growth.

A simple model for nitrogen competition is presented. Here, the competition model of Exercise 60, which applies to optimal growing conditions, is extended by including a procedure for N uptake. This procedure is based on the model of van Keulen (1982b) for the effect of N fertilization on crop growth. Subsequently, below-ground competition for N is introduced into the model.

Soil nitrogen available for uptake Mineral nitrogen (nitrate, ammonium) in the rooted profile is potentially available for uptake by the plants. To avoid the need for a complex model of the soil nitrogen balance, the amount of N actually taken up by the vegetation is tracked as a state variable in the model. Total uptake is calculated from the results of standard fertilizer trials where both yield and uptake of the crop are recorded in response to fertilizer application (Figure 62).

The amount initially available for uptake equals the uptake from unfertilized soil (intercept N_0 in Figure 62). A constant fraction of the fertilizer is eventually recovered in the (above-ground) plant material (linear relation with slope r in Figure 62). Therefore, the amount of soil N at time t which is still to be taken up ($A_{s,t}$) equals the initial amount ($A_{s,0}$) minus the integral of rate of N uptake:

$$A_{s,t} = A_{s,0} - \int (-U_t)dt \quad \text{with} \quad A_{s,0} = A_{us,0} + rF \quad \text{Equation 114}$$

where $A_{s,t}$ is the amount of soil N yet to be taken up at time t (kg N ha^{-1}), U the rate of uptake ($\text{kg N ha}^{-1} \text{ d}^{-1}$), $A_{us,0}$ the uptake from unfertilized soil (kg N ha^{-1}), F the fertilizer rate (kg N ha^{-1}), and r the fraction of fertilizer recovered at harvest in above-ground plant material ($\text{kg N kg}^{-1} \text{ N}$).

Values of the parameters can be derived from reviews of fertilizer experiments given by van Keulen & van Heemst (1982) and van Keulen (1986b). Uptake at

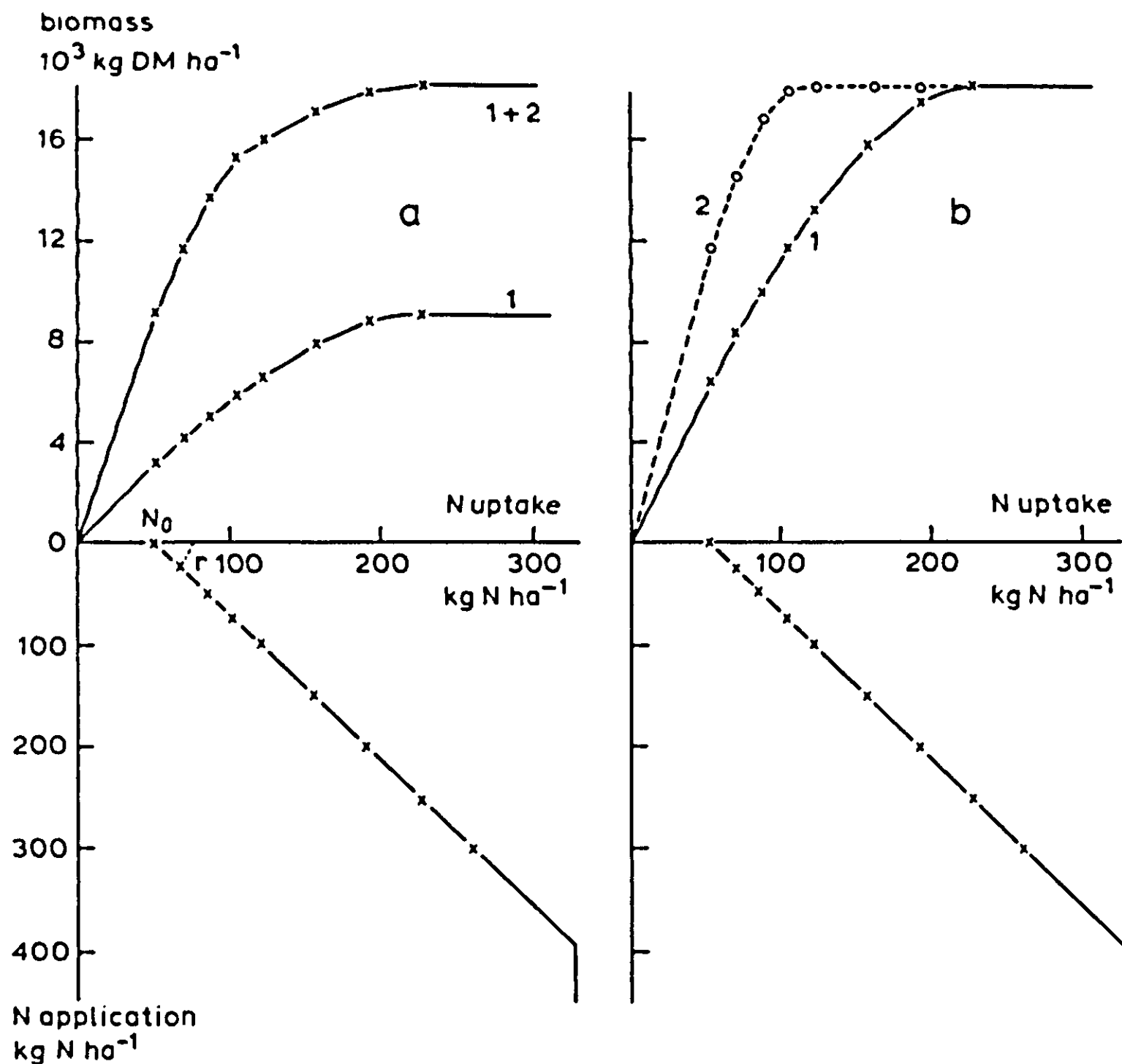


Figure 62. Simulated biomass production of two species and their total N uptake (a) in 1:1 mixture and (b) in monocultures. The lower the soil N availability the greater the relative advantage of the C_4 type (species 2) over the C_3 type (species 1). At low N availability, the C_4 type utilizes the available N almost twice as efficiently as the C_3 type because it is able to dilute the N concentration in its tissues to concentrations that are half as low. Fertilizer recovery ($r = 0.7$) and N uptake from unfertilized soil ($N_0 = 50 \text{ kg N ha}^{-1}$) are depicted in Figure a. See also Exercise 62.

zero application ($A_{us,0}$) is mainly determined by soil characteristics. Typical values for arable lands in the Netherlands are 70 kg N ha^{-1} , 2.2 kg P ha^{-1} , and 40 kg K ha^{-1} . The recovery fraction (r) varies from 0.1 to 0.8 for N and from 0.5 to 0.8 for K, depending on husbandry and soil characteristics. Recovery of phosphorus seldom exceeds 0.3 (Driessen, 1986b); and the relation between P fertilizer rate and uptake often deviates from linearity. Typical recovery fractions for arable lands in the Netherlands are 0.7, 0.2 and 0.7 for N, P and K, respectively.

Uptake The amount of nitrogen in the plants is given by the integral of the rate of uptake. The potential rate of uptake of the vegetation is called its demand. The

demand at time t equals the maximum amount at t minus the actual amount at the previous time $t - 1$:

$$D_t = (NA_{mx,t} - NA_{act,t-1})/T_c = (Y_t \cdot NC_{mx,t} - NA_{act,t-1})/T_c \quad \text{Equation 115}$$

where NA is the amount of nitrogen (kg N ha^{-1}), NC the nitrogen content (kg N kg^{-1} DM) and Y the biomass (kg DM ha^{-1}). Subscripts mx and act refer to the maximum and actual values, respectively. The time coefficient T_c is introduced to account for a delay in uptake, which is of the order of 2 days (Seligman & van Keulen, 1981).

The actual uptake of the vegetation is equal to the minimum of the demand or the maximum supply by the soil:

$$U_t = \text{Min}(D_t, A_{s,t}) \quad \text{Equation 116}$$

Growth reduction When the N content of the vegetation decreases below a certain, critical level, the growth rate is reduced. This growth rate is assumed to be linearly related to the N content:

$$\Delta Y_{t,act} = f_N \Delta Y_{t,pot} = \frac{NC_{act} - NC_{mn}}{NC_{cr} - NC_{mn}} \Delta Y_{t,pot} \quad 0 \leq f_N \leq 1 \quad \text{Equation 117}$$

where Y_{act} and Y_{pot} are the actual and potential growth rates, and NC_{act} , NC_{cr} and NC_{mn} are the actual, critical and minimum nitrogen contents, respectively. The actual content is obtained by dividing the actual amount (NA_{act}) by the present biomass (Y).

Because of stomatal control, the transpiration rate must be reduced in the same way as the growth rate when nutrients are in short supply (Goudriaan & van Keulen, 1979; Wong et al., 1985).

Maximum, critical and minimum nutrient contents For a given nutrient, these key values differ strongly between plant organs, decrease with development stage, and depend to a lesser degree, also upon plant species. For nitrogen, typical values for field-grown annual C_3 grasses can be derived from van Keulen (1982b, p. 240). The maximum N content (NC_{mx}) in leaves decreases linearly with development stage according to $0.055 \cdot (1 - 0.3 \text{ DVS})$, with 0.055 referring to the value at seedling emergence (DVS increases from 0 at emergence to 2 at maturity). Maximum N contents of stems and roots amount to about 0.35 and 0.20, respectively, of the value for leaves. The maximum N content of grass seeds decreases from 0.045 at the onset of seed filling to 0.025 at seed maturity. Critical N contents (NC_{cr}) amount to about 0.65 of the maximum contents. Minimum content (NC_{mn}) of the vegetative parts averages about 0.005, but is somewhat higher for the early stages. The minimum N content of grass seeds is 0.015.

Total uptake (Equation 116) is distributed among the various plant organs in proportion to their demands (van Keulen, 1982b). In the summary model of

Exercise 60, where only the total biomass of each species is considered, averaged N contents are used. The dry matter distribution pattern of annual C₃ grasses suggests a maximum N content of the above-ground parts that decreases from 0.050 at emergence to 0.025 at flowering, and to 0.018 at maturity; a critical content that amounts to 0.65 of the maximum content; and a minimum content of 0.008 kg N kg⁻¹ DM.

Maximum contents of C₄ grasses are probably close to those of the C₃ grasses. However, owing to the C₄ pathway, photosynthesis can continue at much lower contents of carboxylating enzymes (Ku et al., 1979). Critical and minimum N contents of C₄ species are, therefore, about 0.5 of the respective values for C₃ species (Penning de Vries & van Keulen, 1982; Brown, 1985). Maximum N contents of legumes are 30% and those of non-leguminous dicotyledons about 10% higher than those of grasses. Maximum contents of seeds may differ strongly between species.

Phosphorus (P) contents are coupled, to some extent, to nitrogen contents. P/N ratios vary within a range of 0.04 to 0.15 and have a value of 0.10 with ample nutrient supply (Penning de Vries & van Keulen, 1982). At very low levels of N uptake, absorption of P is restricted so that the P/N ratio does not exceed 0.15. At very low P availability, uptake of N is reduced so that the P/N ratio does not decrease below a value of 0.04. Thus, by combining these features with the N model discussed above, a simple model for P is defined.

Potassium (K) contents are of roughly the same order of magnitude as N contents, but vary greatly among plant species and according to soil cation status.

Competition In the case of mobile soil elements, such as water and nitrates, root density has little effect on the total uptake of these elements by the crop, when the conditions are within a normal range (Seligman & van Keulen, 1981; van Noordwijk, 1983). Thus, the total uptake of a mixed vegetation is calculated in a similar way to that outlined above for the weed-free crop.

However, when supply from the soil cannot cover demand, uptake by a species in a mixed vegetation will be related to its share in the total absorbing root length. Below-ground competition for soil elements is modelled analogously to the above-ground competition for light. Just as the fraction of light quanta intercepted by a species was related to its share in total leaf area, the fraction of water molecules or nutrient ions that is intercepted is related to its share in the total root system:

$$U_i = (l_i/\Sigma l) \Sigma U \quad U_i \leq D_i \quad \text{Equation 118}$$

where U_i is the uptake by species i , and ΣU the uptake summed over all species of which the vegetation is composed (kg N ha⁻¹ d⁻¹), D_i the demand of species i (kg N ha⁻¹ d⁻¹), and l the effective root length (m ha⁻¹). Equation 118 shows that the relative, rather than the absolute, root lengths of the species determine their competitive ability.

A species with an extensive root system, relative to its demand, is able to meet its demand up to a lower soil nitrogen supply. In the model, at limited soil supplies, the soil nitrogen not used by such a species is distributed over the other species.

Exercise 62

Combine the nitrogen model with the competition model of Exercise 60. Simulate the effect of a C₄ grass weed on a C₃ cereal, assuming that crop and weed are identical except that the C₄ species has a critical and minimum nitrogen content which is half that of the C₃ species. Assume a value of 2.76 g DM MJ⁻¹ for the light utilization efficiency. Evaluate the effect of N fertilization, assuming a recovery of 0.7 and a zero uptake of 50 kg N ha⁻¹.

The foregoing approach assumes a limited stock of soil nitrogen, which is depleted during the course of the growing season, without periodic replenishment except from fertilizer application. This suggests that the species with the greatest demand will take up most of the nitrogen. After the available soil nitrogen has been depleted, the growth rate of a species is reduced less if it can dilute the nitrogen to lower concentrations in its tissue (e.g. a C₄ type), or has a low potential growth rate. The size of the root system would then be of hardly any importance. In reality, however, small amounts of mineral nitrogen become available throughout the growing season because of the mineralization of soil organic matter. The species with the greatest root capacity benefit most from this release.

Modelling the separate processes of the soil N balance is complex and falls beyond the scope of this Section (for reviews of models see Frissel & van Veen, 1981; de Willigen & Neeteson, 1985). Instead, net mineralization, i.e. the difference between mineralization and immobilization, is accounted for in a very simplified way according to Greenwood et al. (1984). Here, we consider the total mineral soil N instead of only the amount which will be taken up by the vegetation. Equation 114 for available soil N then becomes

$$A_{s,t} = A_{s,0} + \int (M_t - U_t/r)dt \quad \text{with} \quad A_{s,0} = A_0 + F \quad \text{Equation 119}$$

where A_0 is the initial amount of mineral soil N (kg N ha⁻¹), F the fertilizer rate (kg N ha⁻¹), U_t the N uptake by the vegetation (kg N ha⁻¹ d⁻¹) which is divided by the recovery (r) to account for incomplete uptake of mineral soil N, and M_t the net mineralization rate (kg N ha⁻¹ d⁻¹). Mineralization mainly depends on the amount of fresh organic material that can be easily mineralized and, therefore, on the previous crop. For UK arable soils, previously cropped with cereals, Greenwood et al. (1984) give an average of $4.5 \cdot 10^{-5}$ kg N_{min} kg⁻¹ N_{org} d⁻¹ (15°C, $Q_{10} = 2$) and 10 t total organic N ha⁻¹ in the rooted profile.

Exercise 63

Use the model of Exercise 62 to compare the soil N balance according to van Keulen (1982b) (with a zero uptake of 50 kg N ha^{-1}) with that according to Greenwood et al. (1984) with an initial amount of $26.4 \text{ kg N}_{\text{min}} \text{ ha}^{-1}$. Assume a fertilizer rate of 25 kg N ha^{-1} applied in early spring, and a recovery of 0.7. Calculate the effect of a twofold difference in the root length/biomass ratio on yield and N uptake of two C_3 species when grown together in a 1:1 mixture.

In the preceding sections, the state variables referred predominantly to the whole canopy and to the whole rooted zone. For the rate variables, their daily averages were considered. The system becomes more sophisticated when the spatial heterogeneity of canopy and soil, and the temporal heterogeneity during the day is taken into account (Spitters & Aerts, 1983; Baldwin, 1976). Further detail is introduced by accounting for environmental effects on species attributes; e.g. adaptation mechanisms. This involves the effects of shade, water stress and nutrient shortage on the (re)distribution of carbohydrates within the plant, and on specific leaf area, photosynthetic capacity of the leaves (A_m, ϵ) and senescence.

In Exercise 61, a simple procedure was applied to illustrate the effects of weed control. For practical purposes, however, this procedure is clearly too simple. Therefore, with respect to modelling crop-weed competition, the main subject to be enlarged upon is weed control and, in particular, to the interactions between herbicide, dose and timing of application, development stages of crop and weed, and environmental conditions.

4.3 Combination models, crop growth and pests and diseases

R. Rabbinge and L. Bastiaans

4.3.1 *Introduction*

Estimates of yield loss due to pests or diseases are essential in any supervised or integrated control system of pests and diseases (Chapter 1). They form the basis for an economic cost-benefit analysis of control measures and, therefore, help to develop rational crop protection systems. These yield losses may be expressed in mass of product or economic values. Here, both concepts will be used. Yield losses, whether mass of product or financial, are often only based on intelligent guesses made by agronomists or crop protection scientists. They are seldom based on a real knowledge of the nature or level of crop growth reduction due to the presence of pests or diseases. The increasing significance of pests and diseases as growth and production reducing factors (Smith et al., 1984), justifies more detailed analysis of the interaction between the host plant (crop) and its enemies. This may be done in a statistical analysis of the relation between disease severity or infection level and crop loss. Such analyses help to define injury levels under some field conditions and can be used in pest and disease management (Royle et al., 1988). However, they do not provide much insight into the nature of growth and yield reduction and cannot be extrapolated to other, not yet studied, field situations.

There are several ways in which pest or disease populations can affect different physiological processes in plants. They may, for example, reduce crop stands by eliminating the plants, they may reduce inputs such as light, CO₂ or water, they may affect rates of metabolic and growth processes directly or they may remove or consume previously produced material. Simulation models are useful for studying the quantitative consequences of the various effects.

Eventually, these simulation models will provide insight into the mechanism of growth and yield reduction and into the quantification of yield reduction under various conditions, as demonstrated in cereal aphids on winter wheat (Section 4.4).

4.3.2 *Statistical analysis and descriptive models*

In order to make competent decisions on the management of pests and diseases, it is essential to know how the different disease or pest epidemics will reduce yields. In most studies of pest and disease management, the concept of Economic Injury Level (EIL) is introduced as the value at which cost of control is in balance with the expected yield loss. However, because of time lags, control measures are often needed at some action threshold long before this economic

injury level is reached (Chapter 1). The EIL concept, when it was introduced by Stern (e.g. 1973), revolutionized the thinking of crop protection scientists. It presumes a fixed relation between disease or pest intensity and yield loss, irrespective of crop growth conditions. However, results differ greatly under various conditions, as illustrated for the fruit-tree red spider mite on apple, one of the most studied host plant-pest relations. Van de Vrie (1956) showed, for a well kept, well fertilized and intensively controlled 'Beauty of Boskoop' apple orchard in the Netherlands, that a spider mite density of maximally 40 mites leaf⁻¹ and 1080 mite days leaf⁻¹ caused a yield loss of 18% and a reduction in shoot growth of 30%. However, Avery & Briggs (1968a, b), in similar experiments in England with two-year-old 'Lord Lambourne' trees, found that a mite density of 70 mite days cm⁻² did not result in significant differences in apple yield ha⁻¹ or in shoot growth, dry weight of apples or number of buds. In a detailed study from 1965 to 1971 in various apple orchards in England, Light & Ludlam (1972) used different spraying treatments to determine immediate and delayed effects of mites. In their experiments, mite densities varied from 800 mite days leaf⁻¹ to 2000 mite days leaf⁻¹ and densities of up to 40 mites leaf⁻¹ were recorded. This experiment was statistically very well designed, and differences of 500 kg ha⁻¹ were significant. However, these showed up only when the number of mite days leaf⁻¹ exceeded 1350. In the following year, no significant differences in pomological characteristics could be detected.

At Hood River Valley, Oregon (U.S.A.) a four-year study, using individual ten-year-old 'Newton' and 'Golden Delicious' apple trees, was carried out by Zwich et al., (1976). The mite densities were observed at weekly intervals for various spider mite control treatments (timing and method of control). The trees were irrigated when necessary and nitrogen supply was abundant. Chemical control was in accordance with normal farming practices and pruning was done chemically. Maximum densities of 70 mites leaf⁻¹, and maximally 1400 mite days leaf⁻¹, were reached in these experiments. These high mite densities did not result in significant effects on yield or on other pomological characteristics. Only at the highest mite density was the chlorophyll content of the leaves significantly affected. Effects on fruit growth, shoot length, number of buds and trunk diameter were absent in the year following the heavy infestation. Apparently, the apple trees growing under 'optimal' conditions could tolerate high mite densities; up to 1900 mite days leaf⁻¹ or a maximum density of 70 mites leaf⁻¹. These results led Zwich et al. (1976) to fix the economic injury levels of fruit-tree red spider mites at 20-30 mites leaf⁻¹. This is approximately ten times the economic injury level which was proposed at the Technical Expert Meeting of the FAO in 1973.

It seems impossible to explain these conflicting experimental results. It indicates that the economic injury level depends on the conditions that prevail during the experiments, and thus a specific EIL based on field experiments alone is only possible when several experiments are done and statistically analysed. This is both time-consuming and painstaking. It would seem, therefore, attractive to

combine such field experiments with detailed physiological and biological studies on the nature and background of damage. Simulation studies may bridge the gap between both levels. However, crop physiological parameters are very loosely determined in all the experiments described, and neither the cropping history of the experimental orchards nor crop agronomy measures are given. Moreover, the data on spider mite densities are often incomplete, the age composition of the spider mite population is not determined, and accuracy of the population density is not given. Weather conditions during the experiments are also not recorded. This lack of information makes interpretation of the data virtually impossible.

Clearly, the above studies, which can be extended by many others, demonstrate that it is almost impossible to define generally applicable economic injury levels; the results are too conflicting.

Statistical methods are based on a description of the field situation but give no insight into the background of damage. Extrapolating the damage relations to other field situations is, therefore, hazardous, as the consequences of the interaction between pest and crop may vary considerably and could result in a different yield loss-pest density relation. For example, weather conditions may not only affect the epidemiological development of a disease but also the host-pathogen relation (Zadoks & Schein, 1979). Apart from when and where the pest is present, the crop growing conditions may considerably affect the reduction in yield. At high nitrogen contents in the leaves, epidemiological development of many diseases is promoted, because the latency period is shorter and the infectious period longer than under nitrogen-deficient conditions. The effect of the nitrogen conditions on the growth and yield reduction, per unit of disease or pest, is also important.

The effects of pests and diseases are, in general, more significant at higher yield levels. A healthy crop, essential for high yields, and the favourable micro-meteorological conditions in a dense crop, may promote the epidemiological development of many diseases and affect the yield loss-pest density relation. Increase in winter wheat yields in western Europe in the seventies, is largely due to better pest and disease control in crops that already had a high potential (Rabbinge, 1986). Cereal aphids cause progressive damage at increasing yield levels (Section 4.4). Other diseases cause proportional (mildew) or subproportional (Septoria) damage per unit of disease (Rabbinge, 1986). The existence of differential effects limits the use of generally applicable economic injury levels. When such differential effects are absent, well-designed and well-executed field experiments may lead to adequate economic injury levels. Experimentally determining flexible economic injury levels, however, would require a discouraging number of field experiments and, for this reason, the use of dynamic simulation models in combination with experiments would seem to be more appropriate.

4.3.3 *Dynamic explanatory models as a vehicle for development of EILs*

In most models of population dynamics for pest and disease organisms, the crop is considered as a constant substrate which imposes limitations only when all sites are becoming occupied.

However, the crop's condition may, for example, affect the length of the latency or infectious periods, and thus epidemiological development. Such effects are considered by extending the simple epidemiological models of Section 3.1. For instance, the nitrogen content of the leaves can be introduced, or several leaf layers with differing sensitivities to the disease can be distinguished. Leaf layers can be introduced using boxcar trains for the various leaf layers, and crop condition can be introduced as a forcing variable. The epidemiological model of mildew in winter wheat of Exercise 36 (Section 3.1) is used to introduce leaf layers with different nitrogen contents.

Exercise 64

Introduce leaf layers into the model of Exercise 36. Each leaf layer has an LAI of 1.5, so at the beginning one leaf layer and on Day 180 (with the highest leaf mass) three leaf layers are distinguished. After Day 180, leaf dying due to ageing starts from the lowest leaf layer, via the middle and finally reaches the upper leaf layer. Run the model and study its results. Explain the differences with the results of Exercise 36.

The effect of leaf layers on the epidemic may be amplified or reduced when the condition of the leaf layer in terms of nitrogen content is introduced. This is the next step in model development. Crop condition in terms of nitrogen content is introduced as a forcing function that influences the latency and infectious periods. The nitrogen content in the various leaf layers is, for reasons of simplicity, kept constant during the growing season. In the middle leaf layer, layer 2, it is kept at 3.0% and in the first layer, the lower layer, a lower percentage is maintained whereas the third or upper leaf layer has a slightly higher nitrogen percentage. How the various nitrogen contents affect the lengths of the latency and infectious periods is given in Table 15.

Exercise 65

Introduce the nitrogen content of the various leaf layers in the model of Exercise 64 and compute the consequences of the changes in latency and infectious periods for the upsurge of the mildew epidemic. Explain the differences in the results between Exercises 64 and 65.

Table 15. Effect of nitrogen contents in leaves of winter wheat on latency period and infectious period of mildew *Erysiphe graminis* expressed as a multiplication factor.

Proportion nitrogen in leaves (%)	Latency period (multiplication factor)	Infectious period (multiplication factor)
2.0	1.5	0.8
2.5	1.2	0.9
3.0	1.0	1.0
3.5	0.8	1.2

The epidemiological model, although more realistic, is still not complete as it does not account for changes in nitrogen content during the growing season and neglects the effect of mildew on crop performance, which may ultimately result in shifts in the epidemiological parameters. This effect of the disease on crop performance is exemplified in the following paragraphs and in Section 4.4.

The effect of disease or pest on crop performance may vary considerably depending on the place and the method of interaction (Boote et al., 1983). In Table 16, some sites of coupling between crop and pests and diseases are indicated. Various rates may be affected. The rate of photosynthesis may be affected by a direct effect on the light use efficiency through light stealing, or on the assimilation rate at light saturation because of a physiological change. Such a direct effect is found as a result of, for example, mildew-diseased wheat. This disease decreases photosynthesis at light saturation and has no effect on light use efficiency (Rabbinge et al., 1985). Another disease, beet yellows virus (BYV) causes a decrease in both light use efficiency and photosynthesis at light saturation (van der Werf et al., 1989a). The cereal aphid, through its excretion product, honeydew, besides causing direct phloem consumption, also affects light use efficiency and photosynthesis. (Rabbinge et al., 1983).

Maintenance respiration and growth respiration may be affected by mites that drain assimilates from the parenchyma cells and promote suberization. Further growth rate may be affected directly through leaf mass or tissue consumption. Stand reducers may cause loss of plants, which may result in yield loss unless sufficient compensation, and the capability and time to realize this compensation, is available. Some pests and diseases may affect the turgor of cells, either directly or by disrupting the tissue in such a way that transpiration is promoted. Leaf senescence may be promoted and growth of root, stem or storage organ may be directly affected, caused by having to compete for assimilates. Various aspects of growth reduction may be distinguished (Table 16). These aspects are also present in the crop growth model SUCROS87. Therefore, some of the crop growth reducing factors of Table 16 will be discussed below in a way that the order of capturing and use of solar energy is followed as a line. The relational

Table 16. Various examples of crop growth-reducing factors, place and nature of effect.

Type of effect	Yield-loss determining aspects	Example
Stand reducers	<ul style="list-style-type: none"> – number of plants lost – distribution of lost plants – compensation ability of remaining plants 	damping-off fungi
Light stealers	<ul style="list-style-type: none"> – covered area – type of tissue – total or partial absorption 	yeasts
Assimilation rate reducers	<ul style="list-style-type: none"> – effect on AMAX and/or EFF – position of affected leaves 	powdery mildew beet yellows virus
Assimilation sappers	<ul style="list-style-type: none"> – rate of CH₂O consumption – harmful excretion products 	mites
Tissue consumers	<ul style="list-style-type: none"> – type of tissue – rate of consumption 	cereal leaf beetles

diagram of Figure 63 indicates where the effects of the various harmful organisms are focused.

Stand reducers, such as damping-off fungi, reduce plant biomass and the number of plants. Analysis is difficult as it requires similar approaches to those described in Section 4.2 on light or nutrient capturing by weeds. The distribution of the remaining plants in the field and their capacity to compensate should then be considered.

Light stealers Some leaf pathogens have a 'light stealing' effect on crops as they live in dead host tissue which absorbs photosynthetically active radiation, which is caused, for example, by perthotrophic and saprophytic fungi. Leaf coverage due to excretion products or light interception by leaves with necrotic lesions may interfere with photosynthesis. Coverage of leaves with mycelium may also affect light absorption.

Assimilation rate reducers Many pathogens and pests affect the CO₂ assimilation rate; they may affect the photosynthesis rate at light saturation or the light use efficiency. Mechanisms by which pathogens affect photosynthesis have been summarized by Buchanan et al. (1981). Viruses and some fungi may reduce the number of chloroplasts per unit leaf area or alter the chloroplast ultrastructure and components of the electron transport chain, thus decreasing photosynthesis.

ary damage by assimilate consumers, for instance due to honeydew, may result in higher total levels of damage. These secondary effects are mainly caused by a considerable change in the physiological characteristics of the crop due to the pest organisms.

Turgor reducers, such as nematodes that feed on the roots, and root pathogens affect the water balance of the plant. They also affect the crop nutrient balance by disrupting phloem transport to the roots, reducing the energy supply for the active uptake of nutrients such as K, and by disrupting the passive flow of water and nutrients by the eventual decay of that tissue.

Evaluation of the various host plant-pest interactions can be done for the conditions of an optimally functioning crop, when water and nutrients are abundantly available, by introducing damage mechanisms into the model SUCROS87 (Section 4.1).

4.3.4 *SUCROS87 coupled with growth-reducing factors*

Mutilation of leaf mass To demonstrate the effect of a leaf consumer on crop growth, a simplified simulator of population growth of the cereal leaf beetle (*Lema cyanella*) may be attached to the model SUCROS87. Larvae of cereal leaf beetles consume leaf mass at a rate of about $250 \text{ cm}^2 \text{ d}^{-1}$ (= 1.2 g dry matter d^{-1}). Only the larvae consume leaves. After growth and development they pupate, moult and develop into adults that may give rise to another generation. The rate of increase in the number of cereal leaf beetle larvae depends on the egg-laying rate of the adult females. After hatching, the larvae immediately start feeding. Their effect on crop growth is introduced into the model, using the parameters for wheat, by a decrease in the amount of leaves. This rate of decrease in leaf weight is assumed to be proportional to the number of larvae, lumping all development stages of the larvae together. Consumption of leaf mass by the adults is neglected, and the relation of ageing and reproduction rate on food quality are not considered. Population dynamics of the beetles are introduced in a very simple way by distinguishing four morphological stages: eggs, larvae, pupae and adults. The adult population is assumed to be 50% male, so that only 50% of the next generation will produce eggs.

Exercise 66

Develop a simple model of *Lema cyanella* when environmental conditions are considered to be constant and the different development stages last 5, 10, 4, 20 days for the egg, larval, pupal and adult stages, respectively, and when there are initially 100 adult cereal leaf beetles that produce eggs at a rate of 3 per day.

Assume that there is no influence of larval density on the rate of reproduction, and assume during development a constant relative dispersion of one.

The population model can be linked to the crop growth model by introducing a consumption rate of leaves that drains leaf mass. This rate depends on the number of beetle larvae and the daily consumption rate per larva. The leaf area index, LAI, is affected by this decrease in leaf mass due to beetle 'grazing'. There is also another consequence for the crop growth model, as the maintenance respiration is affected by the ratio of weight of green leaves divided by the total leaf weight, $WLVG/WLV$. This ratio (MNDVS) was introduced in SUCROS87 to express the change in maintenance respiration due to ageing or to a decrease in nitrogen content. Since the beetles reduce $WLVG$, they indirectly affect simulated maintenance respiration. To avoid this, the factor expressing the reduced maintenance respiration, due to ageing or low nitrogen content, is transformed into a forcing function, based on the $WLVG/WLV$ ratio, as determined in Section 4.1, in course of time: $MNDVS = AFGEN(MNDVST, DVS)$.

Exercise 67

Link the model SUCROS87 to the simple population model, and use this combination model to evaluate the effects of different cereal leaf beetle attacks. Assume that the adult cereal leaf beetles enter the crop on Day 195. The simulation should reproduce the results of Figure 64.

Tissue death and assimilate consumption Plant mites inject their stylets through the epidermis into the parenchyma cells and swallow the contents. The attacked cells may die and the surrounding cells often demonstrate phenomena such as suberization of cell walls, decreased photosynthetic activity and increased maintenance respiration. Plant mites are found in many agricultural and horticultural crops. They are especially prolific in glasshouse crops but, under suitable conditions, may also cause damage in arable crops such as potato. To illustrate this, the model SUCROS87 for potato is linked to a mite population. The model for the potato crop is changed in two places to introduce the effects of mites.

First, the maintenance respiration is increased by an amount considered to be proportional to the mite density. Although this may be true at relatively low densities, it overestimates the effects of the mites at high densities. Second, an effect of the mites on the photosynthetic activity is introduced. This effect is also mite-density-dependent, the basis of these effects is derived from measurements made by Tomczyk & van de Vrie (1982) and damage data of Sabelis (1981) on chrysanthemums and roses. Mite density is introduced by way of a forcing function, lumping all the different morphological stages together. A more realis-

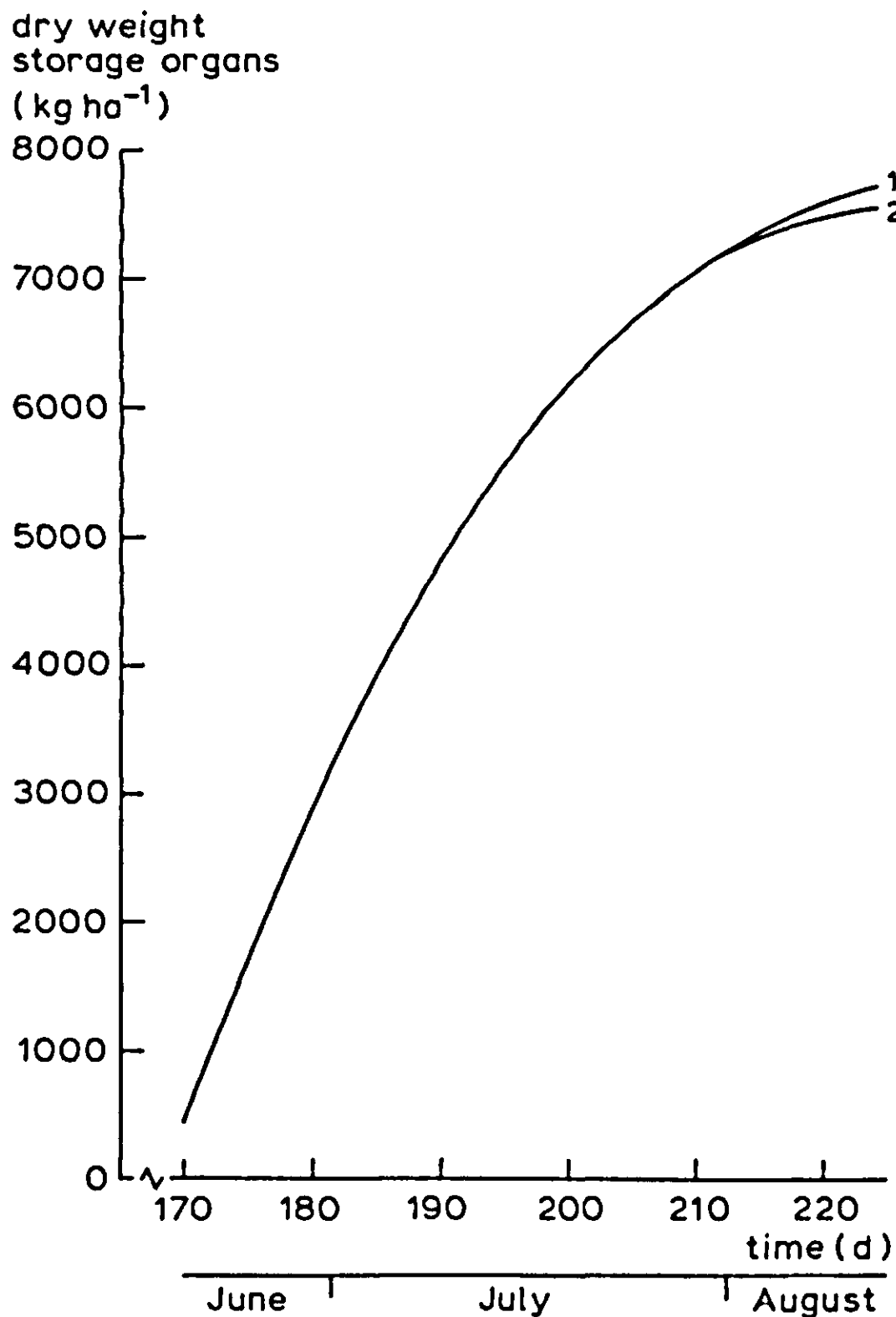


Figure 64. Simulated weight of grains (WSO, kg dry matter ha⁻¹) of a spring wheat crop for different levels of cereal leaf beetle attacks. 1: no beetles; 2: starting with 300 adult beetles on 14 July (Day 195).

tic population model, which may be combined with a comprehensive crop model, should consider the different morphological stages and the sensitivity of the development rate to temperature and food quality (Rabbinge, 1976).

Exercise 68

Introduce the effect of spider mites on maintenance respiration in the model SUCROS87 for potato. Give an imaginary population density curve in course of time, for a mite population that reaches a maximum on 29 July of 2 mites cm⁻², 6 mites cm⁻² or 12 mites cm⁻², respectively. The first mites are found on 30 June, and the last ones have left by 18 August. Presume a linear increase and decrease in the mite population density. Each mite respire 50% of its body weight per day.

An adult mite has a weight of 50 μg . Your calculations should be the same as the results of Figure 65.

Computations using the model of Exercise 68 show that minor changes in the respiration rate, due to the presence of mites, have a major effect on the growth rate of the canopy; consequently, yield is considerably affected. The same is true for the effect on photosynthetic activity. This effect is introduced by a decrease in the assimilation rate at light saturation (Table 17). Computation using the model, which comprises both effects, shows that due to the combined effects of mites on respiration and photosynthesis at light saturation, yield is reduced by 16% when a maximum density of 12 mites cm^{-2} is reached (Table 18). The effect of the

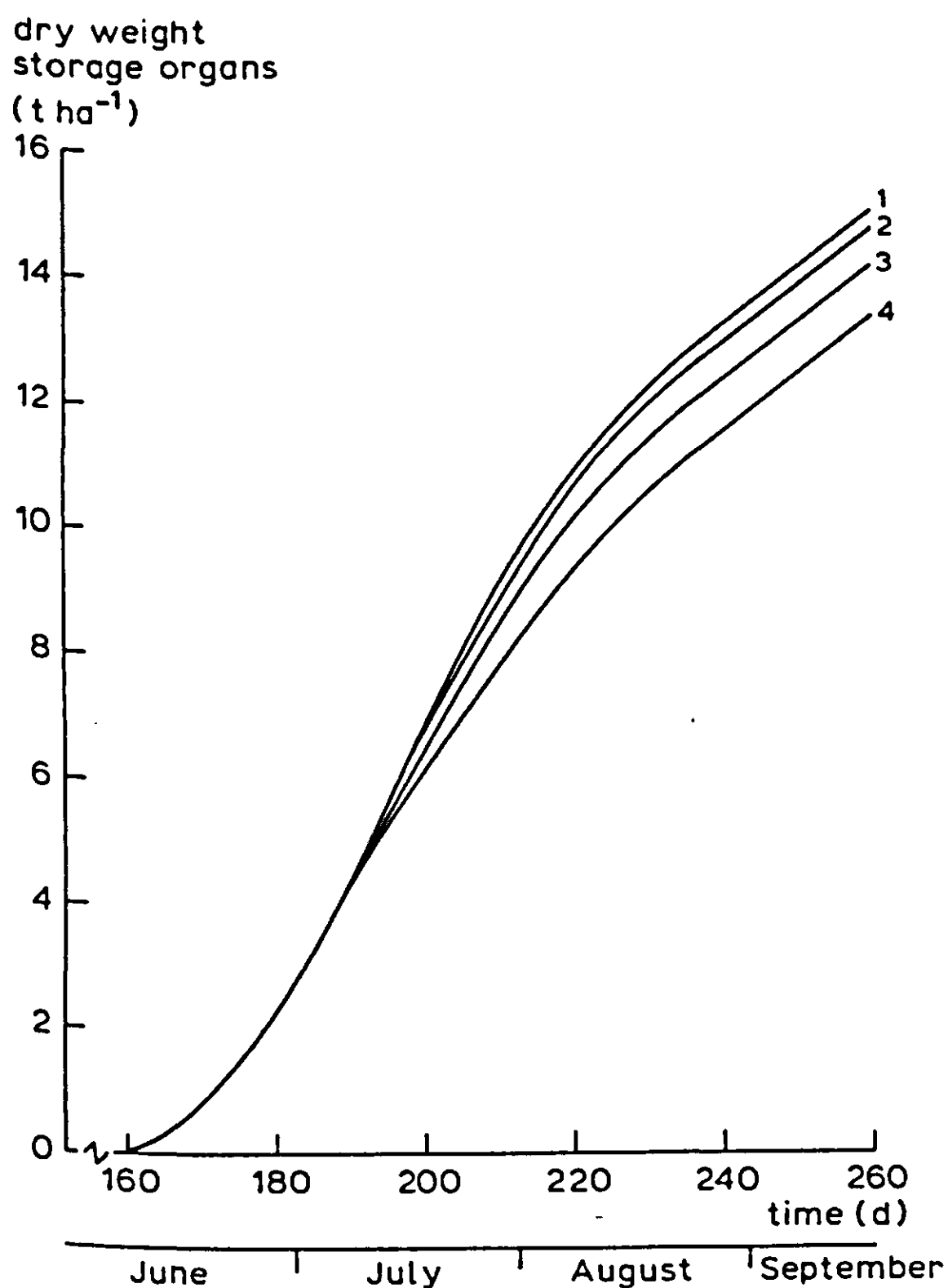


Figure 65. Simulated dry weight of storage organs (WSO, t ha^{-1}) of a potato crop in the presence of a mite population that affects maintenance respiration. A maximum mite density of 0, 2, 6 and 12 mites cm^{-2} leaf (curve 1–4, respectively) is reached on 29 July (Day 210).

Table 17. Decrease in photosynthesis at light saturation of potato leaves at various mite densities, expressed as a multiplication factor.

Mite density (mites cm ⁻²)	Decrease in photosynthesis at light saturation (multiplication factor)
3	1
10	0.75
20	0.3

Table 18. Simulated effect of mites on dry weight yield of storage organs (WSO, kg ha⁻¹) of a potato crop (WSO control = 14950 kg ha⁻¹) at harvest (17 September; Day 260). It is assumed that the mites affect maintenance respiration (MAINT), and/or assimilation rate at light saturation (AMAX).

	Maximum mite density (mites cm ⁻² ; on 29 July (Day 210))					
	2 mites		6 mites		12 mites	
	WSO	reduction	WSO	reduction	WSO	reduction
MAINT	14665.	285.	14096.	854.	13242.	1708.
AMAX	14950.	0.	14816.	134.	14276.	674.
MAINT + AMAX	14665.	285.	13962.	988.	12569.	2381.

increase in maintenance respiration is relatively more important than the effect on photosynthesis at light saturation. Both effects seem to be additive. This is understandable because the places that are affected are independent of each other, and a positive feedback due to growth reduction of leaves is absent, because the mites are not introduced until Day 181 when leaf growth has already stopped. If the mites are introduced earlier, the two effects (on maintenance respiration rate and assimilation rate at light saturation) are no longer additive, as a positive feedback would be present due to reduced leaf growth and consequently leaf area and assimilation rate. At maximum mite densities of 2 or 6 mites cm⁻², yield reduction is almost negligible. The effect on maintenance respiration and photosynthetic activity only occurs when weather conditions are favourable for both crop and pest: high temperature, rapid crop development and limited radiation levels.

Further testing of this hypothesis may be done using this combination model. For example, effects of webbing, which appear sooner than injury symptoms (Sabelis et al., 1983), on light use efficiency and assimilation rate at light saturation, may be evaluated. However, the reliability of such model computations is

doubtful, as too many descriptive relations on the system level are needed, and too many estimates required. Therefore, comprehensive models are needed in this process of hypothesis testing to obtain insight into the consequences of the different effects that spider mites have on plant physiological parameters. This will require additional experiments at the process level, together with well-defined field experiments for model testing.

The ultimate aim of such studies is to develop damage relations, which can be used to control the acarine system under various conditions.

Leaf coverage To demonstrate the effect of organisms that cover the leaves with a thin layer, yeasts such as *Sporobolomyces spp.* (pink yeasts) and *Cryptococcus spp.* (white yeasts) or an organism like the saprophytic fungus *Cladosporium cladosporides* (black moulds), are coupled to the model SUCROS87 for wheat growth (Section 4.1). Yeasts and the saprophytic fungus occur on all surfaces where organic matter, sugars, proteins or other leaf exudates, needed for growth and respiration, are available. When cereal leaves produce exudates or are covered with the cereal aphid excretion product honeydew or with sugary exudates, numbers of up to 10^6 cells cm^{-2} are reached. The light stealing effect of yeasts is evaluated. The yeast epidemic is simulated using the logistic growth equation (Equation 37). A leaf area covered by yeast cells absorbs light before it is captured by the chloroplasts. It is assumed that a linear relation between absorption and the log value of yeast density in cells cm^{-2} exists. The absorption is introduced by multiplying daily photosynthetically active radiation (DPAR) by $(1 - \text{ABSORB})$, in which ABSORB expresses the light absorption by yeast cells.

Exercise 69

Construct a combination model for wheat growth with yeasts, and run it for different initial yeast densities at flowering (DVS = 1., Day 170) of 10, 100 and 10000 yeast cells cm^{-2} , respectively. The relative growth rate of the population $r = 0.8$, and a maximum of 10^6 yeast cells cm^{-2} is assumed. Repeat the calculations when the yeast population starts with an initial density of 10 cells cm^{-2} on Day 185 and Day 200, respectively.

At high yeast densities, light absorption is relatively less than at low yeast densities. This is due to the high number of yeast cell layers that cover a leaf at higher densities. The simulated reduction in grain yield is about 1000 kg ha^{-1} at an initial density of 10 yeast cells cm^{-2} on Day 170. The increase in yield loss at higher initial densities is small, as the maximum density of 10^6 cells cm^{-2} is reached in nearly all cases: the extra yield loss at an initial density of 10 000 cells cm^{-2} is only 500 kg ha^{-1} .

Light stealing may not be as high as assumed, and yeast cells may play an important role by suppressing perthotrophic fungi, such as *Septoria*, by competing for space and exudates (Rabbinge et al., 1984b). Thus, negative effects of yeasts and saprophytic fungi may be smaller than assumed, and positive effects such as competition may be larger, resulting in various net responses of growth and production under various conditions.

Assimilation rate reducer Beet yellows virus (BYV) can cause considerable yield reductions in sugar beet. In a field experiment in 1986, van der Werf et al. (1989a) demonstrated that plants infected on 5 June (8-leaf stage) with beet yellows virus (BYV; closterovirus group) produced only 45 t ha⁻¹ of beet roots (fresh weight), whereas healthy plants produced 93 t ha⁻¹. Plants infected at the 28-leaf stage, on 14 July, produced 87 t ha⁻¹. Thus, timing of virus infection is crucial for yield reduction as both the rate of virus spread and the physiological parameters are affected (van der Werf et al., 1989a, b). The effect of virus infection on physiological parameters has been determined in detailed photosynthesis measurements, and in measurements of optical characteristics of infected leaves. Light reflection and transmission of photosynthetically active radiation are decreased in virus infected plants and, partly as a result of this, light use efficiency is considerably smaller (Table 19). Photosynthesis at light saturation (AMAX, Table 19) is also considerably decreased due to virus infection. Healthy or infected green leaves had similar rates of light-saturated photosynthesis; in leaves with vein clearing symptoms, AMAX had decreased by 30%, and in bright yellow leaves AMAX was four times smaller.

The effects of the virus on light use efficiency and photosynthesis at light saturation (Table 19), were introduced into the model SUCROS87. A possible effect of the position of the infected leaves is neglected. First, crop assimilation is calculated for healthy leaves, and then the same calculations are done for infested leaves with bright yellow symptoms. The weighted average for the actual crop assimilation is then found by multiplying the last computed assimilation rate by the fraction of diseased leaves (FRDIS), and the first computed assimilation rate

Table 19. Normalized values of the maximum assimilation rate at light saturation (AMAX, kg CO₂ ha⁻¹ h⁻¹), light use efficiency (EFF, kg CO₂ ha⁻¹ h⁻¹ W⁻¹ m²) and dark respiration (RD, kg CO₂ ha⁻¹ h⁻¹) for various categories of leaves on BYV infected plants.

Leaf category	AMAX	SD(±)	EFF	SD(±)	RD	SD(±)
healthy	100(37.)	2	100(0.40)	0.04	100(2.9)	0.7
vein clearing	72	2	89	0.04	138	1.1
greenish yellow	46	2	80	0.03	188	0.7
bright yellow	26	2	71	0.03	138	0.7

by $(1. - \text{FRDIS})$. Thus, first calculations of crop assimilation are done, and then the average is determined. This is necessary to prevent errors due to averaging which may occur when the relation between the affected photosynthetic parameters and crop assimilation is curvilinear, see also Sections 3.2 and 3.3.

For the first infection date (5 June), the proportion of yellowed leaves is given by:

```
FRDIS = AFGEN(FRDIST, DAY)
FUNCTION FRDIST = (0., 0.), (172., 0.), (182., 0.15), (192., 0.28), ...
                (212., 0.47), (232., 0.54), (272., 0.63), (292., 0.63)
```

and for the second infection date (14 July) by:

```
FUNCTION FRDIST = (0., 0.), (242., 0.), (252., 0.05), (292., 0.12)
```

Exercise 70

Introduce the effect of the virus on light use efficiency and photosynthesis at light saturation. Run the model for the two infection dates 5 June and 14 July, respectively.

The effect of infection date on growth and yield of sugar beet is given in Table 20. The simulation results demonstrate that a late infection, 14 July, does not do much harm; yield reduction is very limited. An early infection, 5 June, causes a considerable reduction in yield. This confirms field experiments of van der Werf et al., (1989a). However, the measured yield reduction is higher than the simulated yield reduction. This is probably due to the distribution of the virus yellowed leaves, which are mainly found in the upper leaf layers and thus their contribution to light interception is relatively high. Such an effect is not considered in the simulation; infested leaves are homogeneously distributed.

Another reason for the discrepancy between simulation and experimental results may be due to the fact that the increase in dark respiration due to the presence of a virus was neglected. The effect of reduced light use efficiency or reduced photosynthesis at light saturation may be different, because the sensitivity of crop photosynthesis to these parameters is not the same. Of course, the model may be totally inaccurate and, thus, the discrepancy between simulated and field results can be explained. However, this possibility should be considered only after studying the reasons for the discrepancy mentioned above.

Table 20. Simulated production of sugar beet infected by beet yellows virus on various infection dates. The virus affects the assimilation rate at light saturation (AMAX) and/or light use efficiency (EFF). (WSO = sugar beet, kg DM ha⁻¹; WSO control = 14575 kg ha⁻¹, harvest on 17 October, Day 290.)

Effect	Infection date 5 June		Infection date 14 July	
	WSO absolute	WSO %	WSO absolute	WSO %
AMAX	10664	73.2	14377	98.6
EFF	12646	86.8	14479	99.3
AMAX + EFF	10014	68.7	14343	98.4

Exercise 71

Evaluate the effect of the virus on light use efficiency and on photosynthesis at light saturation. Repeat, therefore, the computations of Exercise 70, in case only one photosynthetic parameter is affected. Explain the differences.

The model computations clearly demonstrate the important contribution of both the reduction in photosynthesis at light saturation and the light use efficiency. The effect on light use efficiency and photosynthesis at light saturation is not additive. In absolute terms, the latter effect is more important, due to the strong effect of beet yellows virus (BYV) on photosynthesis at light saturation. However, a relative equal change in light use efficiency and photosynthesis at light saturation shows that the latter effect is relatively less important. Further analysis of the physiological background of the effects, and their consequences for growth and production of sugar beet, is needed to derive damage relations which can be used in crop protection management.

4.3.5 A detailed study of an assimilation rate reducer, mildew in winter wheat

The effect of mildew in wheat, *Erysiphe graminis*, on respiration and assimilation rates have been quantified (Table 21). Mildew clearly affects the assimilation rate at light saturation (Rabbinge et al., 1985). Even with a diseased crop for which the mildew is hardly visible, ca. 4% of the leaf area being covered, both the assimilation and the transpiration rates at light saturation are considerably reduced – by up to 50%. Light use efficiency and dark respiration are not significantly affected.

Tabel 21. Normalized values of the maximum assimilation rate at light saturation (AMAX, kg CO₂ ha⁻¹ h⁻¹), light use efficiency (EFF, kg CO₂ ha⁻¹ h⁻¹ W⁻¹ m) and dark respiration (RD, kg CO₂ ha⁻¹ h⁻¹). Mildew-diseased plants were grouped in classes of percentage of mildew-diseased leaf area (PMI). (Source: Rabbinge et al., 1985).

n ¹	PMI class	AMAX	SD (±)	EFF	SD (±)	RD	SD (±)
11	control	100.0 ² (45) ³	3.9	100.0 (.27)	0.02	100.0 (1.33)	0.21
11	0.1– 0.5	97.1	4.4	101.5	0.03	94.0	0.20
11	0.5– 1.0	86.5	4.1	100.4	0.03	99.2	0.29
9	1.0– 2.0	83.6	4.9	103.4	0.02	111.3	0.37
9	2.0– 3.0	66.8	4.1	94.0	0.03	109.8	0.25
10	3.0– 6.0	57.5	5.2	88.8	0.04	128.6	0.29
9	6.0–10.0	55.3	4.9	84.7	0.03	123.3	0.23
8	≥10.0	40.1	2.6	86.2	0.03	133.8	0.42

¹ Number of replicates.

² Age effects are eliminated.

³ Measured values for the control are given between brackets.

Exercise 72

Introduce the effect of mildew on photosynthesis at light saturation in the model SUCROS87 for growth of spring wheat. The intensity of the mildew disease expressed in severity is introduced using a forcing function:

$$\text{PMI} = \text{AFGEN}(\text{PMIT}, \text{DVS})$$

$$\text{FUNCTION PMIT} = (0., 0.), (0.79, 0.), (0.8, 0.5), (1.0, 7.5), (1.2, 5.), \dots \\ (1.5, 0.5), (2.5, 0.5)$$

Exercise 72 demonstrates how the consequences of detailed physiological observations can be evaluated under field conditions. The difference between the control (7773 kg grains ha⁻¹) and this visible mildew-diseased simulation amounts to 1182 kg grains ha⁻¹.

Evaluating the effects using a multi-layered crop growth model, demonstrated that even at low infection levels considerable reductions in crop growth rate may occur. It was also shown that this effect is more pronounced under a clear sky than when it is overcast (Table 22). The mildew in these simulations is distributed homogeneously over the leaf layers.

However, a homogeneous distribution of mildew will rarely be met in practice. The infection is more often initially located in the lower-leaf layers, and spreads

Table 22. Simulated daily gross assimilation of a wheat crop under an overcast and under a clear sky (DGAO and DGAC, kg CO₂ ha⁻¹ d⁻¹, respectively), at several crop development stages (DC). The mildew (PMI) was homogeneously distributed in the crop. For comparison, AMAX values (kg CO₂ ha⁻¹ h⁻¹) are presented. (Source: Rabbinge et al., 1985).

PMI	Day 143, DC 35, LAI ¹ = 2			Day 160, DC 50, LAI = 4			Day 173, DC 65, LAI = 4		
	DGAO	DGAC	AMAX	DGAO	DGAC	AMAX	DGAO	DGAC	AMAX
0.0	100 (156.) ²	100 (475.)	100 (45.)	100 (206.)	100 (644.)	100 (44.)	100 (207.)	100 (620.)	100 (39.)
0.5	99.2	96.1	91.5	99.3	96.3	91.3	99.1	95.6	90.3
1.0	98.5	92.9	85.0	98.7	93.2	84.7	98.4	91.9	82.9
2.0	97.3	87.8	75.8	97.7	88.4	75.4	97.0	86.1	72.5
4.0	95.6	81.2	65.2	96.2	82.1	64.5	95.0	78.5	60.3
8.0	93.5	74.3	55.4	94.3	75.4	54.5	92.3	70.4	49.2
16.0	91.4	68.4	48.0	92.5	69.8	47.1	89.5	63.6	40.8

¹ Leaf Area Index, in m² m⁻².

² Normalized values, control = 100. For control plants the values calculated by the model are presented in brackets.

from the bottom to the top of the canopy. This location effect was simulated assuming an overall value of the percentage of mildew-diseased crop as before, but with a mildew concentration in specific leaf layers of the canopy (Table 23). The effect on the gross assimilation rate was most marked when the mildew was either uniformly distributed over the canopy or concentrated in the upper-leaf layers. When the mildew was concentrated in the lower-leaf layers, the reduction was less, and the effect of mildew was substantial only when levels above 4% were reached.

Methods of assessing disease and determining the damage threshold should, therefore, take the location of visible mildew-diseased tissue into consideration. The consequences of this effect of mildew on crop growth and production at various locations and under various conditions, is computed using the extended wheat model of Section 4.4 and described by Daamen & Jorritsma (in prep.). Preliminary results of a study of these effects is given by Rabbinge & Rossing (1988).

Table 23. Location effect of the mildew disease on daily gross assimilation under an overcast sky (DGAO) and under a clear sky (DGAC) for crops with LAI¹ = 2 (DC 35) and LAI = 4 (DC 50). Starting from the top, leaf layers (LAI = 1 per layer) are numbered I to IV. The percentage of mildew covered leaf area (PMI) and AMAX (kg CO₂ ha⁻¹ h⁻¹) of the diseased layers are represented by PMIL and AMAXL, respectively.

Infected leaf layers	PMI = 4				PMI = 8			
	PMIL	AMAXL ²	DGAO ²	DGAC ²	PMIL	AMAXL ²	DGAO ²	DGAC ²
LAI = 2, DC 35:								
none	0	100	100	100	0	100	100	100
I	8	55	95	82	16	48	93	78
II	8	55	99	92	16	48	98	90
all	4	65	96	81	8	55	93	74
LAI = 4, DC 50:								
none	0	100	100	100	0	100	100	100
I	16	47	95	83	32	42	94	81
I+II	8	55	95	80	16	47	93	75
IV	16	47	100	98	32	42	100	98
IV+III	8	55	100	96	16	47	100	95
IV+III+II	5.3	60	99	91	10.7	51	98	88
all	4	65	96	82	8	55	95	75

¹ Leaf Area Index, in m² m⁻².

² Normalized values; disease-free = 100.

The results of the combination model are compared with field experiments of Daamen (1988). In these experiments, the mildew epidemic was followed and the growth and production of wheat was measured. The experiments were done at the experimental farm 'Vredepeel', situated on loamy sand (which is sensitive to dry conditions), in the south-east of the Netherlands. The grain yields attained in the control measurements were 6500 kg dry matter ha⁻¹, whereas the potential was 9–12 t ha⁻¹. Water shortage caused a low growth rate during part of the growing season. In the simulation, the yields were higher than 6500 kg ha⁻¹ but, taking into account the water shortage during the growing season (see also Section 4.2), when a water balance was introduced, simulated and measured values corresponded. The mildew expressed as an integrated value of the percentage of mildew-covered leaf area was also introduced into the model and it is shown that the experimental and simulated relative yields at various mildew-diseased levels of the crop correspond rather well (Figure 66).

The preliminary combination model of the growing crop and the disease has been used to evaluate the consequences of an integrated percentage of mildew

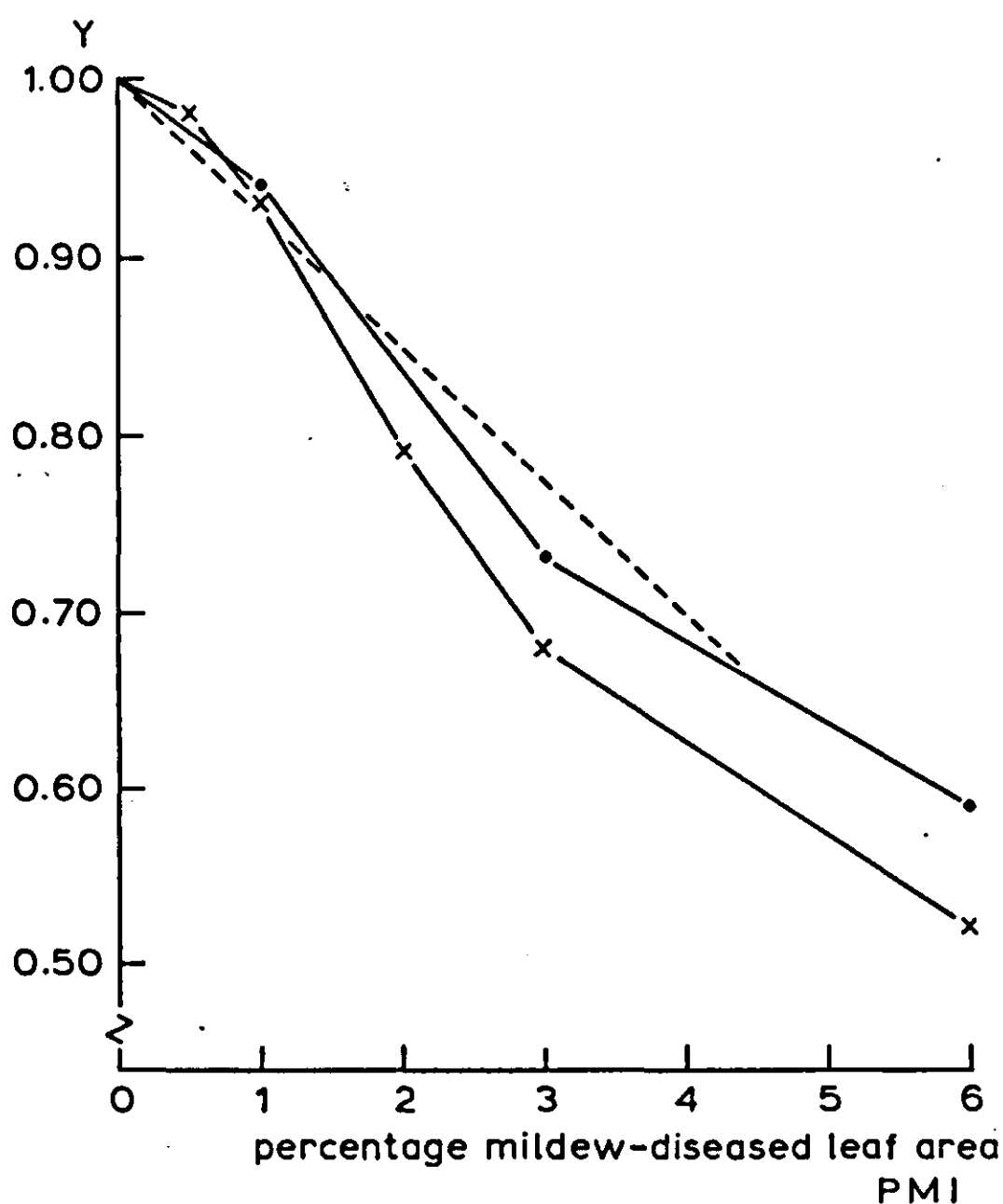


Figure 66. Relative grain yield (Y) at various percentages of mildew-diseased leaf area (PMI), during crop growth from DC 30 until milky ripe. Simulation using SUCROS87 (x), simulation using SUCROS87 combined with a primitive water balance (●) (Section 4.2), and damage function derived from field experiments (----).

severity of 3% during the growing season on crops growing in various production situations, which are dictated by a limited supply of water (Section 1.2). These results (Table 24; Schans, 1984, Internal Report Theoretical Production Ecology) show that yield reduction is proportional to yield, indicating that economic injury levels should be inversely proportional to yield.

A detailed analysis on the physiological background of the considerable effect that mildew has on CO_2 assimilation and transpiration, was done by measuring both rates at various external CO_2 concentrations, at the same time. Assimilation rate at light saturation and transpiration were both affected to the same extent. The assimilation rate/transpiration rate ratio (A/T) was, therefore, not significantly affected by the mildew disease (Table 25). The simultaneous reduction in assimilation and transpiration rates may have been caused by two different mechanisms: one based on a direct effect on carboxylation, and the second based on a direct effect on stomatal behaviour. This is illustrated in Figure 67. Curve A represents the response of assimilation rate (P) to the internal CO_2 concentration (CI). Line B is the CO_2 supply function, describing the diffusion of CO_2 from the atmosphere (with concentration CA) to the intercellular spaces (with concentration CI). The initial slope made by curve A with the abscissa (ϵ) represents the CO_2 use efficiency; i.e. the inverse of the carboxylation resistance. If there was a direct effect on carboxylation (mechanism 1) then the CO_2 flow from the stomatal cavities to the carboxylation sites would decrease. Because of the feedback loop between internal CO_2 concentration, assimilation rate and stomatal conductivity, the stomata would close (Goudriaan & van Laar, 1978; Farquhar & Sharkey, 1982). Consequently, the gas exchange rates would be reduced. If the second mechanism, a direct effect on stomatal behaviour, was taking place, then the ratio of CI/CA would be affected, although the consequences for photosynthesis might be similar to those of mechanism 1.

The stomatal regulation mechanism was studied by Rabbinge et al. (1985). In this study, the CO_2 response of assimilation rate was measured and the carboxylation resistance calculated from the relation between internal CO_2 concentration (CI) and net assimilation rate at an irradiance of 320 W m^{-2} . In Table 26, the CI/CA ratio is given for mildew-diseased and control plants, with an irradiance of 320 W m^{-2} . Mildew had no significant effect on the ratio so that stomatal resistance was not directly affected, although the presence of mechanism 2 may have been masked by the strong effects of mechanism 1. Nevertheless, it can be concluded that mildew does not influence the stomatal regulation mechanism. As a result, the water use efficiency, expressed as the assimilation/transpiration ratio, is rarely influenced by mildew. Whatever the exact nature of this effect may be, it was necessary to quantify both the effect and its consequences. Further analysis of how mildew affects crop behaviour can be done using a detailed model of assimilation and transpiration (BACROS, de Wit et al., 1978) as illustrated by Rabbinge (1982) for a different disease, stripe rust *Puccinia striiformis* in winter wheat.

Table 24. Simulated yield loss due to a mildew load on winter wheat of 3% leaf coverage (PMI = 3) during the growing season starting at DC 30, at various expected yields in kg grains ha⁻¹. (Source: Schans, 1984. Internal Report, Department of Theoretical Production Ecology).

Yield expected (kg ha ⁻¹)	Yield loss (kg ha ⁻¹)
6000	1800
8000	2400
10000	3000

Table 25. The ratio of assimilation (A) and transpiration rates (T) at an irradiance of 320 W m⁻² and an ambient CO₂ concentration of 340 ppm for control and mildew-diseased plants at DC 50. (Source: Rabbinge et al., 1985).

n ¹	PMI class	A/T	SD ±
23	control	10.6	0.95
11	0.1– 0.5	10.4	1.07
11	0.5– 1.0	9.3	0.67
9	1.0– 2.0	9.2	0.65
9	2.0– 3.0	9.4	0.80
10	3.0– 6.0	9.3	0.81
9	6.0–10.0	9.6	0.74
8	≥10.0	8.9	0.53

¹ Number of replicates.

4.3.6 Discussion

The combination models described above show how simulation at each stage of research, can help to provide insight into the quantitative interpretation of changes caused by the presence of pests or diseases in various plant physiological processes. This insight may help to derive damage relations which could be used in practice (Section 4.4). The comprehensive models integrate knowledge and ideas from the various disciplines but thorough testing of the models is still essential.

Thus, experiments still need to be done which will help to define input relations and which will test the simulation results. The explaining level of the disciplines delivers the input relations which are determined under well-defined conditions, and the explanatory level of the field situation produces the data needed for

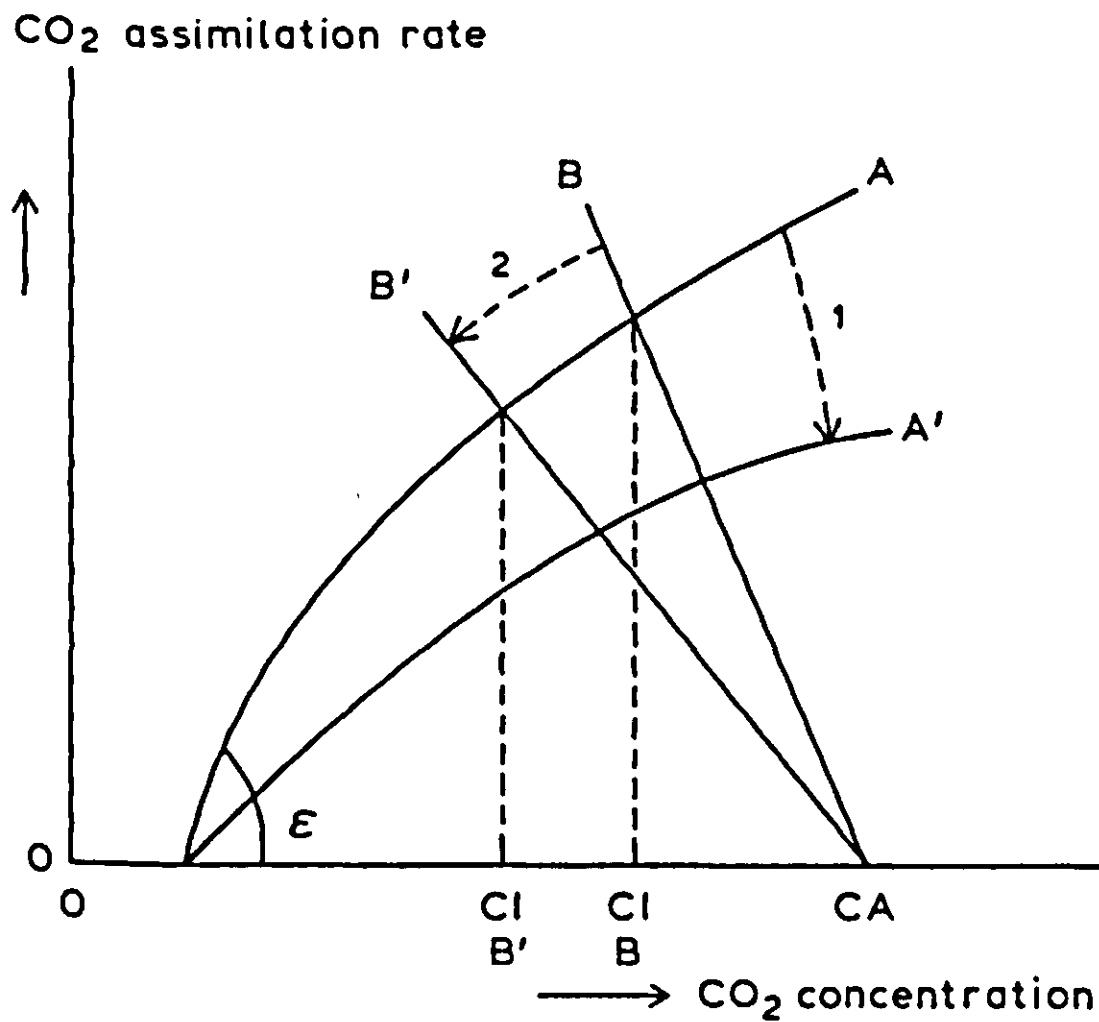


Figure 67. CO_2 assimilation rate at various internal CO_2 concentrations (CI, curve A); and the CO_2 supply function at various internal CO_2 concentrations (line B). Effects of mildew are indicated for two hypothetical mechanisms: (1) Reduced efficiency in CO_2 absorption (ϵ): curve A is transformed into curve A'. (2) Increased stomatal resistance: line B is transformed into line B'.

Table 26. The ratio (CI/CA) of the internal CO_2 concentration (CI) to the ambient CO_2 concentration (CA), for control and mildew-diseased plants at development stages DC 32 and DC 55. (Source: Rabbinge et al., 1985).

Plants	n^1	$\text{CA} = 340 \text{ mg m}^{-3}$		$\text{CA} = 600 \text{ mg m}^{-3}$		$\text{CA} = 1000 \text{ mg m}^{-2}$	
		CI/CA	SD	CI/CA	SD	CI/CA	SD
DC 32: control	2	0.77	0.007	0.77	0.007	0.79	0.028
mildew-diseased	6	0.73	0.049	0.74	0.023	0.78	0.033
DC 55: control	2	0.74	0.014	0.73	0.021	0.71	0.049
mildew-diseased	5	0.73	0.021	0.72	0.029	0.70	0.016

¹ Number of replicates.

testing the models (Rabbinge, 1986). This heuristic way of working is very important, both to biology itself and in its agricultural application.

4.4 Simulation of aphid damage in winter wheat; a case study

W.A.H. Rossing, J.J.R. Groot and H.J.W. van Roermund

4.4.1 Introduction

Winter wheat yields in the Netherlands increased from approximately 4000 kg dry matter ha⁻¹ in 1945 to 8000 kg ha⁻¹ in 1980 (Rabbinge, 1986). This yield increase was the result of improved cultural methods which reduced the significance of yield-limiting factors such as shortages of water and nitrogen, the introduction of short-straw varieties with a higher harvest index and a longer grain-filling period and, finally, the improved control of growth- and yield-reducing factors. The latter are relatively more significant at high yield levels, due to the positive effect of 'good crops' on the increase rate of pests and diseases – mainly as a result of higher nitrogen levels in attacked tissue (e.g. White, 1984). Moreover, in 'good crops' most yield-limiting factors have already been eliminated. This resulted in a tendency to use insurance spraying, i.e. spraying without first establishing the presence of pests or diseases. Overuse of crop protection agents, however, reduces the net profit for a grower, increases environmental side effects and can stimulate secondary pests and diseases by killing their natural enemies.

In the Netherlands, three aphid species occur in winter wheat: the grain aphid, *Sitobion avenae*, the rose grass aphid, *Metopolophium dirhodum*, and the bird cherry oat aphid, *Rhopalosiphum padi*. Usually, *Sitobion avenae* occurs in the highest numbers. Cereal aphids have been economically significant pests in winter wheat since the late sixties. Around that time, top dressings of nitrogen were introduced which prolonged the maturation period of the crop when cereal aphids cause the most damage. It was shown that a high nitrogen content of the crop accelerates aphid population growth by increasing fecundity and inhibiting wing formation (Vereijken, 1979).

Because of their uneconomical turnover of food, aphids take up large amounts of phloem sap. Vereijken (1979) showed that yield losses are not only caused by the feeding on assimilates, but that other factors exist which adversely affect the crop physiology. These are: (1) honeydew, excreted by the aphid, covers the stomata of the leaves and affects photosynthesis, and (2) toxins or growth regulators are injected with the saliva, and may influence the rate of leaf senescence. The latter is considered to be of little significance in the Dutch cereal aphid-winter wheat system.

Relations between aphid density and damage have been developed, based on regression analysis of field observations (Entwistle & Dixon, 1987). Rabbinge et al. (1983) hypothesized that the yield level of the control treatment should be considered when calculating the damage relation. However, conducting new field experiments at various yield levels, under various intensities of pest attack,

would not overcome the limitations of system's description at the system level (cf. Chapter 1). Here, a simulation approach, based on laboratory experiments, is presented which describes the effect of *S. avenae* on the physiology of the winter wheat crop. Thus, with knowledge of the process level, the effects on the system level (yield and yield reduction) are predicted. Although our knowledge on the exact nature of the interaction between pest and crop is incomplete, the simulation model contributes to our understanding of the relative significance of various damage components and will also help in further research.

4.4.2 *The life cycle of Sitobion avenae*

Host plant species of *S. avenae* belong to *Gramineae*. Overwintering takes place as viviparae or as eggs. Starting at the end of May, alatae (winged aphids) can be found in winter wheat, which is preferred to other cereals. The first instar nymphs are produced by parthenogenesis and develop through four nymphal instars before moulting into adults. Most of these nymphs develop into apterous (wingless) adults, whose reproductive rate is higher than that of alate adults. The aphid population usually starts to increase around anthesis (DC 60, Decimal Code for crop development stage, Zadoks et al., 1974), and the population density usually reaches a maximum at the late-milky ripe stage of wheat (DC 77). Ears are preferred to leaves as feeding sites.

The rate of population development depends on food quality, especially the nitrogen content of the crop, and also on temperature and the presence of predators and parasites. The reproductive rate is density-dependent. As a result of high aphid density and a decline in food quality, an increasing proportion of the nymphs born to the apterous adults after DC 73 develops into alate adults. These alatae leave the crop, causing a rapid decline in field populations which is enhanced by the effect of natural enemies.

Under short day conditions in autumn, *S. avenae* produces sexual offspring. First gynoparae and then mostly males. After mating, oviparae are produced, which lay winter eggs on the winter host (Carter et al., 1982).

Exercise 73

The time, needed for a fictitious aphid population to double in size, depends on the food quality (which is related to the crop development stage, coded with the decimal code for crop development) and on the temperature. On Day 0, the decimal code for crop development stage is 50 and the aphid density is 0.05 aphids ear⁻¹. The doubling time for the population (at 20°C) is during DC 50–DC 60: 4 days, DC 60–DC 70: 2.5 days, and for DC 70–DC 77: 6 days, respectively. An increase in temperature of 10 degrees causes the doubling time to reduce to 50% of its value at 20°C. Inversely, a decrease in temperature of 10 degrees results in values of the doubling time which are twice the reference.

The duration of different crop development periods (in days) also depends on temperature:

	DC 50–DC 60	DC 60–DC 70	DC 70–DC 77
10°C	11	10	35
20°C	7	7	27
30°C	4	5	19

- Calculate the aphid density at anthesis (DC 60), at the end of anthesis (DC 70) and at the late-milky ripe stage (DC 77) at a constant temperature of 20°C.
- Assume that a farmer will spray his crop if the aphid density exceeds the threshold of 15 aphids tiller⁻¹. After how many days will the threshold be passed at a temperature of 20°C?
- Write a CSMP program to simulate the population growth of *S. avenae*. Do not distinguish age classes. Assume a sinusoidal daily course of temperature between 12°C and 28°C.

4.4.3 Simulation of crop growth

When simulating the interaction between wheat growth and aphids, only the post-anthesis phase is considered. Growth, the increase in crop dry matter, is simulated as a function of radiation, ambient temperature and nitrogen availability in the soil. The model consists of sink-source relations, which describe the flow of carbohydrates and nitrogen. It is based on models by Groot (1987) for winter wheat and van Keulen & Seligman (1987) for spring wheat. The time step of integration is one day. A simplified relational diagram of the model is given in Figure 68.

Simulation starts at anthesis with measured weight and nitrogen content of the organs (roots, stems, leaves and ears), and the amount of water-soluble carbohydrates (reserves) in the stem as inputs. Generally, 10% to 15% of the stem weight consists of reserves at anthesis. To determine the strength of the only sink, the grains, the number of grains per unit area must be known.

The nitrogen source for grain growth consists of translocatable nitrogen present in biochemical structures which are easily decomposable into amino acids. Some of the nitrogen is permanently incorporated in cell material and this residual nitrogen is not available for translocation to the grains.

The carbohydrate source for grain growth consists of the daily gross photosynthesis and stem reserves (see Figure 68). Photosynthesis is calculated according to the procedure described in Section 4.1. The maximum rate of photosynthesis at light saturation, AMAX, decreases with increasing crop development as proteins are broken down to meet the nitrogen requirements of the sink. In the model, AMAX is proportional to the ratio of the translocatable nitrogen fraction (TNF) of an organ and the translocatable nitrogen fraction at anthesis (TNFA) (Vos, 1981):

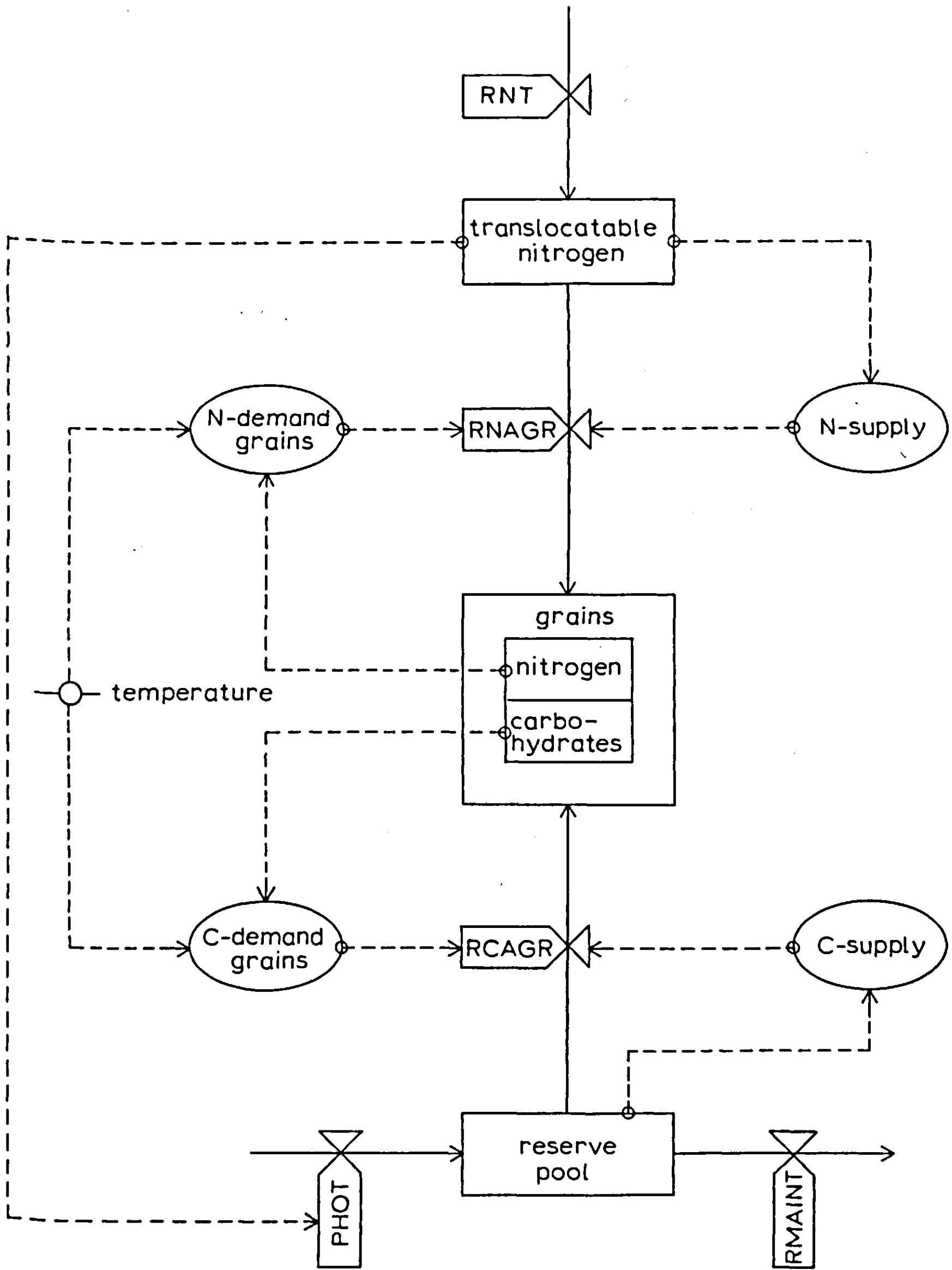


Figure 68. Simplified relational diagram of a crop growth model for winter wheat.

$$AMAX = AMAXA * TNF/TNFA$$

where AMAXA represents AMAX at anthesis. The initial light use efficiency, EFF, is independent of the nitrogen content of green plant material (e.g. van Keulen & Seligman, 1987).

Some of the assimilates are used for maintenance respiration. Maintenance respiration is calculated for each of the plant organs as a product of organ weight (WO) and maintenance respiration coefficient (MAINO, $\text{kg kg}^{-1} \text{d}^{-1}$) (see Section 4.1), with a correction for respiration activity. In active tissues, a continuous protein turnover occurs which requires energy. The respiration activity of an organ (RACT) is assumed to depend on the translocatable nitrogen fraction of an organ, relative to the translocatable nitrogen fraction at anthesis (Vos, 1981):

$$RACT = TNF/TNFA$$

$$TEFF = Q10^{**} (TMPA - REFTMP)/10.$$

$$RMAINT = WO * MAINO * TEFF * RACT$$

TEFF represents the effect of temperature. Q10 is the multiplication at a 10 degree increase or decrease in the ambient temperature (TMPA), relative to the reference temperature (REFTMP).

After subtracting the maintenance requirements of all plant organs from the gross photosynthesis, the available assimilates (AVASS) are allocated to the reserves in the stem. The carbohydrates required for grain growth are supplied from this stem reserve pool. The rate at which carbohydrates are mobilized from the stem reserves (CSUPG) is determined by the time coefficient of the translocation process (TCTR). The time coefficient depends on the reserve level (RESL), which is defined as the amount of reserves (ARES) expressed as a fraction of the vegetative above-ground dry matter (WSTRAW):

$$ARES = INTGRL (ARES1, AVASS-RCAGR)$$

$$RESL = ARES /WSTRAW$$

$$TCTR = AFGEN (TCTR1, RESL)$$

$$\text{FUNCTION TCTR1} = 0., 50., 0.05, 8., 0.1, 2., 0.2, 1., 0.7, 1.$$

$$CSUPG = ARES / TCTR$$

The sink strength or demand of grains (CDEMG) is based on the potential growth rate of individual grains (PGRIG) which depends on the ambient air temperature (TMPA), according to Sofield et al. (1977a), and on the number of grains per hectare as measured in the field (NUMGR). As the potential growth rate of individual grains is measured in terms of dry weight, PGRGR is divided by the conversion efficiency of carbohydrates into grain dry weight (EFCGR), to obtain the demand of the grains in terms of carbohydrates:

$$PGRIG = AFGEN (PGRIG1, TMPA)$$

$$\text{PARAM NUMGR} = 2.46E8$$

$$PGRGR = PGRIG * NUMGR$$

$$CDEMG = PGRGR / EFCGR$$

The rate of carbohydrate accumulation in the grains (RCAGR) will equal the demand of the grains (CDEMG), unless the rate of carbohydrate supply (CSUPG) is limiting. When the carbohydrate supply exceeds the demand, the rate of carbohydrate accumulation in the grains is sink-limited, and the amount of stem reserves will increase. In CSMP, RCAGR is calculated by means of the FORTRAN function AMIN1 which selects the minimum of CDEMG and CSUPG:

$$RCAGR = AMIN1(CDEMG, CSUPG)$$

The rate of grain growth (GRGR) is calculated from the rate of carbohydrate accumulation by multiplying by the conversion efficiency EFCGR to account for the growth respiration of the grains. The weight of the grains (WGR) is obtained by integrating the grain growth rate:

$$GRGR = RCAGR * EFCGR$$

$$WGR = INTGRL(0., GRGR)$$

The nitrogen supply to the grains (NSUPG) depends on the size of the translocatable nitrogen pool and on the rate at which protein decay occurs. The amount of nitrogen available for translocation (ATN) is the difference between the current amount of nitrogen in the vegetative parts and the amount of residual nitrogen, i.e. the nitrogen incorporated in structural cell material. The rate of protein decomposition is characterized by a time coefficient (TCTN), usually of the order of 10 days (Penning de Vries, 1975). Higher temperatures accelerate the process. The temperature effect on protein decomposition has a Q_{10} value of 2, thus the already defined variable TEFF may be used:

$$NSUPG = ATN / TCTN * TEFF$$

$$PARAM TCTN = 10.$$

The nitrogen demand of the grains (NDEMG) is characterized by a potential rate of nitrogen accumulation in individual grains (PNARIG), defined as a function of ambient air temperature (TMPA), according to Sofield et al. (1977b):

$$PNARIG = AFGEN(PNARIT, TMPA)$$

$$NDEMG = PNARIG * NUMGR$$

When the nitrogen supply exceeds the demand, the rate of nitrogen accumulation is sink-limited. Hence, the rate of nitrogen accumulation in the grains will equal the demand of the grains, unless the supply is limiting:

$$RNAGR = AMIN1(NDEMG, NSUPG)$$

Finally, the amount of nitrogen in the grains (ANGR) is obtained by integrating the rate of nitrogen accumulation in the grains:

$$ANGR = INTGRL(0., RNAGR)$$

4.4.4 Simulation of aphid damage

To simulate aphid damage, aphid numbers as counted in the field are introduced into the model as a forcing function. Direct and indirect effects of *S. avenae* on winter wheat are distinguished. Direct effects result from uptake of carbohydrates and nitrogen. Indirect effects are due to honeydew excreted onto green plant surfaces.

Direct effects Conceptually, modelling the effect of aphids feeding on the crop is identical to modelling grain growth (Figure 69). Both aphids and grains are sinks for carbohydrates and nitrogen and the supply is partitioned among them.

Suction rates and honeydew production rates seem to be negatively related to the nitrogen content of the food source (Vereijken, 1979; Ajayi & Dewar, 1982). Concomitantly with nitrogen, carbohydrates in the phloem sap are taken up. Very little quantitative information is available on the relation between the rate of phloem sap uptake and the phloem sap nitrogen content. Coster (1983) and Rabbinge & Coster (1984) measured daily honeydew production rates of *S. avenae* on flag leaves and ears of winter wheat plants at various growth stages. The plants were supplied with sufficient water and fertilizer. The rate of phloem sap uptake was calculated by applying an energy budget approach (Llewellyn, 1988). Their results are listed in Table 27. Suction rates decrease as the crop matures. No data are available on the nitrogen content of phloem sap. Here, it is assumed to be 2% of the dry weight. Furthermore, the demand of the aphids is taken to be fully satisfied at the highest suction rate measured. Lower suction rates are attributed to mechanical and physiological changes associated with ripening of the crop. Thus, a potential suction rate SRAP of $8.92 \cdot 10^{-9}$ kg (N) mg^{-1} (aphid, fresh weight) day^{-1} is found. The nitrogen demand (NDEMA) is found by multiplying the potential suction rate by the average weight of one aphid (AWAP), the number of aphids per tiller (NUMAP) and the number of tillers per hectare (EARHA). Average aphid weight depends on the age distribution of the aphid population. As an approximation, the data of Mantel et al. (1982) are used, which represent average aphid weight at three crop development stages calculated from a large number of field observations.

$$\text{NDEMA} = \text{SRAP} * \text{AWAP} * \text{NUMAP} * \text{EARHA}$$

The demand for carbohydrates (CDEMA) is calculated from the demand for nitrogen, using the ratio of the rates of carbohydrates and nitrogen to the sinks calculated by the model one integration interval previously, to approximate the fraction of carbohydrates in the phloem sap.

Aphids and grains share the supply of nitrogen and carbohydrates. Several hypotheses can be formulated concerning the nature of the partitioning, as the true nature has not been established. Aphids may be the first to utilize the supply of phloem sap, the remainder going to the grains. Alternatively, the supply may be distributed over the sinks in proportion to the respective demands. The

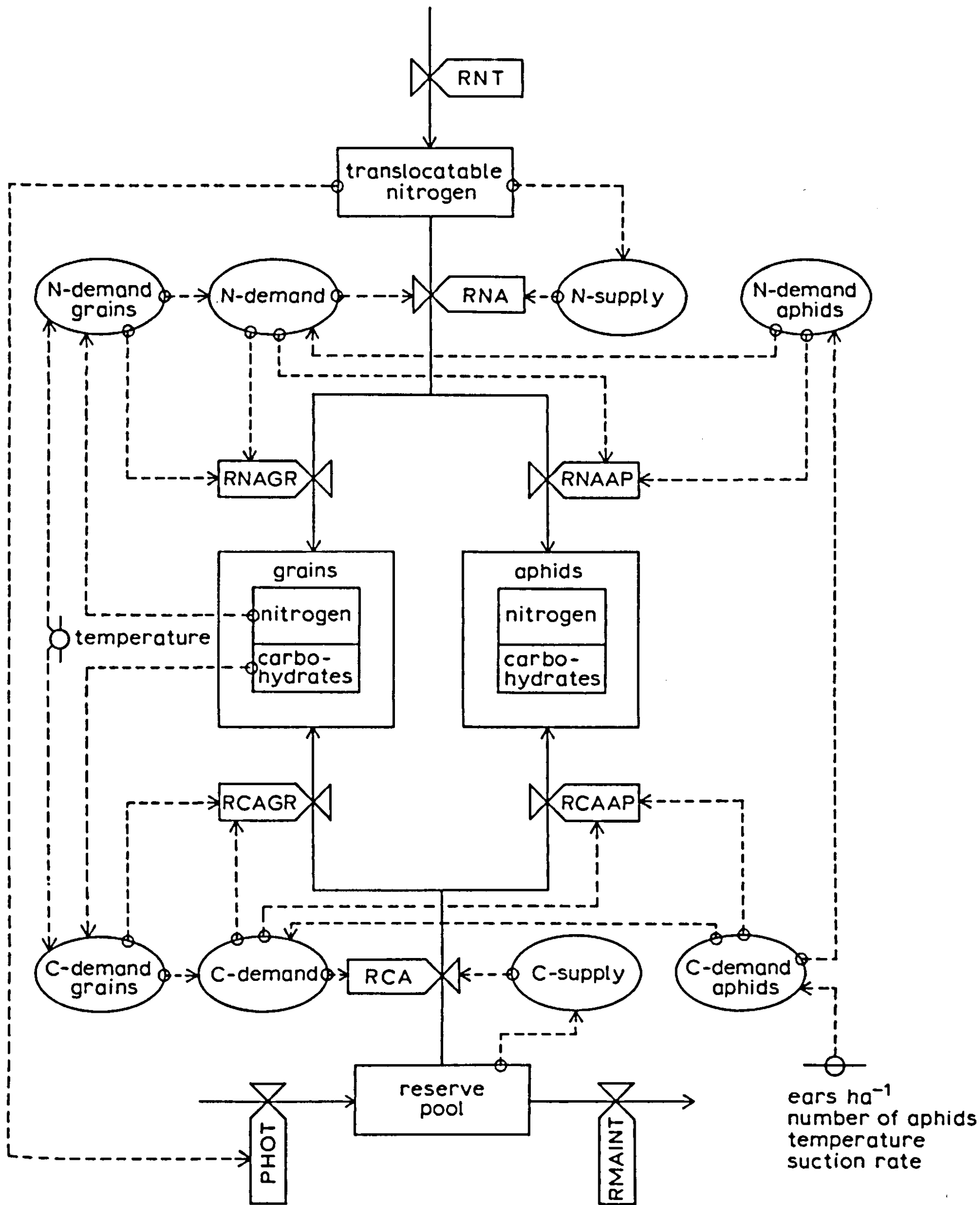


Figure 69. Simplified relational diagram of a model for direct aphid damage in winter wheat.

Table 27. Rate of honeydew production (mg (honeydew dry weight) mg^{-1} (aphid fresh weight) day^{-1}) and suction rate (mg (phloem sap dry weight) mg^{-1} (aphid fresh weight) day^{-1}) of *S. avenae* on spring wheat var. Bastion. Each figure is the average of 10 replicates. (Sources: Coster (1983) and Rabbinge & Coster (1984)).

Feeding position of aphids	Crop stage	Suction rate	Honeydew production rate	N content of flag leaves (f) or grains (gr) (g kg^{-1})
flag leaf	45	0.450	0.148	–
flag leaf	45	0.505	0.188	4.57 (f)
ear	65	0.446	0.180	–
ear	69	0.307	0.086	3.56 (gr)
ear	71	0.326	0.128	2.26 (gr)
ear	73	0.167	0.063	2.47 (gr)
ear	75	0.237	0.082	2.35 (gr)

incomplete fulfilment of grain demand may result in enhanced supply. Thus, total demand will consist of the sum of demands of grains and aphids. Here, two extreme situations are distinguished concerning the direct effect of *S. avenae* on the crop. In the following these are referred to as hypotheses I and II:

I. The total demand equals the sum of demands of grains and aphids; the supply is distributed in proportion to the respective demands.

II. When present, only the grains determine the total demand; the supply is first utilized by the aphids.

The simulation model is used to evaluate the quantitative consequences of these potential modes of interaction to damage.

Exercise 74

Write a CSMP program to simulate direct effect of aphids using hypothesis I.

Exercise 75

A winter wheat crop is infested with 30 *S. avenae* per tiller. Assume the ear density to be 635 m^{-2} . The N content of the phloem sap is 2%. Other data: NSUP = $15 \text{ kg ha}^{-1} \text{ d}^{-1}$, CSUP = $1000 \text{ kg ha}^{-1} \text{ d}^{-1}$, NDEMG = $2 \text{ kg ha}^{-1} \text{ d}^{-1}$ and CDEMG = $50 \text{ kg ha}^{-1} \text{ d}^{-1}$. Calculate numerically the reduction in the flow of carbohydrates to the grains due to *S. avenae*, assuming:

- a. hypothesis I to apply for the direct effects;
- b. hypothesis II to apply for the direct effects.

Indirect effects In experiments in which an artificial honeydew solution is applied to flag leaves of winter wheat, honeydew reduces the maximum rate of leaf photosynthesis, and increases the rate of maintenance respiration two weeks after application. One day after application, no effects are yet detectable (Ros-sing, in prep.). The effects are most pronounced under dry conditions, rain may remove honeydew before it affects the leaf. Here, only the effects found under dry conditions are used, neglecting environmental influences. The assumption is made that the effect increases linearly between one day and 14 days after deposition of the honeydew, and from then on remains constant. Moreover, the total effect is assumed not to exceed the maximum effect measured.

To evaluate the effect of honeydew on crop photosynthesis, the distribution of daily honeydew production over the canopy profile is calculated. The daily honeydew production (in $\text{kg ha}^{-1} \text{ ground day}^{-1}$) is derived from the actual phloem sap suction rate by multiplying by 0.404, a factor calculated from the data of Coster (1983) and Rabbinge & Coster (1984). On its way through the canopy, honeydew is intercepted by ears, leaves and stems, similar to light. The upper layer of the simulated crop consists solely of ears. According to Vereijken (1979), the ears intercept 30% of the honeydew produced. Beneath the ear-layer, the canopy is divided into layers of thickness DL ($\text{ha leaf ha}^{-1} \text{ ground}$). Of the produced honeydew, 70% will be intercepted by those layers or fall on the ground (HDLGHA, $\text{kg ha}^{-1} \text{ ground day}^{-1}$). Analogous to the light distribution inside a canopy, the amount of honeydew not intercepted, is assumed to decrease exponentially with the leaf area index, measured from the top of the canopy, LAI' (Figure 70). The extinction coefficient (k) for honeydew will be higher than the extinction coefficient for light, because no transmission or reflection of honeydew occurs. Here a value of 0.8 is used. The distribution is described by:

$$H_{\text{LAI}'} = H_0 \cdot e^{-k \cdot \text{LAI}'} \quad \text{and}$$

$$\text{HDLGHA} = \int_0^{\infty} H_0 \cdot e^{-k \cdot \text{LAI}'} d\text{LAI}' = H_0/k$$

The amount of honeydew intercepted in a leaf layer (Figure 70) is calculated:

$$\begin{aligned} \text{HDLAY}(z) &= \int_{(z-1) \cdot \text{DL}}^{z \cdot \text{DL}} H_0 \cdot e^{-k \cdot \text{LAI}'} d\text{LAI}' = -H_0/k \cdot e^{-k \cdot \text{LAI}'} \Big|_{(z-1) \cdot \text{DL}}^{z \cdot \text{DL}} \\ &= H_0/k \cdot (1 - e^{-k \cdot \text{DL}}) \cdot e^{-(z-1) \cdot k \cdot \text{DL}} \\ &= \text{HDLGHA} \cdot (1 - e^{-k \cdot \text{DL}}) \cdot e^{-(z-1) \cdot k \cdot \text{DL}} \end{aligned}$$

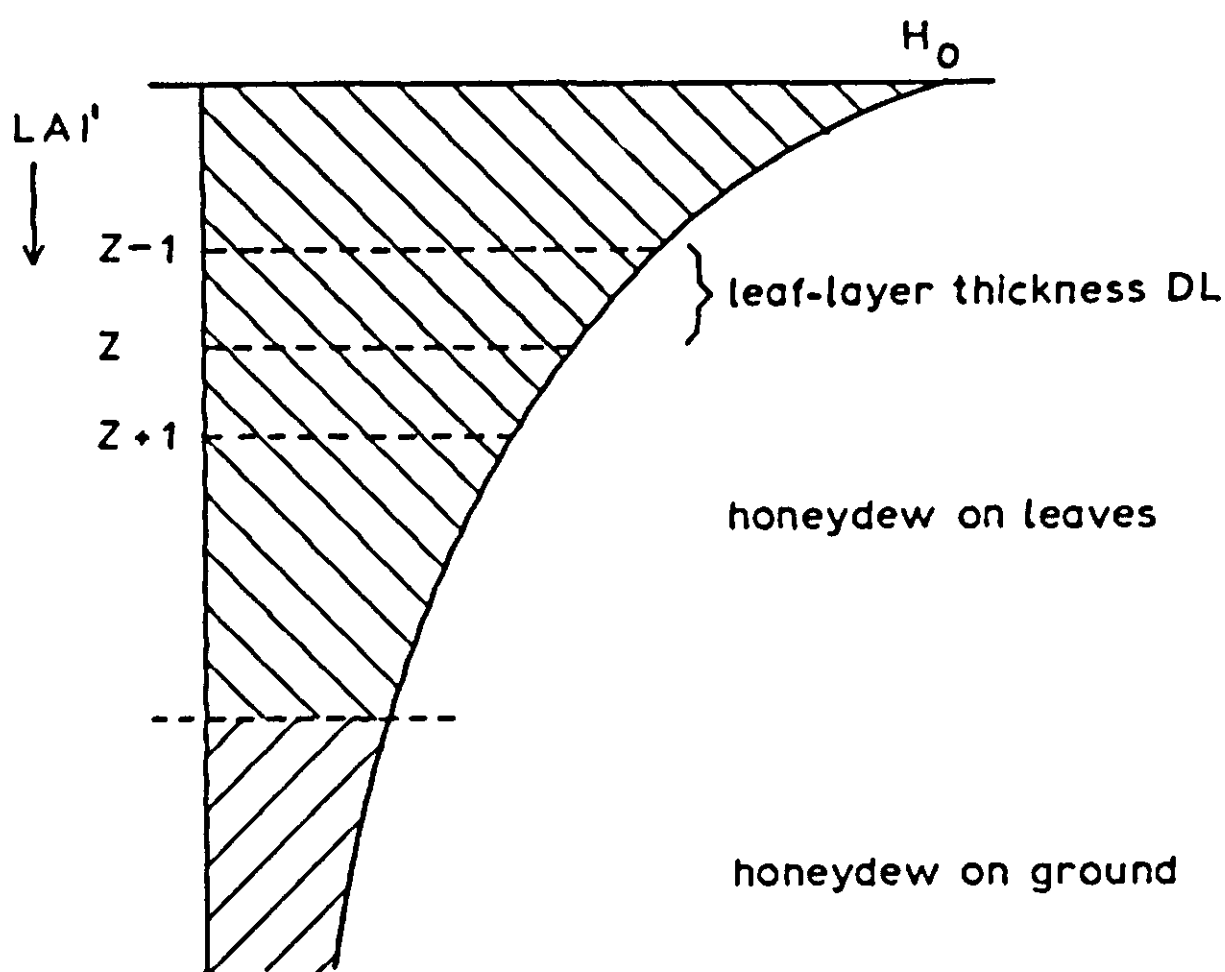


Figure 70. Interception of honeydew in the canopy as a function of the leaf area index (ha leaf ha^{-1} ground).

The total effect of honeydew at a certain depth is calculated by adding the effects of honeydew deposited at various times during grain growth. Thus, interference of honeydew deposited on subsequent days is assumed not to occur. The reduction of the maximum rate of photosynthesis and the increase in maintenance respiration is input for the photosynthesis algorithm of the crop model.

4.4.5 Simulation results

Data for evaluation Six data sets from three locations and two years are used to evaluate the crop model (PAGV1, PAGV2, PAGV3, EEST83, EEST84 and BOUWING84). The data sets represent a range of grain yields which were arrived at under conditions of nitrogen limitation only. Information on the experiments from which the data are derived is given in Table 28. The data sets collected in 1983 pertain to experiments in which the rate of fertilizer application was varied (Groot, 1987). The data sets of 1984 constitute the control treatment without aphids in experiments designed specifically to evaluate the damage model. Diseases, weeds and aphids were controlled on occurrence. Due to rapid

*) H = herbicide, F = fungicide, I = insecticide

**) insecticide treatment aimed at creating various aphid infestations

***) yield without and with aphids, respectively. The final yields for EEST84 were 8114 kg ha^{-1} and 7907 kg ha^{-1} due to delayed harvest. Here, the penultimate yields are shown.

Table 28. General information on the data sets used to evaluate the crop model and damage model.

	PAGV1	PAGV2	PAGV3
Location	Lelystad	Lelystad	Lelystad
Wheat variety	Arminda	Arminda	Arminda
Grain yield (kg ha ⁻¹)	6256	7442	8279
Soil type	Sandy loam	Sandy loam	Sandy loam
Percentage silt	23	23	23
Previous crop	sugar beet	sugar beet	sugar beet
Sowing date	25 Oct 1982	25 Oct 1982	25 Oct 1982
Flowering date	22 June 1983	22 June 1983	22 June 1983
Harvest date	2 August 1983	2 August 1983	2 August 1983
Row spacing (cm)	12.5	12.5	12.5
Sowing density (kg ha ⁻¹)	140	140	140
Total N (kg ha ⁻¹)	120	200	300
Growth regulator	yes	yes	yes
Protective chemicals*	H,F	H,F	H,F
Experimental design	Random block	Random block	Random block
Replicates	8	8	8
No. sampling dates	4	4	4
Sample size (tillers)	25	25	25
	EEST83	EEST84	BOUWING84
Location	Nagele	Nagele	Randwijk
Wheat variety	Arminda	Arminda	Arminda
Grain yield (kg ha ⁻¹)	4496	9290/7778***	8754/8549***
Soil type	Sandy clay	Sandy clay	Clay
Percentage silt	45	33	35-60
Previous crop	potatoes	sugar beet	potatoes
Sowing date	19 Oct 1982	4 Nov 1983	22 Oct 1983
Flowering date	22 June 1983	27 June 1984	20 June 1984
Harvest date	3 August 1983	31 August 1984	23 August 1984
Row spacing (cm)	15	15	24
Sowing density (kg ha ⁻¹)	148	148	138
Total N (kg ha ⁻¹)	94	250	250
Growth regulator	yes	no	no
Protective chemicals*	H,F,I	H,F,I**	H,F,I**
Experimental design	Random block	Random block	Random block
Replicates	8	6	6
No. sampling dates	4	10	9
Sample size (tillers)	25	50	50

increase of aphid numbers in 1984 a slight infestation in the control could not be avoided, affecting the two data sets. At regular time intervals, 0.5 m² of the crop was harvested and taken to the laboratory. There, the following analyses were carried out: dry weight of leaves, stems, ears and grains, nitrogen content of green leaves and dead leaves, amount of soluble carbohydrates in the stems and the green leaf area index.

To evaluate the damage model, data of two experiments carried out in 1984 are available (EEST84 and BOUWING84). In these experiments, various aphid infestations were created by chemical control of a natural aphid infestation at various crop development stages (van Roermund et al., 1986). Here, the data of the plots which received no aphicide treatment are used. At the time of the intermediate crop harvests, aphid density was also established. Statistical analysis of the experimental results showed that grain yield, leaf area index, leaf weight and amount of leaf nitrogen, decreased significantly in EEST84 on a number of harvest dates due to the aphid infestation. For BOUWING84 few significant effects were found. Climatic data were collected from nearby weather stations.

All model runs are carried out with measured temperature, irradiation and soil nitrogen data. The development rate of the crop is fitted to the observed rate.

Evaluation of the crop model Here, both crop and damage models are evaluated by visual inspection of the time course of actual and simulated values of a number of variables. In the context of gaining better understanding of the winter wheat – *S. avenae* system, this approach seems justifiable. The use of quantitative methods is advocated if model results are to be used in a management environment (Teng et al., 1980). The output variables examined are grain yield, weight of the green leaves, amount of reserves, amount of leaf nitrogen and leaf nitrogen content.

For each data set two simulation runs were made, one with simulated leaf area index, the other with the leaf area index as observed in the field. In this way, errors in the simulation of leaf area dynamics, which are still poorly understood, can be identified.

Simulated and observed rates of increase in grain yield compare well in the initial linear phase for all data sets (Figure 71). Also, the onset of grain-filling is simulated satisfactorily, except for BOUWING84 where it is predicted too early. High soil heterogeneity in combination with a warm spell around flowering may have obscured accurate estimation of the date of flowering.

Simulated and actual grain yields compare less well towards the end of the growing season. For PAGV1, PAGV2, PAGV3 and EEST83 underestimation occurs due to overestimation of leaf death. This is especially prominent at low nitrogen fertilizer amounts applied in PAGV1 and EEST83, indicating that the description of leaf death limits the applicability of the model to yield levels above 6000 kg ha⁻¹. Some inconsistencies show up in the data: at low fertilizer rates, grain yield is found to increase for two weeks after the leaf area was estimated to be zero.

For EEST84 and BOUWING84 the grain yield is overestimated. This is partly due to the presence of a light aphid infestation, but more importantly to the presence of photosynthetically active tissue (both simulated and observed) until shortly before harvest. Van Keulen & Seligman (1987) calculate the end of the linear growth of individual grains to occur at 0.72 of the total time between flowering and ripeness. For a crop the end of linear growth is more gradual, due to differences in the onset of grain-filling between grains. Their approach is, therefore, not used in the present model. Nevertheless, the results for EEST84 and BOUWING84 show that decrease in the sink strength at the end of the growing season needs to be considered to avoid overestimating the period of grain-filling.

A more extensive evaluation of the crop model will be given elsewhere (Ros-sing, in prep.). It is concluded that the output variable of most interest, grain yield, is simulated acceptably, but that errors in predicting leaf death limit the applicability of the model to yield levels above 6000 kg ha^{-1} .

Sensitivity analysis of the crop model Sensitivity analysis consists of examining the effect of uncertainty in model parameters (fine sensitivity analysis) and model structure (coarse sensitivity analysis) on the value of output variables. As a measure of model sensitivity, the relative sensitivity $(\Delta z/z)/(\Delta y/y)$ is defined, where z is the value of the relevant model output variable, y the value of the parameter and Δz the change in z caused by a change Δy in y . The size of the perturbation Δy should not exceed the variation of y reported in the literature.

Fine sensitivity analysis is carried out using data sets EEST84 and EEST83. The results of most interest are listed in Table 29. Sink strength for carbohydrates depends on the density of grains and the potential growth rate of an individual grain. An increase in the value of these parameters causes a decrease in grain yield for EEST84, whereas yield increases for EEST83. Two mechanisms working in opposing directions are involved. Due to a higher potential growth rate, the reserves are utilized more quickly resulting in lower maintenance respiration. On the other hand, the reserves are depleted sooner, causing enhanced leaf senescence. For the poorer crop EEST83, the first mechanism is dominant, for the richer crop the second.

Changes in the value of parameters describing leaf photosynthesis have a more significant effect on grain weight than changes in those of ear photosynthesis. The latter apparently contributes less to grain yield.

The amount of nitrogen in the crop is limiting to grain yield, in both data sets. For EEST84, the amount of nitrogen in the soil only becomes limiting after severe reduction of the parameter value (see Table 29).

In the coarse sensitivity analysis, ears are excluded from the photosynthesis model. Runs are made with data of EEST84. Due to higher light absorption by leaves and stems, yield increased by 2%. If ears are assumed to be photosynthetically inactive and only shade the lower plant parts, final grain yield is reduced by 15%.

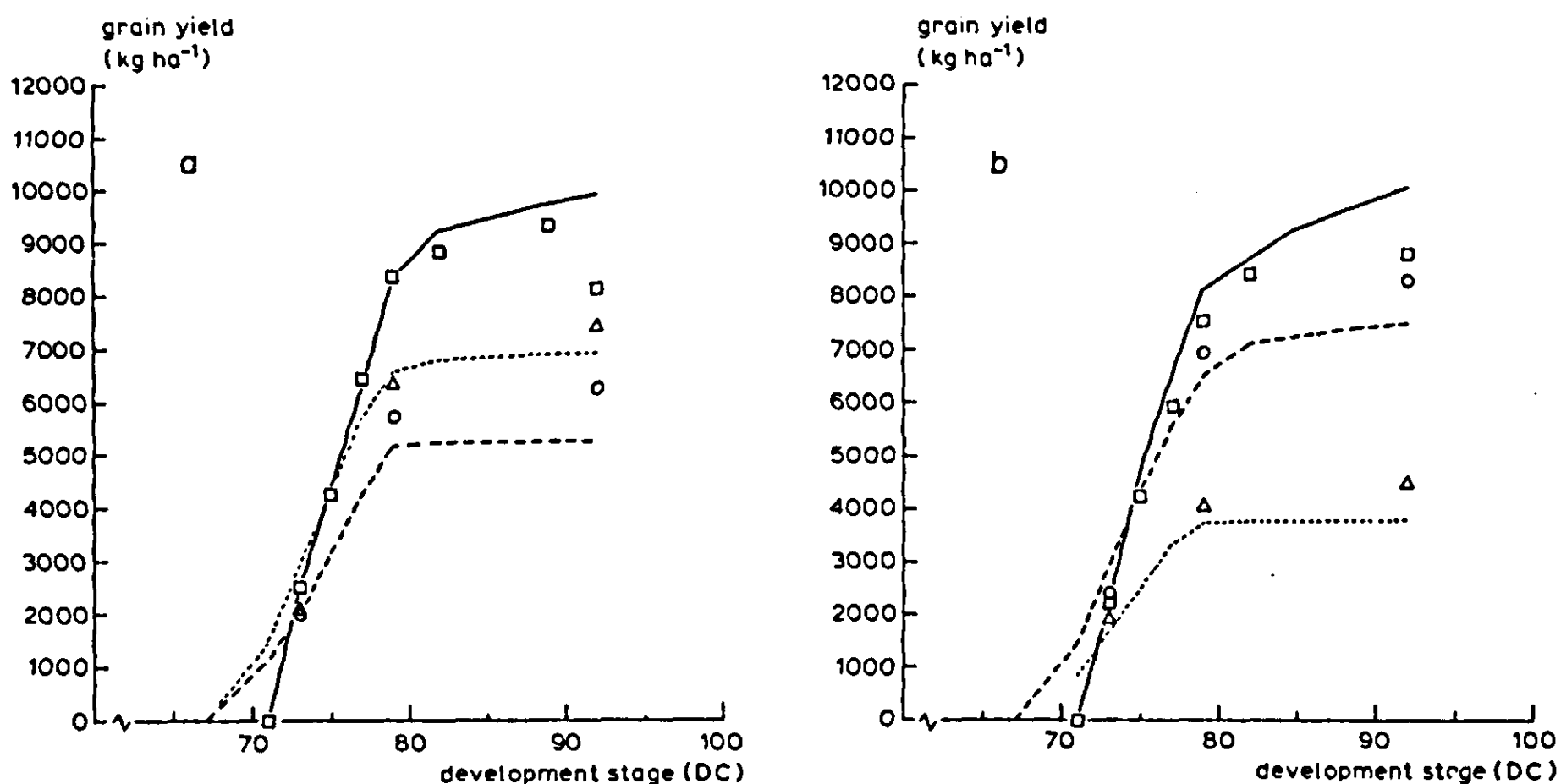


Figure 71. Evaluation of the crop model: simulated and observed grain yields of six data sets. Leaf area index is introduced as forcing function. a) EEST84 (—) simulated, (\square) observed; PAGV1 (---) simulated, (\circ) observed; PAGV2 (---) simulated, (Δ) observed. b) BOUWING84 (—) simulated, (\square) observed; PAGV3 (---) simulated, (\circ) observed; EEST83 (---) simulated, (Δ) observed.

Evaluation of the damage model Two data sets are available for evaluation. Here, only results of model runs for EEST84 are presented, where the effects of aphids are most pronounced. In Figure 72, actual grain yield for the high and low infestation plots of EEST84 is compared with simulation results using the two hypotheses on aphid phloem sap uptake (Subsection 4.4.4). For both hypotheses, grain yield is overestimated at the end of the growing season. This can be partly attributed to the causes identified in the evaluation of the crop model. However, the assumed maximum for the reduction of photosynthesis parameters also needs to be considered as this affects grain yield especially at the end of the season.

When modelling the uptake of phloem sap, assuming an increased demand due to aphid presence (hypothesis I), aphid damage becomes apparent when the process of grain-filling changes from sink-limited to source-limited, i.e. after the reserves have been depleted. If aphids are assumed not to increase total sink strength for carbohydrates and nitrogen (hypothesis II), grain yield is reduced from the onset of the aphid infestation. This agrees with field observations.

Although hypothesis II explains the early reduction of grain yield, the observed reduction of reserves, leaf nitrogen and leaf area index is only simulated using hypothesis I, as in that case aphids interfere with the supply.

Simulating grain yield of the control plots shows that the low aphid infestation certainly had some effect on grain yield.

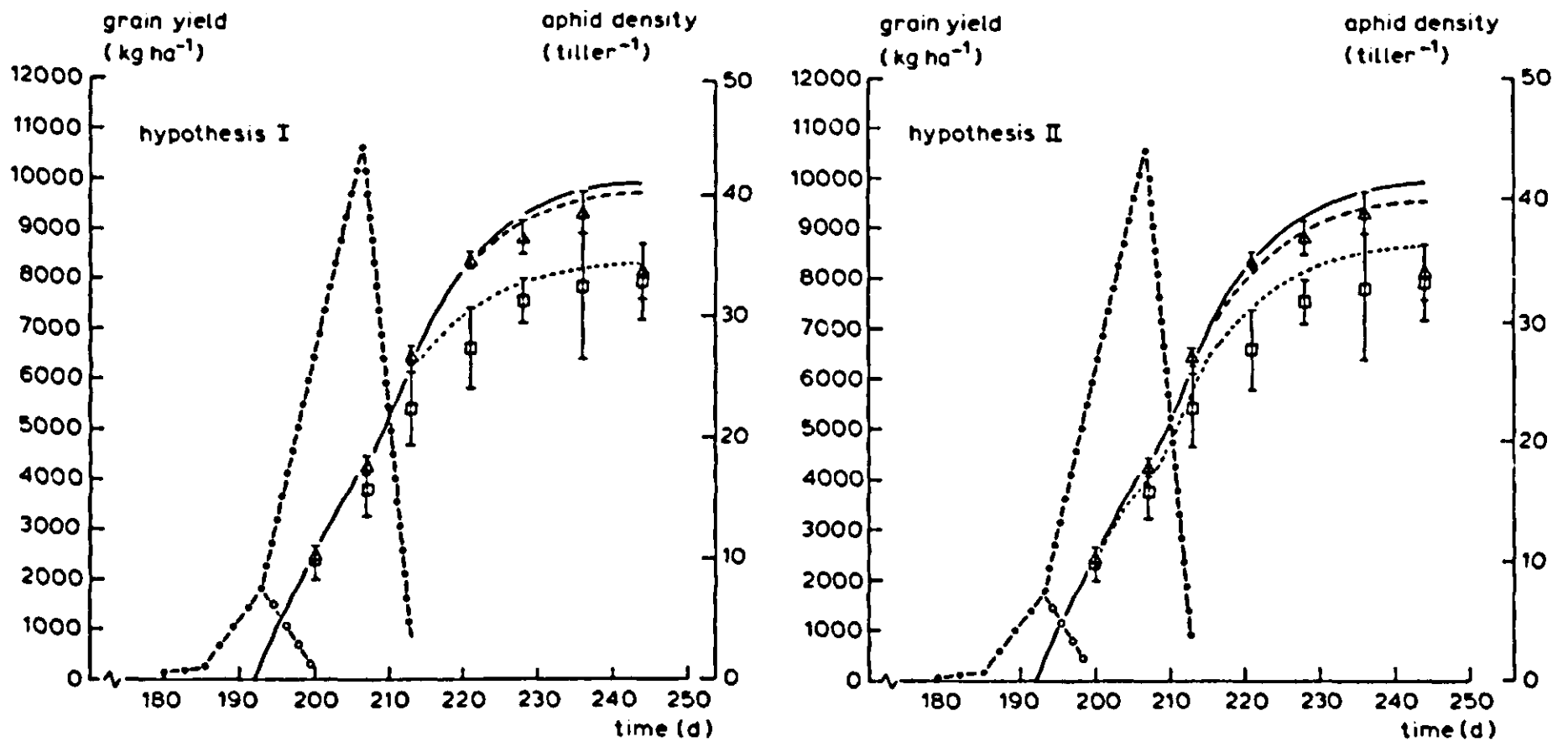


Figure 72. Evaluation of the damage model: simulated and observed grain yields of EEST84, using two alternative hypotheses on the direct effects of *Sitobion avenae* (see also text). Vertical bars represent standard errors of the mean. Simulated grain yield without aphids (—), aphid infestation as in control treatment (---) and high aphid infestation (···). The size of the aphid infestations is shown for the control (-o-o-) and the high infestation (-●-●-).

Sensitivity analysis of the damage model Fine sensitivity analysis is carried out with data of EEST84 using both hypotheses (Table 30a). Relative sensitivity is expressed in terms of grain yield as well as damage.

The greatest effects result from variations in the average aphid weight and the rate of phloem sap uptake. This is not surprising as both influence the direct and the indirect effects. Changes in the parameters describing the effect of honeydew have a relatively small effect.

As part of the coarse sensitivity analysis, the contribution of each of the damage components to total damage is evaluated. The results for EEST84 are listed in Table 30b. Uptake of phloem sap constitutes an important cause of damage. Hypothesis I results in higher damage and a higher contribution of aphid suction than hypothesis II.

Similar analysis at various yield levels using the data sets PAGV1, PAGV2, PAGV3 and EEST83 and an aphid infestation comparable to that of EEST84 shows that, using hypothesis II, the feeding component is more important at lower yield levels. Photosynthesis then compensates less for assimilate loss than at higher yield levels. Using hypothesis I, the contribution of phloem sap uptake is approximately equal at all yield levels.

The contribution of each damage component to total damage in course of time is represented in Figure 73 for EEST84. Under hypothesis I, effects show up from the time grain growth becomes source-limited (Day 213), three days before

Table 29. Relative sensitivity of end-of-season grain yield calculated with the crop model run with data of EEST84 and EEST83. In the runs, the leaf area index was simulated. Reference grain weight is 9898 kg ha⁻¹ for EEST84 and 2864 kg ha⁻¹ for EEST83, respectively. Relative sensitivity is calculated as the ratio of percentage change in grain weight and percentage change in parameter.

Parameter	Unit	Reference value		% change in parameter		Relative sensitivity	
		EEST84	EEST83	EEST84	EEST83	EEST84	EEST83
Maximum rate of leaf CO ₂ assimilation	kg ha ⁻¹ h ⁻¹	35 ^a	35 ^a	+ 14	+ 14	0.33	0.43
Maximum rate of ear CO ₂ assimilation	kg ha ⁻¹ h ⁻¹	25 ^b	25 ^b	+ 20	+ 20	0.15	0.11
Initial efficiency of light use of leaves	kg ha ⁻¹ h ⁻¹ • (J m ⁻² s ⁻¹) ⁻¹	0.45 ^c	0.45 ^c	+ 11	+ 11	0.64	0.45
Initial efficiency of light use of ears	kg ha ⁻¹ h ⁻¹ • (J m ⁻² s ⁻¹) ⁻¹	0.40 ^b	0.40 ^b	+ 13	+ 13	0.12	0.08
Size of an ear	cm ²	10 ^b	10 ^b	+150	+ 50	0.00	0.13
Grain density	ha ⁻¹	2.46 10 ^{8d}	1.41 10 ^{8d}	+ 8	+ 8	-0.47	-0.11
Potential rate of carbohydrate accumulation of grains	kg ha ⁻¹ d ⁻¹	table ^e	table ^e	+ 10	+ 10	0.01	0.00
Amount of nitrogen in the soil	kg ha ⁻¹	50 ^d	table ^d	+ 60	+ 20	0.07	0.00
Maximum rate of nitrogen uptake	kg ha ⁻¹ d ⁻¹	3 ^e	3 ^e	+100	+100	-0.07	0.29
Time coefficient for nitrogen translocation	d	8 ^e	8 ^e	- 67	- 67	0.19	0.22
Potential rate of nitrogen accumulation of grains	kg ha ⁻¹ d ⁻¹	table ^e	table ^e	+ 10	+ 10	-0.47	-0.12
Residual nitrogen fraction of leaves	kg ha ⁻¹ • (kg DM ha ⁻¹) ⁻¹	table ^e	table ^e	- 10	- 10	-0.55	-0.21
Onset of leaf death due to nitrogen shortage	-	0.4-0.9 ^a	0.4-0.9 ^a	as measured in the experiment	0.6-0.8	- 24 ^f	14 ^f

^a basically from van Keulen & Seligman (1987), calibrated on data sets PAGV1 and PAGV3

^b Groot (unpublished data)

^c van Keulen & Seligman (1987)

^d input

^e Groot (1987)

^f Absolute change in output (kg grain dry matter ha⁻¹).

Table 30a. Fine sensitivity analysis of the damage model. Relative sensitivity of end-of-season grain yield calculated with the damage model run with data of EEST84. In the runs the leaf area index was simulated. Reference grain weight is 9898 kg ha^{-1} without aphids, 8389 kg ha^{-1} with aphid damage according to hypothesis I and 8636 kg ha^{-1} according to hypothesis II. Relative sensitivity is calculated as the ratio of percentage change in grain weight and percentage change in parameter value.

Parameter	Unit	Reference value	% change in parameter	Relative sensitivity			
				Hypothesis I		Hypothesis II	
				Yield	Damage	Yield	Damage
Average apterous aphid weight	mg	table ¹	+10	0.63	-0.09	0.60	
Extinction coefficient for honeydew	-	0.8	-25	0.03	0.00	0.03	
Fraction of honeydew deposited on ears	-	0.3	+33	-0.03	0.00	-0.02	
Suction rate	$\text{kg mg}^{-1} \text{ d}^{-1}$	$8.92 \cdot 10^{-9}$	-33	-0.00	0.00	-0.01	
% reduction of AMAX after 15 days	-	24	+10	0.63	-0.09	0.60	
% increase in rate of dark respiration after 15 days	-	35	-10	0.68	-0.09	0.63	
			+20	0.31	-0.06	0.39	
			-20	0.30	-0.06	0.38	
			+20	0.21	-0.04	0.27	
			-20	0.20	-0.04	0.27	

¹ Function of the development stage of the crop.

Table 30b. Coarse sensitivity analysis of the damage model. Contribution of damage components to total damage in percentage of total damage, calculated under both hypotheses on partitioning of phloem sap between grain and aphids. For explanation of the hypotheses see text.

Hypothesis	Total damage (kg ha ⁻¹)	Damage components		
		Feeding (%)	Photosynthesis reduction (%)	Respiration increase (%)
I	1532	51	28	21
II	1323	37	36	27

reserves are depleted in the run without aphids. Damage due to all components increases with time. Damage due to uptake of phloem sap continues to increase after the departure of the aphids (Day 221), as enhanced nitrogen translocation, due to feeding, results in lower photosynthesis and increased rates of leaf death later in the simulation. This accounts for 37% of the total direct damage.

As under hypothesis II the demand of the grains is only partly met as a consequence of aphid feeding, damage occurs from grain set onwards. Damage due to reduction of net photosynthesis starts after grain-filling becomes dependent upon photosynthesis. With the departure of the aphids from the system, damage due to the uptake of phloem sap does not increase, as the rate of nitrogen translocation is assumed to be unaffected, in contrast to hypothesis I.

The effect of rain is evaluated by assuming complete removal of honeydew and its effects after daily precipitation of at least 5 mm, which occurred on Days 190 to 193 for EEST84. The effect on yield is less than 1%.

In experiments (Rossing, in prep.), an increase in the rate of dark respiration up to 56% is found one day after a honeydew application of 64 kg ha⁻¹ onto flag leaves. The efficiency of light use was decreased by 26% in one instance, two weeks after a honeydew application of 109 kg ha⁻¹. These effects were introduced in the model, combined with the reduction of the maximum rate of photosynthesis already described. The consequence for grain yield is an 8% (691 kg ha⁻¹) decrease, due to increased dark respiration and 3% (300 kg ha⁻¹), due to decrease in light use efficiency.

In a preliminary version of the model, van Roermund et al. (1986) modelled the aphid sink using a demand for carbohydrates and the nature of the competition according to hypothesis I. This is repeated here for EEST84, also using hypothesis II. The results are similar to the model runs where aphids exerted a demand for nitrogen.

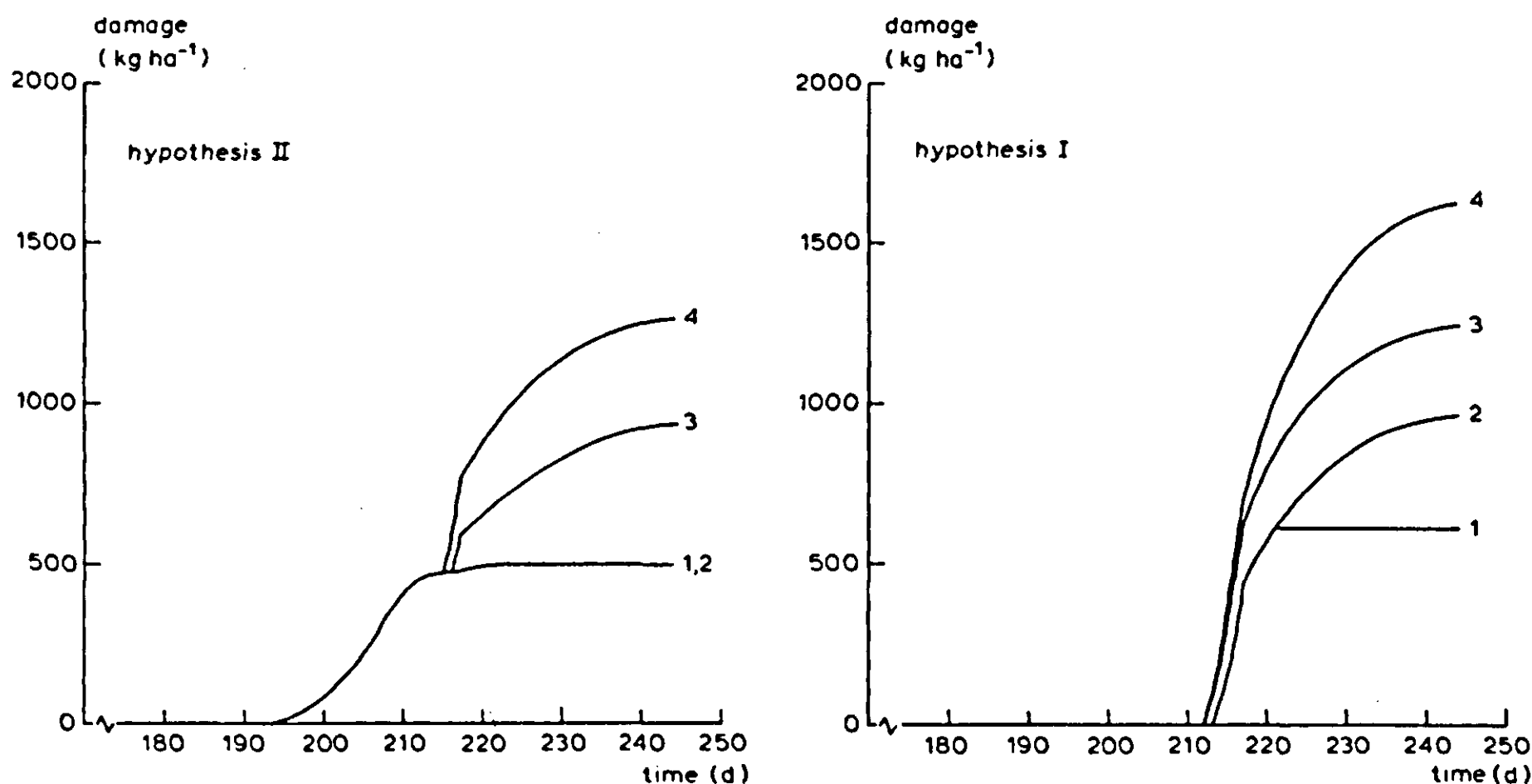


Figure 73. Simulated total damage (grain yield reduction, kg ha^{-1}) and damage components using two alternative hypotheses on the direct effects of *Sitobion avenae*. Data of EEST84, the highest aphid infestation. 1: carbohydrate uptake. 2: carbohydrate and nitrogen uptake. 3: carbohydrate and nitrogen uptake + increased maintenance respiration. 4: carbohydrate and nitrogen uptake + increased maintenance respiration + decreased maximum photosynthesis.

Exercise 76

- Explain the signs of the relative sensitivities in Table 30a.
- Recalculate the absolute damage (in kg ha^{-1}) as it was simulated with the model after the parameter values were changed.

Conclusions Quantitative information available on winter wheat – *S. avenae* interaction, is integrated in a simulation model of growth of winter wheat. As the information on the effect of *S. avenae* on the sink-source relations is incomplete, the model is used to evaluate the quantitative consequences of alternative hypotheses describing the direct effects. Most effects observed in field experiments can be explained by the hypotheses, but each one only provides a partial explanation. The maximum difference between the hypotheses in simulated final yield is 360 kg ha^{-1} .

4.4.6 Application to management

As indicated above, quantitative model evaluation is desirable before results can be used in a management environment. Although the evaluation presented here is only qualitative, the model is used to contribute to the calculation of dynamic economic thresholds as an example of model application. For this purpose, aphid populations of equal relative growth rate, and timing of the peak density as for EEST84, are introduced in the damage model as explained in the previous Subsection. Total damage per aphid per day for the various yield levels is shown in Figure 74. In Table 31 damage per aphid per day is calculated for various periods of crop development. At the higher yield levels, early infestations cause the greater damage as the effects of carbohydrate and nitrogen uptake persist for the rest of the season. At low yield levels, this pattern is obscured by the low values involved and the increasing significance of feeding damage with increasing crop age, as such crops lack compensation by photosynthesis due to their low leaf area indices.

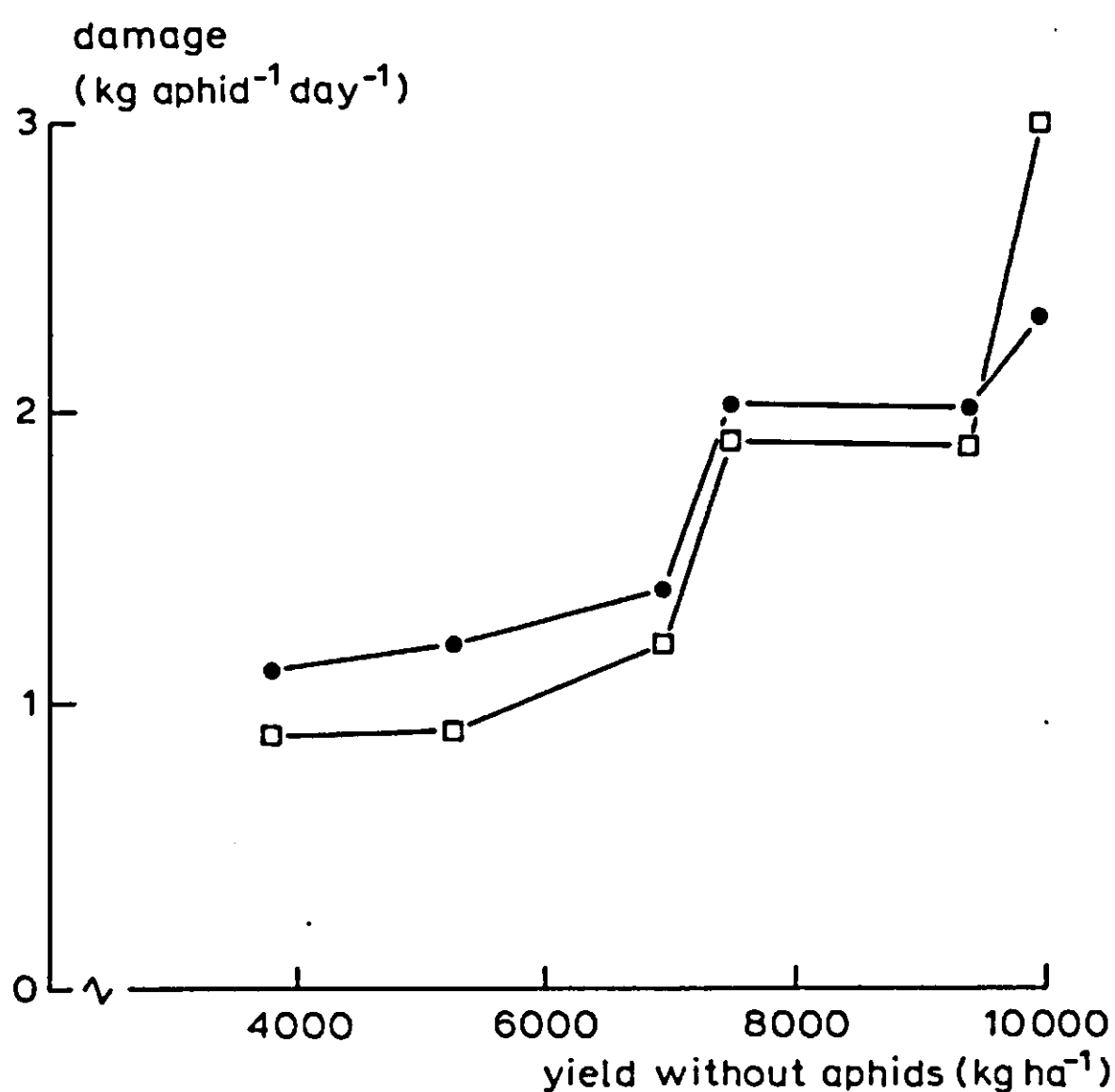


Figure 74. Damage per aphid per day at various yield levels, calculated with the damage model using alternative hypotheses to describe the direct effects of *Sitobion avenae*: hypothesis I (-□-) and hypothesis II (-●-)

Table 31. Simulated damage (kg aphid⁻¹ day⁻¹) for various crop growth stage periods, calculated under hypotheses I and II on aphid-crop interaction.

Data set	Hypothesis	Crop growth stages (Decimal Code)					
		60-65	65-69	69-71	71-73	73-75	75-79
EEST83	I	0.53	0.90	0.65	0.50	1.07	1.17
	II	0.53	1.16	1.14	1.14	1.03	1.22
PAGV1	I	0.57	0.72	0.55	0.54	0.90	1.48
	II	0.57	1.16	1.10	1.08	1.15	1.48
PAGV2	I	1.60	1.41	1.14	1.00	1.19	1.28
	II	1.60	2.19	1.63	1.41	1.23	1.28
PAGV3	I	2.66	3.59	2.60	2.05	1.77	1.12
	II	2.66	3.11	2.60	2.19	1.81	1.43
BOUWING84	I	8.46	5.32	3.73	3.64	1.73	1.08
	II	8.46	5.32	3.88	3.74	1.86	1.25
EEST84	I	11.26	6.72	4.72	4.61	2.79	1.78
	II	11.26	6.72	4.57	3.94	1.91	1.29

5 DECISION MAKING AND MANAGEMENT

5.1 Decision making and data management

F.H. Rijsdijk, J.C. Zadoks and R. Rabbinge

5.1.1 Introduction

Decision making in crop protection management varies widely for different crops. This is because factors such as variety susceptibility, soil type and crop rotation influence the decisions that have to be made.

Often, the use of pesticides plays a major role. Depending on crop and disease, treatments are applied either preventively or immediately after the first observation of the pathogen in the field. Sometimes treatment is delayed until the disease intensity passes a threshold which justifies protective action. In any case, the attitude of the farmers, which vary from risk-avoiding to risk-accepting, is also important. One task of the crop protection scientist is to produce rules and algorithms to assist the farmer in his decision making, and so avoid the unnecessary use of pesticides.

Decision making in crop protection is just part of decision making in general management, and should be understood as such. Interrelation with other cultural measures, such as fertilization and crop husbandry practices, are essential in order to create optimal conditions for the use of decision systems in agricultural practice. In decision making, a distinction is made between strategic decisions and tactical decisions (Chapters 1 and 6). For both types, simulation could be useful.

Comprehensive simulation models on pest and disease epidemics as such are seldom an instrument for decision making in agriculture. Decision making requires algorithms and decision rules that are rarely derived directly from such simulation models, but they may be used to find such rules.

5.1.2 Tactical decision making in disease control

When preventive methods, such as varietal resistance, crop rotation or biological control are no longer sufficient, then chemical control is needed. In order to limit the use of pesticides, and to spray only when really necessary, computer supported disease management becomes desirable and such systems are being developed for many crops.

A management system for the protection of winter wheat is already operational. Decision making in this management system concerns the control of the pathosystem by applying a pesticide only when needed. The decisions require information on the cost/benefit relation of a prospective treatment. Total costs depend on the price of the chemical, labour costs and possible damage to the crop by chemical or spraying equipment. Damage caused by the spraying equipment

(mainly wheel-track damage) depends on the past and present state of the particular field, and is not affected by the pest or disease. The benefit of a treatment depends on how the disease is affecting crop productivity. This may vary from field to field, so that information on both crop and pathogen is needed for each individual field.

Comprehensive explanatory models have shown that in cereal diseases the upsurge of the epidemic is decisive for the amount of damage that may occur later in the season, and that in this very first phase the severity of the disease increases exponentially, as growth limiting factors are absent. The relative growth rate is used as a value to characterize the host-pathogen relationship. This relative growth rate may depend on the development stage of the crop, crop conditions (e.g. nitrogen status) and weather conditions. The severity of the disease in the (near) future, is estimated using a certain time horizon or prognosis period. Future severity is used to compute the expected yield loss. The computation of yield loss may be based on an analysis as given in Sections 4.3 and 4.4.

The types of analysis, given in the previous Sections, were used to construct a supervised disease and pest control system in winter wheat: EIPRE.

5.1.3 EIPRE, a supervised control system of pests and diseases in wheat

EIPRE, developed in the Netherlands, is a system devised to support decision making in pest and disease control in winter wheat. It is an acronym representing EPIdemiology, PREdiction and PREvention. EIPRE is one of the earliest world-wide attempts to develop computerized Integrated Pest and Disease Management systems (IPDM). The word integrated has a double meaning here. EIPRE integrates chemical control with various aspects of varietal choice, crop husbandry, and farm economics. It also integrates the control of six fungal diseases and three aphid pests (Table 32; Zadoks, 1981). Moreover, the aim of EIPRE is to minimize cost of crop protection measures and to reduce pesticide use.

Field monitoring EIPRE's comparative advantage is its field specificity (Zadoks et al., 1984). Each field is registered separately, with its own characteristics, and each field must be monitored for pests and diseases. EIPRE requires the participants to do their own monitoring, for two reasons. The first is educational, the participants should learn how to diagnose their own situations. The second reason is a formal one. With computers, it is 'rubbish in, rubbish out'. To avoid this, it is the responsibility of the participant to provide good input data, and the responsibility of the management to provide good output data from these inputs. Some input errors can be recognized and corrected, but many cannot. An error-spotting algorithm has been in use. The output returned to the participant repeats the original information, as used by the computer, so that the participant can check the inputs used.

Table 32. Pests and diseases on wheat considered by EIPRE. Diseases not mentioned in this table cannot yet be controlled satisfactorily, and thus are not handled by EIPRE.

Latin name	Common name
<i>Erysiphe graminis</i>	Powdery mildew
<i>Pseudocercospora herpotrichoides</i>	Eyespot
<i>Puccinia recondita</i>	Brown rust
<i>Puccinia striiformis</i>	Yellow rust
<i>Septoria nodorum</i>	Glume blotch
<i>Septoria tritici</i>	Leaf blotch
Aphids were treated as a group	
<i>Metopolophium dirhodum</i>	Rose-grass aphid
<i>Rhopalosiphum padi</i>	Bird cherry oat aphid
<i>Sitobion avenae</i>	English grain aphid

Field monitoring takes time, and time is money. About half an hour per field, spent on monitoring, seems to be acceptable to most farmers, if it does not have to be done too frequently. In 1983, the average number of visits per field was $4.2 \text{ h} \pm 1.5$. The costs of the farmers' time, which are relatively independent of field size, were incorporated into the module calculating the net profit according to EIPRE. For the Netherlands, with an average field size of 8 ha, this means an observation time of no more than half an hour per ha; the production of 1 ha of winter wheat, including all agronomical activities, requires about 8 h ha^{-1} under Dutch conditions.

Implementation Implementing EIPRE is a complex affair. The actual program, presented in a modular design, varies with time, conditions and available computers. Only a few points will be raised here, by way of example, according to the 1985 version (Reinink, 1985).

When EIPRE was initiated, the standard objection made by scientists, but not by farmers, was 'we don't know enough'. The standard reply was 'we use whatever knowledge is available here and now'. This reply is still valid, but how much should we 'know' for decision support systems in IPDM? Too much knowledge may result in the system designer going out of business. He simply does not need to know the financial implications of every possible situation, because the majority of these possible situations (e.g. with very little or very much disease) are, in any case, not very interesting (Zadoks, 1984).

A prerequisite for the designer of a decision support system is a good understanding of the decision making process (Norton & Mumford, 1983). Complex simulation models, highly detailed and thoroughly verified, are splendid research

instruments but clumsy extension tools (Zadoks & Rabbinge, 1985). They are too complex and too slow, require too many specifications and provide unnecessary detail for decision making. Also, they are often not available.

For extension purposes, the model should be as simple as possible. So, why use sophisticated equations when the exponential equation, well known from population dynamics, has been proved to be good enough in the situation considered? Population density studies are only of importance during the very first phase of population growth, when exponential growth occurs. Moreover, predictions are made for relatively short prognosis periods, so that updating the input data obtained by monitoring is possible.

The decision maker has, at any time, only two options, he either treats or he does not. However sophisticated the model, which in EIPRE is nothing more than a deterministic yes/no decision model, it must determine the 'action threshold' (Zadoks & Schein, 1979), where *no* just tops over into *yes*. The actual course of disease is of no interest to either the system designer or to the decision maker, except to determine whether or not the disease will pass the action threshold (Zadoks, 1985). The quality of a decision support system does not depend on the amount of underlying knowledge, but on the frequency of its usage and the profits made by using it.

The pragmatism expressed here does not exclude sound biological knowledge from decision support systems. In EIPRE, the model status, the amount of biological knowledge incorporated into the model, varies according to the disease being considered. The following briefly indicates, in descriptive and subjective terms, the model status of the various modules of EIPRE (Reinink, 1985).

Yellow rust The module is based on the oldest European disease simulation model, now outdated. Adequate knowledge of the effects of cultivars, sowing dates, soil types, and fungicides was absent, so that all the parameters had to be estimated by a process of iteration. The resulting model was extensively checked by repeatedly visiting hundreds of fields.

The underestimation of future severity occurs when the distinction level is less than 99.5% or $p < 0.005$ and is corrected at the next observation round. Early samples of yellow rust were used to examine the physiological race involved and to adjust the system before a new race appeared.

Brown rust Little effort was made to model the dynamics of brown rust. However, detailed disease and damage assessment studies have been made in recent years by R.A. Daamen (unpublished), which were applied to the brown rust module.

Powdery mildew The early model, based on the yellow rust module, has been gradually upgraded. Recently, a great deal of knowledge on disease assessment (Daamen, in prep.) and damage assessment (Daamen, in prep.) has been collected and applied to EIPRE. The mildew model also uses recent knowledge about the

physiology of damage caused by powdery mildew (Rabbinge et al., 1985). A special algorithm was developed to warn of unexpectedly severe mildew infestations after treatment, which could be due to the resistance of the mildew to triadimefon (de Waard et al., 1986).

Eyespot Although interesting decision models are available from elsewhere, use is only made of the Dutch extension service. The action threshold at development stage DC 31 (Decimal Code, Zadoks et al., 1974) is about $x = 0.15$, adjusted for variety, DC and expected yield. On sandy soils, no treatment is recommended to avoid stimulation of sharp eyespot (*Rhizoctonia cerealis*). On other soils, treatment is avoided wherever possible to reduce carbendazim resistance in the fungus (Sanders et al., 1986).

Septoria EPIPARE lumps all brown flecks on leaves under the heading *Septoria*, to compensate for the limited diagnostic abilities of the participants. *S. tritici* (*Mycosphaerella graminicola*) and *S. nodorum* (*Leptosphaeria nodorum*) are then 'separated' by means of an algorithm, based on annual disease surveys providing relative frequencies of the two diseases per region and soil type. Treatments recommended only once between crop development stage stem extension and watery ripe, DC 39 and DC 69 respectively, are most effective at about DC 57. The two diseases respond differently to the various fungicides. Information on damage is available (Forrer & Zadoks, 1983). For *S. nodorum*, ear infection must be avoided. On some sandy soils, severe ear infection may appear without any noticeable infection of the leaves in earlier development stages.

Aphids The aphid model in EPIPARE is well substantiated. Aphid monitoring has been studied in detail (Rabbinge & Mantel, 1981; Rabbinge & Carter, 1984; Ward et al., 1985a, b) and explanatory simulation models have been constructed for aphid population biology (Carter et al., 1982). The physiology of aphid damage is well known (Rabbinge et al., 1983, 1984a). In the aphid module, this knowledge is compacted into simple algorithms. Before DC 55 the action threshold is 0.7 (expressed here as the proportion of tillers with at least one aphid; $x = 0.7$). At late milky ripe, DC 77, damage is negligible and no treatment is recommended. After booting, DC 55, and before late milky ripe, $55 < DC < 77$, treatment is never recommended if the proportion of infested tillers is less than 0.2, but always if this proportion is higher than 0.80. In the remaining interval, a calculation is needed. This is done in a similar way to that for the diseases with a superproportionality correction (Section 4.4). The expected damage increases, and is expressed in grain weight from 18 to 80 kg ha⁻¹ for each aphid tiller⁻¹ at the maximum population density when yield increases from 5500 to 9000 kg ha⁻¹.

This summary of the various EPIPARE modules leads to the conclusion that detailed, explanatory simulation models are useful but not indispensable prerequisites for applied IPDM. It is the underlying biological knowledge that is

required, and this can only be obtained by combining modelling with experimental work.

Multiple infection The decision is simple as long as only one disease passes the action threshold. It is complex when several diseases become significant growth- and yield-reducing factors. Then it is necessary to find the best combination of pesticides. Sometimes, two or more diseases are subliminal but, nevertheless, a combination treatment is warranted. Alternating pesticides, to avoid the development of resistance in fungi to fungicides, is then considered and only those aphicides which do not harm beneficial insects, and which respect before-harvest safety periods, are recommended.

How a decision is made The EIPRE data bank contains field data and general data. The field data are specified by the farmer for each field separately (Table 33). They contain core data, once per season, and variable data, from two to five observation dates per season. The field observations made by the farmer follow a certain protocol (Figure 75) and lead to completing an Observation Card (Figure 76). This card contains farmer and field identification data and the variable data, used as inputs for EIPRE. EIPRE responds with a written recommendation (Figure 77) previously sent by mail, but nowadays replaced by a telephone call.

The general data belong to various groups. One group is a list of some 60 varieties with their susceptibility coefficients (Table 34). Another group is a list of some 150 commercially available pesticides with their characteristics and prices. A third group consists of a large set of small tables for operational use by the several EIPRE modules. A fourth group contains the texts of the recommendations to be given.

Table 33. Field data used in EIPRE. (Source: Reinink, 1985).

Variable data	Core data
1. Date	1. Variety
2. Growth Stage = DC	2. Soil type
3. Counts of:	3. Yield expectation
Eyespot	4. Width of spray swath
Yellow rust	5. Labour costs for treatment
Brown rust	6. Costs of pesticides
Powdery mildew	7. Number treatments after 15 May
Leaf flecks (Septorias)	8. Dates/amounts CCC treatment
Aphids	9. Dates/amounts N treatment
4. Recent treatments applied	

Walk over the field in a diagonal line. On 20 locations check 5 stems for the presence of aphids and take 2 stems for disease assessment. For aphid assessment (from DC 49), count the number of stems with at least 1 aphid. Use the 40 stems for the following assessments:

- Determine the development stage using the Decimal Code (Zadoks et al., 1974).
- Eyespot disease, until DC 32. Count the sprouts (stems) with eye spots. The range is from 0 to 40.
- Yellow rust. Inspect the 5 upper leaves of the stems and count the leaves with at least 1 lesion. If 5 leaves per stem are not left, inspect only the green leaves. The range is from 0 to a maximum of 200.
- Brown rust. As yellow rust.
- Powdery mildew. Inspect the upper 3 fully grown leaves of the stems and count the leaves with mildew. The range is from 0 to 120.
- Brown leaf fleck, after DC 39. Inspect the upper 3 fully grown leaves of the stems and count the leaves with brown flecks. The range is from 0 tot 120.

Figure 75. Schematic protocol for field monitoring.

EPIPARE	Observation Card				
	FIELD NR.:	VARIETY:			
	FIELD NAME:				
Date:	Growth stage:				
Eyespot	Yellow rust	Brown rust	Mildew	Leaf flecks	Aphids
TOTALS from scoring list on reverse side					

Figure 76. Example of an EPIPARE observation card, to be completed by the farmer.

Wheat cropping system

EPIPARE recommendation

FIELD

FIELD

NAME: Nearfield

NUMBER: 1312

Variety: Arminda

Lelystad, 8 June 1986

Considering your field observations of 7 June 1986,

Disease	:	Count	:	Damage and costs in kg wheat per ha			
				Expected damage	Labour	Wheel track damage	Costs of pesticides
Yellow rust	:	16	:	Over 500	40	101	107
Brown rust	:	0	:	0	40	101	138
Mildew	:	0	:	0	40	101	107
Leaf flecks	:	17	:	Over 500	40	101	43

We advise you to treat on or shortly before 13 June 1986.

The treatment should aim at

LEAF FLECKS and YELLOW RUST

The ultimate date for the next field observation is 27 June 1986.

We recommend using one of the following pesticides or combinations:
BAYFIDAN, CORBEL or TILT in combination with SPORTAK.

Figure 77. Example of an EPIPARE recommendation.

All possible recommendations have a code number, following a binary numbering system. The code number is calculated from the Decision Module. From its data bank, the computer finds the corresponding text to be sent to the farmer. There are three possibilities per disease: (1) Expected loss is less than the pesticide costs. No treatment is recommended. If there is disease, the date of the next observation will be indicated. (2) Expected loss exceeds the costs of the pesticide but is less than the total treatment costs. A recommendation for treatment is

Table 34. Susceptibility coefficients of varieties.

Disease	Range
Aphids	not used
Eyespot	80–110
Brown rust	77–110
Powdery mildew	70–120
Glume blotch	88–100
Leaf blotch	88–100
Yellow rust	77–100

considered, in combination with other possible treatments. (3) Expected loss exceeds the treatment costs. A recommendation for treatment is given. If a treatment has already been applied, the program will respect the duration of the effective protection period.

The annual variation in the mean number of recommendations is considerable (Table 35), mainly due to variations in long-term weather patterns. The steady replacement of varieties, and the gradual improvement of EIPRE, may also have affected the annual variation.

Procedures The effect of disease intensity on damage and loss (Zadoks, 1985) depends on the development stage of the crop. All calculations are based on the development stages described by the Decimal Code (Zadoks et al., 1974). The following procedural aspects refer to the yellow rust module and reflect the structure of the other modules. Each disease or pest in the system has its own module, with basically the same structure.

The field observation produces a figure n with $0 \leq n \leq 200$, i.e. the number of leaves from 200 inspected leaves with symptoms. This incidence number n is transformed into a disease severity by using the relation between severity and incidence. The disease severity, y , expressed as a fraction of visibly diseased leaf area is, at the low severity levels of interest here, proportional to n :

$$y_0 = 0.00025 \cdot n$$

Expected disease severity, expressed as a fraction y_e ($0 \leq y_e \leq 0.1$), is the disease level expected at some time in the future. Starting with the present observed disease level, y_0 , the future disease level, y_e , is foreseeable only over a short time horizon, the prognosis time, t_p . The prognosis time, t_p , (Table 36) depends on crop development stage, DC. Development rate is directly affected by mean temperature. The exponential equation for disease increase is

$$y_e = y_0 \cdot \exp(t_p \cdot r_e) \quad \text{Equation 120}$$

Table 35. Annual variation in recommendations. Entries represent percentages of fields for which farmers were recommended to treat the disease mentioned in the first column. Also given are the annual mean number of spray recommendations per field for all diseases together, the annual mean recommended Treatment Index (TI represents the actual number of recommended machine runs per field applying pesticides either singly or, more usually, as a mixture), and the total number of fields involved. (Source: Stol, 1985).

Disease	Year			
	1982	1983	1984	1985
Eyespot	—	6	10	19
Yellow rust	0	8	3	2
Brown rust	0	18	3	5
Powdery mildew	13	63	99	53
Septorias	11	37	37	48
Aphids	51	3	38	44
recommendations per field	4.1	3.8	4.8	4.5
recommended TI	0.8	1.6	1.9	1.6
number of fields	1069	1380	1100	816

Table 36. Yellow rust. Prognosis time (t_p) and relative growth rate (r) in relation to development stage, DC. (Source: Reinink, 1985).

DC	t_p	r	
		without N top dressing	with N top dressing
37	28	0.110	0.110
39	28	0.109	0.124
45	23	0.105	0.121
59	16	0.088	0.102
69	6	0.074	0.087

The relative growth rate, r_e , of a disease depends, for example in stripe rust, on variety (susceptible or not), DC and nitrogen status (Table 36). Varieties are placed in one of three groups, susceptible with a compatibility coefficient $CF = 1.$, moderately resistant with $CF = 0.88$, or resistant with $CF = 0.77$. A cultural correction (CC) is applied to express the effect of cultural conditions

on the disease, e.g. for spring wheat $CC = 0.82$. The expected relative growth rate, r_e , is found by multiplication:

$$r_e = r \cdot CF \cdot CC$$

in which r expresses the relative growth rate under optimal conditions. This value is inserted into Equation 120 to obtain the expected severity.

When a treatment is applied, y_e can be reduced by systemic action and t_p by protectant action of the pesticide. Reduction factors RF must be introduced. Equation 120 becomes

$$y_e = y_0 \cdot RF1 \cdot \exp(t_p \cdot RF2 \cdot r_e)$$

Reduction factors may vary per disease and cultivar. The varietal resistance can strongly influence the effectiveness of systemic fungicides. As the literature is rather 'silent' on reduction factors, they are determined empirically using an iterative approach.

As very low levels of disease cause relatively little damage, a no-damage discount y_n (Table 37) is applied to y_e . The expected damage, d_e , is expressed as a multiplier m , again DC-dependent (Table 37). In some cases, damage at high yield levels, resulting from favourable growing conditions, such as high nitrogen levels, is superproportional; i.e. more than proportional to yield (Rabbinge et al., 1981; Rabbinge & Rijsdijk, 1984; Section 4.4). Superproportionality is attained by introducing a factor s , which equals 1.0 up to $Y_e = 7500 \text{ kg ha}^{-1}$ and increases linearly up to $Y_e = 8000 \text{ kg ha}^{-1}$, Y_e being the expected yield specified by the farmer. The expected relative damage, d_e , expressed as a proportion of the expected yield, becomes

$$d_e = y_e \cdot m \cdot s$$

The expected damage D_e , expressed in kg ha^{-1} , is d_e multiplied by the yield expectation, Y_e in kg ha^{-1} :

$$D_e = d_e \cdot Y_e$$

Table 37. Yellow rust. No-damage thresholds (y_n) and damage multipliers (m) depending on development stage, DC. (Source: Reinink, 1985).

DC	y_n	m
30	0.002	5.0
39	0.002	6.7
45	0.002	5.0
61	0.005	2.0

This value is transferred to the decision model, where it is balanced against expected costs.

Data management A decision scheme that uses specific field and crop data, as in EPIPARE, requires structured data storage and management. It is necessary to describe the site characteristics accurately to generate the recommendations. The continuously changing situation during the season is partly due to the growth and development of the crop and pest and disease populations, and it is partly due to man, through cultural measures such as the application of fertilizers, growth regulators and pesticides. Whenever a recommendation is generated, a check of the data is needed which will include the effects of changing parameters. In EPIPARE, data are organized as follows: basic data, being parameters which do not change during one season, such as soil type, variety, farmer's address etc.; fertilizer data, which are added during the season; data on pesticides, which are added during the season; observations, together with recommendations based on these observations. During the season, a data-base is filled gradually, starting from the basic data and finishing with a more or less complete field and crop history. These data can be used afterwards to check any complaints from the farmers, and for scientific analysis, which may lead to improvements of the system.

The techniques of data management will not be treated here. It suffices to recommend modern data-base software packages which enables the easy storage and retrieval of data from a data-base. Many software packages are available, ranging from indexed file systems to well-defined and completely preprogrammed data management systems, such as CODASYL or Relational Database systems.

5.1.4 Pathosystem management as part of crop management

Using EPIPARE, we have demonstrated how a decision system with complex decision algorithms can be developed, and how it can make use of information on crop husbandry practices. It indicates a new line of future developments. Pest and disease management systems must be part of an integrated crop management system, covering all decisions made by the farmer. Some crop management systems (e.g. on small grains) are now ready for experimental use in agricultural practice. These crop management systems are in fact collections of advisory modules which cover most farmers' decisions. They may improve decision making and, in many situations, lead to the reduced use of pesticides.

At present, these decision support systems are run on mainframe computers, which means that the system is completely centralized. However, EPIPARE can also be run on microcomputers, completely decentralized. The advantages of centralization are, rapid updating and upgrading of the system and immediate contact between user and adviser, but time consumption and communication

limitations are a disadvantage. On the other hand, decentralized systems have the disadvantage of slow updating and no guaranteed upgrading.

Another development concerns the introduction of packages in which farmers may choose between various forms of risk-accepting and risk-avoiding behaviour (Section 5.2). This development of steady improvement and upgrading of supervised control systems tends to increase the scientific basis of crop husbandry. Therefore, in the near future, we will see crop management systems where all aspects of crop management are integrated. For their development, much additional interdisciplinary scientific work is needed in which simulation models may play a major integrative role.

5.2 Application of operations research techniques in crop protection

W.A.H. Rossing

5.2.1 Introduction

Management of cropping systems and pathosystems requires (as discussed in Section 5.1) appropriate, well-defined decision procedures and adequate information on the state and dynamics of the system. If these conditions are fulfilled, decisions may be made by evaluating all possible options. This is a feasible and operational method if only a limited number of options exists, and few decisions have to be made. For example, a seedling disease may or may not be controlled chemically; if control measures are taken, the pesticide may be applied as seed dressing or after sowing. However, in crop protection it is a recognized fact that many decisions interact. For example, many pests and diseases react to the nutritional status of the crop which, in turn, is determined by cultural measures such as seedbed preparation and fertilization. Traditionally, the experience of the decision maker plays a major role in such cases. Many combinations or options are ruled out in advance, based on experience and knowledge of the behaviour of the system. However, the approach is not transferable and, although the results may be satisfactory, it is not known whether a different combination of decisions would have led to better results.

The rapidly growing research on expert systems employs empirical experience. Here, researchers try to quantify and make explicit the insight and knowledge of the experienced decision maker. The drawback to this approach is that it freezes the knowledge of the currently 'good' farmer and does not help in the development of better and well transferable information. Previous Sections have shown an approach that may lead to improvement in decision making. Information on the effect of various decisions on the behaviour of the system can be obtained by simulation or by experiments, or by combining both ways. The latter seems the best route.

Decision making is a process which continues throughout the growing season. Methods and techniques developed in operations research can be applied to tune managerial actions to objectives. These objectives need not be economic; they may be, e.g. environmental. With most techniques, however, the objectives must be quantifiable, although sophisticated methods are being developed which can handle qualitative objectives.

One optimization technique which has found wide application, including the scheduling of farm operations, is linear programming. Non-linear regression methods originate from operations research. Dynamic programming, discrete event simulation and goal programming are examples of techniques which have been used in agricultural decision problems, although mainly at the research

level. In this Section, the basic principles of linear programming (LP), dynamic programming (DP) and discrete event simulation for decision making in crop protection are discussed. After studying this Section, the reader should be able to recognize the structure of the optimization methods discussed here. Formulating a specific problem, e.g. an LP-problem, will require more experience as will the choice of one optimization method over an other. Handbooks, e.g. van Beek & Hendriks (1985), Dannenbring & Starr (1981), Hillier & Lieberman (1980) and Wagner (1979) are advised for further study.

Before proceeding to explain the techniques, the general structure of a decision problem should be discussed.

5.2.2 *General structure of a decision problem*

In general, a decision problem involves one or more objective functions, decision variables, constraints and a transformation function. The objective function(s) describe(s) the aim of optimization and measure(s) how 'good' a certain combination of decision variables is. The ways in which the decision maker can intervene in the system are represented by the decision variables. Several combinations of decisions may not be feasible, owing to technical or policy considerations. The feasible combinations are described by the constraints. The transformation function describes the way the system evolves under various decision alternatives.

A solution is optimal only within the boundaries of the constraints. These constraints reflect an opinion on the socio-economic situation and on the technical possibilities. As points of view differ and are incomplete a generally optimal solution does not exist. This can be illustrated by an example from the crop protection practice.

When deciding to apply a pesticide, a farmer usually only weighs costs of treatment against costs due to harmful organisms without treatment. Crop husbandry measures, effects on non-target organisms, pesticide residues, dangers to the health of the person applying the chemical and long-term effects on productivity, constitute technical and policy constraints. Each of these represents a decision problem in itself, but with respect to applying a pesticide, they are treated as given facts which cannot be influenced. The farmer's decision problem is then reduced to: what is the optimum timing of pesticide applications to give the highest financial returns (objective function)? The decision variable is 'treatment' with options 'treat' and 'do not treat'. This concept is called 'supervised control'.

In the 'integrated control' concept, less constraints appear in the decision problem. Here, the constraints of the supervised control problem appear as variables in the objective function. Thus, the number of decision alternatives increases. An example is the explicit minimization of effects on non-target organisms in integrated control, as opposed to 'do not spray more than X active ingredient, to prevent excessive effects on non-target organisms' in supervised

control. In the former case, the concentration of active ingredients occurs in the objective function, in the latter case in the constraints.

Optimization of decisions in agricultural management may occur at different levels:

1. Crop husbandry measures (e.g. optimal timing of fertilizer applications);
2. Cropping system (e.g. timing of fertilizer application in relation to pests and diseases);
3. Farm (e.g. optimization of the choice of crops);
4. Policy (e.g. optimal farming systems).

The higher the level of integration, the more complex the decision problem, as the number of decision alternatives grows. In principle, management science provides techniques to deal with problems at all levels of integration.

5.2.3 *Linear programming*

Linear programming (LP) is a general-purpose technique for determining the best allocation of scarce resources. LP-problems are characterized by an objective function (a way of measuring how good an allocation is), a set of decision variables (the way in which scarce resources can be allocated) and a set of resource constraints (limitations placed on the decision variables to reflect the resource scarcity). The objective function and the resource constraints must be linear in the decision variables. This means that a change of one unit in the decision variables results in a constant change in the value of the objective function and in the resource constraint.

LP-problems cannot be solved analytically. They are solved by an algorithm which involves a finite number of operations, the so-called simplex method, developed by Dantzig in 1947, which has found wide application in managerial decision problems.

In this Subsection, two examples will be presented to convey some idea of the type of problem that can be handled by linear programming. A graphic approach and an algebraic approach to solving LP-problems are given. Finally, some advanced applications are considered.

LP-problem formulation, Example 1 Consider a farmer who wants to maximize financial returns from two crops, potatoes and wheat. One hectare of potatoes gives two-and-a-half times the financial return of one hectare of wheat. The farmer faces three constraints: he only has 6 hectares of arable land, potatoes may not be grown more than once every two years and, for reasons of diversity, the farmer does not want wheat to cover more than two-thirds of his arable land. The farmer wants to know how many hectares he should put under potatoes and wheat, respectively.

LP-problem formulation, Example 2 is taken from animal ecology. A bird may collect food for itself and its nestlings from two isolated areas. One is at 2 minutes

distance, the other at 3. The energy needed to visit the two areas is 5 and 10 Joules, respectively. The prey at the first site has an energy content of 25 Joules per individual, the prey item at the other site 40 Joules. The amount of time needed to find and catch a prey item is 2 minutes at the first site and 1 minute at the second. Once a prey is caught, the bird takes it to its nest. Per day, the predator spends no more than 80 minutes hunting and 120 minutes travelling. To satisfy its own basic energy needs, and that of the nestlings, it requires 600 Joules. How many individuals of each prey species must be caught to maximize the net amount of energy gained?

To solve these problems a more formal notation is useful. Example 1 may be reformulated in this way:

$$\text{maximize } (w = 2x_1 + 5x_2) \quad \text{financial return objective} \quad \text{Equation 121}$$

where x_1 = number of hectares under wheat,
 x_2 = number of hectares under potatoes

subject to

$$x_1 + x_2 \leq 6 \quad \text{total area constraint} \quad \text{Equation 122}$$

$$x_1 \leq 4 \quad \text{area constraint wheat} \quad \text{Equation 123}$$

$$x_2 \leq 3 \quad \text{area constraint potatoes} \quad \text{Equation 124}$$

$$x_1 \geq 0, x_2 \geq 0 \quad x_1 \text{ and } x_2 \text{ cannot be negative} \quad \text{Equation 125}$$

As described in the introduction, the problem consists of an objective function (Equation 121), a number of resource constraints (Equation 122 to 125) and decision variables (x_1 and x_2).

Exercise 77

Give the mathematical representation of Example 2.

Optimal solution to an LP-problem: the iso-profit line approach In Figure 78, a graphic representation is given of the LP-problem of Example 1. The range of values of x_1 and x_2 permitted by the inequalities is indicated by the shaded area in Figure 78a. The set of permitted values of x_1 and x_2 is called the solution set or the feasible region and consists of the polygon OABCD. The points O, A, B, C and D are referred to as corner points of the solution space. Points on the transects connecting these corner points are referred to as extreme points.

The objective function, w , can assume different values as represented by the broken lines in the graph of Figure 78b. Each line consists of combinations of x_1 and x_2 which result in the same amount of profit. Note that these 'iso-profit lines'

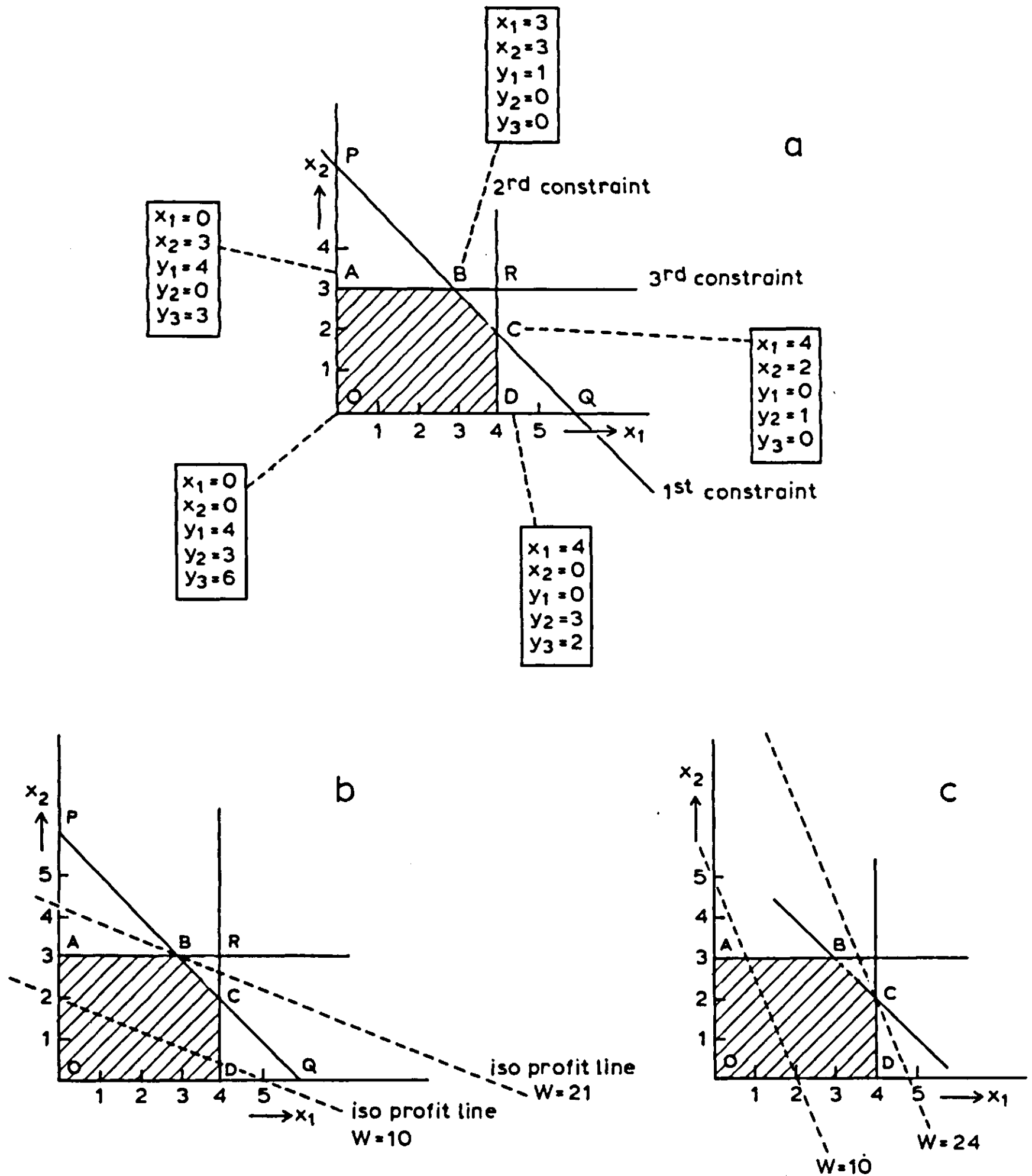


Figure 78. Graphic representation of a linear programming problem. The solution space (shaded) and iso-profit lines (dashed lines).

are perpendicular to the vector $\begin{pmatrix} 2 \\ 3 \end{pmatrix}$, which consists of the coefficients of x_1 and x_2 in the objective function. The combination of x_1 and x_2 within the feasible region OABCD which is situated on the highest iso-profit line is optimal. In Example 1, the optimal solution is point B, where $x_1 = 3$ and $x_2 = 3$. The objective function value here is 21.

It is not a coincidence that the optimal solution is reached in an extreme point. Only points on the border of the feasible region can be optimal. The explanation

can be inferred from Figure 78b. The objective function value can be increased only by moving the iso-profit line 'up' or, more exactly, along the gradient vector $\begin{pmatrix} 2 \\ 5 \end{pmatrix}$. Thus, there are two possibilities: the iso-profit line with the highest objective function value either shares one point with the feasible region or coincides with one of its sides. In both cases, the optimal points are extreme points. In the first case the solution is unique, in the second case there are alternative solutions. Thus, when trying to find the optimal solution the search may be limited to the border of the solution space.

It still remains to be proved that point B is optimal. When moving from one point on the border to another the objective function value either increases, decreases or remains unchanged depending on the constraint describing the intermediate intersect. Proceeding from O (with $x_1 = 0$ and $x_2 = 0$) to A in Figure 78, the objective function increases by the marginal contribution of x_2 (the contribution of one unit x_2) which equals 5, the coefficient of x_2 in the objective function. At A ($x_2 = 3$), therefore, the objective function value is 15.

Going from A to B along the constraint line, x_2 remains unchanged while x_1 increases. The equation describing the line ($x_2 = 3$) shows that x_1 can be increased independent of x_2 until point B is reached. Here $x_1 = 3$ and $x_2 = 3$. The change in x_1 results in a change in the value of the objective function of $2(3) = 6$, so the objective function value is 21. Thus B is preferred to A.

Going from B to C, x_2 decreases while x_1 increases. As dictated by the equation of the intermediate line ($x_1 + x_2 = 6$), each unit of decrease of x_2 is equalled by an increase in x_1 of one unit. Thus, each unit decrease of x_2 results in an increase of the objective function value of $2(1) + 5(-1) = -3$. When moving from B to C, the objective function value decreases. As the objective function is always linear in LP-problems, it can be concluded that any other point is inferior to B, since A and C are inferior.

Exercise 78

Repeat this line of reasoning with the objective function $w = x_1 + x_2$.

Apart from the unique and alternative solutions illustrated above, two other classes of solutions exist, as illustrated in Figures 79 and 80. In Figure 79, the problem has an unbounded solution set. The objective function value can be made arbitrarily large, while still satisfying the constraints. In a practical setting, this situation may exist for a range of values of a variable until another constraint is reached. In Figure 80, a problem is depicted for which no feasible and, therefore, no optimal, solution exists. As an example, consider the case where a certain minimum amount of pesticide is needed to control a pest while this amount exceeds the maximum level tolerated by beneficial insects.

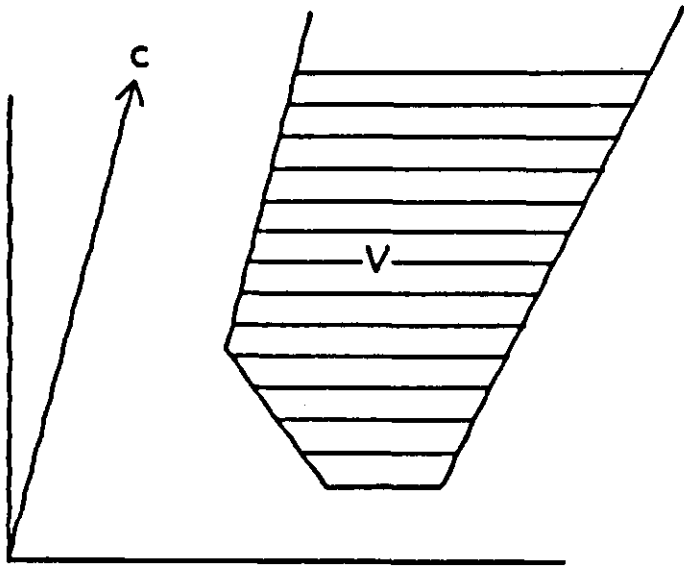


Figure 79. Graphic representation of a linear programming problem with an infinite solution. V is the solution space, c the vector of coefficients of the objective function. (Source: van Beek & Hendriks, 1985).

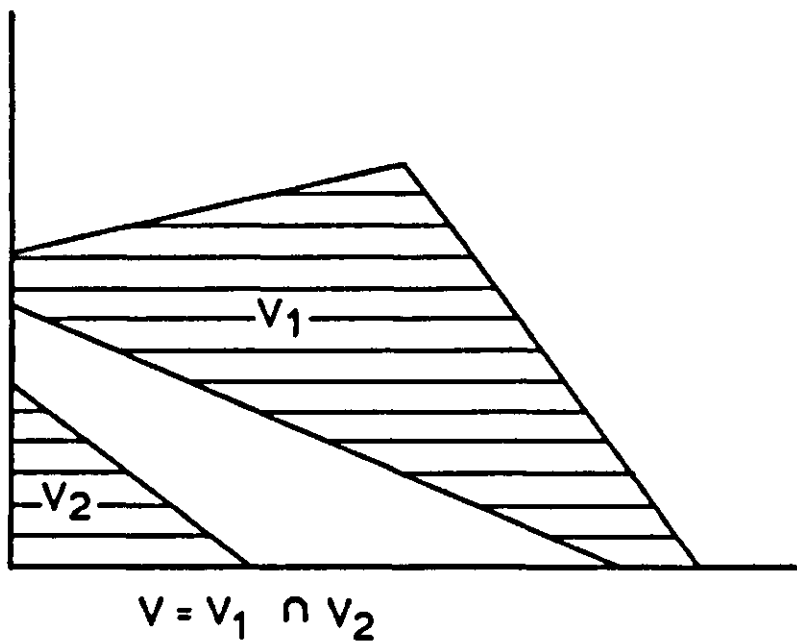


Figure 80. Graphic representation of a linear programming problem without a feasible solution. (Source: van Beek & Hendriks, 1985).

General algebraic form of an LP-problem Two forms of LP-problems are distinguished: the standard form and the canonical form. An LP-problem in the standard form can be written as:

$$\text{maximize } (w = c_1x_1 + c_2x_2 + \dots + c_nx_n) \quad \text{Equation 126}$$

subject to ...

$$\begin{aligned} a_{11}x_1 + a_{12}x_2 + \dots + a_{1n}x_n &= b_1 \\ a_{21}x_1 + a_{22}x_2 + \dots + a_{2n}x_n &= b_2 \\ \vdots & \\ a_{m1}x_1 + a_{m2}x_2 + \dots + a_{mn}x_n &= b_m \end{aligned}$$

$$x_1 \geq 0, x_2 \geq 0, \dots, x_n \geq 0$$

Here c_j , a_{ij} and b_i ($i = 1, 2, \dots, m; j = 1, 2, \dots, n$) are fixed and the decision variables x_i are to be determined.

In the canonical form the LP-problem is

$$\text{maximize } (w = c_1x_1 + c_2x_2 + \dots + c_nx_n)$$

Equation 127

subject to

$$a_{11}x_1 + a_{12}x_2 + \dots + a_{1n}x_n \leq b_1$$

$$a_{21}x_1 + a_{22}x_2 + \dots + a_{2n}x_n \leq b_2$$

⋮

$$a_{m1}x_1 + a_{m2}x_2 + \dots + a_{mn}x_n \leq b_m$$

$$x_1 \geq 0, x_2 \geq 0, \dots, x_n \geq 0$$

A number of transformations exists by means of which any LP-problem may be reformulated in its equivalent standard or canonical form. For example, 'maximize (w)' is equivalent to 'minimize (-w)', and multiplying the objective function by a scalar $k \neq 0$ does not change the optimal solution. Of course, if $k < 0$, a maximization problem becomes a minimization problem and vice versa. An important transformation is: $\sum a_{ij}x_j \leq b_i$ is equivalent to $\sum a_{ij}x_j + y_i = b_i$ (and vice versa), where $y_i \geq 0$. The variable y_i is called a slack variable as it removes the slack in the constraint. It appears in the objective function with coefficient 0.

Exercise 79

Apply the transformation rules to derive the standard form of Example 1 and Example 2.

Optimal solution of an LP-problem: algebraic analysis and simplex algorithm The iso-profit line method with evaluation of extreme border points is only applicable in the case of a two-dimensional LP-problem. For problems of higher dimensionality, the simplex algorithm has been developed. In spite of its name, the method is too complex to be dealt with in detail here. In order to appreciate the hurdles involved in the technique, an algebraic solution to the example in Equations 121–125 will be examined.

Applying the transformations of the previous section, the LP-problem can be rewritten in the standard form:

$$\text{maximize } (w = 2x_1 + 5x_2 + 0y_1 + 0y_2 + 0y_3)$$

Equation 128

subject to

$$x_1 + y_1 = 4$$

Equation 129

$$x_2 + y_2 = 3$$

Equation 130

$$x_1 + x_2 + y_3 = 6$$

Equation 131

$$x_1 \geq 0, x_2 \geq 0, y_1 \geq 0, y_2 \geq 0, y_3 \geq 0$$

Equation 132

The simplex algorithm starts with a feasible solution, checks whether it is optimal, identifies a better solution if optimality is not yet reached and stops if it is. A reasonable initial feasible solution seems to be $x_1 = 0$ and $x_2 = 0$ and the slack variables at their maximum (why?) values $y_1 = 4$, $y_2 = 3$, $y_3 = 6$. As the coefficients of the slack variables in the object function are zero, $w = 0$.

The positive coefficients of x_1 and x_2 in the objective function imply that increasing either x_1 or x_2 results in an increase of w . The marginal contribution of x_2 is greater. Thus, for the purpose of maximizing w , increasing the value of x_2 is most attractive.

To which value can x_2 be increased while still satisfying the constraints? From Equation 130 it can be seen that x_2 may be maximally 3, otherwise y_2 becomes negative. According to Equation 131, x_2 may be maximally 6. Thus, the maximum value of x_2 is 3 according to the most limiting constraint. If $x_2 = 3$, Equation 131 dictates that $y_3 = 3$. The value of x_1 is left at zero, $x_1 = 0$, therefore $y_1 = 4$. The second solution, still feasible, is therefore $x_1 = 0$, $x_2 = 3$, $y_1 = 4$, $y_2 = 0$, $y_3 = 3$ and the objective function value is $w = 15$.

How can this be interpreted graphically? The initial solution involved point O in Figure 78a. The value of the slack variables designated the shortest distance along the x_1 - and x_2 -axis from O to each of the constraints: the distance to constraint Equation 129 was 4 ($y_1 = 4$), etc. Next, x_2 was increased. As can be seen in Figure 78a, values of x_2 greater than 3 are no longer within the solution space. Therefore, the next feasible solution is point A. With $x_2 = 3$ the slack in the first constraint (Equation 129) has not changed and is represented by the intersect AR, whereas the slack in the second constraint (Equation 130) has been eliminated. The slack in the third constraint (Equation 131) is reduced to 3, represented by the intersects AP and AB.

As a next step in the optimization, a criterion is needed to judge whether increasing the value of any other variable results in an increase in w . As $x_2 = 3$, this variable can be eliminated from the constraints by making it explicit in Equation 130 and using it as a so-called pivot to remove x_2 from other equations. This results in:

$$\begin{array}{rcl} x_1 + y_1 & = & 4 \qquad \text{Equation 129} \\ x_2 & = & 3 - y_2 \qquad \text{Equation 133} \\ x_1 + y_3 & = & 3 + y_2 \qquad \text{Equation 134} \end{array}$$

Substituting x_2 described by Equation 133 into the objective function (Equation 128) yields:

$$\text{maximize } (w = 2x_1 + 15 - 5y_2 + 0y_1 + 0y_2 + 0y_3) \qquad \text{Equation 135}$$

The positive sign of the coefficient of x_1 in Equation 135 indicates that increasing x_1 from its original value ($x_1 = 0$) can result in a solution superior to the previous one. Therefore, the solution found so far is not optimal.

To what value can x_1 be increased while still satisfying the constraints? From Equations 129 and 134 it can be inferred that x_1 may not be made larger than 3,

otherwise y_2 and y_3 become negative. By making x_1 explicit in Equation 134 and using it as a pivot, x_1 is eliminated from the other equations:

$$y_1 - y_3 = 1 - y_2 \quad \text{Equation 136}$$

$$x_2 = 3 - y_2 \quad \text{Equation 133}$$

$$x_1 = 3 + y_2 - y_3 \quad \text{Equation 134}$$

From these equations it can be seen that if $x_1 = 3$ and $x_2 = 3$, it follows that $y_1 = 1$, $y_2 = 0$ and $y_3 = 0$.

Substituting x_1 (Equation 134) and x_2 (Equation 133) into the objective function (Equation 128) yields:

$$\begin{aligned} w &= 2x_1 + 5x_2 + 0y_1 + 0y_2 + 0y_3 \\ &= 2(3 + y_2 - y_3) + 5(3 - y_2) + 0y_1 + 0y_2 + 0y_3 \\ &= 21 - 3y_2 - 2y_3 + 0y_1 + 0y_2 + 0y_3 \end{aligned} \quad \text{Equation 137}$$

The coefficients of all variables are zero or negative. Thus, no more improvement can be expected by increasing the value of any variable, and the optimal solution found is: $x_1 = 3$, $x_2 = 3$, $y_1 = 1$, $y_2 = 0$, $y_3 = 0$.

As shown in Figure 78b, the optimal solution coincides with point B. The value of $y_1 = 1$ indicates that not all the 'room' available according to constraint 1 (Equation 129) is used, as represented by the intersect BR. The other slack variables have assumed the value 0, indicating that constraints 2 and 3 (Equations 130 and 131) are exactly satisfied.

The steps made in the simplex algorithm can be summarized as follows:

1. The LP-problem is transformed into its standard form. In the example, this was done by adding slack variables.
2. A feasible solution is determined. In this case we chose the origin. Other initial solutions may be appropriate.
3. The optimality of the solution is checked by examining the potential changes in the objective function value resulting from changes in each of the variables.
4. A promising adjacent corner point is selected. Note that this involves changing variables with a value of zero into variables with a value greater than zero, and vice versa. In the example, x_2 was changed from 0 to 3 in the first step, while y_2 decreased from 3 to 0. Variables with a value of zero are called non-basic, the others are called basic variables. The fundamental theorem of linear programming states that the number of basic variables will always equal the number of constraints. The most promising variable, i.e. the one with the highest coefficient in the objective function, is made basic. The variable to become non-basic is the basic variable in the most limiting constraint (check this in the example).
5. The optimality of the solution is checked. If the solution is optimal, stop. If not, return to step 4.

The different solutions can be clearly arranged in a so-called simplex tableau.

The optimality criterion is also represented in the tableau. For advanced treatment of this subject the reader is referred to handbooks.

Exercise 80

Solve the foraging problem described in Example 2.

Post-optimal analysis A farmer may be interested not only in the optimal solution but also in the conditions under which it holds. These are investigated in the post-optimal analysis. Reconsider the problem of the previous section. The optimal solution was $x_1 = 3$ and $x_2 = 3$. From Figure 78b the consequences of relaxing the constraints for the optimal solution can be seen. By making constraint 1 (Equation 122) less limiting, the optimum moves to R along the third constraint line. Relaxing constraint 3 (Equation 124) moves the optimum to point P along the first constraint line. Relaxing constraint 2 (Equation 123) does not affect the optimal solution, as, with optimality at point B, there is still slack with respect to this constraint.

If the ratio of coefficients of x_1 and x_2 in the objective function were 5:2 (instead of 2:5), the iso-profit lines would be perpendicular to the vector $\begin{pmatrix} 5 \\ 2 \end{pmatrix}$ and the optimum would be point C, as can be seen in Figure 78c. If the coefficients were equal, the highest iso-profit line would coincide with the transect BC (check this). In this case, there is an infinite number of alternative optimal solutions.

Exercise 81

Identify the range of ratios of the coefficients of x_1 and x_2 for which the solution $x_1 = 3$, $x_2 = 3$ is optimal.

Goal programming In most applications, decision problems consist of more than one objective. If absolute weights can be attached to each objective, the multiple objective problem may be transformed into a single objective problem. For example, if the problem is to maximize the hectareage of potatoes and wheat on a farm, subject to a number of constraints, the preference of crops may be expressed in their price per unit area. Thus, the problem is transformed into maximization of financial output of potatoes and wheat.

However, for many objectives, only a priority order may be distinguished rather than a quantifiable priority of one over the other. An example is profit maximization on a farm versus conservation of scenic elements. Goal programming is a method of dealing with this type of problem.

The method requires that the objectives are placed in priority order. Starting with the objective of highest priority, the method attempts to satisfy each goal, or,

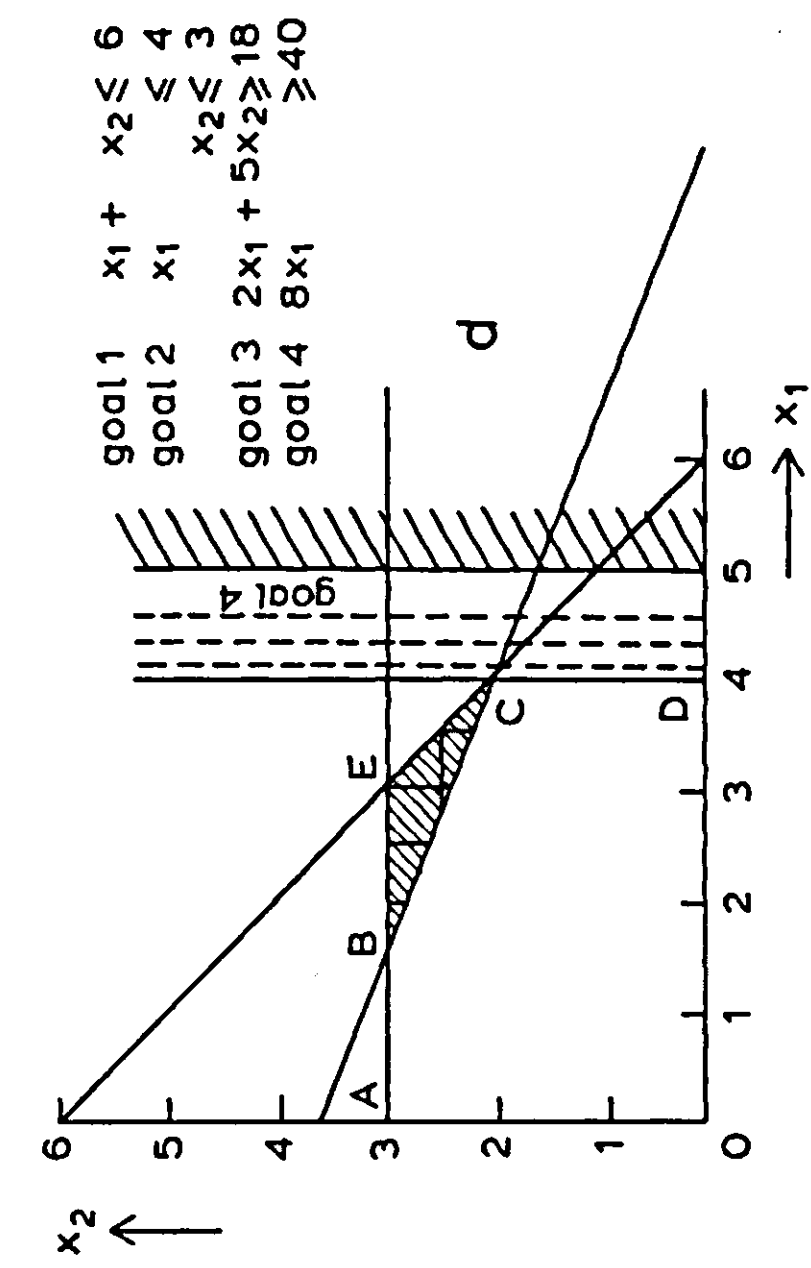
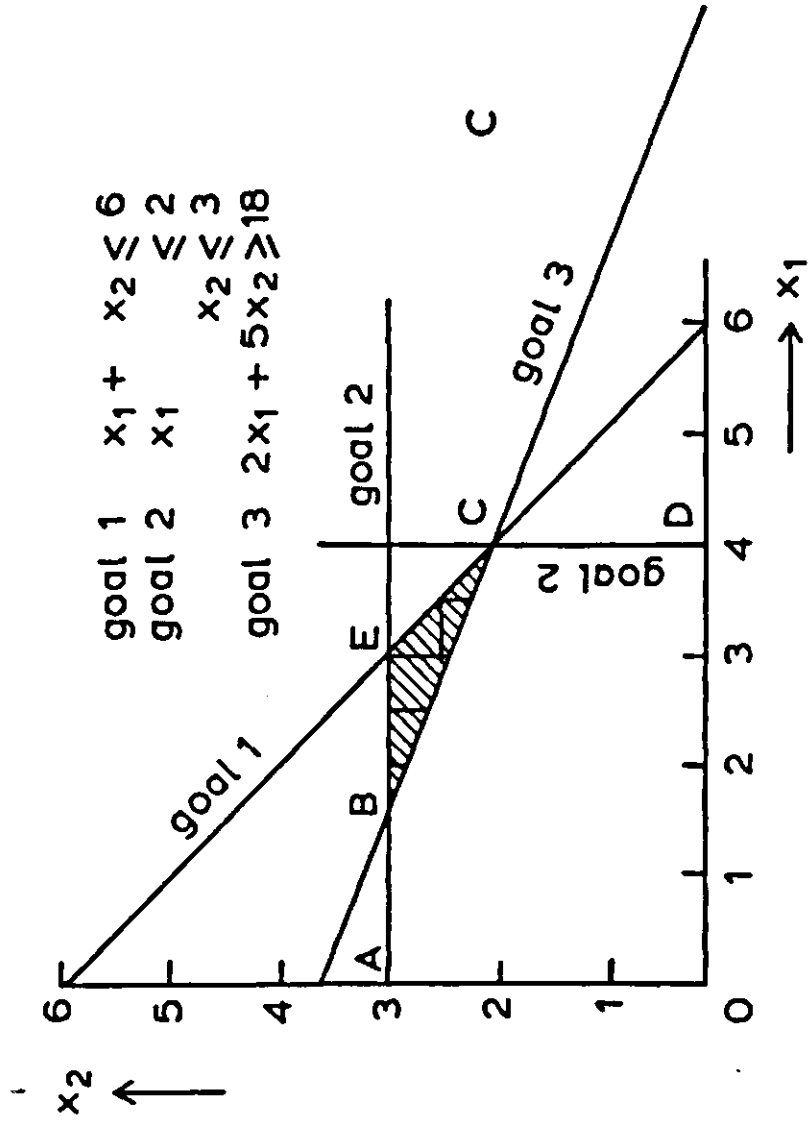
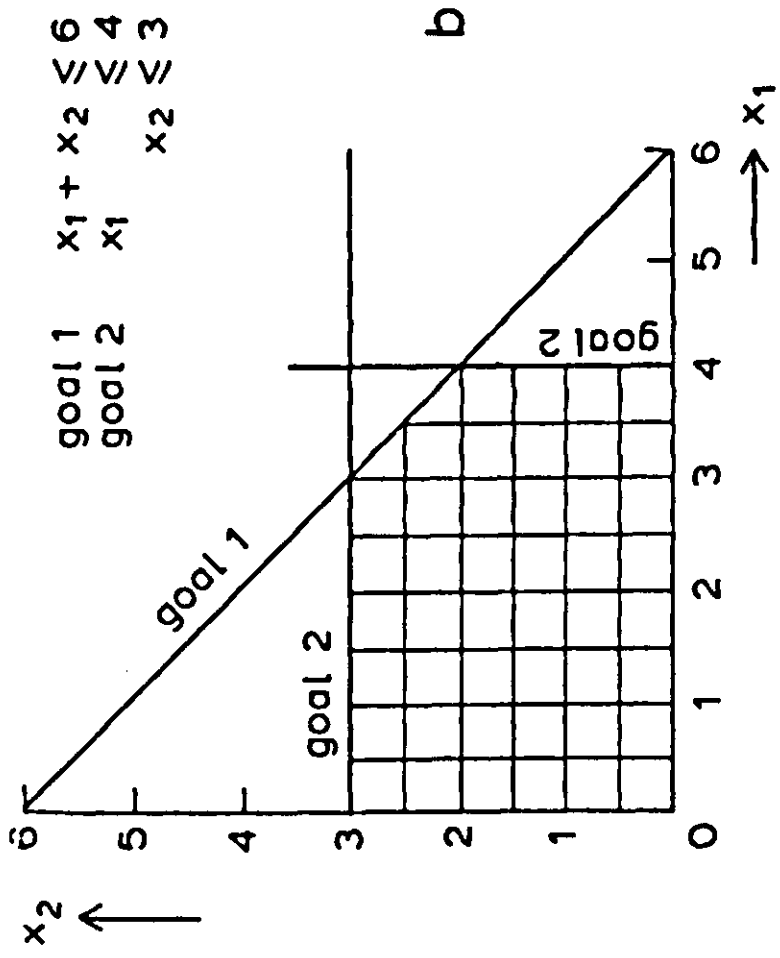
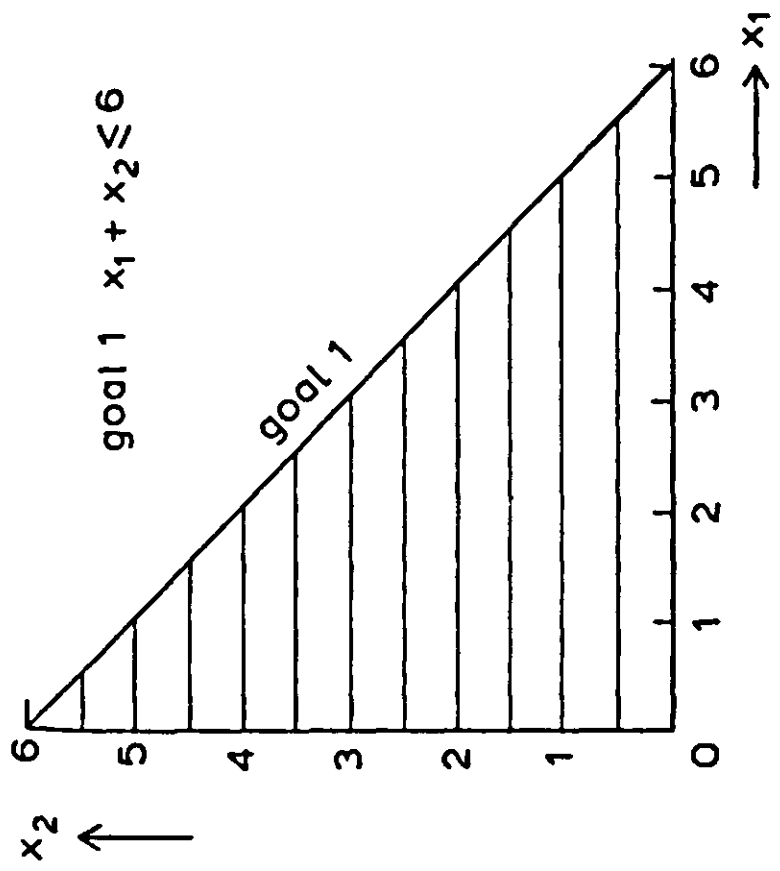


Figure 81. Graphic representation of a goal programming problem. For explanation see text.

failing that, to minimize the undesirable deviations. In this way, a solution can be found that will minimize the amount of underachievement for any goal that cannot be met, without worsening the achievement of any higher-priority goal. Here too, the simplex method can be applied. The following example illustrates the method.

Assume the farmer of Example 1 also wants to produce at least 40 t of wheat to meet a business agreement. His yield expectation for wheat is 8 t ha^{-1} . His goals in order of priority are (1) use maximally 6 hectares of land, (2) obey the constraints with respect to rotation, (3) profit at least equal to 18 and (4) produce at least 40 t of wheat.

This two-dimensional goal programming problem can be solved graphically by repeatedly solving the optimization problem, each time adding an extra goal. Thus, the solution space remains unchanged or, if new goals turn out to be constraints, is decreased. Eventually, a goal may be added that cannot be met by any of the solutions satisfying the higher-priority goals. The solution, feasible with respect to the higher-priority objectives, which deviates least from the unsatisfied goal, is designated as being the optimal solution to the problem.

In Figure 81, this approach is illustrated. After having drawn in the first three goals (Figure 81a, b, c), the solution set with corner points BCE is found. The fourth goal (production ≥ 40) cannot be achieved at any of the points in the solution space. Now a solution has to be found that minimizes the deviation from the fourth constraint and is still feasible. The dashed lines in Figure 81d represent combinations of the decision variables x_1 and x_2 that deviate to the same amount from the fourth constraint. Point C is the first solution encountered which is feasible with respect to the first three goals. Thus, the optimal solution, point C, is to grow 2 ha of potatoes and 4 ha of wheat. The profit is 18 and the deviation from the 40 t level is $1 \cdot 8 = 8 \text{ t}$.

5.2.4 *Dynamic programming*

Dynamic programming (DP) is a technique which efficiently determines the optimal policy in problems with separate but related decisions in a set of sequential time periods. DP is generally compatible with pest management models where decisions are made sequentially. The models may be dynamic, non-linear or stochastic. Because of the ability to handle these types of models, DP is a more suitable tool for problems involving timing of chemical applications than LP.

First, the principle of DP will be explained using a deterministic example. It will become clear why DP is an efficient method. Next, a stochastic problem will be treated.

Shortest route in a network DP-problems can often be formulated as shortest route problems: finding the shortest route from one state in a network to another. Figure 82 represents such a network with four levels or decision stages ($N = 4$).

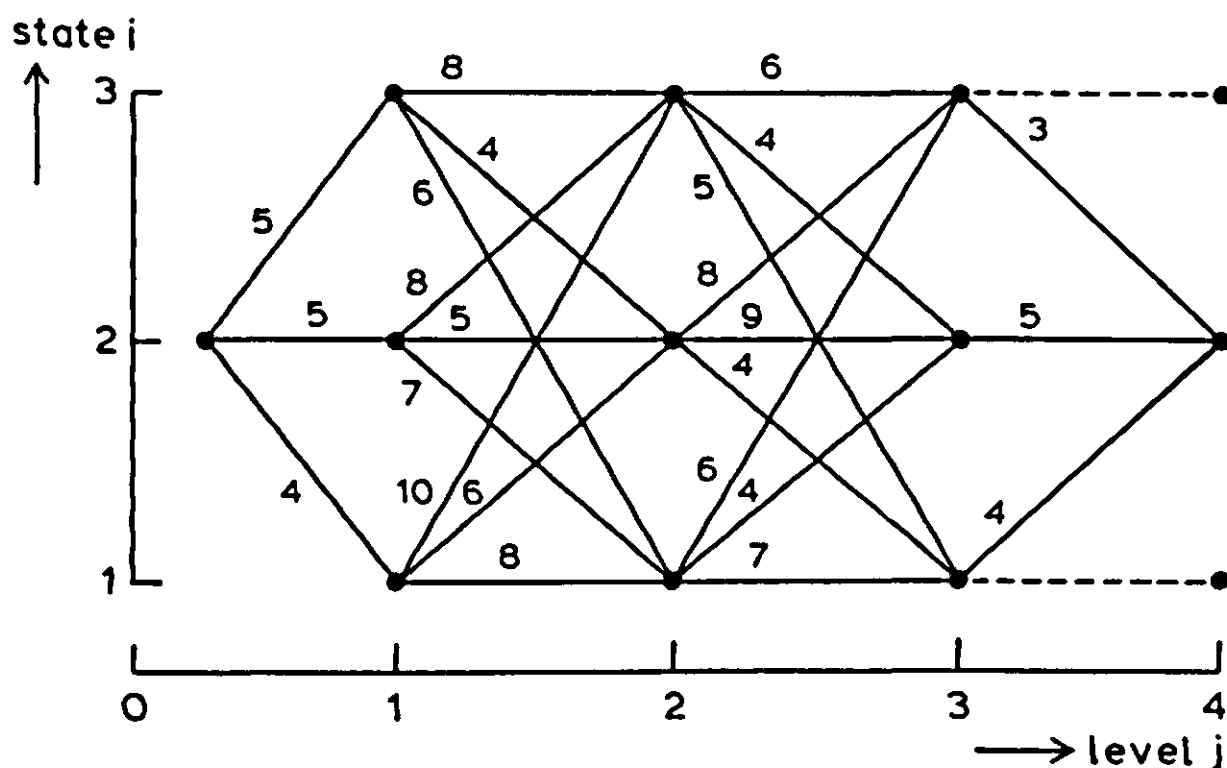


Figure 82. Network representation of a deterministic dynamic programming problem with 4 levels or decision stages. The distance between two nodes or states connected by a branch is indicated.

Each level contains one or more states, nodes in the graphic representation, in which one (the states at the levels 0 and 3) or three decisions (the states on all other levels) are possible. The distances between the nodes vary as indicated in Figure 82. The network may be traversed only from left to right. The problem is to find the shortest route from node 2 at level 0 to the final node 2 at level 4.

Define:

c_{ik} := the distance from node i at an arbitrary level to node k , one level higher

$V_j(i)$:= the shortest route from node (state) i at level j to the final node.

The function V is called the value function. The DP-algorithm states:

$$V_4(2) = 0$$

$$V_j(i) = \underset{k}{\text{minimum}} (c_{ik} + V_{j+1}(k))$$

The second line states that, starting in state i at level j , the decision should always be such that the distance to state k at level $j + 1$ (c_{ik}) plus the minimal distance from state k at level $j + 1$ to the final state ($V_{j+1}(k)$) are minimal. By fixing the value of V at the final (fourth) level and carrying out the calculations starting at the highest level, the algorithm is complete. This procedure can be illustrated using the example of Figure 82.

1. Level 4

The distance from state 2 at level 4 to any subsequent level and state is zero:

$$V_4(2) = 0$$

2. Level 3

Determine the smallest distance from each of the states at level 3 to each of the next states at level 4:

$$V_3(1) = \min_2 (c_{1,2} + V_4(2)) = 4$$

$$V_3(2) = \min_2 (c_{2,2} + V_4(2)) = 5$$

$$V_3(3) = \min_2 (c_{3,2} + V_4(2)) = 3$$

3. Level 2

Determine the smallest distance from each of the states at level 2 to each of the next states at level 3:

$$\begin{aligned} V_2(1) &= \min_{1,2,3} (c_{1,1} + V_3(1), c_{1,2} + V_3(2), c_{1,3} + V_3(3)) \\ &= \min(7 + 4, 4 + 5, 6 + 3) = 9 \quad \text{via state 2 or 3} \end{aligned}$$

Here, the values of the value function $V_3(i)$ which were calculated at level 3 are used.

$$\begin{aligned} V_2(2) &= \min_{1,2,3} (c_{2,1} + V_3(1), c_{2,2} + V_3(2), c_{2,3} + V_3(3)) \\ &= \min(4 + 4, 9 + 5, 8 + 3) = 8 \quad \text{via state 1} \end{aligned}$$

$$\begin{aligned} V_2(3) &= \min_{1,2,3} (c_{3,1} + V_3(1), c_{3,2} + V_3(2), c_{3,3} + V_3(3)) \\ &= \min(5 + 4, 4 + 5, 6 + 3) = 9 \quad \text{via state 1, 2 or 3} \end{aligned}$$

4. Level 1

Determine the smallest distance from each of the states at level 1 to each of the next states at level 2:

$$\begin{aligned} V_1(1) &= \min_{1,2,3} (c_{1,1} + V_2(1), c_{1,2} + V_2(2), c_{1,3} + V_2(3)) \\ &= \min(8 + 9, 6 + 8, 10 + 9) = 14 \quad \text{via state 2} \end{aligned}$$

$$\begin{aligned} V_1(2) &= \min_{1,2,3} (c_{2,1} + V_2(1), c_{2,2} + V_2(2), c_{2,3} + V_2(3)) \\ &= \min(7 + 9, 5 + 8, 8 + 9) = 13 \quad \text{via state 2} \end{aligned}$$

$$\begin{aligned} V_1(3) &= \min_{1,2,3} (c_{3,1} + V_2(1), c_{3,2} + V_2(2), c_{3,3} + V_2(3)) \\ &= \min(6 + 9, 4 + 8, 8 + 9) = 12 \quad \text{via state 2} \end{aligned}$$

5. Level 0

$$\begin{aligned} V_0(2) &= \min_{1,2,3} (c_{2,1} + V_1(1), c_{2,2} + V_1(2), c_{2,3} + V_1(3)) \\ &= \min(4 + 14, 5 + 13, 5 + 12) = 17 \quad \text{via state 3} \end{aligned}$$

By storing the best decisions and associated value functions, the set of optimal decisions is recorded. Thus, the shortest route from state 2 at level 0 to state 2 at level 4 is via states 3, 2 and 1 on the subsequent levels and has length 17.

The algorithm was developed by Bellman (1957), who described the principle of optimality which was applied above as follows: an optimal set of decisions has the property that, whatever the initial state and decision are, the remaining decisions must be optimal with respect to the outcome which results from the initial decision.

The value of the value function V in the state at the final level was arbitrarily chosen to be zero. If there are more states at the last level, the final decision may be directed to a preferred state by attaching appropriately high (in the case of minimization) or low (in the case of maximization) values to value functions in unpreferred states. For example, states 1 and 3 at level 4 may be defined to have value function values of infinity:

$$\begin{aligned} V_4(1) &= \infty \\ V_4(3) &= \infty \end{aligned}$$

Thus, they will never be included in the optimal solution.

The efficiency of DP becomes evident when comparing the number of operations carried out with the number of operations needed when checking all possible routes. The DP-method needed 21 additions, 3 for each node at levels 0 to 2, and 14 comparisons of 2 figures, 2 for each node at levels 0 to 2. In an 'exhaustive search', $3 \cdot 3 \cdot 3 \cdot 1 = 27$ routes have to be checked. This involves $3 \cdot 27 = 81$ additions and 26 comparisons of 2 figures. In problems with more states and levels, the discrepancy between the two methods grows in favour of DP.

Exercise 82

Distinguish the basic components of a decision problem (objective function, decision variables, transformation function and constraints) in the DP-problem formulated in the text.

Stochastic dynamic programming Stochastic dynamic programming concerns the same type of N-step decision problems as deterministic dynamic programming. However, in stochastic DP, the outcome of a decision is not known with certainty in advance. Two or more outcomes may occur, their likelihood described by

a probability distribution. In this case, the optimal policy is the series of decisions which minimizes the expected costs. Calculation is recursive, analogous to the deterministic case. However, the number of computations is generally greater, due to calculation of the expected values.

The algorithm must now be described in more formal terms. Define for $k = 1, 2, \dots, N$:

- x_k := state of the system at level k . The variable x_k is a vector: the state of the system may be characterized by one or more components.
- d_k := describes the decisions to be made between level $k - 1$ and level k .
- r_k := a vector of stochastic variables, the outcome of which is known at level k . The probability distribution of the variables is assumed to be known and the variables are independent. The stochastic vector is indicated by r_k , its outcome by r_k .
- T_k := the transformation function: the function which describes the evolution of the system from state x_{k-1} , decision d_k and outcome r_k to state x_k , yields $x_k = T_k(x_{k-1}, d_k, r_k)$.
- G_k := function describing the costs incurred between levels $k - 1$ and k . These are dependent upon x_{k-1} , d_k and r_k . This yields $G_k(x_{k-1}, d_k, r_k)$.
- V_k := value function on level k . This is the expected value of costs incurred from state x_k at level k to the final level N , if the series of optimal decisions is implemented. V_k is dependent upon x_k : $V_k(x_k)$.

The algorithm now is:

$$V_N(x_N) = 0$$

$$V_{k-1}(x_{k-1}) = \underset{d_k}{\text{minimum}} \{E(G_k(x_{k-1}, d_k, r_k) + V_k(T_k(x_{k-1}, d_k, r_k)))\}$$

where E denotes the expected value.

In the case of stochastic dynamic programming, it is less meaningful to attach different values to $V_N(x_N)$, in order to direct the final outcome towards one preferred state, as the final outcome depends on the chance mechanism.

An example: once a week a decision is made on whether to treat a wheat crop against aphids, based upon the number of aphids and the weather forecast. Two types of weather conditions are distinguished: warm and cool. In the first case, the aphid population grows rapidly and a lot of damage is done. If the weather is cool, the opposite occurs. The decision problem can be formulated in terms of a DP-problem, as illustrated in Figure 83.

The state of the system x_k is described in terms of the number of aphids per wheat tiller. The one-dimensional decision vector consists of the decision to spray or not to spray. Stochasticity is introduced into the system by r_k , describing the probabilities (Pr) of the two weather types. The values of variables defining the system at level $k - 1$ are given in Table 38, which also represents the

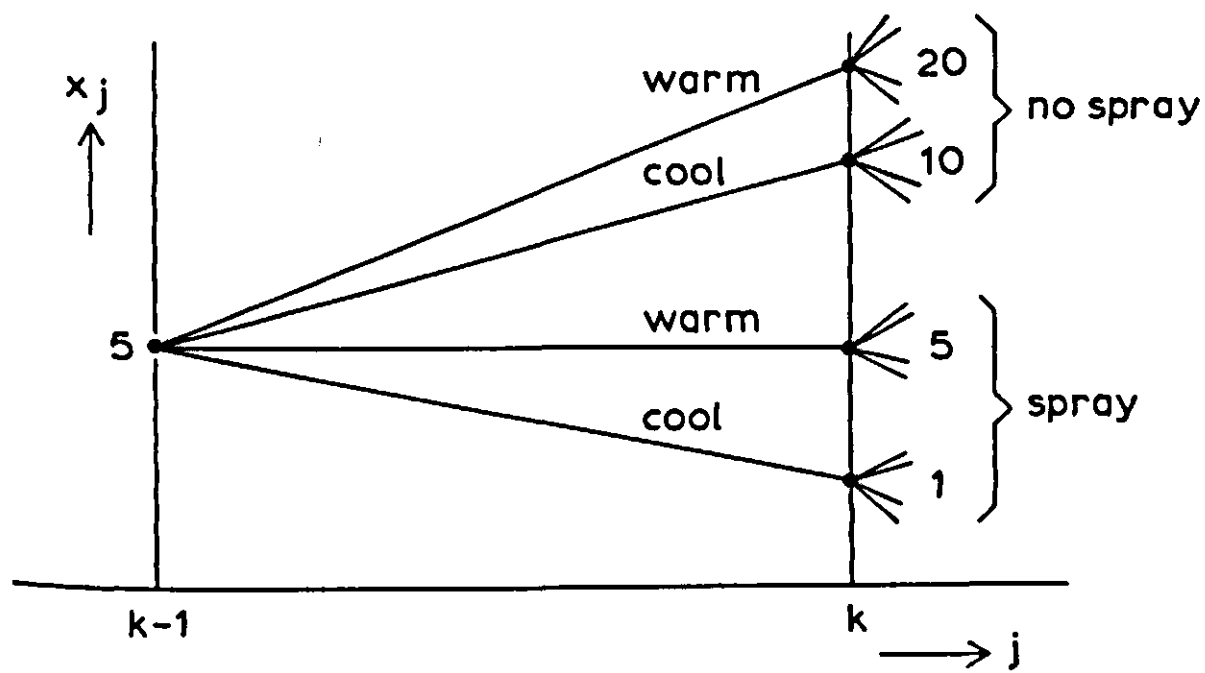


Figure 83. Illustration of a stochastic DP-problem. In each state at each level two decisions may be made: 'spray' or 'no spray.' In each case two type of weather conditions may occur: warm or cool.

Table 38. Chemical control of aphids as an example of stochastic dynamic programming: values of the variable defining the system at level $k - 1$.

$$x_{k-1} = 5$$

$$d_k = \begin{cases} 0 & \text{(no spray)} \\ 1 & \text{(spray)} \end{cases}$$

$$r_k = \begin{cases} 1 & \text{(cool), } \Pr(r_k = 1) = 0.8 \\ 2 & \text{(warm), } \Pr(r_k = 2) = 0.2 \end{cases}$$

T_k for $x_{k-1} = 5$:

r_k	d_k	0	1
1		10	1
2		20	5

G_k for $x_{k-1} = 5$:

r_k	d_k	0	1
1		35	205
2		100	225

evolution of the system from level $k - 1$ to level k . For reasons of clarity, calculation of the value function in only one decision period is discussed. Calculations for the other periods proceed analogously.

The number of aphids in the state vector x_{k-1} is a continuous variable. However, the value function can be calculated only for a finite number of states. Therefore, the value function is calculated for a number of discrete values of x_k and the intermediate values are found by linear interpolation. Suppose $V_k(x_k)$ is known for $x_k = 1, x_k = 5, x_k = 20$. Then $V_k(10) = V_k(5) + 1/3(V_k(20) - V_k(5))$.

The value function for $x_{k-1} = 5$ can now be calculated:

$$V_{k-1}(5) = \min_{d_k=0,1} \left[\begin{array}{c} \text{COOL} \\ \hline 0.8\{G_k(5,0,1) + V_k(10)\} \\ \text{WARM} \\ \hline 0.2\{G_k(5,0,2) + V_k(20)\} \end{array} \right], \text{ no spray} \\ \left[\begin{array}{c} 0.8\{G_k(5,1,1) + V_k(1)\} \\ + 0.2\{G_k(5,1,2) + V_k(5)\} \end{array} \right] \text{ spray}$$

With the value function $V_k(x_k)$ known (the calculation proceeds backwards), $V_{k-1}(5)$ is determined.

5.2.5 Simulation analysis of complex decisions

Both linear and dynamic programming have a number of limitations. Linear programming employs fixed coefficients which may in fact be dynamic. This can be overcome by repeatedly solving the LP-problem with newly calculated coefficients, a time-consuming procedure. Another limitation is the handling of random events. Post-optimal (sensitivity) analysis does not always suffice to estimate the effect of uncertainty in the system. Finally, the model must be linear in the decision variables, a limitation which is hard for many biologists and agronomists to accept, although recently, interesting solutions have been developed (de Wit et al., 1988).

Dynamic programming requires simplified systems with only few state variables, as the computational task soon becomes too large to handle. In the aphid example of Subsection 5.2.4, the number of aphids was the only component describing the state. Other components may include the development stage of the crop, if this interacts with the animal population, or the spraying decisions of previous periods, if residual effects of chemicals are modelled. As a general rule the 'curse of dimensionality' limits the number of state variables to 5 or 6. The inclusion of random events, the number of discrete values of a state component, the complexity of the transformation function and the computer facilities available may alter this figure.

Most of the optimization techniques developed so far are not very suitable for dealing with the combined effects of uncertainty, dynamic interaction between decisions and subsequent events, and complex interdependencies among the variables in the system. When dealing with such a problem, simulation may be a useful tool.

Similar to LP and DP, the system is described in terms of state variables,

decision variables and a transformation function. However, simulation does not involve a fixed algorithm. The effect that the choice of decision variables has on model output is evaluated using an objective function. Different series of decision variables can be fed through the model and assessed with respect to efficacy. Thus, simulation is used as a numerical search method, which is very flexible. However, because of the absence of a prescribed solution structure, convergence of subsequent solutions to an optimal solution is not guaranteed as in LP and DP. This is a serious limitation.

System dynamics are simulated with a fixed-time increment or with an event-step increment. In the former case, the procedure is similar to that described in the previous Sections: the state of the system is updated once per time step. In this way, a continuous process is mimicked. In the latter case, the state of the system is updated at time steps, the length of which is dictated by the occurrence of events defined in advance. An example of a discrete event simulation model is described by Tourigny (1985) who simulated the foraging behaviour of *Rhagoletis pomonella*, the apple maggot fly. This insect searches apple trees for host fruits in which to lay eggs. The fruits are patchily distributed, as they occur in clusters. Once a fruit has been accepted for oviposition, it is marked to avoid secondary parasitism. In the model, three events were defined: (1) systematic search of the host tree for fruit clusters, (2) assessment of the fruits within a cluster for oviposition and (3) oviposition.

The occurrence of an event is a random variable. The time to complete an event is also described by a probability distribution. Events can only occur in a logical order: oviposition is not considered before assessment of fruits has occurred.

In the computer model, an event-list defines the state of the system. The event-list gives the last event that occurred, and its completion time. Upon completion of an event, the next event is added to the list, based upon the outcome of the previous event and the random variables generated. The foraging behaviour of individual flies is thus simulated until they emigrate from the host.

Management simulation models may be either deterministic or stochastic. Deterministic models are useful in retrospective analysis of decisions. An example is the assessment of the efficacy of pesticide applications on cereal aphids by British farmers in 1975 and 1977 (Watt et al., 1984). Based on a model of aphid damage, which was correlated to aphid density, the effect of spray timing was evaluated. The evaluation consisted of the repeated execution of a computer program, each time with a different application date of the chemical. Finally, the optimal decisions were compared with the actual decisions and the differences were expressed in financial terms.

Stochastic management models include random phenomena. In crop protection, these may be weather variables, sampling errors, immigration of pests, etc. The term risk analysis is often applied to such decision models. For example, consider a farmer who wishes to minimize expected costs attributable to aphids, subject to the constraint that the risk of incurring high costs should not exceed a certain threshold. If he does not spray, both the risk and the expected costs are

high. If he sprays frequently, the risk of aphid outbreaks may be sufficiently low, but the expected costs are again high due to the application costs. Less frequent treatment, and appropriate timing, may satisfy the objective. In this situation, simulation of the decision problem is useful since: (1) the number of decisions is large (a farmer may spray every day of the growing season), (2) the interactions between crop, aphids and environment are complex and (3) as a result of (2) no analytical solution exists for the probability distribution of costs.

The usefulness of a stochastic model in this case depends on the extent to which the stochastic variables influence damage. This example is treated in detail by Rossing (1988).

5.2.6 *Final remarks*

Decision-optimization models may be used strategically or tactically. In the first case, the optimal solution for a number of initial conditions is calculated and tabulated or otherwise stored. The decision maker then refers to these tables. In the case of tactical or on-line use, the optimization model is run for one specific set of initial conditions. The approach chosen to disseminate information depends on the problem.

The value of optimization models depends on the quality of the pathosystem description. Poor models of the ecophysiological aspects of population dynamics and damage may yield unrealistic optimal decisions. This is especially true for DP where optimization is carried out over a large planning horizon, i.e. the period of time for which optimal decisions are calculated. Thus, errors when describing the state of the system at the end of the season, affect the first optimal decision calculated. The extent to which this occurs must be evaluated for each case in sensitivity runs with the decision model.

Whether or not further research into certain biological aspects is worthwhile, can be evaluated by sensitivity analysis of the decision model. For efficient planning of biological research activities, it is advisable, therefore, to combine the development of biological models for decision purposes with the development of optimization models.

6 EPILOGUE

6.1 Prospects for simulation and computerized decision making

J.C. Zadoks and R. Rabbinge

6.1.1 Introduction

Simulation is one thing but decision making is quite another. Simulation is a wonderful research tool that provides enlightening insight and helps to define research priorities, while encouraging a certain humility with regard to one's own performance in research. Decision making is very different from simulation; it is usually done without the help of simulation and, certainly in crop protection, simulation is not even a prerequisite. Even so, we claim that simulation is a good tool with which to support management and decision making.

In Chapter 5, preliminary results of a combination of simulation and managerial models were given. Our claim, therefore, will be considered in the light of agro-automation. Before going into detail, some aspects of decision making in agriculture, and more specifically in crop protection, will be discussed.

6.1.2 Agricultural knowledge and decision making

The art of decision making is studied by the managerial sciences. We still call it an art, but art without knowledge is vulnerable when the stakes are high. Experience, skill and insight, combined with intuition and know-how are also essential. The book 'Industrial dynamics' by Forrester (1961), which inspired simulation research more than any other publication, was intended to improve decision making. When the 'system' is relatively limited, as in the manufacturing industry, when the data-base is broad and accurate, and when the decision maker is relatively independent of his environment, simulation can certainly support decision making. The decision models actually used are, however, of another type. Agriculture is different from the manufacturing industry in two respects: the knowledge to be applied and the decisions to be made.

6.1.3 Levels of decision making

Decision making in agriculture, as in other economic sections, occurs at various levels of aggregation. In Chapter 1, these levels were distinguished and it was shown that at each level objectives should be formulated and instruments or tools for decision making should be developed. At the regional/country level the objectives and the way they are reached are mainly subject to political decisions. At farmer, crop and pathogen levels, decision making is based on well-defined technical and economic objectives, which may vary from field to field, and from farm to farm. The following paragraphs mainly concern decision making at the

crop level. Discussions and statements on higher aggregation levels are given elsewhere (de Wit et al., 1987; Zadoks, 1989).

6.1.4 Knowledge in agriculture

Some people have 'green fingers'. Whatever they touch will grow and flourish. 'Green fingers' are an implicit mixture of intuition, experience, attentiveness and foresight. Plant growing can be taught and learned, 'green fingers' cannot. In analogy, we believe in 'green brains', when insight into cause-effect relations and the ability to select the important questions to be addressed are added to the mixture. These psychological qualifications should be seen against the background of phytopathological knowledge which is inherently hazy, as recent studies have indicated. This haziness is partly due to the nature of agricultural processes, which run their genetically programmed courses in manifold interactions among themselves, and within a capricious environment. The haziness is also due to the nature of the decision making process in crop protection, where implicit reasoning, based on the senses seeing, hearing, smelling and feeling, often precedes explicit logic.

6.1.5 Decisions in agriculture

Decisions can be strategic or tactical (Zadoks & Schein, 1980). Strategic decisions are those taken before the start of the growing season. They refer to choices of crop, cultivar, level of inputs required, and so on. Tactical decisions are the day-to-day decisions taken during the growing season, such as 'to treat' or 'not to treat'. Both tactical and strategic decisions are made at two levels, roughly indicated as 'collective' and 'entrepreneurial' (Zadoks & Schein, 1980), here simplified as 'government' and 'grower'. Government has facilities similar to those of an industrial leader; it has access to data, it can outline objectives, and it can apply simulation techniques. Government decisions are usually of the strategic type. The world in which government operates is so complex, that even large simulation models can only provide partial answers to partial questions.

The grower's situation is different. He is always one of many, who consider themselves colleagues rather than competitors. Simulation models are not tools that he can handle, but he welcomes models for decision support. In principle, the grower's situation can be modelled, but we are not aware of any attempts to model his frame of mind or the way he makes decisions, although interesting papers on decision making in crop protection, in theory (Norton, 1976, 1982; Norton & Mumford, 1983) and in practice (Mumford, 1982a, b; Tait, 1978, 1981, 1982), have been published.

When social scientists and agronomists shake hands, the results may be interesting. One result seems to be that decision making is not as logical as a natural scientist might assume it to be. More modestly phrased, his logic does not always result in him obtaining a true picture of the grower's logic. Personal

characteristics play a role, one grower being clearly risk-avoiding, the other accepting risk with an open mind. The two attitudes may dwell together in a single mind. One wheat grower in the Netherlands took a great risk with respect to winter killing, choosing a highly productive but not so winter hardy variety, but started spraying when he saw the first aphid. Where is the logic? Rice farming peasants in the tropics quote insects as the major risk, but by far the most money and effort is spent on weed control. Where is the logic?

Many farmer decisions are based on implicit knowledge, tradition, intuition and social convention. Present efforts aim at rationalizing available knowledge and explaining explicitly the consequences of various options. The contribution of agricultural scientists towards improving agricultural production, may lay in explicitly formulating the consequences of various decisions and thus iteratively improving decision making. Farmers are applying more and more scientific knowledge and, as a result, agricultural production has increased considerably.

One wonders about future developments and about the contribution of systems analysis and simulation to these developments. To address this question, recent developments in the computerization of agriculture will be considered, using the Netherlands as the example.

6.1.6 Agro-computerization in the Netherlands – facts

Computerization in agriculture is the official policy in the Netherlands. A concerted effort by representatives from grower organizations and the Ministry of Agriculture should lead to the formal definition of various farming systems and the decisions taken therein. These studies must ultimately lead to software for decision support in pathosystem management, crop management and farm management. No simulation is foreseen, the aims being packaging the message rather than improving its content. Policy makers seem to be more optimistic about the possibilities of computerization than the scientists.

The actual situation is complex. We distinguish two types of computers, the local computer and the distant computer. The local computer is a process computer or a personal computer on the holding, directly accessible to the grower. The distant computer can be any size, from micro to large mainframe, centralized somewhere in the country, and at the service of the growers. Access is rarely direct, as in the pay-television system VIDITEL (the Dutch version of PRESTEL), but indirect or mediated. An operator is contacted by telephone or letter, and a recommendation is returned by telephone and/or letter.

A sample survey provides a fair picture of computerization in Dutch agriculture (Table 39). Emphasis is clearly on process computers, which either take the decisions, as in the control of glasshouses, or provide rather stringent recommendations, as in dairy cattle feeding. The scientific basis of the process computers in glasshouse climate regulation is still weak and needs further improvement. The technical possibilities developed by the engineers, are now so good that even more physiological insight into crop performance is needed to use these possibili-

Table 39. Computers in Dutch agriculture, 1985, according to a sample survey. (Source: Amro Bank, 1985, 1986).

Branch	Type of application	Number of business units	Computers in use	
			number	%
Horticulture		9 500		
	process		5 200	55
	administration		730	8
Dairy farming		43 200		
	process		5 300	12
	administration		–	0
Arable farming		11 000		
	process		–	0
	administration		550	5
Total		63 700	11 780	18

Table 40. Matching the general and the specific.

System	Subject	Number
SAP	cows (living)	4 500 000
	bulls	100 000
COMZOG	sows	55 000
EPIPPE	fields	1 000

SAP = Sire Advice Program of the Royal Netherlands Cattle Syndicate, Arnhem.

COMZOG = Cooperative Program for the Management of Production Sows, originally designed by a farmer, managed on a distant computer by LARC Ltd (a subsidiary of the organization of cooperatives), Deventer, providing veterinary and zootechnical recommendations to circa 300 holdings.

EPIPPE = Decision support system for crop protection in wheat, managed by the Research Institute for Arable Crops (PAGV, Lelystad), serving about 400 farmers with some 800 fields (1986 data).

ties so that growth and production can be optimized. Decision making in cattle feeding is still largely based on empirical knowledge instead of detailed insight into feeding physiology.

The link between process computer and personal computer for administrative purposes is not yet very strong, although this link is desirable for managerial purposes. A rapid increase in the use of personal computers is to be expected. The use of distant computers for managerial purposes is rather intensive. Table 40 shows only a few examples. The national registration system for dairy cattle and the selection of sires is probably the most extensive system in Dutch agriculture; the ensuing decisions are strategic. In comparison, the crop protection system EPIPARE (Section 5.1) supports tactical decisions.

The pay-television system VIDITEL is being used to transmit commercial information, but its contribution to crop protection is meagre, anno 1986. For fruit growers in the river districts, there is one page available on crop protection. This page was estimated to have been consulted 5000 times in 1986, compared to 29000 consultations for the telephone answering services providing the same message (Zadoks, 1986).

6.1.7 Agro-computerization in the Netherlands – opinions

Decision support systems should satisfy the following criteria:

- simplicity
- time efficiency
- reliability
- solidity
- updating facility
- upgrading facility.

The first set of three criteria speak for themselves. They are partly a matter of packaging the message, that is of programming and screen editing. Several pathosystem management schemes do not comply with these three criteria. Monitoring and sampling may also be too complicated. Their results may be unreliable so that decisions become risky. For this reason, considerable attention in computer-supported decision systems is spent on developing simple, accurate, reliable and time-saving monitoring and sampling techniques (Rabbinge, 1981).

The second set of three criteria refers to more basic characteristics of research, and the resulting software. Solidity refers to the soundness of the recommendations. No combination of data may lead to nonsense recommendations; and they should be in accordance with good agronomic practice. The updating facility is needed for tactical (in-season) adaptations, e.g. to a change in the spectrum of physiological races or in the sensitivity of fungi to fungicides. The upgrading facility is needed for gradual, iterative improvement of the software between growing seasons, as was (and still is) the case with EPIPARE. In this way, the best of our knowledge finds its way directly to the farmer's field. At the same time,

scientists can adjust their research efforts. This is a comparative advantage of computerized decision support systems.

Most of the computerized services require a fee of some kind, some services being strictly commercial, others (e.g. EPIPARE) requiring at least partial coverage of costs. The grower will be prepared to pay a fee if he thinks he can profit from the message obtained. He will not accept a computer-generated message as being imperative (process computers excepted). We expect more and more growers to make a habit of considering computer-generated messages before making a decision. Two points must be made here. (1) A grower will consider both profit and risk, two essentially different concepts. Both are stochastic variables, but present computer-generated messages are deterministic. EPIPARE considers profit but not risk. In another upgrade, variations in profit and risk could be made explicit, even if they could not be calculated accurately. (2) The computer-generated message must be inherently better than messages generated in other ways, especially those generated in print. Speed of delivery is seldom an argument, because the difference in arrival time between a computer-generated and a printed message is only a matter of hours. Any printed message is of a general nature, containing, say, 80% accuracy for 80% of the growers, but this message is possibly wrong for some of them. In this respect, the present VIDITEL messages are little more than modernized press issues, old wine in new bottles.

The comparative advantage of a computer-generated message must be such that a grower is ready to pay for it and, under the present imperfect conditions, to accept some extra inconvenience. The message has additional value if the general knowledge, as provided by the scientist, is matched to the specific situation of the grower. Growers have been trained to do the matching themselves. Scientists, without farm experience, do not know much about specifics. Scientists were never trained to do this matching of the general with the specific. On the contrary, their training was to disregard the specific and to find the general by the process of abstraction. Today's challenge is different (Zadoks, 1986). Successful computerization depends on the scientist's capability to provide messages that do match general knowledge to specific situations. The matching process demands considerable intellectual effort on the part of the scientist. The program selecting the best bull for any specific cow, whose production and inheritance data are available, obeys our matching criterium. The EPIPARE system also does this in the crop protection area. To give just one example: if for some reason yellow rust (*Puccinia striiformis*) on wheat went out of control because of a cultivar's loss of resistance, or because the fungus became resistant to the fungicide normally used (an improbable event), EPIPARE would recommend omitting the last top-dressing of nitrogen. This top-dressing is usually applied just before flowering and by omitting it, the development of the epidemic, which is stimulated by nitrogen-rich leaf material, is no longer stimulated.

6.1.8 *Simulation applied*

Simulation is a tool used by the scientist to model a segment of the real world and to see how that real world might react under a variety of conditions. By either simplification, as in EIPRE (Zadoks, 1988), or by completely different approaches, the resulting messages can be listed as recommendations to the growers. These lists will usually be written in the IF ... THEN ... mode, arranged in a time sequence in the form of a computerized decision support system with a clear comparative advantage. Dynamic simulation provides a good start, but it does not provide the end point. This is true for the grower and, *a fortiori*, is true for a government faced with situations of far greater complexity than those of individual growers.

6.1.9 *Comprehensiveness*

If one wants to develop marketable agro-software, which is really going to gain impetus, there will be a conflict of interest between local computer services and distant computer services. Maybe there will be room for both and, in the long run, possibly a coupling between the two systems. An interim solution is partial decentralization, as foreseen by the cooperative organization in the Netherlands, whose farm advisers will use microcomputers and software provided by one distribution centre. Growers, though willing to use computers if they increase profits, are not computer hobbyists. They will require (1) foolproof systems and (2) systems that have obvious advantages over a few books. Here, we touch on the subject of comprehensiveness.

In the past, simulation models developed like trees trying to incorporate as many variables as could reasonably be useful. As indicated in Chapter 1, an optimum should be found for the number of state variables that harmonizes the conflicting trends towards completeness of the model; i.e. accuracy and practicality. This is not, however, the comprehensiveness intended here. A compromise is needed. The early, simulation-based EIPRE system almost failed to be accepted, not because of its inaccurate predictions, but because it was only concerned with yellow rust (*Puccinia striiformis*). Wheat farmers had more problems than yellow rust alone. Since the fungicide triadimefon, available at that pioneer time, was as good against mildew (*Erysiphe graminis*) as against yellow rust, farmers wanted, as a minimum requirement, recommendations concerning both diseases. In the future, farmers will not readily accept one piece of software with disease warnings, another for nitrogen fertilization, a third for weed control, and still another for bookkeeping and stock administration. Single-issue software is not marketable. Good agro-software should have all these items in one, with easy switching between modules. When a farmer makes and carries out a decision, he only wants to have to enter it once and then expects it to be entered into all relevant registers; simultaneously, all relevant modules should be updated and ready for consultation.

The comprehensiveness outlined here is very demanding on space and speed of hardware and software. The grower-orientated software will, therefore not pay much attention to simulation models for immediate application, but will give preference to simple decision structures such as decision trees or networks (Norton, 1982), or simple projections with a limited time horizon (Zadoks, 1988) for threshold-based (Zadoks, 1985) decisions. Of course, these may have their roots in explanatory simulation models, summary models, or models which emulate simulation techniques. Typical examples are the decision systems for weed control (Aarts & de Visser, 1985; de Visser et al., 1986) advocated by the Research Institute for Arable Crops (PAGV, Lelystad), which were incorporated in a VIDITEL-transmitted advisory system in a 1987 trial run. The best example of a comprehensive package is COMAK^(R), which contains administrative modules, a disease identification module, and an EIPRE-like decision support module. If computerization in agriculture by way of local computers is going to be successful, it will be because of the comprehensiveness of the software available for everyday access.

For services provided through distant computers, with direct or mediated access, there will be plenty of scope. Direct access is good for the fast transmission of general messages, but there are some doubts about the interactive use of distant computers. Matching of general and specific knowledge is needed for managerial purposes. Special purpose services using distant computers, to be consulted at more widely spaced intervals, as in cattle breeding, will remain extremely useful. In view of the expectations outlined here, there seems to be little scope for the use of simulation models in advisory work through distant computers.

6.1.10 Conclusions

Simulation models, be they explanatory or summary, may be a good basis on which to develop decision support systems, but they are not (yet) suitable for immediate on-the-farm application. Decision support systems could be constructed without simulation models. Simulation models should, however, be used to condense, formulate, test and validate that particular mix of intuition, experience and knowledge, which we endearingly call 'green brains'. For the crop-protection scientist, dynamic simulation is a scientific tool of great value, but it is certainly not an end in itself.

Answers to the exercises

Exercise 1

- distance time^{-1} , time^{-1} , time^{-1} .
- the terms that are added or subtracted should have the same dimensions. The dimensions of the expressions on both sides of the equal sign should be identical. In multiplication and division identical dimensions cancel out. The arguments of exponentials, logarithms and angles should be dimensionless.

Exercise 2

- The slopes of the different lines represent the time derivatives of the variable on the y axis.
- (the dimension of the state variable) time^{-1} .
- The numerical value of the slope in the graph depicting Equation 4 does not change; it is equal to the constant c . The numerical values of the slopes in the graphs depicting Equations 5 and 6 increase and decrease, respectively, with increasing time.
- The graphs depicting Equations 1, 2a and 3a give the slopes as a function of time. These time derivatives are constant, increasing and decreasing in time, respectively.

Exercise 3

The results of the numerical integration are:

t	0	2	4	6	8	10
W	0	8	12	14	15	15.5

- The numerical solution overestimates the analytical solution because it is assumed that the rate is constant during the time interval of integration, while in fact it decreases (see graph depicting Equation 3a).
- When the maximum level is reached. This is the case after a long time, in principle when t approaches infinity.
- The process is twice as slow.

Exercise 4

- For $\Delta t = 1 \cdot c^{-1}$ the tank is filled after one time step, no inflow occurs thereafter.
For $\Delta t = 1.5 \cdot c^{-1}$ the amount of water in the tank oscillates about the equilibrium level, but eventually settles at this level.
For $\Delta t = 2 \cdot c^{-1}$ an oscillation about the equilibrium level between the limits 0 and $2 \cdot W_m$ is obtained.
For $\Delta t = 2.5 \cdot c^{-1}$ the result is an oscillation with divergence.
- For $\Delta t \geq c^{-1}$ the results do not reflect reality at all.

- d. Δt should be less than $0.5 \cdot c^{-1}$. As a first approximation Δt should be set at about one-tenth of c^{-1} .

Exercise 5

- a. The rate equation is given by $dW/dt = 1/\tau \cdot (W_m - W)$. The change during a time interval equal to τ , and with a constant rate equals $\tau \cdot 1/\tau \cdot (W_m - W) = W_m - W$. Thus, the difference between the equilibrium value, W_m , and W is eliminated within a single time interval equal to the time coefficient.
- b. In a positive feedback loop in case of exponential growth, the change is directed away from the equilibrium state, so the extrapolation of the tangent must be reversed, and directed towards the unstable equilibrium state; the tangent cuts the horizontal equilibrium line a time coefficient interval earlier.

Exercise 6

- a. The time coefficients are: 0.67; 5; 20 year.
- b. One-tenth of τ . However, these data should be rounded off to the nearest smaller value that is an integral fraction of the output interval. For instance, 0.067 will become 0.05, but 0.5 and 2 years may be appropriate for output intervals.
- c.1. 271.83 after 5 years.
- c.2.
- | | | | | | | |
|---|-----|-----|--------|--------|--------|--------|
| t | 0 | 1 | 2 | 3 | 4 | 5 |
| A | 100 | 121 | 146.41 | 177.16 | 214.36 | 259.37 |
- e. During Δt the rate of increase is assumed to be constant, but in fact it increases exponentially, as shown in the graph depicting Equation 2a. After the first time interval the amount is underestimated, and consequently the rate for the next time interval is underestimated, and so on. As time proceeds, the discrepancy between the numerical and analytical solution becomes larger. This error propagation will be discussed in Section 2.1.7.

Exercise 7

Use Equation 5. Then $t(2) = \tau \cdot \ln 2 \cong 0.7 \cdot \tau$. Similarly, the half-life is defined as the time necessary to reach half the original amount. For exponential decrease, $t(1/2) \cong 0.7 \cdot \tau$.

Exercise 8

The question is whether the average residence time equals τ . This is the case:

$$\tau = \frac{1}{A_0} \int_0^{\infty} A \cdot dt = \int_0^{\infty} e^{-t/\tau} dt = [-\tau \cdot e^{-t/\tau}]_0^{\infty} = \tau.$$

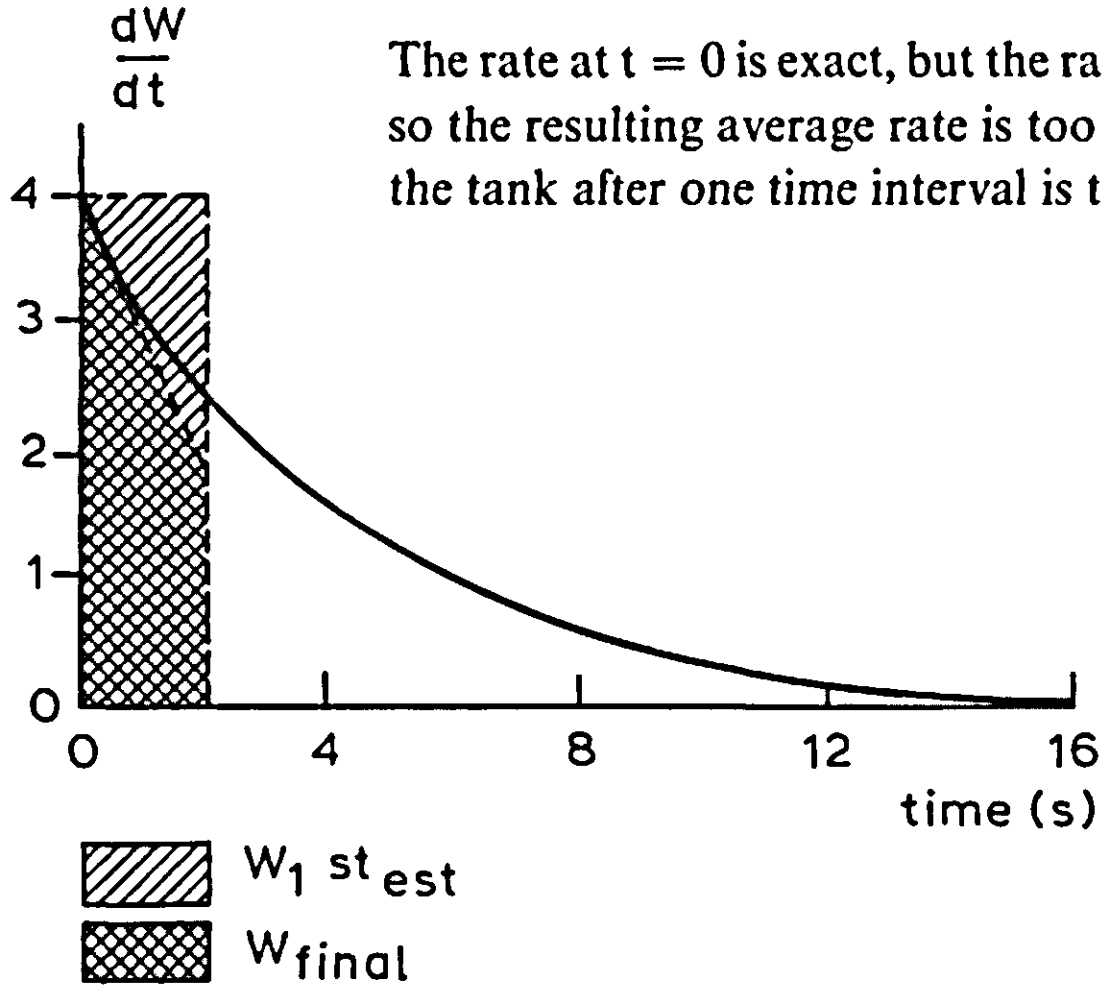
Exercise 9

The results of the numerical integration are:

t	0	2	4	6	8	10
W	0	6	9.75	12.09375	13.5586	14.4741

(Decimals have been given for comparative purposes only.)

- a. The numerical solution underestimates the analytical solution.



Exercise 10

Starting with the values $W_0 = 0$ l; $W_m = 16$ l; $\Delta t = 2$ s; and $c = 0.25$ s⁻¹, the intermediate rates are $R_1 = 4$, $R_2 = 3$, $R_3 = 3.25$ and $R_4 = 2.375$ s⁻¹, resulting in a W at 2 s equal to 6.2916 l. The analytical solution is 6.2955 l.

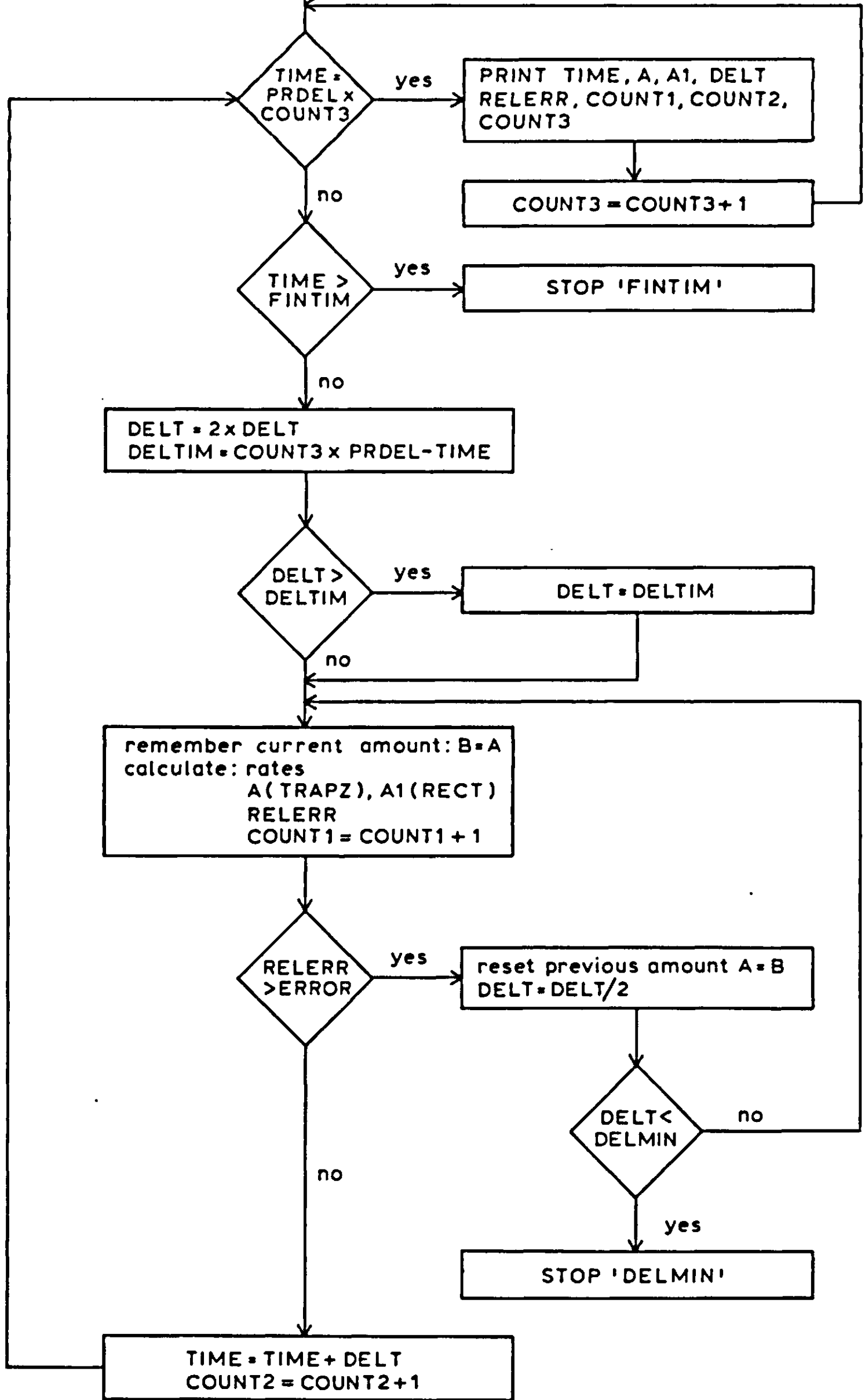
Exercise 11

Flow diagram of listing of Figure 9.

TIAL

setting of initial values of variables:
 time variables: TIME, FINTIM, PRDEL, DELMIN, DELT
 counters: COUNT1, COUNT2, COUNT3
 other variables: A, RGR, ERROR

NAMIC



Exercise 12

- The results of the rectangular- and trapezoidal methods are $A_{t+\Delta t} = 0$ and $A_{t+\Delta t} = 50$, respectively.
- When a division by Δt occurs in a model, the rectangular method must be applied.

Exercise 13

- $\Delta t = 0.02 \cdot \tau$; $\Delta t = 0.12^{\frac{1}{2}} \cdot \tau$; $\Delta t = 28.8^{\frac{1}{2}} \cdot \tau$
- 1.7183; 1.0; 1.8591; 1.7189

Method	Rectangular	Trapezoidal	Runge-Kutta
exact absolute error	$-7.18 \cdot 10^{-1}$	$14.09 \cdot 10^{-2}$	$5.79 \cdot 10^{-4}$
exact relative error	$-4.18 \cdot 10^{-1}$	$8.20 \cdot 10^{-2}$	$3.37 \cdot 10^{-4}$
estimated relative error (Table 3)	$-5.0 \cdot 10^{-1}$	$8.33 \cdot 10^{-2}$	$3.47 \cdot 10^{-4}$

The estimates are good approximations of the relative errors of the numerical integration methods.

Exercise 14

- $\Delta t = 0.02 \cdot \tau$; $\Delta t = 0.06^{\frac{1}{2}} \cdot \tau$; $\Delta t = 1.2^{\frac{1}{2}} \cdot \tau$
- 2.0; 2.5; 2.7083; 2.7183. Note that the initial value of the integral must be added to the analytical result to make a proper comparison with the numerical integration methods.

Method	Rectangular	Trapezoidal	Runge-Kutta
exact absolute error	$-7.18 \cdot 10^{-1}$	$-21.83 \cdot 10^{-2}$	$-9.95 \cdot 10^{-3}$
exact relative error	$-2.64 \cdot 10^{-1}$	$-8.03 \cdot 10^{-2}$	$-3.66 \cdot 10^{-3}$
estimated relative error (Table 3)	$-5.0 \cdot 10^{-1}$	$-16.67 \cdot 10^{-2}$	$-8.33 \cdot 10^{-3}$

The exact relative errors are overestimated by a factor of two by the expressions in Table 3. This discrepancy is due to the large ratio of Δt to τ ; in this case, omission of the higher order terms in the Taylor expansion (Appendix 2) is not justified. When Δt is taken to be about one-tenth of τ , or is adjusted to yield a reasonable error, the estimates are in good agreement with the exact relative errors made.

Exercise 15

It is known that with a fixed sugar concentration the yeast grows exponentially, i.e. as described by Equation 5. Expressing $c (= \mu)$ explicitly in Equation 5 gives:

$\mu = (\ln(y/y_0))/t$. A plot of $\ln(y/y_0)$ versus t will give a straight line with slope μ . Plot the data of Exercise 15 in a graph and calculate μ from $\mu = \Delta(\ln(y/y_0))/\Delta t$.

a. The results should be as follows:

Sugar concentration, c_s	0	0.02	0.05	0.10
$\mu \text{ h}^{-1}$	0.0	$4.17 \cdot 10^{-2}$	$1.04 \cdot 10^{-1}$	$2.08 \cdot 10^{-1}$
$\mu \text{ d}^{-1}$	0.0	1.0	2.5	5.0

b. The general equation for a straight line is $\mu = a \cdot c_s + b$. The intercept $b = 0$ and the slope $a = \mu_{10}/c_{s10}$ thus $\mu = (\mu_{10}/c_{s10}) \cdot c_s$.

c. The concentration of sugar is defined as the weight of sugar per weight of water and is, thus, proportional to the amount of sugar. The same is true for c_{s10} , which is simply a particular value of the sugar concentration. The equation may, therefore, be written as $\mu = \mu_{10} \cdot (s/s_{10})$.

Exercise 16

a. Use the dimension rules of Exercise 1b.

b. From dimensional analysis it follows that 1000 has the dimension kg m^{-3} . Thus, 1000 denotes the density of water.

Note that this number actually varies between 998.2 and 933.7 kg m^{-3} for 0 and 10% glucose, respectively. (Handbook of Chemistry and Physics, 1974–1975 (D205)).

Exercise 17

Expressing t explicitly gives $t = -\tau \cdot \ln(1 - s/s_m)$, so $t_{95} = -\tau \cdot \ln(0.05) \cong 3 \cdot \tau$.

Exercise 18

This time is equal to the volume of the vessel divided by the inflow rate of the sugar solution, which is equal to the time coefficient. Thus, 100% of the equilibrium level is reached after time $t_{100} = \tau$.

Note: in this case the rate is constant during the whole filling period, therefore, the increase of the contents is linear.

Exercise 19

Insert Equation 14 into Equation 13 and set dy/dt equal to zero to obtain Equation 19. Set ds/dt in Equation 17 equal to zero, and write y explicitly to obtain

$$y = \frac{1}{s_y} \cdot \left(c_s \cdot q \cdot 1000 - \frac{s}{\tau} \right)$$

Multiply the first term within brackets by v/v , use Equation 16 to replace the quotient q/v , and replace $c_s \cdot v \cdot 1000$ by s_m to obtain Equation 20.

Exercise 20

$$\begin{aligned} \frac{dy}{d\tau} &= \frac{d}{d\tau} \left(\frac{1}{\tau \cdot s_y} \cdot \left(s_m - \frac{s_{10}}{\mu_{10} \cdot \tau} \right) \right) \\ &= \frac{s_m}{s_y} \cdot \frac{d}{d\tau} \left(\frac{1}{\tau} \right) - \frac{s_{10}}{\mu_{10} \cdot s_y} \cdot \frac{d}{d\tau} \left(\frac{1}{\tau^2} \right) \end{aligned}$$

Apply the rule for differentiating a quotient $y = u/v$ to each term:

$$y' = \frac{u' \cdot v - v' \cdot u}{v^2}, \text{ where } u' \text{ and } v' \text{ stand for the first derivative of the numerator and}$$

the denominator, respectively, both with respect to x (of which u and v are functions).

Take $1/(s_y \cdot \tau^2)$ outside the brackets to obtain Equation 21.

- b. A maximum or minimum occurs when $dy/d\tau = 0$. This is the case when $2 \cdot s_{10}/(\tau \cdot \mu_{10}) = s_m$ or when $\tau = 2 \cdot s_{10}/(\mu_{10} \cdot s_m)$.

Exercise 21

- a. A summary of the dimensions of the individual terms is:

s_{10}, s_m, s : kg of sugar ; μ_{10} : d^{-1} ; τ : d; s_y : kg of sugar per kg of yeast per day.

- b. The optimum τ is given in the answer of Exercise 20b. Substituting that expression in Equation 16, and replacing s_m by $c_s \cdot v \cdot 1000$, gives the flow rate:

$$q = c_s \cdot v^2 \cdot \mu_{10} \cdot 500/s_{10}.$$

Exercise 22

TITLE EGG DELAY

OUTFL = DELAY(20,PERIOD,INFL)

INFL = AFGEN(INFLTB,TIME)

FUNCTION INFLTB = 0.,0., 1.,100., 2.,100.,3.,0., 50.,0.

PERIOD = 20.

TIMER FINTIM = 30., PRDEL = 1., DELT = 1.

METHOD RECT

PRINT INFL, OUTFL

END

STOP

ENDJOB

Exercise 23

Between 6°C and 25°C, the following relation exists:

degree-days = (temperature-threshold temperature) • duration

490 = (TA - 6) • duration

At 10°C, the period will be $490/(10 - 6) = 122.5$ days and the rate of development will be $(15 - 9)/122.5 = 0.049 \text{ day}^{-1}$.

At 20°C, these values will be $490/(20 - 6) = 35$ days and $(15 - 9)/35 = 0.171 \text{ day}^{-1}$, respectively.

Exercise 24

In the same way as in Exercise 23, the development rate at 25°C can be calculated: 0.233 day⁻¹. TA can be set to 10°C or 20°C.

```
TITLE DEVELOPMENT OF RAPE SEED
STAGE = INTGRL(9.,DEVR)
DEVR = AFGEN(DEVRTB,TA)
FUNCTION DEVRTB = 0.,0., 6.,0., 25.,0.233, 30.,0.233
TA = 10.
TIMER FINTIM = 130., PRDEL = 1., DELT = 1.
METHOD RECT
PRINT STAGE, DEVR
END
STOP
ENDJOB
```

Exercise 25

The value of γ is $(15 - 9)/4 = 1.5$. The development rate is the inverse of the duration between stage 9 and stage 15 (in day⁻¹). The resetting occurs after 1.5 stage units (γ), this is after $1/4 \cdot 490 = 122.5$ degree-days.

Exercise 26

$$\left. \begin{array}{l} T_{\text{tot}} = 20 \\ \sigma_{\text{tot}} = 2 \end{array} \right\} \left. \begin{array}{l} \frac{\sigma_{\text{tot}}}{T_{\text{tot}}} = 2/20 = 1/10 \\ \frac{\sigma_{\text{tot}}}{T_{\text{tot}}} = 1/\sqrt{N} \end{array} \right\} N = 100$$

Exercise 27

See text.

Exercise 28

The delay period, calculated by hand, is $1/\text{DEVR} = 1/0.005 = 200$. Its variance, calculated by hand, is :

$$\begin{array}{l} \sigma_{\text{tot}}/T_{\text{tot}} = 1/\sqrt{N} \\ T_{\text{tot}} = 200 \quad \sigma_{\text{tot}}^2 = 200^2/5 = 8000. \\ N = 5 \end{array}$$

The simulated value of ADP and VAR at time 1000 are 200.0 and 7799.8 respectively. These values only mean anything at time 1000, when all individuals have flown out of the last boxcar. Only then does AOUT equal 1.

Exercise 29

Use the listing of Figure 21.

TBR is made constant and set to 1000 girls per year, therefore

$$TBR = 0.$$

and $TBR = TBR + A(I) * AFGEN(RBRTB, AGE(I)) * FRGIRL$

are replaced by the single statement

$$TBR = 1000.$$

The birth rate per age class is now $1000 \cdot \text{length age class}$, in this case 5 years, so that the birth per age class amounts to 5000 girls.

The fraction of survival and the age distribution are calculated by:

STORAGE FS(20), FRACA(20)

$$FS0 = A0/5000$$

$$FRACA0 = A0/ATOT$$

DO I = 1, 20

$$FS(I) = A(I)/5000$$

$$FRACA(I) = A(I)/ATOT$$

ENDDO

TIMER FINTIM = 100., PRDEL = 20., DELT = 1.

PRINT FRACA0, FRACA(1-20), FS0, FS(1-20)

The simulated fraction of survival (FS) and the age distribution after 100 years as a function of the age is:

Mean age	Age distribution	FS
2.5	0.0675	0.987
7.5	0.0667	0.975
12.5	0.0665	0.972
17.5	0.0664	0.971
22.5	0.0663	0.969
27.5	0.0661	0.967
32.5	0.0659	0.964
37.5	0.0656	0.959
42.5	0.0651	0.951
47.5	0.0641	0.937
52.5	0.0626	0.915
57.5	0.0605	0.885
62.5	0.0580	0.848
67.5	0.0541	0.791
72.5	0.0475	0.695
77.5	0.0355	0.520
82.5	0.0177	0.259
87.5	0.0039	0.057
92.5	0.0001	0.001
97.5	0.0000	0.000

Exercise 30

Again, we use the listing of Figure 21

TIMER FINTIM = 1000., PRDEL = 100., DELT = 1.

The total simulated female population grows from $6.42 \cdot 10^6$ (TIME = 0) to $2.89 \cdot 10^{10}$ (TIME = 1000). The simulated age distribution is:

Mean age	Age distribution
2.5	0.0895
7.5	0.0848
12.5	0.0811
17.5	0.0777
22.5	0.0744
27.5	0.0712
32.5	0.0680
37.5	0.0649
42.5	0.0617
47.5	0.0583
52.5	0.0546
57.5	0.0507
62.5	0.0466
67.5	0.0416
72.5	0.0351
77.5	0.0252
82.5	0.0120
87.5	0.0025
92.5	0.0001
97.5	0.0000

Exercise 31

At time $t = 0$ the size of the population is Y_0 , so

$$Y_0 = \frac{Y_m}{1 + K \cdot e^{-r \cdot 0}} = \frac{Y_m}{1 + K \cdot 1}$$

$$(1 + K)Y_0 = Y_m, KY_0 = Y_m - Y_0 \text{ and } K = (Y_m - Y_0)/Y_0$$

Exercise 32

TITLE PARALOGISTIC GROWTH

INITIAL

INCON LATINI=50., INFINI=1., NLINFI=1.
PARAM R=8., LP=4., IP=4.
PARAM NMAX=1.E10

DYNAMIC

LAT =INTGRL(LATINI, RIR - EIR)
INF =INTGRL(INFINI, EIR - REM)
NLINF =INTGRL(NLINFI, REM)

RIR =R * INF * (1.- OCC/NMAX)
EIR =LAT/LP
REM =INF/IP

OCC =LAT + INF + NLINF
LOGLAT=ALOG10(LAT)
LOGINF=ALOG10(INF)
LOGNLI=ALOG10(NLINF)
LOGOCC=ALOG10(OCC)
LOGNMA=ALOG10(NMAX)

TIMER FINTIM=50., DELT=0.05, PRDEL=1.
PRINT LOGLAT,LOGINF,LOGNLI,LOGOCC,LOGNMA
METHOD RECT
END
STOP
ENDJOB

Exercise 33

$$\text{LAT} = Y_t - Y_{t-p}$$
$$\text{INF} = Y_{t-p} - Y_{t-p-i}$$
$$\text{NLINF} = Y_{t-p-i}$$

Exercise 34



The relation between temperature and development rate is given in the figure. The development rates at various temperatures are found by interpolation.

Development stage:

- After 3 days at 15°C development status = $3 \cdot 0.125 = 0.375$;
- $3 \cdot 0.5 \cdot 0.0875 + 3 \cdot 0.5 \cdot 0.2 = 0.131 + 0.300 = 0.431$;
- After 3 days at fluctuating temperatures 12 h 2°C and 12 h 18°C.
 $3 \cdot 0.5 \cdot 0 + 3 \cdot 0.5 \cdot 0.20 = 0.30$ when fluctuating,
 $3 \cdot 0.063 = 0.189$ when constant 10°C for 3 days.

As a result of the non-linearity in the temperature response, the development stages at constant and fluctuating temperatures are different. This difference is stronger when temperatures are below the threshold value, as illustrated in the fluctuation between 2°C and 18°C.

Exercise 35

Relative mortality of the spores (RMRISP), if computed as a proportion of the number of spores, will be considerably underestimated. This is due to the positive feedback in the exponential decrease, which results in a larger relative mortality rate. The relative mortality should be calculated as $Y_t = Y_0 e^{-\text{RMRISP} \cdot t}$, in which t is the germination period. If the proportion of non-germinating spores (dying) spores is large, there is a considerable difference between this proportion and the relative mortality.

$\text{RMRISP} = -\ln(Y_t/Y_0)/\text{GP} = -\ln(\text{GF})/\text{GP}$, in which GF is the germinated fraction and GP the germination period.

GF	(1 - GF) = proportion spores	-ln(GF) = RMRISP (if GP = 1)
.99	.01	.01005
.95	.05	.0513
.9	.1	.105
.8	.2	.223
.5	.5	.69
.1	.9	2.3

This table demonstrates that at low fractions of non-germinating spores, the difference is unimportant, but that at high fractions (GF < 0.8) the errors exceed 10%, and are unacceptable.

Exercise 36

Note: Humidity is not a restriction for the development of a powdery mildew epidemic, so that only the temperature is included as a forcing function.

The number of boxcars introduced into the subroutine is 4 for the latency period and 3 for the infectious period. This is based on the computation of the relative dispersion at different temperatures. At 30°C the relative dispersion (SD/X) of the latency period is 1/2.2, so the upper limit of boxcars is $(2.2/1)^2 = 4.84$, by rule of thumb we take $3/4 \cdot 4.84 = 3.63$, equivalent to 4 boxcars ($N < \text{the minimum value of } (X/SD)^2$).

The other data in the function are based on guesses rather than actual experiments. The time step of integration is based on the shortest residence time in one of the boxcars of INF; at 30°C this is 1 day in 3 boxcars, so 0.33 days in each boxcar; this results in an estimate for the time step of $0.1 \cdot 0.33 = 0.033$ days, so that a time step of 0.05 day is acceptable.

Exercise 37

The values of b and a are: $b = 25 \text{ m}^{-2} \text{ s}^{-1}$; $a = 0.091 \text{ m s}^{-1}$.

The time coefficient is equal to L/a , which has the value 187 s.

Exercise 38

The equilibrium spore concentration is $275 \text{ spores m}^{-3}$.

Integration of $dc_i/dt = b/L - (a/L)c_i$ gives (Equation 44)

$$c_{i(t)} = (c_{i(0)} - b/a) \cdot e^{-(a/L) \cdot t} + b/a$$

or

$$c_{i(t)} = (c_a - c_{eq}) \cdot e^{-(a/L) \cdot t} + c_{eq}$$

After 3 time coefficients ($t = 3 \cdot (L/a)$; ca. 10 minutes) $c_i = 266 \text{ spores m}^{-3}$, that is within 5% of c_{eq} .

Exercise 39

+0.006	-0.006	0	0
-0.005	+0.026	-0.021	0
0	-0.02	+0.161	-0.101
0	0	-0.1	+0.351

 \times

c_1
c_2
c_3
c_4

 $=$

20
0
0
25.1

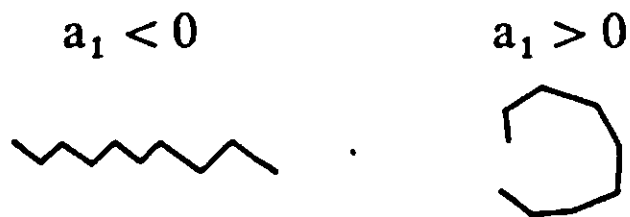
The solution is $c_1 = 4333$, $c_2 = 1000$, $c_3 = 206$ and $c_4 = 130$.

Exercise 40

$$A_s = a_1 A_{s-1} + E_s$$

If $a_1 < 0$, then a left turn will tend to be followed by a right turn, so the overall walking pattern will be relatively straight.

If $a_1 > 0$, however, the animal will tend to continue turning in one direction:



Exercise 41

$$\lambda = 1 \rightarrow Y_p = \{p - (1 - p)\} = -1 + 2p$$

$$E_s = \mu + \sigma Y_p = \mu - \sigma + 2\sigma p$$

i.e. the approximation is perfect

$$\mu - \sigma \leq E_s \leq \mu + \sigma$$

μ expresses the tendency to turn left.

Exercise 42

When the hypothesis is true, a Poisson distribution is expected and the expected number of samples containing i individuals is calculated by

$$E_i = n \cdot P_i = n \cdot m^i e^{-m} / i!$$

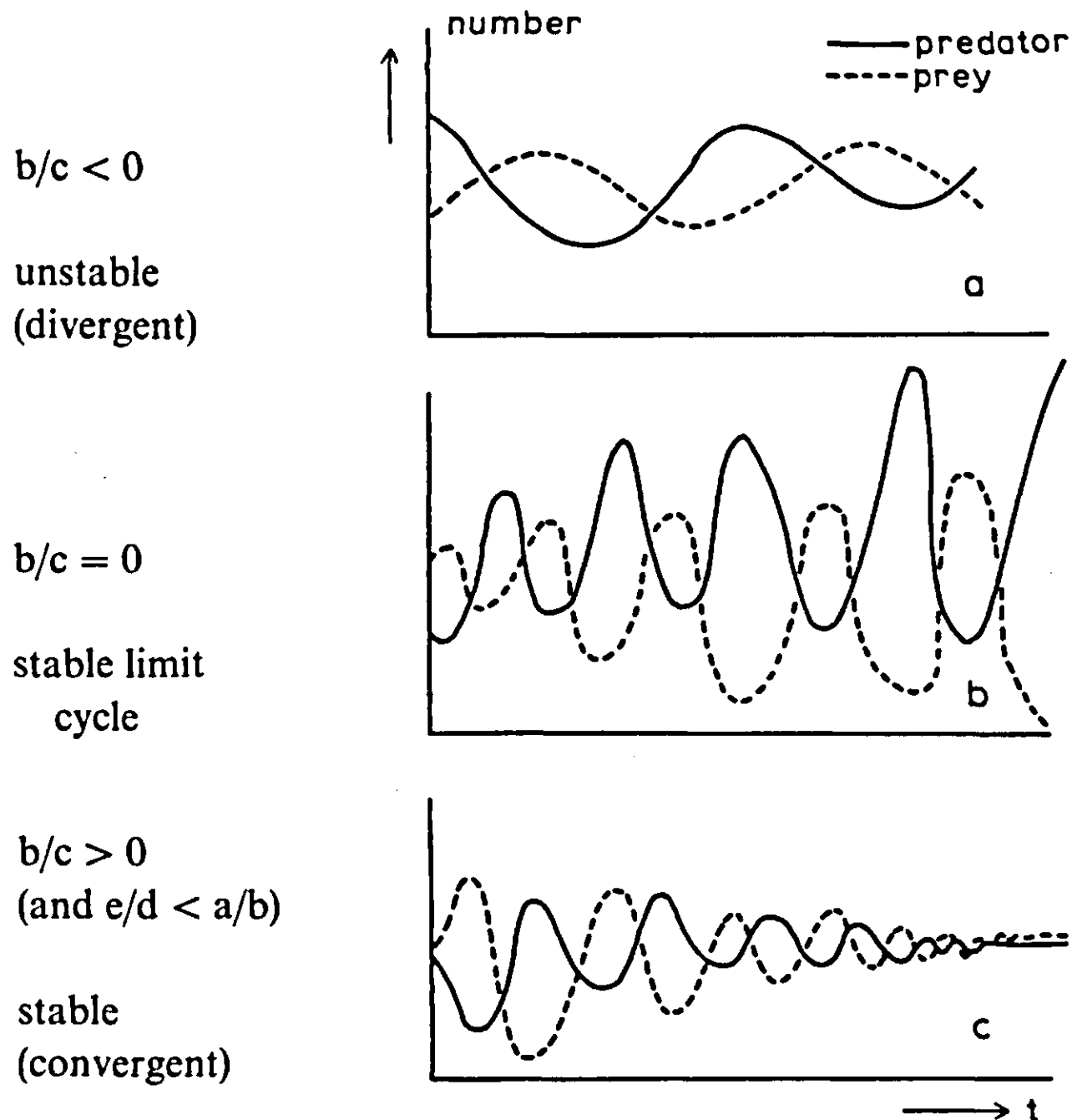
where n is the total number of samples, and m the sample mean (here 2.38 eggs per host larvae). A thorough comparison of observed and predicted distributions involves the calculation of χ^2 :

$$\chi^2 = \sum_i (O_i - E_i)^2 / E_i$$

where O_i is the observed number of host larvae containing i eggs and E_i is the number predicted from the theoretical distribution. In this case $\chi^2 = 20.64$, and from a basic statistical table it is found that $P(\chi_4^2 \geq 20.64) < 0.005$.

Therefore, the observed data do not support our hypothesis, on the contrary, they suggest that the parasitoids have some kind of preference. (4 is the number of degrees of freedom, calculated as (number of classes) - 1 - (number of estimated parameters) = 6 - 1 - 1 = 4).

Exercise 43



Fluctuations in prey and predator densities for different relations between b and c . When the ratio b/c equals 0, so $b = 0$, prey density reduction due to the predator is infinitely more important than prey density reduction due to intraspecific competition. This ratio results in a limit cycle. When $b/c < 0$, so when there is an increase in prey density due to intraspecific competition or due to predation of for example weak individuals, an unstable equilibrium will result with densities that vary with increasing amplitude. When $b/c > 0$, and $e/d < a/b$ a stable convergent equilibrium will result.

Exercise 44

Time coefficients: $1/a$, $1/e$.

Dimensions: a: time^{-1} ; b: $\text{prey}^{-1} \text{time}^{-1}$; c: $\text{pred}^{-1} \text{time}^{-1}$; d: $\text{prey}^{-1} \text{time}^{-1}$; e: time^{-1} .

Exercise 45

TITLE PREDATOR-PREY

INITIAL

INCON PREYI=10., PREDI=2.

PARAM A=0.1732, B=0.0577, C=0.1, D=0.1, E=0.2310

PARAM F=0.1, G=0.1

DYNAMIC

PREY = INTGRL(PREYI,RPREY)

PRED = INTGRL(PREDI,RPRED)

RPREY= (A - B*PREY) * PREY - C * PRED * (1.-EXP(-F*PREY))

RPRED= -E * PRED + D * PRED * PREY * (1.-EXP(-G*PREY))

TIMER FINTIM=50., DELT=0.4, OUTDEL=5.

OUTPUT PREY, PRED

METHOD RECT

END

STOP

ENDJOB

Exercise 46

TITLE STOCHASTIC PREDATION

INITIAL

FIXED M

M=315

PARAM NREP=50.

INCON SUMP=0., COUNT=0.

INCON PI=0.

DYNAMIC

P = INTGRL(PI, C * V**1.5)

V = RNDGEN(M)

PARAM C=8.

NOSORT

M = M+2

TIMER FINTIM=24., DELT=1.

METHOD RECT

TERMINAL

SUMP = SUMP + P

COUNT= COUNT + 1.

IF(COUNT.GE.NREP) GO TO 1

CALL RERUN.

GO TO 3

1 EP= SUMP/COUNT

WRITE (6,2) EP

2 FORMAT (' EP = ', F10.4)

3 CONTINUE

END

STOP

ENDJOB

TITLE DETERMINISTIC PREDATION

INITIAL
INCON PI= 0.

DYNAMIC
P = INTGRL(PI, C * V**1.5)
PARAM V= 0.5, C= 8.

TIMER FINTIM=24., DELT=1., OUTDEL=1.
METHOD RECT
OUTPUT P
END
STOP
ENDJOB

The simulated number of prey killed per day is 67.882 using the deterministic model.

The analytical solution is

$$P = PI + 24 \cdot C \cdot [\varepsilon(V)]^{3/2} \quad P = 0 + 24 \cdot 8 \cdot 0.5^{3/2}$$
$$\varepsilon(V) = 0.5 \quad = 67.9$$

The simulated number of prey killed per day is 77.03 using the stochastic model.

The analytical solution is:

$$P = PI + 24 \cdot C \cdot \varepsilon(V^{3/2})$$

$$\varepsilon(V^{3/2}) = \int_0^1 V^{3/2} dV = \left[\frac{2}{5} V^{5/2} \right]_0^1 = \frac{2}{5} = 0.4$$

$$P = 0 + 24 \cdot 8 \cdot 0.4 = 76.8$$

Exercise 47

With constant relative dispersion, N equals $(1/RD)^2$ (see Subsection 2.2.6), in which RD is the relative dispersion. The minimum value is reached at 30°C:

$$\text{EGG: } N = (5/1.25)^2 = 16$$

$$\text{J : } N = (2.5/0.65)^2 = 14$$

$$\text{JS : } N = (2/0.5)^2 = 16$$

This method can be used only if the relative dispersion is constant during the simulation. According to Table 9, this is only in cases of constant temperature. When the temperature varies, the fractional boxcar train should be used.

TITLE WINTER EGG HATCHING

STORAGE EGGI(12),EGG(12)
FIXED N

*-----
INITIAL
*-----

TABLE EGGI(1-12) = 1000.,11*0.
PARAM N = 12
*N has been calculated as 3/4 * 16
HATCH = 0.

*-----
DYNAMIC
*-----

* temperature during the day
TEMP = AVTMP + AMPTMP*(-COS(2.*PI*TIME))
PARAM PI = 3.141529
AMPTMP = (30.-15.)/2.
AVTMP = 15.+(30.-15.)/2.

*relative mortality rate
RMR = 0.

*DEVRT = 1/residence time
DEVRT = AFGEN(DEVRT,TEMP)
FUNCTION DEVRT= 15.,0.0560, 18.,0.1000, 25.,0.1587, 30.,0.2000

*RD = relative dispersion
* = standard deviation/residence time
RD = AFGEN(RDT,TEMP)
FUNCTION RDT = 15.,0.1670, 18.,0.1600, 25.,0.1680, 30.,0.2500

NOSORT
INFLO = 0.
EGGO,EGG,EGGTOT,MORFL,OUTFL,GAMMA,GCYCL=...
BOXCAR(1,EGGI,DEVRT,RD,RMR,INFLO,N,DELT,TIME)
HATCH=HATCH+OUTFL*DELT
SORT

TOTAL = EGGTOT+HATCH

TIMER FINTIM=15.,PRDEL=0.08,DELT=0.08
PRINT TEMP,EGGO,EGG(1-12),EGGTOT,OUTFL,HATCH,TOTAL
METHOD RECT
END
STOP

C*****C
SUBROUTINE BOXCAR(COUNT,AI,DEVRT,RD,RMR,INFL,N,DELT,TIME,
\$ AO,A,ATOT,MORFL,OUTFL,GAMMA,GCYCL)
C*****C

$$N_t = N_0 \cdot e^{-RMR \cdot t}$$

$$N_t = 0.50 \cdot N_0 \quad 0.50 = e^{-RMR(2.5)} \quad RMR = 0.28$$

At 30°C, t = 2.5 days

Exercise 48

TITLE DEVELOPMENT EGGS INTO ADULTS

STORAGE EGGI(12),EGG(12)
STORAGE JI(10), J(10)
STORAGE JSI(12), JS(12)
FIXED NE, NJ, NJS

*-----

INITIAL

*-----

TABLE EGGI(1-12) = 1000.,11*0.

TABLE JI(1-10) = 10*0.

TABLE JSI(1-12) = 12*0.

PARAM NE=12, NJ=10, NJS=12

*N has been calculated as $3/4 * 16$, $3/4 * 14$ and $3/4 * 16$ resp.

ADULT = 0.

*-----

DYNAMIC

*-----

*temperature during the day

TEMP = AVTMP + AMPTMP*(-COS(2.*PI*TIME))

PARAM PI = 3.141529

AMPTMP = (30.-15.)/2.

AVTMP = 15.+(30.-15.)/2.

*relative mortality rate for each stage

RMRE =0.

RMRJ =0.

RMRJS =0.

*DEVRE = development rate = 1/residence time

DEVRE = AFGEN(DEVRET,TEMP)

FUNCTION DEVRET= 15.,0.0560, 18.,0.1000, 25.,0.1587, 30.,0.2000

DEVREJ = AFGEN(DEVREJT,TEMP)

FUNCTION DEVREJT= 15.,0.0990, 18.,0.1538, 25.,0.2500, 30.,0.4000

DEVREJS = AFGEN(DVRJST,TEMP)

FUNCTION DVRJST= 15.,0.1818, 18.,0.2326, 25.,0.4167, 30.,0.5000

*RD = relative dispersion

* = standard deviation/residence time

RDE = AFGEN(RDET,TEMP)

FUNCTION RDET = 15.,0.1670, 18.,0.1600, 25.,0.1680, 30.,0.2500

RDJ = AFGEN(RDJT,TEMP)

FUNCTION RDJT = 15.,0.1980, 18.,0.2000, 25.,0.2000, 30.,0.2480

RDJS = AFGEN(RDJST,TEMP)

FUNCTION RDJST = 15.,0.2000, 18.,0.1977, 25.,0.2500, 30.,0.2500

NOSORT

INFLO = 0.

EGGO, EGG, EGGTOT, MORFLE, OUTFLE, GAMMAE, GCYCLE=...

BOXCAR(1, EGGI, DEVRE, RDE, RMRE, INFLO, NE, DELT, TIME)

JO, J, JTOT, MORFLJ, OUTFLJ, GAMMAJ, GCYCLJ=...

BOXCAR(2, JI, DEVREJ, RDJ, RMRJ, OUTFLE, NJ, DELT, TIME)

JSO, JS, JSTOT, MRFLJS, OUTFJS, GAMMJS, GCYCJS=...

BOXCAR(3, JSI, DEVREJS, RDJS, RMRJS, OUTFLJ, NJS, DELT, TIME)

ADULT =ADULT+OUTFJS*DELT

SORT

TOTAL = EGGTOT+JTOT+JSTOT+ADULT

```

TIMER FINTIM=25.,PRDEL=1.,DELT=0.03
METHOD RECT
PRINT TEMP,EGGO,EGG(1-12),EGGTOT,JO,J(1-10),JTOT,...
      JSO,JS(1-12),JSTOT,ADULT,TOTAL
END
STOP

```

```

C*****C
      SUBROUTINE BOXCAR(COUNT,AI,DEVR,RD,RMR,INFL,N,DELT,TIME,
      $                AO,A,ATOT,MORFL,OUTFL,GAMMA,GCYCL)
C*****C

```

Exercise 49

Within the subroutine BOXCAR all classes have the same physiological properties. Of course it is possible to calculate an average rate of oviposition, but for each age distribution the average rate of oviposition is different. Therefore, a method with discontinuous shifts should be used, so that mortality during development is considered and age dependence of oviposition is introduced.

Exercise 50

TITLE DEVELOPMENT EGGS INTO ADULTS

STORAGE EGGI(12),EGG(12)
STORAGE JI(10), J(10)
STORAGE JSI(12), JS(12)
STORAGE FLOW(5),RMRF(5),FECUN(5)
FIXED NE, NJ, NJS, NF, I

*-----
INITIAL
*-----

TABLE EGGI(1-12)=1000.,11*0.
TABLE JI(1-10)=10*0.
TABLE JSI(1-12)=12*0.
TABLE FI(1-5) = 5*0.
PARAM MI = 0.
PARAM FOLDI = 0.
PARAM NE=12, NJ=10, NJS=12, NF=5
EGGPRO=0.

*-----
DYNAMIC
*-----

*temperature during the day
TEMP = AVTMP + AMPTMP*(-COS(2.*PI*TIME))
PARAM PI = 3.141529
AMPTMP = (30.-15.)/2.
AVTMP = 15.+(30.-15.)/2.

*relative mortality rate for each stage

RMRE =0.
RMRJ =0.
RMRJS=0.
NOSORT
DO I=1,NF
RMRF(I) = TWOVAR(RMRFIT,TEMP,FLOAT(I))
ENDDO

SORT
FUNCTION RMRFIT,1.=10.,0.011, 15.,0.011, 20.,0.005, 25.,0.005, 30.,0.003
FUNCTION RMRFIT,2.=10.,0.033, 15.,0.031, 20.,0.049, 25.,0.050, 30.,0.027
FUNCTION RMRFIT,3.=10.,0.088, 15.,0.089, 20.,0.061, 25.,0.245, 30.,0.273
FUNCTION RMRFIT,4.=10.,0.150, 15.,0.138, 20.,0.360, 25.,0.504, 30.,0.709
FUNCTION RMRFIT,5.=10.,0.200, 15.,0.150, 20.,0.400, 25.,0.600, 30.,0.800
RMRM = AFGEN(RMRMT,TEMP)
FUNCTION RMRMT=10.,0.088, 15.,0.089, 20.,0.061, 25.,0.245, 30.,0.273

*DEVRE = development rate = 1/residence time

DEVRE = AFGEN(DEVRET,TEMP)
FUNCTION DEVRET= 15.,0.0560, 18.,0.1000, 25.,0.1587, 30.,0.2000
DEVREJ = AFGEN(DEVREJT,TEMP)
FUNCTION DEVREJT= 15.,0.0990, 18.,0.1538, 25.,0.2500, 30.,0.4000
DEVREJS= AFGEN(DVRJST,TEMP)
FUNCTION DVRJST= 15.,0.1818, 18.,0.2326, 25.,0.4167, 30.,0.5000
DEVRF = AFGEN(DEVRFRT,TEMP)
FUNCTION DEVRFRT= 10.,0.0417, 15.,0.0400, 20.,0.0769, 25.,0.1111,...
30.,0.1333

*RD = relative dispersion

* = standard deviation/residence time

RDE = AFGEN(RDET,TEMP)
FUNCTION RDET = 15.,0.1670, 18.,0.1600, 25.,0.1680, 30.,0.2500

```

RDJ = AFGEN(RDJT,TEMP)
FUNCTION RDJT = 15.,0.1980, 18.,0.2000, 25.,0.2000, 30.,0.2480
RDJS = AFGEN(RDJST,TEMP)
FUNCTION RDJST = 15.,0.2000, 18.,0.1977, 25.,0.2500, 30.,0.2500
*PDF = AFGEN(RDFT,TEMP)
*FUNCTION RDFT = 10.,0.6040, 15.,0.4800, 20.,0.3850, 25.,0.4110,...
*
*           30.,0.3200

```

```

NOSORT
DO I=1,NF
    FECUN(I) = TWOVAR(FECTI,TEMP,FLOAT(I))
ENDDO

```

```

SORT
FUNCTION FECTI,1.= 10.,0.6, 15.,1.2, 20.,1.9, 25.,3.1, 30.,4.2
FUNCTION FECTI,2.= 10.,0.5, 15.,1.2, 20.,2.2, 25.,3.7, 30.,5.5
FUNCTION FECTI,3.= 10.,0.5, 15.,1.1, 20.,1.8, 25.,3.1, 30.,3.8
FUNCTION FECTI,4.= 10.,0.4, 15.,1.0, 20.,1.4, 25.,2.0, 30.,1.4
FUNCTION FECTI,5.= 10.,0.2, 15.,0.8, 20.,0.8, 25.,1.0, 30.,0.8

```

```

NOSORT
*call of subroutine boxcar
EGGO,EGG,EGGTOT,MORFLE,OUTFLE,GAMMAE,GCYCLE=...
    BOXCAR(1,EGGI,DEVRE,RDE, RMRE,EGGPRO,NE,DELT,TIME)
JO ,J ,JTOT ,MORFLJ,OUTFLJ,GAMMAJ,GCYCLJ=...
    BOXCAR(2,JI,DEV RJ,RDJ, RMRJ,OUTFLE,NJ,DELT,TIME)
JSO ,JS ,JSTOT ,MRFLJS,OUTFJS,GAMMJS,GCYCJS=...
    BOXCAR(3,JSI,DEV RJ, RDJS, RMRJS,OUTFLJ,NJS,DELT,TIME)

```

```

SORT

```

```

*egg-producing females
F = INTGRL(FI,NFLOW,5)
PUSHF = INSW(OS-1.,0.,1.)
OS = INTGRL(0.,5.*DEVRF-PUSHF/DELT)

```

```

NOSORT
FLOW0 = 0.5*OUTFJS
DO I=1,NF
    FLOW(I) = PUSHF * (F(I)-F(I)*RMRF(I)*DELT)/DELT
ENDDO

```

```

NFLOW(1)=FLOW0-FLOW(1)-F(1)*RMRF(1)
DO I=1,NF
    NFLOW(I)=FLOW(I-1)-FLOW(I)-F(I)*RMRF(I)
ENDDO

```

```

*calculation of total egg production
EGGPRO=0.
DO I=1,5
    EGGPRO=EGGPRO + FECUN(I)*F(I)*DELT
ENDDO
SORT

```

```

*females, not producing eggs anymore (FOLD)
FOLD = INTGRL(FOLDI,FLOW(5)-MRFOLD)
MRFOLD= RMRF(5)*FOLD

```

```

*total females
NOSORT
FTOT=0.
DO I=1,NF
    FTOT=FTOT+F(I)
ENDDO
FTOT=FTOT+FOLD

```

SORT

*males

M = INTGRL(MI,0.5*OUTFJS-MRM)

MRM = RMRM*M

TIMER FINTIM=30., PRDEL=0.03, DELT=0.03

METHOD RECT

PRINT TEMP, EGG0, EGG(1), EGG(12), EGGTOT, JO, J(1), J(10), JTOT, ...
JS0, JS(1), JS(12), JSTOT, F(1-5), FOLD, FTOT, M

END

STOP

C*****C

SUBROUTINE BOXCAR(COUNT, AI, DEVR, RD, RMR, INFL, N, DELT, TIME,
\$ AO, A, ATOT, MORFL, OUTFL, GAMMA, GCYCL)

C*****C

Exercise 51

TITLE GUT CONTENT

INITIAL

*IGUT and GUTMAX expressed in prey-units

INCON IGUT= 0.

PARAM PREY= 10., GUTMAX= 15.

DYNAMIC

GUT = INTGRL(IGUT, UPTAKE-DIGEST)

*PREDR is predation rate, FCONS is prey fraction consumed

*RPR is relative predation rate

UPTAKE= PREDR * FCONS

PREDR = RPR * PREY

RPR = AFGEN(RPRT, GUT/GUTMAX)

FUNCTION RPRT = 0., 0.3, 0.5, 0.1, 1., 0.

FCONS = 1.-GUT/GUTMAX

*RDR is relative digestion rate

DIGEST= RDR * GUT

PARAM RDR = 0.5

TIMER FINTIM=20., PRDEL=1., DELT=0.1

METHOD RECT

PRINT GUT, UPTAKE, DIGEST

END

STOP

ENDJOB

Exercise 52

A CSMP program to simulate the population dynamics of wild oat in spring barley. No account is taken of density dependence of seed production of wild oat:

```
TITLE POPULATION DYNAMICS OF WILD OAT IN BARLEY
INCON NSEEDI=1000.
PARAM PG=0.68, PE=0.15, PB=0.60, SEEDNO=50.
```

```
*No. of plants(NPLWW), seed production(NPS), seeds in soil(NSEED) per m2
NPLWW = NSEED * PG * PE
NPS    = NPLWW * SEEDNO
INCR   = - PG * NSEED + PB * NPS
NSEED  = INTGRL(NSEEDI, INCR)
```

```
TIMER FINTIM=15., DELT=1., PRDEL=1., TIME=1.
PRINT NSEED, NPLWW, NPS
METHOD RECT
END
STOP
ENDJOB
```

Simulation results are represented by the broken line in Figure 54. The linear relation on the logarithmic scale represents an exponential increment of the seed population. The presented model deals with discrete generations as most weeds show only one, quite synchronized reproduction cycle a year. In modelling population dynamics, populations of discrete generations must be distinguished from populations reproducing continuously, such as polycyclic diseases and pests (Begon & Mortimer, 1981, p 31-35).

In the discrete situation, the number of seeds in year t is

$$n_t = n_{t-1} R = n_0 R^t$$

with n_0 = initial number of seeds; R = 'reproductive rate'. The 'interval relative increment rate' is then given by the difference equation

$$(n_t - n_{t-1})/n_{t-1} = R - 1$$

In the continuous situation, the 'instantaneous relative increment rate' is given by a differential equation obtained by differentiation of $\ln n_t$ to t :

$$r = d(\ln n_t)/dt = \ln R$$

which characterizes the slope of the graph of $\ln n_t$ against time t .

Substituting the population parameters of wild oat into Equation 76 gives, for the discrete situation, a relative increment rate of 2.38 yr^{-1} so that $R = 3.38 \text{ yr}^{-1}$. The ln-linear relation of Figure 54 has a slope r of 1.22 yr^{-1} , which is, by definition, equal to $\ln R$.

Exercise 53

See Figure 54 and program listing in Exercise 55.

One barley plant is equivalent to 45/14 wild oat plants. Hence, with respect to inter-specific competition $b_{cc}/b_{cw} = 45/14$ and $b_{ww}/b_{wc} = 14/45$. With respect to intra-specific competition $(1/b_{c0})/(1/b_{w0}) = 45/14$ at $b_{cc} = b_{ww}$. Crop production level is obtained from crop grain yield as $Y_{cc} = 500 \cdot 0.85/0.45 = 944 \text{ g m}^{-2}$. This biomass production amounts to 94% of maximum biomass yield so that $1/b_{cc} = 1004 \text{ g m}^{-2}$. The density response of barley is further characterized by the curvature $b_{cc}/b_{c0} = 0.057 \text{ m}^2 \text{ plant}^{-1}$. With the above relations, the competition coefficients are defined (see program listing in Exercise 55). These coefficients agree well with those estimated from density experiments of barley (Spitters, 1979, p. 80) and from field experiments of barley and wild oat in competition (Peters & Wilson, 1983).

Exercise 54

See Figure 55 and program listing in Exercise 55.

Year of herbicide application is described using the IMPULS function:

$$\text{HERBIC} = \text{IMPULS}(1., \text{HERBYR})$$

so that HERBIC takes the value 1 each HERBYR, otherwise HERBIC = 0. The first argument of the function is the time of the first pulse, and the second argument the time between pulses.

The time interval between two successive sprayings (HERBYR in years) is introduced as a PARAMeter and can thus be invoked by reruns.

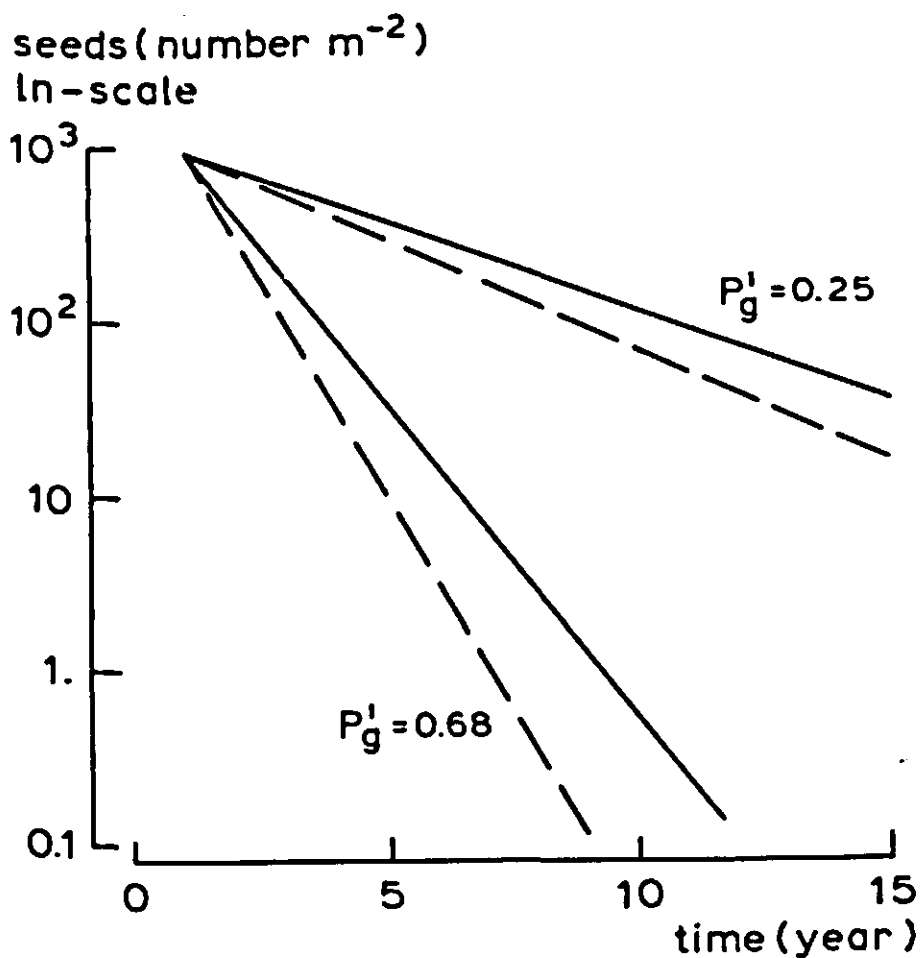


Figure 84. Simulated time course of soil seed population of a species with a persistent seed bank ($P_g' = 0.25$) and a species with a transient seed bank ($P_g' = 0.68$) for an efficiency of weed control of 95% (solid lines) and 100% (broken lines).

Exercise 55

A CSMP program to simulate the population dynamics of wild oat in spring barley. Allowance is made for density dependence of weed seed production, weed control measures, and a separation of soil seed population into surface and subsoil populations, see also Figure 84.

TITLE POPULATION DYNAMICS OF WILD OAT IN BARLEY

INITIAL

* Initial no. of seeds in upper (NSDIU) and lower (NSDIL) soil layer from
* total initial seed no.(NSEEDI) and depth of emergence(DE) and ploughing(DP)
INCON NSEEDI=1000.

NSDIU = NSEEDI*DE/DP

NSDIL = NSEEDI-NSDIU

PARAM DE = 0.04, DP=0.20

DYNAMIC

PARAM PGD=0.68, PED=0.75, PB=0.60

PARAM RE =0.42, SEEDW=0.014

PARAM NPLC=250.

* No. of plants before (NPLWW) and after (NPLW) weeding (no./m2)

NPLWW = NSEED * PED * PGD * DE/DP

NPLW = NPLWW * (1.-KILL*HERBIC)

PARAM KILL=0.95

HERBIC = IMPULS(1.,HERBYR)

PARAM HERBYR=1.

* Seed production (NPS) (no./m2)

NPS = BIOMWC * RE/SEEDW

* No. of seeds in upper(NSEEDU) and lower(NSEEDL) soil layer (no./m2)

INCRU = - PGD * NSEEDU + ((-DP+DE)*NSEEDU+DE*NSEEDL)/DP + PB*NPS

INCRL = - PGD * NSEEDL + ((+DP-DE)*NSEEDU-DE*NSEEDL)/DP

NSEEDU = INTGRL(NSDIU,INCRU)

NSEEDL = INTGRL(NSDIL,INCRL)

NSEED = NSEEDU + NSEEDL

* Competition coefficients; W refers to Weed, C refers to Crop

PARAM BWO=0.00562, BWW=0.000996, BWC=0.00320

PARAM BCO=0.0175, BCC=0.000996, BCW=0.000310

* Biomass of Crop and Weed (g/m2)

BIOMCW = NPLC/(BCO + BCC*NPLC + BCW*NPLW)

BIOMCC = NPLC/(BCO + BCC*NPLC)

BIOMWC = NPLW/(BWO + BWW*NPLW + BWC*NPLC)

RY = BIOMCW/BIOMCC

TIMER FINTIM=15., DELT=1., PRDEL=1., TIME=1.

PRINT NSEED,NPLWW,NPS,BIOMWC,BIOMCW,BIOMCC,RY

METHOD RECT

END

PARAM PGD=0.68, PED=0.75

PARAM KILL=1.00

END

STOP

ENDJOB

Separating the soil seed population into a surface soil and a subsoil population helps when evaluating soil cultivation operations differing in depth of soil disturbance.

Exercise 56

A CSMP program to simulate seedling emergence in relation to temperature:

```
TITLE GERMINATION AS FUNCTION OF TEMPERATURE
* Germinable seeds (NM,no./m2), incubation time (INC,°C day),
* germination probability (PO,1/°C/day), base temperature (TBASE,°C)
PARAM NM=100., INC=35., PO=0.020, TBASE=6.

* Germinated seeds (NGERM,no./m2), Rate of germination (RGERM,no./m2/day)
NGERM = INTGRL(0.,RGERM)
RGERM = AMAX1(0., PGERM * NMAX * (1. - NGERM/NMAX))
* Germinable seeds (NMAX), germination probability (PGERM in 1/day)
NMAX = NM * AVNMT
PGERM = PO * DTSUM * GERM
GERM = INSW(TSUM - INC, 0., 1.)

* Temperature functions
NMT = AFGEN(NMTT,TEMP)
FUNCTION NMTT = 0.,0., 6.,0., 19.,1., 34.,1., 43.,0.
TEMP = AFGEN(TEMPT,TIME)
FUNCTION TEMPT = 0.,10., 30.,20.
TSUM = INTGRL(0., DTSUM)
DTSUM = AMAX1(0., TEMP - TBASE)
* 5-days running average of NMT
AVNMT = INTGRL(AVNMTI, (NMT - AVNMT) / 5.)
INCON AVNMTI = 0.3

TIMER FINTIM=30., DELT=0.1, PRDEL=1.
METHOD RECT
PRINT NGERM,NMAX,PGERM,TSUM,NMT,AVNMT
END
STOP
ENDJOB
```

A simple, approximate formulation of the running average is used:

$$\bar{N}_m = \bar{N}_m + (N_m - \bar{N}_m)/\tau$$

where \bar{N}_m = running average; N_m = actual, instantaneous value; τ = time coefficient (5 days).

Exercise 57

A CSMP program to simulate seedling emergence in relation to temperature and soil moisture. Available soil moisture in the layer from which seedling emergence takes place is tracked by a simple model for the soil water balance:

TITLE GERMINATION AS FUNCTION OF TEMPERATURE AND SOIL MOISTURE
 * Germinable seeds (NM,no./m2), incubation time (INC,°C day),
 * germination probability (PO,1/°C/day), base temperature (TBASE,°C)
 PARAM NM=100., INC=35, PO=0.020, TBASE=6.

* Germinated seeds (NGERM,no./m2), Rate of germination (RGERM,no./m2/day)
 NGERM = INTGRL(0.,RGERM)
 RGERM = AMAX1(0.,PGERM * NMAX * (1. - NGERM/NMAX))
 * Germinable seeds (NMAX), germination probability (PGERM in 1/day)
 NMAX = NM * AVNMT * NMSM
 PGERM = PO * DTSUM * NMSM * GERM
 GERM = INSW(TSUM - INC, 0., 1.)

* Temperature functions
 NMT = AFGEN(NMTT,TEMP)
 FUNCTION NMTT = 0.,0., 6.,0., 19.,1., 34.,1., 43.,0.
 TEMP = AFGEN(TEMPT,TIME)
 FUNCTION TEMPT = 0.,10., 30.,20.
 TSUM = INTGRL(0., DTSUM)
 DTSUM = AMAX1(0.,TEMP - TBASE) * INSW(VSM-VSMWP,0.,1.)
 * 5-days running average of NMT:
 AVNMT = INTGRL(AVNMTI, (NMT - AVNMT) / 5.)
 INCON AVNMTI = 0.3

* Soil moisture functions
 NMSM2 = LIMIT(0., 1., (VSM - VSMWP) / (VSMCR - VSMWP))
 VSMCR = CRSM * (VSMFC-VSMWP) + VSMWP
 PARAM CRSM = 0.50
 NMSM1 = DELAY(2, DELT, NMSM)
 DNMSM = INSW(GERM-0.5, -1., NMSM2 - NMSM1)
 NMSM = INSW(DNMSM,NMSM2,NMSM1 + AMIN1((1.-NMSM1)*DELT*DTSUM/INC,...
 DNMSM))

*** SOIL MOISTURE BALANCE ***
 * Soil moisture in the considered soil layer (SM in dm3 H2O / m2 soil)
 SM = INTGRL(SMI, DSM/DELT)
 * division by DELT because INTGRL-statement assumes rates per day
 INCON SMI = 24.
 * Rate of change in soil moisture (DSM in dm3 H2O / m2 soil / time step)
 * as difference between rainfall, evaporative withdrawal and percolation
 DSM = RAIN - EVAPD - PERC
 * Volumetric soil moisture at field capacity (VSMFC),
 * wilting point (VSMWP), air dryness (VSMAD) in dm3 H2O / m3 soil .
 * and of the considered soil layer (VSM) having depth DEPTH (m)
 PARAM VSMFC=200., VSMWP=50., VSMAD=17., DEPTH = 0.12
 VSM = SM / DEPTH

RAIN = AFGEN(RAINTB,TIME) * IMPULS(0.,1.)
 FUNCTION RAINB = 0,0, 2,0, 3,10, 4,0, 5,0, 6,10, 7,0, 8,0, 9,10,...
 10,0, 11,0, 12,10, 13,0, 21,0, 22,15, 23,0, 24,0, 25,15, 26,0, 30,0
 EVAPD = AMIN1(EVAP * (1. - EXP(-PROP*DEPTH)), SM - VSMAD*DEPTH)
 PERC = AMAX1(0., SM + RAIN - (EVAPD/DELT) - DEPTH*VSMFC)
 * EVAPD/DELT: daily evaporation withdrawal from the soil layer

```

* Soil evaporation (EVAP in mm/time step) from Penman evaporation for
* open water (EPENM) and relative soil moisture content of top 2 cm (VSM2)
EVAP = 0.75 * EPENM * RDFSMT
EPENM = 3. * DELT
RDFSMT = AFGEN (RDFSMT, VSM2)
VSM2 = ((SM2/0.02) - VSMAD2) / (VSMFC2 - VSMAD2)
FUNCTION RDFSMT = -0.5,0., 0.,0., 0.2,0.05, 0.22,0.27, 0.33,0.9,...
    1.,1., 1.5,1.
* or in relation to pF:
FUNCTION RDFPFT = 1.7,1.0, 2.5,1.0, 4.0,0.9, 4.65,0.05, 7.0,0.
SM2 = INTGRL(SM2I, (RAIN - EVAP2 - PERC2) / DELT)
INCON SM2I = 4.
EVAP2 = AMIN1 (EVAP * (1.-EXP(-PROP*0.02)), SM2 - 0.02*VSMAD2)
PERC2 = AMAX1 (0., SM2 + RAIN - (EVAP2/DELTA) - 0.02*VSMFC2)

PARAM PROP = 10., VSMFC2 = 200., VSMAD2 = 17.

TIMER FINTIM=30., DELT=0.1, PRDEL=0.5
PRINT NGERM,NMAX,NMSM,PGERM,TSUM,SM,DSM,EVAP,EVAPD,RAIN,PERC,SM2,RDFSMT
METHOD RECT
END
STOP
ENDJOB

```

The variable NMSM2 defines the soil moisture reduction factor $NMSM (= f_{SM})$ of germination in a drying soil. To account for the fact that a rain shower, following a dry spell, does not immediately generate new seedlings, a maximum is set to the rate of recovery of NMSM:

$$NMSM_t = NMSM_{t-\Delta t} + (1 - NMSM_{t-\Delta t})/i$$

where incubation time i acts as time coefficient. The value of NMSM at the previous time step $t - \Delta t$, is given as NMSM1 and calculated by a DELAY function, the first argument of which gives the number of storage locations allocated for the memory, the second argument the delay time, and the third argument the considered variable. Prior to first germination ($GERM < 0.5$), a negative value is allotted to DNMSM so that $NMSM = NMSM2$ and no delay in recovery of NMSM after rainfall occurs during that stage.

Exercise 58

A CSMP program to simulate the periodicity of seedling emergence during the year as determined by changes in seed dormancy. Germination occurs only when soil temperature meets the temperature requirements of the seed, which change with its degree of dormancy, see also Figures 85 and 60:

```
TITLE SEASONAL PERIODICITY OF GERMINATION
* Viable seeds (NMO,no./m2), incubation time (INC,°C day)
* Germination probability (PGO,1/°C/day), base temperature (TBASE,°C)
PARAM NMO=100., INC=80., PGO=0.003, TBASE=0.

* Germinated seeds(NGERM,no/m2)
* Increment rate of germination(RGERM,no./m2/day)
NGERM = INTGRL(0.,RGERM)
RGERM = PGERM * AMAX1(0.,(NMGERM - NGERM))
* Germinable seeds (NMGERM), germination probability (PGERM,1/day)
NMGERM = NMO * FTEMP
PGERM = PGO * DTSUM * GERM
GERM = INSW(TSUM - INC, 0., 1.)

* Temperature functions
FT = AMIN1( BMN * (TEMP-TMN), BMX * (TMX-TEMP) )
FTEMP = LIMIT( 0., 1., FT)
TSUM = INTGRL(0., DTSUM)
DTSUM = AMAX1(0., TEMP - TBASE)
TEMP = AFGEN(TEMPT, DAY)
FUNCTION TEMPT = 0,3.4, 16,-1.5, 46,-0.2, 75,8.7, 106,16.2, 136,20.0,...
    167,24.5, 197,27.9, 228,27.5, 259,23.9, 289,15.2, 320,10.4,...
    350,4.9, 365,3.4
* NMGERM temperature relationship of Ambrosia artemisiifolia in light
TMN = AFGEN(TMNT, DAY)
FUNCTION TMNT = 0,15., 32,10., 60,4., 91,0., 121,4., 152,21., ...
    182,28., 213,30., 244,30., 274,27., 289,25., 305,23., 335,19., 365,17
TMX = AFGEN(TMXT, DAY)
FUNCTION TMXT = 0,32., 365,32.
BMN = AFGEN(BMNT, DAY)
FUNCTION BMNT = 0,.106, 32,.091, 60,.063, 91,.050, 121,.040, ...
    289,.040, 305,.056, 335,.083, 365,.095
BMX = AFGEN(BMXT, DAY)
FUNCTION BMXT = 0,.189, 32,.204, 60,.187, 91,.144, 121,.042, ...
    152,.005, 289,.005, 305,.011, 335,.060, 365,.095

DAY = AMOD(TIME,365.)
TIMER FINTIM=532., DELT=1., PRDEL=5., TIME=182.
METHOD RECT
PRINT NGERM,RGERM,FTEMP,TEMP
OUTPUT NGERM
PAGE MERGE, NTAB=0
OUTPUT RGERM
PAGE MERGE, NTAB=0
END RERUN
* NMGERM temperature relationship of Ambrosia artemisiifolia in dark
FUNCTION TMNT = 0,16., 32,12., 60,7., 91,13., 121,21., 152,28., ...
    182,32., 274,32., 289,28., 305,23., 335,18., 365,17.
FUNCTION TMXT = 0,32., 365,32.
FUNCTION BMNT = 0,.066, 32,.066, 60,.033, 91,.025, 121,.020, ...
    289,.020, 305,.025, 335,.033, 365,.050
FUNCTION BMXT = 0,.044, 32,.155, 60,.078, 91,.044, 121,.005, ...
    305,.005, 335,.007, 365,.026
END RERUN
```

```

* NMGERM temperature relationship of Lamium amplexicaule in light
FUNCTION TMNT = 0,1., 365,1.
FUNCTION TMXT = 0,23., 32,21., 60,19., 91,18., 121,19., 152,21.,...
    182,23., 213,25., 244,27., 274,28., 305,28., 335,25., 365,24.
FUNCTION BMNT = 0,.143, 365,.143
FUNCTION BMXT = 0,.167, 32,.147, 60,.119, 91,.114,121,.119,152,.116,...
    182,.167, 213,.143, 244,.172, 274,.172, 305,.167, 335,.179, 365,.173
END RERUN
* NMGERM temperature relationship of Lamium amplexicaule in dark
FUNCTION TMNT = 0,1., 152,1., 182,2., 213,3., 244,5., 274,7., ...
    305,8., 335,4., 365,2,
FUNCTION TMXT = 0,17., 32,20., 60,24., 91,16., 121,9., 152,8., ...
    182,8., 213,18., 244,20., 274,22., 305,21., 335,19., 365,18.
FUNCTION BMNT = 0,.10, 32,.10, 60,.06, 91,.04, 121,.02, 244,.02, ...
    274,.04, 335,.04, 365,.10
FUNCTION BMXT = 0,.056, 32,.050, 60,.017, 91,.011, 121,.010,152,.011,...
    182,.020, 213,.025, 244,.017, 274,.015, 305,.016, 335,.028, 365,.042
END
STOP
ENDJOB

```

The modulo (AMOD) function calculates the remainder of an integer division. For example, $AMOD(400,365) = 35$. For a correct interpolation of the FUNCTION tables, values at start (Day 0) and end (Day 365) must be defined.

GROUP MERGE combined with the OUTPUT statement collects ('merges') the results of different reruns into one figure.

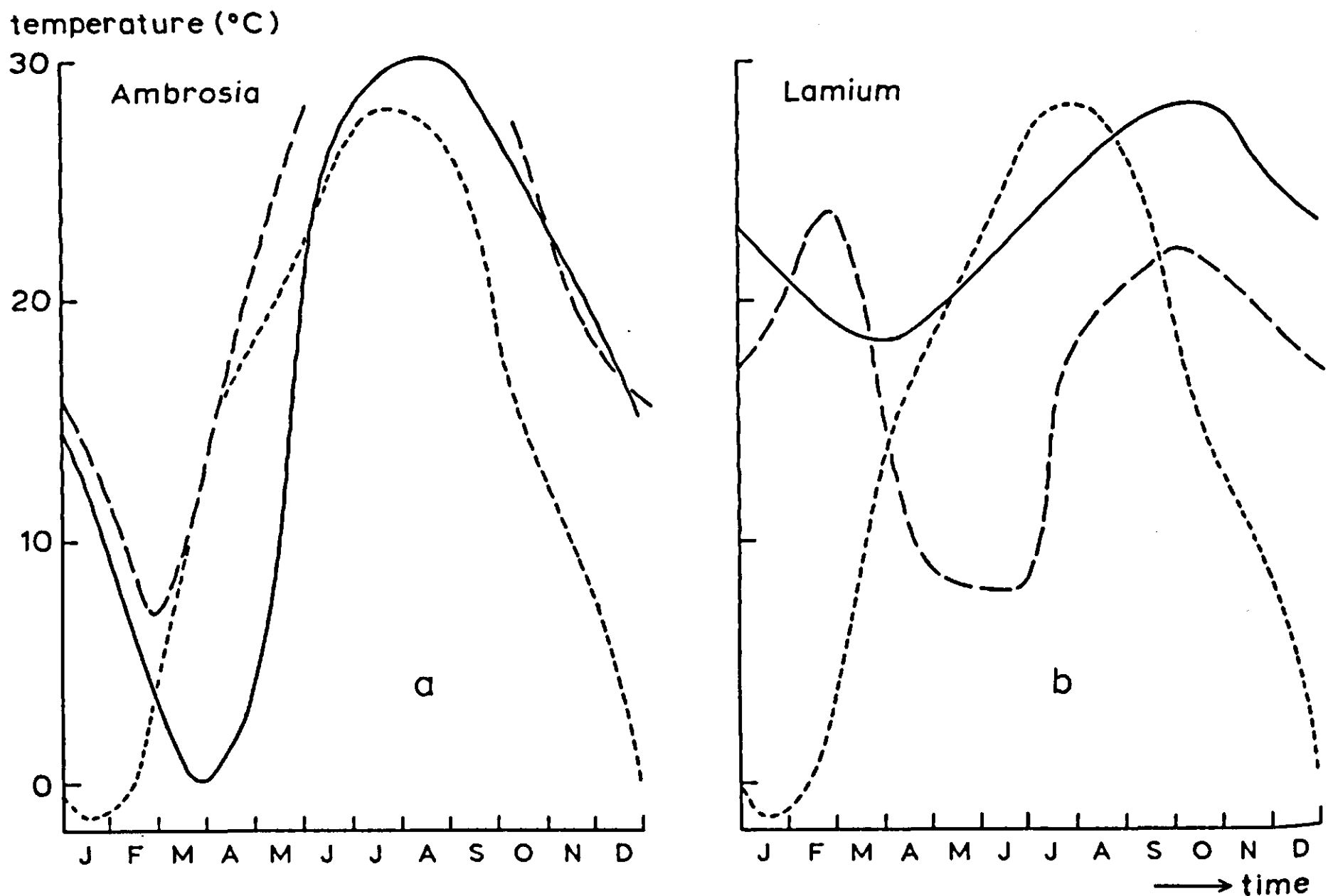


Figure 85. Widening and narrowing of the temperature amplitude of germination of *Ambrosia artemisiifolia* and *Lamium amplexicaule* in relation to the mean seasonal course of temperature (dotted curve). Amplitudes were estimated from data of Baskin & Baskin (1980, 1981) on germination of seeds dug up at monthly intervals after being buried in the soil in Kentucky, U.S. (a) For *A. artemisiifolia*, the apparent minimum temperatures of germination in light (solid curve) and dark (broken curve) are represented. Hence, germination in light is expected from the beginning of March to the end of May but, in the dark, germination will be restricted to perhaps a few seeds at the end of March. In Kentucky, *A. artemisiifolia* is a summer annual germinating only in spring. (b) For *L. amplexicaule*, the apparent maximum temperatures of germination in light (solid curve) and dark (broken curve) are depicted. These suggest that germination in light will be from the end of August to the beginning of May, and in the dark from the end of September to the end of March. In Kentucky, *L. amplexicaule* behaves mainly as a winter annual with the main period of germination in September to October with some seeds germinating during August, March and April.

Exercise 59

A CSMP program to simulate the growth of species in competition. The total growth rate of the mixed vegetation is distributed over the species according to their shares in total leaf area:

```
TITLE GROWTH IN COMPETITION
STORAGE LAI(2)
TABLE YBIOMI(1-2) = 30., 20.
PARAM NS = 2, E = 0.003
* Biomass (kg/ha)
YBIOM = INTGRL(YBIOMI,GTW,2)
* Leaf area ratio (ha green leaves / kg biomass)
LAR = AFGEN (LART,TIME)
FUNCTION LART = 0.,0.0015, 101.,0.
* Leaf area index (ha/ha)
PROCEDURE LAI,LAITOT = LAREA(YBIOM,LAR)
  LAITOT = 0.
  DO K=1,NS
    LAI(K) = LAR * YBIOM(K)
    LAITOT = LAITOT + LAI(K)
  ENDDO
ENDPRO
* Growth rate (kg/ha/day)
PROCEDURE GTW,GTWTOT = GROWTH(LAI,LAITOT)
  GTWTOT = (1.-EXP(-0.7*LAITOT)) * 0.5*RAD * E
  DO K=1,NS
    GTW(K) = GTWTOT * LAI(K)/LAITOT
  ENDDO
ENDPRO
* Incoming solar radiation (MJ/ha/d)
RAD = 14.E4
TIMER FINTIM=100., DELT=1., PRDEL=5.
PRINT YBIOM(1-2),LAI(1-2)
METHOD RECT
END
STOP
ENDJOB
```

Since the growth rate of each species in a mixture is proportional to its leaf area, and the species are only differentiated in initial biomass, the biomass ratio of the species remains equal to the ratio of their initial values of 0.30/0.20.

Exercises 60

A CSMP program to simulate the growth of species in competition. Growth rate of a species in a mixture is proportional to its leaf area and the light intensity at half its plant height, see also Table 14:

```

TITLE GROWTH IN COMPETITION
/   DIMENSION LAR(2), SHARE(2), HS(2), KL(2)
STORAGE HGHT(2), LAI(2), E(2), EXT(2)
TABLE YBIOMI(1-2)=25., 25.
TABLE E(1-2)=0.003, 0.003
TABLE EXT(1-2)=0.7, 0.7
PARAM NS=2

* Biomass (kg/ha)
YBIOM = INTGRL(YBIOMI,GTW,2)
* Leaf area index (ha/ha), plant height (m), growth rate (kg/ha/day)
PROCEDURE LAI,HGHT,GTW = GROWTH(YBIOM,RAD)
  KLTOT = 0.
  DO K=1,NS
    FK=K
    LAR(K) = TWOVAR(LART,TIME,FK)
    LAI(K) = LAR(K) * YBIOM(K)
    KL(K)  = EXT(K) * LAI(K)
    KLTOT  = KLTOT + KL(K)
    HGHT(K) = TWOVAR(HGHTT,TIME,FK)
  ENDDO
* Intercepted photosynthetically active radiation (INTPAR in MJ/ha/day)
  INTPAR = 0.5*RAD * (1.-EXP(-KLTOT))

* Share of each species in total growth
  TSHARE = 0.
  DO K=1,NS
    HS(K) = 0.
    DO J=1,NS
      HS(K) = HS(K) + AMAX1(0.,HGHT(J)-0.5*HGHT(K)) ...
        * EXT(J) * LAI(J) / HGHT(J)
    ENDDO
    SHARE(K) = EXT(K) * LAI(K) * EXP(-HS(K))
    TSHARE   = TSHARE + SHARE(K)
  ENDDO
* Growth rate (GTW in kg/ha/day) of each species
  DO K=1,NS
    GTW(K) = SHARE(K)/TSHARE * INTPAR * E(K)
  ENDDO
ENDPRO
* Leaf area ratio (ha green leaves / kg biomass)
FUNCTION LART,1 = 120.,0.0015, 221.,0.
FUNCTION LART,2 = 120.,0.0015, 221.,0.
* Plant height (m)
FUNCTION HGHTT,1 = 120.,0.01, 200.,1.00, 230.,1.00
FUNCTION HGHTT,2 = 120.,0.01, 200.,1.00, 230.,1.00
* Incoming solar radiation (MJ/ha/day)
RAD = 1.E4 * AFGEN(RADT,TIME)
FUNCTION RADT= 105.,12.4, 135.,16.4, 166.,18.3, 196.,16.2, 227.,14.6
TIMER FINTIM=220., DELT=1., PRDEL=5., TIME=120.
PRINT YBIOM(1-2),LAI(1-2)
METHOD RECT
END
TABLE YBIOMI(1-2)=0., 50.
END
TABLE YBIOMI(1-2)=50., 0.
END
STOP
ENDJOB

```

Exercise 61

The main modifications introduced in the program of Exercise 60 are:

* Herbicide application

HERBIC = IMPULS(HERBTM, 365.)

PARAM HERBTM = 120.

TABLE KILL(1 - 2) = 0.,0.90

*Plant height (m)

HGHT = INTGRL(HGHTI, DHGHT, 2)

TABLE HGHTI(1 - 2) = 0.01, 0.01

DHGHT(K) = 0.01 - HGHT(K)*KILL(K)*HERBIC

*Leaf area index (ha/ha), growth rate (kg/ha/d)

LAI(K) = LAR(K)*YBIOM(K)*(1. - KILL(K)*HERBIC)

GTW(K) = SHARE(K)/TSHARE*INTPAR*E(K) - ...
YBIOM(K)*KILL(K)*HERBIC

Simulation results are depicted in Figure 86.

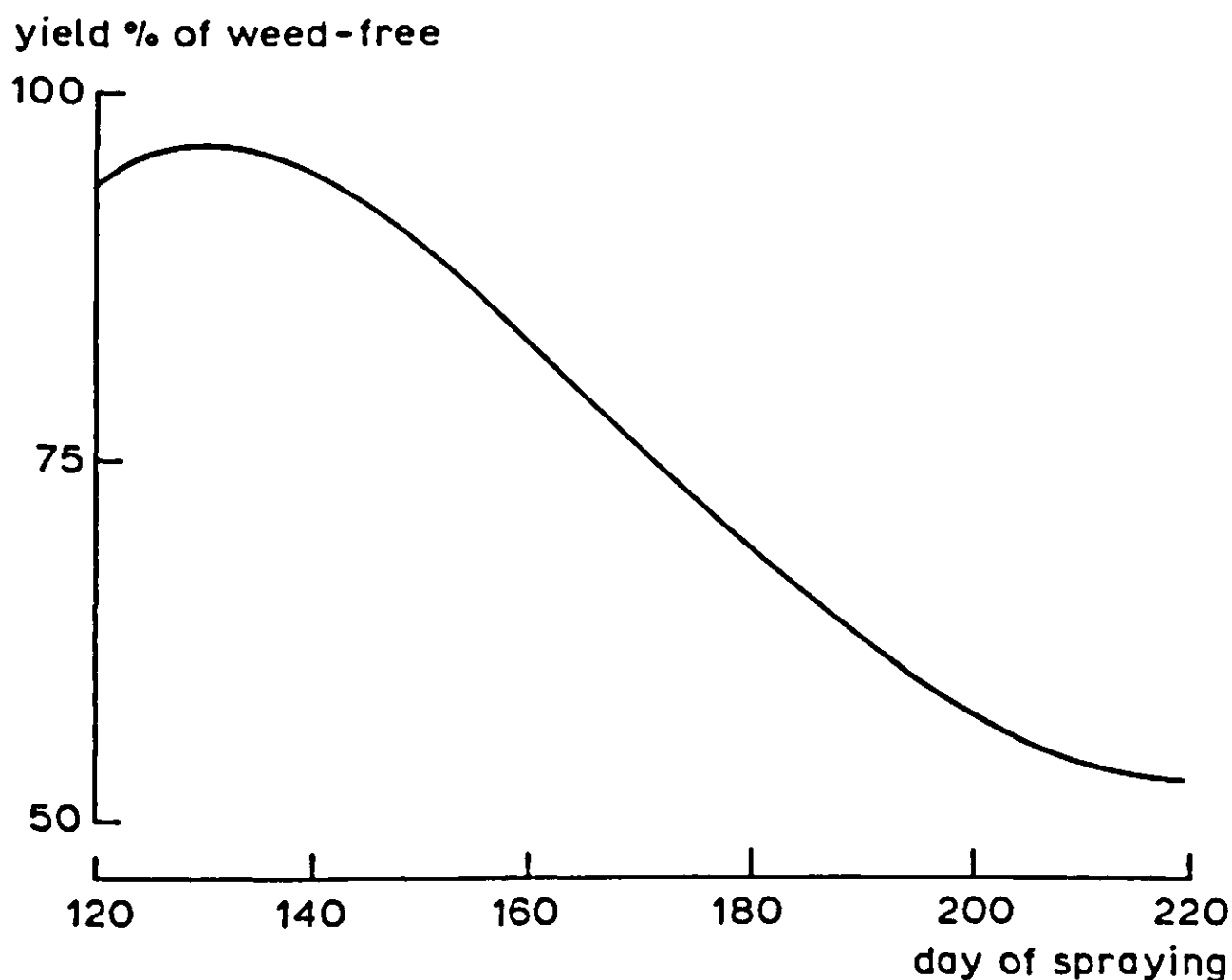


Figure 86. Simulated effect of time of herbicide application (in days since 1 January) on crop yield. Biomass yield of the weed-free crop is 20.2 t ha^{-1} (Exercise 61).

Exercise 62

A CSMP program to simulate competition for nitrogen. Species 1 has the N characteristics of a C_3 cereal, while species 2 represents a C_4 grass. For reasons of simplicity, a nitrogen surplus of a species is allotted to the other species according to their N deficits rather than to the relative capacities of their rooting systems, see also Figure 62:

```

TITLE GROWTH IN COMPETITION WITH NITROGEN LIMITATION
/   DIMENSION LAR(2), SHARE(2), HS(2), KL(2)
STORAGE HGHT(2), LAI(2), E(2), EXT(2)
STORAGE MXN(2), CRN(2), MNN(2), ACTN(2), NDEM(2), REDFN(2)
STORAGE CSP(2), RTL(2), RCAP(2), NDEF(2)
INITIAL
  ANSLI = ANSLU + FERT * RECOV
  PARAM ANSLU=50., RECOV=0.7, FERT=100.
DYNAMIC
TABLE ANBIOI(1-2) = 1.5, 1.5
TABLE YBIOMI(1-2) = 25., 25.
TABLE E(1-2) = 0.00276, 0.00276
TABLE EXT(1-2) = 0.7, 0.7
* Ratios of the species for critical N content (CSP)
TABLE CSP(1-2) = 1., 0.5
* Ratios of the species for root length per unit biomass (RTL)
TABLE RTL(1-2) = 1.,1.
PARAM NS=2

* Biomass (kg/ha)
YBIOM = INTGRL(YBIOMI,GTW,2)
* Leaf area index (ha/ha), plant height (m), growth rate (kg/ha/day)
PROCEDURE LAI,HGHT,GTW = GROWTH(YBIOM,RAD)
  KLTOT = 0.
  DO K=1,NS
    FK=K
    LAR(K) = TWOVAR(LART,TIME,FK)
    LAI(K) = LAR(K) * YBIOM(K)
    KL(K)  = EXT(K) * LAI(K)
    KLTOT  = KLTOT + KL(K)
    HGHT(K) = TWOVAR(HGHTT,TIME,FK)
  ENDDO
* Intercepted photosynthetically active radiation (INTPAR in MJ/ha/day)
  INTPAR = 0.5*RAD * (1.-EXP(-KLTOT))

* Share of each species in total growth
  TSHARE = 0.
  DO K=1,NS
    HS(K) = 0.
    DO J=1,NS
      HS(K) = HS(K) + AMAX1(0.,HGHT(J)-0.5*HGHT(K)) ...
        * EXT(J) * LAI(J) / HGHT(J)
    ENDDO
    SHARE(K) = EXT(K) * LAI(K) * EXP(-HS(K))
    TSHARE = TSHARE + SHARE(K)
  ENDDO
* Growth rate (GTW in kg/ha/day) of each species
  DO K=1,NS
    GTW(K) = SHARE(K)/TSHARE * INTPAR * E(K) * REDFN(K)
  ENDDO
ENDPRO
* Leaf area ratio (ha green leaves / kg biomass)
FUNCTION LART,1 = 120.,0.0015, 221.,0.
FUNCTION LART,2 = 120.,0.0015, 221.,0.
* Plant height (m)
FUNCTION HGHTT,1 = 120.,0.01, 200.,1.00, 230.,1.00
FUNCTION HGHTT,2 = 120.,0.01, 200.,1.00, 230.,1.00

* Incoming solar radiation (MJ/ha/day)
RAD = 1.E4 * AFGEN(RADT,TIME)
FUNCTION RADT= 105.,12.4, 135.,16.4, 166.,18.3, 196.,16.2, 227.,14.6

```

```

* Available nitrogen in soil (ANSL, kg N / ha)
ANSL = INTGRL (ANSLI, -TNUP)
* Actual nitrogen in biomass (ANBIOM, kg N / ha)
ANBIOM = INTGRL (ANBIOI, NUP, 2)

* Uptake of nitrogen

PROCEDURE NUP,REDFN,NDEM,TNUP,ACTN,CRN,MNN = UPTAKE (YBIOM,ANBIOM)
  TNDEM = 0.
  TRCAP = 0.
* Nitrogen contents (kgN/kgDM): maximum, critical, minimum, actual
  DO K=1,NS
    FK = K
    MXN(K) = TWOVAR(MXNT,TIME,FK)
    CRN(K) = 0.65 * MXN(K) * CSP(K)
    MNN(K) = 0.008 * CSP(K)
    ACTN(K) = ANBIOM(K) / YBIOM(K)
* nitrogen demand (kgN/ha/d) and relative root capacity (RCAP)
    NDEM(K) = AMAX1(0.,(YBIOM(K) * MXN(K) - ANBIOM(K))/TC)
    TNDEM = TNDEM + NDEM(K)
    RCAP(K) = RTL(K) * YBIOM(K)
    TRCAP = TRCAP + RCAP(K)
  ENDDO
* nitrogen uptake (kgN/ha/d): total (TNUP) and per species (NUP)
  TNUP = AMIN1 (TNDEM, ANSL/DELT)
  SURPL = 0.
  TNDEF = 0.
  DO K=1,NS
    NUP(K) = TNUP * RCAP(K) / TRCAP
    NDEF(K) = AMAX1 (0., NDEM(K) - NUP(K))
    TNDEF = TNDEF + NDEF(K)
    SURPL = SURPL + AMAX1 (0., NUP(K) - NDEM(K))
  ENDDO
* If under N-shortage some species satisfies its demand, its surplus
* (SURPL) is divided among the other species according to their deficits
  DO K=1,NS
    NUP(K)=AMIN1(NDEM(K),NUP(K) + SURPL*NDEF(K)/(TNDEF+NOT(TNDEF)))
* growth reduction factor
    REDFN(K) = LIMIT (0., 1., (ACTN(K)-MNN(K)) / (CRN(K)-MNN(K)))
  ENDDO
ENDPRO

PARAM TC = 2.
* Maximum nitrogen content (kgN/kgDM)
FUNCTION MXNT,1 = 120.,0.050, 170.,0.025, 220.,0.018
FUNCTION MXNT,2 = 120.,0.050, 170.,0.025, 220.,0.018

TIMER FINTIM=220., DELT=1., PRDEL=5., TIME=120.
PRINT YBIOM(1-2),LAI(1-2),ANBIOM(1-2),REDFN(1-2),NUP(1-2),GTW(1-2),ANSL
METHOD RECT
END
PARAM FERT= (0.,25.,50.,75.,150.,200.,250.,300.,500.,1000.)
END
STOP
ENDJOB

```

Exercise 63

Compared to the program listing in Exercise 62, the following modifications were introduced into the model:

```
ANSLI = ANSL0 + FERT
PARAM ANSL0 = 26.4, RECOV = 0.7, FERT = 25.
*Available nitrogen in soil (ANSL, kg N/ha)
ANSL = INTGRL(ANSLI, NMINR - TNUP/RECOV)
NMINR = 4.5E-5 * ORGNSL
PARAM ORGNSL = 10000.
```

In both models, the amount of N taken up by the vegetation is the same, namely $67.5 \text{ kg N ha}^{-1}$, in addition to the 3 kg N ha^{-1} initially present in the seedlings. In model I (based on van Keulen, 1982b) this is obtained as $50 + 0.7 \cdot 25$, while in model II (based on Greenwood et al., 1984) this is reached as $0.7 \cdot (45 + 26.4 + 25)$.

In model II, where small amounts of nitrogen become continuously available during the growing season, species 1 shows a greater advantage in N uptake and biomass production when grown in a mixture because of its larger root system:

species	kg N ha ⁻¹		kg DM ha ⁻¹	
	1	2	1	2
Model I	35.9	34.6	4213	4070
Model II	39.8	30.5	4062	3357

In model II, total biomass production was smaller at an equal N uptake, because N shortage started sooner, which reduced the peak LAI.

Exercise 64

The structure of the model is not affected by the introduction of three leaf layers. Some calculations are now done three times. The consequences for the model are explained below. The leaf area index, LAI, must be distributed over three leaf layers; in model structure:

```
* the crop
NOSORT
TLBM = AFGEN(TLBMT, DAY)
LAI = TLBM * SLA
LAIMAX = AMAX1(LAIMAX, LAI)
DEADLA = LAIMAX - LAI
DLATOT = DEADLA
LATOT = LAI
DO 10 J = 1,3
  DLA(J) = AMIN1(DLATOT, 1.5)
  DLATOT = DLATOT - DLA(J)
```

```

LA(J)      = AMIN1(LATOT,1.5 - DLA(J))
LATOT     = LATOT - LA(J)

RDYING    = -AMIN1(0.,DERIV(0.,LA(J)))
RMRLA(J)  = RDYING/(LA(J)+NOT(LA(J)))
10 CONTINUE
SORT

```

In this listing, LAIMAX represents the maximum LAI used to calculate the dead leaf area (DEADLA). The total leaf area (DEADLA + LAI) is divided over the leaf layers starting from leaf layer 1. Leaf layer 2 starts dying when the lowest leaf layer is completely dead; thus, the dying process takes place from the bottom of the canopy upwards. The relative mortality rate per leaf layer is, therefore, considerably different for the various leaf layers.

The number of intercepted, ungerminated spores, and the number of germinated spores are computed per leaf layer, using array integrals (see Appendix 5):

```

INTSP     = INTGRL(0., NRINT, 3)
GERSP     = INTGRL(0., NRGER, 3)

```

where NRINT and NRGER are the net rates of change in number of intercepted and number of germinated spores, respectively. These rates are computed per leaf layer, using a DO loop:

```

NOSORT
DO 20 J = 1,3
  IRPSP(J) = R*INFTOT*FINTLL*LA(J)*(1. - (DISL(J)/(LA(J) + NOT(LA(J))))))
  MRISP(J) = RMRISP*INTSP(J)
  GRISP(J) = RGRISP*INTSP(J)
  NRINT(J) = IRPSP(J) - MRISP(J) - GRISP(J)

  MRGSP(J) = RMRGSP*GERSP(J)
  RIR(J)    = RIRGSP*GERSP(J)
  NRGER(J) = GRISP(J) - MRGSP(J) - RIR(J)

  RIRL(J)   = RIR(J)*SLES
20 CONTINUE
SORT

```

The interception rate of produced spores, IRPSP(J), consists of a production term (R*INFTOT), an interception term (FINTLL*LA(J)) and a reduction term (1. - DISL(J)/LA(J)). The first term refers to the entire canopy, since spores produced in leaf layer 1 may land in leaf layer 2 and the other way around. The second and third term only refer to the leaf layer concerned. To prevent zero division in the third term, in case insufficient leaf mass is available, a NOT statement is added.

The development of lesions is also computed per leaf layer; for leaf layer 1:

```
LATO1, LATL1, TLATL1, MRLAT, EIRL1, GAMMA1, GCYCL1 = ...
  BOXCAR(1, ILATL1, DRLAT(1), RDLAT, RMRLA(1), RIRL(1), N1, DELT, TIME)
INFO1, INFL1, TINFL1, MRINF, REML1, GAMMA2, GCYCL2 = ...
  BOXCAR(2, IINFL1, DRINF(1), RDINF, RMRLA(1), EIRL1, N2, DELT, TIME)
NLIFL1 = INTGRL(0., REML1 - RMRLA(1) * NLIFL1)
DISL(1) = TLATL1 + TINFL1 + NLIFL1
```

The computations for leaf layers 2 and 3 are similar and the total latent, infectious and no-longer infectious leaf area is found by summation:

```
TLATLA = TLATL1 + TLATL2 + TLATL3
TINFLA = TINFL1 + TINFL2 + TINFL3
NLIFLA = NLIFL1 + NLIFL2 + NLIFL3
DISLA  = TLATLA + TINFLA + NLIFLA
```

Study of the complete model listing (Appendix 8) demonstrates the need for extra memory storage reservation, due to the use of array-variables. The consequences of introducing leaf layers for the development of the epidemic is given in Figure 87. In the beginning, the course of the epidemic is the same, after Day 180 the three-leaf layer model shows a slower development of the epidemic. This is due to dying of leaf mass, especially in leaf layer 1, where the disease is most prolific. Such an effect is less clear in the non-layered model as, leaf senescence is homogeneously distributed in the canopy, an unrealistic assumption.

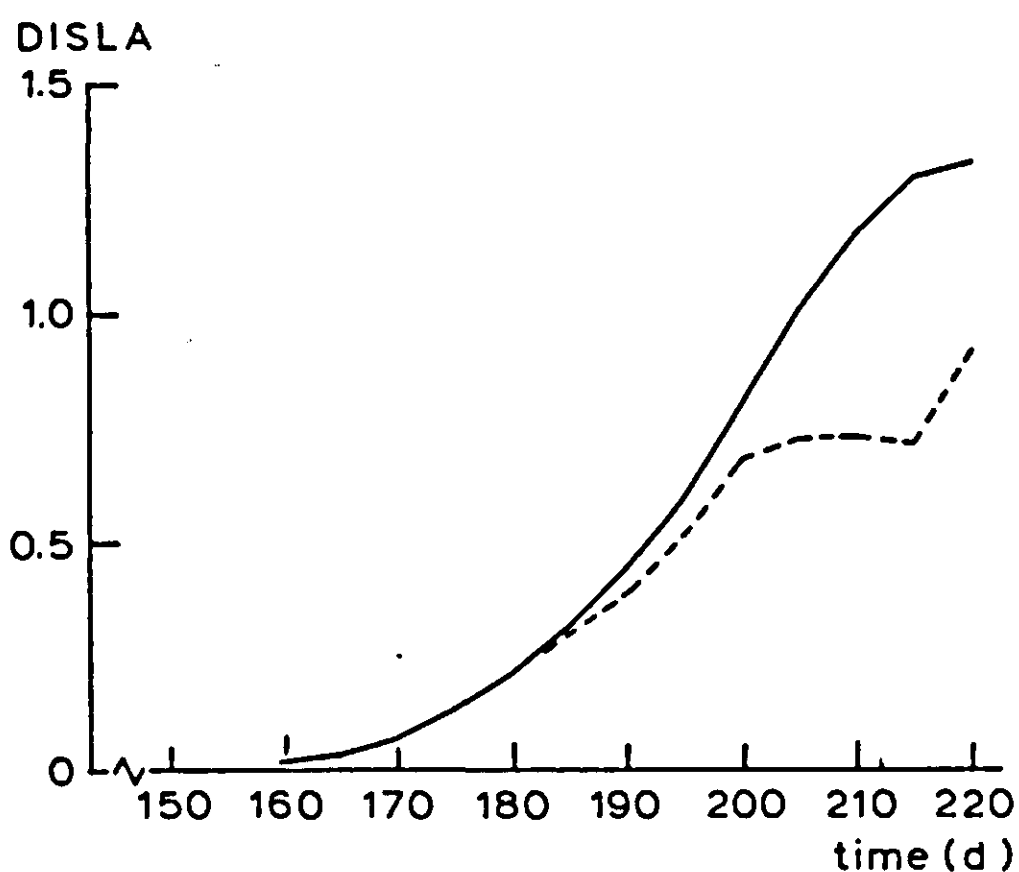


Figure 87. The development of a powdery mildew epidemic expressed in diseased leaf area (DISLA) in course of time. Simulated with a one-leaf layer (—) and a three-leaf layer model (----), respectively.

Exercise 65

The nitrogen content of the leaf layers is assumed to be constant during the growing season and is introduced with a TABLE statement:

```
TABLE NCONT(1 - 3) = 3.0, 3.0, 3.0
```

The inverse of both latency and infectious periods (the development rates) is calculated from the temperature:

```
SDRLAT = AFGEN(DRLATT, TEMP)
```

```
SDRINF = AFGEN(DRINF, TEMP)
```

but both (latency period and infectious period) are affected by the nitrogen content of the leaves. This is introduced using a multiplication factor:

```
NOSORT
```

```
DO 30 J = 1,3
```

```
MFLP = AFGEN(MFLPT, NCONT(J))
```

```
MFIP = AFGEN(MFIPT, NCONT(J))
```

```
DRLAT(J) = SDRLAT/MFLP
```

```
DRINF(J) = SDRINF/MFIP
```

```
30 CONTINUE
```

```
SORT
```

```
FUNCTION MFLPT = 2.0,1.5, 2.5,1.2, 3.0,1.0, 3.5,0.8
```

```
FUNCTION MFIPT = 2.0,0.8, 2.5,0.9, 3.0,1.0, 3.5,1.2
```

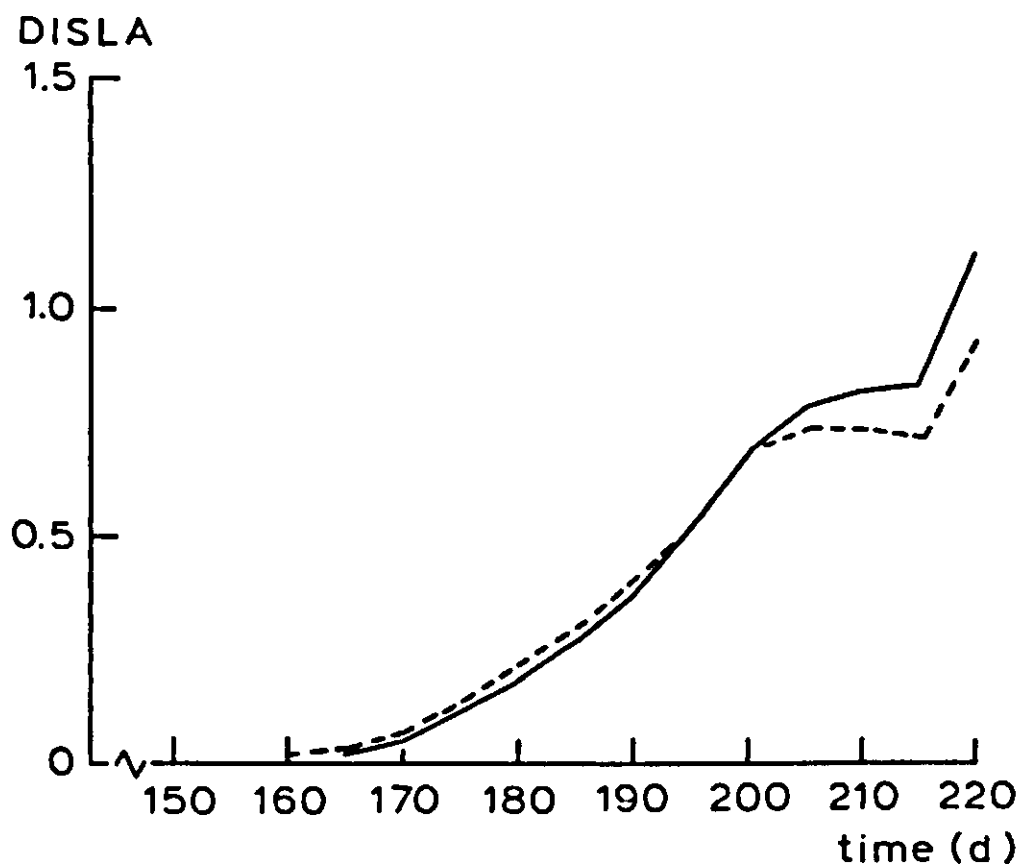


Figure 88. Simulation of the influence of introducing nitrogen content into various leaf layers on the development of a powdery mildew epidemic. (DISLA = diseased leaf area; ---- N content in leaf layer 1-3 = 3.0%; — N content in leaf layer 1, 2, 3 is 2.5, 3.0, 3.5%, respectively).

A complete listing of the model is given in Appendix 8. The results of the modified model are given in Figure 88. When leaf layers 1 and 3 have a nitrogen content which deviates from the average content of 3%, they are 2.5 and 3.5% respectively; the epidemic starts more slowly at the beginning due to the lower nitrogen content of leaf layer 1. Later, this effect is clearly compensated by the higher nitrogen content of leaf layer 3.

Exercise 66

A listing of the straightforward population model of the cereal leaf beetle *Lema cyanella* is given below:

```
TITLE LEMA CYANELLA POPULATION:

INITIAL
INCON IEGG=0., ILARV=0., IPUP=0., IADUL=100.
PARAM RESE=5., RESL=10., RESP=4., RESA=20.
PARAM FERT=3., SR=0.5

DYNAMIC
* Number of organisms per ha in each of 4 development phases
EGG  = INTGRL(IEGG, REPR-LARVR)
LARV = INTGRL(ILARV, LARVR-PUPR)
PUP  = INTGRL(IPUP, PUPR-ADULR)
ADUL = INTGRL(IADUL, ADULR-DEATHR)

* Rates
REPR  = SR * ADUL * FERT
LARVR = EGG/RESE
PUPR  = LARV/RESL
ADULR = PUP/RESP
DEATHR= ADUL/RESA

TIMER FINTIM=50., DELT=.25, PRDEL=2.
PRINT EGG, LARV, PUP, ADUL
METHOD RECT
END
STOP
ENDJOB
```

Exercise 67

Coupling the cereal leaf beetle population model to SUCROS87 is done using the following statements:

```
ADUL  = INTGRL(0., PUSH * IADUL/DELT + ADULR - DEATHR)
PUSH  = IMPULS(195., 1000.)
CONSR = 2.5E-6 * LARV
CONSLA = INTGRL(0., CONSR)
CONSLV = CONSR/SLA
WLVC  = INTGRL(0., CONSLV)
```

where CONSR and CONSLV are the consumption rates of leaves expressed in leaf area and leaf weight, respectively, and CONSLA and WLVC express the total consumed leaf area and leaf weight. The consumption of leaf mass by larvae affects leaf area (LAI) and

green leaf weight (WLVG) of the crop:

$$\text{LAI} = 0.5 * \text{EAI} - \text{CONSLA} + \text{INTGRL}(0., \text{GLAI})$$

$$\text{WLVG} = \text{INTGRL}(0., \text{GLV} - \text{DLV} - \text{CONSLV})$$

$$\text{WLV} = \text{WLVG} + \text{WLVD} + \text{WLVC}$$

The relation between development stage of the crop and the factor expressing the reduced maintenance respiration due to ageing or low nitrogen content, is described by the function:

$$\text{FUNCTION MNDVST} = (0., 1.), (1., 1.), (1.2, 0.6), (1.4, 0.35), \dots \\ (1.6, 0.21), (1.8, 0.12), (2.1, 0.05)$$

The results of the simulation (Figure 64), show that the effect of the beetles on grain growth is very limited. Even at an initial beetle density of 300 beetles m^{-2} the effect on grain growth is almost negligible. Some results of computations for dry weight of storage organs (WSO) with various initial densities are:

IADUL	WSO (kg ha^{-1})
0	7714
50	7691
100	7668
150	7645
200	7621
300	7574

Exercise 68

The mite population density (MITED) is introduced in SUCROS87 for potato as a forcing function. The number of mites per ha (NMITES) is computed from the mite density and the leaf area index of the crop (LAI):

$$\text{MITED} = \text{AFGEN}(\text{MITEDT}, \text{DAY})$$

$$\text{FUNCTION MITEDT} = (0., 0.), (180., 0.), (210., 6.), (230., 0.), (360., 0.)$$

$$\text{NMITES} = \text{MITED} * \text{LAI} * 1.E8$$

The number of mites is used to compute the quantity consumed assimilates (EMAINT) using the consumption rate $\text{day}^{-1} \text{mite}^{-1}$, and this is added to the usual maintenance respiration.

$$\text{EMAINT} = \text{NMITES} * 25.E-9$$

$$\text{MAINT} = \text{AMIN1}(\text{GPHOT}, \text{MAINTS} * \text{TEFF} * \text{MNDVS} + \text{EMAINT})$$

Exercise 69

The model SUCROS87 for spring wheat is extended with a model that computes the logistic growth of the number of yeast cells:

```
INCON IYEAST = 10.  
PARAM RGRY = 0.8, YEASTM = 1.E6  
YEAST = INTGRL(0.,GRY + PUSH * IYEAST/DELT)  
GRY = RGRY * YEAST * (1. - YEAST/YEASTM)  
PUSH = IMPULS(170., 1000.)
```

The computed yeast density in cells cm^{-2} is used to calculate the fraction of intercepted photosynthetically active radiation:

```
ABSORB = 0.05 * LOG10(YEAST + NOT(YEAST))
```

The daily photosynthetically active radiation is reduced by this fraction:

```
DPAR = 0.5 * DTR * (1. - ABSORB)
```

Since DPAR is calculated in the subroutine DRADIA, which is used in the subroutine for the calculation of daily assimilation (DASS), the fraction intercepted photosynthetically active radiation by yeast cells, ABSORB, must be mentioned in the call for the subroutines and in both subroutine statements. This is demonstrated for subroutine DASS:

```
DTGA, DSO = DASS(DAY, LAT, DTR, KDF, SCP, LAI, AMAX, EFF, ABSORB)  
SUBROUTINE DASS (DAY, LAT, DTR, KDF, SCP, LAI, AMAX, EFF,  
                ABSORB, DTGA, DSO)
```

Results of the calculations using the combination model are given below for various initial yeast densities and various days of initiation of the yeast population.

IYEAST at Day 170	WSO (kg ha^{-1})	Initial day (IYEAST = 10)	WSO (kg ha^{-1})
0	7728		
10	6561	170	6561
100	6384	185	7243
10 000	6119	200	7587

Exercise 70

The fraction of leaves belonging to the category bright yellow leaves is read from an AFGEN function. Further, the photosynthetic parameters of bright yellow leaves are calculated from the parameters of healthy leaves:

```
AMAXD = AMAX * 0.26  
EFFD = EFF * 0.71
```

The assimilation rate for shaded leaf area, and the assimilation rate for sunlit leaf area are both computed twice. Once with the parameters for healthy leaves (AMAX, EFF) and once with the parameters for bright yellow leaves (AMAXD, EFFD). The real assimilation rates for shaded leaf area and for sunlit leaf area are computed by weighting the assimilation rate for infected leaf area and the one for non-infected leaf area according to the fraction of infected leaf area:

* assimilation of shaded leaf area (kg CO₂/ha leaf/h)

$$\begin{aligned} \text{ASSSHH} &= \text{AMAX} * (1. - \text{EXP}(-\text{EFF} * \text{PARLSH} / \text{AMAX})) \\ \text{ASSSHD} &= \text{AMAXD} * (1. - \text{EXP}(-\text{EFFD} * \text{PARLSH} / \text{AMAXD})) \\ \text{ASSSH} &= (1. - \text{FRDIS}) * \text{ASSSHH} + \text{FRDIS} * \text{ASSSHD} \end{aligned}$$

* assimilation of sunlit leaf area (kg CO₂/ha leaf/h)

$$\begin{aligned} \text{ASSSLH} &= \text{AMAX} * (1. - (\text{AMAX} - \text{ASSSHH}) * (1. - \text{EXP}(-\text{PARLPP} * \text{EFF} / \dots \\ &\quad \text{AMAX})) / (\text{EFF} * \text{PARLPP})) \\ \text{ASSSLD} &= \text{AMAXD} * (1. - (\text{AMAXD} - \text{ASSSHD}) * \dots \\ &\quad (1. - \text{EXP}(-\text{PARLPP} * \text{EFFD} / \text{AMAXD})) / \dots \\ &\quad (\text{EFFD} * \text{PARLPP})) \\ \text{ASSSL} &= (1. - \text{FRDIS}) * \text{ASSSLH} + \text{FRDIS} * \text{ASSSLD} \end{aligned}$$

As the assimilation rate is computed in the subroutine ASS, which is used in the subroutine for the computation of daily assimilation, DASS, the parameters AMAXD, EFFD and FRDIS must be mentioned in the subroutine statements, as demonstrated for subroutine DASS:

```
DTGA,DSO = DASS(DAY,LAT,DTR,KDF,SCP,LAI,FRDIS,AMAX,AMAXD,...
              EFF,EFFD)
SUBROUTINE DASS(DAY,LAT,DTR,KDF,SCP,LAI,FRDIS,AMAX,AMAXD,
              EFF,EFFD,DTGA,DSO)
```

Exercise 71

When only light use efficiency or photosynthesis at light saturation is affected, a small change in the combination model is required. In the first case, AMAXD = AMAX, in the second EFFD = EFF. The results of the simulations are given in Table 20.

Exercise 72

The assimilation rate at light saturation depends on the mildew disease (Table 21). From this table, the reduction factor for the assimilation rate is calculated.

```
AMPMI = AFGEN(AMPMIT, PMI)
FUNCTION AMPMIT = (0., 1.),(0.3, .97),(0.75, .87), ...
                 (1.5, .84),(2.5, .67),(4.5, .58),(8., .55),(10., .40)
```

This reduction factor is used in the computation of AMAX:

$$\text{AMAX} = \text{AMX} * \text{AMDVS} * \text{AMTMP} * \text{AMPMI}$$

As a result of the mildew infection, the grain yield (7728 kg ha^{-1}) is reduced by 1180 kg.

Exercise 73

a. $N_t = N_0 \cdot e^{rt}$

Until anthesis: $2 \cdot N_0 = N_0 \cdot e^{r \cdot 4}$	$r = \ln 2/4 = 0.17$
At anthesis : $2 \cdot N_0 = N_0 \cdot e^{r \cdot (2.5)}$	$r = \ln 2/2.5 = 0.28$
After anthesis: $2 \cdot N_0 = N_0 \cdot e^{r \cdot 6}$	$r = \ln 2/6 = 0.12$

$N_0 = 0.05$

At anthesis: $N_{t1} = 0.05 \cdot e^{(0.17 \cdot 7)}$	$N_{t1} = 0.16$
At DC 70 : $N_{t2} = 0.16 \cdot e^{(0.28 \cdot 7)}$	$N_{t2} = 1.14$
At DC 77 : $N_{t3} = 1.14 \cdot e^{(0.12 \cdot 27)}$	$N_{t3} = 29.1$

b. $N_{t3} = 1.14 \cdot e^{(0.12 \cdot t)}$
 $N_{t3} = 15 \quad t = 21.5 \text{ days}$

Total time = $7 + 7 + 21.5 = 35.5 \text{ days}$

```
c. TITLE DEVELOPMENT OF SITOBION AVENAE
STORAGE DTAP(3), CDEVR(3)
FIXED PERIOD, INT
INITIAL
INCON IAPHID = 0.05, IPERIO = 1.
PARAM PI = 3.141529, AVTMP = 20., AMPTMP = 8.
PARAM Q10 = 0.5
TABLE DTAP(1-3) = 4., 2.5, 6.
DYNAMIC
NOSORT
* temperature
TEMP = AVTMP + AMPTMP*( -COS(2.*PI*TIME) )
* crop development
PERIOD = INT( PERIO )
CDEVR(PERIOD) = TWOVAR( CDEVRT, TEMP, FLOAT(PERIOD) )
PERIO = INTGRL( IPERIO, CDEVR(PERIOD) )
* aphid development
DTA = DTAP(PERIOD)*Q10**((TEMP-20.)/10. )
RGRA = ALOG(2.)/DTA
GRA = RGRA*APHID
APHID = INTGRL( IAPHID, GRA )
SORT
FUNCTION CDEVRT,1. = 10.,0.0909, 20.,0.1429, 30.,0.2500
FUNCTION CDEVRT,2. = 10.,0.1000, 20.,0.1429, 30.,0.2000
FUNCTION CDEVRT,3. = 10.,0.0286, 20.,0.0370, 30.,0.0526
TIMER FINTIM=38., PRDEL=1., DELT=0.1
METHOD RECT
PRINT PERIO,APHID,RGRA,DTA
END
STOP
ENDJOB
```

Exercise 74

The names of variables used here have been defined in the text, except for RCADEL and RNADEL, which are dummy variables introduced to store RCA and RNA, respectively, of the previous time step. In this way, an approximation is obtained for the nitrogen fraction of the phloem.

* N demand and -supply of aphids and grains

$$\text{NDEMA} = \text{SRAP} * \text{AWAP} * \text{NUMAP} * \text{EARHA}$$

$$\text{NDEMG} = \text{PNARIG} * \text{NUMGR}$$

$$\text{NDEM} = \text{NDEMA} + \text{NDEMG}$$

$$\text{NSUP} = \text{ATN/TCTN} * \text{TEFF}$$

* Flow of nitrogen to aphids and grains

$$\text{RNA} = \text{AMIN1}(\text{NDEM}, \text{NSUP})$$

$$\text{RNAAP} = \text{RNA} * \text{NDEMA}/\text{NDEM}$$

$$\text{RNAGR} = \text{RNA} * \text{NDEMG}/\text{NDEM}$$

* C demand and -supply of aphids and grains

$$\text{CDEMA} = \text{RCADEL}/\text{RNADEL} * \text{NDEMA}$$

$$\text{CDEMG} = \text{PGRIG} * \text{NUMGR}/\text{EFCGR}$$

$$\text{CDEM} = \text{CDEMA} + \text{CDEMG}$$

$$\text{CSUP} = \text{ARES/TCTR}$$

* Flow of carbohydrates to aphids and grains

$$\text{RCA} = \text{AMIN1}(\text{CDEM}, \text{CSUP})$$

$$\text{RCAAP} = \text{RCA} * \text{CDEMA}/\text{CDEM}$$

$$\text{RCAGR} = \text{RCA} * \text{CDEMG}/\text{CDEM}$$

Exercise 75

a. Hypothesis I implies that the total demand for nitrogen is found by adding the demands of aphids and grains. Assume a value of 0.4 mg for AWAP. Applying the algorithm of Exercise 74 yields:

$$\begin{aligned}\text{NDEMA} &= \text{SRAP} * \text{AWAP} * \text{NUMAP} * \text{EARHA} \\ &= 8.92 \cdot 10^{-9} * 0.4 * 30 * 635 \cdot 10^4 = 0.68\end{aligned}$$

$$\text{NDEMG} = 2$$

$$\text{NDEM} = 2.68$$

$$\text{NSUP} = 15$$

The flow of nitrogen to aphids and grains is:

$$\text{RNA} = \text{minimum}(2.68, 15) = 2.68$$

$$\text{RNAAP} = 0.68$$

$$\text{RNAGR} = 2$$

With the information on the N content of the phloem sap, the carbohydrate demands can be calculated:

$$CDEMA = 1/0.02 \cdot 0.68 = 34$$

$$CDEMG = 50$$

$$CDEM = 84$$

$$CSUP = 1000$$

Flow of carbohydrates:

$$RCA = \text{minimum}(84, 1000) = 84$$

$$RCAAP = 34$$

$$RCAGR = 50$$

b. Hypothesis II implies that total demand is equal to the demand of the grains:

$$NDEMA = 0.68$$

$$NDEMG = 2$$

$$NDEM = NDEMG = 2$$

$$NSUP = 15$$

As the supply is first utilized by the aphids, the resulting flows are:

$$RNA = \text{minimum}(2, 15) = 2$$

$$RNAAP = NDEMA = 0.68$$

$$RNAAP = RNA - RNAAP = 1.32$$

Now the demands for carbohydrates are calculated. Total demand is determined by the demand of the grains:

$$CDEMA = 1/0.2 * 0.68 = 34$$

$$CDEMG = 50$$

$$CDEM = 50$$

$$CSUP = 1000$$

Flow of carbohydrates:

$$RCA = \text{minimum}(50, 1000) = 50$$

$$RCAAP = CDEMA = 34$$

$$RCAGR = RCA - RCAAP = 16$$

Conclusion During sink-limited growth, grains are unaffected by aphids if hypothesis I is used to describe the direct effects. However, aphid feeding reduces the rate of grain growth if hypothesis II is applied.

Exercise 76

- a. Relative sensitivity was defined as
 $(\Delta \text{output/output}) / (\Delta \text{param/param})$

If for example the average aphid weight is decreased by 10%, grain yield will increase, and the relative sensitivity is negative. However, the damage becomes smaller, thus the relative sensitivity of damage to average aphid weight is positive.

- b. $r.s. = (\Delta \text{output/output}) / (\Delta \text{param/param})$

For changes in the average aphid weight:

$$-0.13 = (\Delta \text{yield/yield})/0.10$$

$$(\Delta \text{yield/yield}) = -0.013$$

$$\Delta \text{yield} = -129 \text{ kg ha}^{-1}$$

$$\text{yield} = 9898 - 129 = 9769 \text{ kg ha}^{-1}$$

Exercise 77

Mathematical representation of Example 2:

maximize $(w = (25x_1 + 40x_2) - (5x_1 + 10x_2))$ net energy gain

subject to

$$2x_1 + 3x_2 \leq 120 \quad \text{travelling time constraint}$$

$$2x_1 + x_2 \leq 80 \quad \text{searching time constraint}$$

$$20x_1 + 30x_2 \geq 600 \quad \text{minimal energy requirement}$$

$$x_1 \geq 0, x_2 \geq 0; \quad x_1, x_2 \text{ integer}$$

with x_1 the number of prey caught at the first site, and x_2 the number of prey caught at the second site.

Exercise 78

Graphically, the solution can be found to consist of the intersect BC in Figure 78. Thus, there is an infinite number of alternative solutions. This conclusion can also be arrived at by evaluating the objective function values at the points A, B, C and D. In A $x_1 = 0$ and $x_2 = 3$. The objective function value is $w = 3$.

Moving from A to B along the constraint $x_2 = 3$, x_1 increases to $x_1 = 3$. The value function in B is $w = 6$. Going from B to C, x_1 increases and x_2 decreases at the same rate. As the coefficients of x_1 and x_2 are the same in the objective function, no change in w occurs. Therefore, B, C and all intermediate points are equivalent. When going from C to D, x_1 remains unchanged, while x_2 decreases according to the constraint $x_1 = 4$. This results in a decrease of the value of w . Conclusion is that transect BC is optimal.

Exercise 79

The standard form of Example 1 can be obtained by introducing slack variables y_1 and y_2 in the constraints. The variables have coefficients equal to zero in the objective function.

$$\text{maximize } (w = 2x_1 + 5x_2 + 0y_1 + 0y_2 + 0y_3)$$

subject to

$$x_1 + x_2 + y_1 = 6$$

$$x_1 + y_2 = 4$$

$$x_2 + y_3 = 3$$

$$x_1 \geq 0, x_2 \geq 0, y_1 \geq 0, y_2 \geq 0, y_3 \geq 0.$$

The standard form of Example 2 is found in a similar way:

$$\text{maximize } (w = 20x_1 + 30x_2 + 0y_1 + 0y_2 + 0y_3)$$

subject to

$$2x_1 + 3x_2 + y_1 = 120$$

$$2x_1 + x_2 + y_2 = 80$$

$$20x_1 + 30x_2 - y_3 = 600$$

$$x_1, x_2, y_1, y_2, y_3 \geq 0; x_1, x_2 \text{ integer}$$

Exercise 80

The foraging problem is described as:

$$\text{maximize } (w = (25x_1 + 40x_2) - (5x_1 + 10x_2)) \quad (1)$$

Subject to

$$2x_1 + 3x_2 \leq 120 \quad (2)$$

$$2x_1 + x_2 \leq 80 \quad (3)$$

$$20x_1 + 30x_2 \geq 600 \quad (4)$$

$$x_1, x_2 \geq 0 \text{ and integer} \quad (5)$$

Reformulation in the standard form:

$$\text{maximize } (w = 20x_1 + 30x_2) \quad (6)$$

subject to

$$2x_1 + 3x_2 + y_1 = 120 \quad (7)$$

$$2x_1 + x_2 + y_2 = 80 \quad (8)$$

$$20x_1 + 30x_2 - y_3 = 600 \quad (9)$$

$$x_1, x_2, y_1, y_2, y_3 \geq 0; x_1, x_2 \text{ integer} \quad (10)$$

Notice that $x_1 = 0, x_2 = 0$ does not suffice as a first feasible solution in this case. Instead, choose e.g. $x_1 = 40, x_2 = 0$. This implies for the slack variables: $y_1 = 40, y_2 = 0, y_3 = 200$.

Check if the solution is optimal by making x_1 explicit in Equation 8 and substituting it in the objective function:

$$\text{maximize } (w = 20(40 - \frac{1}{2}x_2 - \frac{1}{2}y_1) + 30x_2) \quad (11a)$$

which is equivalent to

$$\text{maximize } (w = 800 + 20x_2 - 10y_1) \quad (11b)$$

The coefficient of x_2 in the objective function is positive, or, in other words, increasing the value of x_2 contributes to the maximization of w . The constraints can be written with x_1 in Equation 8 as pivot:

$$\begin{aligned} 2x_2 &= 40 - y_1 + y_2 \\ x_1 &= 40 - \frac{1}{2}x_2 - \frac{1}{2}y_2 \\ 20x_2 &= -200 + 10y_2 + y_3 \end{aligned}$$

Evaluation of the constraints shows that the feasible values for x_2 lie in the interval $[20, 40]$. A new solution, therefore, is $x_2 = 20$, $x_1 = 30$, $y_1 = 0$, $y_2 = 0$, $y_3 = 600$. Substituting $x_2 = 20$ in the objective function results in:

$$\text{maximize } (w = 1200 - 10y_1)$$

The coefficients of x_1 and x_2 have become zero or, in other words, we have a case with alternative solutions, as long as x_2 remains within the interval $[20, 40]$, which is dictated by the constraints. The value of the objective function is 1200.

Exercise 81

The solution $x_1 = 3$, $x_2 = 3$ is unique as long as the objective function coincides with neither transect AB nor BC. In the former case, the ratio of coefficients is 0:3, in the latter case 1:1.

Thus, the solution $x_1 = 3$, $x_2 = 3$ is optimal in the range of ratios of the coefficients in the objective function from 0 to 1.

Exercise 82

The DP-problem may be formulated as a problem of finding the solution to

$$\text{minimize } (w = C_{0k} + C_{1k} + C_{2k} + C_{3k})$$

where k represents the decision variables and C_{ik} represents the transformation function, describing the effect of proceeding from one state to the next. Constraints are absent.

Appendix 1

Derivation of the relative error in the rectangular integration method, for an exponential rate curve given as a function of time (i.e. integration without feedback).

After cancelling $v_0 \cdot \Delta t$:

$$E_{rel,1} = \frac{1}{\frac{1}{2} + \frac{1}{2} \cdot e^{c \cdot \Delta t}} - 1$$

The formula for the Taylor expansion is:

$$f(x) = f(x_1) + f'(x_1) \cdot (x - x_1) + \frac{f''(x_1)}{2!} \cdot (x - x_1)^2 + \frac{f'''(x_1)}{3!} \cdot (x - x_1)^3 + \dots$$

where x_1 indicates the reference point, with regard to which the function of x , $f(x)$, is expanded; $(x - x_1)$ is the distance between the value of x , for which the function is being calculated, and x_1 ; and $f'(x_1)$, $f''(x_1)$, etc. are the first, second and higher derivatives of the function of $f(x)$ with respect to x , at point x_1 .

Taking $x_1 = 0$, e^x gives the following result after expansion:

$$e^x = 1 + x + \frac{1}{2} \cdot x^2 + \frac{1}{6} \cdot x^3 + \frac{1}{24} \cdot x^4 + \dots,$$

and after some algebra, $E_{rel,1}$ is:

$$E_{rel,1} = \frac{1}{1 + \frac{1}{2} \cdot c \cdot \Delta t + \frac{1}{4} \cdot c^2 \cdot \Delta t^2 + \frac{1}{12} \cdot c^3 \cdot \Delta t^3 + \dots} - 1$$

Omitting second and higher order terms, and setting both terms over a common denominator, yields:

$$E_{rel,1} \cong - \frac{\frac{1}{2} \cdot c \cdot \Delta t}{1 + \frac{1}{2} \cdot c \cdot \Delta t} \quad \text{Equation A.1}$$

For $x_1 = 0$, the Taylor approximation to a function of the type $\frac{x}{1+x}$ is:

$$\frac{x}{1+x} = x - x^2 + x^3 - x^4 + \dots;$$

applying this to Equation A.1 gives:

$$E_{rel,1} \cong -\frac{1}{2} \cdot c \cdot \Delta t + \frac{1}{4} \cdot c^2 \cdot \Delta t^2 - \frac{1}{8} \cdot c^3 \cdot \Delta t^3 + \dots$$

Omitting second and higher order terms once more gives Equation 11 of Subsection 2.1.7.

Appendix 2

Derivation of the relative error in the rectangular integration method for an exponential rate curve which is not known as a function of time. (i.e. integration with feedback).

The surface areas obtained by the rectangular and trapezoidal integration methods are substituted in Equation 10:

$$E_{rel,1} = \frac{A_t \cdot (1 + \Delta t \cdot c)}{A_t \cdot (1 + \Delta t \cdot c + (\Delta t \cdot c)^2/2)} - 1$$

Cancelling A_t and setting 1 over the common denominator gives

$$E_{rel,1} = \frac{- (\Delta t \cdot c)^2/2}{1 + \Delta t \cdot c + (\Delta t \cdot c)^2/2}$$

Omitting higher order terms in the denominator yields

$$- \frac{1}{2} \cdot (\Delta t \cdot c) \cdot ((\Delta t \cdot c)/(1 + \Delta t \cdot c))$$

the second part of this expression is similar in form to Equation A.1 in Appendix 1. Expansion according to Taylor, and omission of higher order terms once more, gives Equation 12 (Subsection 2.1.7):

$$E_{rel,1} \cong -(\Delta t \cdot c)^2/2 = -(\Delta t/\tau)^2/2$$

Appendix 3

Residual variance in the escalator boxcar train

There is no dispersion caused by exchange between adjacent boxcars, but still some dispersion occurs due to internal mixing within a boxcar. During a development cycle, γ , the inflow is collected in boxcar number zero, and whatever variation there might be in the inflow, it is levelled out.

The strongest possible concentration of inflow is in the form of a single pulse. The outflow from the last boxcar will occur delayed over a period T_{total} , and also dispersed over a time span τ , equal to γ/v . The variance around the average time of outflow t_d can be derived as:

$$\sigma_{\text{tot}}^2 = \frac{1}{A_0} \int_{t_d - 0.5\tau}^{t_d + 0.5\tau} (t - t_d)^2 Q_{\text{out}} dt$$

Since, during the time span τ , an amount A_0 must flow out, Q_{out} will be made equal to A_0/τ and A_0 cancels. Substitution, and solving the integral, gives

$$\sigma_{\text{tot}}^2 = (1/12) \tau^2$$

The relative dispersion RD is

$$\sigma_{\text{total}}/T_{\text{total}} = \sqrt{(\tau^2/12)/(N\tau)} = 1/(N\sqrt{12})$$

This equation permits the choice of an appropriate number of boxcars if the observed RD is small. For instance, when it is 3%, 8 boxcars are required. An entirely dispersion-free boxcar train is not possible.

Appendix 4

$$\text{Evaluation of } \sigma^2 = \int_0^{\infty} (t - \tau)^2 \frac{1}{\tau} \exp(-t/\tau) dt$$

First, the upper boundary of integration is changed from infinity to a very large value t_f , which can later be made arbitrarily large:

$$\sigma^2 = \frac{1}{\tau} \int_0^{t_f} (t - \tau)^2 \exp(-t/\tau) dt$$

By replacing $t - \tau$ by t_* , this expression can be rewritten as

$$\sigma^2 = \exp(-\tau/\tau) \frac{1}{\tau} \int_{-\tau}^{t_f - \tau} t_*^2 \exp(-t_*/\tau) dt_*$$

or

$$\sigma^2 = -\frac{\exp(-1)}{\tau} \tau \exp(-t_*/\tau) (t_*^2 + 2\tau t_* + 2\tau^2) \Big|_{-\tau}^{t_f - \tau}$$

Now we let t_f approach infinity, so that the value of the integral at the upper boundary approaches zero:

$$\sigma^2 = 0 - \exp(-1) \exp(1) (\tau^2 - 2\tau^2 + 2\tau^2) = \tau^2$$

Appendix 5

A.5 CSMP, Continuous System Modeling Program

H.H. van Laar and P.A. Leffelaar

A.5.1 Introduction

CSMP stands for Continuous System Modeling Program, version III. It has been extensively described in the Program Reference Manual by IBM (SH19-7001-3, 1975). CSMP is a specific dynamic simulation language used to integrate rate equations to obtain the state of the model as a function of time. CSMP is a non-procedural language, which means that the user can write programs in a conceptual order and CSMP will sort the statements in a computational order. An important feature in CSMP is the availability of numerical integration routines which are easy to use. Moreover, CSMP automatically keeps track of time in dynamic simulation. CSMP provides special functions (e.g. interpolation), and as its source program is written in FORTRAN (FORMula TRANslation), the researcher may use FORTRAN statements as well as all FORTRAN library functions in more advanced models. Tabular and/or graphical output can be obtained by just listing the variables on a special label.

A.5.2 The structure of the model

One starts a program with a TITLE label containing a short identification of the program. In a CSMP program, 3 segments can be distinguished: INITIAL,

TITLE CSMP STRUCTURE	
INITIAL	sorting
.....	
NOSORT	no sorting
.....	
SORT	sorting
.....	
DYNAMIC	sorting
.....	
NOSORT	no sorting
.....	
SORT	sorting
.....	
TERMINAL	no sorting
.....	
END	
STOP	
ENDJOB	

Figure A.1. General layout of a CSMP program. Sorting: sorted by CSMP. No sorting: must be sorted by the user.

DYNAMIC and **TERMINAL**. These statements (labels) indicate that the computations must be performed before, during and after a simulation run, respectively (Figure A.1). If one is using these segments, then each segment label closes the former segment. To close the entire program, one must use the statements **END**, **STOP** and **ENDJOB**, respectively, each on a separate line, and **ENDJOB** must start in the first column.

In the **INITIAL** segment, computations are executed only once per run. The use of the segment is optional. The **INITIAL** segment can be used for computing the results which are used as input data for the dynamic section of the program. All initial conditions and parameters can be given values in this segment. The segment where the simulation takes place is the **DYNAMIC**. This segment is normally the most extensive one in a model. It contains the complete description of the model dynamics, together with any other computation required during the simulation. For some models, the program consists of just the **DYNAMIC** segment. The segment may be declared explicitly by the label **DYNAMIC**, but if there is no **INITIAL** or **TERMINAL** segment, the **DYNAMIC** label can be omitted. The **TERMINAL** segment can be used for computations required at the end of the run, after completing the simulation. This can be a calculation based on the final values of one or more variables. As in the **INITIAL** segment, the computations are executed only once. Also the **TERMINAL** segment is optional.

CSMP is provided with a sorting algorithm to free the user from the task of correctly sequencing the statements. The user can then focus his attention on defining the problem, and can put the statements in a conceptual order. The statements will be put in computational order during the translation phase, and are then written into **UPDATE**, a subroutine created by the **CSMP** compiler which contains the structure of the model with sorted **FORTRAN** statements. All statements in the **INITIAL** and **DYNAMIC** segments are placed in computational order. The statements in the **TERMINAL** segment, however, must be sorted by the user.

It is sometimes desirable for statements in the program not to be sorted by the compiler, for instance where branching conditions are desired, or a decision must be made. In that case the statements, written either in **CSMP** or **FORTRAN**, must stay in a fixed order. There are two ways in **CSMP** to avoid sorting the statements. The simplest method is to divide the **INITIAL** and **DYNAMIC** segments into sections by means of the labels **NOSORT**, which prevents the statements from being sorted, and **SORT**, which ends a **NOSORT** section. Thus, the program will be split into individual blocks. The program blocks between the **NOSORT-SORT** sections will now be sorted individually, and during the translation phase, statements from one **SORT** section cannot be moved to another **SORT** section. Since this usually gives computational problems, it is recommended to write full sections in **NOSORT** or to use **PROCEDURES**. **FORTRAN** statements must always be sequenced in computational order and can be defined only in a non-sortable section.

A more elegant method of defining sections which are not sorted by the CSMP compiler, but which may be sorted as a whole, is to define PROCEDURES. The PROCEDURE is treated as an entity. It is sorted as a functional block on the basis of input and output names given by the user when defining the PROCEDURE. These names correspond with those of the statements in the functional block. A PROCEDURE is defined as:

```

PROCEDURE OUTP1,OUTP2=NAME(INPUT1,INPUT2)
....
....
....
....
ENDPROCEDURE

```

} CSMP and/or FORTRAN
} statements
} sorted by the user

} sorted by
} CSMP

The statements describing the PROCEDURE are placed between the statements labelled PROCEDURE and ENDPROCEDURE and are not sorted internally. Variables defined within a PROCEDURE block and not appearing in the definition, e.g. because they are not needed to sort the block, are not available for data output by means of PRINT or OUTPUT (see also section 'Labels'). If these variables are needed for output, they should be included as output names in the PROCEDURE definition. A PROCEDURE is a block of sequenced statements which is executed where defined. Contrary to PROCEDURES, SUBROUTINES can be called for more than once in a program.

SUBROUTINES are another way of structuring programs. SUBROUTINES can be called from within the CSMP program, but are defined between the labels STOP and ENDJOB. The simplest way to use SUBROUTINES will be discussed below. A SUBROUTINE is called for by the sortable statement:

$$\text{OUT1,OUT2} = \text{SUBNAM}(\text{IN1,IN2,IN3}) \quad \text{Equation (A.2)}$$

where the variables on the left hand side of the equals-sign are the results of the calculations performed in the SUBROUTINE named SUBNAM. (Note that there must be at least two variables on the left hand side, otherwise the translator accepts SUBNAM as a FUNCTION; for details see below.) The input variables for these calculations are listed between brackets following the name of the SUBROUTINE. The variable names, either referring to reals, integers or arrays, serve different purposes: (1) they are used to sort the statement within the CSMP program, as in the case of a PROCEDURE, (2) they attend to the communication between the CSMP program and the SUBROUTINE. The CSMP compiler interprets Equation A.2 as:

```
CALL SUBNAM(IN1,IN2,IN3,OUT1,OUT2)
```

which is placed in UPDATE. Thus, the output variables are placed just after the input variables without changing their sequence. Statements placed between STOP and ENDJOB are not processed by the CSMP compiler. Thus SUBROU-

TINE definitions are directly placed into UPDATE, and the arguments in the definition must agree with the call to the SUBROUTINE as generated by the CSMP translator:

```
SUBROUTINE SUBNAM(IN1,IN2,IN3,OUT1,OUT2)
```

The positions of the variable names in the call statement and in the definition of the SUBROUTINE correspond to one another, but need not have the same names. However, corresponding places in the list of variables must contain the same type of variable.

All the usual FORTRAN rules apply to SUBROUTINES. Some important rules are:

1. Statements begin in column 7 or higher; numbers of continuation labels must be placed in the first 5 columns; column 6 is reserved to indicate whether the line is a continuation of the preceding one by, for example, placing a dollar (\$) sign there.
2. Variables beginning with I, J, K, L, M or N are considered integer, while others are considered real. This may be cumbersome, as in CSMP all variables are considered real except those placed on the FIXED label. It is good practice to apply this rule to FORTRAN as well by introducing the statements:

```
    IMPLICIT REAL(A-Z)
```

```
    INTEGER ...
```

directly after the line which defines the SUBROUTINE. The first statement declares all variables beginning with A up to and including Z real; subsequently, the specific variables listed after the INTEGER label are declared integer. The INTEGER label in FORTRAN is equivalent to the FIXED label in CSMP.

3. Array variables in SUBROUTINES need memory storage:

```
    DIMENSION A(100),...
```

Here, 100 locations are reserved for the variable A. The DIMENSION label in FORTRAN is equivalent to the STORAGE label in CSMP.

4. More than one RETURN statement may be used to return to the place in the CSMP program where the SUBROUTINE was called. However, a SUBROUTINE is always terminated by the statements:

```
    RETURN
```

```
    END
```

The general layout of a SUBROUTINE is shown in Figure A.2.

In the call of a SUBROUTINE in CSMP, at least two variables must be listed on the left hand side of the equals-sign. If there is only one variable listed, the CSMP compiler interprets the statement as a so-called function subroutine, where the result of the calculation is returned to the calling program using the name of the subroutine rather than the output variable. This implies also that only a single variable can be output from a function subroutine, while often array

column

1234567

```
SUBROUTINE SUBNAM(NLOC,IN1,IN2,IN3,INTB,OUT1,OUT2)
IMPLICIT REAL(A-Z)
INTEGER NLOC, ....
DIMENSION ....
.
.
OUT1 = AFGEN(NLOC,INTB,IN1)
.
.
RETURN
END
```

Figure A.2. General layout of a SUBROUTINE.

results are needed, and that can only be achieved by arguments in subroutines. The function subroutine is not discussed here, but when there is one output variable in the subroutine, misinterpretation by the CSMP compiler is avoided by including a dummy variable in the list of output variables. This dummy variable must also be given in the definition.

Many CSMP functions may be used within SUBROUTINES, but specifically excluded is the INTGRL function. The use of functions such as LIMIT, EXP and SQRT is similar to their use in CSMP. When functions starting with I, J, K, L, M or N are used (e.g. INSW or LIMIT, which are examples of function subroutines) the name needs to be declared real either by:

```
REAL INSW, LIMIT
```

or implicitly as explained above. History functions require both past and present values of the inputs to calculate their outputs. When history functions, e.g. AFGEN or NLFGEN, are used in SUBROUTINES, storage locations must be indicated. This is done in the CSMP program by:

```
HISTORY SUBNAM(5)
```

at the beginning of the program. The number '5' corresponds to the number of storage locations for an AFGEN function, which is used in SUBROUTINE SUBNAM. For the use of other functions, reference is made to the CSMP manual. The function which is interpolated by AFGEN is transferred to the SUBROUTINE by including its name in the list of input variables. The combination of the HISTORY label and the call for the SUBROUTINE SUBNAM:

```
OUT1,OUT2=SUBNAM(IN1,IN2,IN3,INTB)
```

where INTB is the function name, causes the generation of the following UP-

```

column
1234567
      SUBROUTINE SUBNAM(IN1,IN2,IN3,OUT1,OUT2)
      IMPLICIT REAL(A – Z)
      INTEGER ....
      DIMENSION ....
      .
      .
      IF(.....) RETURN
      .
      .
10    CONTINUE
      .
      .
      RETURN
      END

```

Figure A.3. General layout of a SUBROUTINE containing a history function.

DATE statement:

```
CALL SUBNAM(1,IN1,IN2,IN3,INTB,OUT1,OUT2)
```

The first argument between brackets, e.g. 1, contains a number corresponding with the first storage location assigned to the SUBROUTINE. The SUBROUTINE definition must agree with the call generated by the CSMP compiler. The general layout of a SUBROUTINE containing an AFGEN function is shown in Figure A.3. The integer variable NLOC (Figure A.3) takes the value assigned by the CSMP compiler in the SUBROUTINE call in UPDATE. Figure A.4 summarizes all this. This demonstration program simulates the change in the amount of water in two lakes connected in series when an instantaneous doubling of water inflow occurs.

A.5.3 Some elements of CSMP

Numeric constants There are two types of constants: integer and real. Integers are whole numbers with a maximum of 10 digits without a decimal point. Real (floating-point) constants are numbers written with a decimal point, with a maximum of 7 digits. A real constant may be followed by a decimal exponent written as the letter E, followed by a signed or unsigned one or two digit integer constant. The decimal E format forms a real constant that is the product of the real constant portion multiplied by 10 raised to the desired power; e.g. $213.15 = 2.1315E2 = 2131.5E-01$. Real constants are restricted to a total of 12 characters.

Figure A.4. Example of the use of subroutines in CSMP.

```

TITLE Demonstration program on how a subroutine can be used
INITIAL
HISTORY INICON(5), FLOWS(5)
FIXED N
STORAGE FLOW(3)
***** Defenition of parameters *****
PARAM DTSYS=8., N=2

***** Timer variables and integration method *****
TIMER FINTIM=14., OUTDEL=2., DELT=2.
METHOD RECT

***** Output results *****
OUTPUT H(1), H(2)

***** Function defining inflow rate into the first reservoir
FUNCTION INTB = 0.0,100., 1.99,100., ...
                2.0,200., 14.0,200.

***** Initial calculations *****
REALN =N
TC     =DTSYS/REALN

***** Initial conditions of reservoirs *****
IH,DUM1      =INICON(N,INTB,TIME,TC)

*****
*****
DYNAMIC
H            =INTGRL(IH,NETFLO,2)

***** Net flow for each reservoir *****
NETFLO,DUM2  =NETFLS(N,FLOW)

***** Individual flows into and out of each reservoir *****
FLOW,DUM3    =FLOWS(N,INTB,TIME,TC,H)

END
STOP
*****
***** Subroutines called from initial *****
*****

      SUBROUTINE INICON(NLOC,N,INTB,TIME,TC,
$           IH,DUM1)
      IMPLICIT REAL(A-Z)
      INTEGER      I,N,NLOC
      DIMENSION    IH(2)
      IN           =AFGEN(NLOC,INTB,TIME)
      DO 10 I =1,N
         IH(I)=IN*TC
10  CONTINUE
      RETURN
      END

```

 ***** Subroutines called from dynamic *****

```

SUBROUTINE NETFLS(N, FLOW,
$              NETFLO, DUM2)
  IMPLICIT REAL(A-Z)
  INTEGER      I, N
  DIMENSION   FLOW(3), NETFLO(2)
  DO 10 I = 1, N
    NETFLO(I) = FLOW(I) - FLOW(I+1)
10 CONTINUE
  RETURN
  END

```

```

SUBROUTINE FLOWS(NLOC, N, INTB, TIME, TC, H,
$              FLOW, DUM3)
  IMPLICIT REAL(A-Z)
  INTEGER      I, N, NLOC
  DIMENSION   H(2), FLOW(3)
  IN          = AFGEN(NLOC, INTB, TIME)
  FLOW(1) = IN
  DO 10 I = 2, N+1
    FLOW(I) = H(I-1) / TC
10 CONTINUE
  RETURN
  END

```

 ENDJOB

Variables The name of a variable can contain one to six characters and the first character must be a letter. No blanks or special characters (e.g. +,*(-:/).) are allowed. For so-called 'reserved words' one is referred to the Reference Manual. All names of labels, functions and data statements are reserved words. In CSMP programs, before the label STOP all variables are declared real. When using integer variables in a program, these variables should be explicitly declared at the beginning of the program by the label FIXED.

Operators As in FORTRAN, the operators and the order in which operations are performed are:

()	grouping of variables and/or constants	1st
**	exponentiation	2nd
*	multiplication	} 3rd
/	division	
+	addition	} 4th
-	subtraction	
=	replacement	5th

Functions and expressions within parentheses are always evaluated first. For operators of the same order, the component operations of the expression are performed from left to right. There is an exception for exponentiation, where the evaluation is performed from right to left. Thus, the expression $A^{**}B^{**}C$ is evaluated as $A^{**}(B^{**}C)$.

Functions A description of various CSMP and FORTRAN functions is given in Tables A.1 and A.2. Extra attention will be given here to the INTGRL and AFGEN functions. The general instruction to execute computations with relation to numerical integration is:

$$A = \text{INTGRL}(IA, \text{RATE})$$

in which A is the output of an integrator, RATE is the rate of change of A, which is integrated over time, and IA is the initial condition of A in a simulation run. Initial conditions are introduced using an INCON label. The feature of integrator arrays is very useful when simulating spatially distributed systems, e.g. gas diffusion through water, or dispersion in time (exponential delays), where space or time is divided into layers or classes. Each class or layer is represented by an integrator and, between layers, transport takes place (Figure A.4 gives an example of the use of an integrator array of length 2). One can use array integrals with subscripted variables for computations that have a similar structure. The statement:

$$A = \text{INTGRL}(IA, \text{RATE}, 10)$$

specifies an array of 10 integrators in which A(I), IA(I) and RATE (I) are, respectively, the output, initial conditions and input variables. The third argument, 10, is an integer constant. The initial conditions of an integrator array must be given by means of a TABLE statement, e.g.

$$\text{TABLE } IA(1-10) = 10 * 5.$$
$$\text{TABLE } IA(1-10) = 2., 4., 6., 3., 7., 1., 4 * 0.$$

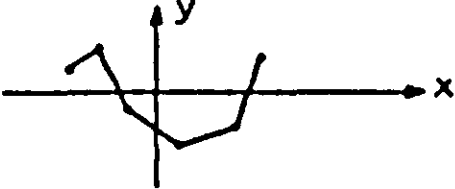
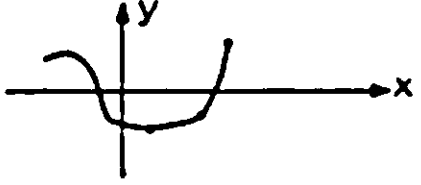
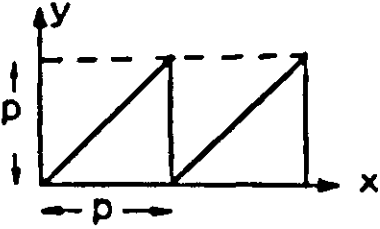
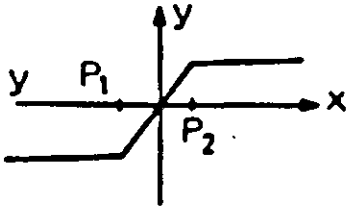
In the latter TABLE statement, the first 6 numbers represent real numbers, the '4' represents an integer number to indicate that the last four numbers have the same value (e.g. zero). For subscripted variables, one usually needs to reserve memory storage. For variables in integrator arrays, however, this happens automatically. The computer system generates:

$$\text{STORAGE } A(10), IA(10), \text{RATE}(10)$$

The rates RATE(1) to RATE(10) can be computed in a DO loop:

```
DO 100 I = 1,10
  RATE(I) = .....
100 CONTINUE
```

Table A.1. Some CSMP functions.

CSMP III Functions	Equivalent Mathematical Expression
Integrator $Y = \text{INTGRL}(IC, X)$ where: $IC = y_{t_0}$	$y(t) = \int_{t_0}^t x dt + y(t_0)$ where: $t_0 = \text{start time}$ $t = \text{time}$
Arbitrary function generator (linear interpolation) $Y = \text{AFGEN}(\text{FUNCT}, X)$	$y = f(x)$ 
Arbitrary function generator (quadratic interpolation) $Y = \text{NLFGEN}(\text{FUNCT}, X)$	$y = f(x)$ 
Modulo function $Y = \text{AMOD}(X, P)$	$y = x - nP$ n is an integer value such that $0 \leq y < P$ 
Limiter $Y = \text{LIMIT}(P1, P2, X)$	$y = P_1 ; x < P_1$ $y = P_2 ; x > P_2$ $y = x ; P_1 \leq x \leq P_2$ 
Not $Y = \text{NOT}(X)$	$y = 1 \text{ if } x < 0$ $y = 0 \text{ if } x > 0$
Input Switch Relay $Y = \text{INSW}(X1, X2, X3)$	$y = x_2 \text{ if } x_1 < 0$ $y = x_3 \text{ if } x_1 \geq 0$

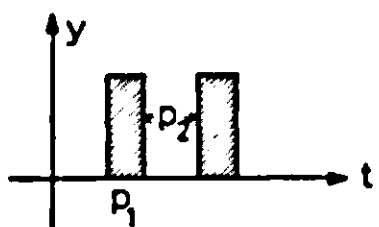
in which 100 is the 'name' of the DO loop, I is a counter which takes the values 1, 2, 3, ... 10, successively so that all RATEs will be computed. I should be an integer variable; therefore, it must be declared integer by the statement FIXED I. A DO loop cannot be sorted by CSMP, so it must be put in a NOSORT-SORT section, a PROCEDURE or in a SUBROUTINE.

The INTGRL statement merely indicates that the specified RATEs have to be integrated. The numerical integration method has still to be specified. This is done on the METHOD label, e.g. METHOD RECT, which causes rectangular integration to take place.

The Arbitrary Function GENERator (AFGEN function) in CSMP interpolates linearly between supplied points (e.g. x_1, y_1 and x_2, y_2). The function value \hat{y} for a certain x is then calculated by the expression:

$$y = y_1 + (x - x_1) \cdot (y_2 - y_1) / (x_2 - x_1)$$

Table A.1. Continued.

<p>Dead time (DELAY)</p> <p>Y=DELAY(N,P,X)</p> <p>where: P=delay time N=number of points sampled in interval p (integer constant) and must be ≥ 3, and $\leq 16,378$</p>	<p>$y=x(t-p) ; t > p$</p> <p>$y=0 ; t < p$</p> <p>Equivalent Laplace Transfer Function: $\frac{Y(s)}{X(s)} = e^{-ps}$</p>
<p>Implicit function</p> <p>Y=IMPL(IC,P,FOFY)</p> <p>where: IC=first guess P = error bound FOFY=output name from final statement in algebraic loop definition</p>	<p>$y = f(y)$</p> <p>$y - f(y) \leq p y$</p>
<p>Impulse generator</p> <p>Y=IMPULS(P1,P2)</p> <p>where: P1=time of first pulse P2=interval between pulses</p>	<p>$y=0 ; t < p_1$</p> <p>$y=1 ; (t-p_1) = kp_2$</p> <p>$y=0 ; (t-p_1) \neq kp_2$</p> <p>$k = 0, 1, 2, 3, \dots$</p> 

and is written in CSMP: $Y = \text{AFGEN}(\text{XYTB}, X)$

FUNCTION XYTB = (0.,0.),(2.,0.4),(6.,0.1)

where the first number of a pair represents the variable x; the values of x must increase monotonically. In most models, linear interpolation suffices. For higher order interpolation methods, reference is made to the CSMP manual.

A.5.4 Labels

Output control statements:

- TITLE** allows the user to identify the program, and the title appears on top of each page of the output listing;
- PRINT** is used to specify upto 55 variables whose values will be printed at each PRDEL interval in a tabular form (only real and not integer variables!). The PRINT label can be used only once in a CSMP program, as a second label would override the first;
- OUTPUT** is used to obtain printed output together with graphical output of

Table A.2. Some FORTRAN functions, which can be used in CSMP statements.

FORTRAN Functions	Equivalent Mathematical Expression
Exponential Y = EXP (X)	$y = e^x$
Trigonometric sine (argument in radians) Y = SIN (X)	$y = \sin (x)$
Trigonometric cosine (argument in radians) Y = COS (X)	$y = \cos (x)$
Square root Y = SQRT (X)	$y = \sqrt{x}$
Largest value (Real arguments and output) Y = AMAX1 (X1, X2)	$y = \max (x_1, x_2)$
Smallest value (Real arguments and output) Y = AMIN1 (X1, X2)	$y = \min (x_1, x_2)$

upto 5 variables at each OUTDEL interval. When the number of OUTPUT variables exceeds 5, graphical output is suppressed and printed output (of upto 55 variables) is given alone.

PRINT is used to organize the graphical OUTPUT.

A useful option is the following example:

```
PAGE GROUP, NTAB = 0, WIDTH = 80
OUTPUT A(1), A(3)
OUTPUT A(1), A(10)
PRINT A(1), A(3), A(10)
```

Here the graphical output of A(1) and A(3), and A(1) and A(10) may easily be compared as these variables are plotted on the same scale (PAGE GROUP). On the plots no tabular output is given (PAGE NTAB = 0), so as to obtain the largest possible graphs.

Tabular output for these variables is obtained by the PRINT statement.

The statement PAGE WIDTH = 80 causes the graphs to be inspected on the computer terminal. A PAGE statement preceding all the OUTPUT statements applies to the whole group. A PAGE statement that follows an OUTPUT statement is assigned to that statement.

Execution control statements:

Values of timing variables are specified with the TIMER statement:

FINTIM final value of time for terminating a simulation;

OUTDEL time interval for graphical output;

PRDEL time interval for tabular output;

DELT integration interval;

TIME initial value of time, to be specified only if not zero.

Example: TIMER FINTIM = 100., PRDEL = 5., OUTDEL = 5.
TIMER DELT = 1.
TIMER TIME = 10.

METHOD identifies the desired integration routine. Note that if the integration method is not specified, the integration routine RKS is default.

Example: METHOD RECT

END completes the specifications of the model;

STOP terminates the simulation run;

ENDJOB terminates the job.

If a simulation is to be repeated with new data and/or execution control statements, the statements are to be placed between two END statements:

Example:
PARAM A = 10.
TIMER FINTIM = 50.
END
PARAM A = 20.
TIMER FINTIM = 100.
END
STOP
ENDJOB

Data statements:

PARAM assignment of a numeric value to a parameter;

CONST assignment of a numeric value to a constant;

INCON assignment of a numeric value to an initial condition;

TABLE assignment of numeric values of (initial) constants to arrays;

FUNCTION assignment of the numeric relation between two variables.

Example: PARAM A = 10., B = 20.
CONST PI = 3.1415
INCON IA = 0., IB = 5.
TABLE A(1-5) = 1., 2., 3., 4., 5.
FUNCTION TEMPTB = (0., 0.), (10., 1.), (40., 1.5)

A.5.5 Syntax

Some syntax rules may be helpful to make programs more readable:

- try to split up your program into an INITIAL, a DYNAMIC and, if necessary, a TERMINAL segment. Remember that statements in a TERMINAL segment must be sequenced by the user;
- lump all parameter specifications at the beginning of your program, so as to have a better overview of them;
- place all INTGRL statements together, e.g. just at the beginning of the DYNAMIC;
- lump all FUNCTIONS that remain unchanged between simulation runs at the end of the CSMP part of your program before the label END. Other FUNCTIONS can be put near the parameter specifications at the beginning of the program.
- start CSMP statements in the first column;
- start FORTRAN statements in the seventh column;
- make short comments in your program in the proper place;
- use ***** to begin comments in CSMP;
- use C***** to begin comments in FORTRAN subroutines;
- use blank lines and ***-lines to distinguish between different program parts;
- use blanks (spaces) to line up, e.g. equals-signs (=) and to distinguish between pairs of data in FUNCTION statements;
- continue CSMP statements on the next line by typing three dots (...) on the line to be continued;
- continue FORTRAN statements in subroutines by typing a dollar sign (\$) in the sixth column of the line following the line which is to be continued;
- when the history function AFGEN is used within a subroutine, the user should reserve 5 storage locations using the label HISTORY SUBNAM(5) in the CSMP program. Here, SUBNAM stands for the name of the subroutine where the AFGEN is to be used. If AFGEN is used in the CSMP program itself, memory is automatically allocated by the translator .

Appendix 6

Listing of a model to describe the competition for light and soil moisture. Parameter values are for maize and barnyard grass (*Echinochloa crus-galli*). References to the values for maize were given in Figure 51. The parameter values for barnyard grass were derived from various field experiments of Spitters, de Groot, Kropff, Vossen & Coster (unpublished data). Most of the abbreviations are explained in Table 12.

```

TITLE COMPETITOR - A MODEL FOR INTER-PLANT COMPETITION
* Species 1=maize, 2=Echinochloa crus-galli
FIXED I,J,K,NS,PRSNC
/      DIMENSION MAINTS(2),DVRV(2),DVRR(2),RDRDV(2),RDRSL(2)
STORAGE GPHOT(2),DTGA(2),AMAX(2),AMX(2),AMDVS(2),AMTMP(2),EFF(2)
STORAGE MAINT(2),MAINSO(2),MNDVS(2),ASRQ(2),ASRQSO(2)
STORAGE SLA(2),GLAI(2),DLAI(2),KDF(2),TADRW(2),WLVG(2),RDR(2)
STORAGE FSH(2),FLV(2),FST(2),FSO(2),FRT(2),GTW(2),GSH(2)
STORAGE DAYEM(2),PRSNC(2),NPL(2),LAO(2),RGRL(2),DTEFF(2)
STORAGE HMAX(2),HB(2),HS(2),HDECR(2),DVSD(2)
STORAGE P(2),CRPF(2),PTRAN(2),TRAN(2),TRANRF(2),VSMCR(2),FRABS(2)

* Dry weights of leaves(green and dead),stems,storage organs,roots
* and total above-ground biomass (kgDM/ha) as integrals of growth rates
  WLV  = INTGRL(0.,GLV,2)
  WLVD = INTGRL(0.,DLV,2)
  WST  = INTGRL(0.,GST,2)
  WSO  = INTGRL(0.,GSO,2)
  WRT  = INTGRL(0.,GRT,2)
  PROCEDURE WLVG,TADRW = DRYWT (WLV,WLVD,WST,WSO)
  DO K=1,NS
    WLVG(K) = WLV(K) - WLVD(K)
    TADRW(K) = WLV(K) + WST(K) + WSO(K)
  ENDDO
  ENDPRO

* Leaf area index (ha leaf / ha soil)
  LAI = INTGRL(0.,NGLAI,2)
  GLAI,LAIT = XGLA (DAY,DAYEM,DTEFF,DVS,NPL,LAO,RGRL,DELT,...
    SLA,LAIT,GLV,NS)
  PROCEDURE NGLAI = NETLAI (GLAI,DLAI)
  DO K=1,NS
    NGLAI(K) = TRANRF(K) * GLAI(K) - DLAI(K)
  ENDDO
  ENDPRO
  PROCEDURE SLA = LAREA (DVS)
  DO K=1,NS
    FK=K
    SLA(K) = TWOVAR (SLAT,DVS(K),FK)
  ENDDO
  ENDPRO

```

* Leaf photosynthesis rate at light saturation (kg CO2/ha leaf/h)
 PROCEDURE AMAX,AMDVS,AMTMP = PHOTO (AMX,DVS,DDTMP)

```

DO K=1,NS
  FK=K
  AMDVS(K) = TWOVAR(AMDVST,DVS(K),FK)
  AMTMP(K) = TWOVAR(AMTMPT,DDTMP,FK)
  AMAX(K) = AMX(K) * AMDVS(K) * AMTMP(K)
ENDDO
ENDPRO

```

* Potential daily total gross assimilation (DTGA, kg CO2/ha/d)
 DTGA,DSO,FRABS,FRD = XDASSH (DAY,LAT,DTR,KDF,LAI,AMAX,EFF,NS,HGHT)

* Actual total growth rate (GTW, kg DM/ha/d)
 PROCEDURE GTW,GPHOT,MAINT = GROWTH (DTGA,ASRQ,TRANRF)

```

DO K=1,NS
* Conversion from assimilated CO2 to CH2O
  GPHOT(K) = DTGA(K) * 30./44.
* Maintenance respiration (kg CH2O/ha/d)
  TEFF = Q10**((DAVTMP-25.)/10.)
  MAINTS(K) = 0.03*WLV(K) + 0.015*WST(K) + 0.015*WRT(K) + ...
              MAINSO(K)*WSO(K)
  MNDVS(K) = WLVG(K) / (WLV(K) + NOT(WLV(K)))
  MAINT(K) = AMINI(GPHOT(K), MAINTS(K) * TEFF * MNDVS(K))
* Total growth rate (kg DM/ha/d)
  GTW(K) = (GPHOT(K) - MAINT(K)) / ASRQ(K) * TRANRF(K)
ENDDO
ENDPRO
PARAM Q10 = 2.

```

* Developmental stage (DVS: 0=emergence, 1=flowering, 2=maturity)
 DVS=INTGRL(0.,DVR,2)

```

PROCEDURE DVR=DEVEL(DAVTMP)
DO K=1,NS
  FK=K
  DVRV(K) = TWOVAR(DVRVT,DAVTMP,FK)
  DVRR(K) = TWOVAR(DVRRT,DAVTMP,FK)
  DVR(K) = INSW(DVS(K) -1., DVRV(K), DVRR(K)) ...
           * INSW(DAY-DAYEM(K),0.,1.) * PRSNC(K)
ENDDO
ENDPRO

```

PROCEDURE FSH,FLV,FST,FSO,FRT,ASRQ = DISF(DVS)

* Fraction of dry matter growth allocated to shoots, leaves, stems,
 * storage organs and roots

```

DO K=1,NS
  FK=K
  FSH(K) = TWOVAR(FSHTB,DVS(K),FK)
  FLV(K) = TWOVAR(FLVTB,DVS(K),FK)
  FST(K) = TWOVAR(FSTTB,DVS(K),FK)
  FSO(K) = 1. - FLV(K) - FST(K)
  FRT(K) = 1. - FSH(K)
* Assimilate requirements for dry matter conversion (kgCH2O/kgDM)
  ASRQ(K) = FSH(K) *(1.47*FLV(K) + 1.52*FST(K) + ...
            ASRQSO(K)*FSO(K)) + 1.45*FRT(K)
ENDDO
ENDPRO

```

* Growth rates of shoots(leaves, stems, storage organs) and roots (kgDM/ha/d)

PROCEDURE GSH, GLV, GST, GSO, GRT = GROWTH (GTW, FSH, FLV, FST, FSO, FRT)

DO K=1, NS

GSH(K) = FSH(K) * GTW(K)

GLV(K) = FLV(K) * GSH(K)

GST(K) = FST(K) * GSH(K)

GSO(K) = FSO(K) * GSH(K)

GRT(K) = FRT(K) * GTW(K)

ENDDO

ENDPRO

* Death rate of leaves (DLAI in ha/ha/d, DLV in kg DM/ha/d)

PROCEDURE DLAI, DLV = SENESC(RDR)

DO K=1, NS

DLAI(K) = LAI(K) * (EXP(RDR(K) * DELT) - 1.)

DLV(K) = WLVG(K) * DLAI(K) / (LAI(K)+NOT(LAI(K)))

ENDDO

ENDPRO

* Upper height of photosynthetic surface (m)

HGHT = INTGRL (0., RHG, 2)

PROCEDURE RHG = HEIGHT (DVR)

DO K=1, NS

RHG(K) = DVR(K) * HMAX(K) * HS(K) * HB(K) * EXP(-HS(K)*DVS(K))...
 /(1. + HB(K) * EXP(-HS(K)*DVS(K)))**2 * TRANRF(K)

IF(DAY.EQ.DAYEM(K)) RHG(K) = PRSNC(K) * HMAX(K)/(1.+HB(K))

IF(DVS(K).GT.DVSD(K)) RHG(K) = - HDECR(K) * DVR(K)

ENDDO

ENDPRO

*** SOIL MOISTURE BALANCE ***

* Soil moisture in the root zone (kg H2O/m2 = mm)

SMRTZ = INTGRL(SMRTZI, RAIN - EVAP - TRANT - PERC)

INCON SMRTZI = 132.

* Volumetric soil moisture contents (kgH2O/m3; 10 kgH2O/m3 = 1 vol%) at
 * field capacity (VSMFC), wilting point (VSMWP), and air dryness (VSMAD)

PARAM VSMFC = 120., VSMWP = 30., VSMAD = 10.

* Volumetric soil moisture content of root zone (VSM)

VSM = SMRTZ / RTD

* Maximum rooting depth (m)

PARAM RTD = 1.10

* Rainfall and percolation (kgH2O/m2/day)

RAIN = AFGEN(RAINT, DAY)

PERC = AMAX1(0., SMRTZ + RAIN - EVAP - TRANT - RTD*VSMFC)

* Soil evaporation (EVAP) from Penman evaporation (EPENM) (kgH2O/m2/day),

* fraction of solar radiation transmitted through the canopy (FRD)

* and relative soil moisture content of root zone

EVAP = 0.75 * EPENM * FRD * LIMIT(0., 1., (VSM-VSMAD)/(VSMFC-VSMAD))

* Potential transpiration (PTRAN, mm/day) from Penman evaporation (EPENM),

* crop factor (CRPF), and absorbed solar radiation (FRABS)

```

* Actual transpiration (TRAN) from PTRAN and soil moisture content (VSM)
PROCEDURE PTRAN,TRANRF,TRAN,TRANT=TRANSP(EPENM,VSM,FRABS)
  TRANT=0.
  DO K=1,NS
    FK=K
    PTRAN(K) = EPENM * CRPF(K) * FRABS(K) / 0.85
    P(K) = TWOVAR(PTB, EPENM, FK)
    VSMCR(K) = (1.-P(K)) * (VSMFC-VSMWP) + VSMWP
    TRANRF(K) = LIMIT(0., 1., (VSM-VSMWP) / (VSMCR(K)-VSMWP))
    TRAN(K) = PTRAN(K) * TRANRF(K)
    TRANT = TRANT + TRAN(K)
  ENDDO
ENDPRO
* Crop factor (CRPF) to compute crop transp. from open water evaporation
* for C3-species 0.9, for C4-species 0.7 in temperate and 0.9 in warm climates
TABLE CRPF(1-2) = 0.7, 0.7
* Soil moisture depletion factor (P) for a temperate climate
FUNCTION PTB,1 = 0.,0.7, 1.,0.6, 5.,0.4, 7.,0.3
FUNCTION PTB,2 = 0.,0.7, 1.,0.6, 5.,0.4, 7.,0.3

***                               WEATHER                               ***
* Daily global radiation (J/m2/d)
  DTR = AFGEN(DTRT,DAY) * 1.E6
* Daily temperature (C): maximum, minimum, average, daytime
  DTMAX = AFGEN(TMAXT,DAY)
  DTMIN = AFGEN(TMINT,DAY)
  DAVTMP= 0.5 * (DTMAX+DTMIN)
  DDTMP = DTMAX - 0.25 * (DTMAX-DTMIN)
* Reference evapotranspiration (mm/d) for short grass in the Netherlands
* (Makkink) and estimated Penman evaporation for open water.
* (Ratio EPENM/EREF is based on a regression for data of the Netherlands;
* on average EPENM/EREF = 1./0.8)
  EREF = 0.65 * (SLOPE/(SLOPE+GAMMA)) * DTR / LABDA
  SLOPE = 4158.6 * SVP / (DAVTMP+239.)**2
  SVP = 6.11 * EXP(17.4*DAVTMP/(DAVTMP+239.))
  PARAM LABDA = 2454.E3, GAMMA = 0.658
  EPENM = EREF * AFGEN(EPERT, DAY)
  FUNCTION EPERT = 74,1.35, 105,1.30, 135,1.30, 166,1.31, ...
    196,1.27, 227,1.19, 258,1.17, 288,1.00

***                               Simulation run specifications                               ***
  DAY = AMOD(TIME,365.)
TIMER TIME=126., FINTIM=271., DELT=1., PRDEL=5.
METHOD RECT
PRINT DVS(1-2),TADRW(1-2),LAI(1-2),DTGA(1-2),GTW(1-2),WSO(1-2),...
  HGHT(1-2),PTRAN(1-2),TRAN(1-2),TRANRF(1-2),SMRTZ,EVAP

***                               WEATHER DATA                               ***
* Wageningen, The Netherlands, 1951 - 1980
* Daily global radiation (MJ/m2/d)
FUNCTION DTRT = 15,2.1, 46,4.4, 74,7.8, 105,13.0, 135,16.3, ...
  166,17.5, 196,15.6, 227,13.8, 258,10.0, 288,5.8, 319,2.7, 349,1.7
* Daily maximum and minimum temperature (C)
FUNCTION TMAXT = 15,4.3, 46,5.4, 74,8.9, 105,12.4, 135,17.3, ...
  166,20.5, 196,21.4, 227,21.5, 258,18.9, 288,14.3, 319,8.6, 349,5.5
FUNCTION TMINT = 15,-0.7, 46,-0.6, 74,1.2, 105,3.3, 135,7.3, ...
  166,10.3, 196,12.2, 227,12.0, 258,9.7, 288,6.5, 319,2.9, 349,0.6
* Rainfall (mm/d) (Recommendation: use daily data as input) dummy:
FUNCTION RAIN = 1,2., 180,2., 185,0., 210,0., 215,2., 365,2.

```

*** FIELD PARAMETERS ***

* Latitude of the site
 PARAM LAT = 52.
 * Number of species
 PARAM NS = 2
 TABLE PRSNC(1-2) = 1, 1
 * Day of emergence
 TABLE DAYEM(1-2) = 135., 140.
 * Plant density (plants/m²)
 TABLE NPL(1-2) = 11.11, 100.

*** SPECIES PARAMETERS: 1 = Maize, 2 = Echinochloa crus-galli ***

* Initial leaf area (cm²/plant) and relative leaf growth rate (cm²/cm²/Cd)
 TABLE LA0(1-2) = 6.69, 0.368
 TABLE RGRL(1-2) = 0.0294, 0.0326
 * Effective temperature for leaf area growth (C)
 PROCEDURE DTEFF = EFFTMP (DAVTMP)
 DTEFF(1) = AMAX1 (0., DAVTMP-10.)
 DTEFF(2) = AMAX1 (0., DAVTMP-10.)
 ENDPRO

* Potential photosynthesis rate at light saturation (kg CO₂/ha leaf/h)
 TABLE AMX(1-2) = 70., 70.
 * Effect of DVS on AMX
 FUNCTION AMDVST,1 = 0.,1.0, 1.3,1.0, 1.6,0.5, 2.0,0.25, 2.5,0.25
 FUNCTION AMDVST,2 = 0.,1.0, 1.3,1.0, 1.6,0.5, 2.0,0.25, 2.5,0.25
 * Effect of daytime temperature on AMX
 FUNCTION AMTMPT,1=-10,.01, 9,.05, 16,.80, 18,.94, 20,1., 30,1., 40,.75
 FUNCTION AMTMPT,2=-10,.01, 9,.05, 16,.80, 18,.94, 20,1., 30,1., 40,.75
 * Initial light use efficiency ((kg CO₂/ha leaf/h)/(J/m²/s))
 TABLE EFF(1-2) = 0.45, 0.45

* Extinction coefficient for diffuse PAR
 TABLE KDF(1-2) = 0.65, 0.80
 * Scattering coefficient for PAR
 PARAM SCP = 0.20
 * Maintenance coefficient for storage organs (kg CH₂O/kg DM/d)
 TABLE MAINSO(1-2) = 0.01, 0.01
 * Assimilate requirement for DM conversion in storage organs (kgCH₂O/kgDM)
 TABLE ASRQSO(1-2) = 1.49, 1.49

* Pre- and post-flowering development rate(1/d) as a function of temp.
 FUNCTION DVRVT,1 = 0.,0., 10.,0., 30.,0.0471
 FUNCTION DVRVT,2 = 0.,0., 10.,0., 30.,0.0571
 FUNCTION DVRRT,1 = 0.,0., 10.,0., 30.,0.0471
 FUNCTION DVRRT,2 = 0.,0., 10.,0., 30.,0.0571
 * Maize: emergence to silking 425 Cd (Tbase=10 C) or 730 Cd (Tbase=6 C)
 * Maize: silking to maturity 425 Cd (Tbase=10 C) or 730 Cd (Tbase=6 C)
 * Echinochloa: emergence to flowering 350 Cd (Tb=10 C) or 600 Cd (Tb=6 C)
 * Fraction of total dry matter growth allocated to shoots (FSH)
 * fraction of shoot DM growth allocated to leaves (FLV) and stems (FST)
 * as a function of DVS
 FUNCTION FSHTB,1= 0.0,0.60, 0.1,0.63, 0.2,0.66, 0.3,0.69, 0.4,0.73,...
 0.5,0.77, 0.6,0.81, 0.7,0.85, 0.8,0.90, 0.9,0.94, 1.0,1.0, 2.5,1.0
 FUNCTION FSHTB,2= 0.0,0.60, 0.1,0.63, 0.2,0.66, 0.3,0.69, 0.4,0.73,...
 0.5,0.77, 0.6,0.81, 0.7,0.85, 0.8,0.90, 0.9,0.94, 1.0,1.0, 2.5,1.0
 FUNCTION FLVTB,1=0.,.70, .25,.70, .80,.15, .95,0., 2.5,0.

```

FUNCTION FLVTB,2=0.,.70, .3,.55, .6,.25, .8,0., 2.5,0.
FUNCTION FSTTB,1=0.,.30, .25,.30, .80,.85, .95,1.0, 1.1,1.0, ...
1.2,0., 2.5,0.
FUNCTION FSTTB,2=0.,.30, .3,.45, .6,.75, .8,.80, .9,.70, 1.2,0., 2.5,0.
* Maize: FSO(=1.-FLV-FST) = stems + leaf sheaths + empty cobs
* Echinochloa: FSO(=1.-FLV-FST) = panicles + seeds
* Seed production of Echinochloa at DVS=2 from WSO (incl. fallen seeds!):
* No. of seeds/m2 = WSO(panicle weight) * 0.76 (fractional weight of seeds)
* * 1.8 mg (weight per seed)
* Seed fall starts at DVS=1.15 and amounts to about 0.015*TADRW per day

```

```

* Specific leaf area of new leaves (ha leaf / kg leaf) as a function of DVS

```

```

FUNCTION SLAT,1=0.,0.0040, 0.7,0.0010, 2.5,0.0010
FUNCTION SLAT,2=0.,0.0022, 0.5,0.0044, 0.8,0.0030, 2.5,0.0030
* Relative death rate (1/d) of leaves as a function of temperature

```

```

PROCEDURE RDR = DTH(DAVTMP)
  RDR(1) = INSW (DVS(1)-1.0, 0., AMAX1(RDRDV(1),RDRLT,0.001))
  RDRDV(1) = RDRSL(1) * (DAVTMP - 8.)
  RDRSL(1) = INSW (DVS(1)-1.35, 0.0005, 0.0030)
  RDRLT = INSW (DVS(1)-1.25, 0., LIMIT(0.,1.,(6.-DAVTMP)/6.))
  RDR(2) = INSW (DVS(2)-0.8, 0., AMAX1(RDRDV(2),0.01))
  RDRDV(2) = RDRSL(2) * (DAVTMP - 10.)
  RDRSL(2) = INSW (DVS(2)-1.25, 0.003, 0.007)

```

```

ENDPRO

```

```

* Constants of logistic height function: HMAX (m), HB (-), HS (1/dvs)

```

```

TABLE HMAX(1-2) = 2.05, 1.01
TABLE HB(1-2) = 32.8, 57.4
TABLE HS(1-2) = 6.29, 6.54

```

```

* Decrease of height of photosynthetic tissue (m/dvs) after stage DVSD

```

```

TABLE HDECR(1-2) = 0.5, 0.15
TABLE DVSD(1-2) = 1.3, 1.0

```

```

END

```

```

TABLE PRSNC(1-2) = 1, 0

```

```

TABLE NPL(1-2) = 11.11, 0.

```

```

END

```

```

TABLE PRSNC(1-2) = 0, 1

```

```

TABLE NPL(1-2) = 0., 100.

```

```

END

```

```

STOP

```

```

* -----
* Subroutine XGLA:
* computes daily increase of leaf area index (ha leaf/ ha ground/ d)
* -----

```

```

SUBROUTINE XGLA (DAY, DAYEM, DTEFF, DVS, NPL, LAO, RGRL, DELT, SLA,
$              LAI, GLV, NS,
$              GLAI, LAIT)
  IMPLICIT REAL (A-Z)
  INTEGER NS, K
  DIMENSION GLAI(NS), DAYEM(NS), DTEFF(NS), DVS(NS), NPL(NS), LAO(NS)
  DIMENSION RGRL(NS), SLA(NS), LAI(NS), GLV(NS)

```

```

  LAIT = 0.
  DO K=1, NS
    LAIT = LAIT + LAI(K)
  ENDDO

```

```

  DO K=1, NS

```

```

*   during mature plant growth:
      GLAI(K) = SLA(K) * GLV(K)
*   during juvenile growth:
      IF ((DVS(K).LT.0.3).AND.(LAIT.LT.0.75)) THEN
          GLAI(K) = LAI(K) * (EXP(RGRL(K) * DTEFF(K) * DELT) - 1.)
      ENDIF
*   at day of seedling emergence:
      IF ((DAY.GE.DAYEM(K)) .AND. (LAI(K).EQ.0.))
$       GLAI(K) = NPL(K) * LAO(K) * 1.E-4
*   before seedling emergence:
      IF (DAY.LT.DAYEM(K)) GLAI(K) = 0.
      ENDDO
      RETURN
      END

* -----
* Subroutine XDASSH
* computes potential daily assimilation (DTGA, kgCO2/ha/d) in a mixed stand
* by integrating analytically leaf photosynthesis over LAI per species,
* using a rectangular hyperbola for daily photosynthesis-light response of
* single leaves.
* The canopy is stratified into NS horizontal layers.
* Leaf area is assumed to be distributed uniformly with height for each sp.
* Soil moisture balance: fraction of shortwave radiation absorbed (FRABS)
* and transmitted (FRD)
* -----
      SUBROUTINE XDASSH (DAY,LAT,DTR,KDF,LAI,AMAX,EFF,NS,HGHT,
$                      DTGA,DSO,FRABS,FRD)
      IMPLICIT REAL (A-Z)
      INTEGER NS,I,K,J
      DIMENSION HGHT(NS),HT(16),DTGA(NS),FRABS(NS)
      DIMENSION LA(15),LAI(NS),KDF(NS),AMAX(NS),EFF(NS)

*   daylength (h)
      CALL ASTRO (DAY,LAT,
$              DAYL,SINLD,COSLD,DSINB,DSINBE,DSO)
*   daily photosynthetically active radiation (J/m2/d)
      DPAR = 0.50 * DTR

*   Boundaries (HT,m) of the successive layers, ranked from top to bottom
      DO I=1,NS
          HT(I)=HGHT(I)
      ENDDO
      HT(NS+1)=0.
      DO I=1,NS-1
          DO J=NS,I+1,-1
              IF(HT(I).LT.HT(J)) THEN
                  AUX=HT(J)
                  HT(J)=HT(I)
                  HT(I)=AUX
              ENDIF
          ENDDO
      ENDDO
      CROPHT = HT(1)

*   Light intensity (IPAR,J/m2/s), relative radiation level(FRD), and

```

```

* daily gross assimilation (DTGA, kgCO2/ha/d) at top of canopy
  IPAR = (1.-0.08) * DPAR / (DAYL * 3600.)
  FRD = 1.
  DO K=1,NS
    DTGA(K) = 0.
    FRABS(K) = 0.
  ENDDO

* In DO loop 20, leaf area and daily ass. are calculated for each layer I
  DO 20 I=1,NS
    LAIT=0.
    KLT=0.
* Leaf area of species K (LA(K)) and of all species (LAIT) in layer I
    DO K=1,NS
      IF(HGHT(K).LE.HT(I+1)) THEN
        LA(K) = 0.
      ELSE
        LA(K) = LAI(K) * (HT(I)-HT(I+1)) / HGHT(K)
        LAIT = LAIT + LA(K)
        KLT = KLT + KDF(K) * LA(K)
      ENDIF
    ENDDO
* Daily assimilation of species K, cumulated down to layer I (kgCO2/ha/d)
    IF (KLT.LE.0.) GOTO 10
    DO 10 K=1,NS
      DTGA(K) = DAYL * KDF(K)*LA(K)/KLT *
$          AMAX(K)/KDF(K) * ALOG((AMAX(K)+EFF(K)*IPAR*KDF(K))
$          /(AMAX(K)+EFF(K)*IPAR*KDF(K)*EXP(-KLT))) + DTGA(K)
* Absorbed solar radiation(FRABS)
* (Ext.coeff. of solar radiation is 0.7 * ext.coeff. of PAR)
      FRABS(K) = FRABS(K) + KDF(K)*LA(K)/KLT
$          * (1.-EXP(-0.7*KLT)) * FRD
    10 CONTINUE
* Light intensity (IPAR) and rel. radiation (FRD) at top of next layer
    IPAR = IPAR * EXP(-KLT)
    FRD = FRD * EXP(-0.7*KLT)
  20 CONTINUE
  RETURN
  END

* See Figure 46 for subroutine:
* SUBROUTINE ASTRO (DAY,LAT,
* $ DAYL,SINLD,COSLD,DSINB,DSINBE,DSO)
ENDJOB

```

Appendix 7

Listing of a detailed model to describe competition for light. In subroutine XASSNM, the canopy is stratified into a number of horizontal leaf layers. For each species, light absorption and assimilation are calculated per layer, in which sunlit and shaded leaf area are treated separately. Summation over the various layers gives the assimilation rate for each species in the mixed canopy.

In subroutine XASSGS, total assimilation per species is calculated by performing a Gaussian integration over the plant height of each species separately. Integration over plant height according to the Gaussian principle was proposed by C. Rappoldt & S.A. Weaver (pers. commun.) who proved that this approach is equivalent to the above one with integration over a stratified canopy. The Gaussian integration is performed by calling for XASSGS instead of XASSNM in subroutine XDASS.

The model can be linked to the program listed in Appendix 6 and subsequently calling for XDASS instead of XDASSH. The principles of the calculation of light distribution and assimilation are explained in Section 4.1 and abbreviations are defined in Table 12.

TITLE CALCULATION OF DAILY CO₂ ASSIMILATION IN A MIXED CANOPY

STORAGE LAI(2),DTGA(2),KDF(2),AMAX(2),EFF(2),HGHT(2)

FIXED NS

* Daily incoming solar radiation (J/m²/d)

PARAM DTR = 14.E6

PARAM LAT=52., DAY=230.

* Species characteristics: leaf area index (LAI), plant height (HGHT),

* photosynthesis characteristics (AMAX,EFF),

* extinction coeff. for diffuse p.a.r.(KDF), leaf scattering coeff.(SCP)

PROCEDURE LAI = LAREA(TIME)

DO K=1,NS

FK=K

LAI(K) = TWOVAR(LAITB,TIME,FK)

ENDDO

ENDPRO

FUNCTION LAITB,1=0,0., 1,0.25, 2,0.5, 3,1., 4,2., 5,2.5, 6,3., 7,5.

FUNCTION LAITB,2=0,0., 1,0.25, 2,0.5, 3,1., 4,2., 5,2.5, 6,3., 7,5.

TABLE HGHT(1-2) = 1., 0.5

TABLE AMAX(1-2) = 40., 40.

TABLE EFF(1-2) = 0.45, 0.45

TABLE KDF(1-2) = 0.716, 0.716

PARAM SCP=0.2

PARAM NS = 2

* Daily total gross assimilation (DTGA, kgCO₂/ha/d) per species in mixture
DTGA,DSO = XDASS(DAY,LAT,DTR,KDF,SCP,LAI,AMAX,EFF,NS,HGHT)

```

METHOD RECT
TIMER FINTIM=7., DELT=1., PRDEL=1., TIME=0.
PRINT LAI(1-2),DTR,DTGA(1-2),HGHT(1-2)
END
STOP

```

```

* -----
* Subroutine XDASS
* computes potential daily assimilation (DTGA, kgCO2/ha/d) in a mixed stand
* -----

```

```

SUBROUTINE XDASS (DAY,LAT,DTR,KDF,SCP,LAI,AMAX,EFF,NS,HGHT,
$ DTGA,DSO)
IMPLICIT REAL (A-Z)
INTEGER T,K,NS
DIMENSION DTGA(NS),FGROS(15),HGHT(NS),GSDST(3),GSWT(3)
DATA GSDST /0.112702, 0.5, 0.887298/
DATA GSWT /0.277778, 0.444444, 0.277778/
* daylength (h) and daily extra-terrestrial radiation (J/m2/d)
CALL ASTRO (DAY,LAT,
$ DAYL,SINLD,COSLD,DSINB,DSINBE,DSO)
* daily radiation above the canopy (J/m2/d)
CALL DRADIA (DSO,DTR,
$ FRDF,DPAR)

DO K=1,NS
DTGA(K) = 0.
ENDDO
DO T = 1,3
HOUR = 12. + DAYL*0.5*GSDST(T)
CALL XASSNM (HOUR,DAYL,SINLD,COSLD,DSINB,DSINBE,DTR,
$ FRDF,DPAR,KDF,SCP,LAI,AMAX,EFF,NS,HGHT,
$ FGROS)
* integration of instantaneous assimilation to a daily total (DTGA)
DO K=1,NS
DTGA(K) = DTGA(K) + FGROS(K) * DAYL * GSWT(T)
ENDDO
ENDDO
RETURN
END

```

```

* -----
* Subroutine XASSNM
* computes instantaneous assimilation (FGROS, kgCO2/ha/h) in a mixed stand
* For each species, light absorption and assimilation are calculated per
* layer, in which shaded and sunlit leaf area are treated separately.
* Assimilation rates per species are summed over the various foliage layers.
* -----

```

```

SUBROUTINE XASSNM (HOUR,DAYL,SINLD,COSLD,DSINB,DSINBE,DTR,
$ FRDF,DPAR,KDF,SCP,LAI,AMAX,EFF,NS,HGHT,
$ FGROS)
IMPLICIT REAL (A-Z)
INTEGER I,ISN,K,NS,NLL
DIMENSION FGROS(15),LAI(NS),KDF(NS),CLUSTF(15),AMAX(NS),EFF(NS)
DIMENSION PARLSH(15),ASSSH(15),ASSSL(15),FSLLA(15),HGHT(NS)
DIMENSION KBL(15),KDRT(15),LA(15)

* radiation above the canopy: PAR (J/m2/s)
CALL RADIAT (HOUR,SINLD,COSLD,DSINB,DSINBE,FRDF,DPAR,
$ PARDF,PARDR,SINB)

```

```

* height (m) of vegetation
CROPHT = 0.
DO K=1,NS
  CROPHT = AMAX1 (CROPHT,HGHT(K))
ENDDO
* number of canopy layers (NLL) and depth of each layer (DL,m)
NLL = 20.
DL = CROPHT / NLL

* extinction coeff. for direct component(KBL) and total direct flux(KDRT)
REFL = (1.-SQRT(1.-SCP)) / (1.+SQRT(1.-SCP))
DO K=1,NS
  CLUSTF(K) = KDF(K) / (0.8*SQRT(1.-SCP))
  KBL(K) = (0.5/SINB) * CLUSTF(K)
  KDRT(K) = KBL(K) * SQRT(1.-SCP)
ENDDO
* components of photosynthetically active radiation at top of canopy
VISDF = PARDF
VIST = PARDR
VISDR = PARDR
FSL = 1.

* in DO loop 400, assimilation (kgCO2/ha/h) is calculated per species
* per layer and summed over the NLL layers
DO K=1,NS
  FGROS(K)=0.
ENDDO
HU = CROPHT
DO 400 I=1,NLL
  KDFL = 0.
  KDRTL = 0.
  KBLL = 0.
  TLA = 0.
  CLUST = 0.
* leaf area of species K (LA(K)) in layer I from its cumulative
* LAI function (LAI cumulated from top (h=HGHT(K)) to bottom (h=0))
DO K=1,NS
* upper (HUK) and lower (HLK) height of the layer
HUK = AMIN1 (HU,HGHT(K))
HLK = AMIN1 (HU-DL,HGHT(K))
IF (HGHT(K).GT.0.) THEN
* rectangular leaf area density function
* LA(K) = LAI(K) * (HUK-HLK) / HGHT(K)
* parabolic leaf area density function
* LA(K) = ( 3.*(HUK**2-HLK**2) / HGHT(K)**2
$ - 2.*(HUK**3-HLK**3) / HGHT(K)**3) * LAI(K)
ELSE
  LA(K) = 0.
ENDIF
  KDFL = KDFL + KDF(K) * LA(K)
  KDRTL = KDRTL + KDRT(K) * LA(K)
  KBLL = KBLL + KBL(K) * LA(K)
  TLA = TLA + LA(K)
  CLUST = CLUST + CLUSTF(K) * LA(K)
ENDDO
* cluster factor averaged over the species in layer I
IF (TLA.GT.0.) CLUST = CLUST / TLA
IF (TLA.LE.0.) CLUST = 1.

```

```

* PAR absorbed by layer I per unit ground area (PARG.. in J/m2 ground/s):
* diffuse flux(PARGDF), total direct flux(PARGT), its direct component(PARGDR)
  PARGDF = (1.-REFL) * VISDF * (1.-EXP(-KDFL))
  PARGT  = (1.-REFL) * VIST  * (1.-EXP(-KDRTL))
  PARGDR = (1.-SCP)  * VISDR * (1.-EXP(-KBLL))

```

```

IF(KDFL.LE.0.) GOTO 300
DO 300 K=1,NS

```

```

* visible radiation absorbed by shaded leaves (PARLSH)
  PARLSH(K) = KDF(K)/KDFL * (PARGDF + PARGT - PARGDR)
* direct PAR absorbed by leaves perpendicular on direct beam (PARLPP)
  PARLPP = PARDR * (1.-SCP) / SINB
* assimilation of shaded and sunlit leaf area (kg CO2/ha leaf/hr)
* (sunlit leaves: assimilation summed over 5 leaf angle classes)
  ASSSH(K) = AMAX(K) * (1.-EXP(-EFF(K)*PARLSH(K)/AMAX(K)))
  ASSSL(K) = 0.
  DO ISN = 1,5
    SN = (ISN-0.5) * 0.2
    PARLSL = PARLSH(K) + SN * PARLPP
    ASSSUN = AMAX(K) * (1. - EXP(-PARLSL * EFF(K)/AMAX(K)))
    ASSSL(K) = ASSSL(K) + 0.20 * ASSSUN
  ENDDO
* fraction sunlit leaf area
  FSLLA(K) = FSL*KBL(K)*TLA * (1.-EXP(-KBLL)) / KBLL**2 * CLUST
* canopy assimilation (kg CO2/ha soil/hr) cumulated over layers
  FGROS(K) = FGROS(K) + LA(K) * ((1.-FSLLA(K))*ASSSH(K)
    $ + FSLLA(K)*ASSSL(K))
300 CONTINUE

```

```

* Visible radiation and fraction sunlit leaf area at top (HU) of next layer
  HU = HU - DL
  VISDF = VISDF * EXP(-KDFL)
  VIST  = VIST  * EXP(-KDRTL)
  VISDR = VISDR * EXP(-KBLL)
  FSL   = FSL   * EXP(-KBLL)
400 CONTINUE
RETURN
END

```

```

* -----
* Subroutine XASSGS
* computes instantaneous assimilation (FGROS, kgCO2/ha/h) in a mixed stand
* For each species, light absorption and assimilation are calculated at
* 5 selected plant heights. Assimilation rates per species are obtained by
* Gaussian integration over the canopy.
* -----

```

```

SUBROUTINE XASSGS (HOUR, DAYL, SINLD, COSLD, DSINB, DSINBE, DTR,
$                FRDF, DPAR, KDF, SCP, LAI, AMAX, EFF, NS, HGHT,
$                FGROS)
IMPLICIT REAL (A-Z)
INTEGER FK, K, NS, I, L
DIMENSION GSDST5(5), GSWT5(5), LAD(15), KBL(15), KDRT(15)
DIMENSION FGROS(15), LAI(NS), KDF(NS), AMAX(NS), EFF(NS), HGHT(NS)
DATA GSDST5 /0.046910, 0.230753, 0.5, 0.769247, 0.953090/
DATA GSWT5 /0.118464, 0.239314, 0.284444, 0.239314, 0.118464/

```

```

* radiation above the canopy: PAR (J/m2/s)
CALL RADIAT (HOUR, SINLD, COSLD, DSINB, DSINBE, FRDF, DPAR,

```

```

$          PARDF,PARDR,SINB)
DO K=1,NS
  FGROS(K) = 0.
ENDDO
DO K=1,NS
  FK = K
  DO L=1,5
*    plant height (HT) for which the assimilation rate is calculated
*    (For each species, integration only over that section of
*    plant height that contains photosynthesizing organs)
    HT = HGHT(K) * GSDST5(L)
    CALL XRDPRF (PARDF,PARDR,SINB,KDF,SCP,HGHT,LAI,HT,LAD,FK,NS,
$          PARLSH,PARLSL,PARLPP,FSLLA)
*    assimilation of shaded and sunlit leaf area (kg CO2/ha leaf/hr)
    ASSSH = AMAX(K) * (1.-EXP(-EFF(K)*PARLSH/AMAX(K)))
    ASSSL = 0.
    DO I = 1,5
      PARLSL = PARLSH + PARLPP*GSDST5(I)
      ASSSL = ASSSL + AMAX(K) *
$        (1. - EXP(-PARLSL * EFF(K)/AMAX(K))) * GSWT5(I)
    ENDDO
*    assimilation (kg CO2/ha soil/hr) cumulated over canopy layers
    FGROS(K) = FGROS(K) + ((1.-FSLLA)*ASSSH + FSLLA*ASSSL)
$    * LAD(K) * HGHT(K) * GSWT5(L)
  ENDDO
ENDDO
RETURN
END

```

```

* -----
* Subroutine XRDPRF
* computes the radiation profile in a mixed foliage, giving instantaneous
* values of absorbed radiation at a given plant height (HT) for each species
* -----

```

```

SUBROUTINE XRDPRF (PARDF,PARDR,SINB,KDF,SCP,HGHT,LAI,HT,LAD,FK,NS,
$          PARLSH,PARLSL,PARLPP,FSLLA)
IMPLICIT REAL (A-Z)
INTEGER FK,J,NS
DIMENSION LAI(15),HGHT(15),KDF(15),KBL(15),KDRT(15),CLUSTF(15)
DIMENSION LA(15),LAD(15)
REFL = (1.-SQRT(1.-SCP)) / (1.+SQRT(1.-SCP))
* extinction coeff. for direct component(KBL) and total direct flux(KDRT)
* as affected by micro-clustering (cluster factor CLUSTF)
DO J=1,NS
  CLUSTF(J) = KDF(J) / (0.8*SQRT(1.-SCP))
  KBL(J) = (0.5/SINB) * CLUSTF(J)
  KDRT(J) = KBL(J) * SQRT(1.-SCP)
ENDDO

```

```

* sums of leaf area indices (LA) above height HT,
* weighted by the extinction coefficients
KDFL = 0.
KDRTL = 0.
KBLL = 0.
LAC = 0.
CLUST = 0.
DO J=1,NS
  CALL LADF (LAI(J),HGHT(J),HT,
$          LA(J),LAD(J))

```

```

      KDFL = KDFL + KDF(J) * LA(J)
      KDRTL = KDRTL + KDRT(J) * LA(J)
      KBLL = KBLL + KBL(J) * LA(J)
      LAC = LAC + LA(J)
      CLUST = CLUST + AMIN1(1.,CLUSTF(J)) * LA(J)
ENDDO
* cluster factor averaged over the species down to height HT
  IF (LAC.GT.0.) CLUST = CLUST / LAC
  IF (LAC.LE.0.) CLUST = 1.
* PAR absorbed at height HT (PARL..in J/m2 leaf/s):diffuse flux(PARLDF),
* total direct flux(PARLT), its direct component(PARLDR)
  PARLDF = (1.-REFL) * PARDF * KDF(FK) * EXP(-KDFL)
  PARLT = (1.-REFL) * PARDR * KDRT(FK) * EXP(-KDRTL)
  PARLDR = (1.-SCP) * PARDR * KBL(FK) * EXP(-KBLL)
* visible radiation absorbed by shaded leaves (PARLSH)
  PARLSH = PARLDF + (PARLT - PARLDR)
  PARLSL = PARLSH + (1.-SCP) * KBL(FK) * PARDR
* direct PAR absorbed by leaves perpendicular on direct beam (PARLPP)
  PARLPP = PARDR * (1.-SCP)/SINB
* fraction sunlit leaf area
  FSLLA = EXP(-KBLL) * CLUST
  RETURN
  END

* -----
* Subroutine LADF
* calculates leaf area index (LAI) above height HT, and
* leaf area density (LAD, m2 leaf/ m2 ground/ m height) at HT from
* the leaf area density distribution of the species.
* -----
      SUBROUTINE LADF (LAI,HGHT,HT,
$                   LA,LAD)
      IMPLICIT REAL (A-Z)
      IF (HT.LT.HGHT) THEN
*       Rectangular leaf area density function:
*       LA = LAI * (HGHT - HT) / HGHT
*       LAD = LAI / HGHT
*       Parabolic leaf area density function:
      LA = LAI * (1. + 2.*HT**3/HGHT**3 - 3.*HT**2/HGHT**2)
      LAD = 6.*LAI * (HT/HGHT**2 - HT**2/HGHT**3)
      ELSE
      LA = 0.
      LAD = 0.
      ENDIF
      RETURN
      END

* See Figure 46 for the subroutines:
* SUBROUTINE ASTRO (DAY,LAT,
* $ DAYL,SINLD,COSLD,DSINB,DSINBE,DSO)
* SUBROUTINE DRADIA (DSO,DTR,
* $ FRDF,DPAR)
* SUBROUTINE RADIAT (HOUR,SINLD,COSLD,DSINB,DSINBE,FRDF,DPAR,
* $ PARDF,PARDR,SINB)
ENDJOB

```

Appendix 8

TITLE EPIDEMIC POWDERY MILDEW

```
STORAGE DLA(3) ,LA(3) ,RMRLA(3) ,NCONT(3)
STORAGE IRPSP(3) ,MRISP(3) ,GRISP(3) ,MRGSP(3) ,RIR(3) ,RIRL(3)
STORAGE DRLAT(3) ,DRINF(3)
STORAGE ILATL1(4) ,LATL1(4) ,IINFL1(3) ,INFL1(3)
STORAGE ILATL2(4) ,LATL2(4) ,IINFL2(3) ,INFL2(3)
STORAGE ILATL3(4) ,LATL3(4) ,IINFL3(3) ,INFL3(3)
STORAGE DISL(3)
FIXED N1,N2,J
```

INITIAL

```
*crop-parameters
PARAM SLA=20.E-4
TABLE NCONT(1-3)=3.0,3.0,3.0
*parameters connected with the fungus
PARAM STDAY=100.,N1=4,N2=3
TABLE ILATL1(1-4)=5.E-4,3*0., IINFL1(1-3)=3*0.
TABLE ILATL2(1-4)=4*0., IINFL2(1-3)=3*0.
TABLE ILATL3(1-4)=4*0., IINFL3(1-3)=3*0.
PARAM SLES=3.5E-10,R=1.E3,FINTLL=0.01
```

DYNAMIC

```
DAY =STDAY + TIME
TEMP =AFGEN(TEMPT,DAY)
```

*the crop

```
NOSORT
TLBM =AFGEN(TLBMT,DAY)
LAI =TLBM * SLA
LAIMAX=AMAX1(LAIMAX,LAI)
```

DEADLA=LAIMAX-LAI

DLATOT=DEADLA

LATOT =LAI

DO 10 J=1,3

```
DLA(J) =AMIN1(DLATOT,1.5)
DLATOT =DLATOT-DLA(J)
LA(J) =AMIN1(LATOT,1.5-DLA(J))
LATOT =LATOT-LA(J)
```

```
RDYING =-AMIN1(0.,DERIV(0.,LA(J)))
RMRLA(J) =RDYING/(LA(J)+NOT(LA(J)))
```

10 CONTINUE

SORT

*the fungus

**spores

INTSP =INTGRL(0.,NRINT,3)

GERSP =INTGRL(0.,NRGER,3)

```

INFTOT=TINFLA/SLES
RMRISP=AFGEN(RMRIST,TEMP)
RGRISP=AFGEN(RGRIST,TEMP)
RMRGSP=AFGEN(RMRGST,TEMP)
RIRGSP=AFGEN(RIRGST,TEMP)
RIRLA =0.

```

```

NOSORT

```

```

DO 20 J=1,3
  IRPSP(J) =R*INFTOT*FINTLL*LA(J)*(1.-(DISL(J)/(LA(J)+NOT(LA(J))))))
  MRISP(J) =RMRISP*INTSP(J)
  GRISP(J) =RGRISP*INTSP(J)
  NRINT(J) =IRPSP(J) - MRISP(J) - GRISP(J)

```

```

  MRGSP(J) =RMRGSP*GERSP(J)
  RIR(J) =RIRGSP*GERSP(J)
  NRGER(J) =GRISP(J) - MRGSP(J) -RIR(J)
  RIRL(J) =RIR(J) * SLES
  RIRLA =RIRLA + RIRL(J)

```

```

20 CONTINUE

```

```

SORT

```

```

**infected leaf area

```

```

*Development Rate

```

```

SDRLAT =AFGEN(DRLATT,TEMP)

```

```

SDRINF =AFGEN(DRINFT,TEMP)

```

```

NOSORT

```

```

DO 30 J=1,3

```

```

  MFLP =AFGEN(MFLPT,NCONT(J))

```

```

  MFIP =AFGEN(MFIPT,NCONT(J))

```

```

  DRLAT(J)=SDRLAT/MFLP

```

```

  DRINF(J)=SDRINF/MFIP

```

```

30 CONTINUE

```

```

SORT

```

```

*Relative Dispersion

```

```

RDLAT =AFGEN(RDLATT,TEMP)

```

```

RDINF =AFGEN(RDINFT,TEMP)

```

```

NOSORT

```

```

LATO1,LATL1,TLATL1,MRLAT,EIRL1,GAMMA1,GCYCL1=...

```

```

  BOXCAR(1,ILATL1,DRLAT(1),RDLAT,RMRLA(1),RIRL(1),N1,DELT,TIME)

```

```

INFO1,INFL1,TINFL1,MRINF,REML1,GAMMA2,GCYCL2=...

```

```

  BOXCAR(2,IINFL1,DRINF(1),RDINF,RMRLA(1),EIRL1,N2,DELT,TIME)

```

```

NLIFL1 =INTGRL(0.,REML1 - RMRLA(1)*NLIFL1)

```

```

DISL(1) =TLATL1+TINFL1+NLIFL1

```

```

LATO2,LATL2,TLATL2,MRLAT,EIRL2,GAMMA3,GCYCL3=...

```

```

  BOXCAR(3,ILATL2,DRLAT(2),RDLAT,RMRLA(2),RIRL(2),N1,DELT,TIME)

```

```

INFO2,INFL2,TINFL2,MRINF,REML2,GAMMA4,GCYCL4=...

```

```

  BOXCAR(4,IINFL2,DRINF(2),RDINF,RMRLA(2),EIRL2,N2,DELT,TIME)

```

```

NLIFL2 =INTGRL(0.,REML2 - RMRLA(2)*NLIFL2)

```

```

DISL(2) =TLATL2+TINFL2+NLIFL2

```

```

LATO3,LATL3,TLATL3,MRLAT,EIRL3,GAMMA5,GCYCL5=...

```

```

  BOXCAR(5,ILATL3,DRLAT(3),RDLAT,RMRLA(3),RIRL(3),N1,DELT,TIME)

```

```

INFO3,INFL3,TINFL3,MRINF,REML3,GAMMA6,GCYCL6=...

```

```

  BOXCAR(6,IINFL3,DRINF(3),RDINF,RMRLA(3),EIRL3,N2,DELT,TIME)

```

```

NLIFL3 =INTGRL(0.,REML3 - RMRLA(3)*NLIFL3)

```

```

DISL(3) =TLATL3+TINFL3+NLIFL3

```

```

SORT

```

```

TLATLA = TLATL1 + TLATL2 + TLATL3
TINFLA = TINFL1 + TINFL2 + TINFL3
NLIFLA = NLIFL1 + NLIFL2 + NLIFL3
DISLA = TLATLA + TINFLA + NLIFLA

```

```

FUNCTION TLBMT = 0., 75., 70., 75., 90., 100., 115., 200.,...
                130.,1250., 150.,2200., 180.,2250., 200.,2000.,...
                220.,1300., 240., 1., 300., 1.
FUNCTION RMRIST= 0.,0.12, 10.,0.12, 15.,0.36, 20.,0.46, 25.,0.92,...
                30.,1., 35.,1.
FUNCTION RGRIST= 0.,0., 7.,0., 10.,0.0333, 15.,0.1000, 20.,0.1250,...
                25.,0.2500, 30.,0.3333
FUNCTION RMRGST= 0.,20., 10.,16., 15.,18., 20.,20., 30.,24.
FUNCTION RIRGST= 0., 1., 10.,1.8, 15., 2., 20.,2.2, 30.,2.4
FUNCTION DRLATT= 0.,0., 7.,0., 10.,0.0625, 15.,0.1250, 20.,0.2500,...
                25.,0.4000, 30.,0.4540
FUNCTION MFLPT = 2.0,1.5, 2.5,1.2, 3.0,1.0, 3.5,0.8
FUNCTION DRINFT= 0.,0., 7.,0., 10.,0.1000, 15.,0.2500, 20.,0.3333,...
                25.,0.5000, 30.,1.0000
FUNCTION MFIPT = 2.0,0.8, 2.5,0.9, 3.0,1.0, 3.5,1.2
FUNCTION RDLATT= 0.,0., 7.,0., 10.,0.1875, 15.,0.2500, 20.,0.3750,...
                25.,0.4000, 30.,0.4545
FUNCTION RDINFT= 0.,0., 7.,0., 10.,0.3000, 15.,0.5000, 20.,0.3333,...
                25.,0.2500, 30.,0.2500
FUNCTION TEMPT = 0.,2., 60.,8., 120.,15., 180.,28., 240.,15., 300.,2.

```

```

METHOD RECT
TIMER FINTIM=120., DELT=0.05, PRDEL=5.
PRINT DAY,TLBM,LAI,DISLA,TLATLA,TINFLA,NLIFLA,DEADLA,RIRLA

```

```

END
STOP

```

```

C*****C
SUBROUTINE BOXCAR(COUNT,AI,DEVR,RD,RMR,INFL,N,DELT,TIME,
$              AO,A,ATOT,MORFL,OUTFL,GAMMA,GCYCL)
C*****C

```

```

C To use this subroutine, memory storage has to be reserved for
C the initial- and actual values of each boxcar of a particular boxcar
C train by typing in the INITIAL-part: STORAGE AI(N),A(N)
C in which AI and A are the names of the arrays of that boxcar train.
C For N, the total number of boxcars in that boxcar train has to be
C substituted. N is an integer, which has to be declared by: FIXED N
C The initial conditions of AI can be given by means of a
C TABLE statement: TABLE AI(1-N)=...,,, or can be calculated in
C a DO loop.
C N has to be calculated as a function of the residence time and
C its standard deviation and has to be given as a parameter in the
C main program. For a fractional boxcar train:
C N < minimum of 1/RD**2
C Usually 3/4 * minimum of 1/RD**2 is taken.(In practice a value of
C N=4 usually seems to mimick delay and dispersion very well).

```

```

IMPLICIT REAL(A-Z)
INTEGER I,N,COUNT
DIMENSION AI(N),A(N),MORR(50)

```

```

C-----C
C Initiation of the boxcar train C
C-----C
IF (TIME.EQ.0.) CALL BOXINI(AI,N,AO,A,GAMMA,GCYCL)

```

```

C-----C
C   Calculation of fraction  $\bar{r}$  C
C-----C
      CALL FRACT(COUNT,DEVR,RD,N,DELT,GAMMA,F)

C-----C
C   Calculation of the rates C
C-----C
      IF (TIME.EQ.0.) GO TO 10
C-----the rate of inflow (INFL) is given or calculated in the main program

C-----mortality rate (MORR) and total mortality flow (MORFL)
      MORRO =RMR * A0
      MORFL =MORRO
      DO 100 I=1,N
          MORR(I) =RMR * A(I)
          MORFL =MORFL + MORR(I)
100 CONTINUE

C-----the rate of outflow (OUTFL) is calculated
C-----note the outflow is also subject to mortality
      CN =A(N)/(GAMMA - GCYCL)
      OUTFL =DEVR * CN * (1. - RMR * DELT)

C-----C
C   Calculation of the states (integrals) C
C-----C
C-----development
      GCYCL =GCYCL + DEVR*DELT
C-----amount in each boxcar (A), after mortality flow and
C-----inflow and outflow in respectively A0 and A(N)
      A0 =A0 - MORRO*DELT + INFL*DELT
      DO 110 I=1,N-1
          A(I) =A(I) - MORR(I)*DELT
110 CONTINUE
      A(N) =A(N) -MORR(N)*DELT - OUTFL*DELT

C-----amount in each boxcar (A), after shift (discontinuous process)
      IF(GCYCL.GE.F*GAMMA) CALL SHIFT(N,F,A0,A,GAMMA,GCYCL)

10 CONTINUE

C-----total amount in boxcar train (ATOT)
      ATOT= A0
      DO 120 I=1,N
          ATOT =ATOT + A(I)
120 CONTINUE

      RETURN
      END

C*****C
      SUBROUTINE BOXINI(AI,N,AO,A,GAMMA,GCYCL)
C*****C
      IMPLICIT REAL(A-Z)
      INTEGER I,N
      DIMENSION AI(N),A(N)

      GCYCL =0.
      GAMMA =1./FLOAT(N)

```

```

      AO      =0.
      DO 200 I=1,N
          A(I) = AI(I)
200  CONTINUE

      RETURN
      END

```

```

C*****C
      SUBROUTINE FRACT(COUNT,DEVR,RD,N,DELT,GAMMA,F)
C*****C

```

```

      IMPLICIT REAL(A-Z)
      INTEGER      N,COUNT

```

```

      F      = 1. - N * RD * RD

```

```

C-----DELT has to be smaller than a fraction F of the smallest time coefficient
C of one boxcar

```

```

      IF (DELT.GT.(F*GAMMA/(DEVR+1.E-10))) THEN
          WRITE (6,'(A,I2,A)') ' Delt too large for boxcar no: ',COUNT
          $           , ' or too many boxes N: F too small '

```

```

      CALL EXIT
      ENDIF

```

```

      RETURN
      END

```

```

C*****C
      SUBROUTINE SHIFT(N,F,AO,A,GAMMA,GCYCL)
C*****C

```

```

      IMPLICIT REAL(A-Z)
      INTEGER      I,N
      DIMENSION    A(N)

```

```

      A(N) = A(N) + A(N-1)*F
      DO 300 I=N-1,2,-1
          A(I)=A(I)*(1.-F) + A(I-1)*F

```

```

300  CONTINUE
      A(1)=A(1)*(1.-F) + AO
      AO = 0.

```

```

      GCYCL =GCYCL - F*GAMMA

```

```

      RETURN
      END

```

```

C-----C

```

```

ENDJOB

```

References

- Aarts, H.F.M. & C.L.M. de Visser, 1985. A management information system for integrated weed control in winter wheat. *Proceedings British Crop Protection Conference (BCPC) – Weeds*: 679-686.
- Acock, B., D.A. Charles-Edwards, D.J. Fitter, D.W. Hand, L.J. Ludwig, J. Warren Wilson & A.C. Withers, 1978. The contribution of leaves from different levels within a tomato crop to canopy net photosynthesis: an experimental examination of two canopy models. *Journal of Experimental Botany* 29: 815-827.
- Acock, B., D.A. Charles-Edwards & S. Sawyer, 1979. Growth response of a *Crysanthemum* crop to the environment. III. Effects of radiation and temperature on dry matter partitioning and photosynthesis. *Annals of Botany* 44: 289-300.
- Ajayi, O. & A.M. Dewar, 1982. The effect of barley yellow dwarf virus on honeydew production by the cereal aphids, *Sitobion avenae* and *Metopolophium dirhodum*. *Annals of applied Biology* 100: 203-212.
- Allen, R.N., 1983. Spread of banana bunchy top and other plant virus diseases in time and space. In: *Plant virus epidemiology*. Eds. R.T. Plumb & J.M. Thresh. Blackwell, Oxford. p. 51-59.
- Amro-Bank, 1985. Modernisering in de melkveehouderij en akkerbouw. Rapport, Amsterdam. 22 p.
- Amro-Bank, 1986. Modernisering in de glastuinbouw. Rapport, Amsterdam. 22 p.
- Amthor, J.S., 1984. The role of maintenance respiration in plant growth. *Plant, Cell and Environment* 7: 561-569.
- Angus, J.F., R.B. Cunningham, M.W. Moncur & D.H. Mackenzie, 1981. Phasic development in field crops. I. Thermal response in the seedling phase. *Field Crops Research* 3: 365-378.
- Aust, H.J., 1981. Ueber den verlauf von Mehlten epidemien innerhalb des Agro-Oekosystems Gerstenfeld. *Acta Phytomedica*, Heft 7.
- Avery, D.J. & J.B. Briggs, 1968a. Damage to leaves caused by fruit tree red spider mite, *Panonychus ulmi* (Koch). *Journal of Horticultural Science* 43: 463-473.
- Avery, D.J. & J.B. Briggs, 1968b. The aetiology and development of damage in young fruit trees infested with fruit tree red spider mite, *Panonychus ulmi* (Koch). *Annals of Applied Biology* 61: 277-288.
- Ayres, P.G., 1981. *Effects of disease on the physiology of the growing plant*. Cambridge University Press, Cambridge.
- Baldwin, J.P., 1976. Competition for plant nutrients in soil; a theoretical approach. *Journal of Agricultural Science* 87: 341-356.
- Balen, J.H. van, 1973. A comparative study of the breeding ecology of the Great Tit *Parus major* in different habitats. *Ardea* 61: 1-93.

- Barnett, K.H. & R.B. Pearce, 1983. Source-sink ratio alteration and its effect on physiological parameters in maize. *Crop Science* 23: 294-299.
- Baskin, J.M. & C.C. Baskin, 1980. Ecophysiology of secondary dormancy in seeds of *Ambrosia artemisiifolia*. *Ecology* 61: 475-480.
- Baskin, J.M. & C.C. Baskin, 1981. Seasonal changes in the germination responses of buried *Lamium amplexicaule* seeds. *Weed Research* 21: 299-306.
- Beek, P. van & Th.H.B. Hendriks, 1985. *Optimaliseringstechnieken, principes en toepassingen*. 2e druk. Bohn, Scheltema & Holkema, Utrecht/Antwerpen. 277 p.
- Begon, M. & M. Mortimer, 1981. *Population ecology*. Sinauer Associates, Sunderland, Mass., U.S.A. 200 p.
- Bellman, R., 1957. *Dynamic programming*. Princeton University Press. Princeton, New York. 340 p.
- Berger, R.D. & J.W. Jones, 1985. A general model for disease progress with functions for variable latency and lesion expansion on growing host plants. *Phytopathology* 75: 792-797.
- Bewley, J.D. & M. Black, 1982. *Physiology and biochemistry of seeds in relation to germination*. 2. Viability, dormancy and environmental control. Springer, Berlin. 375 p.
- Bierhuizen, J.F., 1973. The effect of temperature on plant growth, development and yield. In: *Plant response to climatic factors*. Ed. R.O. Slatyer, Unesco, Paris. p. 89-98.
- Bierhuizen, J.F. & R.A. Feddes, 1973. Use of temperature and short wave radiation to predict the rate of seedling emergence and the harvest date. *Acta Horticulturae* 27: 269-277.
- Bierhuizen, J.F. & W.A. Wagenvoort, 1974. Some aspects of seed germination in vegetables. 1. The determination and application of heat sums and minimum temperature for germination. *Scientia Horticulturae* 2: 213-219.
- Bloc, D., J.P. Gay & J.P. Gouet, 1983. Influence de la temperature sur le développement du maïs. *Bulletin Organisation Européenne pour la Protection des Plantes (OEPP)* 13: 163-169.
- Boote, K.J., J.W. Jones, J.W. Mishoe & R.D. Berger, 1983. Coupling pests to crop growth simulators to predict yield reductions. *Phytopathology* 73: 1581-1587.
- Bridge, D.W., 1976. A simulation model approach for relating effective climate to winter wheat yields on the Great Plains. *Agricultural Meteorology* 17: 185-194.
- Brockington, N.R., 1979. *Computer modelling in agriculture*. Oxford University Press, Oxford. 154 p.
- Brown, R.H., 1985. Growth of C₃ and C₄ grasses under low N levels. *Crop Science* 25: 954-957.
- Bruin, H.A.R. de, 1987. *From Penman to Makkink*. TNO Committee on Hydrological Research, The Hague, the Netherlands. *Proceedings and Information* 39: 5-32.
- Buchanan, B.B., S.W. Hutcheson, A.C. Magyarosy & P. Montalbini, 1981. Photosynthesis in healthy and diseased plants. In: *Effects of disease on the physiology of the growing plant*. Ed. P.G. Ayres. Cambridge University Press, Cambridge. p. 13-28.
- Burton, W.G., 1963. Concepts and mechanism of dormancy. In: *The growth of the potato*. Eds. J.D. Irvin & F.L. Milthorpe, Butterworths, London. p. 17-41.

- Burton, W.G., 1964. The respiration of developing potato tubers. *European Potato Journal* 7: 90-101.
- Burton, W.G., 1974. The oxygen uptake, in air and in 5% O₂, and the carbon dioxide output, of stored potato tubers. *Potato Research* 17: 113-137.
- Carter, N., A.F.G. Dixon & R. Rabbinge, 1982. Cereal aphid population: biology, simulation and prediction. *Simulation Monographs*, Pudoc, Wageningen. 91 p.
- Causton, D.R. & J.C. Venus, 1981. *The biometry of plant growth*. Edward Arnold, London. 307 p.
- Chamberlain, A.L., 1972. Deposition of spores and other particles on vegetation and soil. *Annals of Applied Biology* 71: 141-158.
- Collares-Pereira, M. & A. Rabl, 1979. The average distribution of solar radiation-correlations between diffuse and hemispherical and daily and hourly insolation values. *Solar Energy* 22: 155-164.
- Collins, M.D., S.A. Ward & A.F.G. Dixon, 1981. Handling time and the functional response of *Aphelinus thomsoni*, a predator and parasite of the aphid *Drepanosiphum platanoidis*. *Journal of Animal Ecology* 50: 479-487.
- Cooper, A.J. & J.H.M. Thornley, 1976. Response of dry matter partitioning, growth, and carbon and nitrogen levels in the tomato plant to changes in root temperature: experiment and theory. *Annals of Botany* 40: 1139-1152.
- Coster, G., 1983. De zuigsnelheid van *Sitobion avenae* op tarwe. Internal Report of the Department of Theoretical Production Ecology, Agricultural University, Wageningen. 55 p.
- Cousens, R., 1985. A simple model relating yield loss to weed density. *Annals of Applied Biology* 107: 239-252.
- Curry, G.L. & D.W. De Michele, 1977. Stochastic analysis for the description and synthesis of predator-prey systems. *Canadian Entomologist* 109: 1167-1174.
- Daamen, R.A., 1981. Surveys of diseases and pests of winter wheat in the Netherlands, 1979-1980. *Mededelingen Faculteit Landbouwwetenschappen Rijksuniversiteit Gent*, 46(3): 933-937.
- Daamen, R.A., 1988. Effects of nitrogen fertilization and cultivar on the damage relation of powdery mildew (*Erysiphe graminis*) in winter wheat. *Netherlands Journal of Plant Pathology* 94: 69-80.
- Dannenbring, D.G. & M.K. Starr, 1981. *Management Science*. McGraw-Hill, New York. 763 p.
- Dixon, A.F.G., 1959. An experimental study of the searching of the predatory beetle *Adalia decempunctata* (L.). *Journal of Animal Ecology* 28: 259-281.
- Deinum, B. & J. Knoppers, 1979. The growth of maize in the cool temperate climate of the Netherlands: Effect of grain filling on production of dry matter and on chemical composition and nutritive value. *Netherlands Journal of Agricultural Science* 27: 116-130.
- Dobben, W.H. van, 1962. Influence of temperature and light conditions on dry matter distribution, development rate and yield in arable crops. *Netherlands Journal of Agricultural Science* 10: 377-389.

- Doorenbos, J. & W.O. Pruitt, 1977. Crop water requirements. FAO Irrigation and Drainage Paper 24, FAO, Rome. 144 p.
- Doorenbos, J. & A.H. Kassam, 1979. Yield response to water. FAO Irrigation and Drainage Paper 33, FAO, Rome. 193 p.
- Downton, W.J.S., 1975. The occurrence of C₄ photosynthesis among plants. *Photosynthetica* 9: 97-105.
- Driessen, P.M., 1986a. The water balance of the soil. In: Modelling of agricultural production: weather, soils and crops. Eds. H. van Keulen & J. Wolf, Simulation Monographs, Pudoc, Wageningen. p. 76-117.
- Driessen, P.M., 1986b. Nutrient demand and fertilizer requirements. In: Modelling of agricultural production: weather, soils and crops. Eds. H. van Keulen & J. Wolf, Simulation Monographs, Pudoc, Wageningen. p. 182-200.
- Dwyer, L.M. & D.W. Stewart, 1986. Effect of leaf age and position on net photosynthetic rates in maize (*Zea mays* L.). *Agricultural and Forest Meteorology* 37: 29-46.
- Dye, M.H., 1973. Basidiocarp development and spore release by *Stereum purpureum* in the field. *New Zealand Journal of Agricultural Research* 17: 93-100.
- Edmeades, G.O. & T.B. Daynard, 1979. The relationship between final yield and photosynthesis at flowering in individual maize plants. *Canadian Journal of Plant Science* 59: 585-601.
- Ehleringer, J.R., 1978. Implications of quantum yield differences on the distributions of C₃ and C₄ grasses. *Oecologia (Berl.)* 31: 255-267.
- Ehleringer, J. & R.W. Pearcy, 1983. Variation in quantum yield for CO₂ uptake among C₃ and C₄ plants. *Plant Physiology* 73: 555-559.
- Entwistle, J.C. & A.F.G. Dixon, 1987. Short-term forecasting of wheat yield loss caused by the grain aphid (*Sitobion avenae*) in summer. *Annals of applied Biology* 111: 489-508.
- Faber, D.C., 1986. The use of agronomic information in the socio-economic models of the Centre for World Food Studies. In: Modelling of agricultural production: weather, soils and crops. Eds. H. van Keulen & J. Wolf, Simulation Monographs, Pudoc, Wageningen. p. 329-340.
- Farquhar, G.D. & T.O. Sharkey, 1982. Stomatal conductance and photosynthesis. *Annual Review of Plant Physiology* 33: 317-345.
- Farquhar, G.D., S. van Caemmerer & J.A. Berry, 1980. A biochemical model of photosynthetic CO₂ assimilation in leaves of C₃ species. *Planta* 149: 78-90.
- Feddes, R.A., 1987. Crop factors in relation to Makkink reference-crop evapotranspiration. TNO Committee on Hydrological Research, The Hague, the Netherlands. *Proceedings and Information* 39: 33-46.
- Ferrari, Th.J., 1978. Elements of system-dynamics simulation; a textbook with exercises. Pudoc, Wageningen. 89 p.
- Fick, G.W., W.A. Williams & R.S. Loomis, 1973. Computer simulation of dry matter distribution during sugar beet growth. *Crop Science* 13: 413-417.
- Firbank, L.G., R.J. Manlove, A.M. Mortimer & P.D. Putwain, 1984. The management of grass weeds in cereal crops, a population biology approach. *Proceedings 7th Interna-*

- tional Symposium on Weed Biology, Ecology and Systematics. COLUMA/EWRS, Paris. p. 375-384.
- Firbank, L.G. & A.R. Watkinson, 1985. On the analysis of competition within two-species mixtures of plants. *Journal of applied Ecology* 22: 503-517.
- Forrer, H.R. & J.C. Zadoks, 1983. Yield reduction in wheat in relation to leaf necrosis caused by *Septoria tritici*. *Netherlands Journal of Plant Pathology* 89: 87-98.
- Forrester, J.W., 1961. *Industrial Dynamics*. Massachusetts Institute of Technology Press, Cambridge, Massachusetts, U.S.A. 464 p.
- Foth, H.D., 1962. Root and top growth of corn. *Agronomy Journal* 54: 49-52.
- Fransz, H.G., 1974. The functional response to prey density in an acarine system. *Simulation Monographs*, Pudoc, Wageningen. 149 p.
- Frère, M. & G.F. Popov, 1979. Agrometeorological crop monitoring and forecasting. *Plant Production and Protection Paper 17*, FAO, Rome. 64 p.
- Frissel, M.J. & J.A. van Veen (Eds.), 1981. *Simulation of nitrogen behaviour of soil-plant systems*. Pudoc, Wageningen. 277 p.
- Froud-Williams, R.J., R.J. Chancellor & D.S.H. Drennan, 1984. The effects of seed burial and soil disturbance on emergence and survival of arable weeds in relation to minimal cultivation. *Journal of applied Ecology* 21: 629-641.
- Gausman, H.W. & W.A. Allen, 1973. Optical parameters of leaves of 30 plant species. *Plant Physiology* 52: 57-62.
- Geng, S., F.W.T. Penning de Vries & I. Supit, 1985a. Analysis and simulation of weather variables. Part I: Rain and wind in Wageningen. *Simulation Report CABO-TT 4*, Centre for Agrobiological Research, Wageningen. 55 p.
- Geng, S., F.W.T. Penning de Vries & I. Supit, 1985b. Analysis and simulation of weather variables. Part 2: Temperature and solar radiation. *Simulation Report CABO-TT 5*, Centre for Agrobiological Research, Wageningen. 74 p.
- Gosse, G., C. Varlet-Grancher, R. Bonhomme, M. Chartier, J.-M. Allirand & G. Lemaire, 1986. Production maximale de matière sèche et rayonnement solaire intercepté par un couvert végétal. *Agronomie* 6: 47-56.
- Goudriaan, J., 1973. Dispersion in simulation models of population growth and salt movement in the soil. *Netherlands Journal of Agricultural Science* 21: 269-281.
- Goudriaan, J., 1977. *Crop micrometeorology: a simulation study*. *Simulation Monographs*, Pudoc, Wageningen. 257 p.
- Goudriaan, J., 1982. Some techniques in dynamic simulation. In: *Simulation of plant growth and crop production*. Eds. F.W.T. Penning de Vries & H.H. van Laar. *Simulation Monographs*, Pudoc, Wageningen. p. 66-84.
- Goudriaan, J., 1986. A simple and fast numerical method for the computation of daily totals of crop photosynthesis. *Agricultural and Forest Meteorology*, 38: 251-255.
- Goudriaan, J., 1988. The bare bones of leaf angle distribution in radiation models for canopy photosynthesis and energy exchange. *Agricultural and Forest Meteorology* 43: 155-169.
- Goudriaan, J. & H.H. van Laar, 1978. Calculation of daily totals of the gross CO₂-assimilation of leaf canopies. *Netherlands Journal of Agricultural Science* 14: 373-383.

- Goudriaan, J. & H. van Keulen, 1979. The direct and indirect effects of nitrogen shortage on photosynthesis and transpiration in maize and sunflower. *Netherlands Journal of Agricultural Science* 27: 227-234.
- Greenwood, D.J., A. Draycott, P.J. Last & A.P. Draycott, 1984. A concise simulation model for interpreting N-fertilizer trials. *Fertilizer Research* 5: 355-369.
- Groot, J.J.R., 1987. Simulation of crop growth and nitrogen behaviour in a winter wheat-soil system. Simulation Report CABO-TT 13, Centre for Agrobiological Research, Wageningen. 69 p.
- Groot, J.J.R., M.J. Kropff, F.J.H. Vossen, C.J.T. Spitters & R. Rabbinge, 1986. A decimal code for the development stages of maize and its relation to accumulated heat units. *Netherlands Journal of Agricultural Science* 34: 67-73.
- Grosclaude, C., 1969. Le plomb des arbres fruitiers. VII. Observations sur les carpophores et les spores du *Stereum purpureum*. *Annales de Phytopathologie* 1(1): 75-85.
- Gutierrez, A.P., L.A. Falcon, W.B. Loew, P.A. Leipzig & R. van den Bosch, 1975. An analysis of cotton production in California: a model of Acala cotton and the effect of defoliators on its yield. *Environmental Entomology* 4: 125-136.
- Gutierrez, A.P., J.B. Christensen, C.M. Merritt, W.B. Loew, C.G. Summers & W.R. Cothran, 1976. Alfalfa and the Egyptian alfalfa weevil (Coleoptera: Curculionidae). *Canadian Entomologist* 108: 635-648.
- Hadley, P., E.H. Roberts, R.J. Summerfield & F.R. Minchin, 1984. Effects of temperature and photoperiod on flowering in soya bean (*Glycine max* (L.) Merrill): a quantitative model. *Annals of Botany* 53: 669-681.
- Hagan, R.M. & J.I. Stewart, 1972. Water deficits – irrigation design and programming. *Proceedings of the American Society of Civil Engineers. I. Irrigation and Drainage Division* 98 (IRZ): 220-226.
- Handbook of Chemistry and Physics, 1974-1975. CRC, 55th Edition.
- Hanway, J.J., 1962. Corn growth and composition in relation to soil fertility: I. Growth of different plant parts and relation between leaf weight and grain yield. *Agronomy Journal* 54: 145-148.
- Hanway, J.J., 1963. Growth stages of corn (*Zea mays* L.). *Agronomy Journal* 55: 487-491.
- Hassell, M.P., 1978. The dynamics of anthropod predator-prey system. Princeton University Press.
- Hassell, M.P. & R.M. May, 1973. Stability in insect host-parasite models. *Journal of Animal Ecology* 42: 693-726.
- Heemst, H.D.J. van, 1986. The distribution of dry matter during growth of a potato crop. *Potato Research* 29: 55-66.
- Hegarty, T.W., 1978. The physiology of seed hydration and dehydration, and the relation between water stress and the control of germination: a review. *Plant, Cell and Environment* 1: 101-119.
- Heydecker, W. (Ed.), 1973. Seed ecology. *Proceedings 19th Easter School in Agricultural Science 1972*, Nottingham. Butterworths, London.
- Hillier, F. & G.J. Lieberman, 1980. Introduction to operations research. 3rd Edition. Holden-Day, San Francisco. 829 p.

- Hodanova, D., 1981. Photosynthetic capacity, irradiance and sequential senescence of sugar beet leaves. *Biologia Plantarum* 23: 58-67.
- Holling, C.S., 1966. The functional response of invertebrate predators to prey density. *Memoires of the Entomological Society of Canada* 48: 1-86.
- Hunt, R., 1982. Plant growth curves. Edward Arnold, London. 248 p.
- Hunt, E.R., J.A. Weber & D.M. Gates, 1985. Effects of nitrate application on *Amaranthus powellii* Wats. I. Changes in photosynthesis, growth rates, and leaf area. *Plant Physiology* 79: 609-613.
- IBM, 1975. Continuous system modeling program III (CSMP III), Program Reference Manual. IBM SH19-7001-3. Technical Publication Department, White Plains, USA. 206 p.
- Ingram, K.T. & D.E. McCloud, 1984. Simulation of potato crop growth and development. *Crop Science* 24: 21-27.
- Institut International de Recherches Betteravières (IIRB), 1980. Storage of sugar beet. *Compte Rendy* 43. IIRB, Bruxelles, Belgium. 392 p.
- Jansen, D.M., R.T. Dierkx, H.H. van Laar & M.J. Alagos, 1988. PCSMP on IBM PC-AT's or PC-XT's and compatibles. Simulation Report CABO-TT 15, Centre for Agrobiological Research, Wageningen. 64 p.
- Janssen, J.G.M., 1974. Simulation of germination of winter annuals in relation to microclimate and microdistribution. *Oecologia* 14: 197-228.
- Johnson, I.R. & J.H.M. Thornley, 1983. Vegetative crop growth model incorporating leaf area expansion and senescence, and applied to grass. *Plant, Cell and Environment* 6: 721-729.
- Jones, C.A. & J.R. Kiniry (Eds), 1986. CERES-maize: a simulation model of maize growth and development. Texas A&M University Press, Texas. 194 p.
- Jones, J.W. & J.D. Hesketh, 1980. Predicting leaf expansion. In: Predicting photosynthesis for ecosystem models. Eds. J.D. Hesketh & J.W. Jones. CRC Press Inc., Boca Raton, Florida, U.S.A., Vol. 2. p. 85-122.
- Jong, M.D. de, 1988. Risk to fruit trees and native trees due to control of black cherry (*Prunus serotina*) by silver fungus (*Chondrostereum purpureum*). PhD thesis, Wageningen Agricultural University, the Netherlands. 138 p. (in Dutch, with English summary).
- Jong, M.D. de & P.C. Scheepens, 1985. Analyse van risico bij bestrijding van Amerikaanse vogelkers (*Prunus serotina*) met *Chondrostereum purpureum* voor planten waartegen de bestrijding niet is gericht. Centre for Agrobiological Research Report 58, Wageningen, (in Dutch).
- Karssen, C.M., 1982. Seasonal patterns of dormancy in weed seeds. In: The physiology and biochemistry of seed development, dormancy and germination. Ed. A.A. Khan. Elsevier Biomedical Press. p. 243-270.
- Kase, M. & J. Catský, 1984. Maintenance and growth components of dark respiration rate in leaves of C₃ and C₄ plants as affected by leaf temperature. *Biologia Plantarum* 26: 461-470.
- Keulen, H. van, 1975. Simulation of water use and herbage growth in arid regions. Simulation Monographs, Pudoc, Wageningen. 176 p.

- Keulen, H. van 1982a. Crop production under semi-arid conditions, as determined by moisture availability. In: Simulation of plant growth and crop production. Eds. F.W.T. Penning de Vries & H.H. van Laar. Simulation Monographs, Pudoc, Wageningen. p. 159-174.
- Keulen, H. van, 1982b. Crop production under semi-arid conditions, as determined by nitrogen and moisture availability. In: Simulation of plant growth and crop production. Eds. F.W.T. Penning de Vries & H.H. van Laar. Simulation Monographs, Pudoc, Wageningen. p. 234-249.
- Keulen, H. van, 1986a. A simple model of water-limited production. In: Modelling of agricultural production: weather, soils and crops. Eds. H. van Keulen & J. Wolf, Simulation Monographs, Pudoc, Wageningen. p. 130-153.
- Keulen, H. van, 1986b. Crop yield and nutrient requirements. In: Modelling of agricultural production: weather, soils and crops. Eds. H. van Keulen & J. Wolf, Simulation Monographs, Pudoc, Wageningen. p. 153-181.
- Keulen, H. van & H.D.J. van Heemst, 1982. Crop response to the supply of macronutrients. Agricultural Research Reports 916. 46 p.
- Keulen, H. van & W.A.J. de Milliano, 1984. Potential wheat yields in Zambia – A simulation approach. Agricultural Systems 14: 171-192.
- Keulen, H. van & J. Wolf (Eds), 1986. Modelling of agricultural production: weather, soils and crops. Simulation Monographs, Pudoc, Wageningen. 479 p.
- Keulen, H. van & N.G. Seligman, 1987. Simulation of water use, nitrogen nutrition and growth of a spring wheat crop. Simulation Monographs, Pudoc, Wageningen. 310 p.
- Keulen, H. van, F.W.T. Penning de Vries & E.M. Drees, 1982. A summary model for crop growth. In: Simulation of plant growth and crop production. Eds. F.W.T. Penning de Vries & H.H. van Laar. Simulation Monographs, Pudoc, Wageningen. p. 87-94.
- Kroon, A.G. & H.P.J.M. Driessen, 1982. Een simulatiemodel voor de parasitering van *Sitobion avenae* door *Aphidius rhopalosiphi*. Internal Report, Theoretical Production Ecology, Agricultural University, Wageningen.
- Ku, M.S.B., M.R. Schmitt & G.E. Edwards, 1979. Quantitative determination of RuBP carboxylase – oxygenase protein in leaves of several C₃ and C₄ plants. Journal of Experimental Botany 30: 89-98.
- Legg, B.J. & F.A. Powell, 1979. Spore dispersal in a barley crop: a mathematical model. Journal of Agricultural Meteorology 20: 1-127.
- Lenteren, J.C. van, K. Bakker & J.J.M. van Alphen, 1978. How to analyse host discrimination. Ecological Entomology 3: 71-75.
- Leverenz, J.W. & G. Öquist, 1987. Quantum yields of photosynthesis at temperatures between -2°C and 35°C in a cold-tolerant C₃ plant (*Pinus sylvestris*) during the course of one year. Plant, Cell and Environment 10: 287-295.
- Lighth, W.I. & F.A.B. Ludlam, 1972. The effects of fruit tree red spider mite, *Panonychus ulmi* (Koch) on the yield of apple trees in Kent. Plant Pathology 21: 175-181.
- Llewellyn, M., 1988. Aphid energy budgets. In: World Crop Pests: Aphids. Volume 2B. Eds. A.K. Minks & P. Harrewijn. Elsevier, Amsterdam. p. 109-117.
- Loomis, R.S., R. Rabbinge & E. Ng, 1979. Explanatory models in crop physiology. Annual Reviews Plant Physiology 30: 339-367.

- Lotka, A.J., 1925. Elements of physical biology. Williams and Wilkens, Baltimore.
- Makkink, G.F., 1957. Testing the Penman formula by means of lysimeters. *Journal of the Institution of Water Engineers* 11: 277-288.
- Mantel, W.P., R. Rabbinge & J. Sinke, 1982. Effekten van bladluizen op de opbrengst van winter tarwe. *Gewasbescherming* 13: 115-124.
- McDermitt, D.K. & R.S. Loomis, 1981. Elemental composition of biomass and its relation to energy content, growth efficiency, and growth yield. *Annals of Botany* 48: 275-290.
- Milthorpe, F.L. & J. Moorby, 1974. An introduction to crop physiology. Cambridge University Press, Cambridge. 244 p.
- Mols, P.J.M., 1989. Searching behaviour of the carabid beetle *Pterostichus coerulescens*. Ph.D. thesis. Agricultural University, Wageningen (in prep.).
- Monsi, M. & T. Saeki, 1953. Ueber den Lichtfaktor in den Pflanzengesellschaften und sein Bedeutung fuer die Stoffproduktion. *Japan Journal of Botany* 14. 22 p.
- Monteith, J.L., 1965. Evaporation and environment. *Proceedings Symposium Society of Experimental Biology* 19: 205-234.
- Monteith, J.L., 1969. Light interception and radiative exchange in crop stands. In: *Physiological aspects of crop yield*. Eds. J.D.Eastin, F.A.Haskins, C.Y.Sullivan & C.H.M.van Bavel, American Society of Agronomy, Crop Science Society of America, Madison, Wisconsin, U.S.A. p. 89-111.
- Mortimer, A.M., 1983. On weed demography. In: *Recent advances in weed research*. Ed. W.W. Fletcher. Commonwealth Agricultural Bureaux, England. p. 3-40.
- Mumford, J.D., 1982a. Perceptions of losses from pests of arable crops by some farmers in England and New Zealand. *Crop Protection* 1: 282-288.
- Mumford, J.D., 1982b. Farmers' perceptions and crop protection decision making. *Proceedings British Crop Protection Conference, BCPC Monograph* 25. p. 13-19.
- Murdoch, A.J. & E.H. Roberts, 1982. Biological and financial criteria for long-term control strategies for annual weeds. *Proceedings British Crop Protection Conference on Weeds, 1982*. p. 741-748.
- Nachman, G., 1981. A mathematical model of the functional relationship between density and the spatial distribution of a population. *Journal of Animal Ecology* 50: 453-460.
- Ng, E. & R.S. Loomis, 1984. Simulation of growth and yield of the potato crop. *Simulation Monographs*, Pudoc, Wageningen. 147 p.
- Noordwijk, M. van, 1983. Functional interpretation of root densities in the field for nutrient and water uptake. In: *Root ecology and its practical application*. International Symposium Gumpenstein, 1982, Bundesanstalt Gumpenstein, A-8952 Irdning. p. 207-226.
- Norton, G.A. 1976. Analysis of decision making in crop protection. *Agro-Ecosystems* 3: 27-44.
- Norton, G.A., 1982. A decision-analysis approach to integrated pest control. *Crop Protection* 1: 147-164.
- Norton, G.A. & J.D. Mumford, 1983. Decision making in pest control. *Advances Applied Biology* 8: 87-119.

- Onstad, D.W. & R. Rabbinge, 1985. Dynamic programming and the computation of economic injury levels for crop disease control. *Agricultural Systems* 18: 207-226.
- Parsons, A.J. & M.J. Robson, 1981. Seasonal changes in the physiology of S24 perennial ryegrass (*Lolium perenne* L.). 2. Potential leaf and canopy photosynthesis during the transition from vegetative to reproductive growth. *Annals of Botany* 47: 249-258.
- Pearcy, R.W. & J. Ehleringer, 1984. Comparative ecophysiology of C₃ and C₄ plants. *Plant, Cell and Environment* 7: 1-13.
- Penman, H.L., 1948. Natural evaporation from open water, bare soil and grass. *Proceedings Royal Society London, Series A*, 193. p. 120-146.
- Penning de Vries, F.W.T., 1975. The cost of maintenance processes in plant cells. *Annals of Botany* 39: 77-92.
- Penning de Vries, F.W.T., 1980. Simulation models of growth of crops, particularly under nutrient stress. *Proceedings 15th Colloquium International Potash Institute: Physiological aspects of crop productivity*. Wageningen. p. 213-226.
- Penning de Vries, F.W.T. & H. van Keulen, 1982. La production actuelle et l'action de l'azote et du phosphore. In: *La productivité des pâturages sahéliens*. Eds. F.W.T. Penning de Vries & M.A. Djiteye. Pudoc, Wageningen. p. 196-226.
- Penning de Vries, F.W.T. & H.H. van Laar, 1982. Simulation of growth processes and the model BACROS. In: *Simulation of plant growth and crop production*. Eds. F.W.T. Penning de Vries & H.H. van Laar. *Simulation Monographs*, Pudoc, Wageningen. p. 114-135.
- Penning de Vries, F.W.T., A.H.M. Brunsting & H.H. van Laar, 1974. Products, requirements and efficiency of biosynthesis: a quantitative approach. *Journal of Theoretical Biology* 45: 339-377.
- Penning de Vries, F.W.T., J.M. Wiltage & D. Kremer, 1979. Rates of respiration and of increase in structural dry matter in young wheat, ryegrass and maize plants in relation to temperature, to water stress and to their sugar content. *Annals of Botany* 44: 595-609.
- Penning de Vries, F.W.T., H.H. van Laar & M.C.M. Chardon, 1983. Bioenergetics of growth of seeds, fruits, and storage organs. In: *Potential productivity of field crops under different environments*. International Rice Research Institute, Los Banos, Philippines. p. 37-59.
- Peters, N.C.B. & B.J. Wilson, 1983. Some studies on the competition between *Avena fatua* L. and spring barley. II. Variation of *A. fatua* emergence and development and its influence on crop yield. *Weed Research* 23: 305-311.
- Pielou, E.C., 1974. *Population and community ecology: principles and methods*. Gordon & Breach Science Publishers. New York, Paris, London.
- Pielou, E.C., 1977. *Mathematical ecology*. Wiley, New York. 385 p.
- Pitter, R.L., 1977. The effect of weather and technology on wheat yields in Oregon. *Agricultural Meteorology* 18: 115-131.
- Plank, J.E. van der, 1963. *Plant diseases. Epidemics and control*. Academic Press, New York. 349 p.
- Rabbinge, R., 1976. Biological control of fruit-tree red spider mite. *Simulation Monographs*, Pudoc, Wageningen. 234 p.

- Rabbinge, R., 1981. Introduction. Proceedings of Symposium IX International Congress of Plant Protection, Washington. p. 163-166.
- Rabbinge, R., 1982. Pests, diseases and crop production. In: Simulation of plant growth and crop production. Eds. F.W.T. Penning de Vries & H.H. van Laar. Simulation Monographs, Pudoc, Wageningen. p. 253-265.
- Rabbinge, R., 1985. Aspects of damage assessment. In: Spider mites their biology, natural enemies and control. Eds. W.Helle & M.W.Sabelis. Volume 1B, Elsevier Science Publishers BV, Amsterdam. p. 261-272.
- Rabbinge, R., 1986. The bridge function of crop ecology. Netherlands Journal of Agricultural Science 3: 239-251.
- Rabbinge, R. & P.H. Vereijken, 1980. The effect of diseases or pest upon the host. Zeitschrift für Pflanzenkrankheiten und Pflanzenschutz 87(7): 409-422.
- Rabbinge, R. & W.P. Mantel, 1981. Monitoring for cereal aphids in winter wheat. Netherlands Journal of Plant Pathology 87: 25-29.
- Rabbinge, R. & N. Carter, 1984. Monitoring and forecasting of cereal aphids in the Netherlands: a subsystem of EPIPARE. In: Pest and pathogen control. Strategic, tactical and policy models. Ed. G.R. Conway, International Series on Applied Systems Analysis, IIASA, Austria. Wiley, Chichester. p. 242-253.
- Rabbinge, R. & G. Coster, 1984. Some effects of cereal aphids on growth and yield of winter wheat. In: Proceedings of the Fourth Australian Applied Entomology Research Conference. Eds. P.Barley & D.Swinger. University of Adelaide, Australia, 24-28 Sept. 1984. p. 163-169.
- Rabbinge, R. & F.H. Rijdsijk, 1984. Epidemiological and crop physiological foundation of EPIPARE. In: Cereal production. Ed. E.J. Gallagher, Butterworths, London. p. 227-235.
- Rabbinge, R. & W.A.H. Rossing, 1988. Dynamic explanatory models as a tool in the development of flexible Economic Injury Levels. In: Pest and disease models in forecasting, crop loss appraisal and decision-supported crop protection systems. Eds. D.J. Royle, R. Rabbinge & C.R. Flückiger. International Organization for Biological and Integrated Control of Noxious Animals and Plants/West Palaearctic Regional Section. IOBC/WPRS. Working Group: Models in integrated crop protection, 1988/XI/2. p. 48-61.
- Rabbinge, R., E.M. Drees, M. van der Graaf, F.C.M. Verberne & A. Wesselo, 1981. Damage effects of cereal aphids in wheat. Netherlands Journal of Plant Pathology 87: 217-232.
- Rabbinge, R., C. Sinke & W.P. Mantel, 1983. Yield loss due to cereal aphids and powdery mildew in winter wheat. Mededelingen Faculteit Landbouwwetenschappen, Rijksuniversiteit Gent, 48/4. p. 1159-1168.
- Rabbinge, R., A.G. Kroon & H.P.J.M. Driessen, 1984a. Consequences of clustering in parasite-host relations of the cereal aphid *Sitobion avenae*: a simulation study. Synopsis Netherlands Journal of Agricultural Science 32: 237-239.
- Rabbinge, R., A. Brouwer, N.J. Fokkema, J. Sinke & T.J. Stomph, 1984b. Effects of saprophytic leaf mycoflora on growth and productivity of winter wheat. Netherlands Journal of Plant Pathology 90: 181-197.

- Rabbinge, R., I.T.M. Jorritsma & J. Schans, 1985. Damage components of powdery mildew in winter wheat. *Netherlands Journal of Plant Pathology* 91: 235-247.
- Raghavendra, A.S. & V.S.R. Das, 1978. The occurrence of C₄ photosynthesis: a supplementary list of C₄ plants reported during late 1974 – mid 1977. *Photosynthetica* 12: 200-208.
- Rawson, H.M. & A.K. Bagga, 1979. Influence of temperature between floral initiation and flag leaf emergence on grain number in wheat. *Australian Journal of Plant Physiology* 6: 391-400.
- Rawson, H.M., J.H. Hindmarsh, R.A. Fischer & Y.M. Stockman, 1983. Changes in leaf photosynthesis with plant ontogeny and relationships with yield per ear in wheat cultivars and 120 progeny. *Australian Journal of Plant Physiology* 10: 503-514.
- Reddy, V.M. & T.B. Daynard, 1983. Endosperm characteristics associated with rate of grain filling and kernel size in corn. *Maydica* 28: 339-355.
- Reede, R.H. de & H. de Wilde, 1986. Phenological models for *Pandemis heparana* (DENN et SCHIFF) and *Adoxophyes orana* (F.v.R) (Lepidoptera: Tortricidae) for timing the application of Insect Growth Regulators with juvenile-hormone activity. *Entomologia experimentalis et applicata* 40: 151-159.
- Rees, A.R. & J.H.M. Thornley, 1973. A simulation of tulip growth in the field. *Annals of Botany* 37: 121-131.
- Reinink, K., 1985. PAGV Tarweteelt-begeleidingssysteem: bestrijding van ziekten en plagen. Beschrijving EPIPPE-model. Lelystad, PAGV. Internal Report.
- Reinink, K., I. Jorritsma & A. Darwinkel, 1986. Adaptation of the AFRC wheat phenology model for Dutch conditions. *Netherlands Journal of Agricultural Science* 34: 1-13.
- Rommelzwaal, A.J. & A. Habekotté, 1986. Simulatie van de fenologische ontwikkeling van winterkoolzaad in de IJsselmeerpolders. Rijks IJsselmeerpolder rapport, Lelystad (in Dutch).
- Richards, F.J., 1959. A flexible growth function for empirical use. *Journal of experimental Botany* 10: 290-300.
- Richards, F.J., 1969. The quantitative analysis of growth. In: *Plant Physiology VA: Analysis of growth. Behaviour of plants and their organs*. Ed. F.C. Steward. Academic Press, New York. p. 3-76.
- Ridder, N. de, N.G. Seligman & H. van Keulen, 1981. Analysis of environmental and species effects on the magnitude of biomass investment in the reproductive effort of annual plants. *Oecologia* 49: 263-271.
- Rijsdijk, F.H., 1983. Decision making in the practice of crop protection. The EPIPPE system. *Proceedings British Crop Protection Council Symposium 1982*. p. 65-76.
- Roberts, E.H., 1972. Dormancy: a factor affecting seed survival in the soil. In: *Viability of seeds*. Ed. E.H. Roberts. Chapman and Hall, London. p. 321-359.
- Roberts, E.H. & S. Totterdell, 1981. Seed dormancy in *Rumex* species in response to environmental factors. *Plant, Cell and Environment* 4: 97-106.
- Roberts, H.A., 1984. Crop and weed emergence patterns in relation to time of cultivation and rainfall. *Annals of Applied Biology* 105: 263-275.
- Roermund, H.J.W. van, J.J.R. Groot, W.A.H. Rossing & R. Rabbinge, 1986. Simulation

- of aphid damage in winter wheat. *Netherlands Journal of Agricultural Science* 34: 488-493.
- Rossing, W.A.H., 1988. A decision model for chemical control of aphids in winter wheat with quantification of risk. *Kwantitatieve Methoden* 27: 95-114.
- Royle, D.J., R. Rabbinge & C.R. Flückiger (Eds.), 1988. Pest and disease models in forecasting, crop loss appraisal and decision-supported crop protection systems. International Organization for Biological and Integrated Control of Noxious Animals and Plants/West Palaearctic Regional Section. IOBC/WPRS. Working Group: Models in integrated crop protection, 1988/XI/2. 95 p.
- Sabelis, M.W., 1981. Biological control of two-spotted spider mites using phytoseiid predators. Part I: Modelling the predator-prey interaction at the individual level. *Agricultural Research Reports* 910. Pudoc, Wageningen. 242 p.
- Sabelis, M.W. et al., 1983. Experimental validation of a simulation model of the interaction between *Phytoseiulus persimilis* and *Tetranychus urticae* on cucumber. *International Organization of Biological Control Bulletin* 1983/VI/3. p. 207-229.
- Sanders, P.L., M.A. de Waard & W.M. Loerakker, 1986. Resistance to carbendazim in *Pseudocercospora herpotrichoides* from Dutch wheat fields. *Netherlands Journal of Plant Pathology* 92: 15-20.
- Schapendonk, A.H.C.M. & P. Gaastra, 1984. A simulation study on CO₂ concentration in protected cultivation. *Scientia Horticulturae* 23: 217-229.
- Scheid, F., 1968. Numerical analysis. Schaum's outline series. McGraw-Hill Book Company, New York. p. 125-149.
- Scott, S.J., R.A. Jones & W.A. Williams, 1984. Review of data analysis methods for seed germination. *Crop Science* 24: 1192-1199.
- Seligman, N.G. & H. van Keulen, 1981. PAPRAN: A simulation model of annual pasture production limited by rainfall and nitrogen. In: *Simulation of nitrogen behaviour of soil-plant systems*. Eds. M.J. Frissel & J.A. van Veen. Pudoc, Wageningen. p. 192-220.
- Sheehy, J.E., J.M. Cobby & G.J.A. Ryle, 1980. The use of a model to investigate the influence of some environmental factors on the growth of perennial ryegrass. *Annals of Botany* 46: 343-365.
- Shirota, Y., N. Carter, R. Rabbinge & G.W. Ankersmit, 1983. Biology of *Aphidius rhopalosiphii*, a parasitoid of cereal aphids. *Entomologia experimentalis et applicata* 34: 27-34.
- Sinclair, T.R. & C.T. de Wit, 1975. Photosynthate and nitrogen requirements for seed production by various crops. *Science* 189: 565-567.
- Smith, I.M., L. Chiarappa & N.A. van der Graaff, 1984. World crop losses: an overview. In: *Plant diseases, infection damage and loss*. Eds. R.K.S. Wood & G.J. Jellis. Blackwell Scientific Publications, Oxford. p. 213-225.
- Snedecor, G.W. & W.G. Cochran, 1980. *Statistical methods*. Iowa State University Press. Ames, Iowa, U.S.A. 507 p.
- Sofield, I., L.T. Evans, M.G. Cook & I.F. Wardlaw, 1977a. Factors influencing the rate and duration of grain filling in wheat. *Australian Journal of Plant Physiology* 4: 785-797.
- Sofield, I., I.F. Wardlaw, L.T. Evans & S.Y. Zee, 1977b. Nitrogen, phosphorus and water

- content during grain development and maturation in wheat. *Australian Journal of Plant Physiology* 4: 799-810.
- Southwood, T.R.E., 1978. *Ecological methods* (2nd edition). Chapman and Hall, London. 391 p.
- Spiertz, J.H.J., 1977. The influence of temperature and light intensity on grain growth in relation to the carbohydrate and nitrogen economy of the wheat plant. *Netherlands Journal of Agricultural Science* 25: 182-197.
- Spiertz, J.H.J. & H. van Keulen, 1980. Effects of nitrogen and water supply on growth and grain yield of wheat. *Proceedings 3rd International Wheat Conference, Madrid, 1980.* p. 595-610.
- Spitters, C.J.T., 1979. Competition and its consequences for selection in barley breeding. *Agricultural Research Reports* 893, Pudoc, Wageningen. 268 p.
- Spitters, C.J.T., 1983. An alternative approach to the analysis of mixed cropping experiments. 1. Estimation of competition effects. *Netherlands Journal of Agricultural Science* 31: 1-11.
- Spitters, C.J.T., 1984. A simple simulation model for crop-weed competition. *Proceedings 7th International Symposium on Weed Biology, Ecology and Systematics. COL-UMA/EWRS, Paris.* p. 355-366.
- Spitters, C.J.T., 1986. Separating the diffuse and direct component of global radiation and its implications for modeling canopy photosynthesis. II. Calculations of canopy photosynthesis. *Agricultural and Forest Meteorology* 38: 231-242.
- Spitters, C.J.T. & R. Aerts, 1983. Simulation of competition for light and water in crop-weed associations. *Aspects of Applied Biology* 4: 467-483.
- Spitters, C.J.T. & Th. Kramer, 1986. Differences between spring wheat cultivars in early growth. *Euphytica* 35: 273-292.
- Spitters, C.J.T., H.A.J.M. Toussaint & J. Goudriaan, 1986. Separating the diffuse and direct component of global radiation and its implications for modeling canopy photosynthesis. I. Components of incoming radiation. *Agricultural and Forest Meteorology* 38: 217-229.
- Stapper, M. & G.F. Arkin, 1980. CORNF: a dynamic growth and development model for maize (*Zea mays* L.). Texas Agricultural Experiment Station, Blackland Research Center, Temple, Texas, U.S.A. Program and Model Documentation 80-2. 91 p.
- Stern, V.M., 1973. Economic thresholds. *Annual Review of Entomology* 18: 259-280.
- Stol, W., 1985. EPIPPE-advies per telefoon succesvol. *Boer en Tuinder* 17 oktober 1985. p. 24-25.
- Stroosnijder, L., 1982. Simulation of the soil water balance. In: *Simulation of plant growth and crop production.* Eds. F.W.T. Penning de Vries & H.H. van Laar. Simulation Monographs, Pudoc, Wageningen. p. 175-192.
- Szeicz, G., 1974. Solar radiation for plant growth. *Journal of Applied Ecology* 11: 617-636.
- Tait, E.J., 1978. Factors affecting the usage of insecticides and fungicides on fruit and vegetable crops in Great Britain. *Journal of Environmental Management* 6: 127-151.
- Tait, E.J., 1981. Environmental perception and pest control. IOBC Special Issue Conference Future Trends Integrated Pest Management, Bellagio, 30 May – 4 June, 1980. International Organization of Biological Control, Paris. p. 55-60.

- Tait, E.J., 1982. Farmers' attitudes and crop protection decision making. Proceedings British Crop Protection Conference – BCPC Monograph 25. p. 43-52.
- Tamm, E., 1933. Weitere Untersuchungen über die Keimung und das Auflaufen landwirtschaftlicher Kulturpflanzen. II. Mitteilung. Archiv für Pflanzenbau 10: 297-312.
- Tanaka, A., 1983. Physiological aspects of productivity in field crops. In: Potential productivity of field crops under different environments. International Rice Research Institute, Philippines. p. 61-80.
- Taylor, L.R., 1961. Aggregation, variance and the mean. Nature (London) 189: 732-735.
- Taylor, L.R., I.P. Woiwod & J.N. Perry, 1978. The density-dependence of spatial behaviour and the rarity of randomness. Journal of Animal Ecology 47: 383-406.
- Teng, P.S., M.J. Blackie & R.C. Close, 1980. Simulation of the barley leaf rust epidemic: structure and validation of BARSIM-I. Agricultural Systems 5: 85-103.
- Thompson, L.M., 1969. Weather and technology in the production of corn in the U.S. Corn Belt. Agronomy Journal 61: 453-456.
- Thompson, K. & J.P. Grime, 1979. Seasonal variation in the seed banks of herbaceous species in ten contrasting habitats. Journal of Ecology 67: 893-921.
- Thornley, J.H.M., 1972. A balanced quantitative model for root/shoot ratios in vegetative plants. Annals of Botany 36: 431-441.
- Tollenaar, M., 1977. Sink-source relationships during reproductive development in maize. A review. Maydica 22: 49-75.
- Tomczyk, A. & M. van de Vrie, 1982. Physiological and biochemical changes in three cultivars of chrysanthemum after feeding by *Tetranychus urticae*. Proceedings 5th International Symposium Insect-Plant Relationships, Wageningen. p. 391-392.
- Tourigny, G., 1985. A general dynamic and stochastic discrete-event simulation model of the foraging behaviour of *Ragoletis pomonella* (Walsh), the apple maggot fly. Master of Pest Management Professional Paper. Simon Fraser University, Canada. 293 p.
- Vegis, A., 1964. Dormancy in higher plants. Annual Review Plant Physiology 15: 185-224.
- Vereijken, P.H., 1979. Feeding and multiplication of three cereal aphid species and their effect on yield of winter wheat. Agricultural Research Reports 888. Pudoc, Wageningen. 58 p.
- Versteeg, M.N. & H. van Keulen, 1986. Potential crop production prediction by some simple calculation methods, as compared with computer simulations. Agricultural Systems 19: 249-272.
- Vertregt, N. & F.W.T. Penning de Vries, 1987. A rapid method for determining the efficiency of biosynthesis of plant biomass. Journal of Theoretical Biology 128: 109-119.
- Vickerman, G.P. & K.D. Sunderland, 1975. Arthropods in cereal crops: nocturnal activity, vertical distribution and aphid predation. Journal of Applied Ecology 12: 755-765.
- Visser, C.L.M. de, H.F.M. Aarts & W.A. Dekkers, 1986. Een geautomatiseerd systeem ter ondersteuning van de herbicide-keuze. Gewasbescherming 17(5): 143-151.
- Volterra, V., 1931. Variations and fluctuations of the number of individuals in animal species living together. In: Animal Ecology. Ed. R.N. Chapman. McGraw-Hill, New York.
- Vos, J., 1981. Effects of temperature and nitrogen supply on post-floral growth of wheat;

- measurements and simulations. Agricultural Research Reports 911. Pudoc, Wageningen. 164 p.
- Vrie, M. van de, 1956. Over de invloed van spintaantasting op de opbrengst en groei van vruchtbomen. Tijdschrift voor Plantenziekten 62: 243-257.
- Waard, M.A. de, E.M.C. de Kipp, M.N. Horn & J.G.M. van Nistelrooy, 1986. Variation in sensitivity to fungicides which inhibit ergosterol biosynthesis in wheat powdery mildew. Netherlands Journal of Plant Pathology 92: 21-32.
- Wagenmakers, P.S., 1984. Simulatie van de sporeverspreiding van *Chondrostereum purpureum* in een bos. Internal Report of the Department of Theoretical Production Ecology, Agricultural University, Wageningen, (in Dutch). 58 p.
- Wagner, H.M., 1979. Principles of operations research with application to managerial decisions. 2nd Edition. Englewood Cliffs, New York. 1039 p.
- Ward, S.A., R. Rabbinge & W.P. Mantel, 1985a. The use of incidence counts for estimation of aphid populations. 1. Minimum sample size for required accuracy. Netherlands Journal of Plant Pathology 90: 181-197.
- Ward, S.A., R. Rabbinge & W.P. Mantel, 1985b. The use of incidence counts for estimation of aphid populations. 2. Confidence intervals from fixed sample size. Netherlands Journal of Plant Pathology 91: 100-105.
- Washitani, I. & A. Takenaka, 1984. Germination responses of a non-dormant seed population of *Amaranthus patulus* Bertol. to constant temperatures in the sub-optimal range. Plant, Cell and Environment 7: 353-358.
- Watt, A.D., G.P. Vickerman & S.D. Wratten, 1984. The effect of the grain aphid, *Sitobion avenae* (F.), on winter wheat in England: an analysis of the economics of control practice and forecasting systems. Crop Protection 3(2): 209-222.
- Weir, A.H., P.L. Bragg, J.R. Porter & J.H. Rayner, 1984. A winter wheat crop simulation model without water or nutrient limitations. Journal of Agricultural Science 102: 371-382.
- Werf, W. van der, N.P.C. Mul, L.E.E.M. Spätjens & R. Rabbinge, 1989a. Effects of beet yellows virus on photosynthesis and dry matter production in sugarbeet. (In prep.).
- Werf, W. van der, P.R. Westerman, R. Verwey & D. Peters, 1989b. The effect of the date of primary virus infection on spread of beet yellows virus and beet mild yellowing virus in sugarbeet. (In prep.).
- White, T.C.R., 1984. The abundance of invertebrate herbivores in relation to the availability of nitrogen in stressed food plants. Oecologia (Berlin) 63: 90-105.
- Williams, L.E., 1985. Net photosynthetic rate and stomatal and intracellular conductances subsequent to full leaf expansion in *Zea mays* L.: effect of leaf position. Photosynthetica 19: 397-401.
- Willigen, P. de & J.J. Neeteson, 1985. Comparison of six simulation models for the nitrogen cycle in the soil. Fertilizer Research 8: 157-171.
- Wilson, B.J., 1981. A review of the population dynamics of *Avena fatua* L. in cereals with special reference to work at the Weed Research Organization. Grass Weeds in Cereals in U.K. Conference, 1981. p. 5-14.
- Wilson, B.J., R. Cousens & G.W. Cussans, 1984. Exercises in modelling populations of *Avena fatua* L. to aid strategic planning for the long term control of this weed in cereals.

- Proceedings 7th International Symposium on Weed Biology, Ecology and Systematics. COLUMA/EWRS, Paris. p. 287-294.
- Wilson, D., 1975. Variation in leaf respiration in relation to growth and photosynthesis of *Lolium*. *Annals of Applied Biology* 80: 323-338.
- Wit, C.T. de, 1970. Dynamic concepts in biology. In: Prediction and measurement of photosynthetic productivity. Proceedings IBP/PP technical meeting, Trebon, 1969. Ed. I. Setlík. Pudoc, Wageningen. p. 47-50.
- Wit, C.T. de, 1982. Coordinations of models. In: Simulation of plant growth and crop production. Eds. F.W.T. Penning de Vries & H.H. van Laar. Simulation Monographs, Pudoc, Wageningen. p. 26-31.
- Wit, C.T. de & J. Goudriaan, 1978. Simulation of ecological processes. Revised version. Simulation Monographs, Pudoc, Wageningen. 175 p.
- Wit, C.T. de & F.W.T. Penning de Vries, 1982. L'analyse des systèmes de production primaire. In: F.W.T. Penning de Vries & M.A. Djiteye (Eds.). La productivité des pâturages sahéliens. Agricultural Research Reports 918. Pudoc, Wageningen. p. 20-27.
- Wit, C.T. de & F.W.T. Penning de Vries, 1985. Predictive models in agricultural production. *Philosophical Transactions of the Royal Society London, B* 310: 309-315.
- Wit, C.T. de et al., 1978. Simulation of assimilation, respiration and transpiration of crops. Simulation Monographs, Pudoc, Wageningen. 140 p.
- Wit, C.T. de, H. Huisman & R. Rabbinge, 1987. Agriculture and its environment: Are there other ways? *Agricultural Systems* 23: 211-236.
- Wit, C.T. de, H. van Keulen, N.G. Seligman & I. Spharim, 1988. Application of interactive multiple goal programming techniques for analysis and planning of regional agricultural development. *Agricultural Systems* 26: 211-230.
- Wood, R.K.S. & G.J. Jellis, 1984. Plant diseases, infection damage and loss. Blackwell Scientific Publications, Oxford. 325 p.
- Wong, S.C., I.R. Cowan & G.D. Farquhar, 1985. Leaf conductance in relation to rate of CO₂ assimilation. *Plant Physiology* 78: 821-834.
- Wratten, S.D., 1975. The nature of the effect of the aphids *Sitobion avenae* and *Metopolophium dirhodum* on the growth of wheat. *Annals of Applied Biology* 79: 27-34.
- Zadoks, J.C., 1971. Systems analysis and the dynamics of epidemics. *Phytopathology* 61: 600-610.
- Zadoks, J.C., 1981. EPIPARE: a disease and pest management system for winter wheat developed in the Netherlands. European Plant Protection Organization (EPPO) Bulletin 11: 365-369.
- Zadoks, J.D., 1984. EPIPARE, a computer-based scheme for pest and disease control in wheat. In: Cereal production. Ed. E.J. Gallagher, Butterworths, London. p. 215-225.
- Zadoks, J.C., 1985. On the conceptual basis of crop loss assessment: Threshold theory. *Annual Review Phytopathology* 23: 455-473.
- Zadoks, J.C., 1986. A Dutch perspective of computerization in crop protection. Proceedings British Crop Protection Conference (BCPC) – Pest and Diseases. p. 713-718.
- Zadoks, J.C., 1988. EPIPARE, a computer-based decision support system for pest and

- disease control in wheat: Its development and implementation in Europe. *Plant disease epidemiology* 2: 3-29.
- Zadoks, J.C. (Ed.), 1989. *Development of Farming Systems-evaluation of the five-year period 1980-1984*. Pudoc, Wageningen, 90 p.
- Zadoks, J.C. & P. Kampmeijer, 1977. The role of crop populations and their deployment, illustrated by means of a simulator, EPIMUL, 1976. *Ann. New York Acad. Sci.* 287: 164-190.
- Zadoks, J.C. & R.D. Schein, 1979. *Epidemiology and plant disease management*. Oxford University Press, New York. 427 p.
- Zadoks, J.C. & R.D. Schein, 1980. *Epidemiology and plant disease management, the known and the needed*. In: *Comparative epidemiology. A tool for better disease management*. Eds. J. Palti & J. Kranz. Pudoc, Wageningen. p. 1-17.
- Zadoks, J.C. & R. Rabbinge, 1985. *Modelling to a purpose*. *Advances in Plant Pathology* 3: 231-244.
- Zadoks, J.C., T.T. Chang & C.F. Konzak, 1974. A decimal code for the growth stages of cereals. *Weed Research* 14: 415-421.
- Zadoks, J.C., F.H. Rijdsdijk & R. Rabbinge, 1984. EIPRE: A systems approach to supervised control of pests and diseases of wheat in the Netherlands. In: *Pest and pathogen control. Strategic, tactical and policy models*. Ed. G.R. Conway, Wiley, Chichester. p. 344-351.
- Zwich, R.W., G.J. Fields & W.M. Mellenthin, 1976. Effects of mites population density on 'Newton' and 'Golden Delicious' apple tree performance. *Journal of the American Society of Horticultural Science* 101: 123-125.

Index

- action threshold 217, 269
- ageing 47, 48, 136
- Amblyseius potentillae* 131
- Ambrosia artemisiifolia* 198, 340
- analytical
 - integration 21, 42
 - solution 19, 22, 42, 85, 127
- angular deviation 108
- annual relative decrease 28
- annual relative increase 28
- Aphidius rhopalosiphi* 117
- aphids 11, 269
 - bird cherry oat 240
 - grain (cereal) 221, 240
 - rose grass 240
- assimilate and tissue consumers 223
- assimilation rate reducers 222, 230
- average delay 54, 55

- beet yellows virus 221, 230
- biological control 111, 265
- boxcar train 49, 91, 136
 - escalator 50, 51, 55, 56, 61
 - fixed 51, 53, 55
 - fractional 51, 56, 69, 71
- boxcar width 51, 52, 59, 77
- boxcar zero 52, 58, 61, 69, 77
- brown rust 268

- Chenopodium album* 189
- Chondrostereum purpureum* 99
- clustering 112
- CO₂ assimilation
 - canopy 158, 160, 205
 - leaf 159, 204
 - light use efficiency 159, 172, 211, 232
 - maximum rate 159, 172, 221, 227
- CO₂ concentration 237
- competition 184, 199
- COMPETITOR 211
- constraints 279

- control
 - supervised 279
 - integrated 279
- crop growth rate 147, 200
- crop growth reducing factors 221
- crop protection 265
- crop rotation 265
- crops
 - apple 218
 - barley 182, 187
 - C₃, C₄ 172, 173, 200, 208, 214
 - maize 165, 169, 178, 211
 - potato 165, 179
 - sugar beet 165, 180
 - wheat 11, 164, 165, 169, 178
 - wild oats 182, 187
- CSMP 4, 365
- AFGEN 68
- AMIN1 64, 91
- AMOD 339
- DELAY 48, 56
- DERIV 91
- DIMENSION 65, 71
- DYNAMIC 64, 144
- FUNCTION 65
- IMPULS 60
- INITIAL 64, 144
- INTGRL 60
- METHOD 60
- NOSORT 61
- PARAM 61
- RNDGEN 109
- STORAGE 61
- TERMINAL 144
- TIMER 61
- cyclic development stage 52, 58, 64

- damage 224
- data management 276, 301
- decision making 265, 268, 278, 301
- decision 278

- strategic 265
- support system 267, 268, 276
- tactical 265
- variable 279
- degree-days 49
- degree of freedom 113
- delay 47, 54, 71
 - 1st order exponential 53
 - Nth order 56
- demographic problem 65
- density class 116
- deposition 102
- descriptive 109, 114, 115
- development 47, 94
 - distribution curve 52
 - drift 50, 53
 - epidemiological 220
 - phenological 175
 - rate 48, 53, 59, 88, 164
 - stage 48, 164
- differential equation 19, 38, 43
- dimensions 20
- discontinuities 34, 39
- disease severity 273
- dispersal 91, 99, 106
- dispersion 47, 71, 91, 99, 109, 114
 - in time 90, 94
 - numerical 51, 78
 - relative 56, 69, 77, 90
- distribution 108
 - Chaucy 109
 - logistic 109
 - NBD 113, 114
 - normal 109
 - Poisson 112, 114
 - spatial 111, 116
 - uniform 109, 127
- driving force 36
- dry matter distribution 165, 175
- dynamic behaviour 42
- dynamic equilibrium 43
- dynamic programming (DP) 278
 - deterministic 293
 - stochastic 293
- Echinochloa crus-galli* 193, 197, 211
- economic damage thresholds 13
- Economic Injury Levels 13, 217, 237
- elementary system units 19
- EPIPPE 266
- Erysiphe graminis* 89, 221, 232
- evapotranspiration 208
- equations
 - auxiliary 24
 - descriptive 85
 - difference 170
 - differential 19, 20, 38, 42, 86, 170
 - integral 86
 - logistic growth 84
 - rate 19, 20, 41, 86
 - stiff 143
- equilibrium 23, 27, 42, 43, 103, 130
 - stable 120
- error analysis 35, 38
- errors 19, 32
 - numerical 39
 - relative 36, 37, 39
- evaluation 252
- evaporation 194
- event list 297
- expected relative damage 275
- exponential growth 21, 36, 38, 83, 273
- exponential decrease 40
- exponential delay first order 53
- extinction coefficient 159, 171, 201
- extreme point 282
- eyespot 269
- feasible region 282
- feedback 19, 23, 35, 38, 44
 - negative 4, 23
 - positive 2, 24
- field monitoring 267
- finish conditions 70
- fixed time interval 32
- forcing function 7, 90
- form
 - canonical 284
 - standard 284
- FORTTRAN 4, 365
- fractional repeated shift 57
- fraction of survival 65
- functional response 124
- Galium aparine* 189
- generation 131

- germination 91, 190
 - dormancy 197
 - light 198
 - soil cultivation 192, 198
 - soil moisture 194
 - temperature 192
- goal programming 278
- growth
 - sink-limited 254
 - source-limited 254
- grain growth 166
- heuristic 8, 239
- honeydew 221, 224, 229, 246
- host-parasite 119
- hybridizing 57
- implementation 59, 267
- infectious period 84, 85, 87, 88, 220
- initialization 176
- integration
 - accuracy of 32
 - analytical 21, 43
 - Euler 31
 - driving force 35
 - Gaussian 160
 - numerical 19, 24, 30, 35, 85
 - rectangular 30, 31, 33, 40
 - Runge-Kutta 30, 31
 - trapezoidal 30, 31, 33
- IPDM 269
- iso-line profit 281
- iteration 112
- Lamium amplexicaule* 198, 340
- latency period 48, 84, 88, 220
- leaf
 - area 90, 95, 169, 175
 - area index 85, 102
 - biomass 90
 - coverage 229
 - senescence 170
 - wetness 91
- Lema cyanella* 224
- level of organization 5
- light
 - absorption 229
 - reflection 230
 - stealing 222, 229
 - transmission 230
- light utilization efficiency 200
- limit to Δt 27
- linearity 115
- linear programming (LP) 278, 280
- logistic growth 84, 119
- logit transformation 84
- logit value 84
- maximum likelihood 112, 115
- management 276, 278
- Metopolophium dirhodum* 240
- mildew 91, 221, 232
- mites 221
- models 3, 19
- models
 - combination 143, 217
 - comprehensive 8
 - comprehensive explanatory 122, 266
 - conceptual 8, 122
 - descriptive 4, 5, 6, 99, 109, 217
 - deterministic 124
 - dynamic 4, 19, 43
 - empirical 177
 - epidemiological 220
 - explanatory 4, 5, 111, 308
 - four-layer 104
 - mathematical 3
 - mechanistic 177
 - numerical 83, 99, 124
 - one-layer 101
 - paralogistic 85
 - population 83, 131
 - predator-prey 119
 - static 4, 43
 - stochastic 124
 - summary 8, 147, 308
- Monte Carlo analysis 129
- Negative Binomial Distribution 111
- network 290
- nitrogen contents 220
- non-linear regression 278
- numerical
 - dispersion 51
 - integration 19, 24, 30, 35, 85
 - search method 297
- nutrients 211

- objective function 279
- operation research 278
- optimization 279
- oviposition 136

- Pandemis heparana* 71
- Panonychus ulmi* 131
- paralogistic growth 84, 85, 90
- parameter
 - clustering 115
 - physiological 40
 - technical 40
- pathosystem 3, 276, 278, 303
- pesticides 265
- physiological age 135
- pivot 286
- planning horizon 298
- population dynamics 15, 97, 111, 182, 268
- population growth 84, 97
- population models 83, 131
- post-optimal analysis 288
- powdery mildew 85, 268
- predator 106, 119, 138
- predation 123, 137
- predator-prey 97, 119
- preference 138
- prey 119, 142
- prey utilization 137
- probability 111
- Production Situations 10, 11
- Prunus serotina* 100
- Puccinia striiformis* 268, 306

- queuing technique 129

- radiation
 - diffuse 158
 - direct 158
 - photosynthetically active 159, 171, 200
 - shortwave 158
- random number generator 109, 126
- rates 9
- rate variable 7, 20
- real infection rate 94
- recommendation 269, 277

- relational diagram 7, 19, 23, 24, 25, 40, 85
- relative dispersion 56, 69, 77, 90, 134, 363
- relative death rate 28
- relative growth rate 20, 28, 83, 84, 91, 170
- relative mortality rate 83, 91
- relative reproduction rate 83
- reserves 166
- resetting event 52
- resistance
 - carboxylation 237
 - exchange 101, 106
- respiration
 - dark 232
 - growth 163, 174, 211
 - maintenance 162, 174, 211, 225
- response time 7
- Rhopalosiphum padi* 240
- risk accepting 265, 277, 303
- risk analysis 297
- risk avoiding 265, 277, 303

- sedimentation 102
- semi-parallel 29
- sensitivity
 - analysis 106
 - coarse analysis 253
 - fine analysis 253
 - relative 253
- Septoria 269
- shift
 - fractional repeated 57
- simplex
 - algorithm 285
 - tableau 287
- simulation 3, 301
 - compound 129, 130
 - deterministic 125
 - discrete event 278
 - dynamic 19, 29
 - stochastic 125
- sink-source relationship 166, 242, 254
- Sitobion avenae* 240
- solution
 - alternative 283
 - analytical 22
 - unbounded 283
- spatial heterogeneity 118
- specific leaf area 176

spore
 concentration 102
 dispersal 100
 'effective' 91
 exchange 104
 germination 91
 population 118
 production 102, 104
 production layer 100
 stand reducers 221, 222
 states 9
 state-variable approach 6, 19
 state variable 7, 34
 stiff equations 143
 stochastic process 118, 124, 293
 stomatal conductivity 237
 subroutine
 BOXCAR 69, 85
 SHIFT 61, 65
 success ratio 106, 137
 SUCROS87 147, 221, 224
 sugar beet 165, 180
 superproportionality 275
 systems 3, 19, 301
 systems
 agroeco- 3
 analysis 3
 cropping 3
 decision support 267, 268, 276
 elementary 25
 farming 3
 management 12
 recurring 4
 recurring ecological 5
 repeatable 4, 5
 state determined 7
 unique 4
 unique ecological 4

 Taylor expansion 36, 361, 362
 temperature sum 165, 193
 time
 average residence 28, 41, 58
 coefficient 7, 20, 24, 27, 28, 55, 103
 constant 28
 delay 28
 doubling 29
 extinction 29
 relaxation 29
 residence 51, 134
 transmission 28
 time interval of integration 7
 time step 107
 total variance 59
 transformation function 279
 transpiration 208, 210
 turbulent exchange 102, 103
 turgor reducers 224

 validation 9
 variables
 auxiliary 7, 9
 driving 6, 19, 21
 forcing 9, 21
 rate 6, 7, 19
 slack 285
 state 6, 7, 19
 variance 55, 59, 108, 363
 verification 9, 252

 walking pattern 106, 109
 weeds 182
 control 187, 203
 competition 184
 germination 190
 population dynamics 183
 soil seed population 183
 wheat 11, 164, 178
 wind speed 102

 yeast 40
 yellow rust 268, 306
 yield
 loss 217, 229
 potential 9
 reduction 228, 231
 yield-determining factors 9
 yield-limiting factors 9, 13, 240
 yield-reducing factors 10, 11, 13, 240

Simulation Monographs 32

This textbook introduces the reader step by step to simulation and systems analysis, and to their application in crop protection. It explains the systems analysis of crop growth, yields and losses, the population dynamics of pests, diseases and weeds, and the assembly of these analyses into various models.

Understanding of how pathosystems function and the way basic processes affect their behaviour is gained by the combination of experiment and modelling. Comprehensive models of crop growth, the population dynamics of pests, diseases and weeds, and the interaction between crop growth and pathogens are presented and explained.

Comprehensive models are scientific tools and not aims in themselves. The way these models can be used to develop crop and disease management systems is illustrated. It is shown how pathosystems management can make use of simple summary models based on the insight gained by simulation. Management tools making use of data banks, dynamic programming and other optimization techniques are described.

The book is written as an elementary text for laymen in this field and it contains many exercises to help students to familiarize themselves with the way of thinking and experimenting needed for simulation and systems management in crop protection.

ISBN 90 220 0899 1
NUGI 835



Pudoc Wageningen